

UNCLASSIFIED

AD NUMBER
AD921522
NEW LIMITATION CHANGE
TO Approved for public release, distribution unlimited
FROM Distribution authorized to U.S. Gov't. agencies only; Test and Evaluation; 28 FEB 1974. Other requests shall be referred to Space and Missile Systems Organization, Los Angeles, CA 90045.
AUTHORITY
SAMSO, USAF ltr, 17 Jun 1977

THIS PAGE IS UNCLASSIFIED

AD-921522

FILE COPY

R-74-034

SAMSO-TR-74-181

SYSTEM/DESIGN  
TRADE STUDY REPORT  
FOR  
GLOBAL POSITIONING SYSTEM  
CONTROL/USER SEGMENTS

CS/UE DEFINITION CONTRACT  
F04701-73-C-0298

Prepared for  
Space and Missiles Systems Organization  
Los Angeles, California 90045

DATA ITEM A002  
FEBRUARY 28, 1974



**GENERAL DYNAMICS**  
*Electronics Division*  
P.O. Box 81127, San Diego, California 92138 714 279-7331

5

91

## **DISCLAIMER NOTICE**

**THIS DOCUMENT IS BEST QUALITY  
PRACTICABLE. THE COPY FURNISHED  
TO DDC CONTAINED A SIGNIFICANT  
NUMBER OF PAGES WHICH DO NOT  
REPRODUCE LEGIBLY.**

## 1. INTRODUCTION

This Trade Study Report documents the decision rationale used to resolve configuration design approaches. The trade studies presented are the major decision efforts required during this concept Definition Phase. The design of the Global Positioning System (GPS) for Phase I required evaluation of alternatives for a variety of design problems. The trade studies contained in this report are:

<u>No.</u>	<u>Title</u>
1.	Satellite Memory Loading
2.	Satellite Orbits
3.	Monitor Station Sites
4.	Control Segment Computers
5.	User Segment Computer
6.	User Cost/Performance
7.	User Ionospheric Model
8.	User Ephemeris Model
9.	Ephemeris Determination

The Satellite Memory Loading trade study investigates the alternatives for uploading and storing in satellite memory that portion of the user navigation data frame generated by the Master Control Station (MCS). The alternatives considered dealt with the implementation and error contributions of the upload station design, upload message format, satellite receiver and decoder configuration, data verification method, and downlink communication channel to the ground.

The Satellite Orbits trade study investigates the selection of the satellite constellation and orbits for the Phase I. The important parameters are GDOP's and visibility over the expected test areas.

The Monitor Station Sites trade study investigates the possible locations of Upload Station (ULS), Monitor Stations (MS) and Master Control Station for collecting, processing, and uploading pseudo-range and clock data of the satellites. The satellite visibility and viewing times of these sites must be compatible with satellite navigation system updates prior to testing over southwestern CONUS.

The Control Segment Computers trade study investigates the computational equipment required by the Master Control Station and Monitor Stations for Phase I. This effort is to perform a preliminary evaluation and sizing of computer equipment that will satisfy the mandatory requirements of the stations. The computers must be capable of supporting a constellation of 12 satellites.

The User Segment Computer trade study investigates the computational equipment required by the User Segment equipments for Phase I. This effort is to perform an initial evaluation of potential computer equipment to determine those equipments that meet the expected minimum set of design requirements.

The User Cost/Performance trade study investigates design-to-cost criteria of user equipment with respect to predicted design performance. The areas of importance are the requirements of maximum commonality, hardware versus software implementation, digital or analog circuitry for minimal life cycle cost.

The User Ionospheric Model trade study investigates potential algorithms for predicting the ionospheric delay of the ranging signal. The algorithms must be compatible with the spare bits and time spans of the user navigation data frame.

The User Ephemeris Model trade study investigates possible mathematical models of satellite position that will permit the users to determine the satellite location via the L-band user navigation data. The models must not overburden the user navigation data frame and provide an error of less than 1 foot with respect to the MCS predicted satellite orbit.

The Ephemeris Determination trade study investigates potential methods of computing the predicted satellite position and orbit based on measurement made by the Monitor Stations. The computational complexity, accuracy and convergence properties of the algorithm are the important evaluation parameters.

## 2. TRADE STUDIES RESOLVE GPS DESIGN

The Global Positioning System (GPS), Phase I, is a space-based radio navigation system which will provide suitably equipped users system time and three-dimensional position and velocity within designated test areas. The GPS is composed of four system segments: Space System Segment, User System Segment, Control System Segment, and Navigation Technology Segment. It is the purpose of this effort to resolve design tradeoffs within the User System Segment and Control System Segment. Because of the critical interfaces between the ground and space segments careful consideration must be taken to insure minimal impact on the satellite design.

All of the trade studies performed can be directly related to interfaces between system segments or the individual system segment components. The Satellite Orbit trade study is a minor exception since its purpose is to document the effort devoted to defining the most effective orbits for Phase I of GPS. The relationship of the trade studies to the system segments is shown in the functional block diagram of Figure 1. The design of the unload station-satellite interface and procedure is selected by the Satellite Memory Loading trade study. The resulting design will be suitable through Phase II of the GPS program since operation with at least twelve satellites is planned.

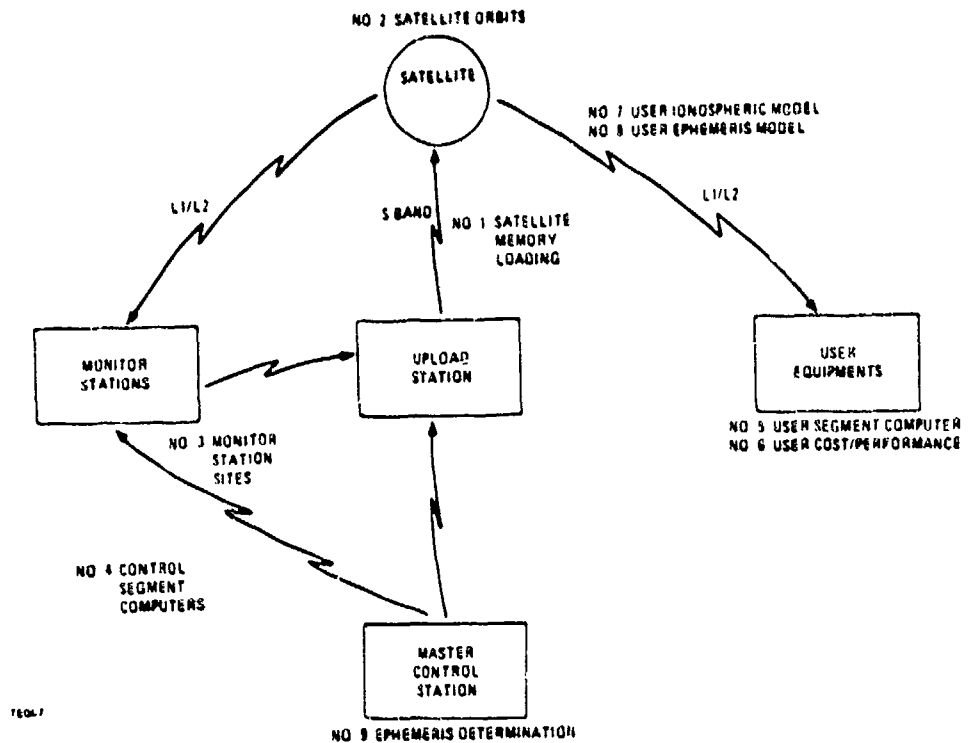


Figure 1. Relationship of Trade Studies and System Segments

The selection of configuration and orbit parameters for the initial 4 satellites is documented in the Satellite Orbit trade study. Since only 4 satellites were considered and their orbits were optimized for specific test areas, the results are only applicable to GPS Phase I.

The analysis for the selection of sites for the MS, ULS, and MCS are documented in the Control Segment Site trade study. These evaluations are also considered only system geometry requirements for specific test areas and therefore are applicable to GPS. Phase I.

The purpose of the Control Segment Computer trade study is to identify those computers that will satisfy the mandatory computational requirements of the Master Control Station and Monitor station. In terms of future phase requirements it is desired that the computer selection be made assuming that the configuration be adequate at least until the latter stages of GPS Phase II or possibly the beginning of GPS Phase III.

The User Segment Computer and User Cost/Performance trade studies deal directly with user equipment design for Phase I and on. Since it is an objective not to develop any new computers for Phase I, the computer selection is limited to existing computers that can satisfy the computational requirements of Phase I. The cost/performance analyses have much greater scope since the intent of the trade study was to generate user equipment configurations that will develop valid design-to-cost criteria.

The purpose of the User Ionospheric and Ephemeris Model trade studies is to develop analytic models that will provide to the user from the Master Control Station, via the satellite, accurate knowledge of the ionospheric delay and satellite ephemeris. These models must be compatible with the low data rate channel available with the  $L_1/L_2$  navigation channels and require a minimum computational burden upon the user equipment. It is desirable that these models be suitable for all Phases of the GPS program. Changes within the constraints of the communication capacity of the system are possible during the test portion of Phase I with little impact upon user software.

The Ephemeris Determination trade study provides the computational approach that yields the detail of the interface between the Master Control Station software and the Monitor Station pseudo-range measurements. The resulting computational approach should be adequate for all phases of the GPS program.

### 3. RESULTS

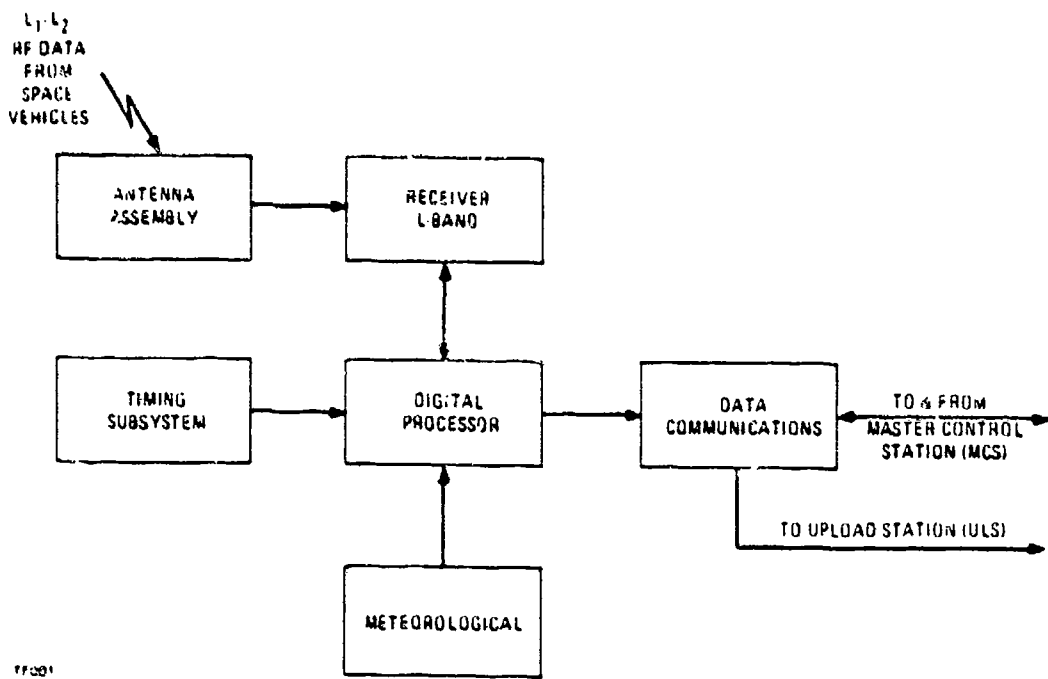
This section details the selection resulting from each trade study analysis. Only conclusions are presented and no attempt is made to justify the determinations in this presentation. For the rationale and corresponding analysis, that led to these conclusions, the reader is referred to the individual trade studies following this survey.

#### 3.1 Satellite Memory Loading

The recommended satellite loading method is S-band uplink/L-band downlink with on-board verification of upload messages and the AFSCF is its backup. The S-band upload frequency is one of the standard SGLS frequencies with a 3 tone FSK data modulation. The L-band downlink is the TLM words of the user navigation data frame; they will contain the addresses of erroneous blocks.

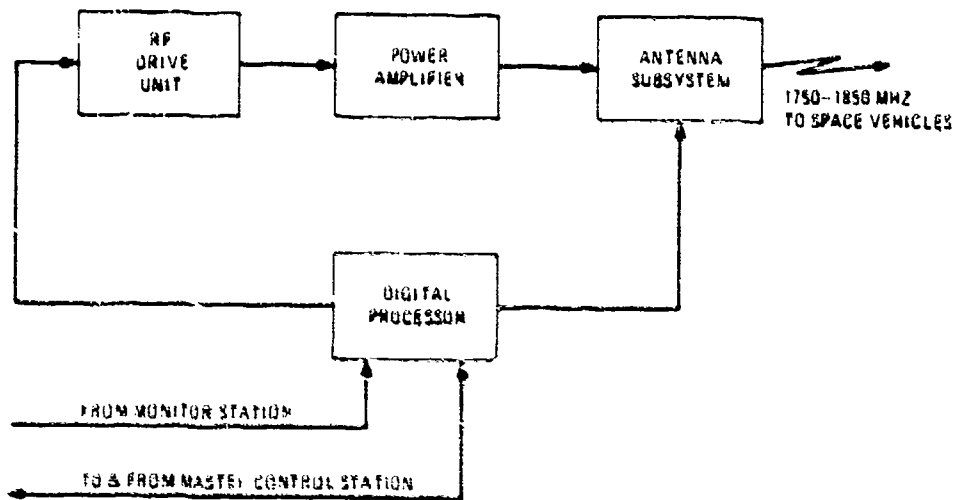
3.1.1 Upload Station. Figure 2 illustrates the functional block diagram of the Monitor Station/Upload Station. The recommended station consists of a 14-ft antenna, S-band TWT transmitter, formatter, display, antenna drive, computer and modems for communication with the Master Control Station computer and Monitor Station computer. This configuration has the advantages of being moved to another monitor station location or being remotely located from its monitor station with a minimum of interface disconnections.

3.1.2 Satellite. A functional block diagram of a feasible satellite configuration for loading the memory is shown in Figure 3. The function of the SGLS R-23 and command decoder is to receive the access words for the GPS decoder. It is suggested that the GPS access commands storage be capable of many days of unattended operation to circumvent AFSCF impact on operation.



17301

Monitor Station



17302

Upload Station

Figure 2. Monitor Station/Upload Station



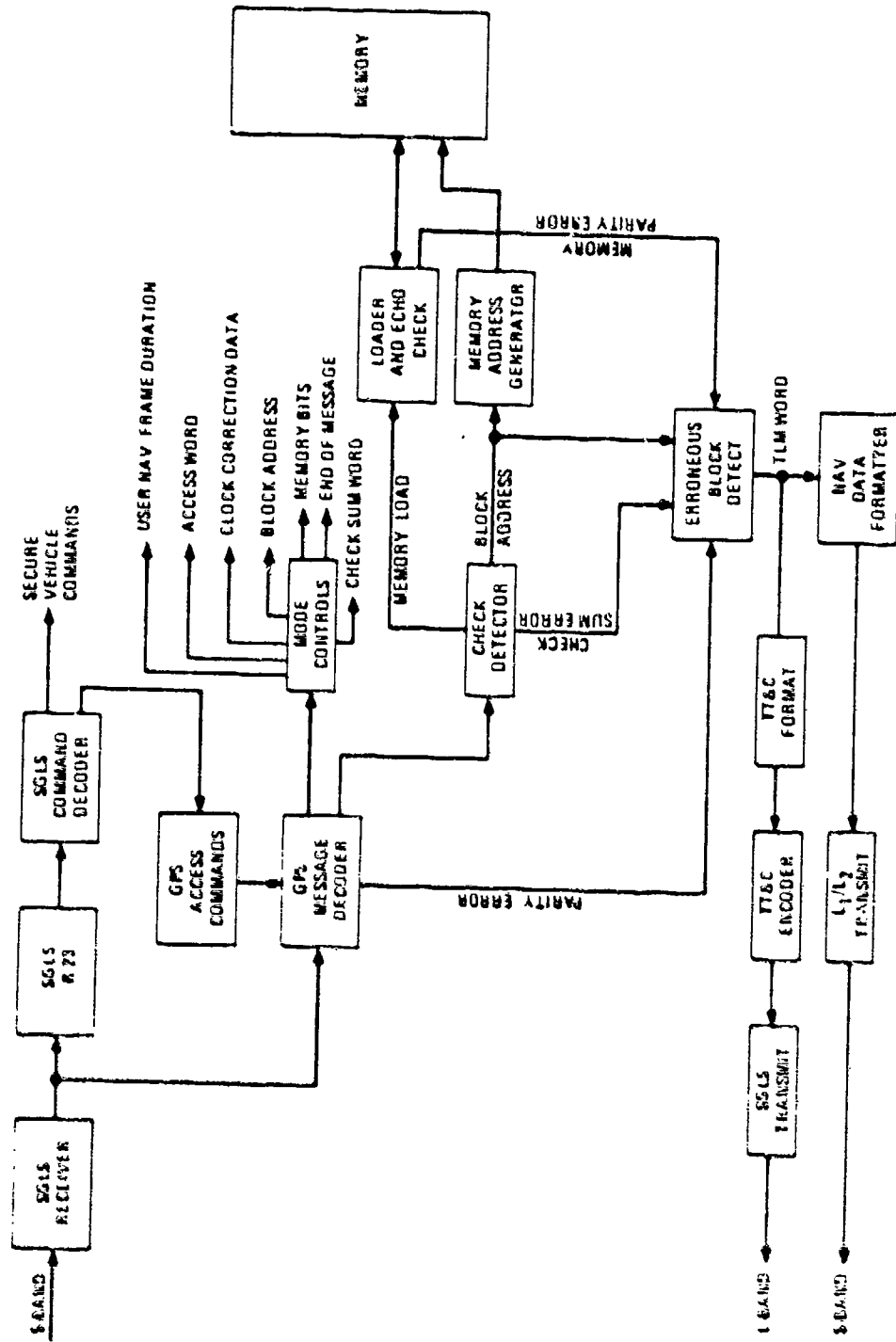


Figure 3. Satellite Configuration for Loading Memory

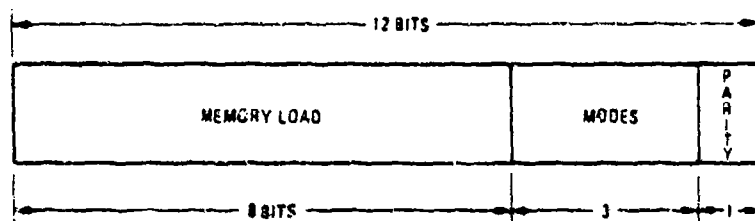
The reception of a memory load is enabled by an access word that will enable the GPS decoder to accept data words and blocks. The digital word received by the GPS decoder should contain memory bits, mode bits and a parity bit. In addition, each block of data will end with a check sum word since both horizontal and vertical parity checks are required to obtain an undetected bit error rate of  $10^{-15}$ . Anytime an error is discovered, the erroneous block address will be incorporated into the TLM word and provided to the SGLS TT&C format if the loading verification is in the backup mode.

As the words are decoded by the GPS decoder, the block address is loaded into the memory address generator and the memory is loaded word by word from the memory address corresponding to the received block address. As a word is loaded into memory, it would be advisable to immediately re-read (echo) the word from memory and perform a parity check on the word using the parity bit required for the user navigation data transmission. Again, a parity error would enable transmission of the erroneous block address to the upload station. The echo check of the memory load can be performed by cycle sharing since the incoming data has a rate of only 1 kilobit per second.

The purpose of the mode bits is to provide control information to the satellite that identifies the purpose of the load and the type of word received. This type of data is considered overhead and must be distinguishable from any memory data. Therefore, separate bits are recommended to provide these modes. Three bits should be sufficient to provide these modes.

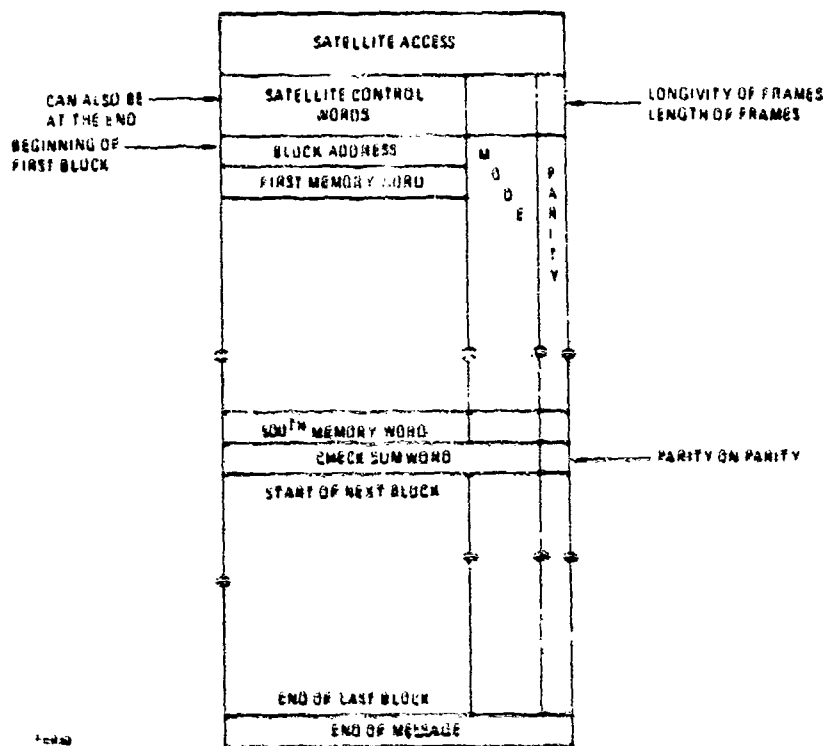
3.1.3 Message Format. The message format refers to the size and structure of the upload message and downlink data. The upload message will consist of blocks both for the initial transmission and subsequent retransmissions. During retransmissions only, blocks found in error will be uploaded again.

Given that the portion of the user navigation frame stored in the satellite is composed of 4 bit bytes, the minimum word size feasible for uploading is 12 bits. These 12 bits include 4 bits for memory, 3 bits for modes and 1 bit of parity. For an uplink BER of  $10^{-6}$ , the maximum block size of 375 words is imposed to meet the undetected bit error rate of  $10^{-15}$ . The recommended word format is shown in Figure 4. The recommended block size is 302 twelve-bit words. The 302 words will provide for 300 eight-bit words for the memory. This results in the transmission of exactly 25 blocks for a total memory load of 100,000 bits. Slightly over 6 seconds are required to transmit each block, therefore a TLM word will always be available for erroneous block addresses and no additional satellite storage is required. The resulting message format for uploading is shown in Figure 5.



14020

Figure 4. Recommended Word Format



14020

Figure 5. Message Format for Uploading

3.1.4 Performance Parameters. The significant performance parameters of the recommended uploading approach are:

Uplink Frequency	S-Band - Standard SGLS
Downlink Frequency	L-Band. L <sub>1</sub> , L <sub>2</sub> , TLM data words
Uplink BER	10 <sup>-6</sup>
Downlink PER	10 <sup>-5</sup>
Word Size	12 Bits
Block Size	502 Words
Undetected Bit Error Rate in Memory	10 <sup>-15</sup>
Error Detection	Word parity and block check sum
Overhead	2024 bits per 4000 bits of memory data
Message Flexibility	One or more blocks can be sequentially loaded
Modes	At least eight separate satellite command words are available.
Access	Via GPS decoder using stored bit patterns

### 3.2 Satellite Orbits

The purpose of the satellite orbit selection trade study is to optimize the duration of test area coverage by all four satellites GDOP factor over the test area, and pre-visibility for monitor and upload stations for tracking, clock evaluation, and satellite memory uploading prior to testing. The results of computer evaluation indicates that the 2/2/0 Aerospace Final Constellation provides the best compromise between the requirements of GDOP, test area co-visibility and pre-visibility. The characteristics of the orbital parameters of this constellation are:

Satellite Number	Longitude of the Ascending Node (deg)	Argument of Perigee (deg)	Orbit Inclination (deg)	Orbital Period (min)
1	240	330	63.0	718.0343
2	240	3	63.0	718.0342
3	120	0	63.0	718.0342
4	120	70	63.0	718.0342

The performance of this satellite constellation in terms of Holloman, Yuma, and Vandenberg test site coverage and GDOP and the period of time all satellites are visible prior to the Holloman visibility are:

**PERFORMANCE**

<u>Test Area</u>	<u>Coverage Time</u>	<u>GDOP Range</u>
Holloman	2 Hours 32 Minutes	4.2 to 7.2
Yuma	2 Hours 11 Minutes	4.2 to 9.1
Vandenberg	2 Hours 4 Minutes	4.2 to 10.8

**PRE-VISIBILITY**

<u>Location</u>	<u>Pre-visibility Time (all four satellites)</u>
Vandenberg, Ca.	20 Minutes
Wahiawa, Hawaii	1 Hour 20 Minutes
Elmendorf, Alaska	1 Hour 45 Minutes

**3.3 Monitor Station Sites**

The acceptability of site locations for Monitor Stations and the Upload Station must be determined with respect to a defined satellite orbit and specified test area. The satellite orbits used for the evaluation is the 2/2/0 Aerospace Final Constellation which was the orbit selection of Trade Study No. 2. The test areas assumed for this effort were the Holloman and Yuma Test Ranges. By locating the Monitor and Upload Stations where satellite tracking and clock monitoring can be performed and fresh user navigation data can be uploaded into the satellite memory just prior to satellite visibility over the test area.

The recommended control segment configuration based upon the satellite viewing time and tracking geometry analysis is given in Table 1. Originally, the fourth Monitor Station site was located at Prospect Harbor, Maine. It is felt that it should be relocated to provide more effective satellite monitoring prior to entering the test area. Considerations which are not visible to this contractor will drive the final selection by the JPO. Those considerations include the future plans for the utilization of existing network sites, availability of existing buildings to house the Control Segment equipments and, finally, the willingness of host commands to share facilities for the GPS Program.

Table 1. Control Segment Configuration

Function	Location/Type
Monitor Sites	1. Wahiawa, Hawaii 2. Vandenberg AFB, California 3. Elmendorf AFB, Alaska 4. TBD
Master Site	Vandenberg AFB, California
Upload Station	Vandenberg AFB, California Command Date - AFSCF
Telemetry	AFSCF
Off-line Computations	NWL
Data Communications	Commercial Dial-up

### 3.4 Control Segment Computers

The purpose of this trade study was to identify potential suppliers and types of candidate computers for the Master Control Station and Monitor Station. At this juncture, a final selection of computers is impossible without a formal submission of vendor proposals that guarantee their hardware, software and service capabilities. Therefore, all types of computers that satisfy the mandatory requirements of the Master Control Station and Monitor Stations are identified. These candidate computers and their manufacturers (Table 2) are limited to manufacturers capable of supplying both the Master Control Station and Monitor Station Computers. If possible, candidate computers should be selected from the same family thereby, simplifying support and maintenance requirements.

Table 2. Candidate Computers

Manufacturer	MCS Candidate	MS Candidate
Data General Corporation	840	Nova 2
Digital Equipment Corporation	11/45	11/40
Hewlett-Packard Co.	3000	2100
Modular Computer System	IV	II
Varian Associates	V73	V73 or 620

The question not resolved is whether or not it is feasible to employ the User Segment computer for the Monitor Station. Analysis is continuing to resolve this question. Computers that appear feasible to satisfy both User Segment and Monitor Station requirements are: the Data General, ROLM Rugged Nova 1602R; Digital Equipment, 11/20/R; Hewlett-Packard 2100; and Varian Associates R620. The HP 2100 is not ruggedized but undergoes more stringent testing and has been successfully used in more airborne, and maritime applications than any other standard version of minicomputer.

### 3.5 User Segment Computer

The purpose of this trade study was to survey the multitude of computer candidates and determine those machines capable of satisfying the mandatory requirements of a User Segment Computer. From the analysis, it was determined that a very small number of candidates can satisfy the mandatory requirements of higher order language capability, floating point double precision hardware, and proven reliability. At this time the preliminary evaluation indicates that the ROLM rugged Nova-1502R is the superior selection. However, there are other computers that merit serious consideration: General Electric CP32A, Univac MPC-16, Honeywell 516, and Rockwell D216.

This analysis is continuing in terms of desirable features such as ability to interface with auxiliary sensors and the ability to perform the computational and control functions of a monitor station. This analysis will continue through the evaluation of formal proposals from capable vendors.

### 3.6 User Cost/Performance

The purpose of this trade study is to identify specific design techniques that have significant impact upon the cost and performance of User Segment equipment. The primary emphasis on the user equipment design is to develop a minimum cost set of user systems that will provide adequate operational capability for a specified military mission. Table 3 summarizes candidate design techniques, range of cost deltas, and performance range.

In all cases, the cost/performance evaluations are not finalized. It is expected that these and other design techniques will be continually quantified through out the Phase I testing program as the performance of GPS is verified.

Table 3. Cost/Performance Range

Candidate	Cost Delta Range	Performance Range
Oscillator Stability for Direct Acquisition	\$53 - \$190	10 - 100 times longer operation
Standard Oscillator Frequencies	\$200/unit	Logistics and maintenance only
Error Correcting Codes	\$300/unit	2-3dB Lower Threshold
IMU Calibration and Modeling	\$100/unit	2dB AJ increase
IMU Dynamic Aiding	\$300/unit	Lower Acquisition & reacquisition time - values TBD
Dual Ionospheric Frequency Measurement	\$680/unit	Residual error less than 10 ft.
Plated wire memory hardening	TBD	Nuclear threat protection
Kepler Alert Program	\$60/unit	Improved best GDOP selection aids direct acquisition by factor of six.
Analog vs. Digital Circuits	Implementations known cost - TBD	TBD
Hardware vs. Software Implementations	Software Cost increase \$200/unit - hardware cost savings- TBD	Software has 0.5 to 1 dB sensitivity loss



### 3.7 User Ionospheric Model

Most of General Dynamics work and that of earlier SAMSO contractors has addressed the development of a dynamic ionosphere model — one that depends on time and certain measured solar indices. We have recently undertaken investigation of static models — i.e., simple models which are simply stored in the User Computer and are not updated. General Dynamics intends to further explore this type model and will update the radar study input to include results at a later date.

The recommended dynamic ionospheric model for determination of atmospheric delay by the user is a series representation of the line-of-sight signal delay. This method is referred to as the Satellite Transmit Delay model. It provides a polar coordinate model of the signal propagation delay in terms of range, azimuth, and coelevation angle from a known subsatellite point. This approach saves considerable user computation complexity because the signal delay is obtained directly from the model without an intermediate step of computing the total electron content of the atmosphere along the ray path of the signal.

The series model of ionospheric line-of-sight delay is obtained by the Master Control Station computer. The computations performed are:

1. An empirical grid of ionospheric vertical electron density and height is generated from the Bent Model. The grid pattern is a set of evenly spaced locations in concentric circles centered at the subsatellite point, out to the termination of the satellite's field of view.
2. Using the vertical electron density and ionospheric height at each grid point, the line-of-sight delay to the satellite is computed for each grid point at some time,  $t$ .
3. The line-of-sight at each grid point is then least squares fit with a function that is power series in coelevation angle and trigonometric functions of azimuth angle.
4. The resulting coefficients of the series are quadratic functions of time and it is these coefficients that are transmitted to the user.

The model parameters, transmission requirements, user storage, and performance are:

Number of Coefficients	24
Resolution of Coefficients	5 bits
Model Duration	1 hour
Data Transmission	127 bits per satellite per data frame
User Storage	508 bits
RSS Error	23% to 35% of total atmospheric delay
RSS Error (feet)	10 feet average along line-of-sight

The model duration can be increased as desired, however, the penalty paid is increased error. It should be noted that evaluations of these modeling techniques is continuing and that the above results are the best to date.

An alternate approach to the dynamic ionosphere model involves a cross grid of magnetic latitude and longitude (i.e., a one-dimensional dependence on latitude combined with a multiplying factor which depends on longitude and other independent variables; solar activity, year, month, day.) We are still investigating this approach.

We are also investigating two static models: 1) A simple tabulation of total electron content versus magnetic latitude and longitude versus local time of day; and 2) A simple tabulation of total electron content versus only local time of day. The determination of the best static model and evaluation of residual statistics is continuing.

### 3.8 User Ephemeris Model

The recommended ephemeris model for determination of the satellite position by the user is the Keplerian orbit computation. A set of 13 parameters is required to solve for the satellite position in an inertial frame of reference using the classical two body configuration for Newtonian mechanics. Of the 13 parameters, 9 are fixed, 3 are variable and the last is time or mean anomaly.

By using the inertial coordinate frame of reference, it will be necessary to describe the deviation of the satellite from a perfect Kepler ellipse. With a 12-hour orbit, these deviations are very small in magnitude and will change very slowly. Therefore, it should be possible to describe these variable coefficients in a functional format with very few coefficients of small magnitude and adequate accuracy over a long time span. The 3 variable parameters for satellites at an orbital height of 11,000 nautical miles and where the effect of gravity anomalies and their rate of change is small, will be represented with less than 51 bits to provide for a resolution of 0.1 meters.

The use of an inertial coordinate system to describe the satellite position in space as a function of time is recommended. Although the user must convert to earth fixed coordinates to compute a fix, alert calculations for predetermining approximate satellite position prior to acquisition are easily performed. Also, as stated above, the variable parameters are better behaved.

Although the Kepler method requires more user computations than other methods, the added complexity will be very small when compared to the overall cost of even the least expensive GPS user equipment. For low cost equipment, a microcomputer will be employed to perform the position fix calculations. The use of Kepler orbit parameters will require a modest increase in the size of this microprocessor memory. The additional memory considered sells today for less than \$10 in 100 lot quantities. The additional computation time of less than one second per position fix seems negligible for the low cost user since a fix update rate of every 6 to 10 seconds appears more than adequate.

The physical parameters, performance and requirements of the Keplerian approach are:

Satellite reference frame	Inertial
User Program Storage	1,352 bits
Computation time	333 msec (Intel 8080)
Bits transmitted	416 bits, maximum
Data frame longevity	Up to 4 hours
RMS Position error	1.0 ft. from MCS predicted orbit
RMS velocity error	Less than 0.05 ft/sec

It should be noted that Phase I is an ideal time to evaluate and refine both Keplerian orbit and polynomial representations of satellite position. Excellent models of gravity anomalies and force fields will be available. Also, modifications to US and MCS software can be easily performed with a minimum of logistical impact because of the few number of user equipments. The user impact assessment of the Keplerian orbit is a very recent result. Therefore, the System Specifications were prepared assuming a user ephemeris model using a power series polynomial representation of each coordinate of satellite position.

TRADE STUDY NO. 1

SATELLITE MEMORY LOADING

D. D. Thornburg



**GENERAL DYNAMICS**

*Electronics Division*

P.O. Box 81127, San Diego, California 92138 · 714-279-7301

## 1. INTRODUCTION

The configuration of the GPS requires that the satellite provide to the user the system data required to compute his position. This data consists of satellite ephemeris, system time and ionospheric correction data. Since the satellite is in subsynchronous orbit, the data must be loaded into the satellite memory for future distribution to the user. The purpose of this trade study is to resolve the methods for uploading of this data and verifying its accuracy after reception by the satellite.

Conceptually, the satellite memory loading requires an uploading station for communicating with the satellite, compatible receiving equipment in the satellite, a downlink from the satellite to permit data transfer back to the uploading station, a method of verifying correct reception of data by the satellite, efficient message formatting for both the up and downlink, and a communication channel between the uploading station and the master station computer where the user navigation data is generated. The message format, uploading station and satellite must also be compatible with the AFSCF network that will be used as backup.

Although the present upload station specifications are for GPS Phase I, it is important that the requirements of GPS Phases II and III be considered. Conceptually, the upload requirements for GPS Phases II and III will remain unchanged. The major differences are the capability to support the additional satellites of later Phases and the physical design requirements necessary for possible relocation of the upload station because of future operational objectives.

## 2. REQUIREMENTS

### 2.1 Functional

The upload station is a collection of automatic data processing, radio frequency and data communication equipment which with a set of data bases and algorithms serve to relay navigation subsystem messages from the Master Control Station (MCS) to the space vehicles and vehicles and verify proper receipt of the messages by the space vehicles. Source: SS-GPS-101A, para. 3.7.3.3.

### 2.2 Design

- a. The upload station shall generate a radio frequency environment that is compatible with the space vehicle (SGLS). The upload link and verification technique shall provide an undetected bit error rate of  $10^{-15}$ . Source: SS-GPS-101A, para. 3.2.1.2.3.1.

- b. Data communication between the upload station and the Master Control Station will be performed at the minimum rate needed to support twelve closely spaced satellites; the use of conditioned lines will be avoided if possible. Source: SS-GPS-101A, para. 3.2.1.2.3.2.
- c. The upload station will automatically attempt to reload all segments of any space vehicle navigation subsystem memory in which a load error has been discovered through analysis of the L-band or S-band message from the space vehicle. The number of additional attempts required shall be controlled by software or manual intervention. Source: SS-GPS-101A, para. 3.2.1.2.3.3.

### 2.3 Ground Rules

- a. The maximum message size required by the satellite memory is 100 K bits in length. Computational analysis assumes an overhead factor of 25%.
- b. The satellite memory is partitioned in a manner such that a partial uploading or loading of a particular block of data into memory is possible.
- c. The frequency of the uplink is S-band and will be one or more of the SGLS standard frequencies.
- d. A SGLS receiver, secure address device and message decoder will be available in the satellite to receive and decode messages.
- e. The backup mode in case of failure or unavailability of the uploading station is the AFSCF.
- f. An uplink data rate of 1 Kbps is used throughout. The modulation technique for the uplink data is FSK using 3 tones to represent the symbols of "one", "zero" and "space".
- g. A TT and C data rate of 1 Kbps is used throughout. The modulation is biphase PSK-PCM compatible with the AFSCF. The bit error rate of this link is  $10^{-5}$ .
- h. The user navigation data message contains a 16 bit block of data that is sent every 6 seconds. This data block is dedicated to the uploading verification procedure.

### 2.4 Evaluation Criteria

The following evaluation criteria will be employed to select the preferred uploading protocol.

- differential satellite cost
- differential upload station cost
- mean loading time including one retransmission

- probability of a bit error in memory
- word and block size for probability of an undetected bit error of  $10^{-15}$
- message size flexibility

### 3. CANDIDATES

There are two basic methods for loading the satellite and verifying the contents of the memory after loading. They are checking the data in the satellite for errors and transmitting the data after it is stored in memory back to the uploading station for ground verification. Six candidate configurations are potential methods for performing these type of loading and verification. These methods are identified and explained in Table 3.1-1. The first two methods utilize error detection coding to determine transmission errors at the satellite. The remaining methods - 3, 4, 5 and 6, retransmit the contents of the satellite memory back to the ground for a comparative verification with the transmitted message. Methods 4, 5 and 6 will not be considered further since retransmission over the L-band navigation channel would disrupt the user navigation mode. Methods 1 and 2 are basically identical except the information retransmitted to the ground is sent on L-band user navigation data and S-band SGLS TT&C, respectively. Since the use of the AFSCF is a required backup mode, if method 1 is selected, the satellite must have the capability for using either L-band or S-band. The only difference is that the uploading station would require access to an SGLS TT&C receiver and data demodulator to receive data for method 2. A conceptual diagram of methods 1, 2, and 3 are shown in Figure 3.1-1.

Table 3.1-1. Satellite Loading Methods

Method	Up-Link	Where Verified	Format	Down-Link
#1	S-Band	Satellite	TLM Bits in NAV Data	L-Band
#2	S-Band	Satellite	TT & C	S-Band
#3	S-Band	Ground	Bit-By-Bit	S-Band
#4	S-Band	Ground	Bit-By-Bit, Replaces NAV Data Message	L-Band L-Band Feed on XMTR Dish
#5	S-Band	Ground	Bit-By-Bit, in Quadrature to P-Code	$L_2$
#6	S-Band	Ground	Bit-By-Bit, Use $L_2$ as Comm Link	$L_2$

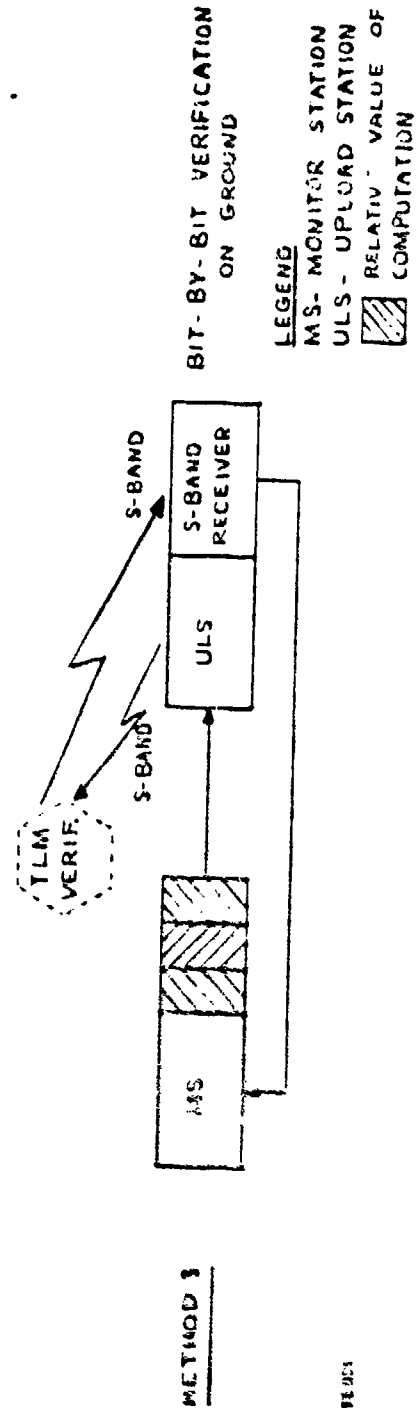
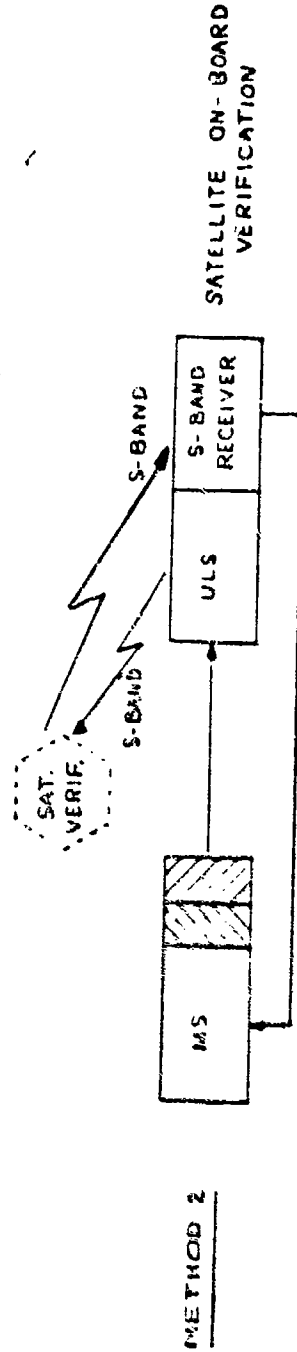
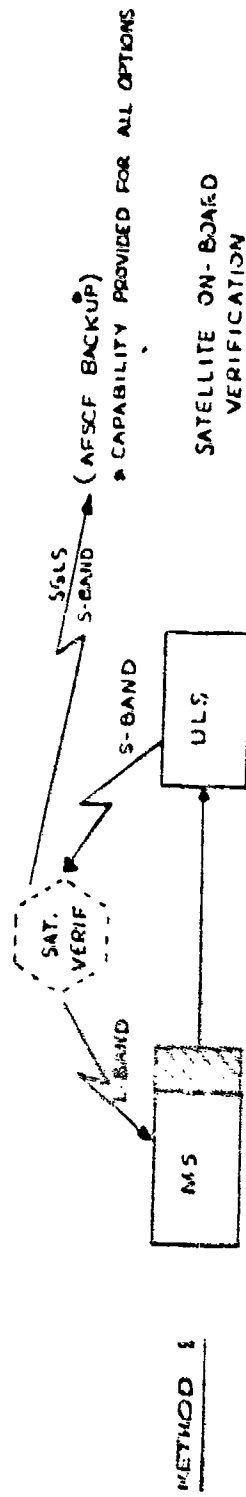


Figure 3.1-1. GPS Upload Station Option Methods



A functional block diagram of the GPS satellite for methods 1 and 2, are shown in Figure 3.1-2. The S-band command receiver receives the upload message. After appropriate access procedures have been satisfied, the digital bit stream is decoded by the command decoder. This decoder can be either the SGLS command decoder or a new GPS message decoder. Outputs from the decoder are parity and check sum verification, the data bits for memory, block address for memory loading, and modes to determine the operation of the memory loading. If an error is detected upon reception or after memory loading, the erroneous block is identified and its address is read into storage for transmission to the ground. The use of either L-band or S-band for transmission to the ground identifies method 1 or method 2.

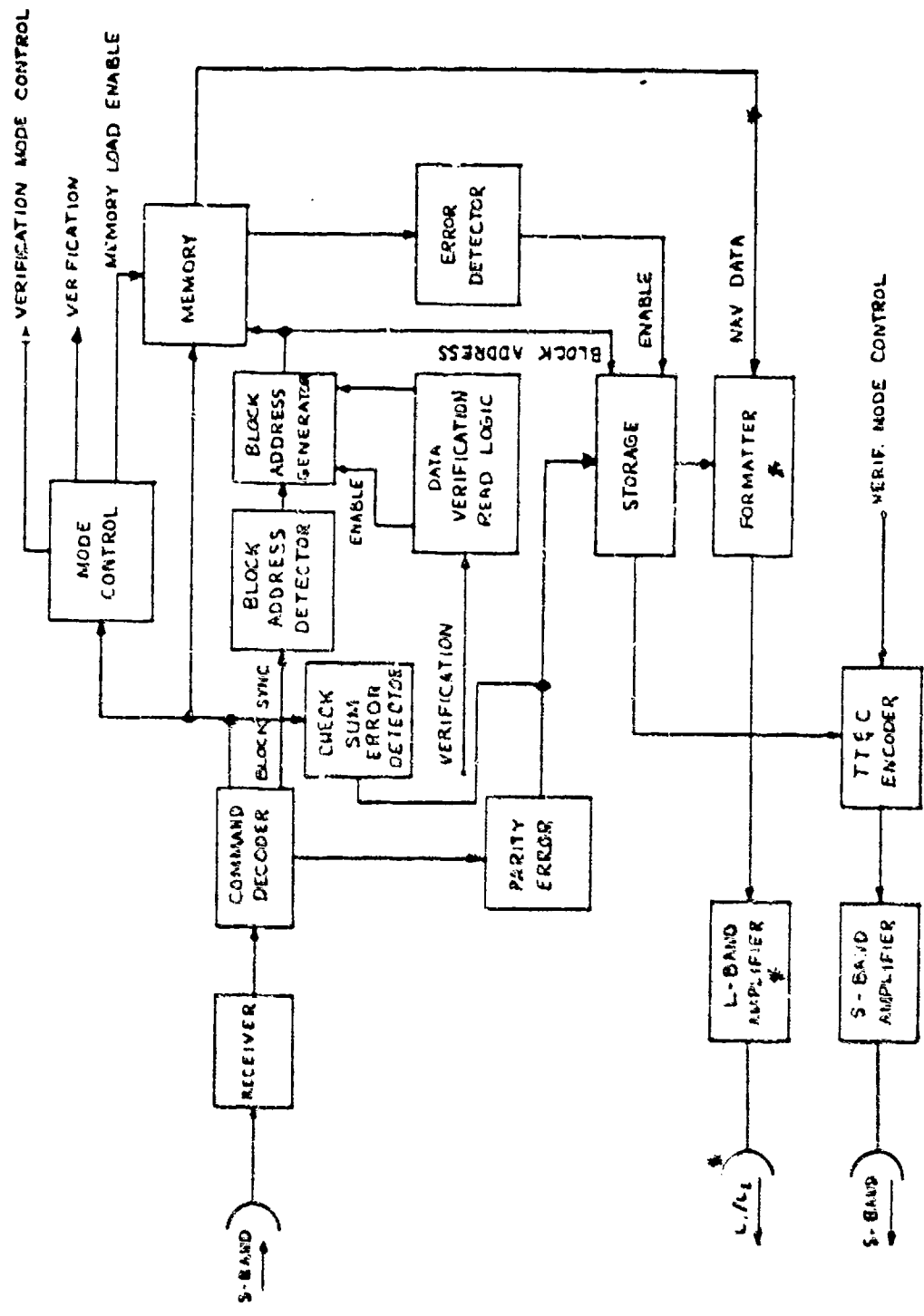
The functional block diagram of the satellite for the ground verification approach used in method 3 is shown in Figure 3.1-3. Conceptually, the method 3 satellite configuration is similar to that of methods 1 and 2. The only difference being that the error detection circuitry is eliminated. After reception of a memory increment (can be a block or total memory load) the memory read logic is enabled and the entire memory increment is dumped. This data is formatted and transmitted back to the upload station via the SGLS TT&C link for comparison with the original memory load. If an error is found, the block received in error will be retransmitted to the satellite and verified again on the ground.

The functional block diagram of upload station for method 1 is given in Figure 3.1-4. The data to be uploaded is received by the station from MCS. Upon command the computer, shown to be the monitor computer but can be separate, generates the data blocks, their parity and appropriate mode bits. The resulting message is then formatted into SGLS compatible three level signalling and transmitted to the satellite. Depending upon satellite configuration selected, an encryptor may be required prior to FSK modulation and transmission. If parity errors are found by the satellite the corresponding block address will be placed in the TLM word of the user navigation data. During the uploading process these erroneous blocks will be identified by the monitor station L-band receiver and the necessary retransmission will be performed.

For methods 2 and 3, the functional block diagram is shown in Figure 3.1-5. In method 2, the operation of the upload station is identical to that of method 1 except that the erroneous block addresses are received by the S-band, SGLS, TT&C receiver located at the upload station. For method 3, the entire message increment is received by the TT&C receiver. Upon demodulation the message increment is compared to the data previously transmitted that is resident in the upload station storage. If an error is found the erroneous block is retransmitted to the satellite and the verification procedure is repeated.

#### 4. ANALYSES

The analysis of the methods for loading the satellite require an understanding of the interrelation between the particular design features and the evaluation criteria. Four areas have been identified as subdivisions of the total uploading requirement. These areas are satellite, control segment, transmission link and message protocol. Figure 4-1 illustrates these



\*-FOR OPTION 2 DELETE THESE FUNCTIONS.  
 14003

Figure 3.1-2. GPS Satellite Methods 1 & 2 On-board Verification

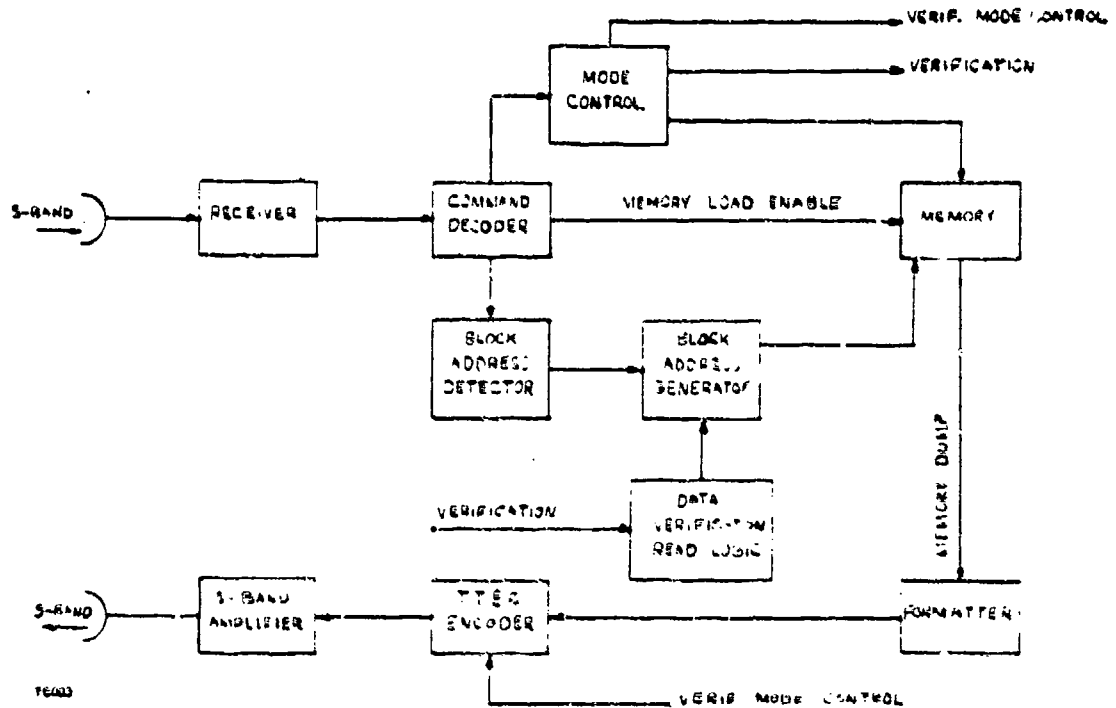
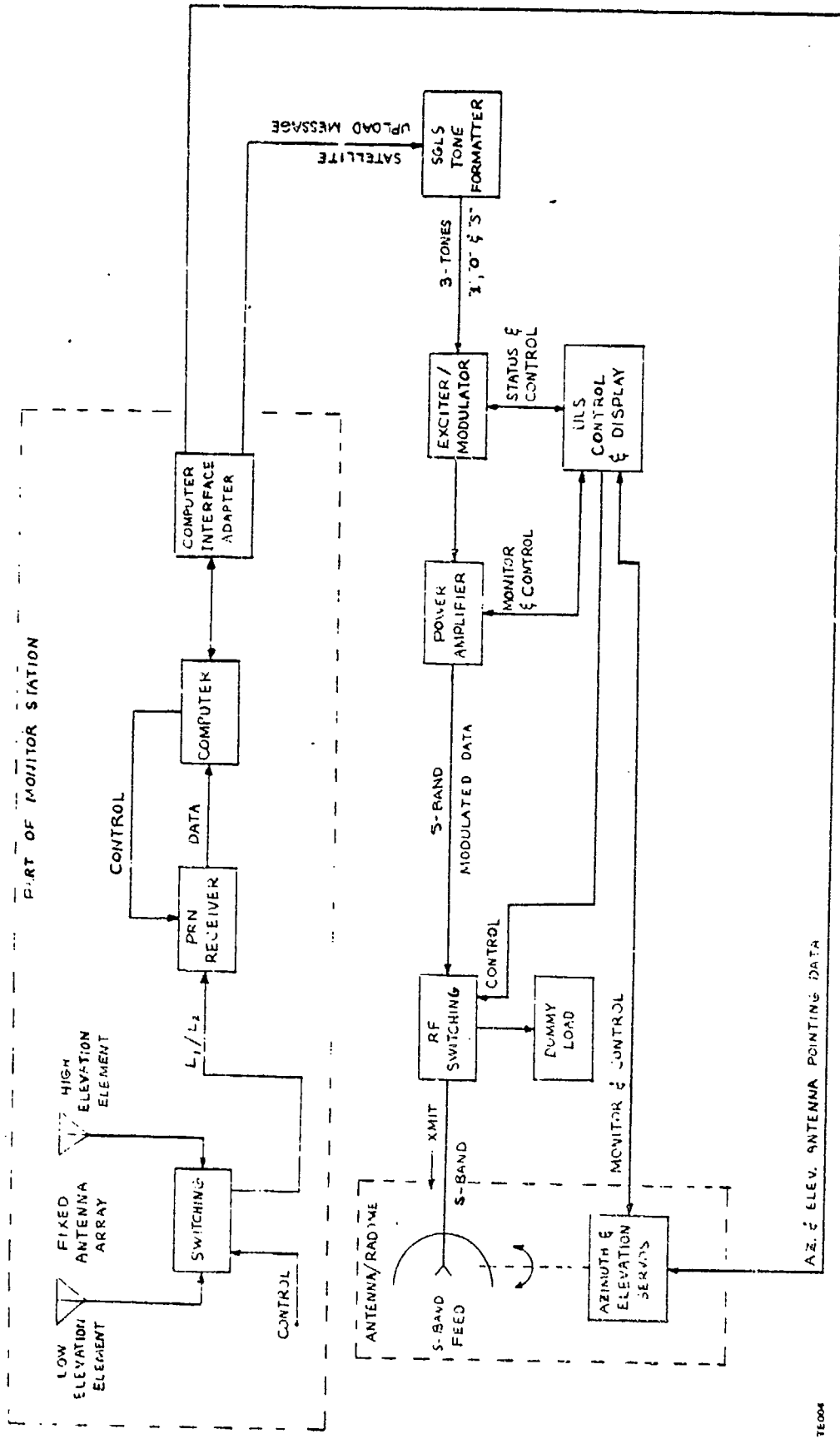


Figure 3.1-3. GPS Satellite Method 3 Ground Verification

areas and the major topics of consideration within these areas. The errors indicate the flow of the analysis presented in the following sections.

The analysis will begin with the satellite and end with message protocol. The results of these analyses are summarized in the comparison matrix presented in the next section.



TE004

Figure 3.1-4. GPS S-Band Up/I-Band Down Upload Station Method 1

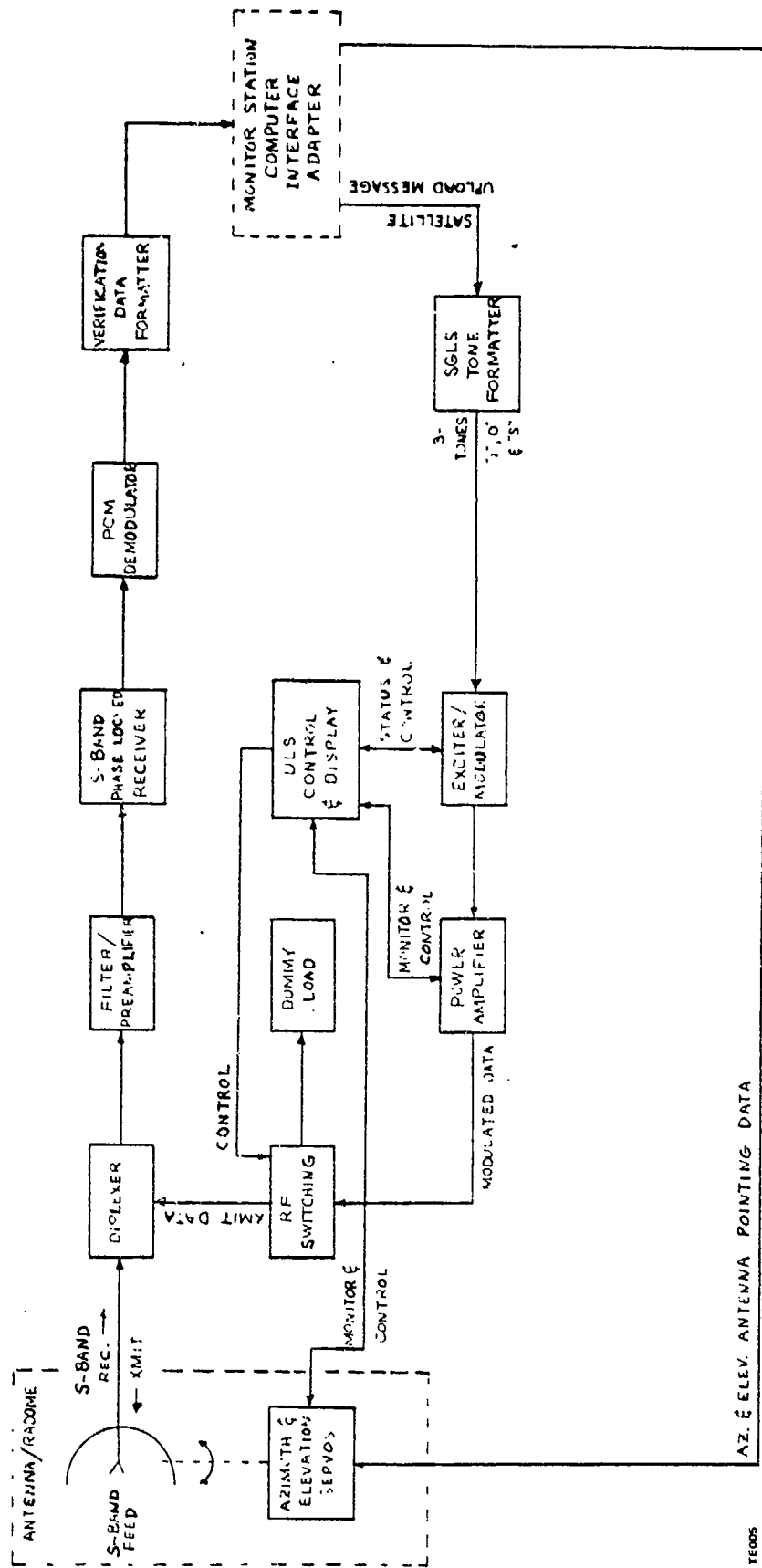
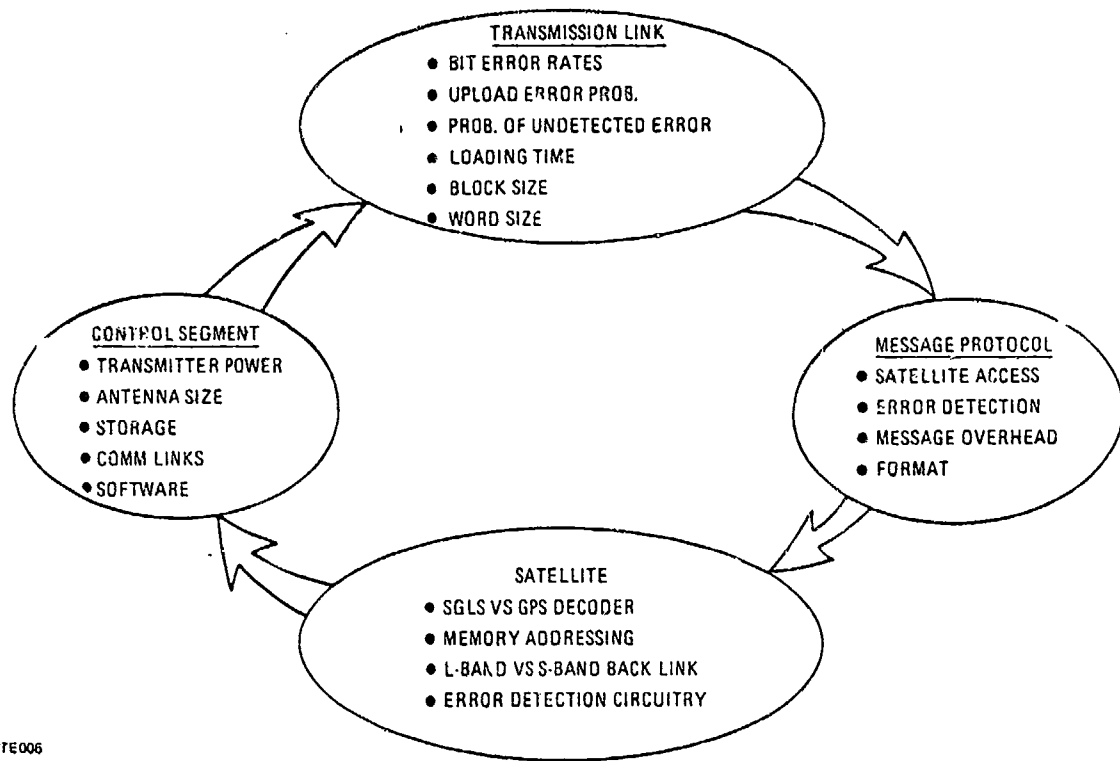


Figure 3.1-5. GPS S-Band Up/S-Band Down Upload Station Methods 2 & 3



TE006

Figure 4-1. Trade-off Concepts

#### 4.1 Comparison Matrix

The comparison matrix compares the analytical and cost results determined for the various evaluation criteria for the three candidate methods. The three candidate methods have been expanded to include different bit error rates and two uploading approaches for methods 1 and 2. The two uploading approaches are breaking the total message into blocks and transmitting the total message as a single block.

The significant results of the comparison matrix given in Table 4.1-1 are: Method 3 will not provide undetected bit error rates in memory of less than  $10^{-15}$ ; total message approaches for methods 2 and 3 are satisfactory only for a uplink BER of  $10^{-7}$  and Method 1 is the least expensive, this is because SGLS receive capability is not required at the upload station.

Methods 1 and 2 using a message block format are the most efficient uploading approaches. For a BER of  $10^{-6}$  or less and block size of less than 700 -8 bit words or 390 -16 bit words, the average transmission times are 173 and 153 seconds for Methods 1 and 2, respectively. Because of the lower cost, Method 1 is selected as the preferred approach. The remainder of Section 4 provides the analysis for the determination of the evaluation criteria. In Section 5, the details of the selected method are presented.

#### 4.2 Satellite

The satellite components are functionally similar for methods 1, 2, and 3. The four basic components of concern in this analysis are:

- Access and Decoding
- Error Detection
- Memory Addressing
- Downlink Communication channel

4.2.1 Access and Decoding. The satellite is required to provide protection against spoofing and determine the purpose of the words received. Figure 4.2.1-1 illustrates four





possible methods of providing access protection and word decoding of the incoming bit stream. Approach A utilizes the existing SGLS decryptor and command decoder to receive the uploading data. This approach requires that all upload data be encrypted with a format compatible with the R-23 device. In approach B, the R-23 device is enabled by appropriate commands, this permits the transmission of a message that enables a bypass circuit around the R-23. Therefore, the remaining portion of the message is in the clear and is decoded by the SGLS command decoder. The output of the command decoder is either secure vehicle commands for satellite health, attitude and control or the clear GPS message that is to be stored in the satellite memory. Both A and B approaches have the disadvantage of requiring that secure vehicle commands and the GPS message be decoded by the same command decoder. The dual functions of the decoder results in increasing the possibility of catastrophic error in the secure vehicle commands caused by bit errors in the upload message unless suitable interlocks are used.

Approaches C and D circumvents erroneous secure vehicle commands by the use of separate GPS decoder for the navigation functions. C and D differ only in the implementation of the access protection. In approach C, the SGLS command decoder provides an enable to the GPS decoder after the satellite is properly entered via the R-23 and SGLS command decoder. This requires that the upload station contain a K-23 encryptor and that the R-23 and SGLS be accessed just prior to every load and after the memory loading is complete the circuitry must be returned to its normal state. Approach D eliminates the need to continually access the secure system by providing periodic update/stored access procedure for the GPS decoder. The keys (access words) will be transmitted from the AFSCF to the satellite well in advance of the uploading of the navigation message. These keys will be stored and changed as desired.

The message overhead required to use these four approaches is an important consideration since the number of overhead bits is directly related to the time to upload the navigation data into the satellite. Method A, because of the security requirements of the R-23, requires at least 64 bits to transmit 16 bits of navigation data. This amount of overhead is clearly excessive since a single transmission would require 82 minutes per satellite to upload the 100 K bits of satellite memory data\*. All other approaches are equivalent in terms of message overhead requirements.

In terms of design, the approach D appears the most attractive because the interface with the secure functions of vehicle commands is minimized.

---

\* Private conversation with C. Hoff, Aerospace Corp. , January 29, 1974.

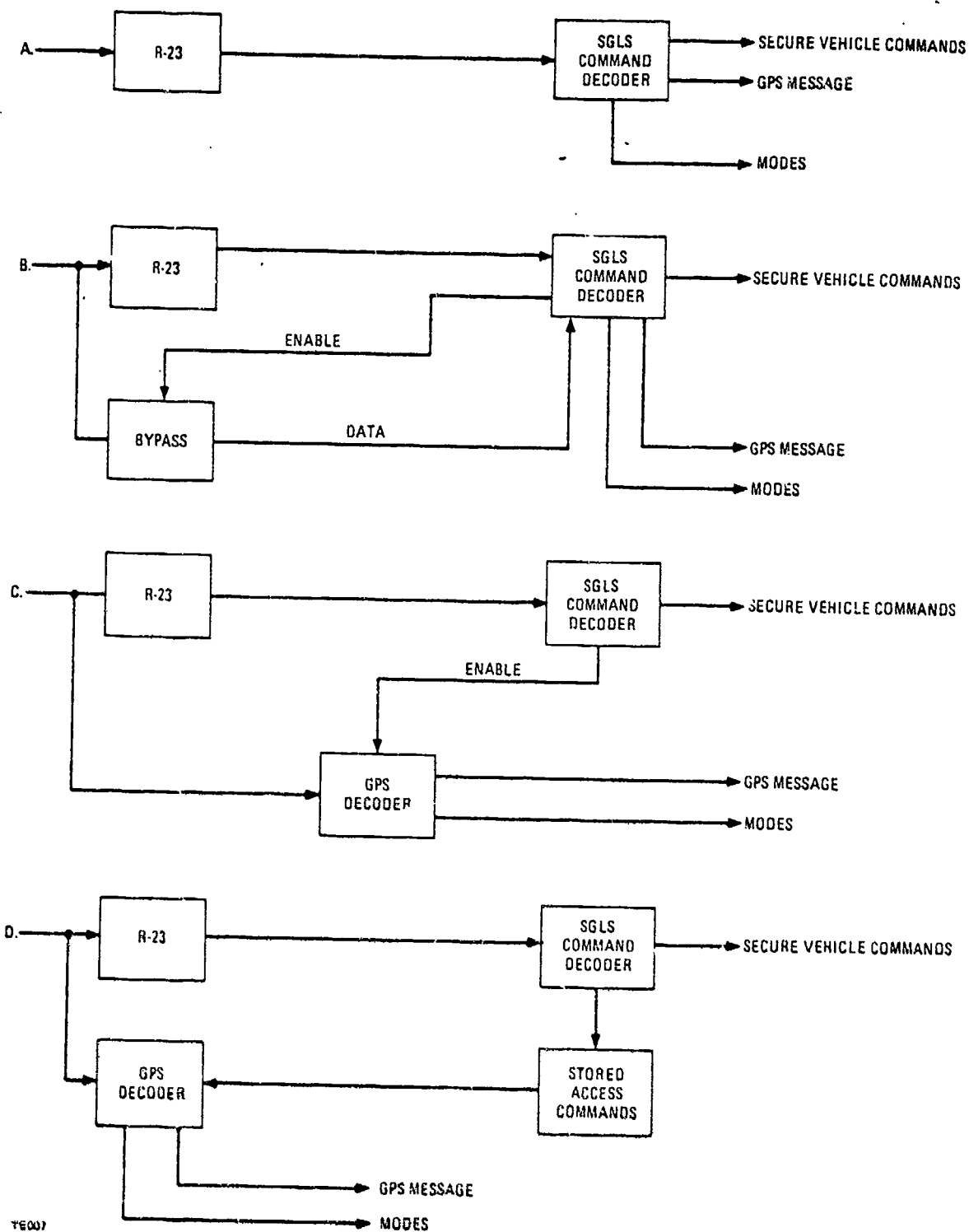


Figure 4.2.1-1. Access and Decoding

Table 4.2.1-1 summarizes the cost deltas for the approaches A, B, C and D with respect to uplink methods 1, 2, and 3. These costs are for the four (4) satellite configuration of Phase 1.

4.2.2 Error Detection. The use of error detection in the satellite is required to check for errors received in the word decoded by the vehicle decoder and to verify the data loaded into memory. For methods 1 and 2, both types of error detection are required. However, for method 3 the only error detection required is the verification of the mode portion of GPS decoder word. The error detection types that are feasible in this application are a parity check bit for each word and a check sum word for each block of words. To obtain the requirement of  $10^{-15}$  for the probability of an undetected bit error in memory, analysis indicates that both check sum and word parity are required for methods 1 and 2.

The possible implementations for performing error detection must consider the decoder and memory interface. Error detection can be performed as:

- a parity check for a word (memory data and mode bits) by the GPS decoder
- a check sum algorithm while storing a data block into memory
- an echo parity check immediately after loading a word into memory
- a parity check of the words of a memory increment after storage
- a check sum comparison of a block (or memory increment) after storage.

For Method 3, the only error detection required is a parity check of the mode bits to ensure correction identification of block address words and memory bits.

The operation of methods 1 and 2 can be best implemented to perform a parity check of a received word in the command decoder; a check sum computation for each block can be performed while the block is being loaded into memory; and performing an echo check on

Table 4.2.1-1. GPS Satellite Cost Impacts

ULS Method	Satellite Configuration			
	A	B	C	D
1	34K	34K	300K	320K
2	34K	34K	282K	316K
3			250K	270K

the memory loading for each word by cycle sharing. The echo check can be performed by loading a word into memory then immediately reading it out and checking the parity of the word by using the inherent parity bit incorporated for user error detection. This is much easier to implement than dedicated parity check and should be more than adequate to verify the data through the hardwired interface between the GPS decoder and memory. The echo parity check will also detect bad memory cells. This configuration deletes the requirement of storing the check sum parity bits when verifying the memory in a dedicated manner.

4.2.3 Memory Addressing. Memory addressing refers to the method of determining the locations in memory that a block of data is to be loaded. The standard method for determining the starting point of a memory load is to precede the bits to be loaded with a word that identifies the memory address of the first word of the block. This word is called the block address.

If an error is detected in a message, there are two approaches for retransmitting the data from the upload station to the satellite. The two approaches are: 1) only the erroneous blocks are retransmitted and 2) the total message is retransmitted if there is an error in any block. Obviously the latter approach is only reasonable if the block size is large, i.e., a high percentage of the total message. The final selection depends upon the available transmission link bit error rate (BER) and will be determined in the Section 4.4 on Transmission Links.

4.2.4 Downlink Channel. In all methods considered, the satellite must have a means of communicating with the upload station. Since the AFSCF is a required backup mode, one of these communication links must be the SGLS TT&C channel. This is the link used in methods 2 and 3. For method 1, the user navigation data present on  $L_1$  and  $L_2$  has available the TLM bits for communication. Note that method 1 must also have the SGLS TT&C to be compatible with the backup mode.

The use of L-Band and S-Band in method 1 has the advantage of better reliability since there are two links to the control segment. The use of the SGLS TT&C of method 2 has the advantage of slightly simpler circuitry in the satellite. These results will be considered when the selection is made.

### 4.3 Control Segment

The control segment portion of the uploading station consists of the transmitter, antenna, data storage, computer, software to perform the upload function, and the power budget for the link to obtain a particular BER. Also, included in this section will be the cost deltas between methods 1, 2, and 3.

4.3.1 Uplink Power Budget. This section provides the analysis to determine the effective radiated power relative to an isotropic antenna, EIRP, necessary at the upload station to

obtain BERs of  $10^{-5}$ ,  $10^{-6}$  and  $10^{-7}$ . The SGLS satellite receiver is designed for a BER versus received power as shown in Table 4.3.1-1.\*

Assuming an omni-directional antenna on the satellite, a one (1) dB duplexer loss, a one (1) dB RF loss, and 0.5 dB polarization loss, the required signal strength at the antenna input is -124dBW, -125dBW, and -126dBW for bit error rates of  $10^{-7}$ ,  $10^{-6}$ , and  $10^{-5}$ , respectively. Using this result, it is possible to compute the required transmitter power for a given uploading station antenna. The following illustrates that computation:

Path Loss	185.5dB	
Signal Margin	6.0dB	
Assignable Path Loss	191.5dB	
Less Required Available Satellite Antenna Power	-124.0dBW	(BER= $10^{-7}$ )
Ground EIRP	67.5dBW	
Upload Station Antenna Gain (14' dish including losses)	-31.5dB	
Transmitter Power (BER= $10^{-7}$ )	36.0dBW	(4 K watts)
Transmitter Power (BER= $10^{-6}$ )	35.0dBW	(3.15 K watts)
Transmitter Power (BER= $10^{-5}$ )	34.0dBW	(2.5 K watts)

Table 4.3.1-1. SGLS Receiver Performance

BER	Signal Level (dBW)		
	Theoretical	Measured	Acceptable Specification
$10^{-5}$	-130.5	-129.5	-129.5
$10^{-6}$	-	-	-129.5
$10^{-7A}$	-	-	-130.5

A - The noise floor of the receiver is inherently capable of supporting BER below  $10^{-7}$ .

\*These results were obtained from Motorola Corp. by private correspondence and relate to their noncoherent SGLS receiver design.

equivalent results for the AFSCF indicate that for a 1 K watt transmitter and 14' antenna there is no margin for a BER of  $10^{-7}$ . If the 14' antenna is replaced with a 46' antenna then the additional margin for a BER of  $10^{-7}$  is greater than 10dB.

4.3.2 Transmitting System. The transmitting system for the upload station consists of the transmitter, antenna, radome, and an additional SGLS receiver and associated hardware required for methods 2 and 3.\* The block diagram of the transmitter is shown in Figure 4.3.2-1. This configuration can be either TWT or Klystron. It is recommended that the TWT be used since its bandwidth is sufficient to cover the range of frequencies possible for the SGLS uplink transmission without retuning. Figure 4.3.2-2 illustrates the cost for the A&E, antenna, radome and transmitter as a function of the antenna diameter. It can be seen that for a 14 foot antenna the estimated TWT transmitting system cost is \$610,000. This cost is directly applicable to the method 1 candidate configuration. For methods 2 and 3, a SGLS TT&C receiver and an S-band diplexer would be required at the upload station. The estimated cost for these devices are \$36,000 and \$9,000, respectively.

4.3.3 Computer and Software. The function of the computer is to control the uploading process, receive data from the master control facility, and store the satellite memory

\*These results were extracted from DRB D9000527B and the presentation made to SAMSO January 23, 1974.

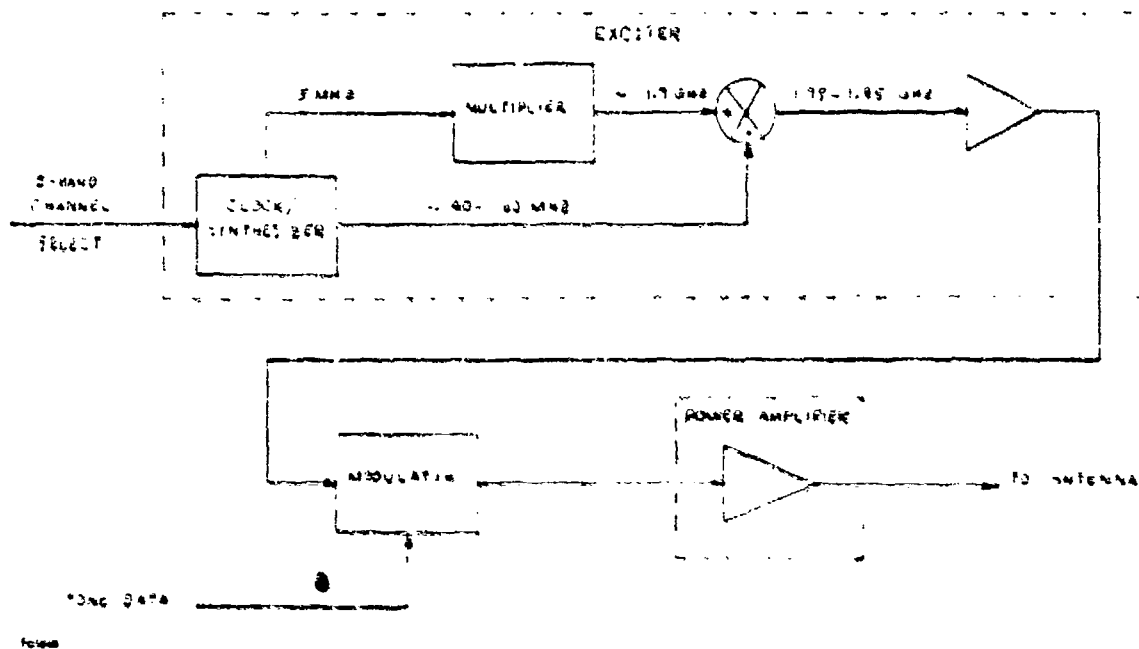


Figure 4.3.2-1. S-Band Exciter/Modulator

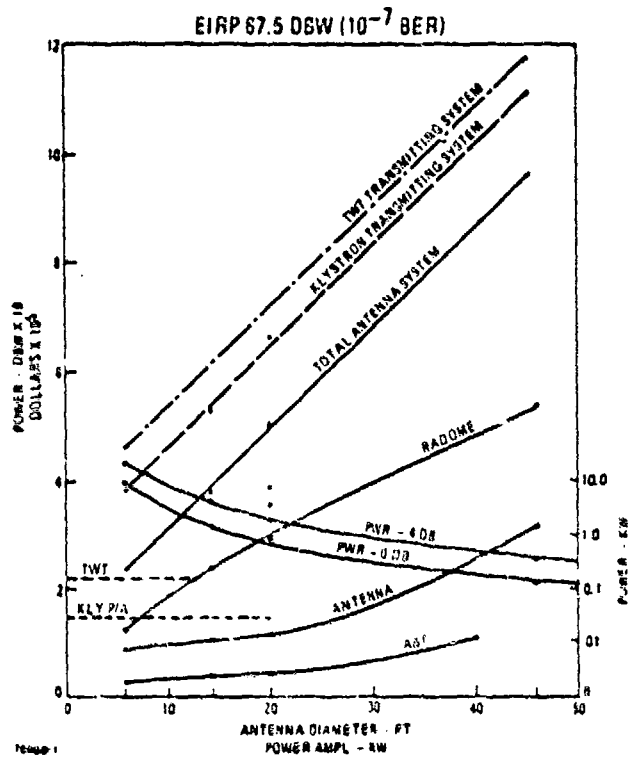


Figure 4.3.2-2. Upload Transmitter System Trade-offs

load during the loading process. There are three approaches in the selection of computer capability for the upload station. \* They are:

- A single computer and software package perform monitor and upload station functions simultaneously.
- A single computer and software package that can only perform either the monitor station or uploading functions.
- A separate computer and software package dedicated to the uploading function.

Figures 4.3.3-1, -2, and -3 illustrate the configuration and cost of the various computer approaches. The separate computer appears advantageous because of the requirements of transportability of the upload station, and possible interference problems with other monitor station computers, and the potential need for near simultaneous loading and satellite clock evaluation by the monitor station. This result is the same for all candidate uploading methods. The only cost differential between the three candidate methods results from a minor increase in software complexity for method 3 because of the file searching and comparison techniques required for ground verification. This additional cost increment is estimated to be \$2,000.

\*Reference preceding page

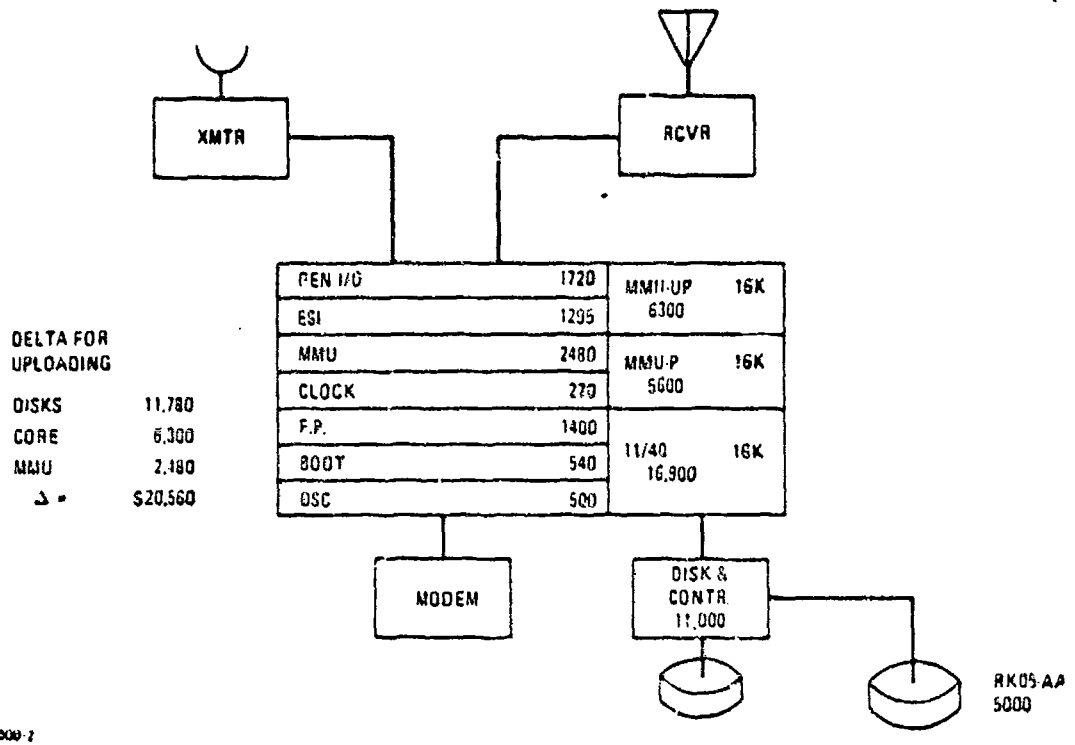


Figure 4.3.3-1. Monitor-Upload Station

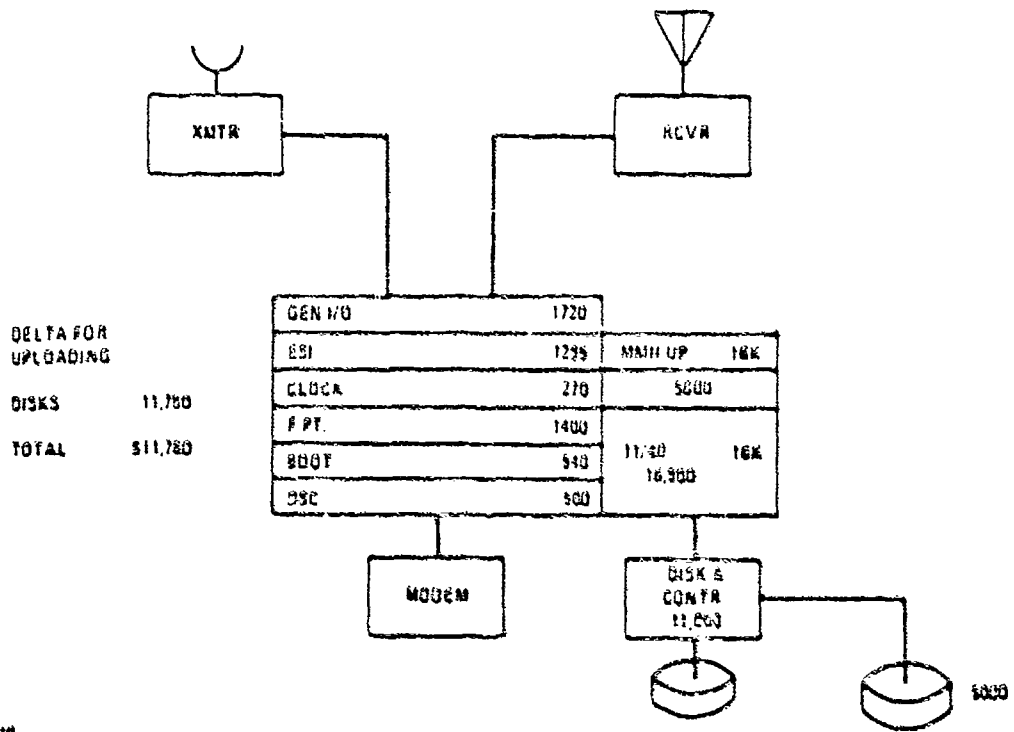
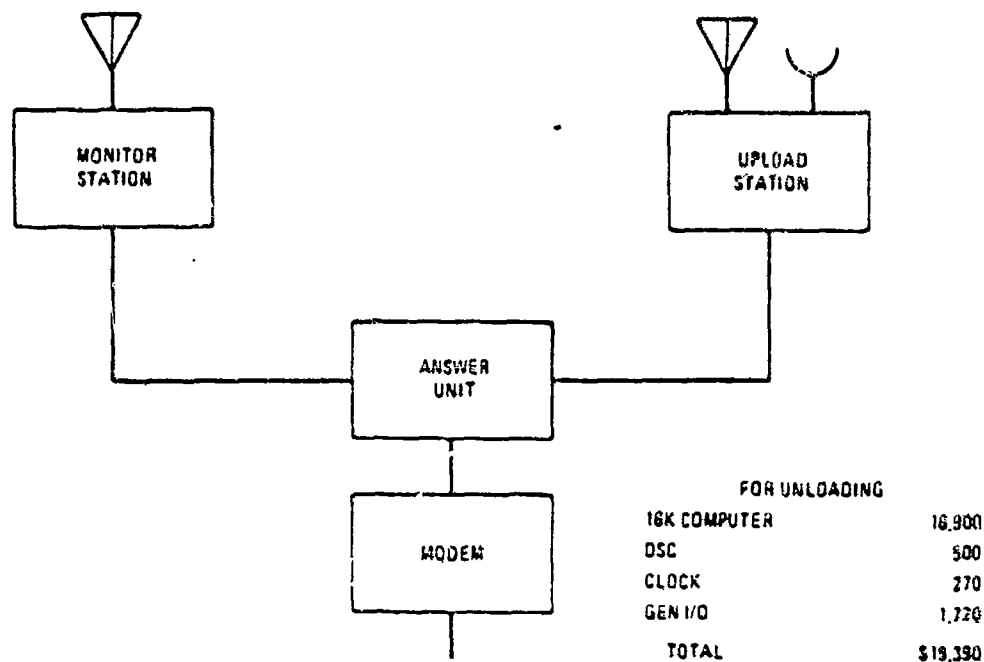


Figure 4.3.3-2. Overlaying Monitor/Uploading Station





TE011

Figure 4.3.3-3. Separate Uploading Computer

#### 4.4 Transmission Links

The transmission links include analyses for the S-band uplink, L-band downlink, and S-band downlink. The particular combination required depends upon the uploading method. As stated above, methods 1 and 2 are identical except for the use of L-band or S-band for the downlink. Method 3 also utilizes S-band for the downlink.

**4.4.1 Satellite Verification.** Methods 1 and 2 employ error detection bits in the uplink data stream for data verification in the satellite. Since the verification is performed in the satellite, the downlink information consists of a request to perform a retransmission. The uplink approaches for the message structure and incorporating error detection bits are:

- a. Blocks of N words
  - (1) parity for each word
  - (2) check sum word for each block
  - (3) iterative code (parity and check sum) for each block

b. Total message in one block

- (1) parity for each word
- (2) check sum word for entire message
- (3) iterative code for entire message

Computations within this section will assume a memory load size of 100 K bits and an estimated overhead to the memory load of 25%.

The most important evaluation criteria is the word length and block size required to obtain the desired probability of a undetected bit error in memory. For word parity or check sum words, the probability of an undetected bit error in memory is given by

$$P_{ue} = 1 - \sum_{k=0, \text{ odd}}^B \binom{B}{k} (1-P_e)^{B-k} P_e^k \quad (1)$$

where  $B$  = bits per word for parity or words per check sum bit

$P_e$  = transmission link BER

The probability of an undetected error in the total memory for parity or check sum error detection is

$$P_{me} = 1 - (1 - P_{ue})^{\lceil 100K(1+H)/N \rceil} \quad (2)$$

where  $H$  = overhead factor (25% = .25)

$N$  = number of bits per block

$\lceil \ ]$  = designates the greatest integer function

Equation (2) can be approximated by

$$\begin{aligned} P_{me} &= 1 - \left( 1 - \lceil 100K(1+H)/N \rceil P_{ue} \right) \\ &= \lceil 100K(1+H)/N \rceil P_{ue} \end{aligned} \quad (3)$$

Equation (3) is plotted in Figure 4.4.1-1 for bit error rates,  $P_e$ , of  $10^{-5}$ ,  $10^{-6}$  and  $10^{-7}$ . It can be seen that for  $P_e = 10^{-7}$  and  $B = 4$ , the value of  $P_{me} = 2 \times 10^{-9}$  this corresponds to a  $P_{ue}$  of approximately  $6 \times 10^{-15}$  which is not adequate to satisfy the design requirement of  $P_{ue} = 10^{-15}$ . The same result is also true for approach A. Therefore, parity bits and check sum words when used alone are not sufficient to obtain a probability of an undetected bit error in memory of less than  $10^{-15}$ .

For approach B, the case of a combination parity and check sum, (iterated code) error detection must be investigated. To do this, a theorem is required from Peterson.\* This theorem states that "for a binary symmetric channel, if one code has a probability of error  $f_1(P)$  and another  $f_2(P)$ , their product is capable of decoding with a probability of error no greater than  $f_2 \left[ f_1(P) \right]$ ." This means that if a channel has a BER =  $P_e$  and a parity check

\*Peterson, W. W., Error Correcting Codes, MIT Press, 1961, page 82

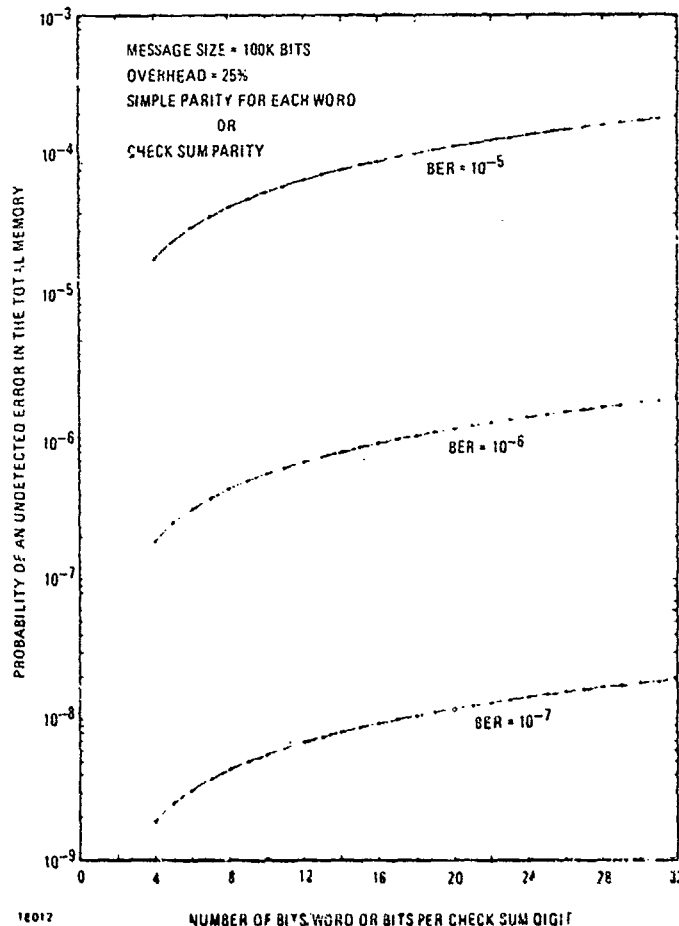


Figure 4.4.1-1. To Determine the Probability of Undetected Bit Errors in Memory

yields an undetected bit error probability  $P_{ue1} = f_1(P)$  then the addition of check sum error detection will yield an undetected bit error probability of  $P_{ue2} \leq f_2(P_{ue1})$ . Therefore the undetected bit error probability of the combination of parity and check sum can be bounded.

The above result can be used with (1) to obtain the bound on the probability of an undetected bit error in a block that has been encoded with both parity and check sum. The result is

$$P_{ue}' \leq 1 - \sum_{j=0, \text{odd}}^K \binom{K}{j} (1-P_{ue})^{K-j} P_{ue}^j \quad (4)$$

where  $P_{ue}$  = probability of an undetected bit error due to parity

$K$  = the number of words per block

If the total message consists of one block, then  $K$  is the number of words in the total message. Results obtained indicate that for bits per word of 8, 16 and 32 and  $P_e = 10^{-7}$ , a value of  $P_{ue}' \leq 10^{-15}$  is possible for transmissions of a block equal to the total message.

Equation (4) can also be used directly for block sizes less than the message length. Figures 4.4.1-2 through -10 give the upper bound for the probability of an undetected bit error in memory versus number of words per block for word lengths of 8, 16, and 32 and transmission link BER of  $10^{-5}$ ,  $10^{-6}$ , and  $10^{-7}$ . The results of these graphs can be summarized in the Table 4.4.1-1 for satisfying the undetected bit error rate. This gives the limits for the number of words per block and number of bits per block to obtain the undetected bit error rate of  $10^{-15}$ .

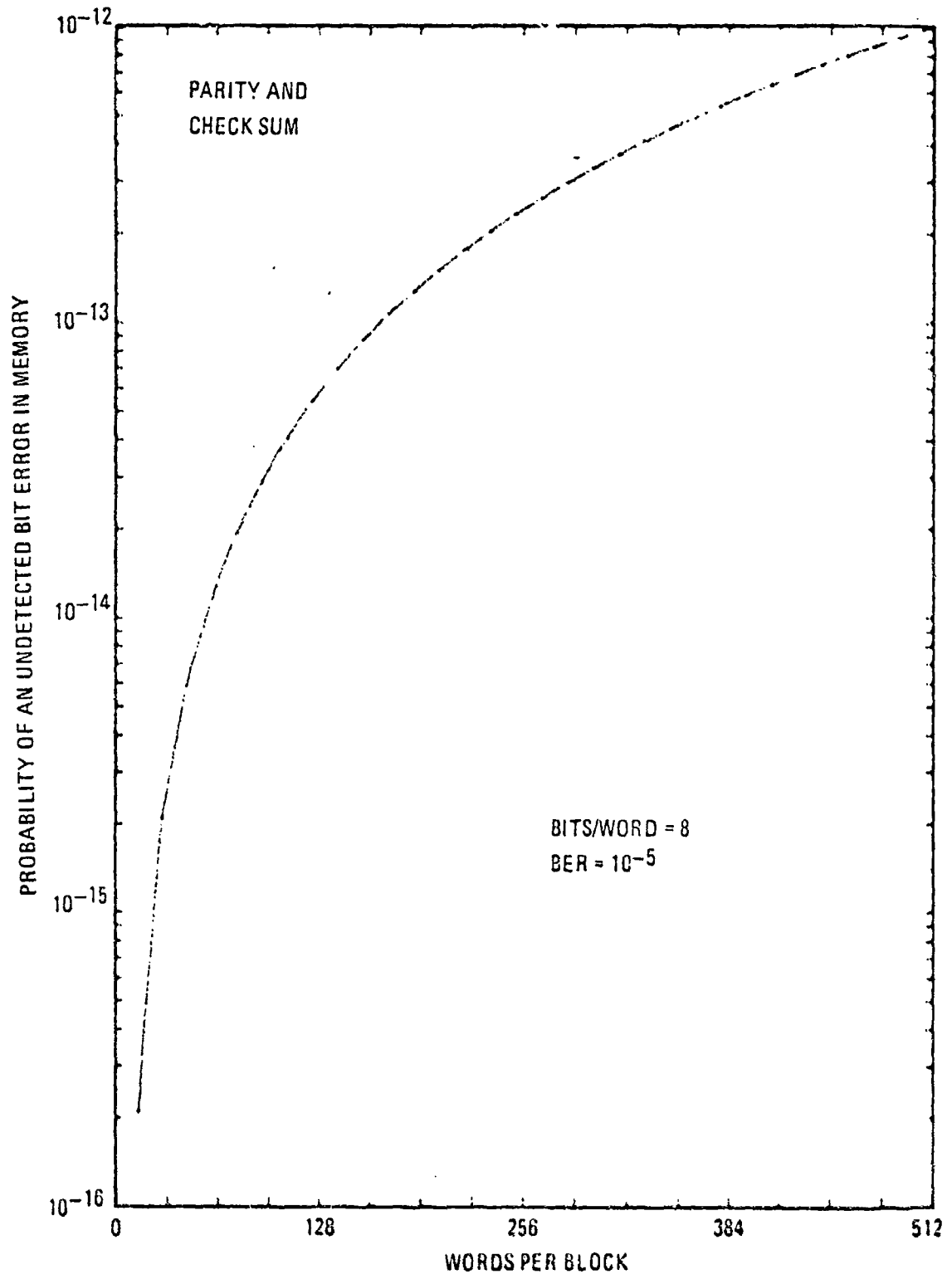
For approaches A and B there are two evaluation criteria yet to be analyzed. They are the mean loading time and probability of a correct load after a given number of attempts. In both approaches, the time required for the initial loading attempt,  $T_o$ , is fixed. The value of  $T_o$  is given by

$$T_o = \frac{M(1+H)}{R} \quad (5)$$

where  $M$  = number of bits to be stored in memory

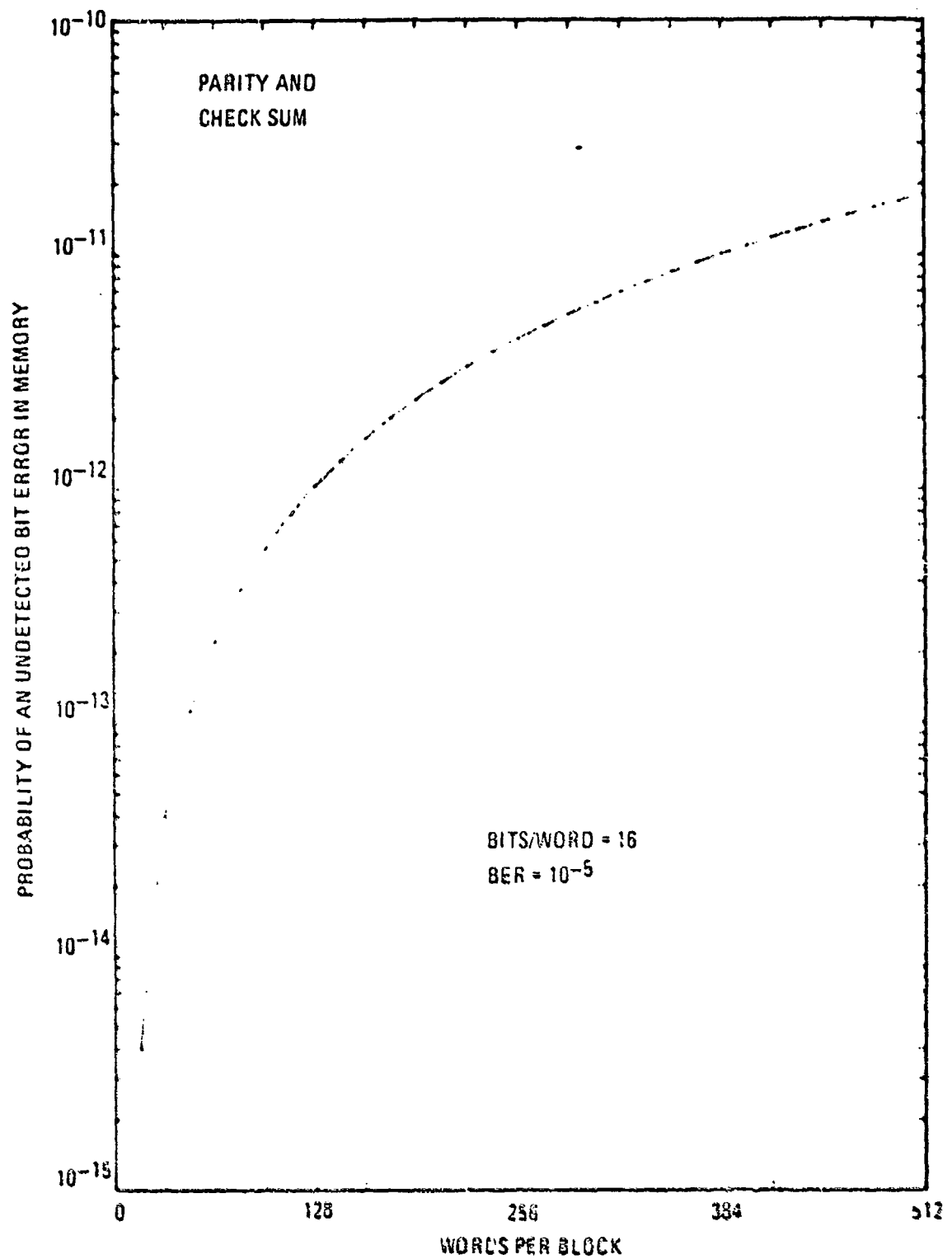
$H$  = overhead factor

$R$  = data rate of upload link



TE01J

Figure 4.4.1-2. Undetected Bit Error Rate For Bits/Word = 8, BER =  $10^{-5}$



FE014

Figure 4.4.1-3. Undetected Bit Error Rate For Bits/Word = 16, BER = 10<sup>-5</sup>

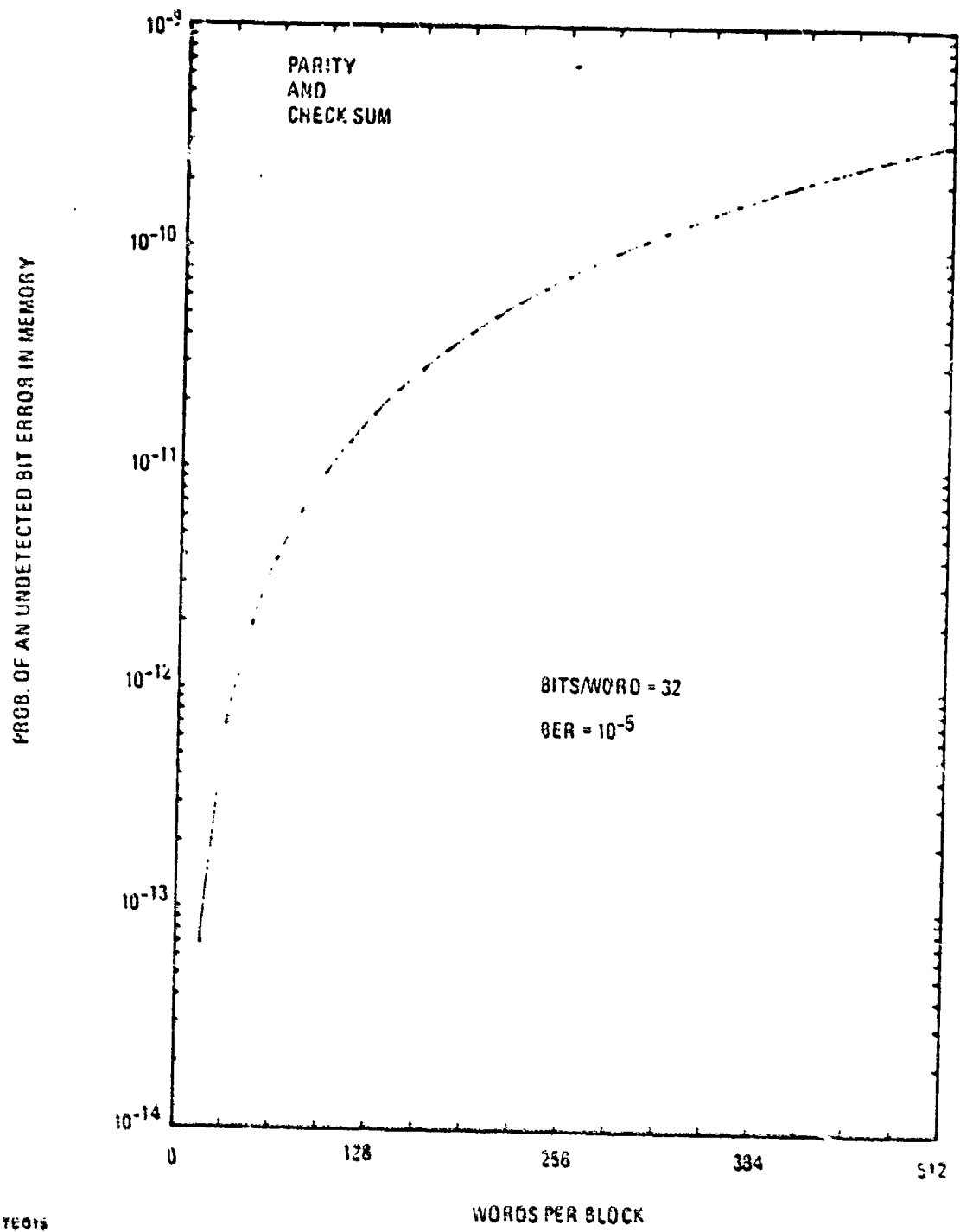
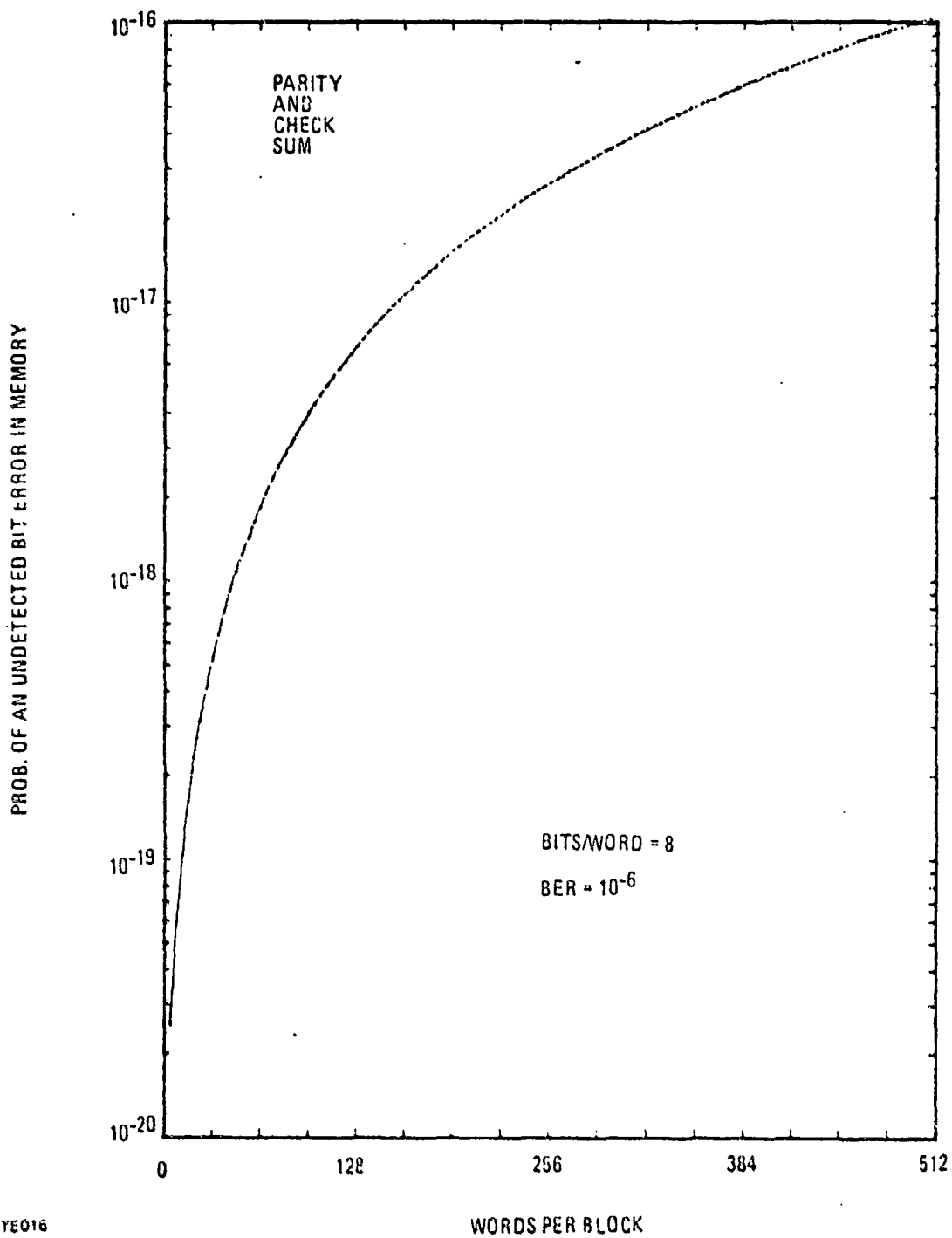


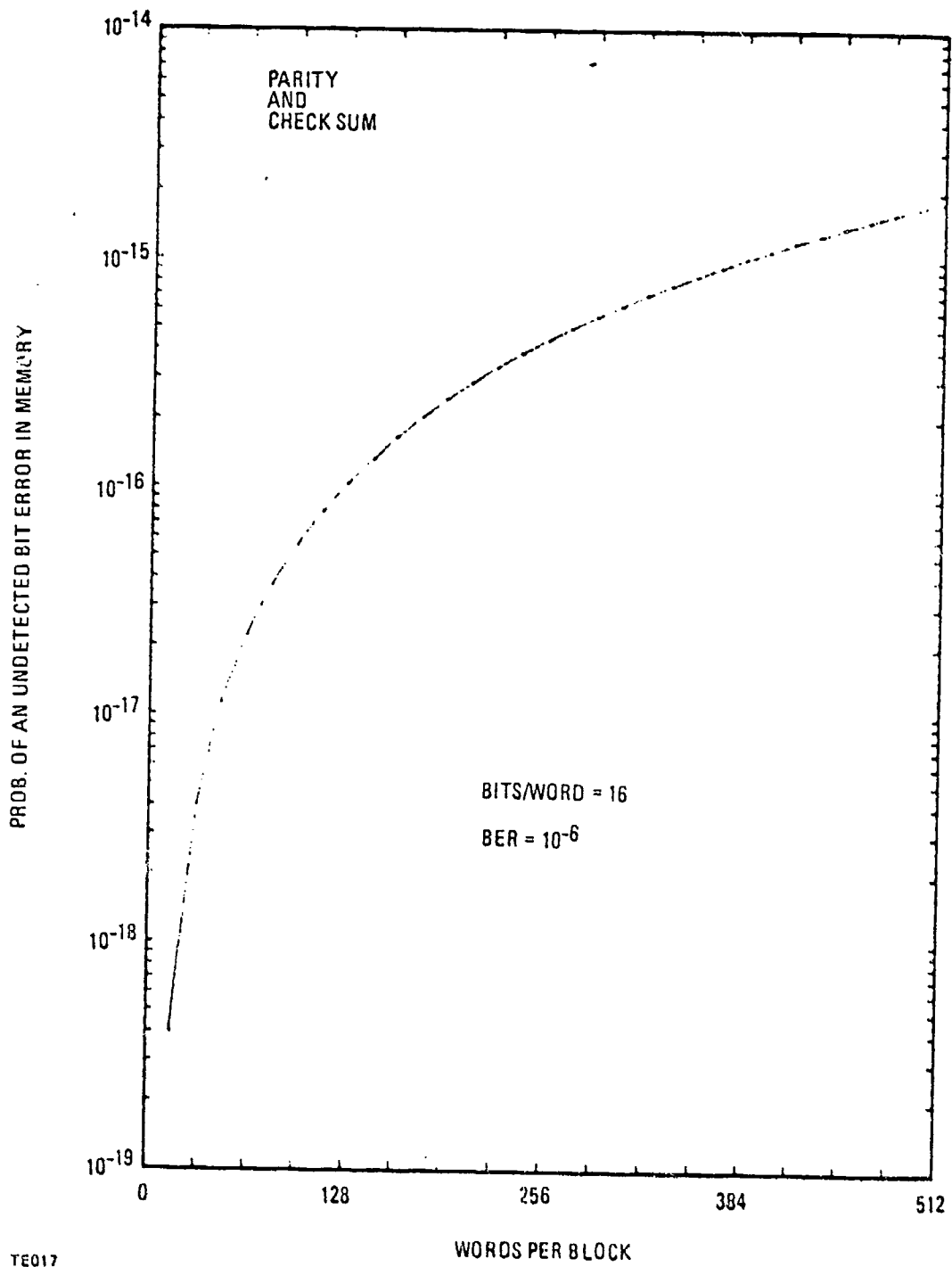
Figure 4.4.1-4. Undetected Bit Error Rate For Bits/Word = 32, BER = 10<sup>-5</sup>



YE016

Figure 4.4.1-5. Undetected Bit Error Rate For Bits/Word = 8, BER =  $10^{-6}$





TE017

Figure 4.4.1-6. Undetected Bit Error Rate For Bits/Word = 16, BER =  $10^{-6}$

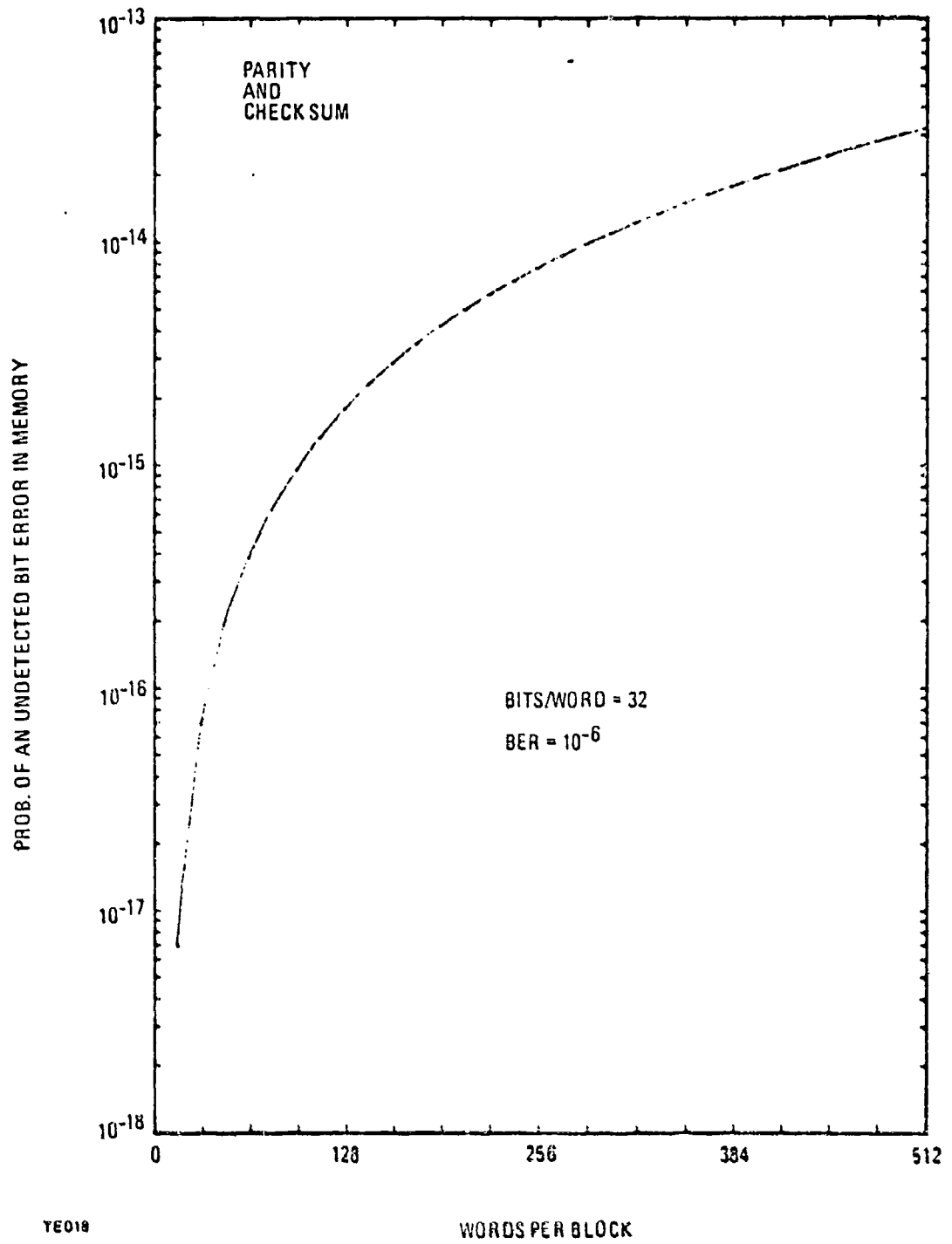
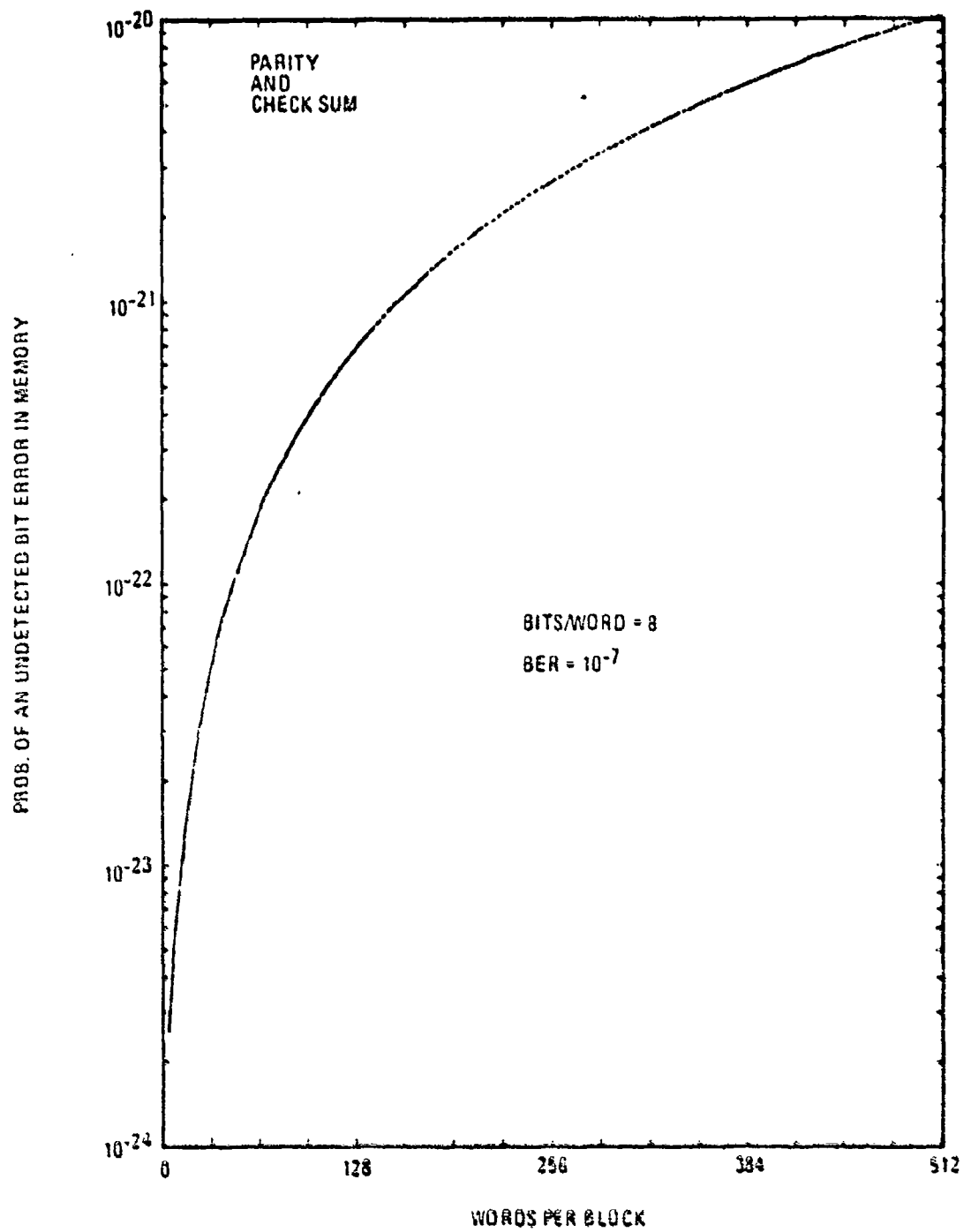


Figure 4.4.1-7. Undetected Bit Error Rate For Bits/Word = 32, BER =  $10^{-6}$



TE019

Figure 4.4.1-8. Undetected Bit Error Rate For Bits/Word = 8, BER =  $10^{-7}$

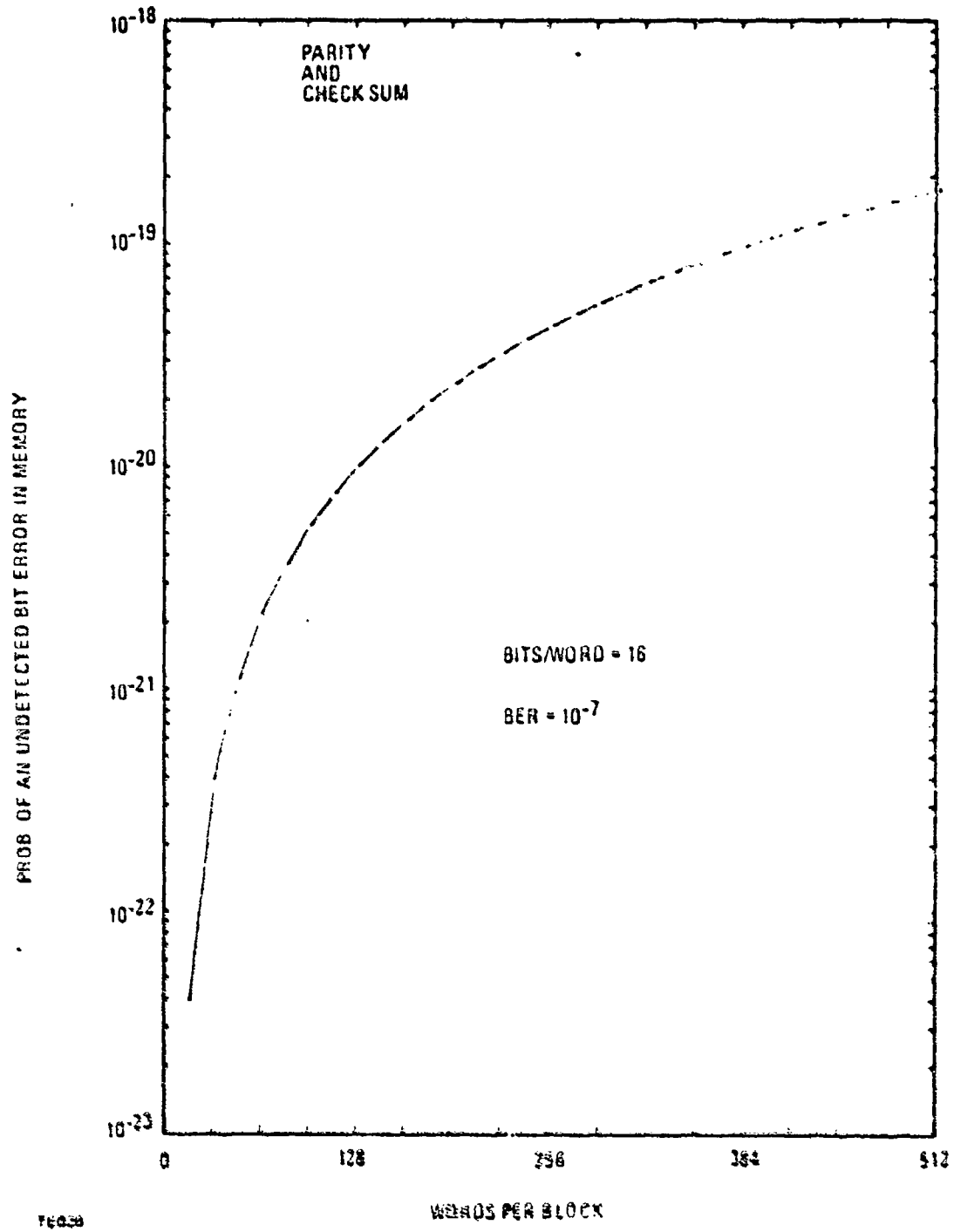


Figure 4.4.1-9. Undetected Bit Error Rate For Bits/Word = 16, BER =  $10^{-7}$

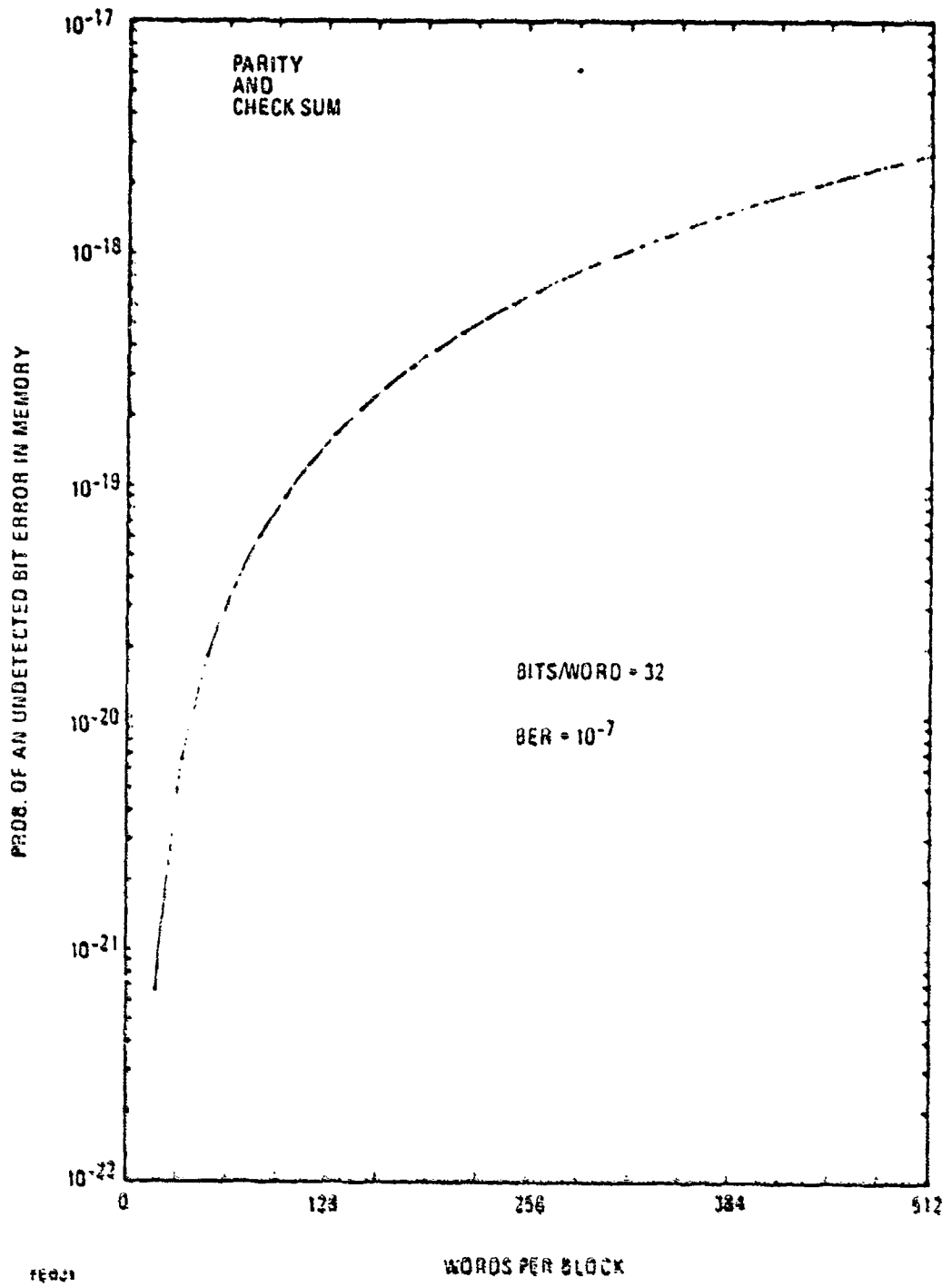


Figure 4.4.1-10. Undetected Bit Error Rate For Bits/Word = 32, BER = 10<sup>-7</sup>

Table 4.4.1-1. Maximum Allowable Words Per Block

Bits Per Word	Maximum Words Per Message Block		
	Transmission Link BER		
	$10^{-5}$	$10^{-6}$	$10^{-7}$
8	16	≈ 700	≈ 16000
16	-	390	≈ 8000
32	-	100	≈ 4000

To consider the total load time the method of down linking the erroneous blocks or message to the upload station must be considered. There are two viable approaches for methods 1 and 2. They are:

- (i) notify the upload station of erroneous block address
- (ii) request request retransmission of total message

Approaches (i) would use the TLM word or the S-band TT&C link to send the address of the erroneous block to the upload station. Approach (ii) will use the same link to send a bit pattern requesting retransmission of the total message. In both cases, since the bit error rate is limited, considerable care must be taken to insure that the message is received correctly and errors are detected. In the case of a detected error that prevents correct determination of the erroneous block address, little remains to do but restart the loading of the satellite. There are design methods to circumvent this problem. An effective method is given in Section 5.

The mean transmission time for initial upload, downlink transmission and one retransmission can now be determined. The equation is

$$\bar{T} = T_0 + \bar{T}d_1 + \bar{T}_1 \quad (6)$$

where  $\bar{T}d_1$  = average downlink transmission time after initial upload  
 $\bar{T}_1$  = average transmission for first retransmission

The value of  $\bar{T}d_1$  is given by

$\bar{T}d_1 = (6 \times D \times \text{probability that a block is in error in the initial upload}) \text{ sec}$   
 assuming one TLM word required per block address and D equals the number of blocks per message. The value of  $\bar{T}$  versus number of words per block for various bit error

rates and bits per word is presented in Figure 4.4.1-11 for retransmission of blocks. Using equations (5) and (6) the average transmission time including one retransmission for approaches (i) and (ii) for methods 1 and 2 can be determined. These results are given in Table 4.4.1-2. It is easily seen that retransmitting only erroneous blocks is much more efficient than total message retransmission.

The probability of a correct load after a given number of transmission attempts is equivalent to the probability of a bit error after a given number of transmission attempts. Because of the undetected error requirement, the number of transmission attempts must be sufficient to result in a bit error probability of less than  $10^{-15}$ . The important result is the number of transmission attempts since the total load time can then be estimated.

For approach (i), the probability of an error in a block is given by

$$P_b = 1 - (1 - P_e)^{KB} \quad (7)$$

where

$P_e$  is the transmission link BER,

$K$  is the number of words per block, and

$B$  is the number of bits per word.

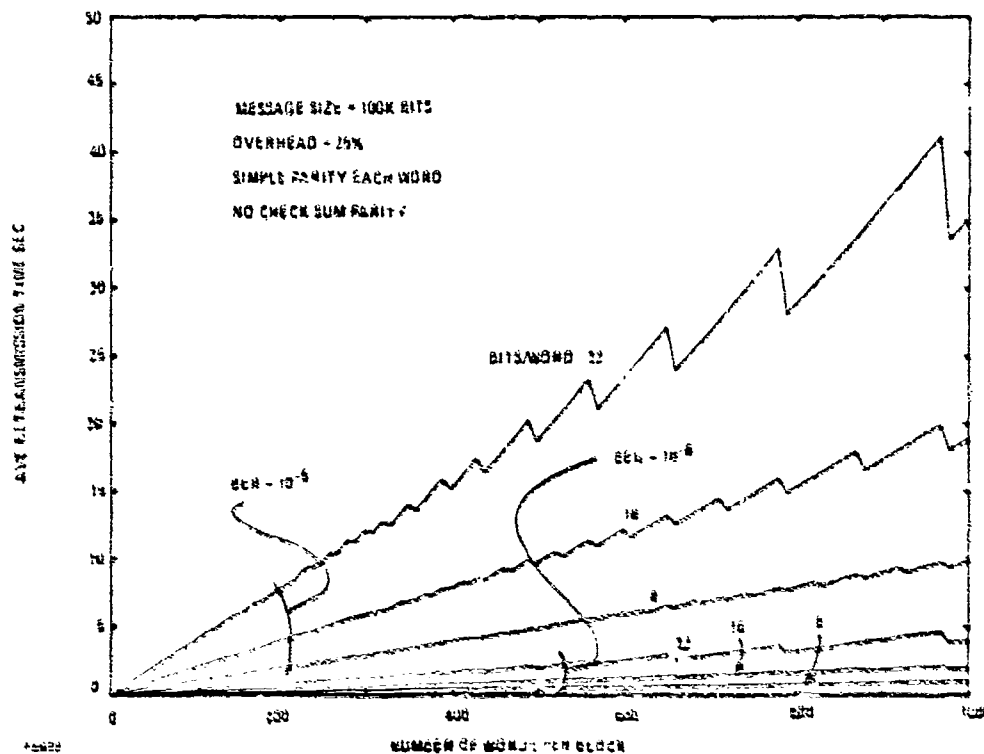


Figure 4.4.1-11. Average Retransmission Time

Table 4.4.1-2. Average Transmission Time

	Average Transmission Time Including One Retransmission (SEC)*		
	Uplink Bit Error Rate		
	$10^{-5}$	$10^{-6}$	$10^{-7}$
Method 1			
(i) Block	142	132	131.5
(i) Message	256	256	255
Method 2			
(i) Block	137	137	137
(ii) Message	251	251	250.5

\*Assumes 8 bits/word, 500 words/block and total upload message of 125,000 bits

The probability that a block has at least one error after n transmissions is given by

$$P_n = 1 - \sum_{i=0}^{n-1} (1-P_b)^i P_b \quad (8)$$

The probability that a message has at least one error is

$$P_m = (1-P_n)^{[100K(1+H)/N]} \quad (9)$$

The probability of a memory bit being in error becomes

$$P_b = \frac{1}{100K(1+H)} P_m \quad (10)$$

Equation (7) is plotted in Figure 4.4.1-12 for bit error rates of  $10^{-5}$  and  $10^{-6}$  and bits per word of 8, 16, and 32. For the case of 8 bit words and 500 words per block, the values of  $P_b$  for various bit error rates and number of transmissions are shown in Table 4.4.1-3. It is seen from the results of this analysis that a probability of a bit error in memory of less than  $10^{-15}$  is attainable for all uplink BER's. On the average, the number of transmissions required are 9, 5 and 4 for bit error rates of  $10^{-5}$ ,  $10^{-6}$  and  $10^{-7}$  respectively.



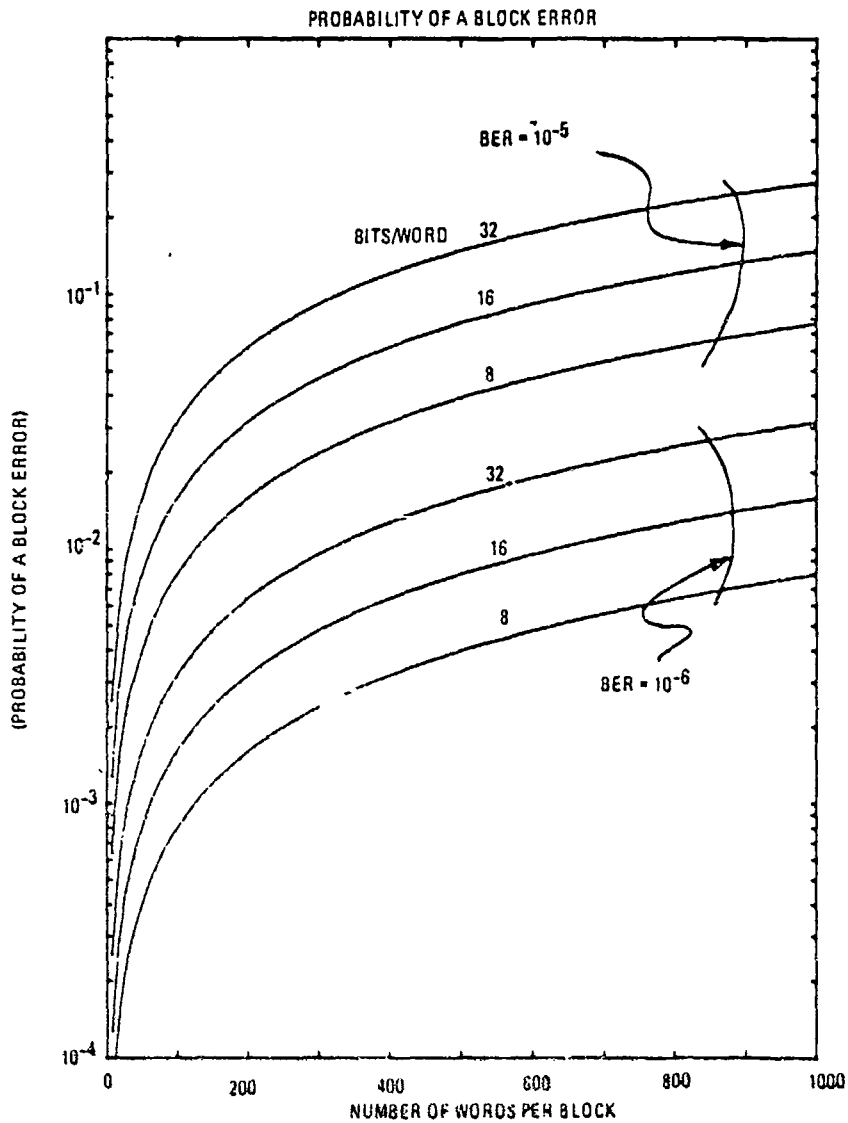


Figure 4.4.1-12. Probability of an Error Block

For approach (ii), the results have been previously reported.\* These results are summarized in Table 4.4.1-4. Only after 5 transmissions and an uplink BER of  $10^{-7}$  can the  $10^{-15}$  undetected bit error rate be reasonably assured. The time required to perform 5 transmissions, in this case, is approximately 650 seconds for both methods 1 and 2.

\*Presentation made to SAMSO, January 28, 1974 and DRB D9000S27B.

Table 4.4.1-3. Bit Error Rate in Memory Versus Number of Transmissions

Number of Trar smissions	Probability of Bit Error in Memory		
	Uplink BER		
	$10^{-5}$	$10^{-6}$	$10^{-7}$
1	$4.7 \times 10^{-6}$	$6.7 \times 10^{-7}$	$7.0 \times 10^{-8}$
2	$2.4 \times 10^{-7}$	$2.4 \times 10^{-9}$	$2.4 \times 10^{-11}$
3	$8.6 \times 10^{-9}$	$8.6 \times 10^{-12}$	$8.5 \times 10^{-15}$
4	$3.0 \times 10^{-10}$	$3.0 \times 10^{-14}$	$3.0 \times 10^{-18}$
5	$1.0 \times 10^{-11}$	$1.0 \times 10^{-15}$	$10^{-18}$
6	$3.7 \times 10^{-13}$	$3.7 \times 10^{-19}$	$10^{-18}$
7	$1.3 \times 10^{-14}$	$10^{-19}$	$10^{-18}$
8	$4.5 \times 10^{-15}$	$10^{-19}$	$10^{-18}$
9	$1.5 \times 10^{-17}$	$10^{-19}$	$10^{-18}$

Table 4.4.1-4. Probability of a Bit Error for Total Message Reiloading

Number of Transmissions	Probability of Bit Error in Memory		
	Uplink BER		
	$10^{-5}$	$10^{-6}$	$10^{-7}$
1	$5.6 \times 10^{-6}$	$8 \times 10^{-7}$	$8 \times 10^{-8}$
2	$3.2 \times 10^{-6}$	$8 \times 10^{-8}$	$8 \times 10^{-10}$
3	$2.4 \times 10^{-6}$	$8 \times 10^{-9}$	$8 \times 10^{-12}$
4	$1.3 \times 10^{-6}$	$8 \times 10^{-10}$	$8 \times 10^{-14}$
5	$8 \times 10^{-7}$	$8 \times 10^{-11}$	$8 \times 10^{-16}$

4.4.2 Ground Verification (Method 3). The concept of ground verification requires that the SGLS TT&C downlink be required to transmit to the ground the information loaded in the satellite memory. For a TT&C link of 1 Kbps with a bit error rate of  $10^{-5}$ , it was found that the overall loading performance was limited by the backlink. Because of this inherent limitation, the probability of an undetected bit error within the satellite memory does not approach the requirement of  $10^{-15}$ . In fact, an undetected bit error probability of approximately  $10^{-5}$  is the theoretical limitation. Because of this result, Method 3 is eliminated from further analysis.

#### 4.5 Message Protocol

Message protocol refers to the sequence of events required to load a message, the message overhead, the form of the uplink word, block size, and in information in the downlink data. The sequence of events required to load a message are access to the satellite memory, determine block address, verify data (Methods 1 and 2), load memory, request erroneous blocks retransmitted (Methods 1 and 2), downlink memory load for ground verification (Method 3), and retransmit erroneous block to the satellite.

The message overhead are those bits required for selecting satellite modes, error detection bits, block addresses, and synchronization bits. The form of the uplink word is the relation of memory load data, error detection bits and satellite mode bits. A typical word structure is shown in Figure 4.5-1. The block size is directly related to the overall message format.

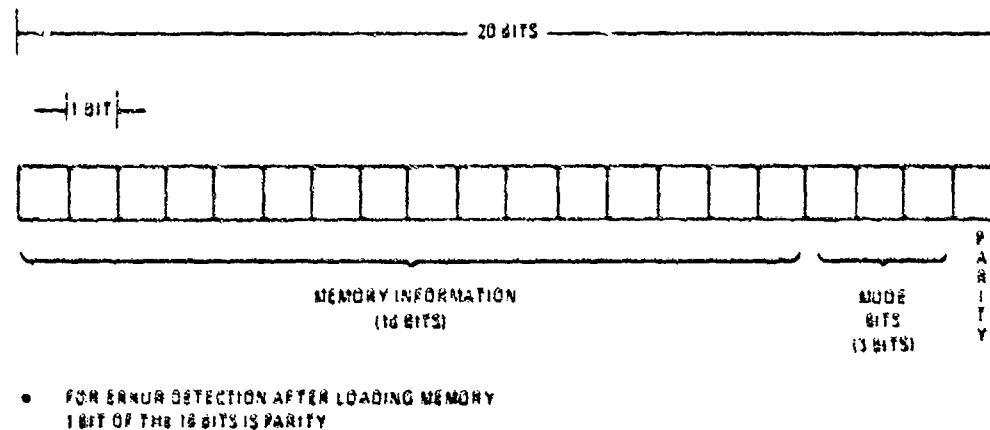


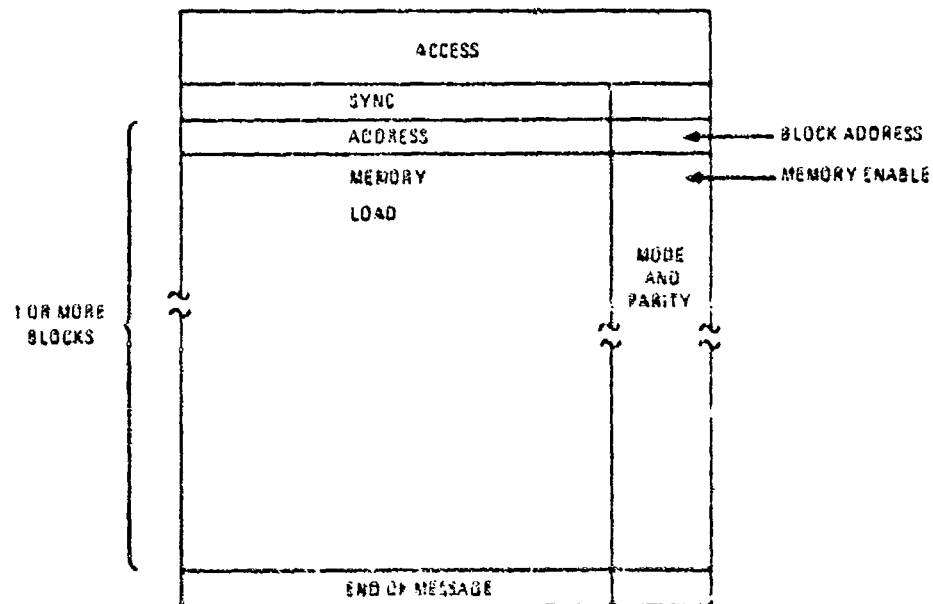
Figure 4.5-1. Typical Word Structure

Message format provides the definition of the total message sent to the satellite including access, sync, and data words. The concept of message format is shown in Figure 4.5-2.

The downlink information obviously depends upon the method used. For Method 1, the TLM words will be used to transmit to the upload station the address of erroneous blocks. For Method 2, the SGLS TT&C link will perform the same function and requires an appropriate message format. For Method 3, the SGLS TT&C link is again used. The downlink message consists of the memory load and an appropriate message format.

## 5. SELECTION

Candidate Method 1 is selected as the most promising uploading system because of minimum cost and minimum required uplink BER (see Section 4.1). An overview showing the relation between the upload station and the other elements of the GPS is given in Figure 5-1. The upload station has interfaces with the satellite constellation, monitor station and master control station. The satellite interface is the S-band uplink. The monitor station interface is the receipt from the monitor station L-band receiver the TLM words transmitted via the L<sub>1</sub>/L<sub>2</sub> user navigation data. The master control station interface is to receive the control data, upload data, and antenna pointing data from the master station computer.



FE025

Figure 4.5-2. Message Format Concept

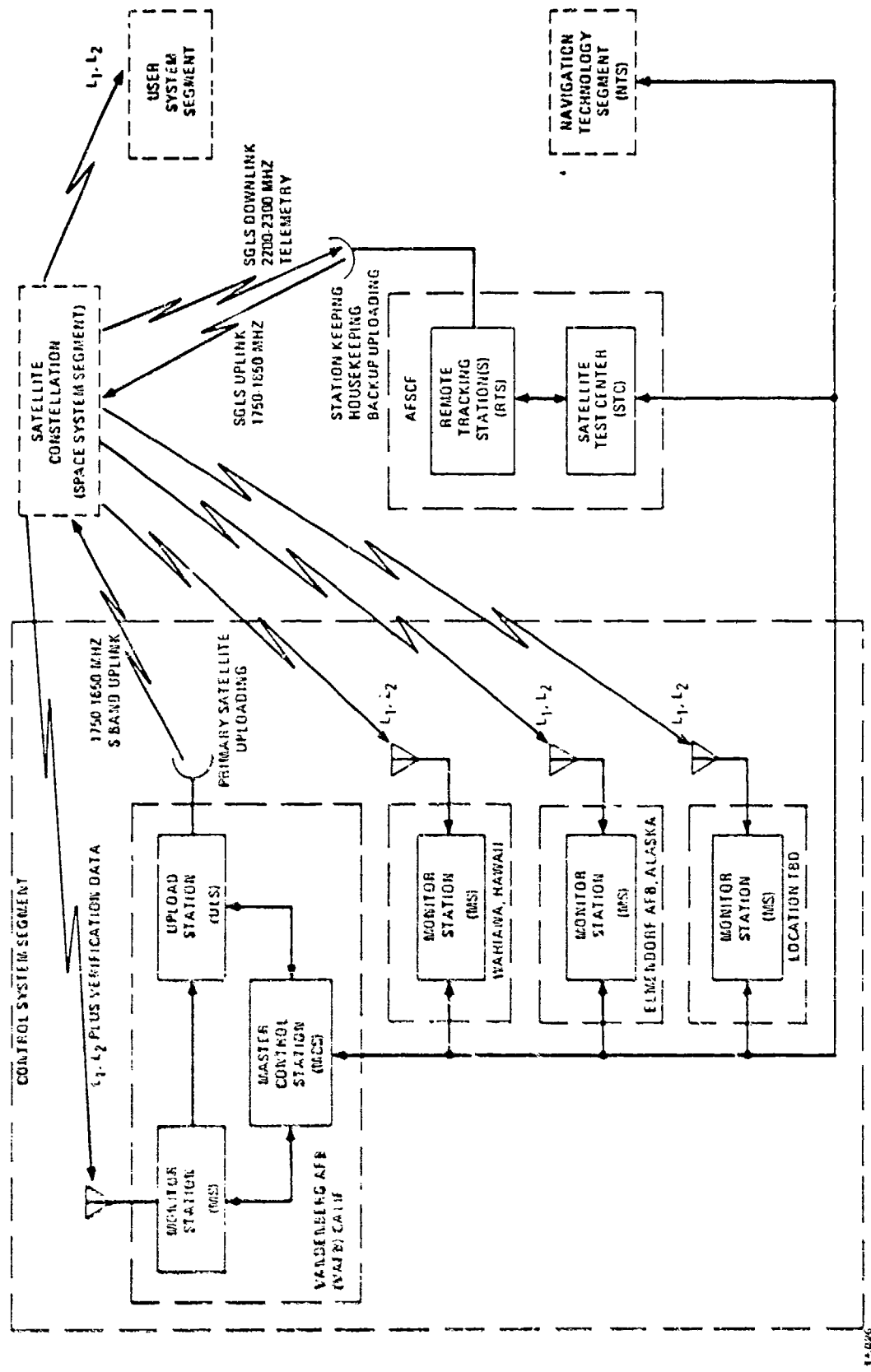


Figure 5-1. Global Positioning System (GPS) Overview Interface

## 5.1 Upload Station

Figure 5.1-1 illustrates the functional block diagram of the Monitor Station/Upload Station. The upload station consists of a 14-foot antenna, S-band TWT transmitter, formatter, display, antenna drive, computer and modems for communication with the Master Control Station computer and Monitor Station computer. This configuration has the advantages of being moved to another Monitor Station location or being remotely located from its Monitor Station with a minimum of interface disconnections.

## 5.2 Satellite

A functional block diagram of a feasible satellite configuration for loading the memory is shown in Figure 5.2-1. The function of the SGLS R-23 and command decoder is to receive the access words for the GPS decoder. It is suggested that the GPS access commands storage be capable of many days of unattended operation to circumvent AFSCF impact on GPS operation.

The reception of a memory load is enabled by an access word that will enable the GPS decoder to accept data words and blocks. The digital word received by the GPS decoder should contain memory bits, mode bits and a parity bit. In addition, each block of data will end with a checksum word since both horizontal and vertical parity checks are required to obtain an undetected bit error rate of  $10^{-15}$ . Anytime an error is discovered, the erroneous block address will be incorporated into the TLM word and provided to the SGLS TT&C if the loading and verification is in the backup mode.

As the words are decoded by the GPS decoder, the block address is loaded into the memory address generator and the memory is loaded word by word from the memory address corresponding to the block address. As a word is loaded into memory, it would be advisable to immediately re-read (echo) the word from memory and perform a parity check on the word using the parity bit required for the user navigation data transmission. Again, a parity error would enable transmission of the erroneous block address to the upload station. The echo check of the memory load can be performed by cycle sharing since the incoming data has a rate of only one (1) kilobit per second.

The purpose of the mode bits is to provide control information to the satellite that identifies the purpose of the load and the type of word received. This type of data is considered overhead and must be distinguishable from any memory data. Therefore, separate bits are recommended to provide these modes. Three (3) bits should be sufficient to provide these modes.

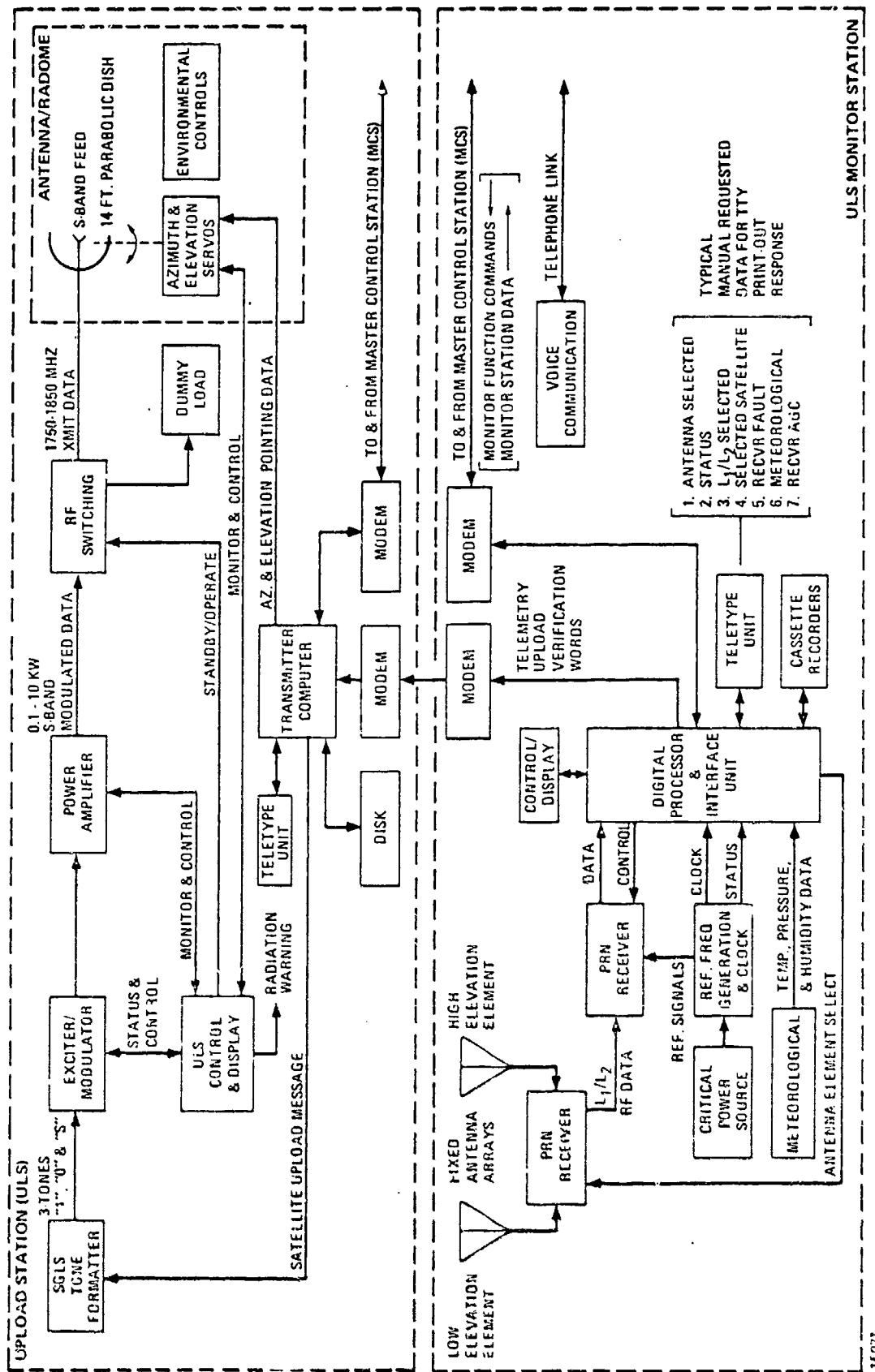


Figure 5. 1-1. GPS Monitor Station/Upload Station Functional Diagram Specification Baseline

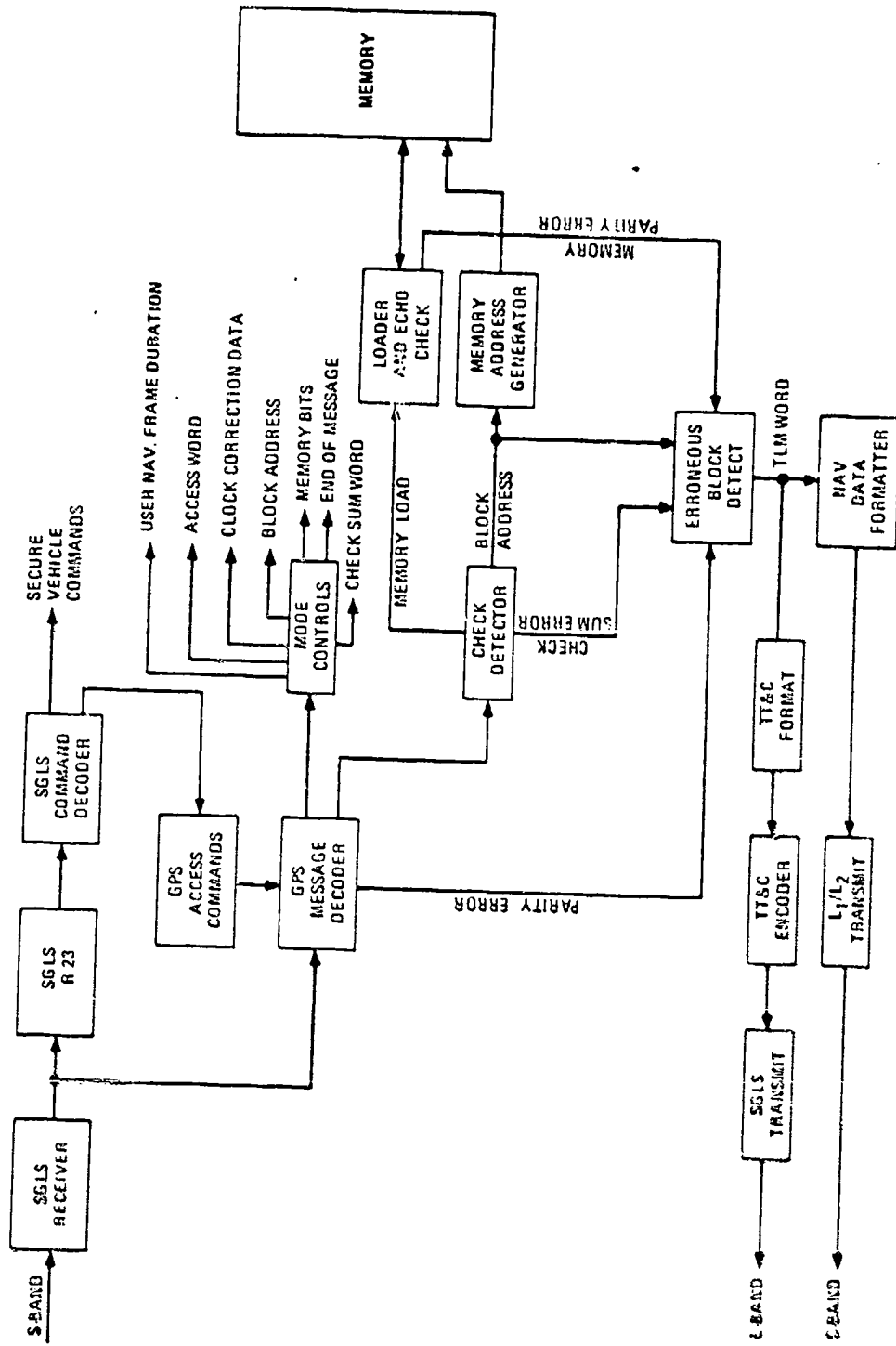


Figure 5.2-1. Satellite Functional Block Diagram for Loading Memory



### 5.3 Message Format

The message format refers to the size and structure of the upload message and downlink data. The upload message will consist of blocks both for the initial transmission and subsequent retransmissions. During retransmissions only, blocks found in error will be uploaded again.

Given that the portion of the user navigation frame stored in the satellite is composed of 8 bit bytes, the minimum word size feasible for uploading is 12 bits. These 12 bits include 8 bits for memory, 3 bits for modes and 1 bit of parity. For an uplink BER of  $10^{-6}$ , the maximum block size of 575 words is imposed to meet the undetected bit error rate of  $10^{-15}$ . The recommended word format is shown in Figure 5.3-1.

To determine the number of words per block, consider the case of an error in the TLM word in the downlink. If an error occurs, it is easy to determine that it has occurred by error detection. However, the determination of the correct block address is difficult without the use of an error correcting code; such encoding would not be cost effective for this task. Consider the result if the uplink transmission time of a block is 6 or more seconds in length. First, storage of erroneous block addresses would not be required prior to transmission. Second, each TLM word could easily be associated with the last block sent to the satellite. Other requirements are that an integer number of blocks be required to load the 100K bit satellite memory, the number of possible block addresses be less than the eight bits of usable data in an uplink word, and the maximum block address binary number fit into the TLM word. The number of words per block can be determined as follows. Since the uplink has a data rate of 1K bits/sec, 6000 bits can be transmitted in a 6-second interval. If there are 12 bits per word, 500 words can be sent per 6-second interval. A block must be started with the block address word and end with the checksum word. Therefore, if a block contained 502 words each of 12 bits, each block would contain 4,000 bits for storage in memory and a total memory load would require 25 blocks exactly. The 25 blocks require 5 bits which is less than the 8 bits available for the block address in the first word of the uploaded block. The resulting message format for uploading is shown in Figure 5.3-2.

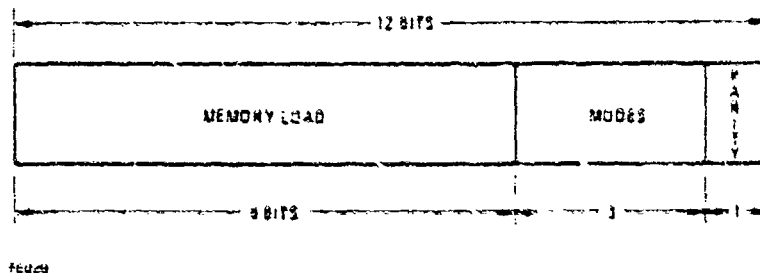


Figure 5.3-1. Upload Word Structure is 12 Bits

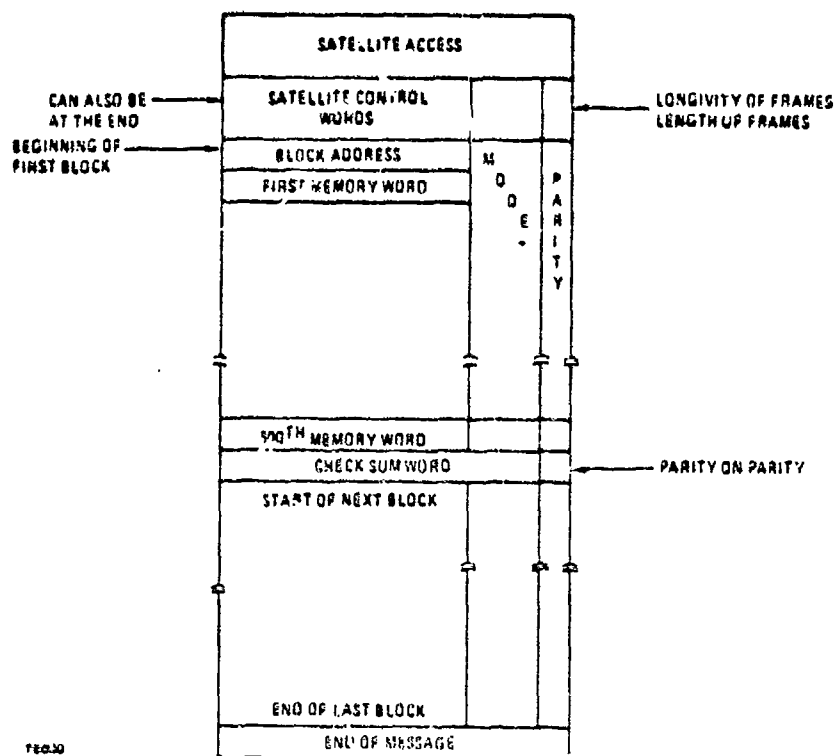


Figure 5.3-2. Recommended Message Format

The remaining portion of the satellite loading procedure is the form of the TLM word. It is recommended that the 16 bits of the TLM word be made up of a block address repeated three (3) times and possibly a parity bit. This will permit some error correction and allow the upload station to compare its last block transmitted information with the erroneous block address received via the TLM word. Since the TLM word will contain an erroneous block address then the satellite does not detect an error and a null number will be required. Either all zeros or all ones word is recommended. In addition, a unique TLM word should be provided to indicate that the satellite memory has been correctly accessed and the loading function is underway.

TRADE STUDY NO. 2

SATELLITE ORBITS

A. Arcidiacono



**GENERAL DYNAMICS**  
*Electronics Division*  
P.O. Box 81127, San Diego, California 92128 TEL 379-7201

## 1. INTRODUCTION

### 1.1 Purpose

The purpose of the satellite orbit selection is to optimize the duration of test area coverage and provide the best possible GDOP for the user. It is not unusual to trade these parameters. In fact, the Aerospace final 2/2/0 constellation does sacrifice the GDOP over Holloman test area to increase the four-satellite co-visibility by approximately one-half hour.

### 1.2 Orbit Concept

For the best possible GDOP, a Y-shaped configuration of the satellites over the test area is desirable. Since all the satellites are moving, the GDOP parameter is affected by the changing geometry of the satellite constellation. The optimization of the GDOP dictates the spacing of the orbital planes and the location of the satellites within them. The orbital injection of the satellite is such that at least once a day the co-visibility and GDOP parameters are obtained over a given test area. This requirement is accompanied by obtaining orbital information via Monitor Stations controlled and supported by a Master Station equipped with computation facilities for the refinement and generation of the satellite ephemerides. This study has considered the stations of various existing networks and the results are presented herein.

### 1.3 Impact of Phases

The above concept applies basically to the Phase I of the GPS Program for the performance evaluation of the system. Nevertheless, the basic concept of optimum GDOP for the user and the location of the Monitor Stations, the Master Station and the satellite update station will be closely related in later phases of the system.

The GPS phases to follow will involve a greater number of satellites (up to 24). The major impact is expected to occur in the satellite spacing, or phasing and number of satellites within the basic three orbital planes studied in Phase I. This study will delineate the basic functional requirements pertinent to the satellites' orbital constellation, and the basic navigation accuracy objectives of the system and the user.

## 2. REQUIREMENTS

### 2.1 Functional Requirements

The initial deployment of the Satellite Segment consists of four satellites in subsynchronous orbit providing simultaneous visibility to system users over a large geographic area including most of CONUS for a period of 1.5 to 3 hours per day. Source: Annex 1, Paragraph 3.1, 16 October 1973.

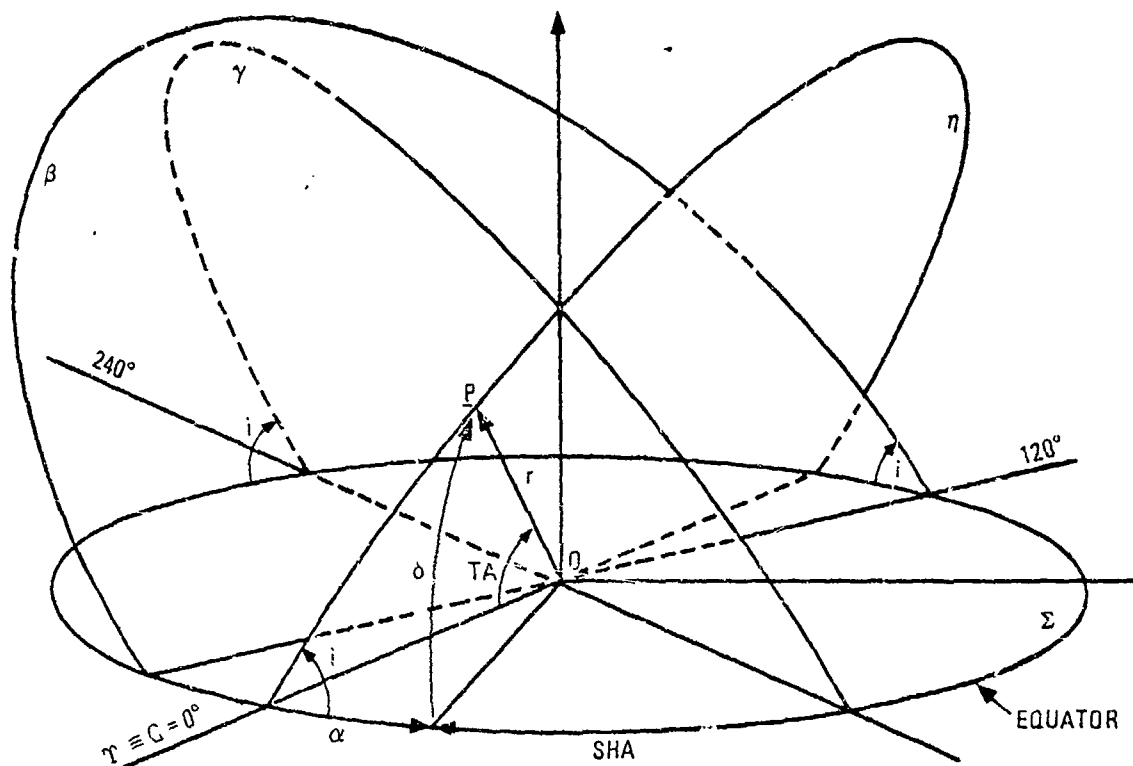
### 2.2 Design Requirements

The basic orbital parameters and requirements of the satellite deployment are:

- A. Geometric quality to satisfy basic navigation accuracy objectives.
- B. Circular Orbit (subsynchronous).
- C. Orbit Period,  $\approx$ 12 hours.
- D. Orbit Inclination, 60 to 65 degrees.
- E. Up to three orbital planes (at least two).
- F. Orbital plane spacing 120 degree (inertial).
- G. A total of four satellites.
- H. An Orbital altitude of 10,900 NMI.

Source: Annex I, Paragraph 3.2, 16 October 1973.

In a geocentric equatorial system of coordinates, the circular paths of the satellites are located in three orbital planes spaced at 120 degrees and inclined 63.4 degrees with respect to the equatorial plane as shown in Figure 2.2 -1. The origin of the system lies at the center of the Earth; the plane of the equator is used as reference plane along which is measured the longitude of the satellite orbit ascending node,  $N$ . The longitude of the satellite position,  $P$ , is measured starting from the vernal equinox,  $T$ , and the Greenwich meridian plane coincidence, eastward (right ascension,  $\alpha$ ) or westward (sidereal hour angle,  $SHA$ ). The latitude of the satellite, better known as declination,  $\delta$ , is measured from the equatorial plane in the North or South direction. The satellite position  $P$ , in its orbital plane, can also be identified by its right ascension angle  $\alpha$  and its true anomaly angle,  $TA$ .



- LEGEND:  $\Sigma$  = EQUATORIAL PLANE  
 $\tau$  = VERNAL EQUINOX ALIGNMENT (TYPICAL)  
 $G$  = GREENWICH MERIDIAN ALIGNMENT (TYPICAL)  
 $O$  = EARTH SPHEROID CENTER  
 $i$  = SATELLITE ORBIT INCLINATION  
 $\beta, \gamma, \eta$  = SATELLITE ORBITAL PLANES  
 $\alpha$  = RIGHT ASCENSION OF  $P$  (SATELLITE)  
 $SHA$  = SIDEREAL HOUR ANGLE OF  $P$   
 $r$  = POSITION VECTOR OF  $P$   
 $\delta$  = DECLINATION OF  $P$   
 $TA$  = TRUE ANOMALY ANGLE

TE043

Figure 2.2 -1. Satellite Orbital Plane Representation

### 2.3 Ground Rules

The computer simulations for the orbital optimization of the satellite constellation were performed by the Convair Aerospace Division. The constellations, the satellite position, the geometric dilution of precision (GDOP), and the coverage data were provided by this team for performing coverage analyses, selecting the ground station sites, and assisting in the optimization of the user error determination.

### 2.4 Evaluation Criteria

The criteria for the evaluation of the optimum constellation and sites was based on the following parameters:

- (1) GDOP over the test areas.
- (2) Co-visibility (4-satellite) time over test areas.
- (3) Pre-visibility of the four-satellite before entering the test area for latest ephemerides update.

The resulting data for the evaluation is presented in the appendices of this trade study. The data consists of several types including earth traces, GDOP plots, and contact opportunity charts.

A preliminary coverage analysis shows the existence of long visibility periods, nevertheless the GDOP opportunity window poses a constraint that is reflected in the time available to the Monitor Stations to gather satellite position data, transmit the data to the Master Station, process the data at the Master Station, prepare the satellite update message, transmit it via landlines to the SCF, and verify the satellite loading. GDOP and visibility permitting, it is highly desirable to have a recent satellite updating when coming over the test area.

### 3. CANDIDATES

Of the three possible constellations, 3/1/0, 2/2/0, and 2/1/1, only data for the 3/1/0 and 2/2/0 constellations will be compared for the final evaluation. The 2/1/1 was abandoned in the early phases of the analyses because of very poor GDOP, nevertheless, GDOP data of this configuration is presented in Appendix E for comparative purposes.

Two 2/2/0 constellations were analyzed. These two constellations will be identified as Aerospace "preliminary" and "final" constellations. The major difference being the satellite's phasing

in their orbital planes. These two constellations were suggested by Aerospace and tend to emphasize the coverage over Yuma (the 2/2/0 preliminary) and the coverage over Holloman (the 2/2/0 final). The General Dynamics Convair generated 2/2/0 constellation data is presented in Appendix B for comparison purposes only. All available constellations were considered in the coverage and GDOP tradeoff.

The characteristics of the orbital parameters of final constellations used in this study are listed below. The parameters are the satellite number (SAT. NO.), the longitude of the ascending node (LAN), the argument of perigee (AOP), orbit inclination (INCL), and orbital period in minutes.

1. Constellation 3/1/0

<u>SAT NO.</u>	<u>LAN(Deg)</u>	<u>AOP(Deg)</u>	<u>INCL(Deg)</u>	<u>PERIOD (Min.)</u>
1	230	240	63.4	720
2	230	270	63.4	720
3	350	165	63.4	720
4	230	325	63.4	720

2. Constellation 2/2/0 Aerospace Preliminary

<u>SAT NO.</u>	<u>LAN (Deg)</u>	<u>AOP(Deg)</u>	<u>INCL(Deg)</u>	<u>PERIOD (Min.)</u>
1	0	63.33	63.4	718.0342
2	0	103.33	63.4	718.0342
3	240	90.00	63.4	718.0342
4	240	160.00	63.4	718.0342

3. Constellation 2/2/0 Aerospace Final

<u>SAT NO.</u>	<u>LAN(Deg)</u>	<u>AOP(Deg)</u>	<u>INCL(Deg)</u>	<u>PERIOD(Min.)</u>
1	240	330	63.0	718.0342
2	240	5	63.0	718.0342
3	120	0	63.0	718.0342
4	120	70	63.0	718.0342



4. Constellation 2/2/0 General Dynamics

<u>SAT NO.</u>	<u>LAN(Deg)</u>	<u>AOP(Deg)</u>	<u>INCL(Deg)</u>	<u>PERIOD (Min.)</u>
1	230	240	63.4	720
2	230	280	63.4	720
3	350	165	63.4	720
4	350	235	63.4	720

5. Constellation 2/1/1 General Dynamics

<u>SAT NO.</u>	<u>LAN(Deg)</u>	<u>AOP(Deg)</u>	<u>INCL(Deg)</u>	<u>PERIOD (Min.)</u>
1	230	362.5	63.4	720
2	230	317.5	63.4	720
3	350	270.0	63.4	720
4	110	15.0	63.4	720

The argument of perigee (AOP) parameter is often interchanged with the true anomaly (TA) parameter. Both are used to indicate the orbital position of the satellite in their own plane at the time  $t = 0$ . The longitude of the ascending node parameter is also referred to the time  $t = 0$  reference.

4. ANALYSES

4.1 Comparison Matrix

Table 4.1-1 summarizes the coverage duration and GDOP variation over the Holloman, Yuma and Vandenberg stations. P. Mugu or San Clemente Island station data was used for the Vandenberg station whenever not available. The data pertinent to other stations is available in the respective appendices of this study.

The data presented in Table 4.1-1 illustrates the very high GDOP obtained from the 2/1/1 satellite configuration thereby eliminating it from further consideration. The General Dynamics 2/2/0 and Aerospace Preliminary 2/2/0 constellation compare favorably. The General Dynamics result has higher co-visibility at Holloman, 2 hours and 48 minutes compared to 2 hours and 8 minutes, while the Aerospace Preliminary 2/2/0 has lower GDOP, 3.8 to 5.0 compared to 4.8 to 9.8.

A comparison between the General Dynamics 3/1/0 and the Aerospace Final 2/2/0 constellations shows that in terms of GDOP and test site visibility, the former provides higher performance. However from the pre-visibility considerations shown in Table 4.1-2, the Aerospace

Final 2/2/0 constellation provides the necessary tracking, clock evaluation and uploading period prior to testing. Table 4.1-2 also shows how long four satellite constellations are visible by the candidate monitor, master and upload stations prior to visibility over the test areas. In addition to an adequate pre-visibility period, it is required that the pre-visibility and co-visibility periods overlap over the test area.

The pre-visibility for the 3/1/0 constellation turns out to be very poor as compared to the 2/2/0 constellations. The Aerospace final 2/2/0 shows that a total of nine stations have pre-visibility for a total of 8 hours as compared to the 7 stations and 5-1/3 hours of the 2/2/0 Aerospace preliminary and zero stations and zero time for the 3/1/0 constellation. It is concluded that the 2/2/0 Aerospace Final constellation appears to provide a good compromise among the basic parameters presented above, usually the pre-visibility, coverage and GDOP.

#### 4.2 Analysis Support Data and Topics

The above analysis reflects data delegated into the appendices of this study. The data was generated by a satellite communication opportunity computer program with the assistance of interactive graphics techniques for the optimization of the constellations. All station rise and set times are based on a satellite elevation angle of 5 degrees and on typical tracking station obscurities. The data contained in the appendices was divided as follows:

<u>Appendix</u>	<u>Title</u>
A	3/1/0 General Dynamics Constellation Data
B	2/2/0 General Dynamics Constellation Data
C	2/2/0 Aerospace Preliminary Constellation Data
D	2/2/0 Aerospace Final Constellation Data
E	2/1/1 General Dynamics Constellation Data

#### 5. SELECTION

Phase I is certainly a test for the evaluation of the performance of the GPS functional requirements and navigation accuracy objectives. However, it is clear that the duration of tests over a given test area is of primary importance in this particular phase. The Aerospace 2/2/0 final constellation appears to provide a good compromise between the relatively low GDOP (4.2 to 7.2) and the test duration (2 hours, 32 minutes) parameters supported by a test area pre-visibility array of at least nine and thirteen stations for the 4 and 3 satellite co-visibility cases, respectively.

TABLE 4.1-1  
TEST AREAS COVERAGE/GDOP SUMMARY

Station Con- stellation	COVERAGE (HR. MIN.)			GDOP*		
	HOLLOMAN	YUMA	Vandenberg	HOLLOMAN	YUMA	Vandenberg
3/1/0 GD	2 hr 54 min	N/A	2 hr 15 min	3.9 to 7.2	N/A	3.9 to 5.8
2/2/0 GD	2 hr 48 min	N/A	2 hr 30 min	4.8 to 9.8	N/A	4.8 to 8.4
2/2/0 Acro. Pre	2 hr 8 min	N/A	2 hr 10 min <sup>Ⓞ</sup>	3.8 to 5.0	N/A	3.8 to 7.0 <sup>Ⓞ</sup>
2/2/0 Acro. Final	2 hr 32 min	2 hr 11 min	2 hr 4 min <sup>ⓄⓄ</sup>	4.2 to 7.2	4.2 to 9.1	4.2 to 10.8 <sup>ⓄⓄ</sup>
2/1/1 GD	4 hr 6 min	N/A	2 hr 45 min	7.3**	N/A	7.6**

NA = Not available

\* = Minimum and Maximum Value within Coverage

\*\* = Lowest Value

Ⓞ = Ft. Mugu Data

ⓄⓄ = San Clemente Island Data

TABLE 4.1-2  
PRE-VISIBILITY TIME OVER CANDIDATE STATIONS (2 & 3 SATELLITE)

STATION CONSTELLATION	NHS	KTS	IOS	GUAM	MILAB	HTS	FAB	LMB	SAMOA	ELM	PT. MUGU	WAHI.	ROSEN.	PROSPECT	CZON	VTS	T. of Ocean	PREVISIBILITY STATION	
																		Total Time	Count
3/1/0 CID	0	0	0	0	0	0	0	0	0	NA	NA	NA	NA	NA	0	0	NA	0	0
2/2/0 Acro Final	0	1 1/2	0	0	0	0	3/4	0	2	NA	NA	NA	NA	NA	0	1	NA	5-1/4	4
2/2/0 Acro Final	0	1 3/4	0	0	0	3/4	NA	NA	NA	1 1/3	1 1/3	1 1/2	NA	1 1/8	NA	1 1/3	NA	5-1/3	7
2/2/0 Acro Final	1 1/2	2 1/2	0	0	2	3 1/4	NA	NA	NA	1 2/3	1 3/8	7 3/8	NA	1 1/4	NA	1 3/4	NA	23-1/2	9
2/2/0 Acro Final	0	1 1/4	0	0	0	1 1/3	1 1/4	1 1/8	0	1 1/4	1 1/5	1 1/3	1 1/4	0	NA	1 1/3	0	8	9
2/2/0 Acro Final	1 1/2	2 1/8	0	0	2 1/3	1 1/2	2 1/5	2 1/5	0	7 1/8	3	3 1/2	1 1/5	1 1/2	NA	7 2/8	1 1/4	30-1/2	13

Times shown are in hours  
 NA - Data not available.  
 \* - Two hours are available.

APPENDIX A

General Dynamics

3/1/0 CONSTELLATION DATA

<u>Figure</u>		<u>Page</u>
A-1	Satellite Earth Traces .....	A-2
A-2	Satellite Coverage Vs Tracking Stations .....	A-3
A-3	Tracking Stations Coverage Vs Satellites .....	A-4
A-4	GDOP for Holloman AFB .....	A-5
A-5	GDOP for Vandenberg AFB .....	A-6
A-6	GDOP for Conus Center .....	A-7
A-7	GDOP for Seattle .....	A-8
A-8	GDOP for Canal Zone .....	A-9

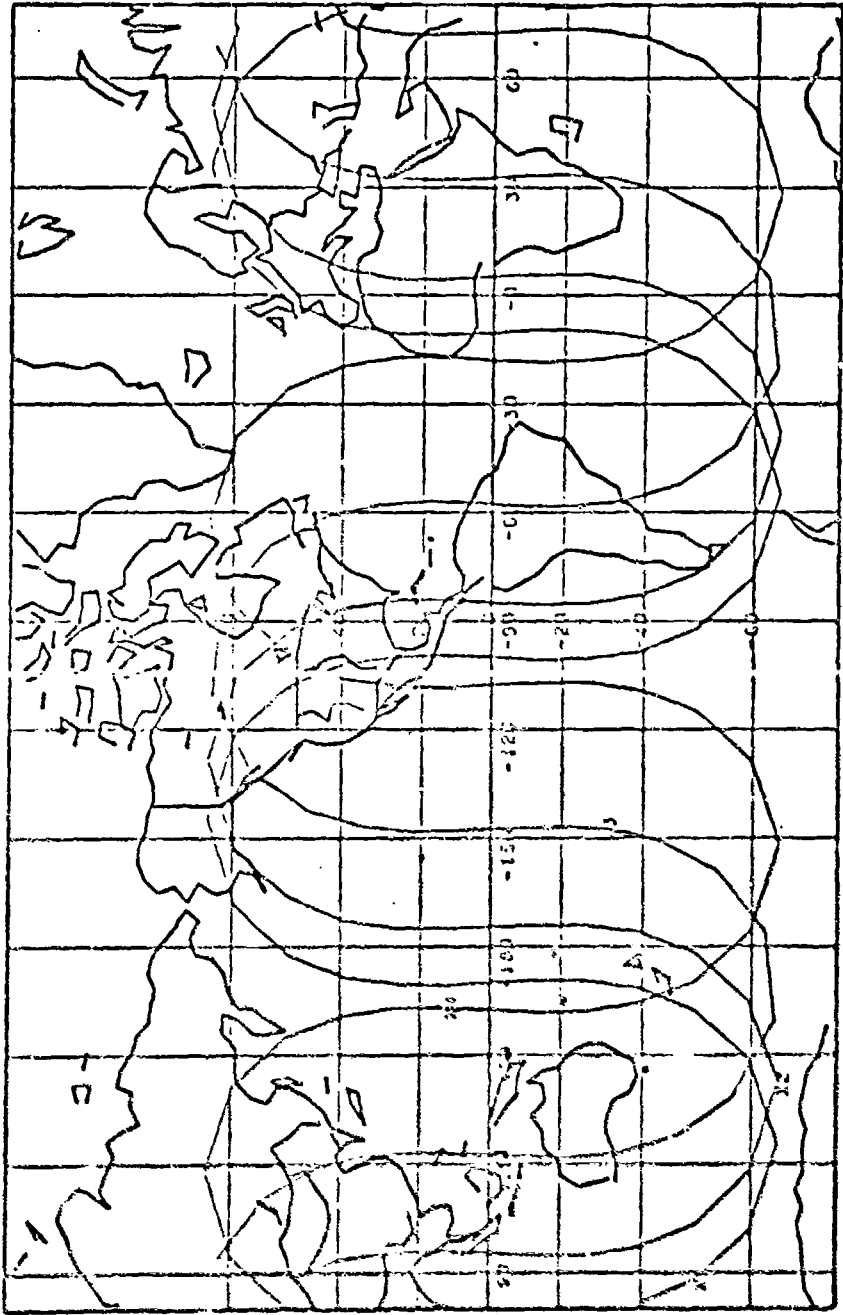


Figure A-1. Satellite Earth Traces

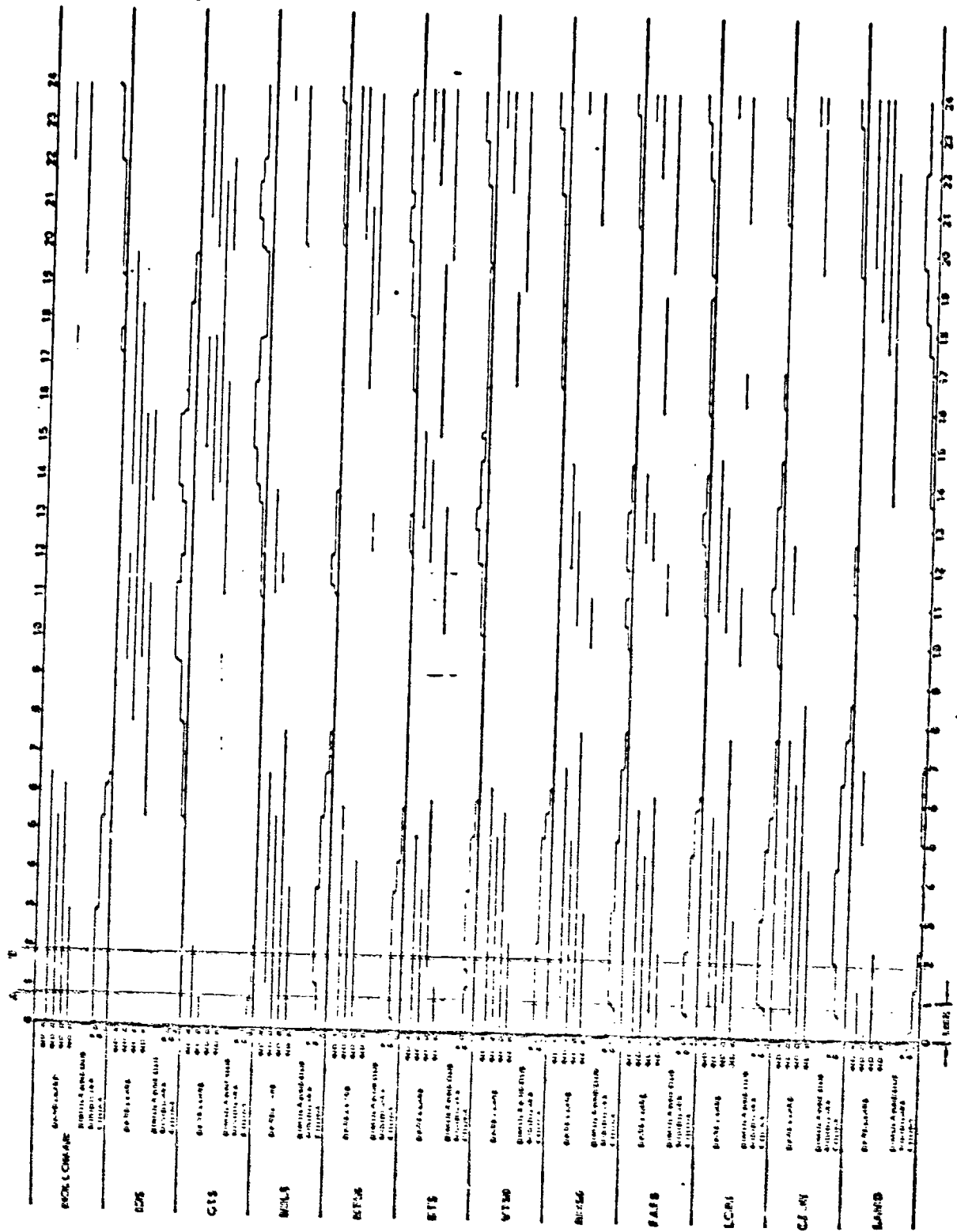


Figure A-2. Satellite Coverage Vs Tracking Stations

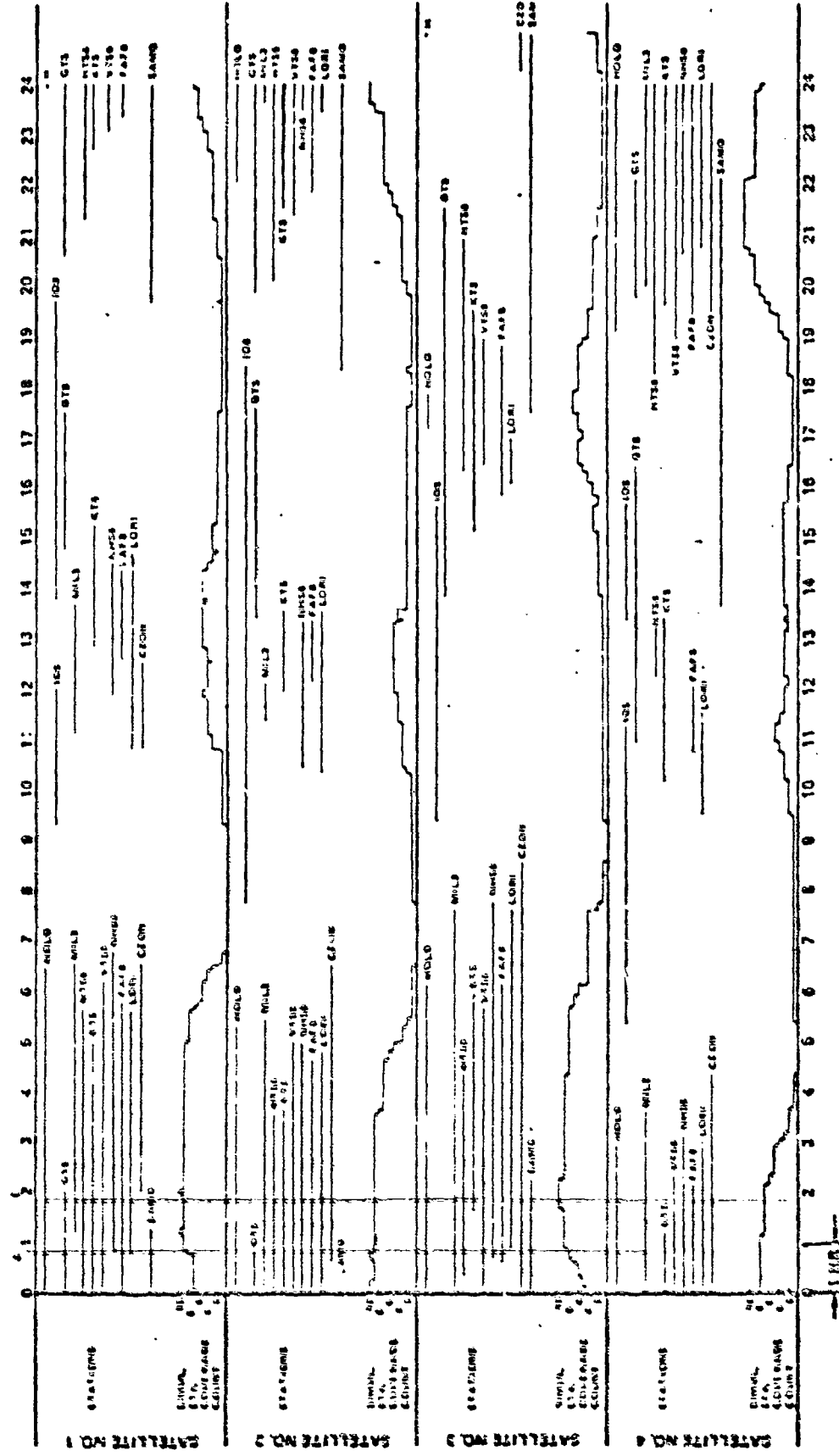
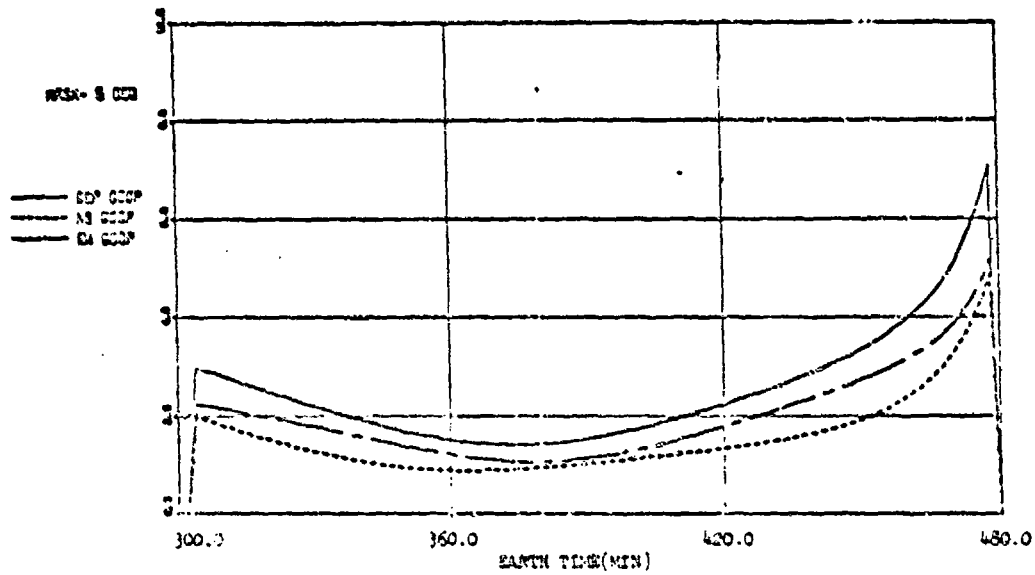


Figure A-3. Tracking Stations Coverage Vs Satellites



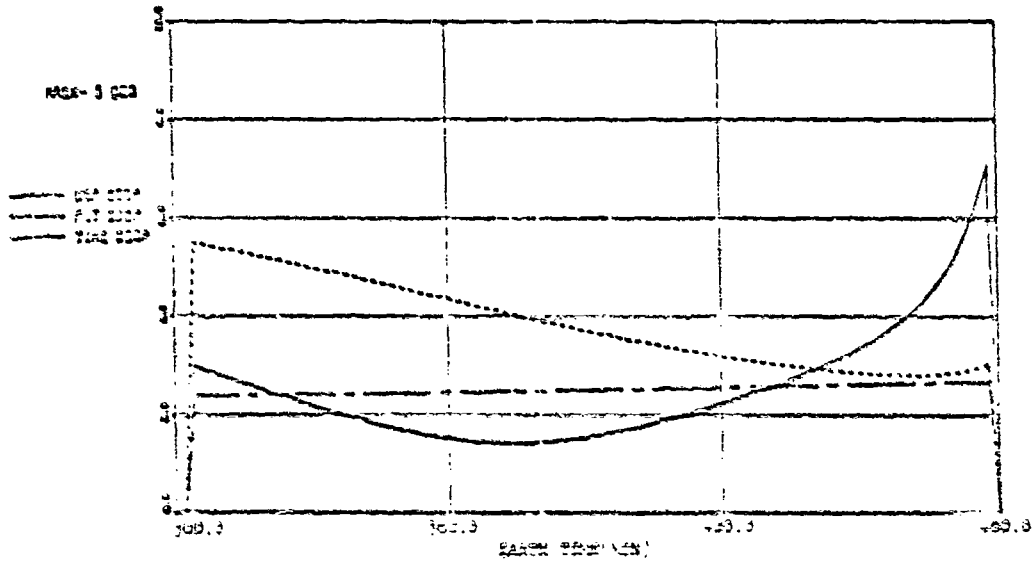
HOLLOWMAN LNG--103.00 LAT- 32.80



SAT	LAN	AOP	B	INC	TA(MIN)	R(MIN)
1	210.0	0.0	.00	63.4	480.0	720.0
2	210.0	0.0	.00	63.4	340.0	720.0
3	330.0	0.0	.00	63.4	30.0	720.0
4	210.0	0.0	.00	63.4	420.0	720.0

(3/1/0 Constellation)

HOLLOWMAN LNG--103.00 LAT- 32.80

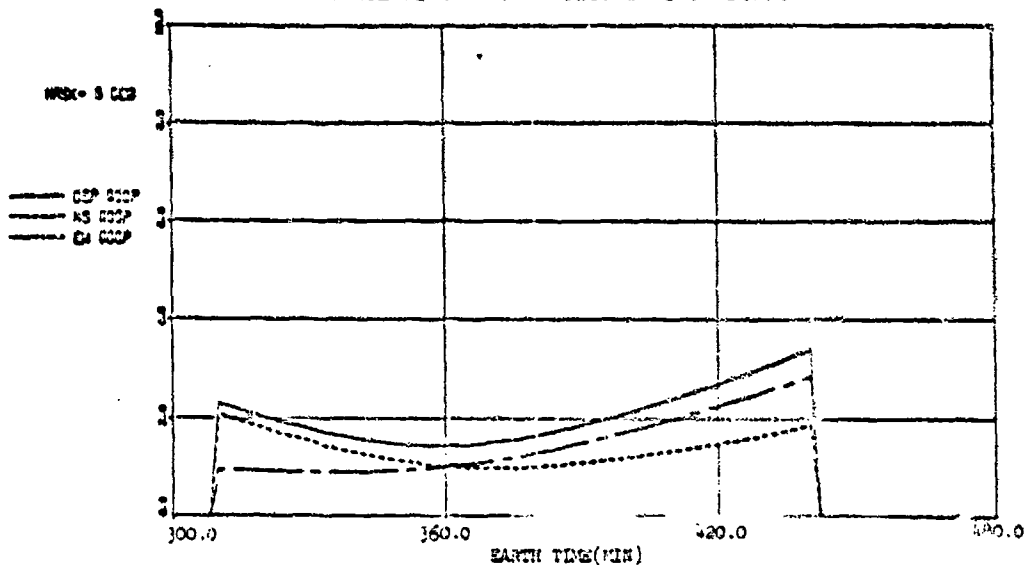


SAT	LAN	AOP	B	INC	TA(MIN)	R(MIN)
1	210.0	0.0	.00	63.4	480.0	720.0
2	210.0	0.0	.00	63.4	340.0	720.0
3	330.0	0.0	.00	63.4	30.0	720.0
4	210.0	0.0	.00	63.4	420.0	720.0

(3/1/0 Constellation)

Figure A-4. GDOP for Hollowman AFH

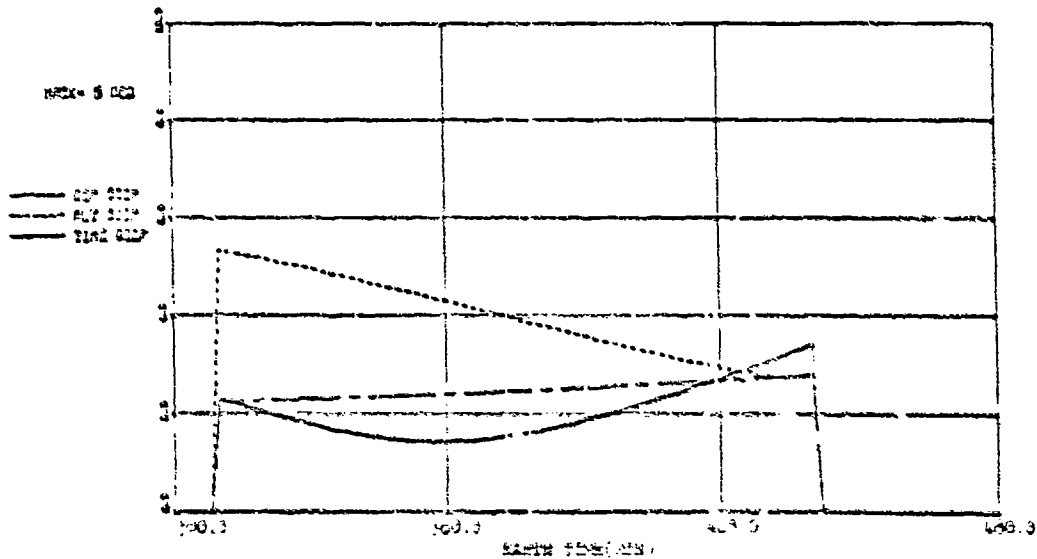
VANDENBERG LONG--120.50 LAT- 34.82



SAT	LAN	AOP	E	INC	TA(MIN)	P(MIN)
1	230.0	0.0	.00	63.4	480.0	720.0
2	230.0	0.0	.00	63.4	540.0	720.0
3	350.0	0.0	.00	63.4	300.0	720.0
4	230.0	0.0	.00	63.4	650.0	720.0

(3/1/0 Constellation)

VANDENBERG LONG--120.50 LAT- 34.82

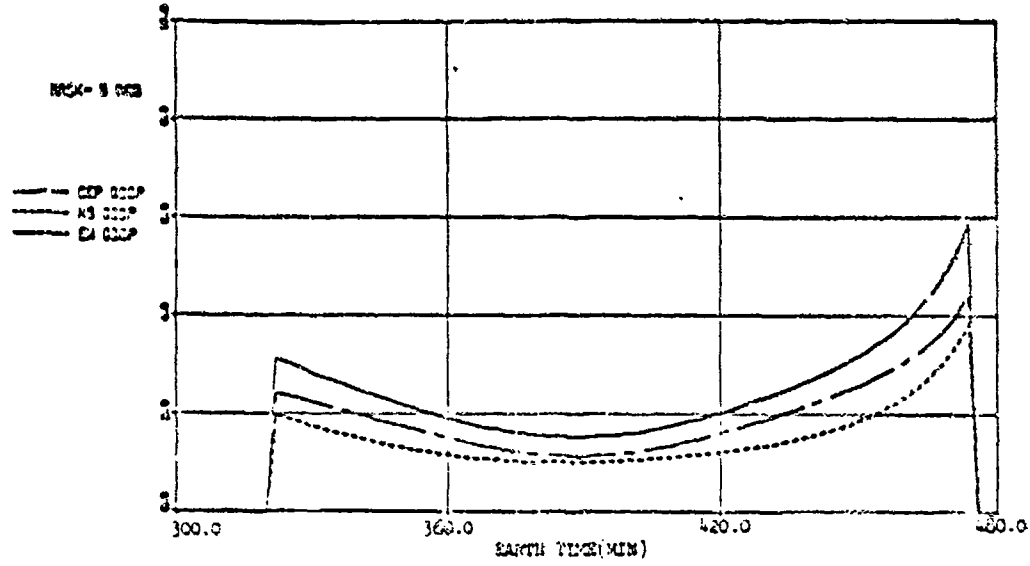


SAT	LAN	AOP	E	INC	TA(MIN)	P(MIN)
1	230.0	0.0	.00	63.4	480.0	720.0
2	230.0	0.0	.00	63.4	540.0	720.0
3	350.0	0.0	.00	63.4	300.0	720.0
4	230.0	0.0	.00	63.4	650.0	720.0

(3/1/0 Constellation)

Figure A-5. GDOP for Vandenberg AFB

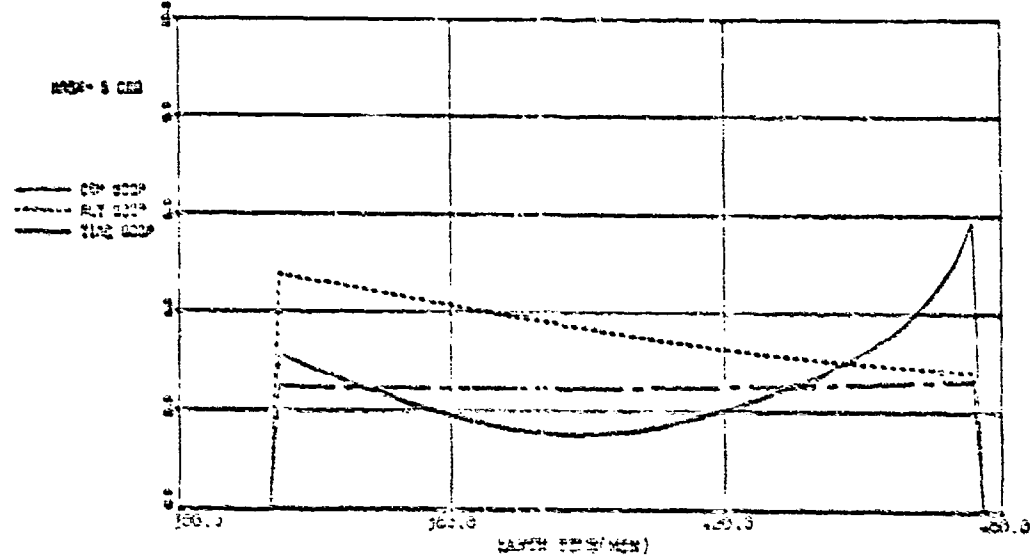
CONUS CENT LNS--100.00 LAT- 40.00



SAT	LAN	AOP	E	INC	TA(MIN)	H(MIN)
1	210.0	0.0	.00	63.4	420.0	720.0
2	210.0	0.0	.00	63.4	340.0	720.0
3	210.0	0.0	.00	63.4	310.0	720.0
4	210.0	0.0	.00	63.4	570.0	720.0

(1/1/0 Constellation)

CONUS CENT LNS--100.00 LAT- 40.00

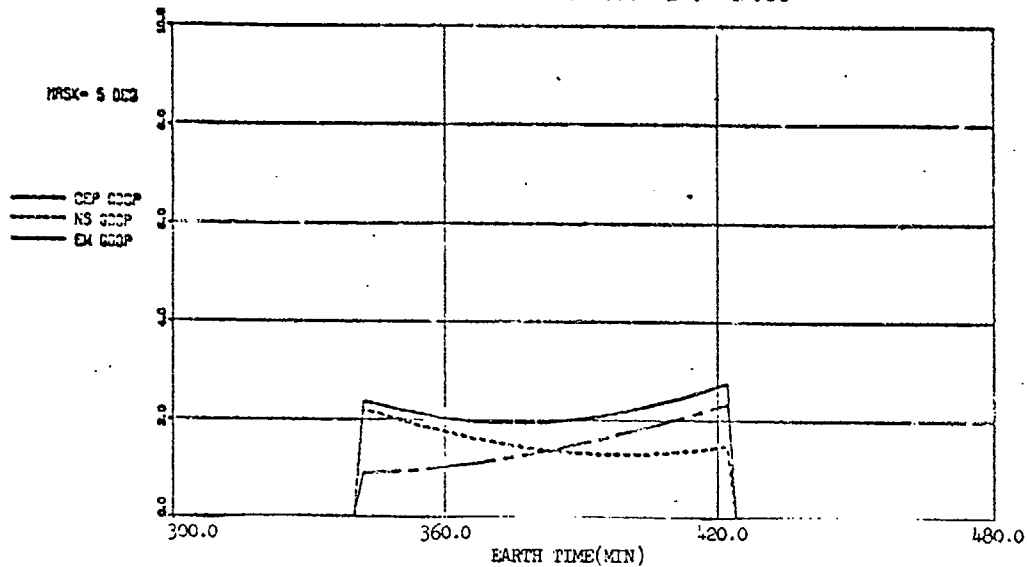


SAT	LAN	AOP	E	INC	TA(MIN)	H(MIN)
1	210.0	0.0	.00	63.4	420.0	720.0
2	210.0	0.0	.00	63.4	340.0	720.0
3	210.0	0.0	.00	63.4	310.0	720.0
4	210.0	0.0	.00	63.4	570.0	720.0

(1/1/0 Constellation)

Figure A-6. GDOF for Conus Center

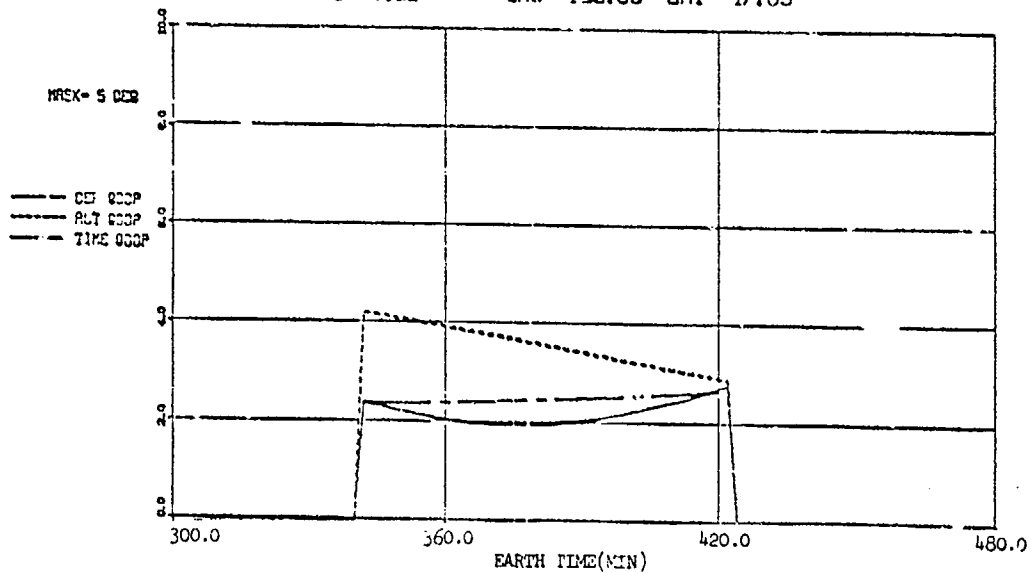
SEATTLE LNG--122.35 LAT- 47.63



SAT	LAN	AOP	E	INC	TA(MIN)	P(MIN)
1	230.0	0.0	.00	63.4	480.0	720.0
2	230.0	0.0	.00	63.4	540.0	720.0
3	350.0	0.0	.00	63.4	330.0	720.0
4	230.0	0.0	.00	63.4	650.0	720.0

(3/1/0 Constellation)

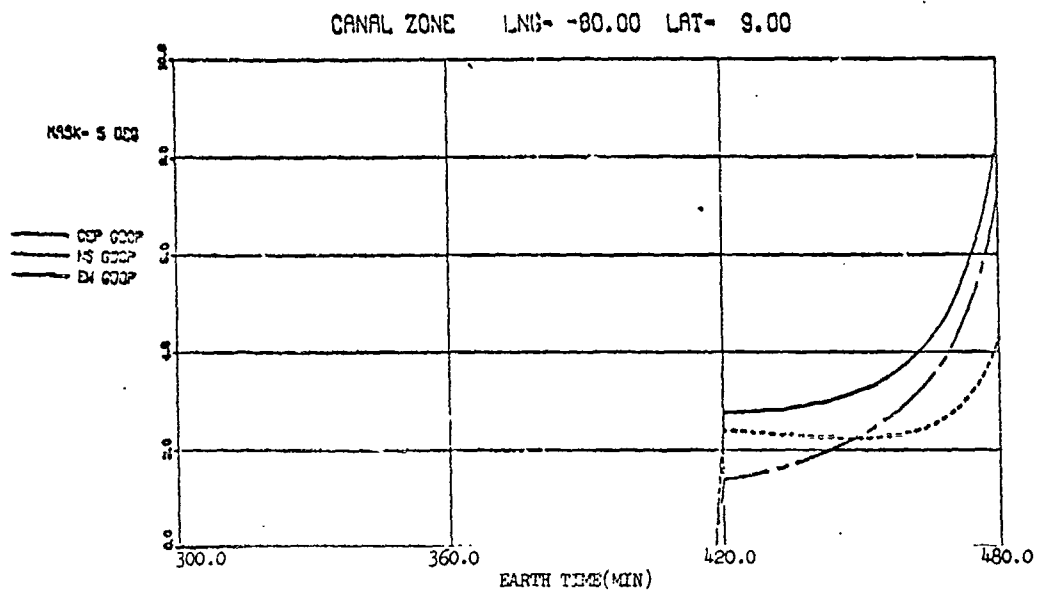
SEATTLE LNG--122.35 LAT- 47.63



SAT	LAN	AOP	E	INC	TA(MIN)	P(MIN)
1	230.0	0.0	.00	63.4	480.0	720.0
2	230.0	0.0	.00	63.4	540.0	720.0
3	350.0	0.0	.00	63.4	330.0	720.0
4	230.0	0.0	.00	63.4	650.0	720.0

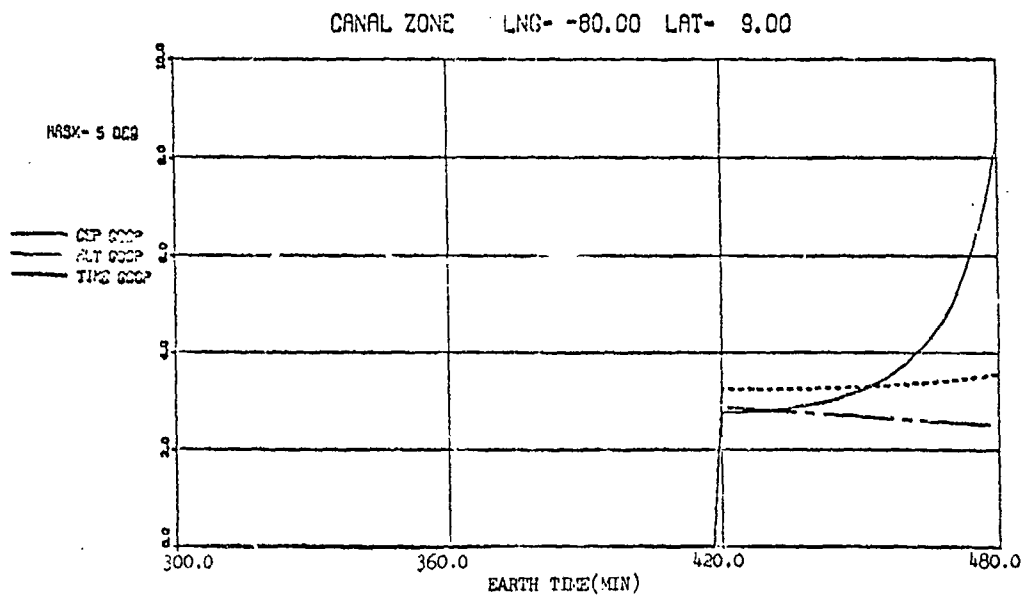
(3/1/0 Constellation)

Figure A-7. GDOP for Seattle



SAT	LAN	AOP	E	INC	TA(MIN)	P(MIN)
1	230.0	0.0	.00	63.4	480.0	720.0
2	230.0	0.0	.00	63.4	540.0	720.0
3	350.0	0.0	.00	63.4	330.0	720.0
4	230.0	0.0	.00	63.4	650.0	720.0

(3/1/0 Constellation)



SAT	LAN	AOP	E	INC	TA(MIN)	P(MIN)
1	230.0	0.0	.00	63.4	480.0	720.0
2	230.0	0.0	.00	63.4	540.0	720.0
3	350.0	0.0	.00	63.4	330.0	720.0
4	230.0	0.0	.00	63.4	650.0	720.0

(3/1/0 Constellation)

Figure A-8. GDOP for Canal Zone

APPENDIX B

General Dynamics

2/2/0 CONSTELLATION DATA

<u>Figure</u>		<u>Page</u>
B-1	Satellite Coverage Vs Tracking Stations .....	B-2
B-2	Tracking Stations Coverage Vs Satellites .....	B-3
B-3	GDOP for Holloman AFB .....	B-4
B-4	GDOP for Vandenberg AFB .....	B-5
B-5	GDOP for Conus Center .....	B-6
B-6	GDOP for Pease .....	B-7
B-7	GDOP for Cape Kennedy .....	B-8
B-8	GDOP for Canal Zone .....	B-9

TO BE SUPPLIED LATER

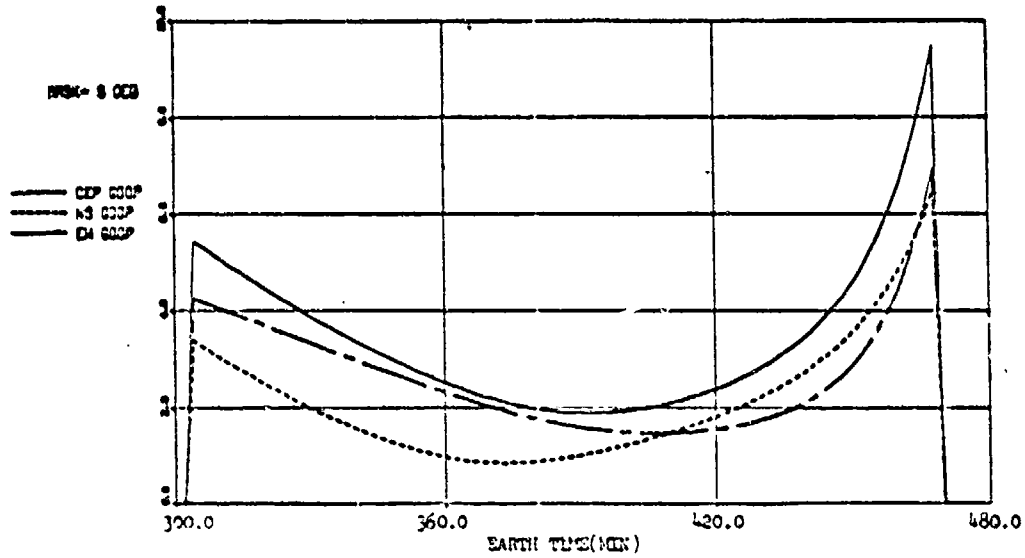
Figure B-1. Satellite Coverage Vs Tracking Stations

TO BE SUPPLIED LATER

Figure B-2. Tracking Stations Coverage Vs Satellites



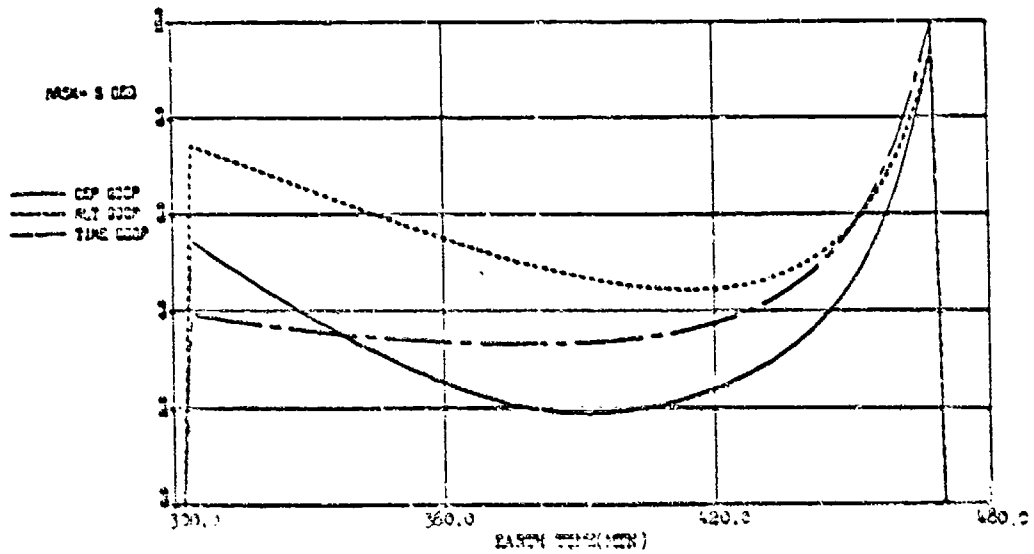
HOLLOMAN LNG--106.00 LAT- 32.88



SAT	LAT	AOP	E	INC	TA(MIN)	P(MIN)
1	237.0	0.0	.00	63.4	480.0	720.0
2	237.0	0.0	.00	63.4	360.0	720.0
3	350.0	0.0	.00	63.4	330.0	720.0
4	350.0	0.0	.00	63.4	470.0	720.0

(2/2/0 Constellation)

HOLLOMAN LNG--106.00 LAT- 32.88

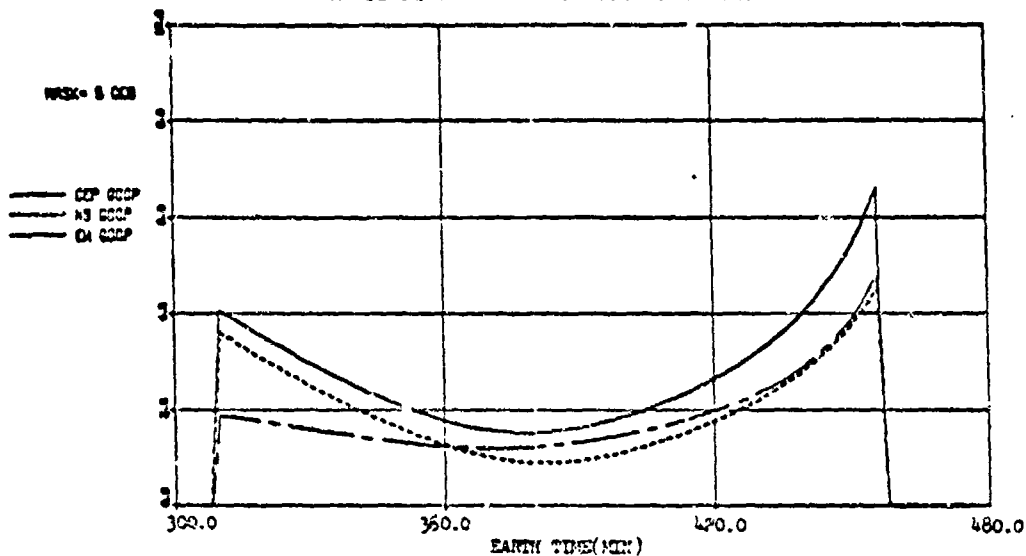


SAT	LAT	AOP	E	INC	TA(MIN)	P(MIN)
1	237.0	0.0	.00	63.4	480.0	720.0
2	237.0	0.0	.00	63.4	360.0	720.0
3	350.0	0.0	.00	63.4	330.0	720.0
4	350.0	0.0	.00	63.4	470.0	720.0

(2/2/0 Constellation)

Figure B-3. GDCP for Holloman AFB

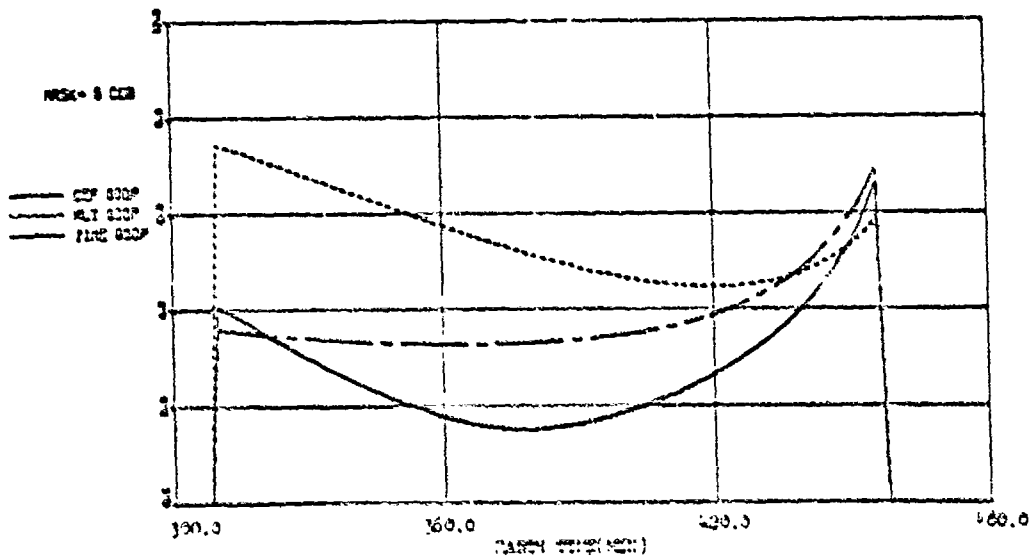
VANDENBERG LNG--120.50 LAT- 34.82



SAT	LAT	AOP	Z	INC	TA(MIN)	P(MIN)
1	230.0	0.0	.00	63.4	450.0	720.0
2	230.0	0.0	.00	63.4	560.0	720.0
3	350.0	0.0	.00	63.4	330.0	720.0
4	350.0	0.0	.00	63.4	470.0	720.0

(2/2/0 Constellation)

VANDENBERG LNG--120.50 LAT- 34.82



SAT	LAT	AOP	Z	INC	TA(MIN)	P(MIN)
1	230.0	0.0	.00	63.4	450.0	720.0
2	230.0	0.0	.00	63.4	560.0	720.0
3	350.0	0.0	.00	63.4	330.0	720.0
4	350.0	0.0	.00	63.4	470.0	720.0

(2/2/0 Constellation)

Figure B-4. GDP for Vandenberg AFB

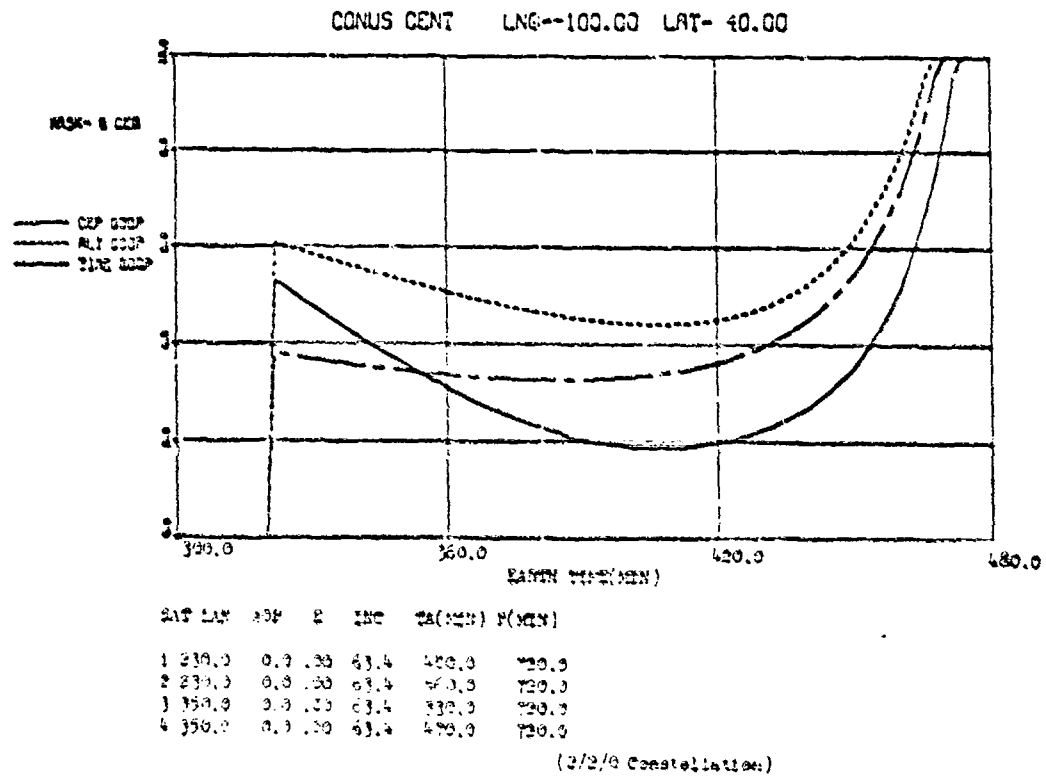
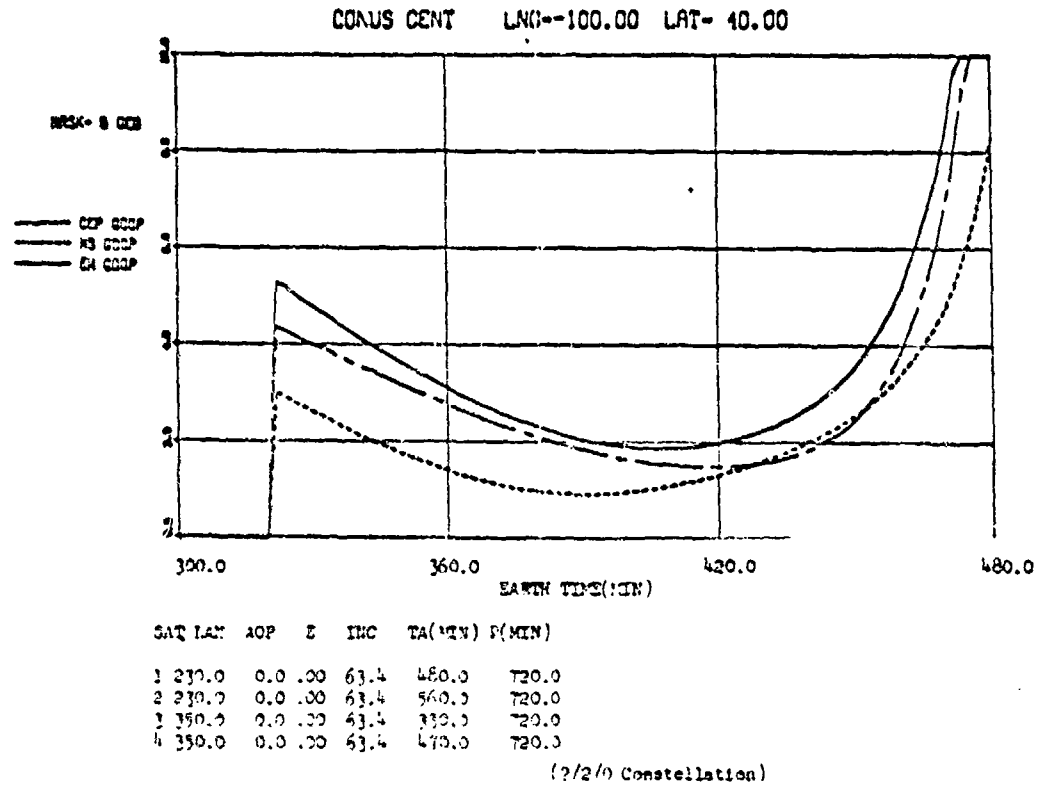
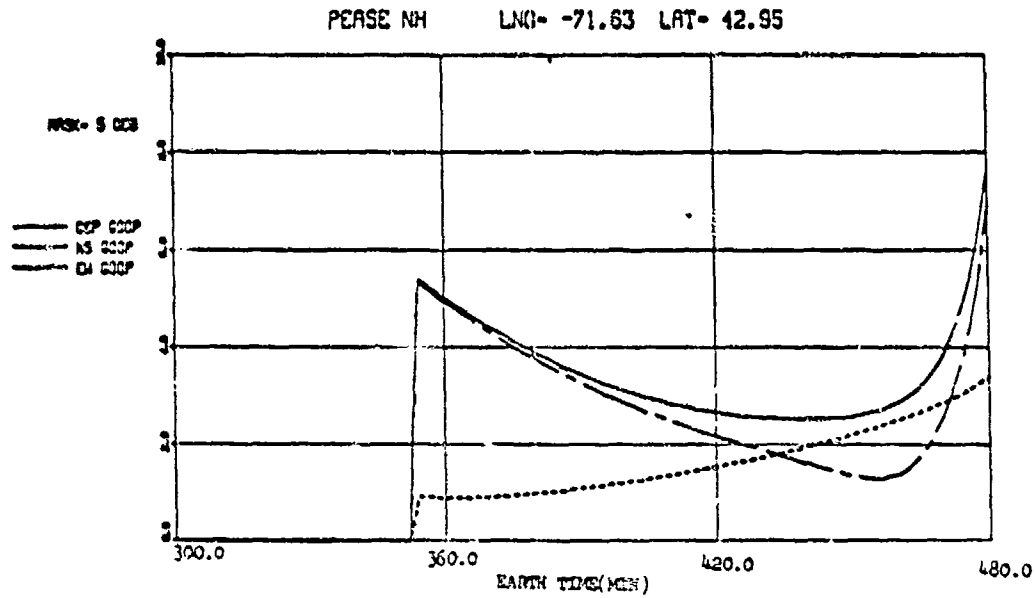
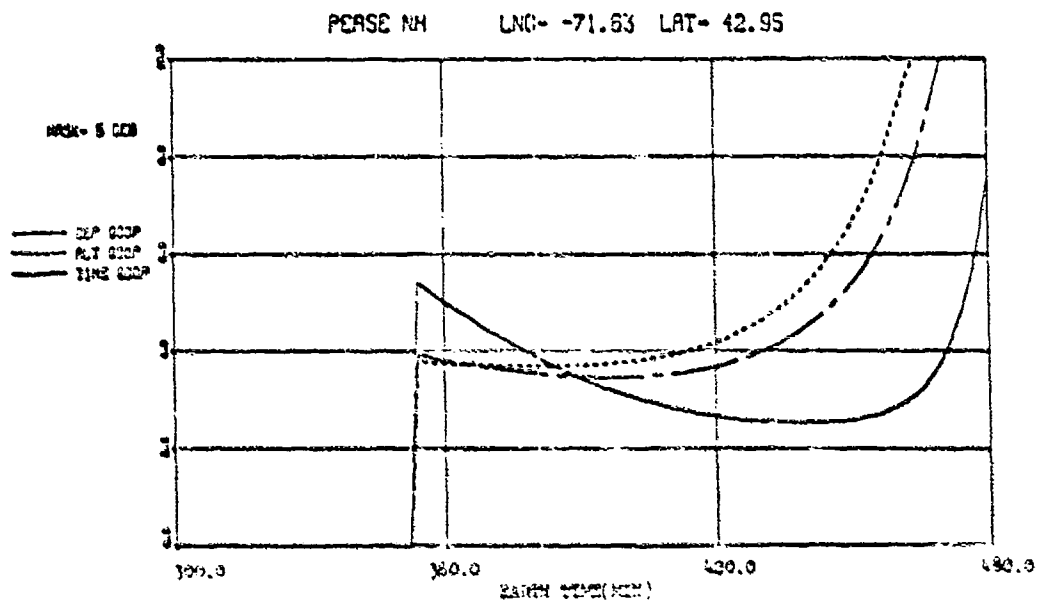


Figure B-5. GDOP for Conus Center



SAT	LAT	AOP	E	INC	TA(MIN)	TA(MIN)
1	230.0	0.0	100	63.4	480.0	720.0
2	230.0	0.0	100	63.4	480.0	720.0
3	350.0	0.0	100	63.4	360.0	720.0
4	350.0	0.0	100	63.4	470.0	720.0

(2/2/0 Constellation)



SAT	LAT	AOP	E	INC	TA(MIN)	TA(MIN)
1	230.0	0.0	100	63.4	480.0	720.0
2	230.0	0.0	100	63.4	480.0	720.0
3	350.0	0.0	100	63.4	360.0	720.0
4	350.0	0.0	100	63.4	470.0	720.0

(2/2/3 Constellation)

Figure B-6. GDOP for Pease

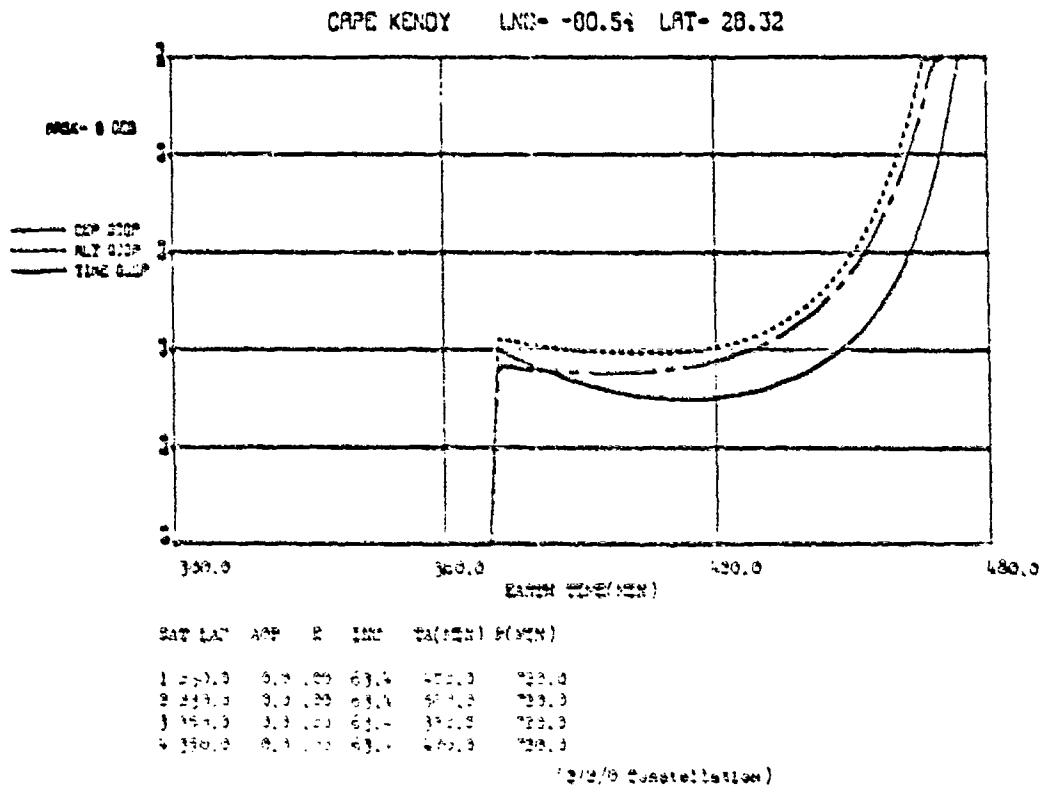
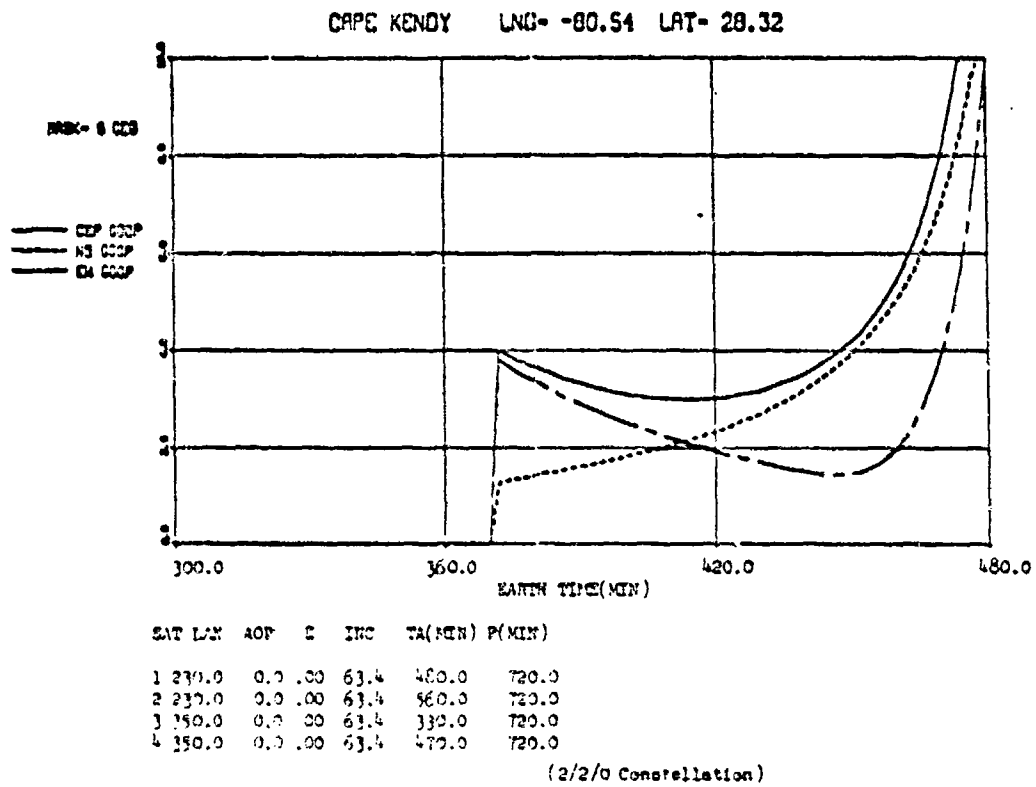
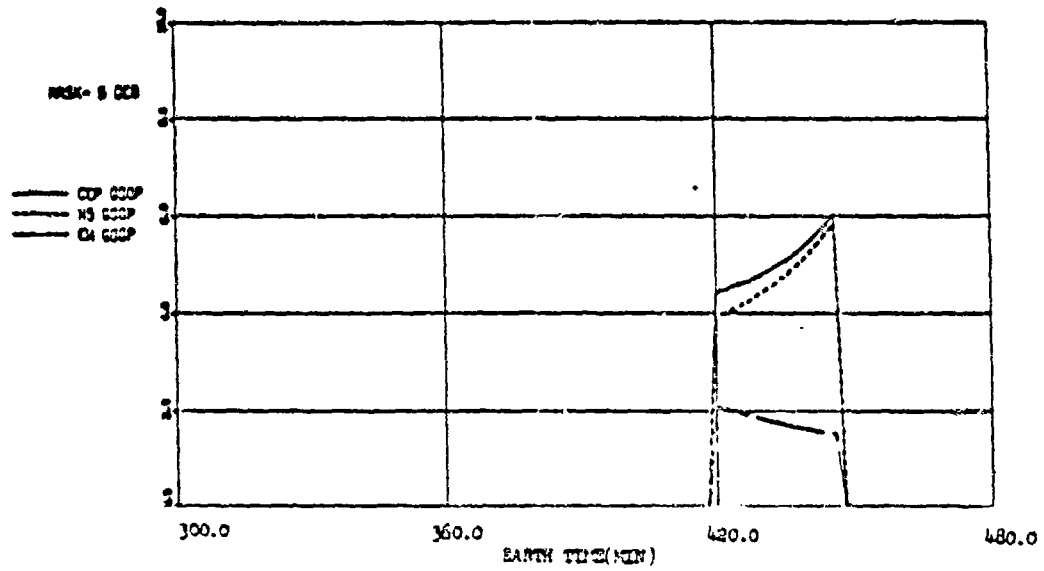


Figure B-7. GDOP for Cape Kennedy

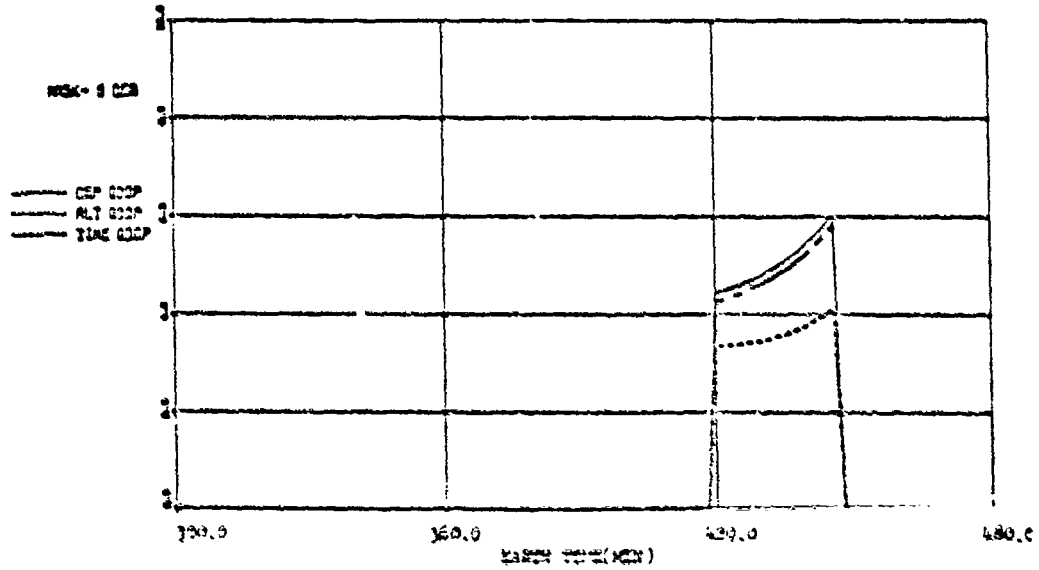
CANAL ZONE LNG- -80.00 LAT- 9.00



SAT	LAT	AOP	E	INC	TA(MIN)	P(MIN)
1	230.0	0.0	.00	63.4	460.0	720.0
2	230.0	0.0	.00	63.4	540.0	720.0
3	350.0	0.0	.00	63.4	330.0	720.0
4	350.0	0.0	.00	63.4	470.0	720.0

(2/2/0 Constellation)

CANAL ZONE LNG- -80.00 LAT- 9.00



SAT	LAT	AOP	E	INC	TA(MIN)	P(MIN)
1	230.0	0.0	.00	63.4	460.0	720.0
2	230.0	0.0	.00	63.4	540.0	720.0
3	350.0	0.0	.00	63.4	330.0	720.0
4	350.0	0.0	.00	63.4	470.0	720.0

(2/2/3 Constellation)

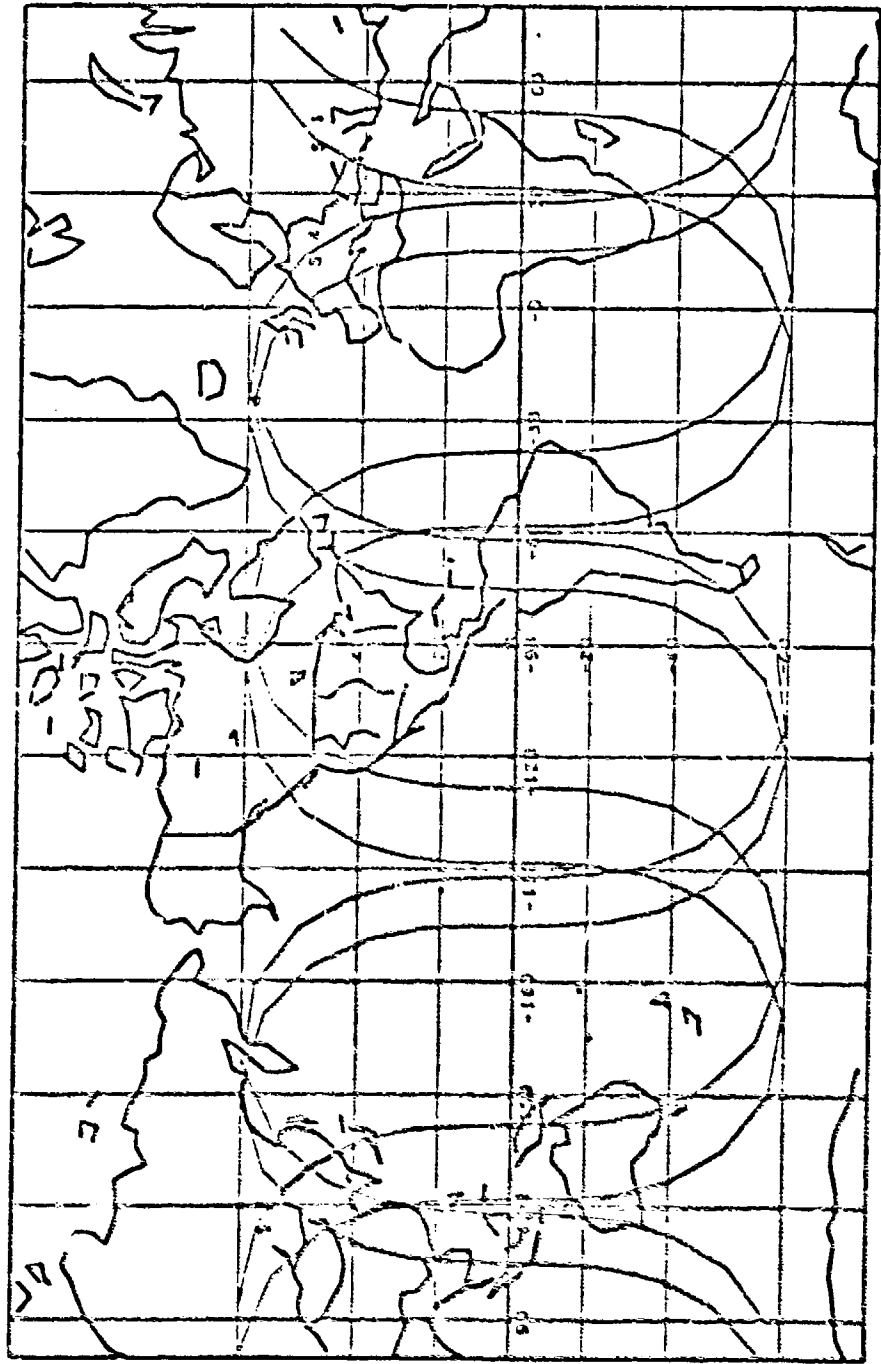
Figure B-8. GDOP for Canal Zone

APPENDIX C

Aerospace Preliminary

2/2/0 CONSTELLATION DATA

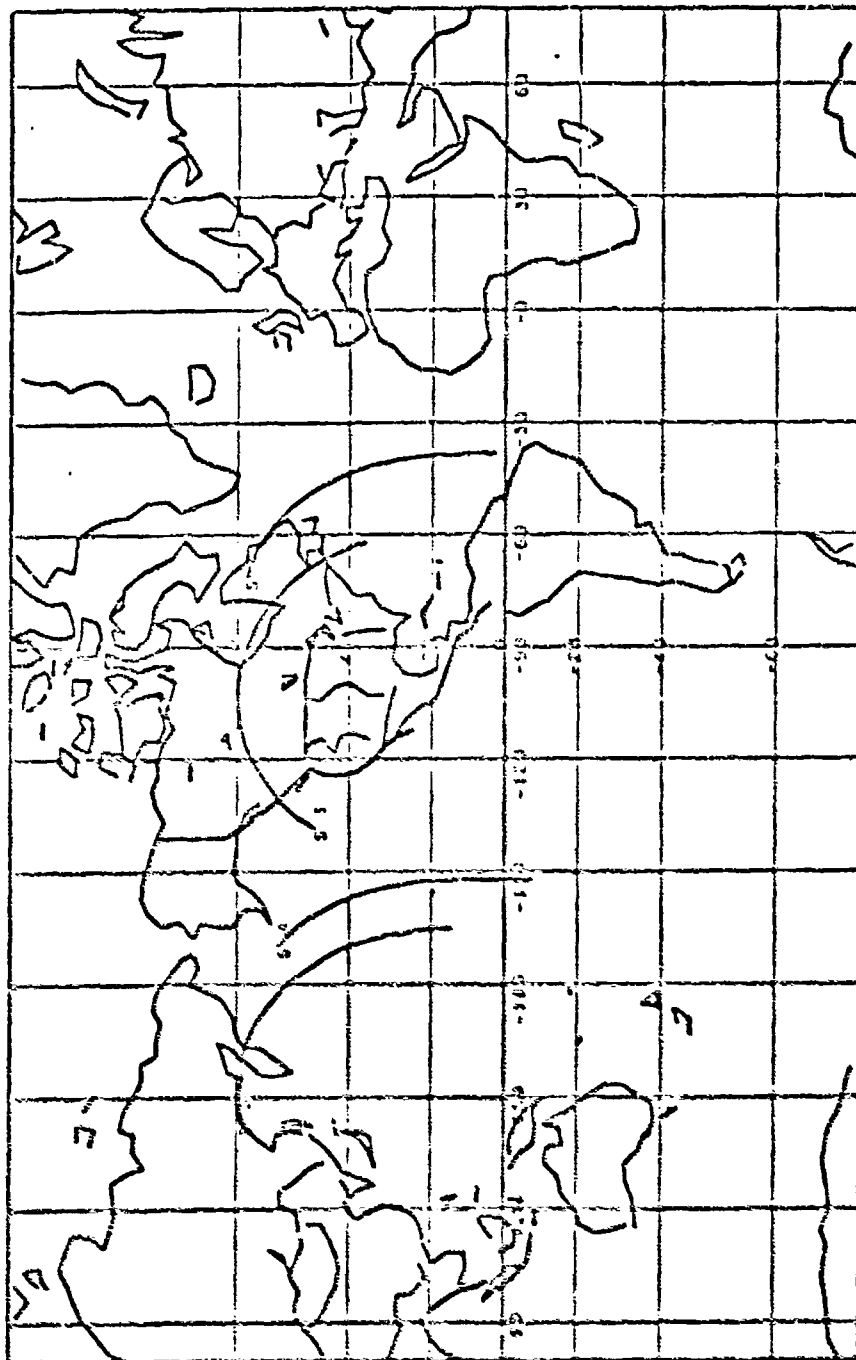
<u>Figure</u>		<u>Page</u>
C-1	Earth Traces . . . . .	C-2
C-2	Satellite Covisibility Earth Traces . . . . .	C-3
C-3	GPS Stations Coverage by Station . . . . .	C-4
C-4	GPS Stations Coverage by Satellite . . . . .	C-5
C-5	SCF Stations Coverage by Station . . . . .	C-6
C-6	SCF Stations Coverage by Satellite . . . . .	C-7
C-7	GDOP for Holloman AFB . . . . .	C-8
C-8	GDOP for Holloman AFB . . . . .	C-9
C-9	GDOP for Pt. Mugu . . . . .	C-10
C-10	GDOP for Pt. Mugu . . . . .	C-11
C-11	GDOP for Elmendorf . . . . .	C-12
C-12	GDOP for Elmendorf . . . . .	C-13
C-13	GDOP for Wahiawa . . . . .	C-14
C-14	GDOP for Wahiawa . . . . .	C-15
C-15	GDOP for Wahiawa . . . . .	C-16
C-16	GDOP for Prospect Harbor . . . . .	C-17
C-17	GDOP for Prospect Harbor . . . . .	C-18
C-18	GDOP for Conus Center . . . . .	C-19



0 DAYS GFSDF - 12 HOUR ORBITS - 2/2/70 AEROSPACE CONFIS MERCATOR

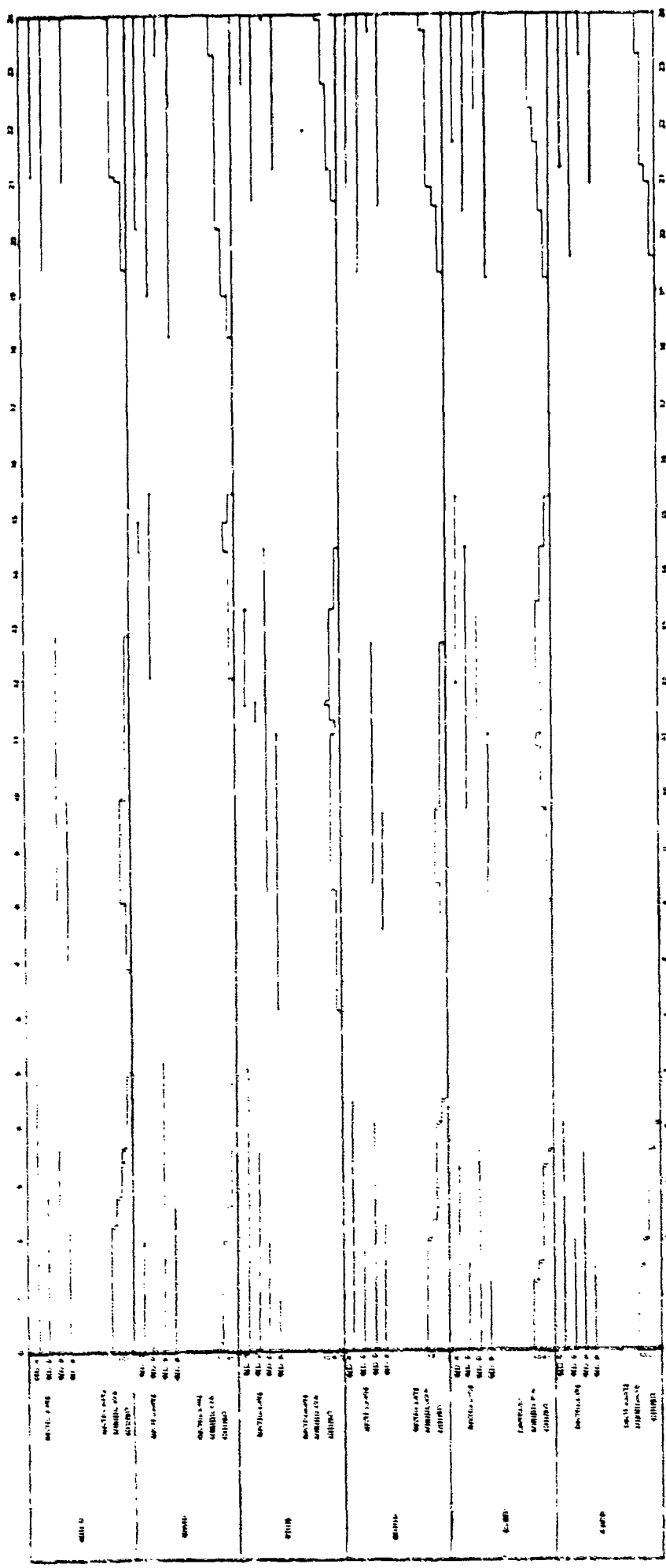
Figure C-1. Earth Traces





9 DAYS SPSEF - 12 HOUR ORBITS - 2/2/70 AEROSPACE CONFIGURATOR

Figure C-2. Satellite Covisibility Earth Traces



STATION IDENTIFICATION OF GPS STATIONS IN AREA  
 APPROXIMATE LONGITUDE AND LATITUDE COORDINATES

Figure C-3. GPS Stations Coverage by Station

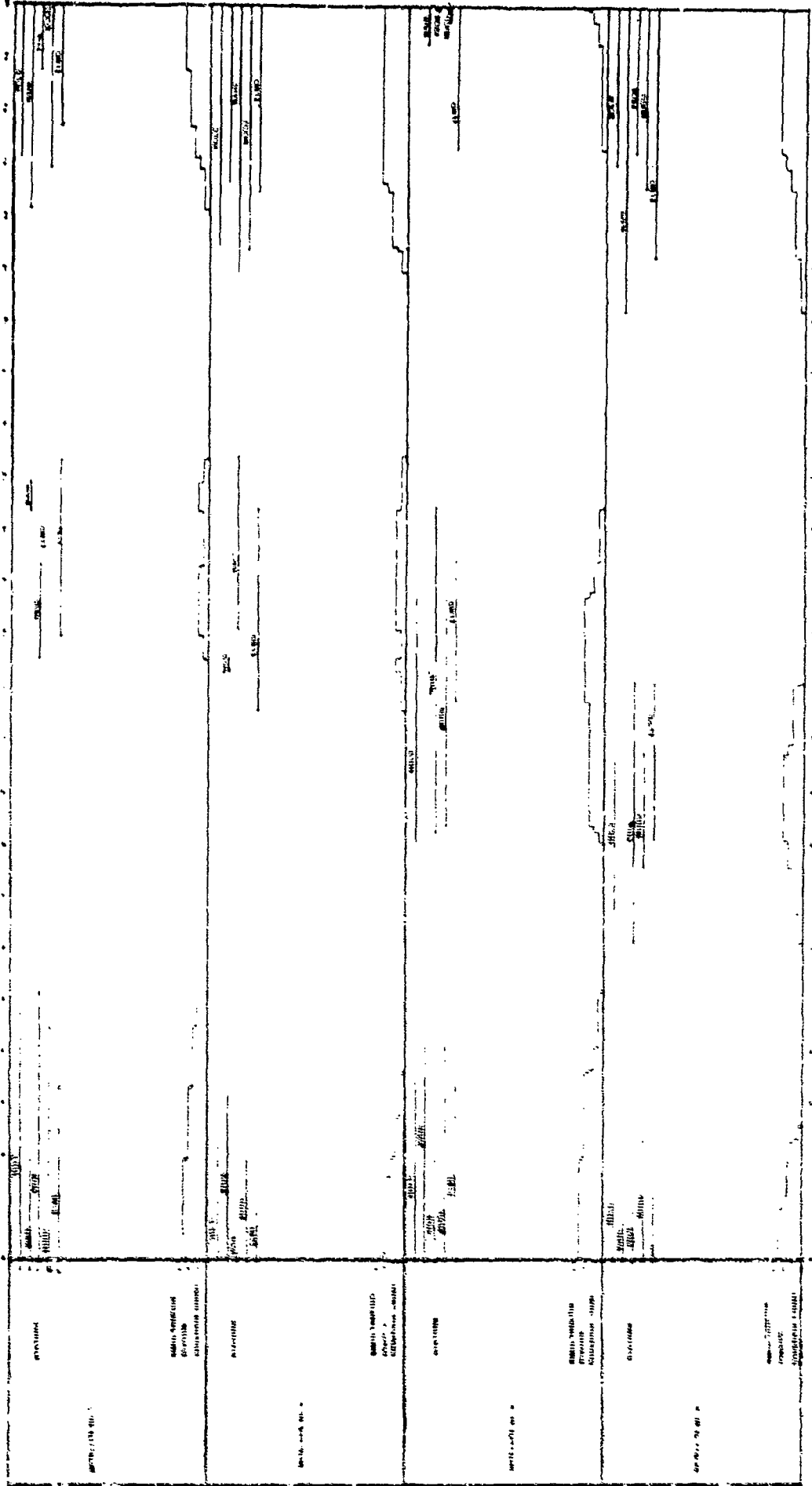


Figure C-4. GPS Stations Coverage by Satellite

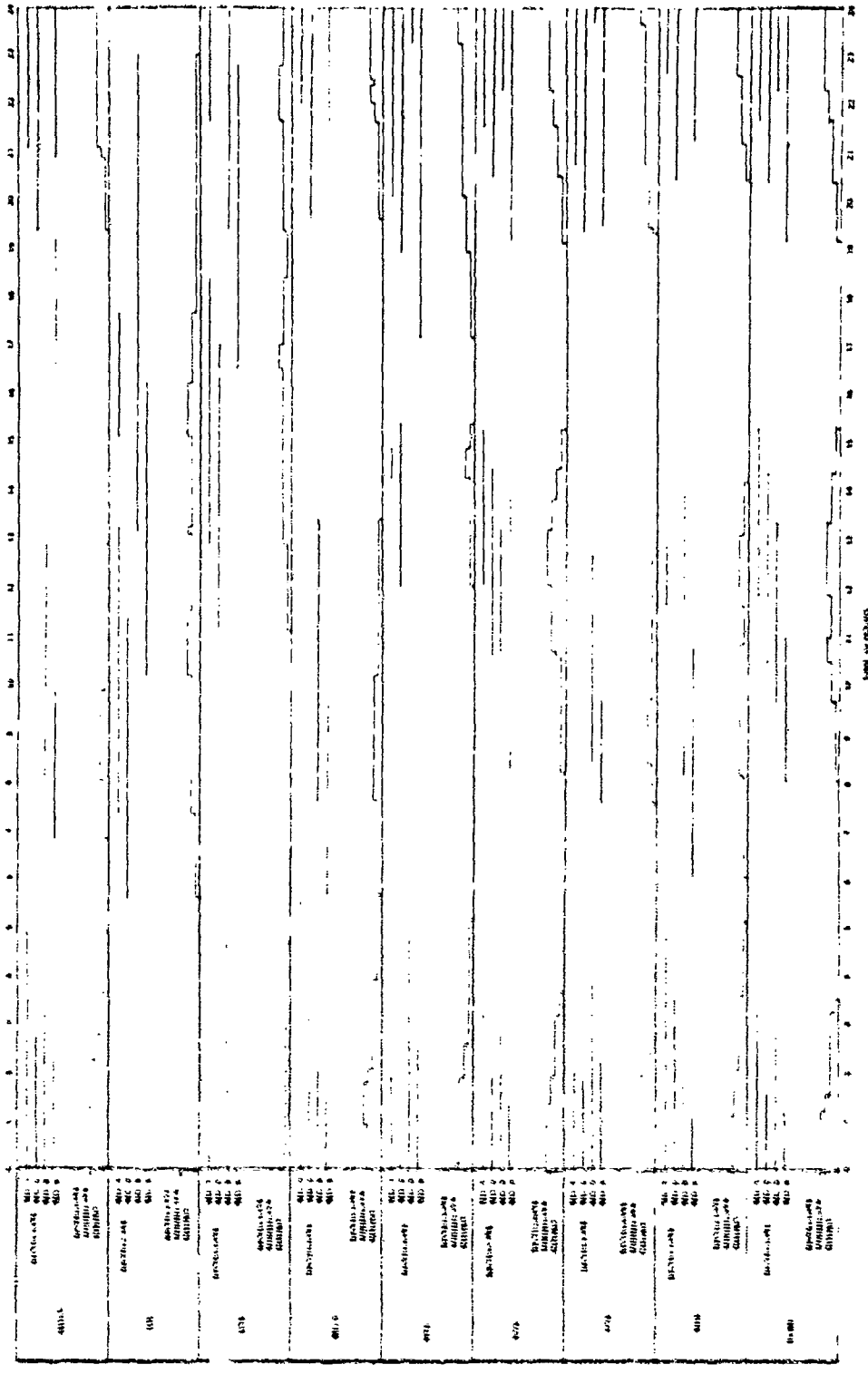


Figure C-5. SCF Stations Coverage by Station

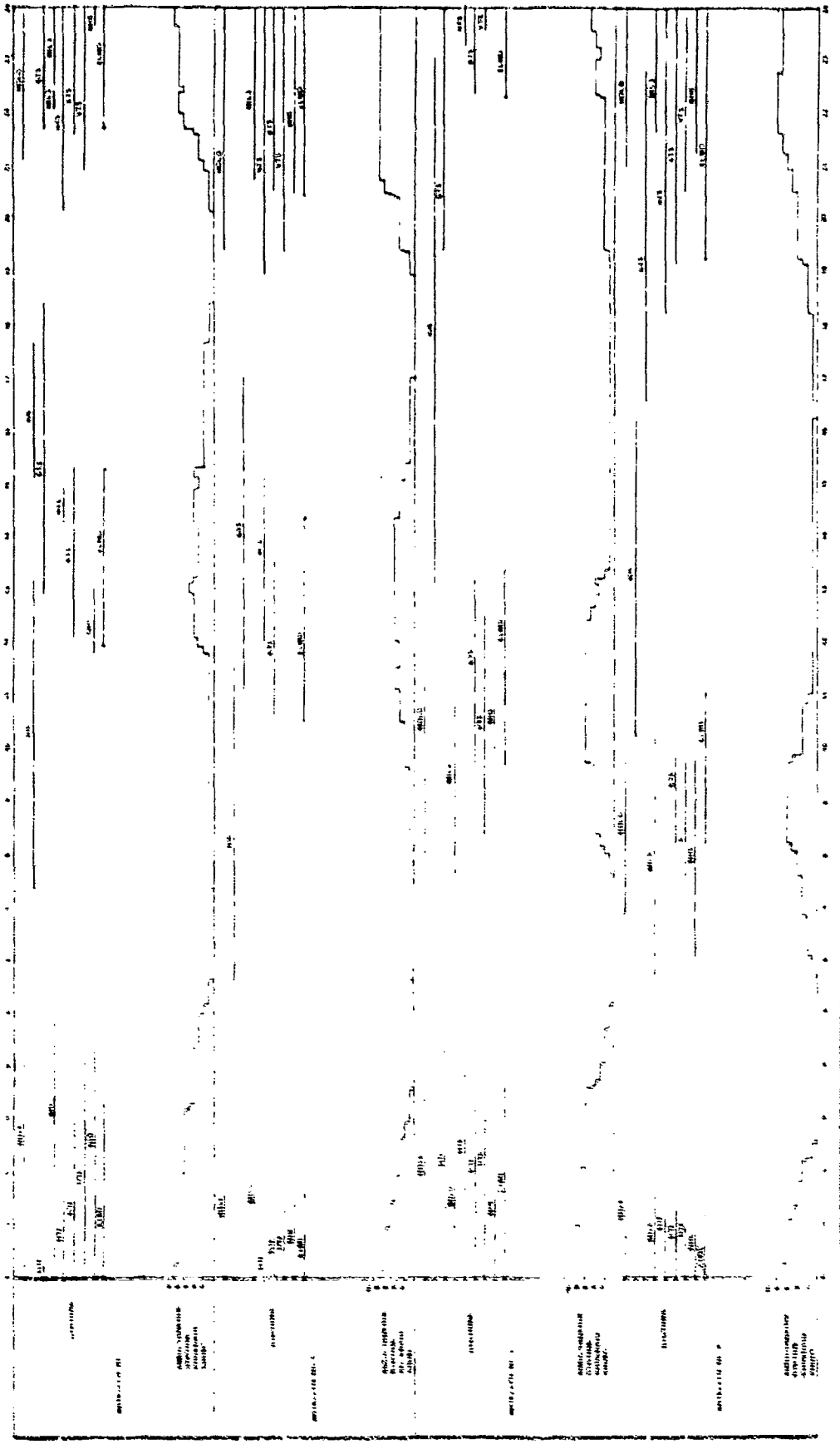
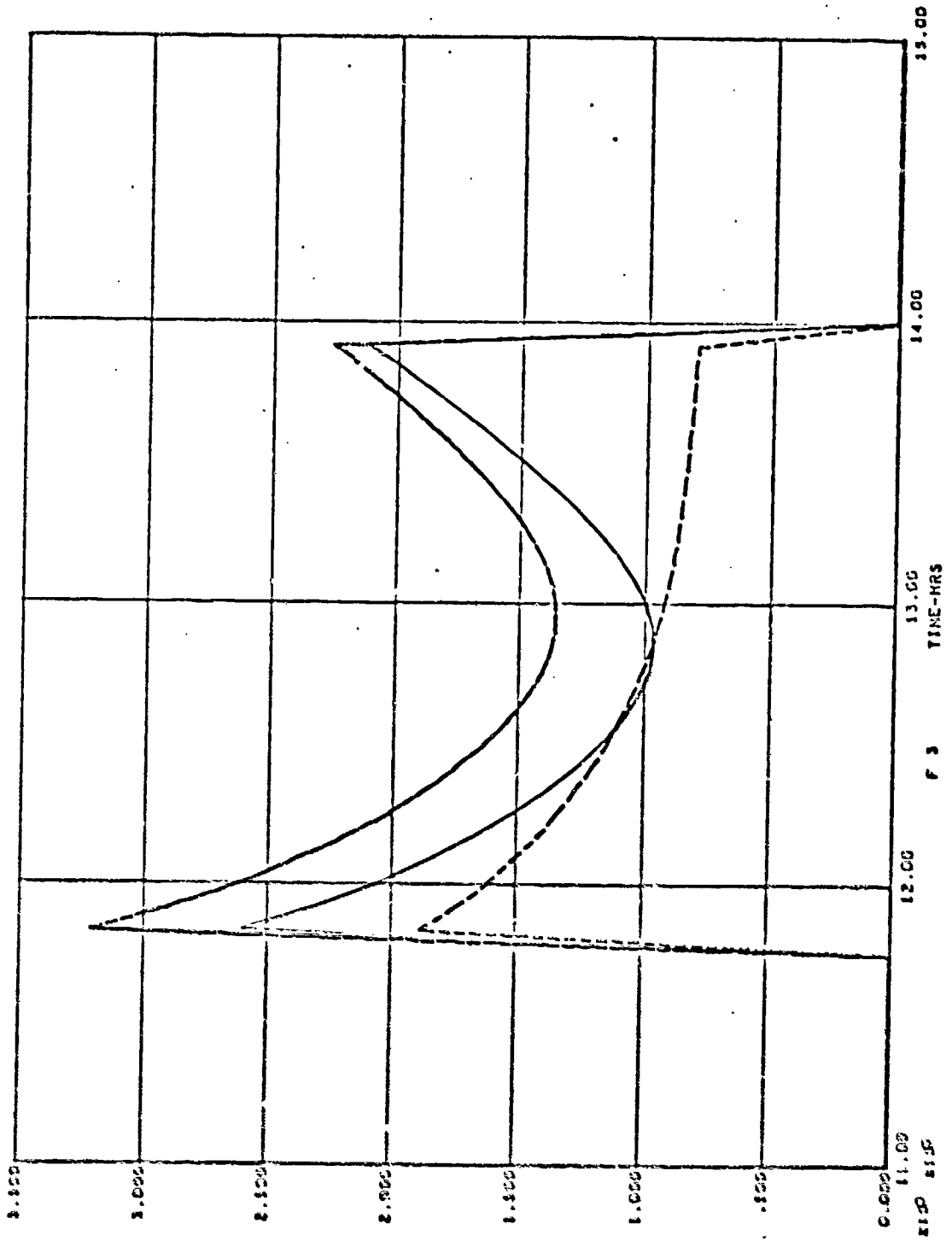


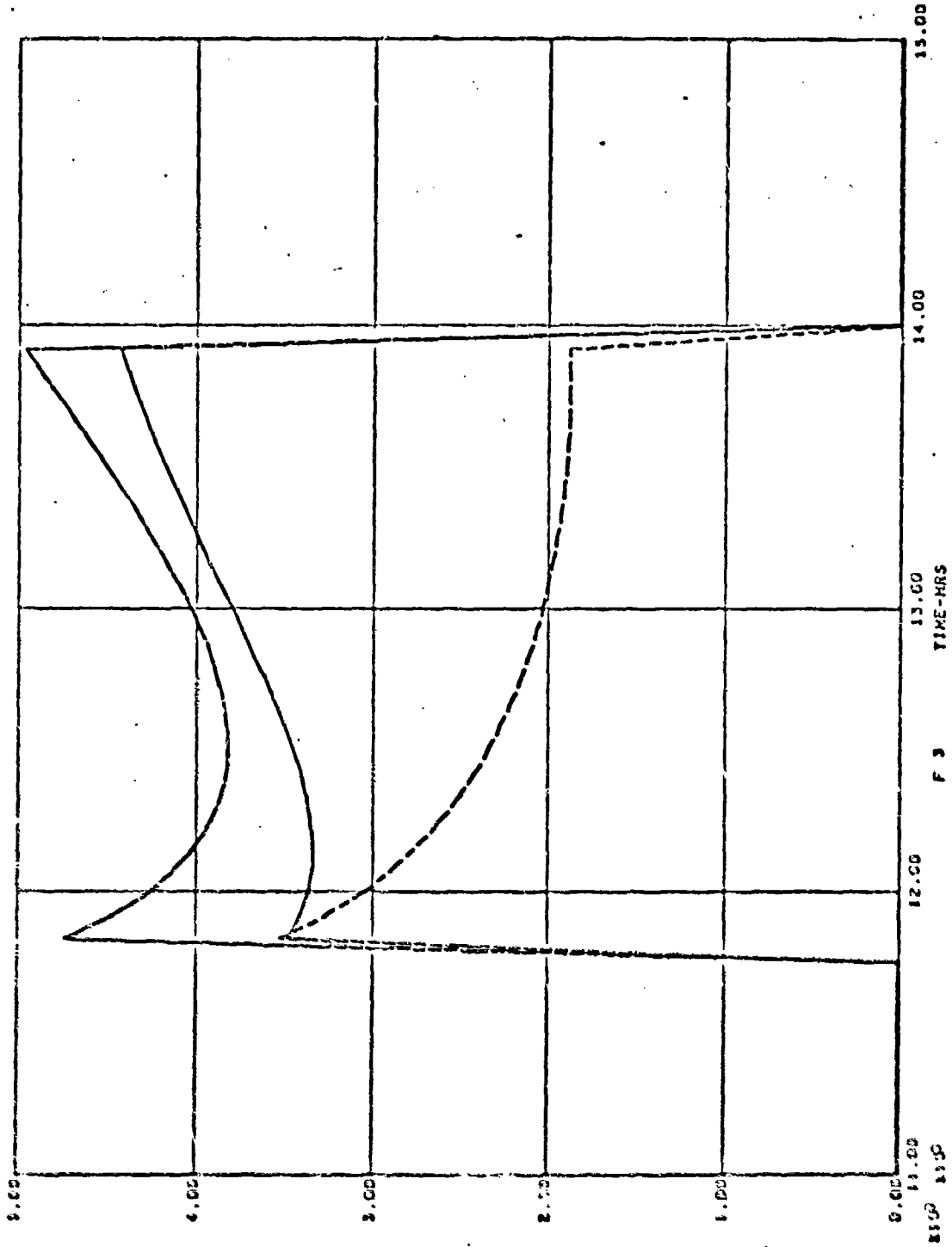
Figure C-6. SCF Stations Coverage by Satellite



FILE 3 0 DAYS GPSPD - AEROSPACE 2/2/0 CONFIGURATION

Figure C-7. GDOP for Holloman AFB

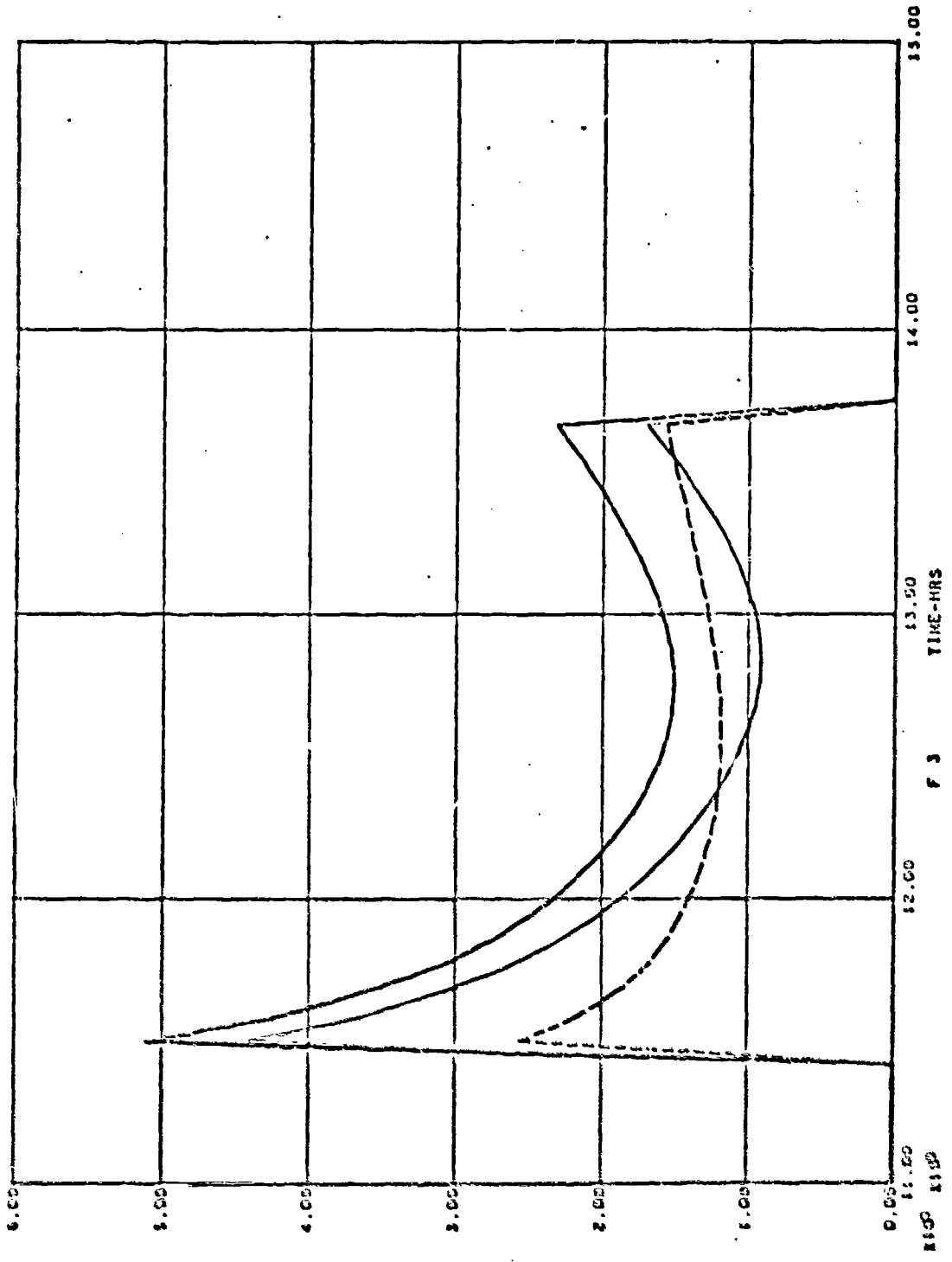
F F 3 | | | | | C 130 0000 MOJJOX4 H  
 F F 3 | | | | | C 17 0000 MOJJOX4 H  
 F F 3 | | | | | C 17A 0000 MOJJOX4 H



F 3 ———— 4.5 0002 NOJJOR4H  
 F 3 ———— 4.5 0002 NOJJOR4H  
 F 3 ———— 4.5 0002 NOJJOR4H

FILE 3 0 DAYS GPSP - AEROSPACE 2/2/0 CONFIGURATION

Figure C-8. GDOP for Holloman AFB



0 2 3 1000 POINT 1000  
 0 2 3 2000 POINT 2000  
 0 2 3 3000 POINT 3000

FILE 3 0 DAYS GPSP - AEROSPACE 2/2/0 CONFIGURATION

Figure C-9. GDOP for Pt. Mugu



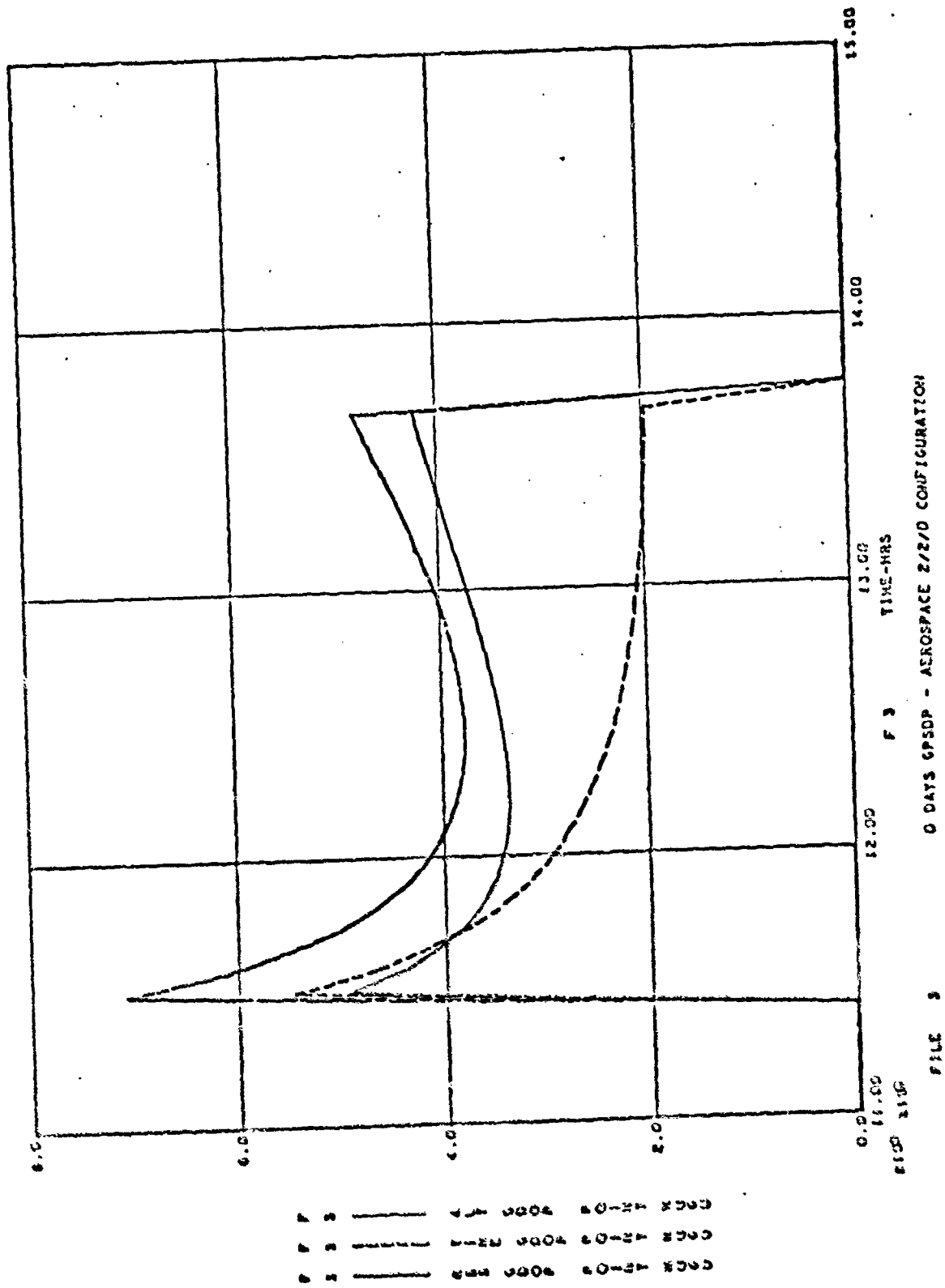
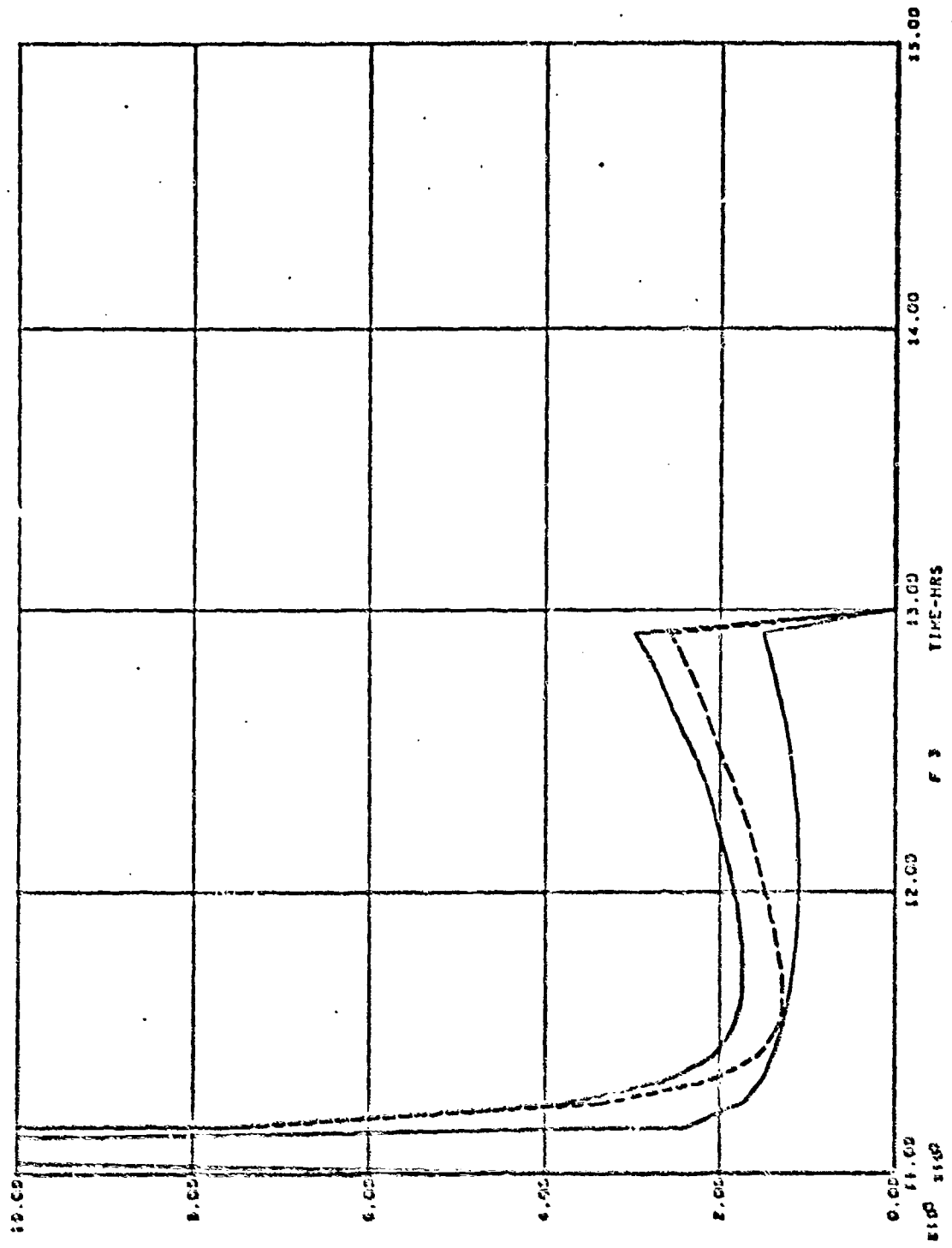


Figure C-10. GDP for Pt. Mugu



0000 0000  
 0000 0000  
 0000 0000

FILE 5 0 DAYS GPSP - AEROSPACE 2/2/0 CONFIGURATION

Figure C-11. GDOP for Elmdorf

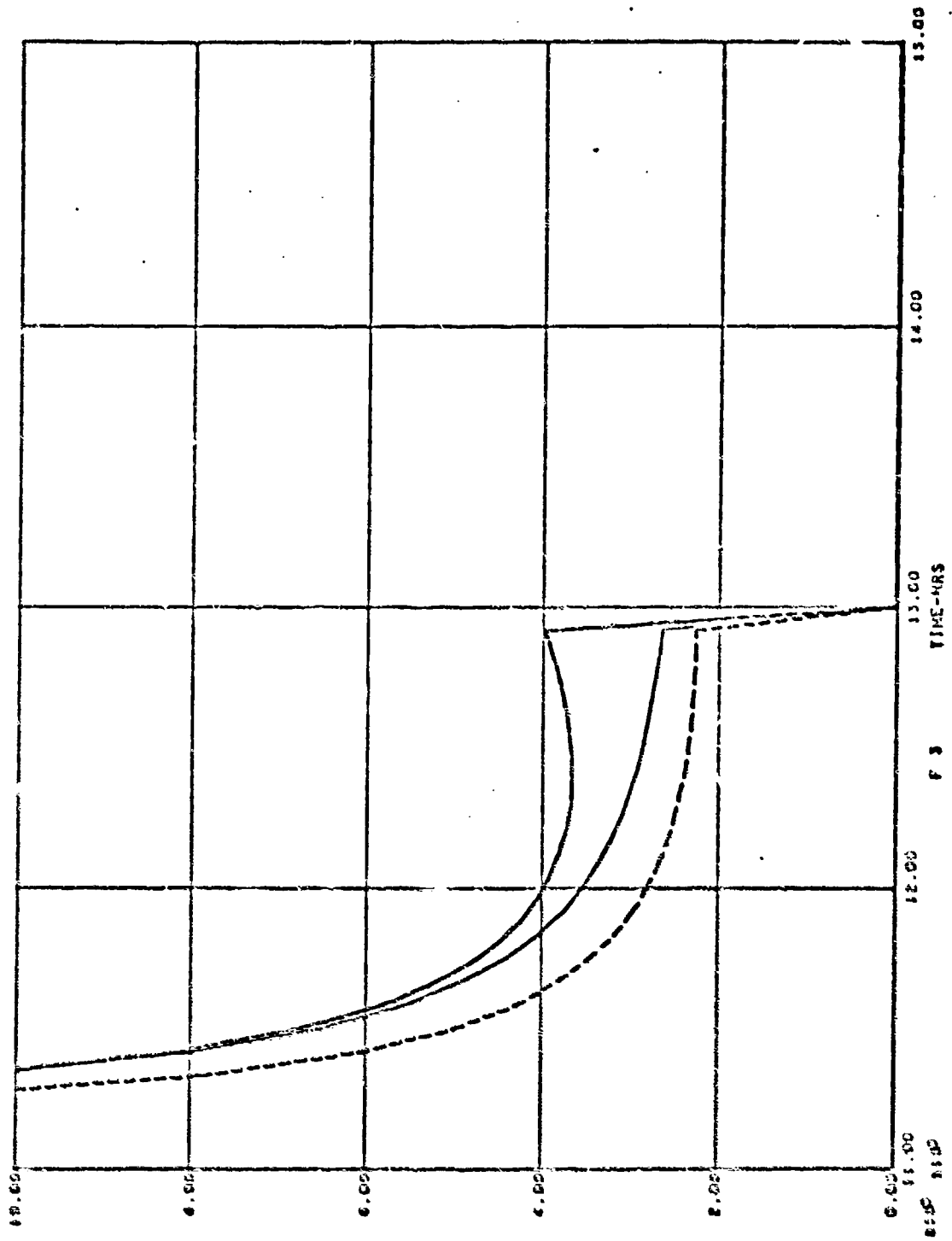
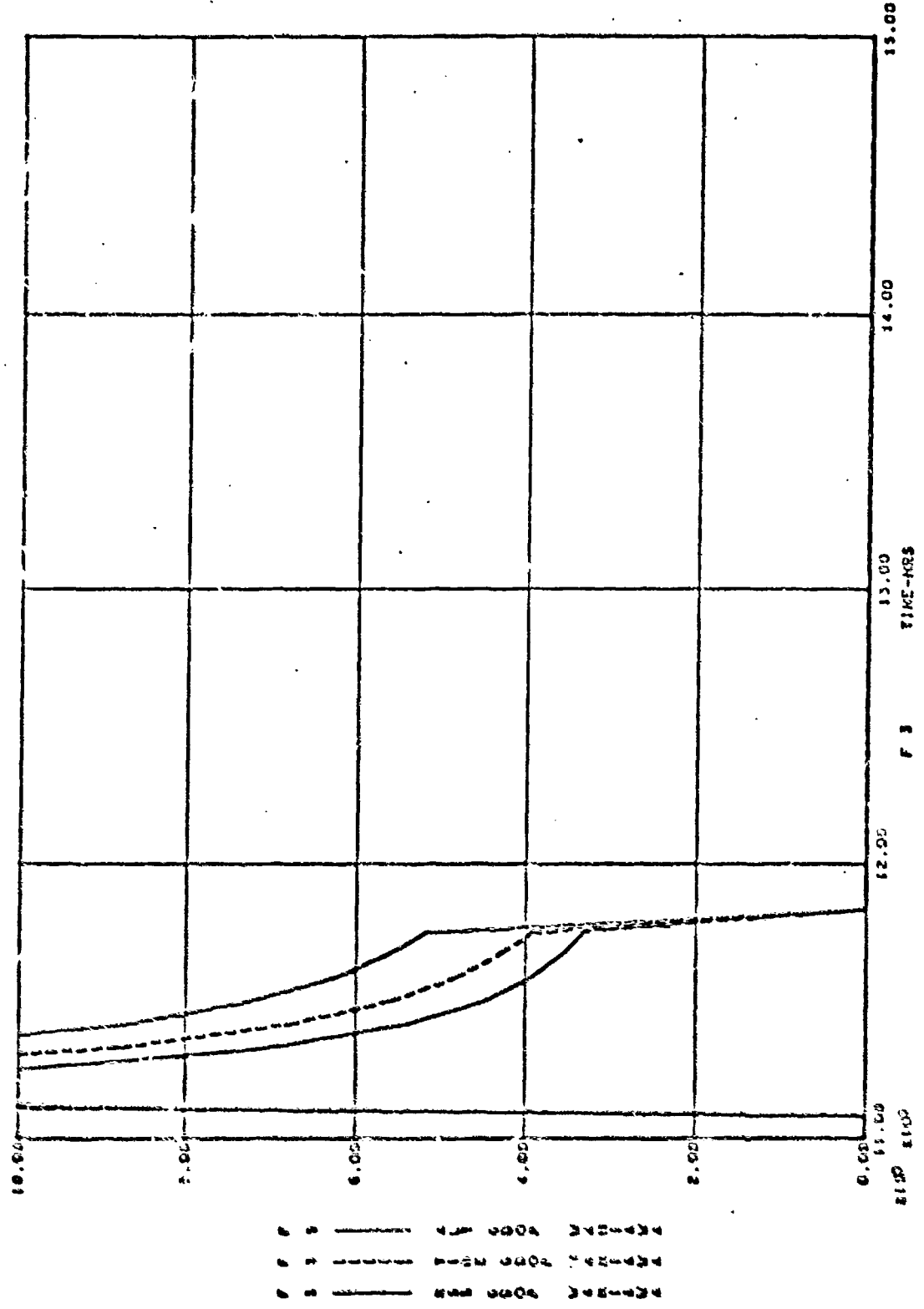


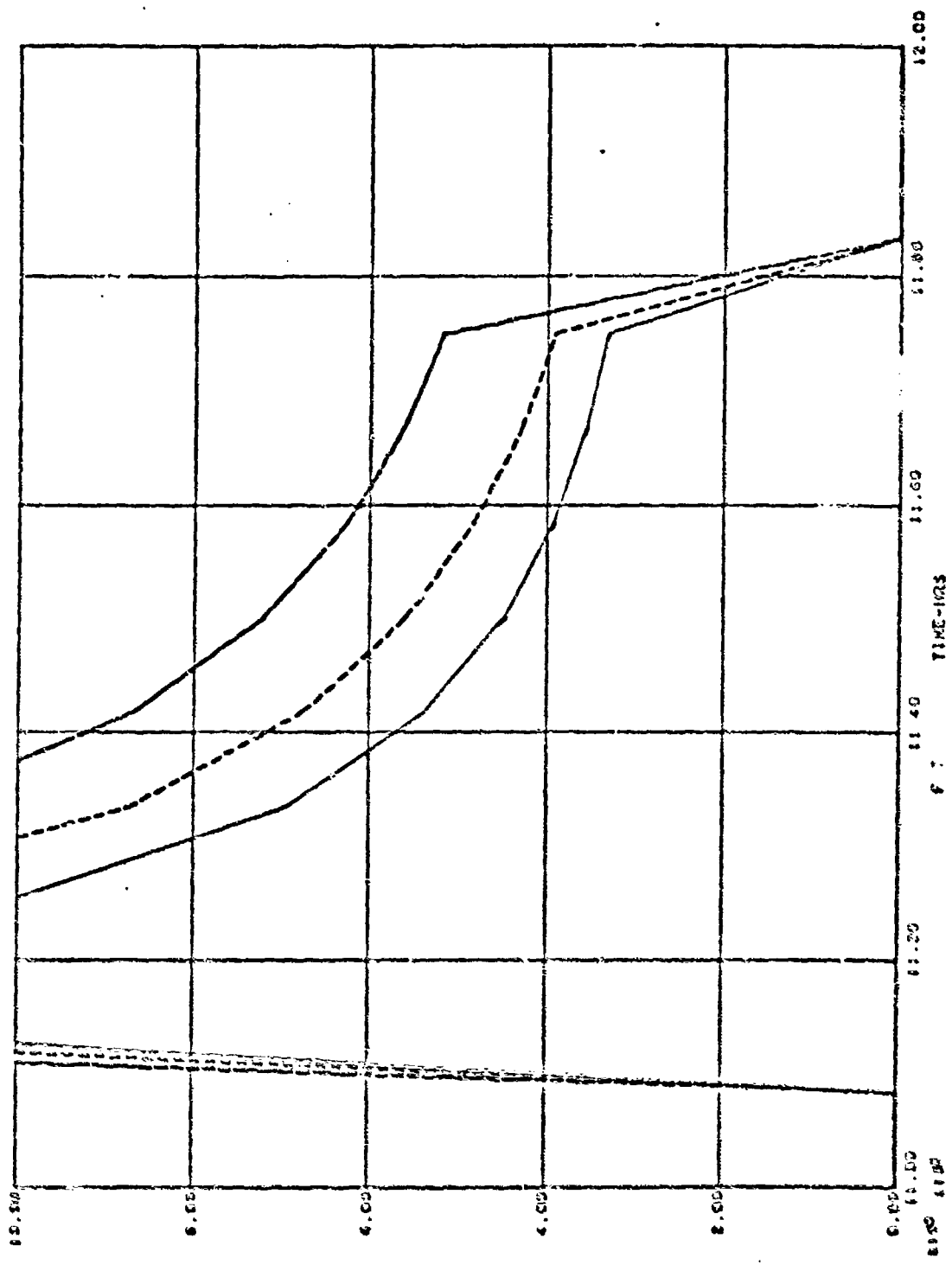
FIGURE 3 G DAYS GPSP - AEROSPACE 2/2/0 CONFIGURATION

Figure C-12. GDOP for Elmendorf

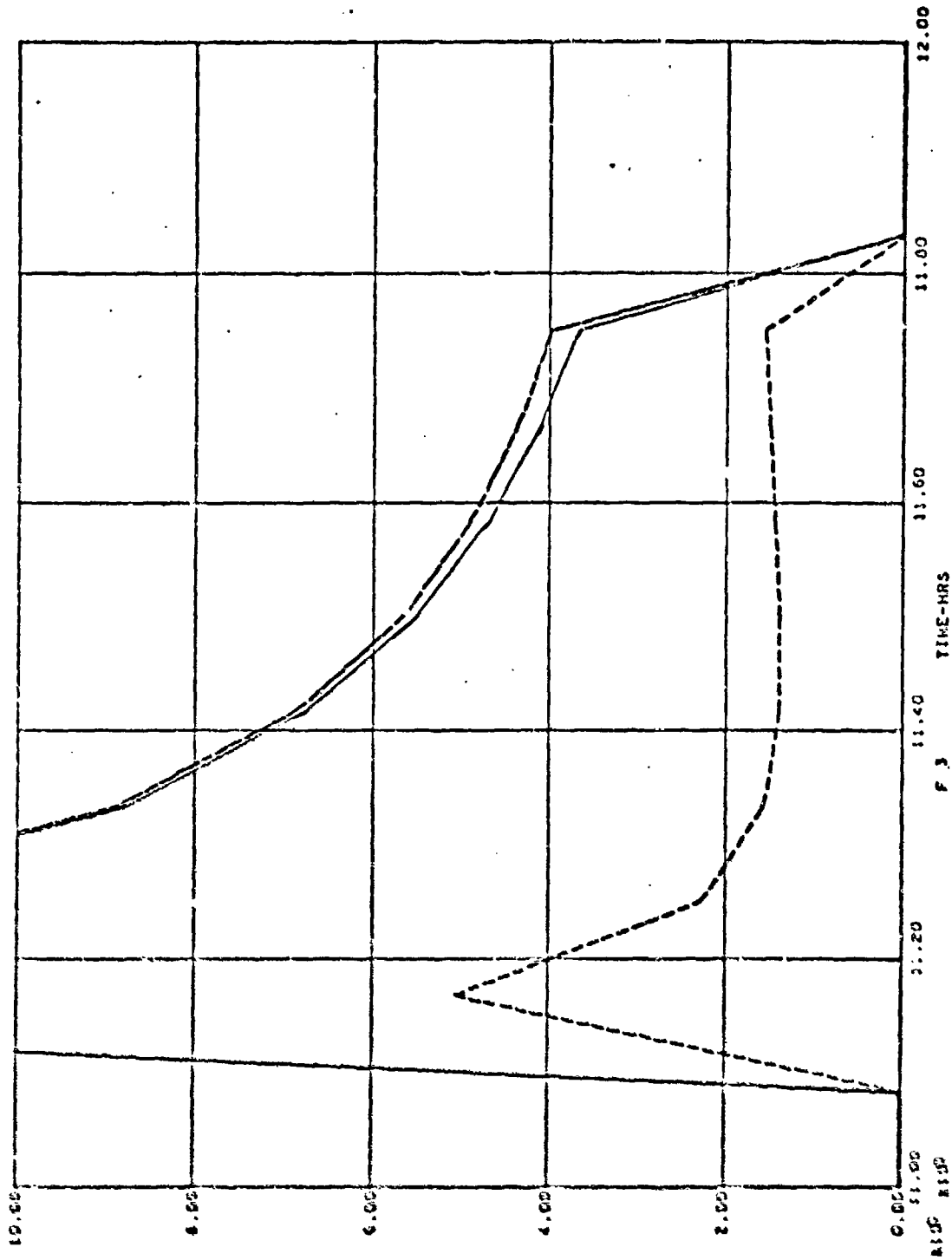


FILE 3 0 DAYS GPSP - AEROSPACE 2/2/0 CONFIGURATION

Figure C-13. GDOP for Wahaiwa



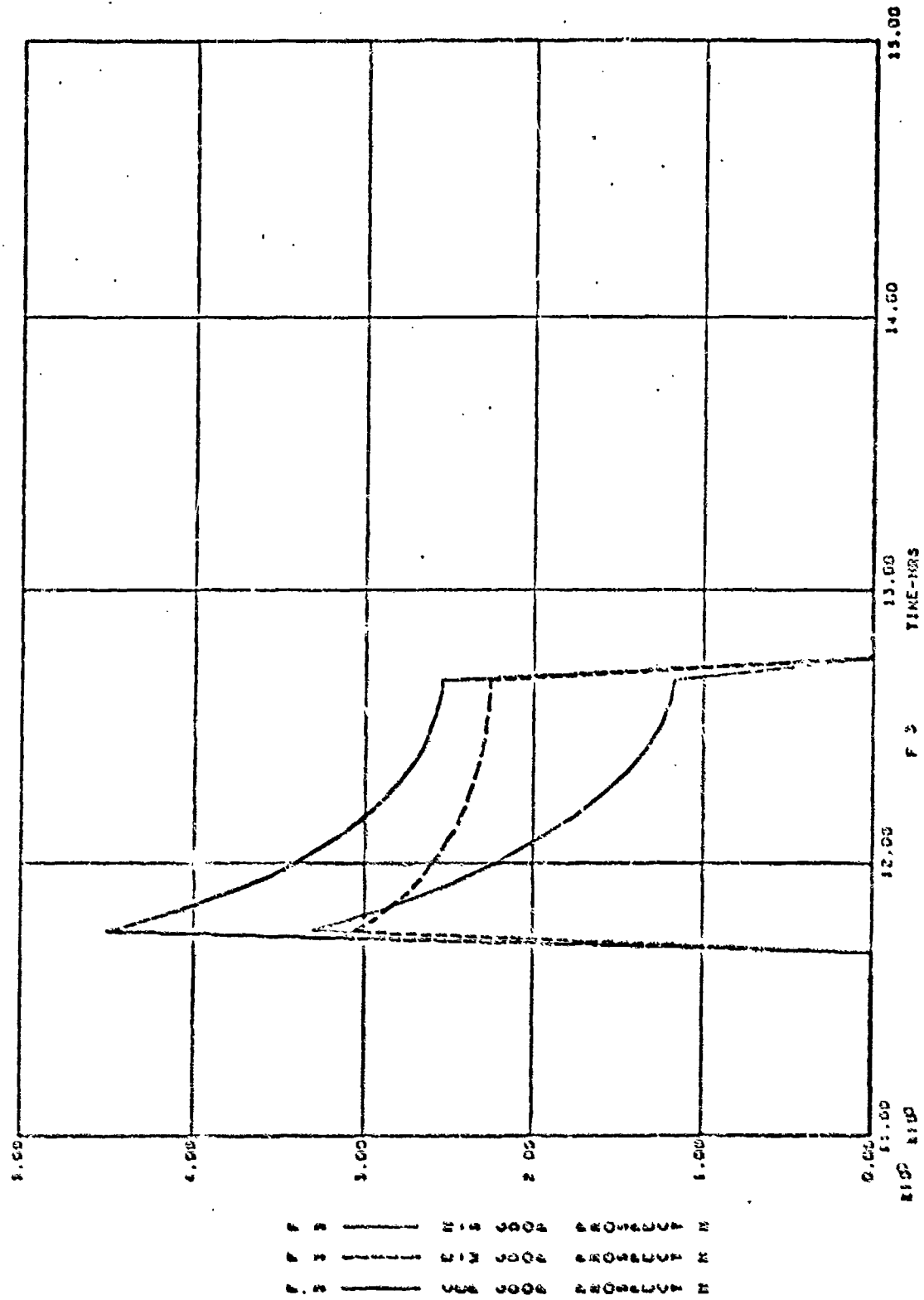
FILE 3  
 0 DAYD GPSD - AEROSPACE 8/2/0 CONFIGURATION  
 Figure C-14. GDOP for Wahiawa



N-15 8006 WASHINGTON  
 C-15 8006 WASHINGTON  
 C-15 8006 WASHINGTON

FILE 3 0 DAYS GPSDF - AEROSPACE 2/2/D CONFIGURATION

Figure C-15. GDOP for Wahiawa



FILE 3 0 DAYS GPSP - AEROSPACE 2/2/0 CONFIGURATION

Figure C-16. GDOP for Prospect Harbor

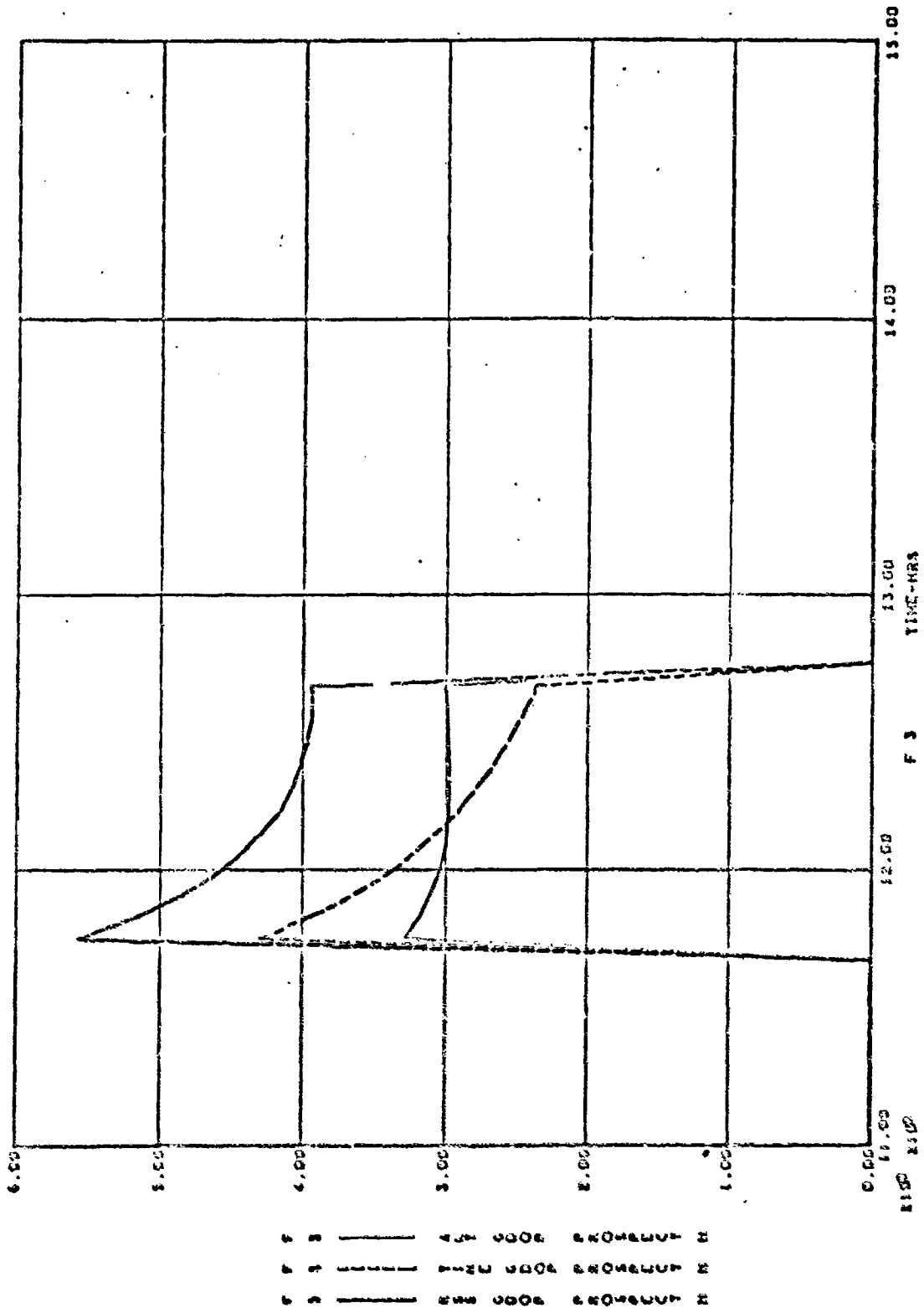
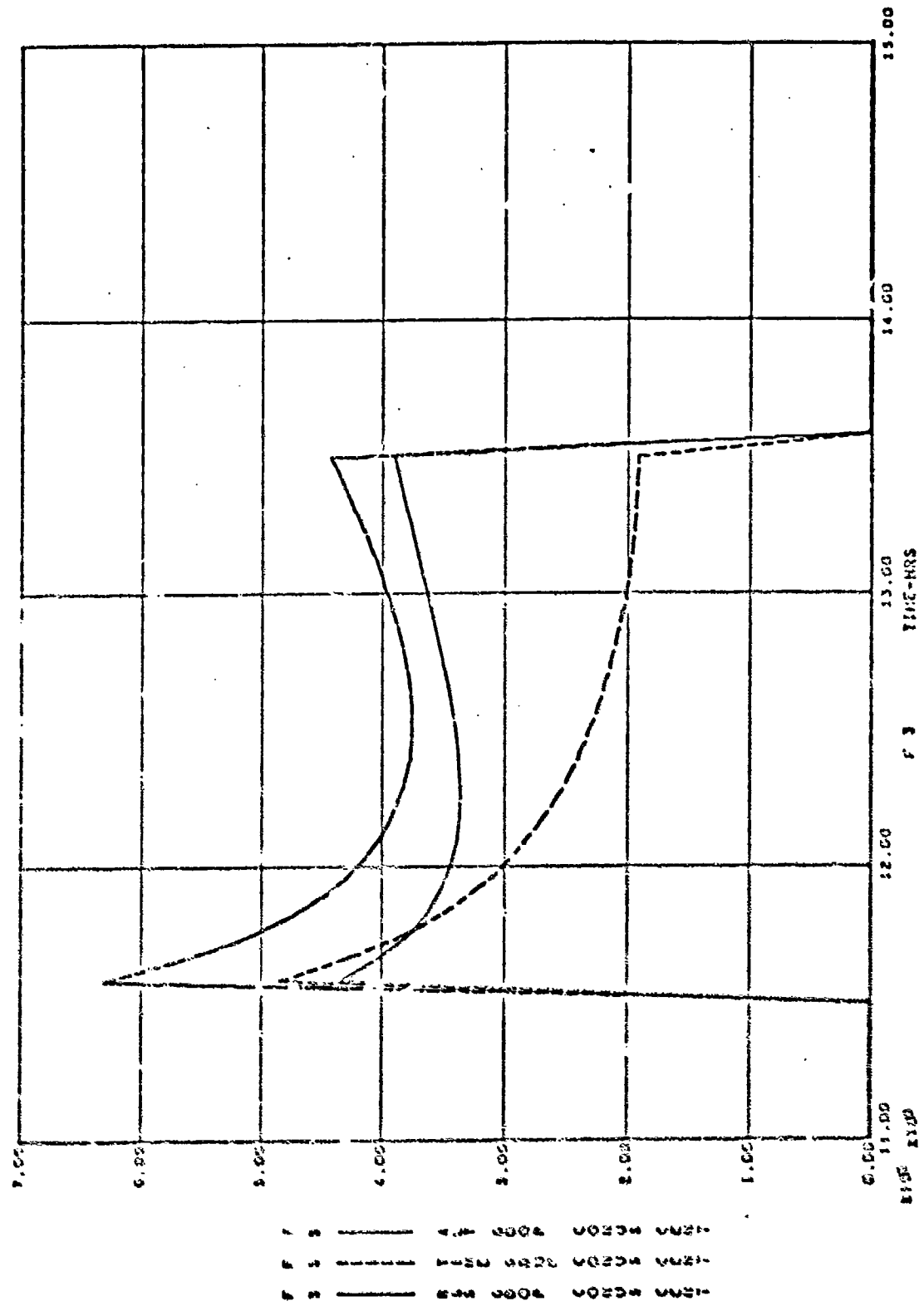


Figure C-17. CDOP for Prospect Harbors





FILE 3 0 DAYS GPSCP - AEROSPACE R/270 CONFIGURATION

Figure C-13. GDDM for Census Center

APPENDIX D

Aerospace Final

2/2/0 CONSTELLATION DATA

<u>Figure</u>		<u>Page</u>
D-1	Satellite Earth Traces . . . . .	D-2
D-2	Satellite Covisibility Earth Traces (Holloman) . . . . .	D-3
D-3	Satellite Covisibility Earth Traces (Yuma) . . . . .	D-4
D-4	Satellite Covisibility Earth Traces (San Clemente 1) . . . . .	D-5
D-5	Satellite Covisibility Earth Traces (Toungue of Ocean) . . . . .	D-6
D-6	Visibility Time Contours (4 Satellites) . . . . .	D-7
D-7	Visibility Time Contours (3 Satellites) . . . . .	D-8
D-8	Satellites/Station Visibility Period . . . . .	D-9
D-9	Test Area Covisibility Chart (4 Satellites) . . . . .	D-10
D-10	Stations Covisibility Opportunity Chart (3 Satellites) . . . . .	D-11
D-11	GDOP for Holloman AFB . . . . .	D-12
D-12	GDOP for Yuma, Arizona . . . . .	D-13
D-13	GDOP for Yuma, Arizona . . . . .	D-14
D-14	GDOP for San Clemente Island . . . . .	D-15
D-15	GDOP for Toungue of Oceans (Bahamas) . . . . .	D-16
D-16	GDOP for Toungue of Oceans (Bahamas) . . . . .	D-17

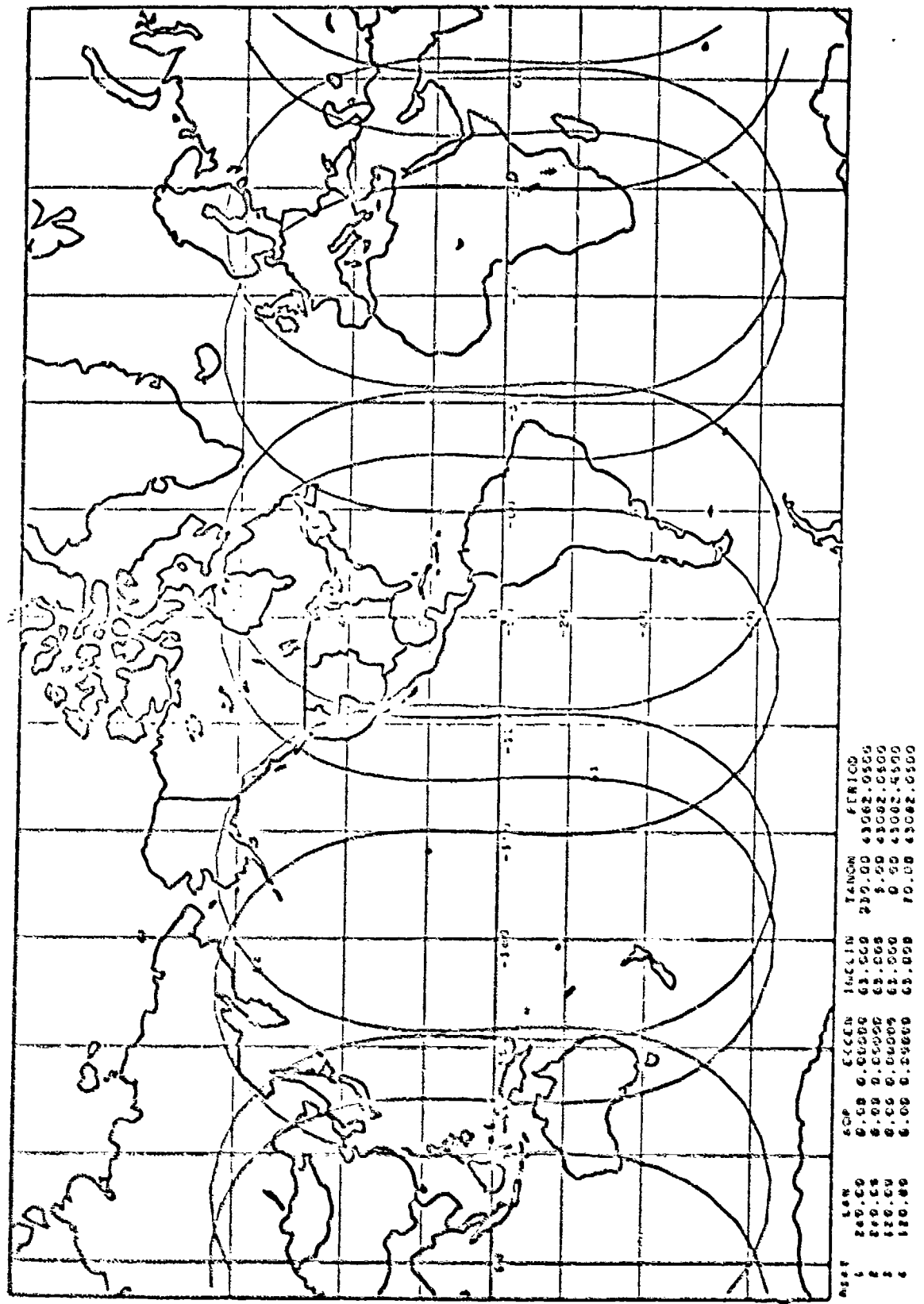


Figure D-1. Satellite Earth Traces

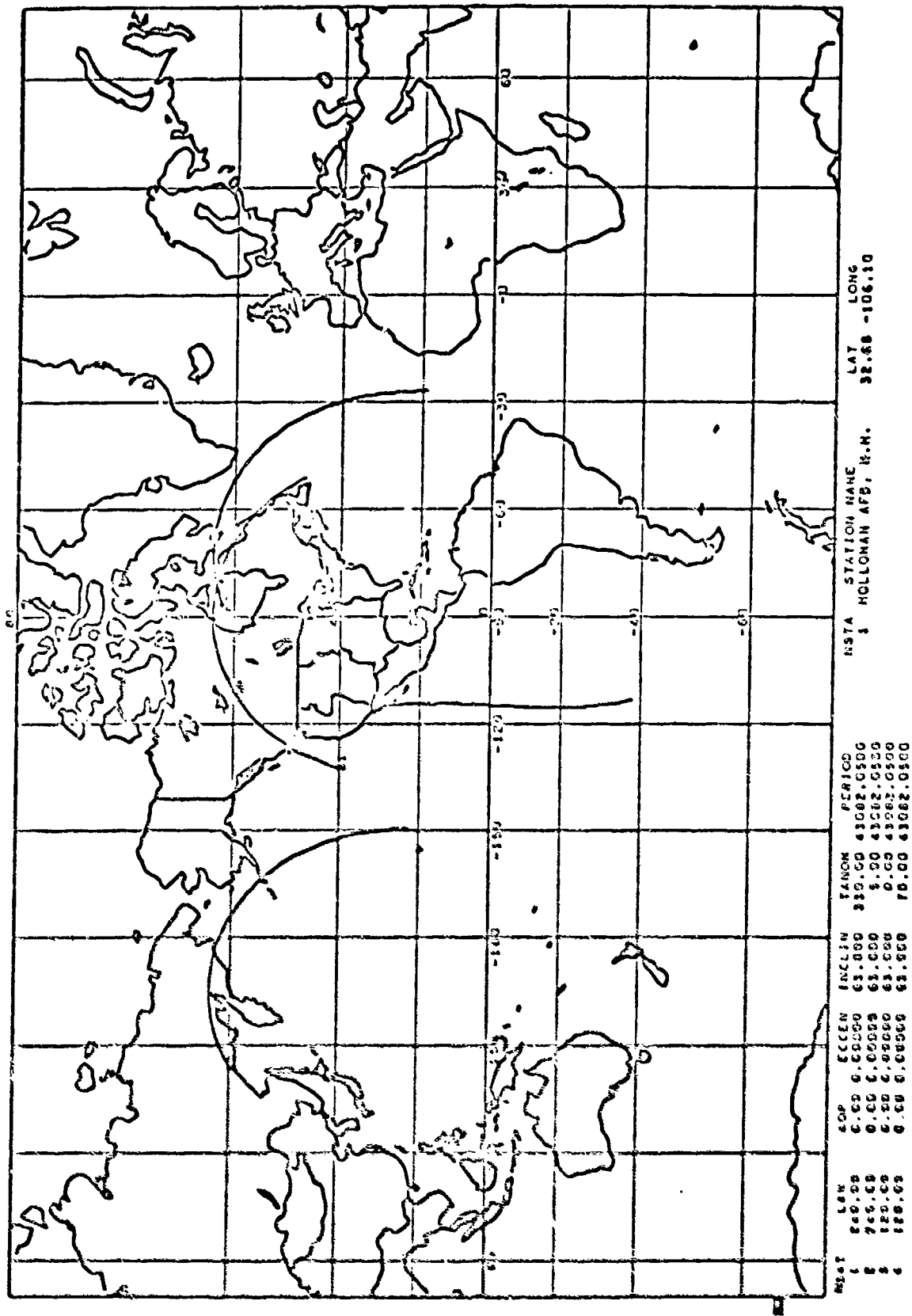


Figure D-2. Satellite Covisibility Earth Traces (Holloman)

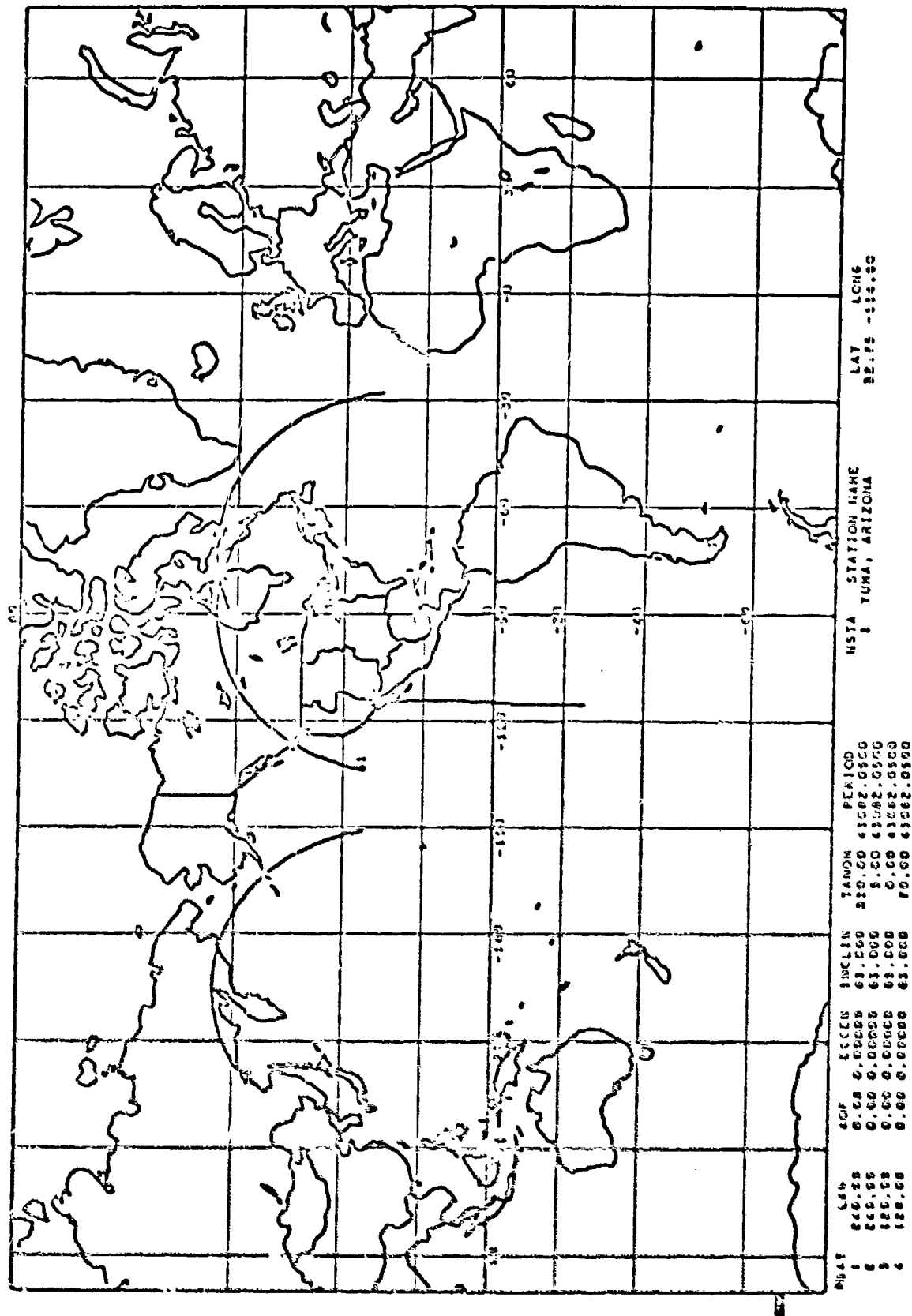


Figure D-3. Satellite Covisibility Earth Traces (Yuma)

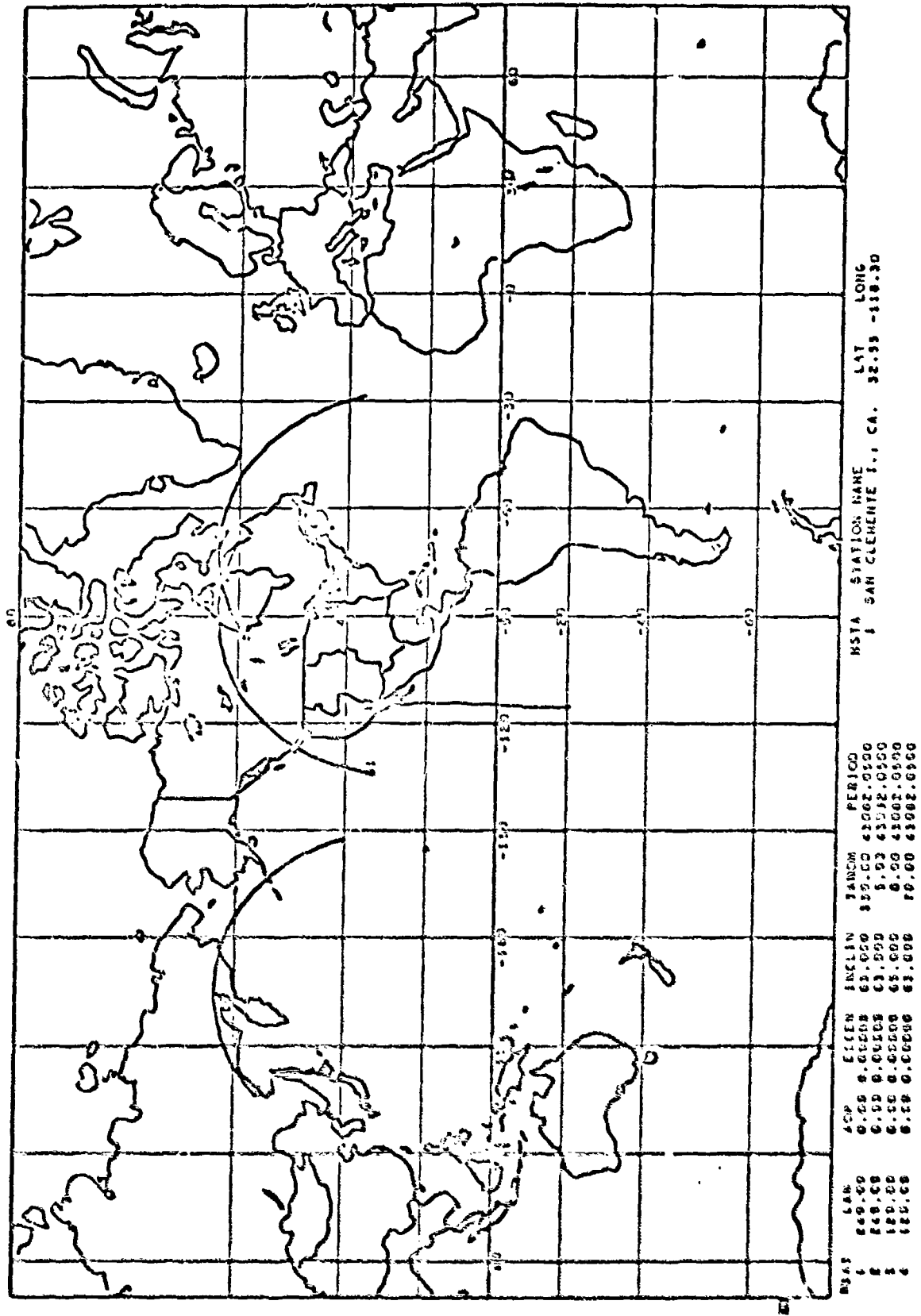


Figure D-4. Satellite Covisibility Earth Traces (San Clemente I)

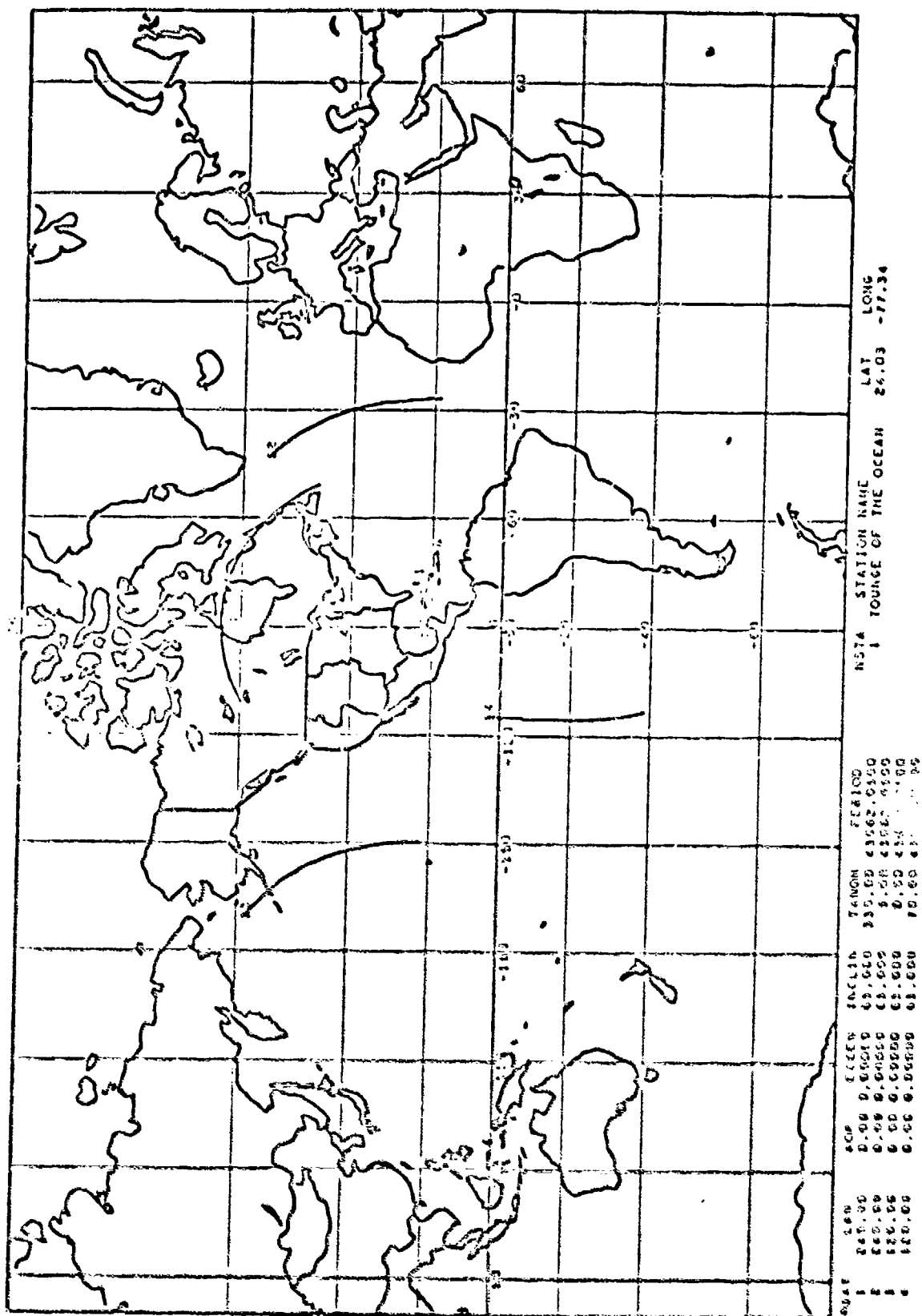


Figure D-5. Satellite Visibility Earth Traces (Tourge of Ocean)

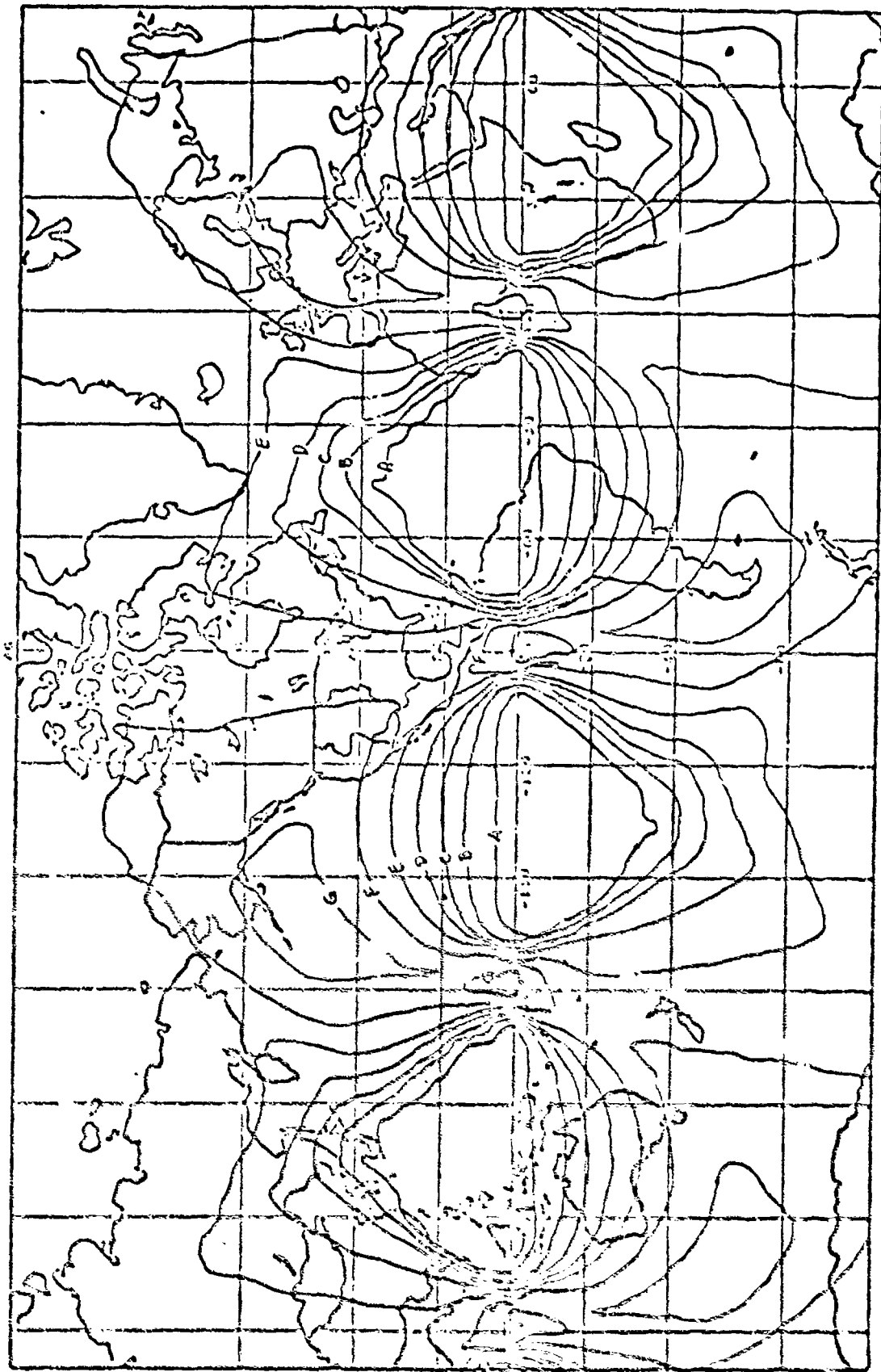
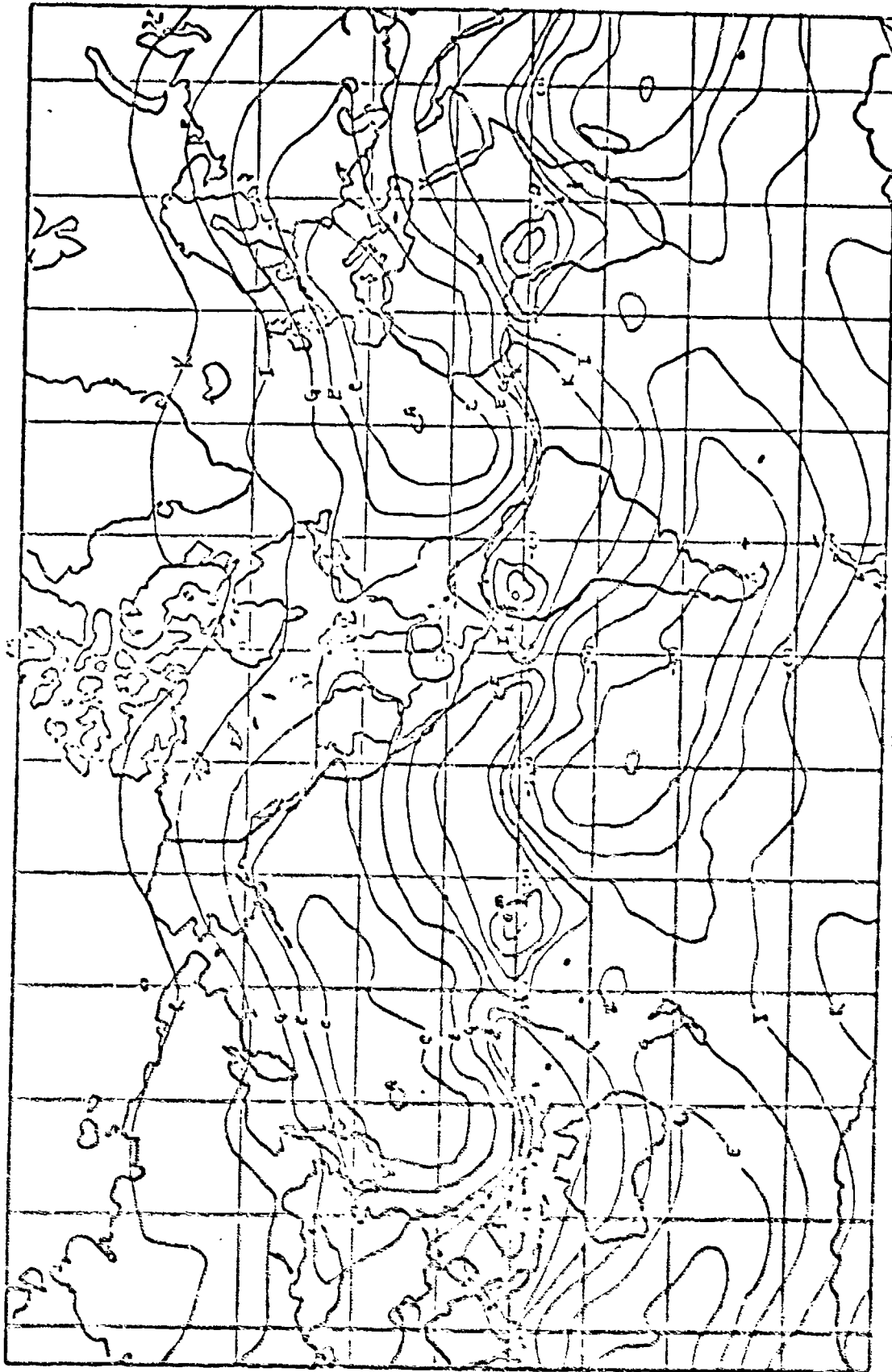


Figure D-6. Visibility Time Contours (4 Satellites)

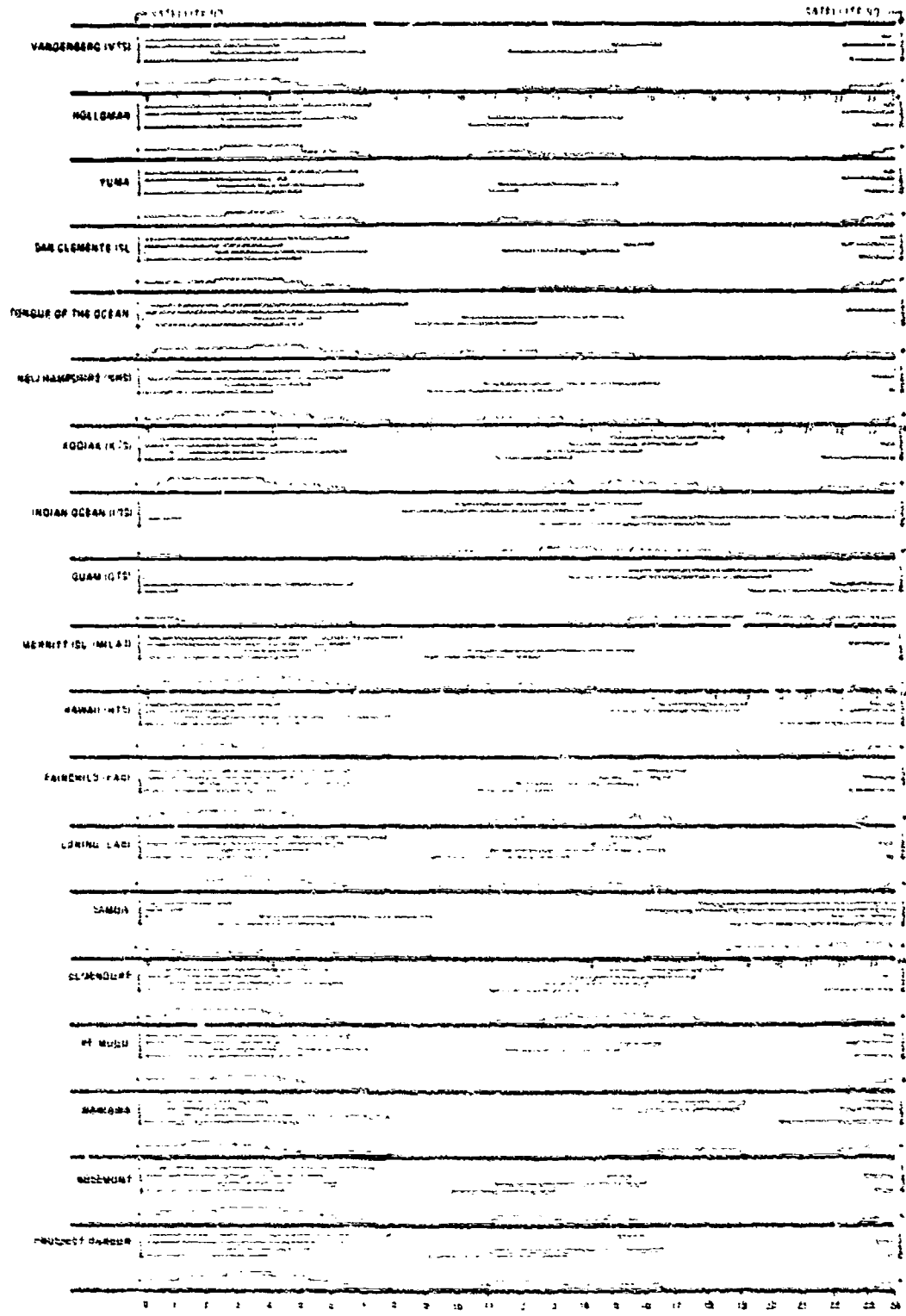




3 SATELLITES

- A 0 sec
- B 1000
- C 1500
- D 2000
- E 2500
- F 3000
- G 3500
- H 4000
- I 4500
- J 5000
- K 5500
- L 6000
- M 6500
- N 7000
- O 7500

Figure D-7. Visibility Time Contours (3 Satellites)



ORBITAL MECHANICS

SATELLITE	LONG. OF ASC. NODE	ARG. OF PER.	DOC	PERIOD (HR)	REMARKS
1	100°	100°	8	11.27	ORBITAL STATION VISIBILITY PERIODS
2	100°	90°	8	11.27	22.0 PERCENTAGE OF TIME IN VISIBILITY
3	100°	90°	8	11.27	100 PERCENTAGE VISIBILITY
4	100°	90°	8	11.27	

Figure D-5. Satellites/Station Visibility Period

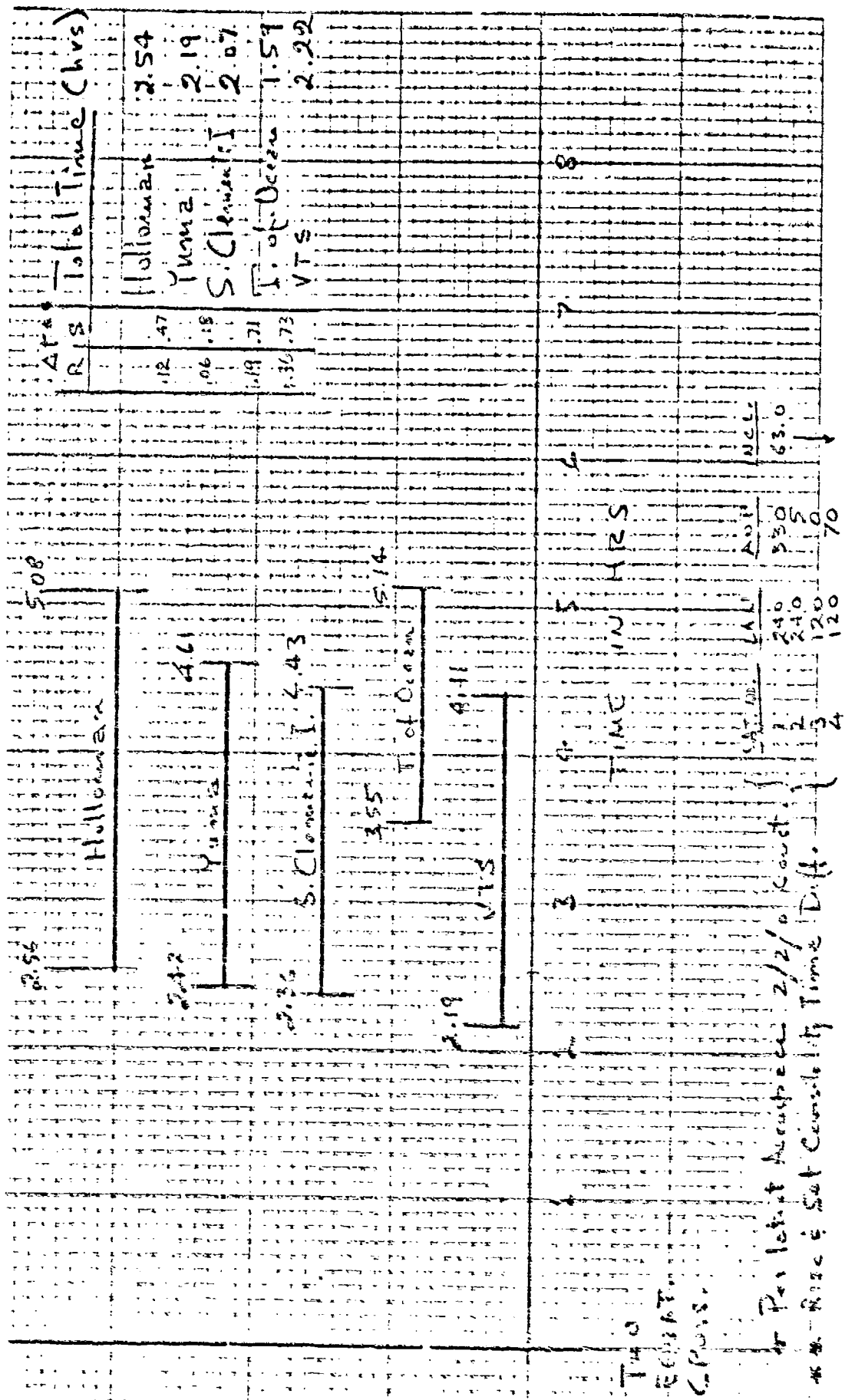


Figure D-9. Test Area Covisibility Chart (4 Satellites)

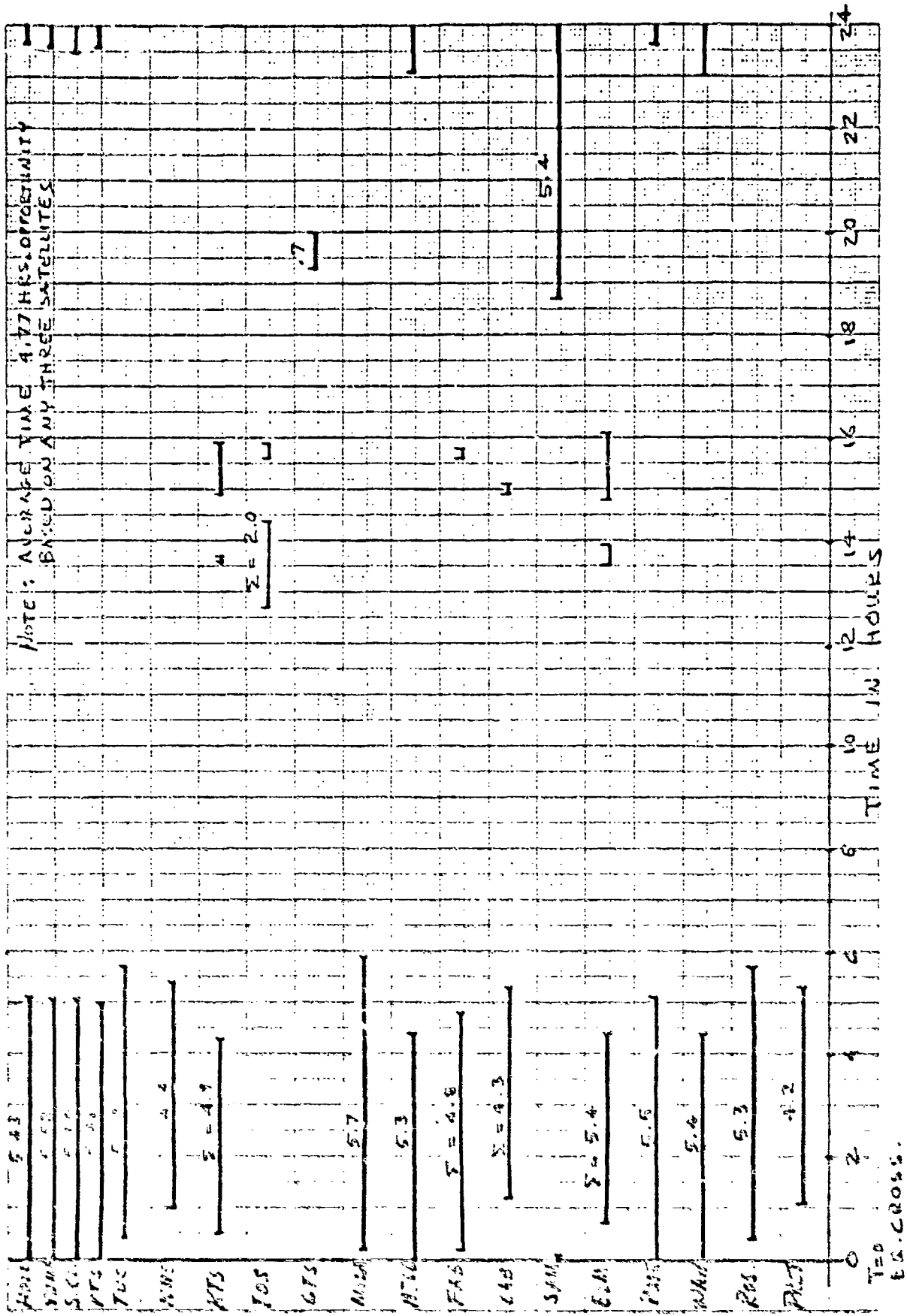
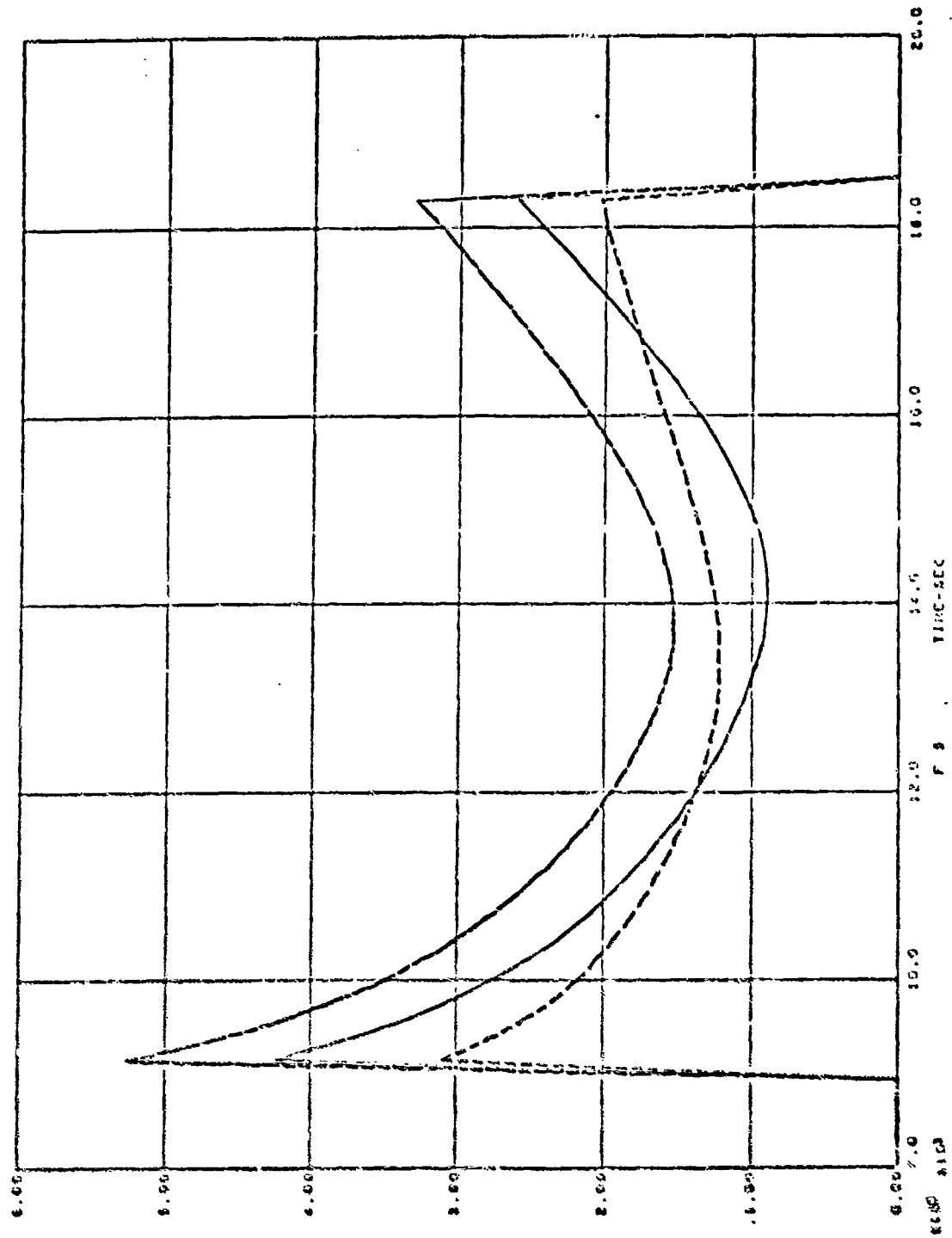


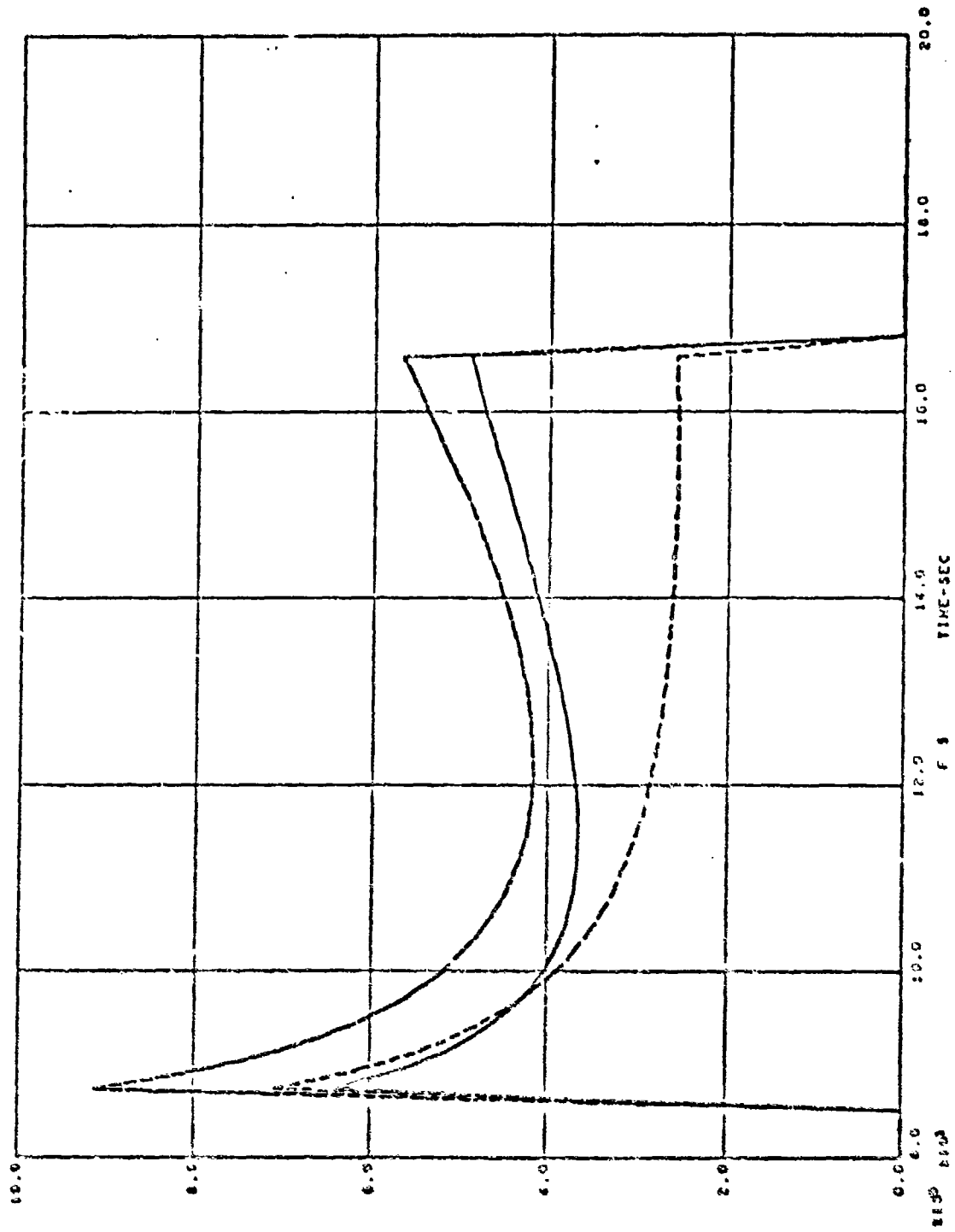
Figure D-10. Stations Covisibility Opportunity Chart (3 Satellites)



10001  
 10002  
 10003

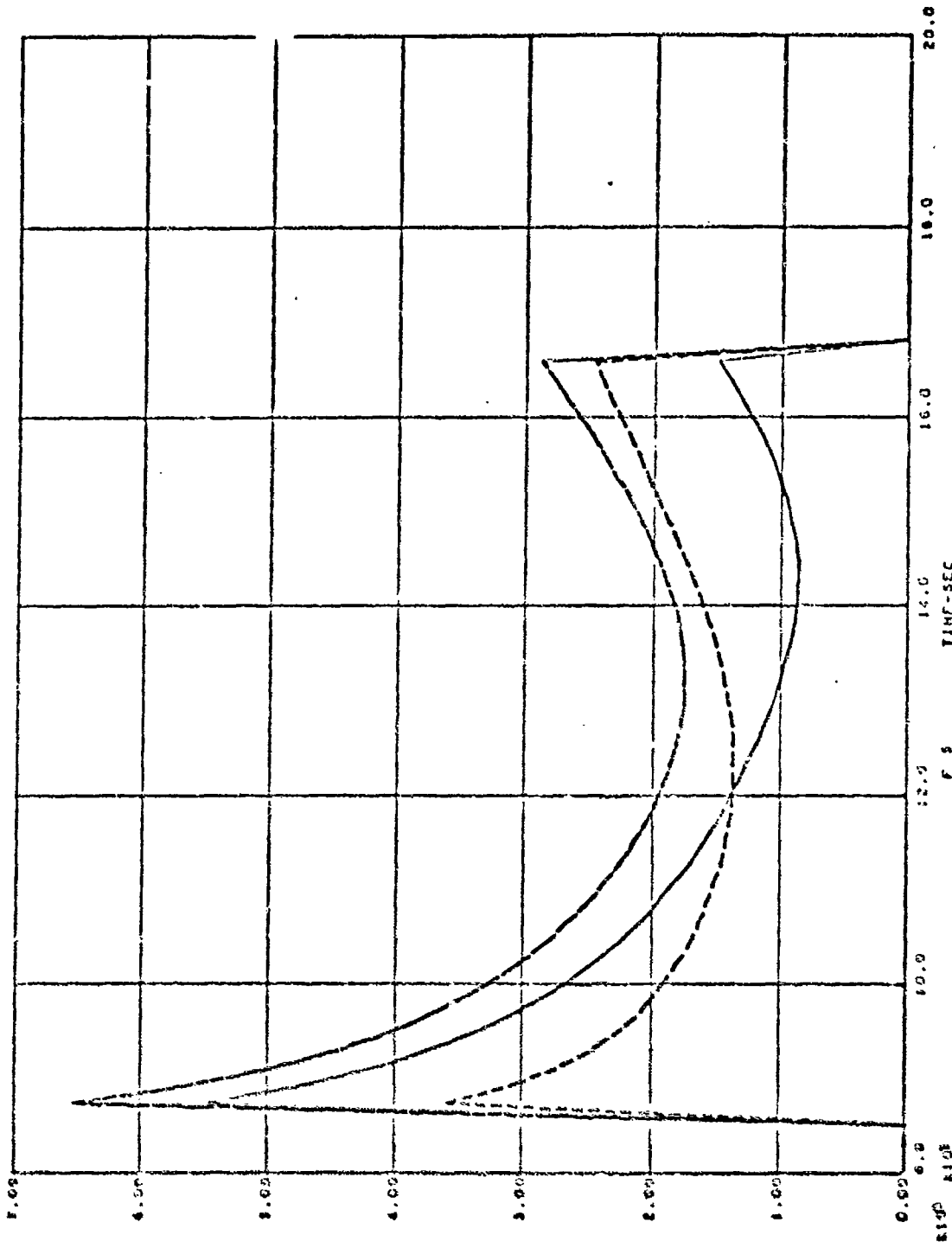
FILE 8 O DAYS GPS - PHASE 1 - 2/2/0 CONFIGURATION

Figure D-11. GDOP for Holloman AFB



FILE 5 0 DAYS CP9 - PHASE I - R/Z/O CONFIGURATION  
 Figure D-12. GDOP for Yuma, Arizona

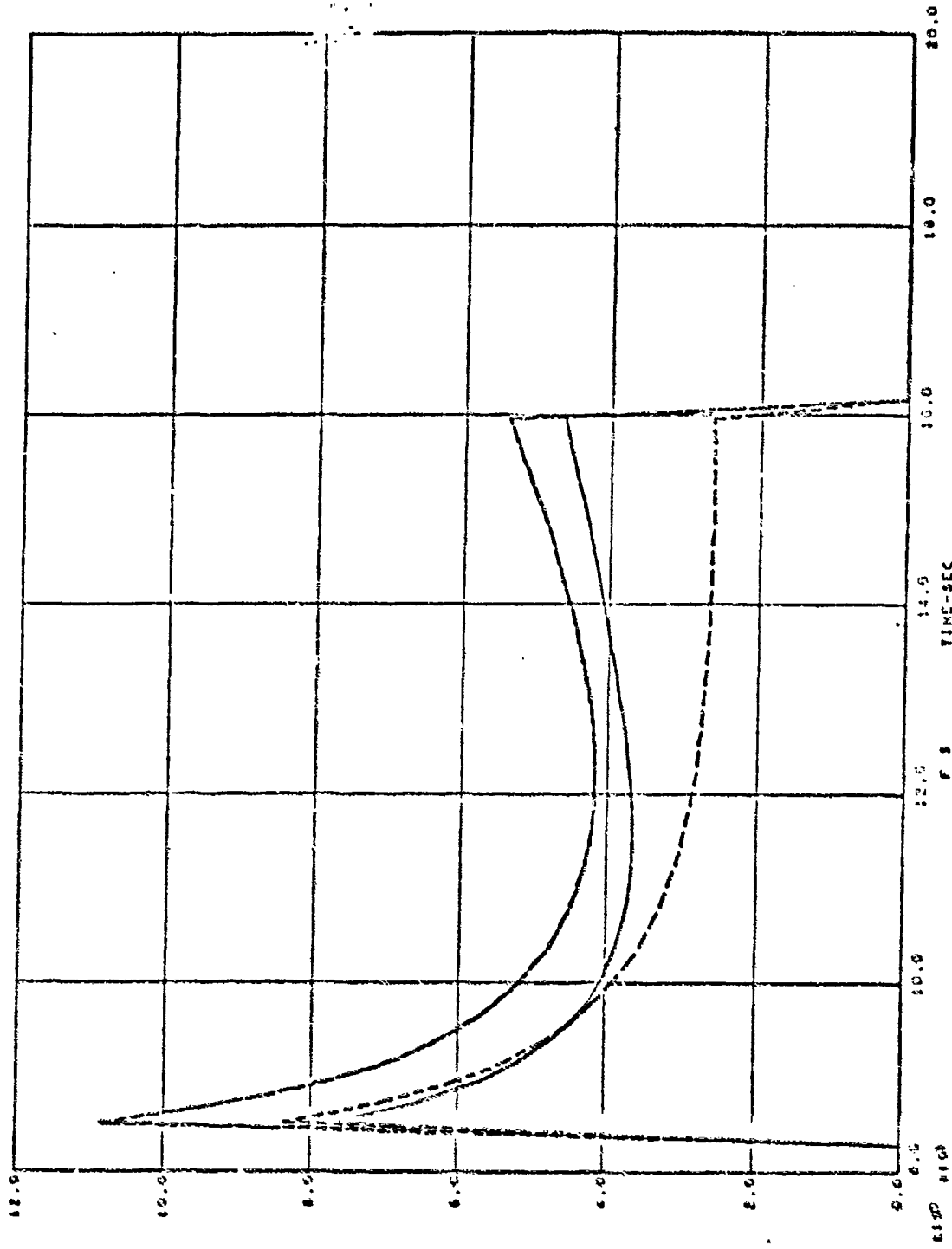
1 0 11111 417 0004 1024 - 4612  
 2 0 11111 420 0004 1024 - 4612  
 3 0 11111 422 0004 1024 - 4612



P 5 | | | | | 5.00 5.00 5.00 5.00 5.00  
 P 5 | | | | | 4.00 4.00 4.00 4.00 4.00  
 P 5 | | | | | 3.00 3.00 3.00 3.00 3.00

FILE # 0 DAYS GPS - PHASE 1 - 2/2/0 CONFIGURATION

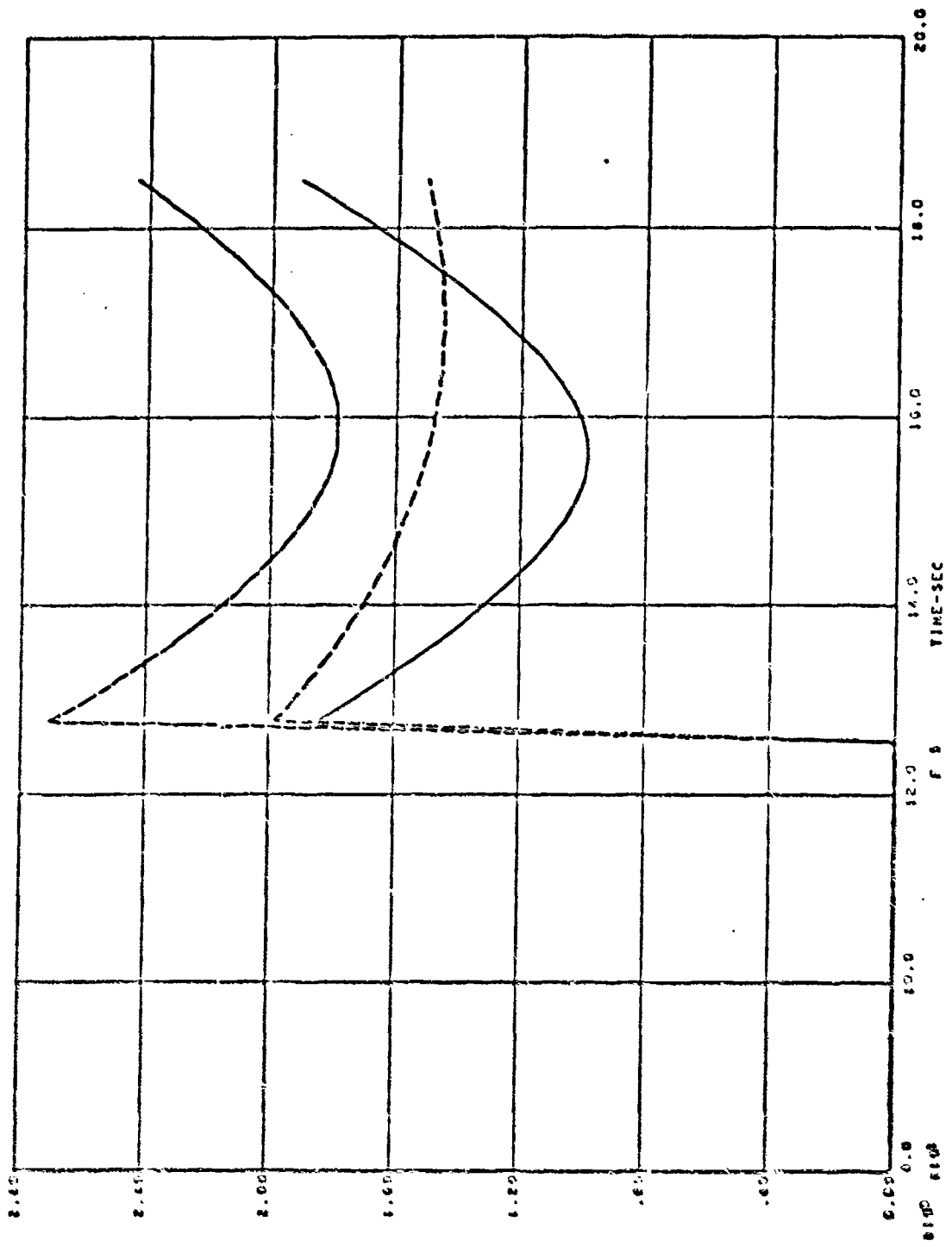
Figure D-13. GDP for Yuma, Arizona



FILE 3 0 DAYS GPS - PHASE 1 - 2/2/0 CONFIGURATION

Figure D-14. GDOP for San Clemente Island

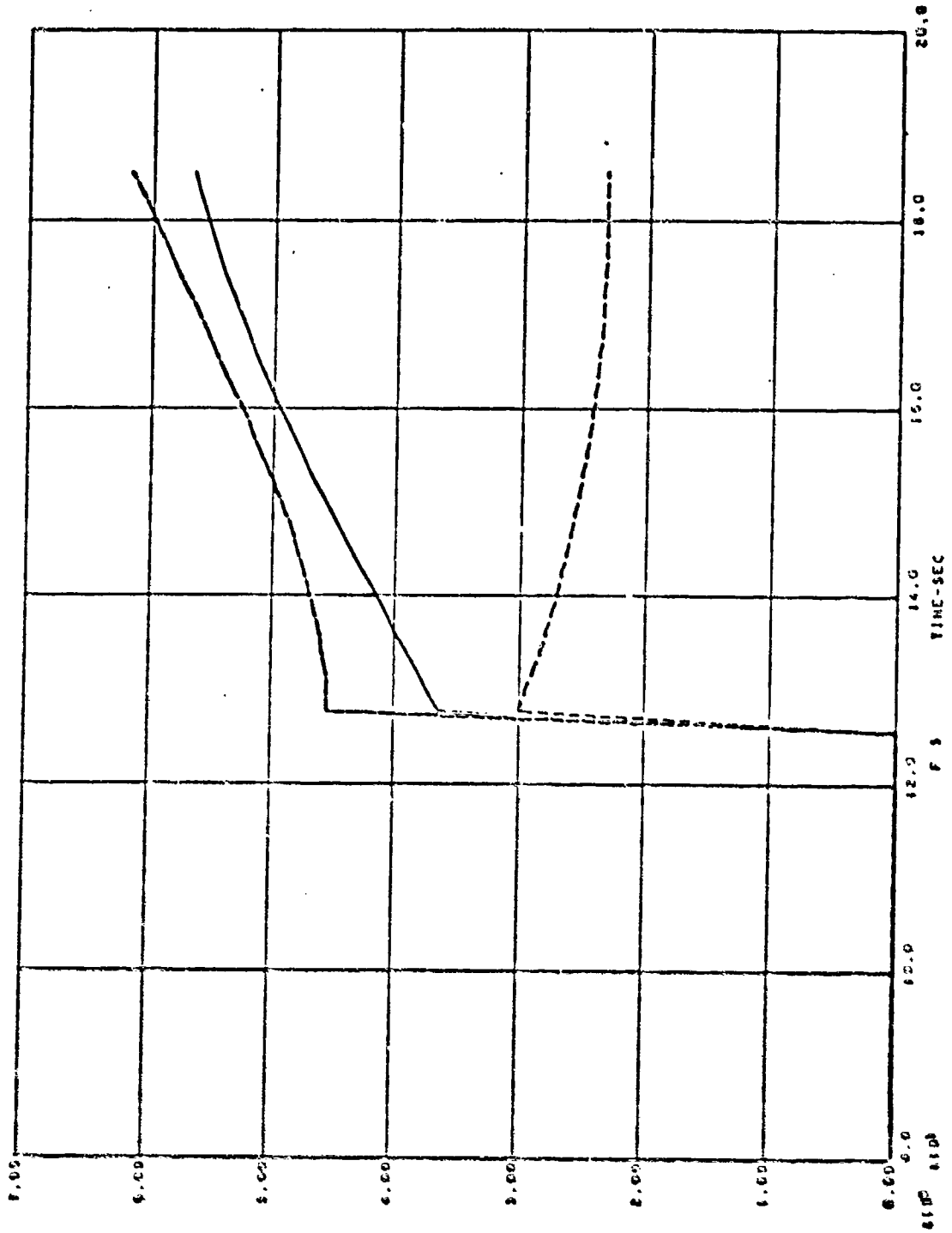




FILE 8 0 DAYS GPS - PHASE I - R/2/0 CONFIGURATION

Figure D-15. GDOP for Tongue of Occinus (Bahamas)

4 0 1 3 3004 1 0 9 9 9 9 9 9  
 4 0 2 3 3004 1 0 9 9 9 9 9 9  
 4 0 3 3 3004 1 0 9 9 9 9 9 9



FILE 6 0 DAYS GFS - PHASE I - R/2/O CONFIGURATION

Figure D-16. GDP for Tongue of Oceans (Bahamas)

6 1 1111111 1 1 1111111 1 1 1111111 1 1  
 6 2 1111111 1 1 1111111 1 1 1111111 1 1  
 6 3 1111111 1 1 1111111 1 1 1111111 1 1

APPENDIX E

General Dynamics

2/1/1 CONSTELLATION DATA

<u>Figure</u>		<u>Page</u>
E-1	GDOP for Holloman AFB .....	E-2
E-2	GDOP for Vandenberg AFB .....	E-3
E-3	GDOP for Conus Center .....	E-4
E-4	GDOP for Cape Kennedy .....	E-5

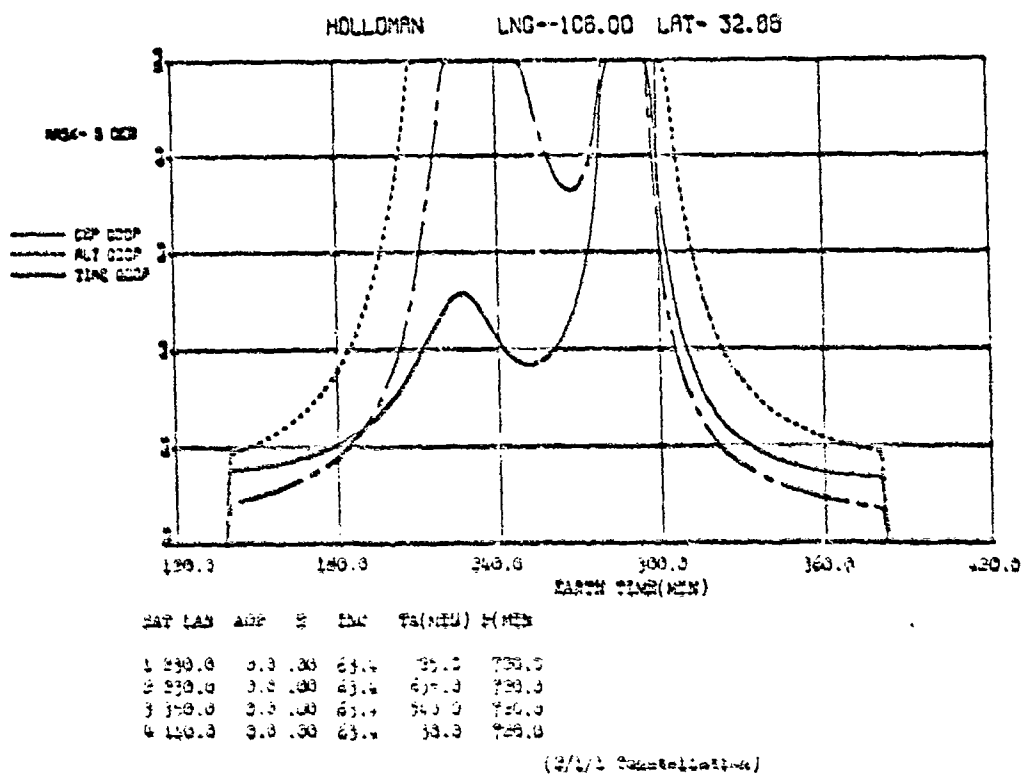
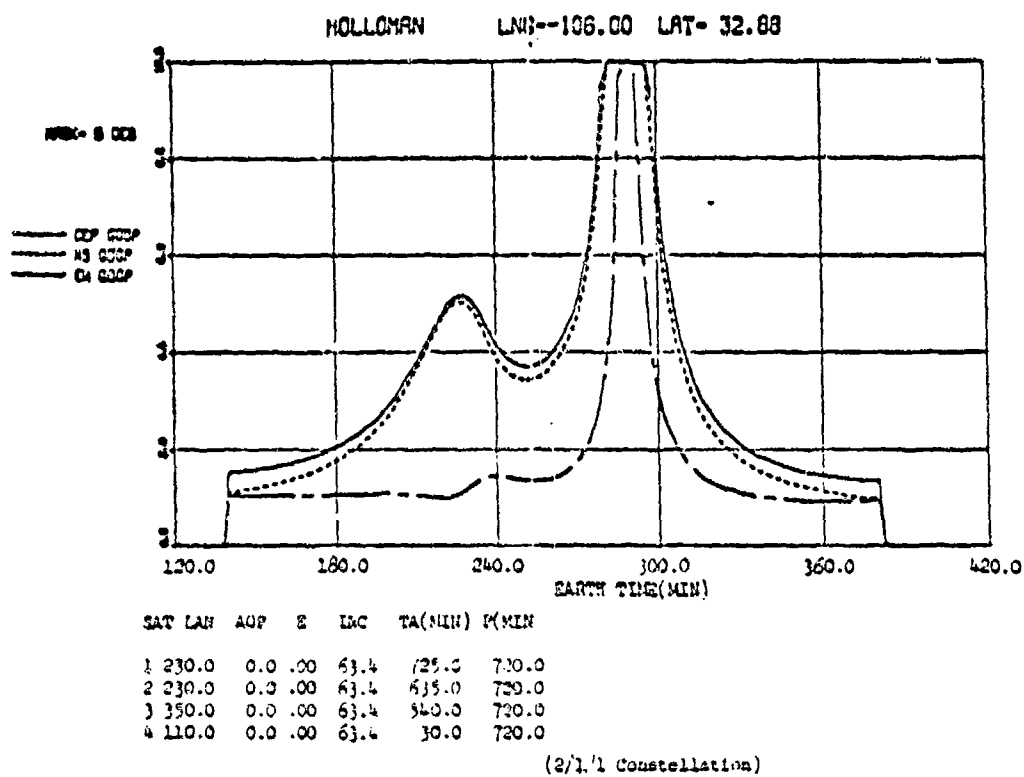
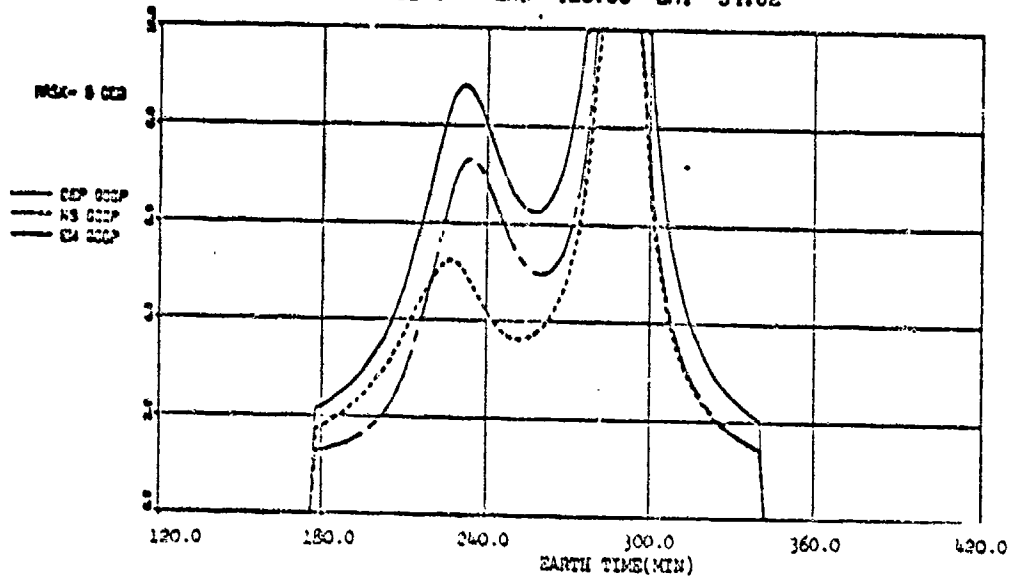


Figure E-1. GDOP for Holloman AFB

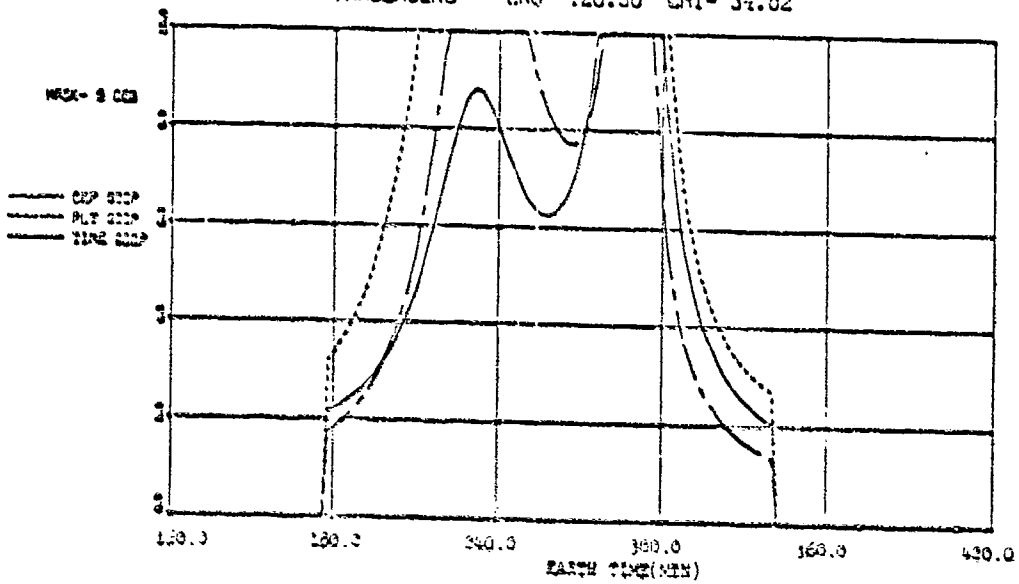
VANDENBERG LNG--120.50 LAT- 34.02



SAT	LAN	AOP	E	INC	TA(MIN)	P(MIN)
1	230.0	0.0	.00	63.4	735.0	770.0
2	230.0	0.0	.00	63.4	615.0	730.0
3	350.0	0.0	.30	63.4	540.0	730.0
4	110.0	0.0	.00	63.4	30.0	720.0

(2/1/1 Constellation)

VANDENBERG LNG--120.50 LAT- 34.02



SAT	LAN	AOP	E	INC	TA(MIN)	P(MIN)
1	230.0	0.0	.00	63.4	735.0	770.0
2	230.0	0.0	.00	63.4	615.0	730.0
3	350.0	0.0	.30	63.4	540.0	730.0
4	110.0	0.0	.00	63.4	30.0	720.0

(2/1/1 Constellation)

Figure E-2. GDOP for Vandenberg AFB

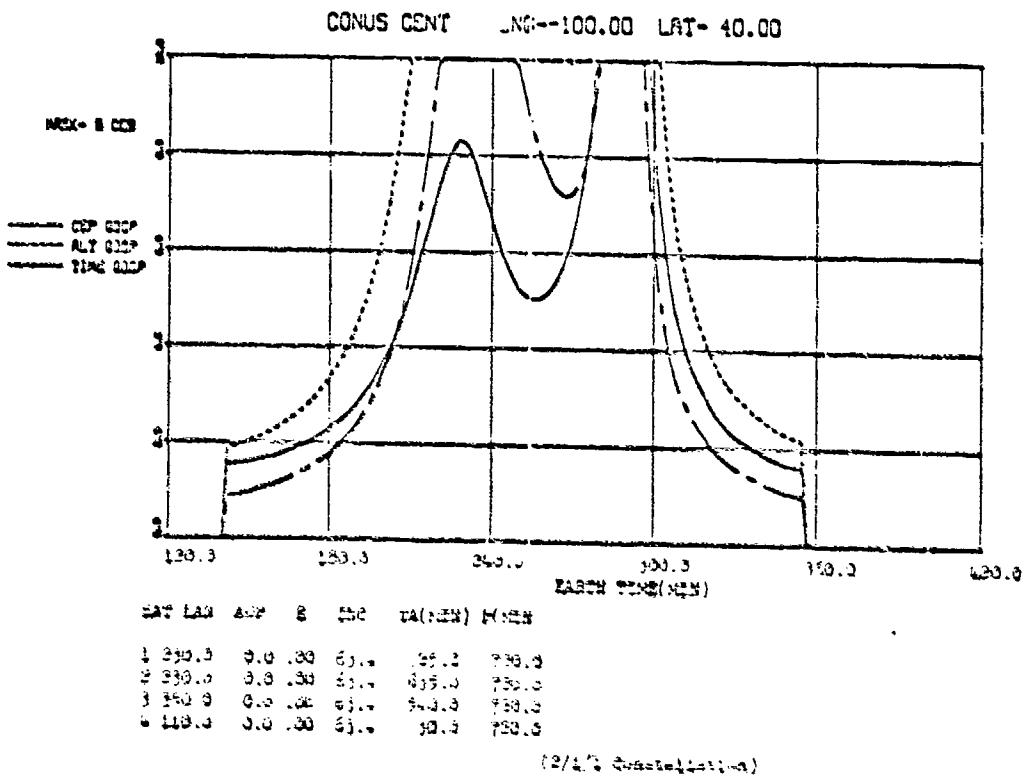
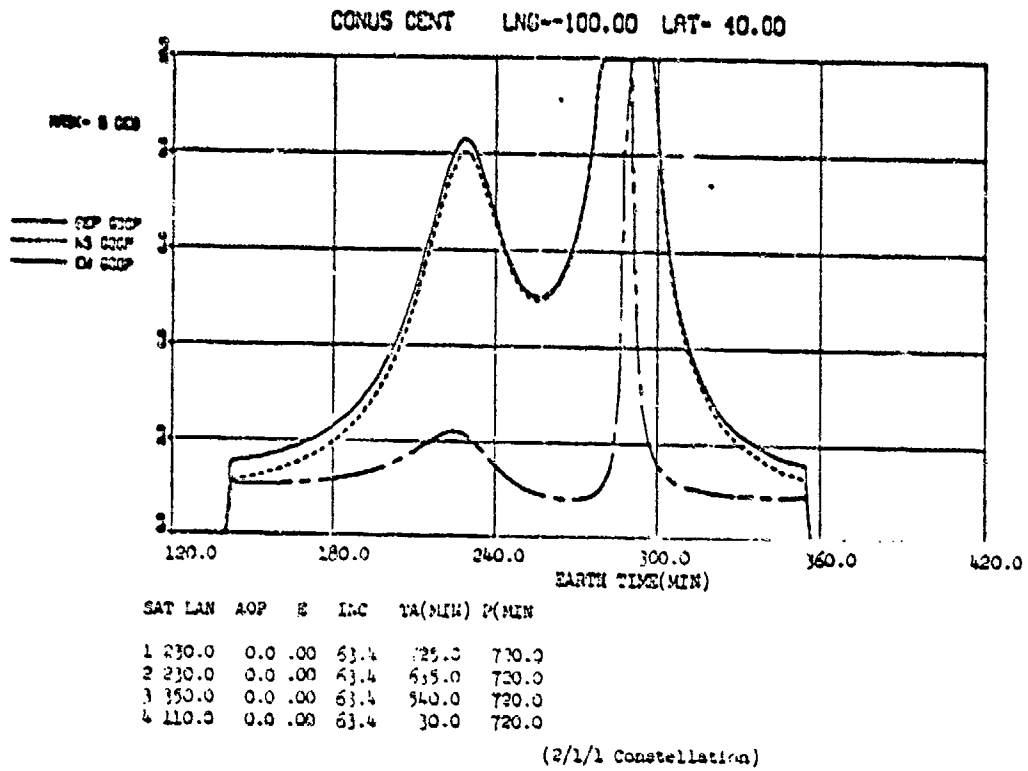
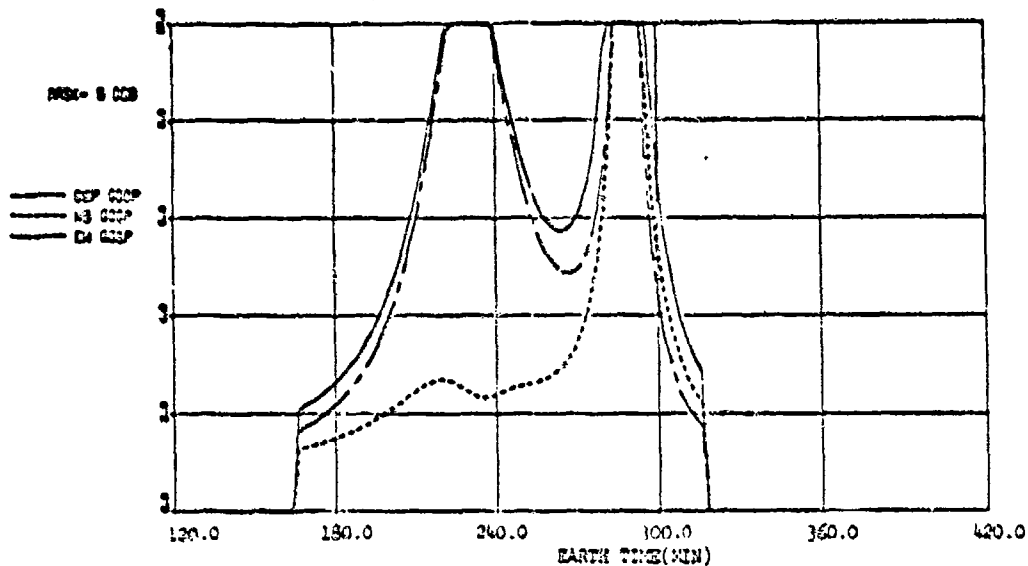


Figure E-3. GDOP for Conus Center

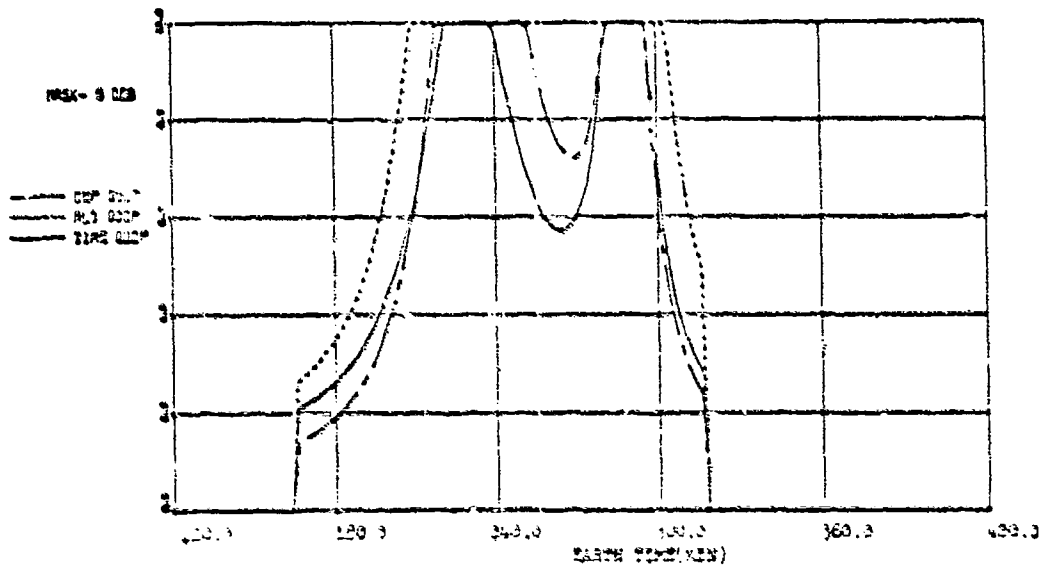
CAPE KENDY LNK- -80.54 LAT- 28.32



SAT	LAN	AOZ	E	INC	TA(MIN)	T(MIN)
1	230.0	0.0	.00	63.4	720.0	720.0
2	230.0	0.0	.00	63.4	615.0	720.0
3	350.0	0.0	.00	63.4	540.0	720.0
4	110.0	0.0	.00	63.4	30.0	720.0

(2/1/1 Constellation)

CAPE KENDY LNK- -80.54 LAT- 28.32



SAT	LAN	AOZ	E	INC	TA(MIN)	T(MIN)
1	230.0	0.0	.00	63.4	720.0	720.0
2	230.0	0.0	.00	63.4	615.0	720.0
3	350.0	0.0	.00	63.4	540.0	720.0
4	110.0	0.0	.00	63.4	30.0	720.0

(2/1/1 Constellation)

Figure E-4. GDOF for Cape Kennedy

TRADE STUDY NO. 3

MONITOR STATION SITES

J. E. Coxey  
A. Arcidiacono



**GENERAL DYNAMICS**

*Electronics Division*

P.O. Box 81127, San Diego, California 92168 616-279-7201



## SITE SELECTION

### 1. INTRODUCTION

#### 1.1 Purpose

The purpose of this trade study is to identify acceptable combinations of sites in existing DOD networks, for the location of GPS Control Segment functions for the Phase I Development, Test and Evaluation program.

#### 1.2 Concept

The Control Segment functions are grouped in a Master Control Station (MCS), four Monitor Stations (MS) and an Upload Station (ULS).

The monitor stations obtain pseudo range data from the PN code transmitted by the satellite's navigation subsystem, time-tags the data, accomplishes preliminary processing, and relays the data to the Master Station.

The MCS is the prime computational facility of the system. This station processes the MS data to determine the satellite's measured ephemeris and computes user navigation data to be loaded into the satellite.

The ULS receives the user navigation data from the MCS and transmits the navigation message to the satellites.

It is important to note that the acceptability of site locations for Monitor Stations and the Upload Station must be evaluated with respect to: (1) a defined satellite constellation and (2) specified user equipment test and/or use location.

#### 1.3 Site Selection Impact on Future Phases

Subsequent phases of the program may be better served by relocating some Control Segment functions. For example, satellite clock accuracy will be a systems accuracy constraint for some time into the future. The world-wide effect of this error source on the User (these are considerations for diverse test locations in Phase I and for Phases II and III) will be significantly

reduced by monitoring and updating the satellite clock and/or clock error polynomial just prior to satellite visibility at the User site. An Upload Station location that will provide this capability may not be required for Phase I but is a probable requirement for Phases II and III. Additional Monitor and Upload elements may also be required for the Phase II and Phase III Control Segment to compensate for the satellite clock accuracy limitations.

## 2. REQUIREMENTS

### 2.1 Functional Requirements

The Monitor Station is the primary means of collecting the space vehicle tracking information necessary for determining the orbit parameters of each space vehicle. Source: SS-GPS-101A (1/29/74), Paragraph 3.7.3.2.

The Monitor Stations will be located to provide measurement geometry for accurate ephemeris and calibration of space vehicle time prior to testing over southwestern CONUS for Phase I. Source: Air Force memo, Technical Direction to the Definition Contractors, 5 February 1974, from William L. Stateham.

### 2.2 Design Requirements

The GPS error budget allocates a one sigma error of 12 feet for the Space Vehicle Ephemeris determination. Source: SS-GPS-101A (1/29/74), Paragraph 3.2.1, Table I.

### 2.3 Ground Rules

2.3.1 Satellite Constellations and Test Sites. In performing this analysis, it was necessary to define the satellite constellation configuration in order to determine the adequacy of viewing times and tracking geometry. On the basis of maximizing the time duration of favorable User GDOP's at the Holloman Test Range and at the Yuma Test Range, a constellation was defined (see Trade Study No. 2). This constellation is used in the simulations for evaluating candidate sites.

2.3.2 Viewing Constraints. The monitor network geometry analysis determined site visibility times, using a 5 degree minimum elevation angle viewing criteria "mask", for candidate sites, on the selected satellite constellation. In cases where known obstruction

constrained viewing to higher than 5 degree elevation angles, the higher angles were used as the constraint.

System simulations investigating parameter sensitivities indicated that the satellite clock errors dominated the ephemeris error for clock updating intervals of more than 24 hours. Tracking data for satellite ephemeris determination need not be obtained just prior to visibility of the constellation over the test area; however, determining satellite clock errors and updating that aspect of the User navigation data was essential to achieving best system performance over the test site.

**2.3.3 Upload Station (Navigation Data and Satellite Commands).** The requirement exists for SGLS compatibility for User navigation data uploading and satellite housekeeping functions and telemetry data. This capability is available from all AFSCF remote tracking sites and the Aerospace Applications Group network (after incorporation of modifications now under contract). The navigation data and satellite commands can be considered separate functions and performed at separate sites as is done in Alternate IV (See Section 3 for definition of alternates).

Until significant satellite clock performance advances are made, it is recommended that capability for updating the operational phase satellite clocks twice each day should be considered a growth requirement of the Upload Station. This requirement may also be satisfied by providing an Upload Station that is easily relocatable for subsequent phases.

The present day utilization of the existing networks favors the Aerospace Applications Group network. This net can accommodate the growth of the GPS system through all three phases with legacy in software, operational procedures and trained personnel. The sites are also judged to be less vulnerable than most AFSCF sites, which is a consideration for the Phase III GPS. Alternate IV includes a GPS dedicated Upload Station for navigation data loading into the satellite and utilizes AFSCF for the satellite command function.

**2.3.4 Data Communications.** Data communications to and from monitor sites and the Master Station and the uplink facility were considered in evaluating candidate sites. The data messages are easily transmitted over standard voice grade telephone lines with reasonable short duration messages on the order of five minutes for one hour of tracking. One site considered at Samoa would use an FAA data link on an as-available basis to relay data to Hawaii.

For the comparative evaluation of alternatives, a minimum number of links and minimum length of links was considered most desirable from a system reliability/vulnerability point of view. The cost of voice grade dedicated leased lines is estimated at \$2,000/link/month. The minimum number of links and minimum communications cost are achieved by co-locating one monitor site, the Master Station and the uplink facility. Link reliability is also judged to be enhanced by locating all sites within CONUS.

2.3.5 Master Site. This computational facility has no critical location requirement. This is the control site for the GPS and for minimizing data communication links, should be co-located with the Upload Station and/or with a Monitor Station.

2.3.6 Computation-Off-Line. Periodic processing of data will be accomplished off-line to provide a reference trajectory and for refinement of models and values employed in the on-line state vector computation. These programs may be executed on any of several existing computer facilities at Aerospace Corporation, the contractor's plant, NWL, APL and others.

2.3.7 Telemetry. SGLS compatibility is required and is available through the AFSCF or AAG network; therefore, consideration of these requirements is the same as the Upload Station discussion.

Telemetry data from the satellites would be preprocessed and converted into engineering units by the existing networks and relayed to the GPS Control Segment Master Station for further analysis.

2.3.8 Growth Potential. Growth potential from the Phase I program to the Phase III program was assessed for the networks evaluated. For example, it may be reasonable to assume that the AFSCF may handle the Phase I upload requirement of daily loading four satellites at specified time-of-day, but it is less reasonable to assume that the AFSCF can handle loading of 24 or more satellites on a daily basis in addition to the support required by other programs. The growth potential is not amenable to being quantized but is of considerable importance in evaluating alternatives.

#### 2.4 Evaluation Criteria

The evaluation criteria employed to select the preferred sites are as follows:

Monitor Station:	Satellite Viewing Time/Tracking Geometry Adequacy
Monitor Station:	Data Communications - Existing Network Shared or Commercial Service Available
Master Site:	Operational Interface Complexity
Master Site:	Number and Length of Data Links
Upload Station (Nav Data):	Availability

DOD Site Possession

Vulnerability

SGLS Compatibility

Upload Opportunity

### 3. CANDIDATES

Five existing networks, selected individual sites, and selected combinations of network stations are analyzed for applicability to GPS. The networks include:

- (1) Air Force Satellite Control Facility (AFSCF)
- (2) Naval Astronautics Group (NAG)
- (3) 4000th Aerospace Applications Group (AAG)
- (4) TRANET
- (5) Navigation Technology Satellite (NTS)

The sites comprising these networks are identified in Appendix I.

From these candidate networks, four alternate site configurations were defined and evaluated by computer simulations for tracking visibility and geometry adequacy. The definition of the alternate configurations follows:

#### Alternate I

Monitor Sites:	FAIR LIZA Vandenberg or Pt. Mugu Cape Kennedy area
Master Site:	BELT
Uplink Facility:	FAIR (Nav. Data & Satellite Commands)
TLM:	FAIR
Off-Line Computations:	NWL

Alternate II

Monitor Sites:                      Wahiawa, Hawaii  
  Pt. Mugu, California  
  Rosemont, Minnesota  
  Prospect Harbor, Maine

Master Site:                           Pt. Mugu, California

Uplink:                                Vandenberg, Kodiak, or FAIR (Nav.  
  Data & Satellite Commands)

TLM:                                    AFSCF or AAG

Off-Line Computations:              NWL

Alternate III

Monitor Sites:                      Hawaii  
  Guam  
  Vandenberg  
  Samoa

Master Site:                          AFSTC, Sunnyvale, California

Uplink:                                Kodiak or Vandenberg (Nav. Data &  
  Satellite Commands)

TLM:                                    AFSTC, Sunnyvale, California

Off-Line Computations:              NWL

Alternate IV

Monitor Sites:                      Hawaii  
  Vandenberg  
  Elmendorf AFB, Alaska  
  Prospect Harbor, Maine

Master Site:                          Vandenberg

Uplink Facility:                      GPS - Vandenberg (Nav. Data)

TLM:                                    AFSTC (Satellite Commands)

Off-Line Computations:

NWL

In addition, generalized viewing opportunity computations were performed for all candidate sites on the "optimized" satellite constellations.

#### 4. ANALYSIS

A significant result of this analysis is the verification by simulation of the geometric adequacy of all four candidate Control Segment configurations. This conclusion is valid for the satellite constellation defined by Trade Study No. 2 (and shown in Appendix II) and for User equipment tests in Southwestern CONUS.

Due to the nature of this trade study topic, the analysis is not in complete accord with the prescribed format for trade studies, however all elements of the format are included.

##### 4.1 Comparison Matrix

The comparison matrix that follows ranks on a relative basis only the discernible variations between the acceptable configurations. Criteria met by all configurations and not included in the matrix are: Present DOD site possession, vulnerability, SGLS compatibility, and upload opportunity.

FUNCTION	CRITERIA	Alternates			
		I (AAG)	II (NAG)	III (AFSCF)	IV (JPO)
Monitor Site:	Location:				
	Satellite Viewing Time/ Tracking Geometry Adequacy	2	2	1	2
	Data Communications:				
	Share Existing Network or Commercial Service Available	2	3	4	1
Master Site:	Operational Interface Complexity	2	3	3	1
	Number & length of Data Links	1	2	3	2
Upload Station: (Nav. Data)	Availability	<u>2</u>	<u>3</u>	<u>3</u>	<u>1</u>
	Relative Ranking Point Totals:	9	13	14	7
	Order of Preference:	2	3	4	1

#### 4.2 Viewing Opportunities and Tracking Geometry

The results of computations performed to determine satellite viewing opportunities is summarized in Appendix II. The results of simulations performed to verify the geometric adequacy of the four alternate configurations are presented in Appendix III.

#### 4.3 Other Data Sources\*

For information other than viewing opportunities and tracking geometry, the primary sources for deriving the relative rankings are:

- (1) Visits to the networks<sup>(1,2)</sup>
- (2) Extensive experience with the AFSCF network by our subcontractor Mellonics Division of Litton<sup>(3,4,5)</sup>

Alternatives I, II and III were defined by the contractor. The Alternative IV configuration was defined and evaluated as a result of JPO correspondence<sup>(6,7)</sup>.

The information in this Trade Study supersedes the preliminary analysis presented in the first issue of Design Requirements Bulletin D9000529B.

---

#### \*References:

- (1) Trip Report: Visit to 4000th Aerospace Applications Group, Nov. 13 through 15, 1973, by J. E. Coxey, H. Newman and R. DiPalma.
- (2) Trip Report: Visit to NAG facility, December 13, 1973, by J. E. Coxey, H. Newman and R. DiPalma.
- (3) D9000532B Monitor/Master Data Interface Analysis
- (4) D9000535B Master/SCF Interface Analysis
- (5) D9000536B SCF/Satellite Interface Analysis
- (6) AF letter dated 29 December 1973, with attachments, to attention of F. E. Huggin from Lt. Col. R. H. Jessen, Subject: GP3 Control Segment Alternatives.
- (7) AF letter dated 5 February 1974: Technical Direction to the Definition Contractors; signed by William L. Statham.



## 5. SELECTION

Based upon the criteria and relative ranking point totals in paragraph 4.1, Alternative IV is the preferred Control Segment configuration. The only exception to the configuration defined is that the Monitor Station located at Prospect Harbor, Maine, should be relocated to be more effective.

### Preferred Alternate IV configuration:

Monitor Sites:	(1) Wahiawa, Hawaii (2) Vandenberg AFB, California (3) Elmendorf AFB, Alaska (4) TBD
Master Site:	Vandenberg AFB, California
Upload Station:	Nav. Data - Dedicated GPS ULS at Vandenberg AFB Command Data - AFSCF
Telemetry:	AFSCF
Off-line Computations:	NWL
Data Communications:	Commercial Dial-up

The objective of this trade study has been satisfied and completed by the identification of four technically acceptable Control Segment configurations. Considerations which are not visible to this contractor will drive the final selection by the JPC. Those considerations include the future plans for the utilization of existing network sites, availability of existing buildings to house the Control Segment equipments and, finally, the willingness of host commands to share facilities for the GPS Program.

For two test locations in Southwestern CONUS and for two possible ocean test sites, the viewing opportunities for monitoring and upload functions, for all candidate sites, are shown in Appendix II.

User GDOP's and world-wide viewing opportunities for both three and four satellites are an outgrowth of the constellation optimization analysis and are presented in Trade Study No. 2.

**APPENDIX I**

**NETWORK SITE LOCATIONS**

## NETWORK SITE LOCATIONS

<b>AFSCF:</b>	Satellite Test Center (STC) Remote Tracking Sites (VTC) NHS HTS KTS IOS GTS OL-5	Sunnyvale, California Vandenberg AFB, California New Hampshire Hawaii Kodiak Indian Ocean Guam (Classified Location)
---------------	---	---

**NAG:**

- Pt. Mugu, California
- Wahiawa, Hawaii
- Laguna Peak, California
- Rosemont, Minnesota
- Prospect Harbor, Maine

<b>AAG:</b>	BELT LIZA FAIR	Classified Location Classified Location Classified Location
-------------	----------------------	---

<b>TRANET:</b>	<u>Station</u>	<u>Location</u>
	008	Sao Jose dos Campos, Brazil
	013	Misawa AB, Japan
	014	Elmendorf AFB, Alaska
	016	Barton Stacey, England (British operated)
	018	Thule AFB, Greenland
	020	Mahe, Seychelles Islands, Indian Ocean
	021	Brussels, Belgium (Belgian operated)
	022	NAVCOMMSTAPHIL, San Miguel, Republic of the Phillippines
	023	PWC, NAVSTA, Guam
	103	Las Cruces, New Mexico
	105	Pretoria, South Africa
	110	Smithfield, Australia (Australian operated)
	117	Tafuna, American Samoa
	192	Austin, Texas (University of Texas/ARL operated)
	197	Shemya AS, Alaska
	350	NAF Sigonella, Sicily
	351	Mould Bay, Price Patrick Island, Canada

**NTS Net:**

**Blossom Point, Md (Command only)**

**Guam (Pacific Ocean)**

**Seychelles (Indian Ocean)**

**Samoa (Pacific Ocean)**

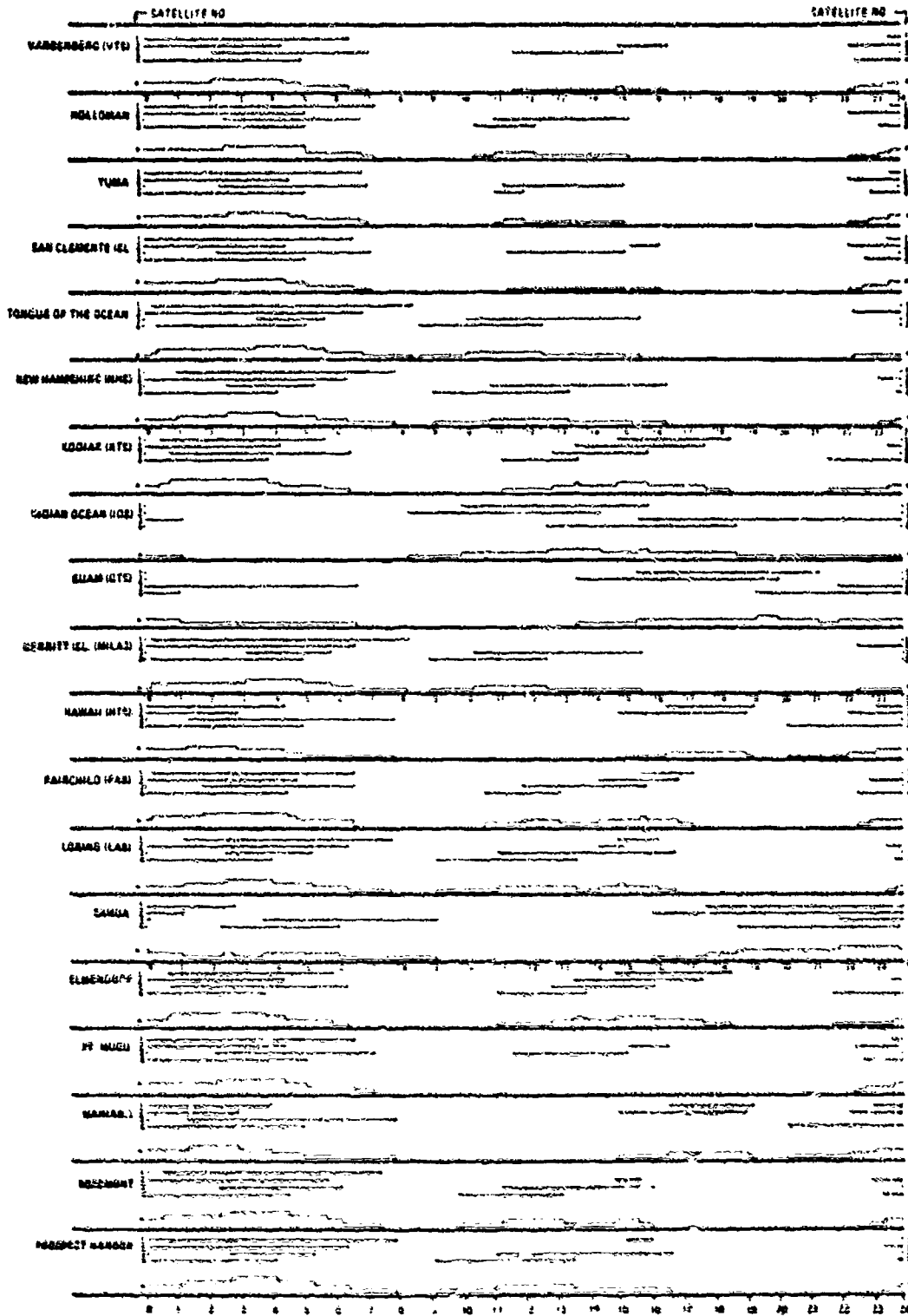
**Richmond, Florida**

**Chesapeake Bay, Md. (about 20 miles S.E. of Washington, D.C.)**

**Hawaii (possibly command links also)**

**APPENDIX II**

**SITE VIEWING OPPORTUNITIES**



QUALITY INDICATIONS BY STATION

SATELLITE	LONG	TR	ACC	WIND	TEMP	PR	REL	ECG	PERIOD	TIME
1	100	100	100	100	100	100	100	100	100	100
2	100	100	100	100	100	100	100	100	100	100
3	100	100	100	100	100	100	100	100	100	100
4	100	100	100	100	100	100	100	100	100	100

SATELLITE STATION NUMBER  
DO NOT WRITE IN THIS COLUMN

APPENDIX III

SIMULATION RESULTS

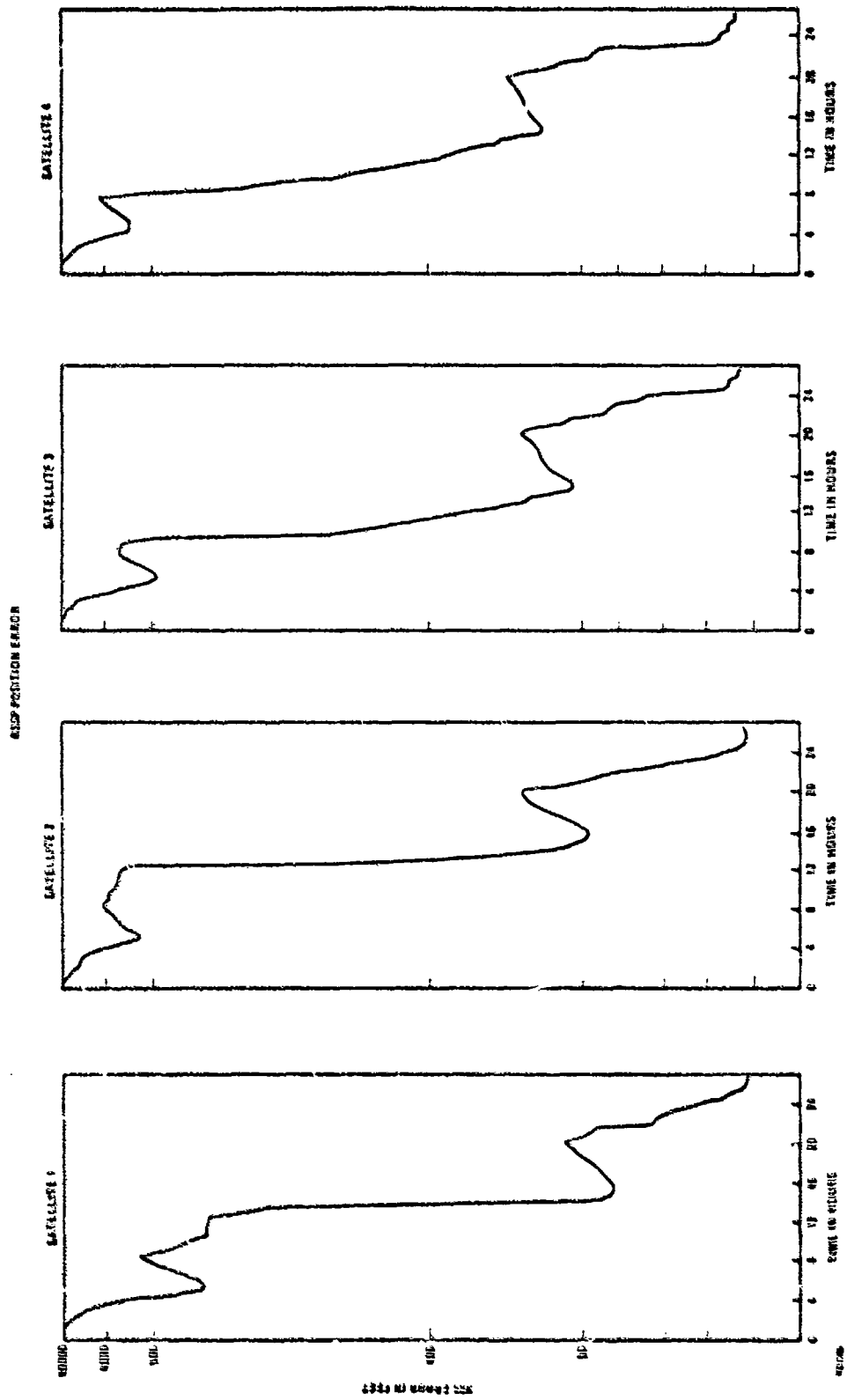
## SIMULATION RESULTS

The relative effectiveness of four alternative tracking station networks was evaluated using the GPS simulation computer programs. This program simulates the real-world dynamics and generates pseudorange measurements which are utilized to update a Kalman filter that provides a current best estimate of satellite positions, velocities, clock offset and clock drifts. The covariance matrix of the solution vector is the statistical estimate of the accuracy of the Kalman filter solution. The charts shown in the following figures are plots depicting the relative accuracy of the four alternative tracking station networks for each of the four satellites in the constellation. The data plots show the square root of the trace of the predicted covariance matrix (just prior to update for measurements) as a function of time for each satellite:

$$\text{RSSP} = \left( \sigma_{x_i}^2 + \sigma_{y_i}^2 + \sigma_{z_i}^2 \right)^{1/2} \quad i = 1, 2, 3, 4$$

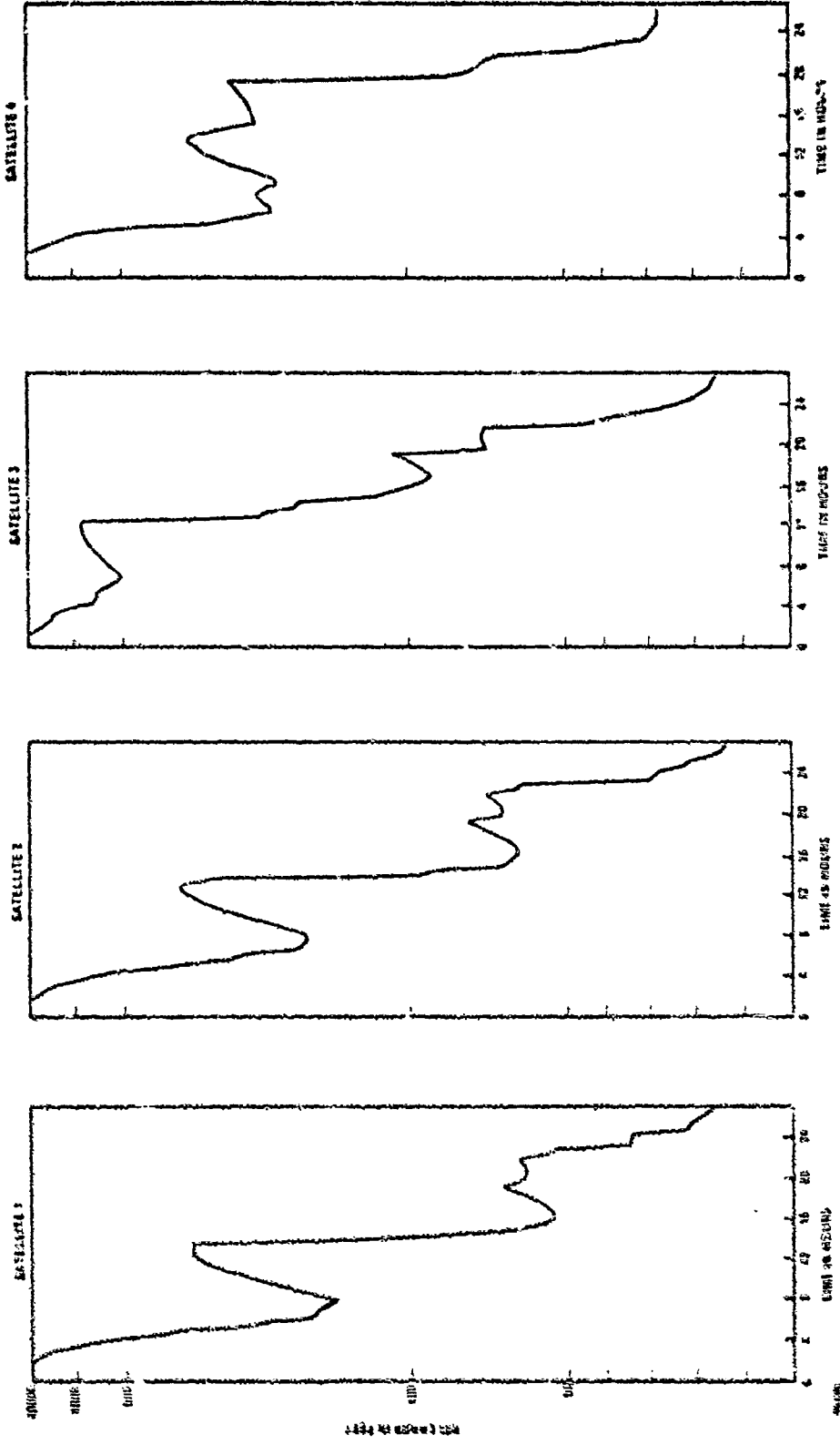
Where  $i$  is the satellite identification.



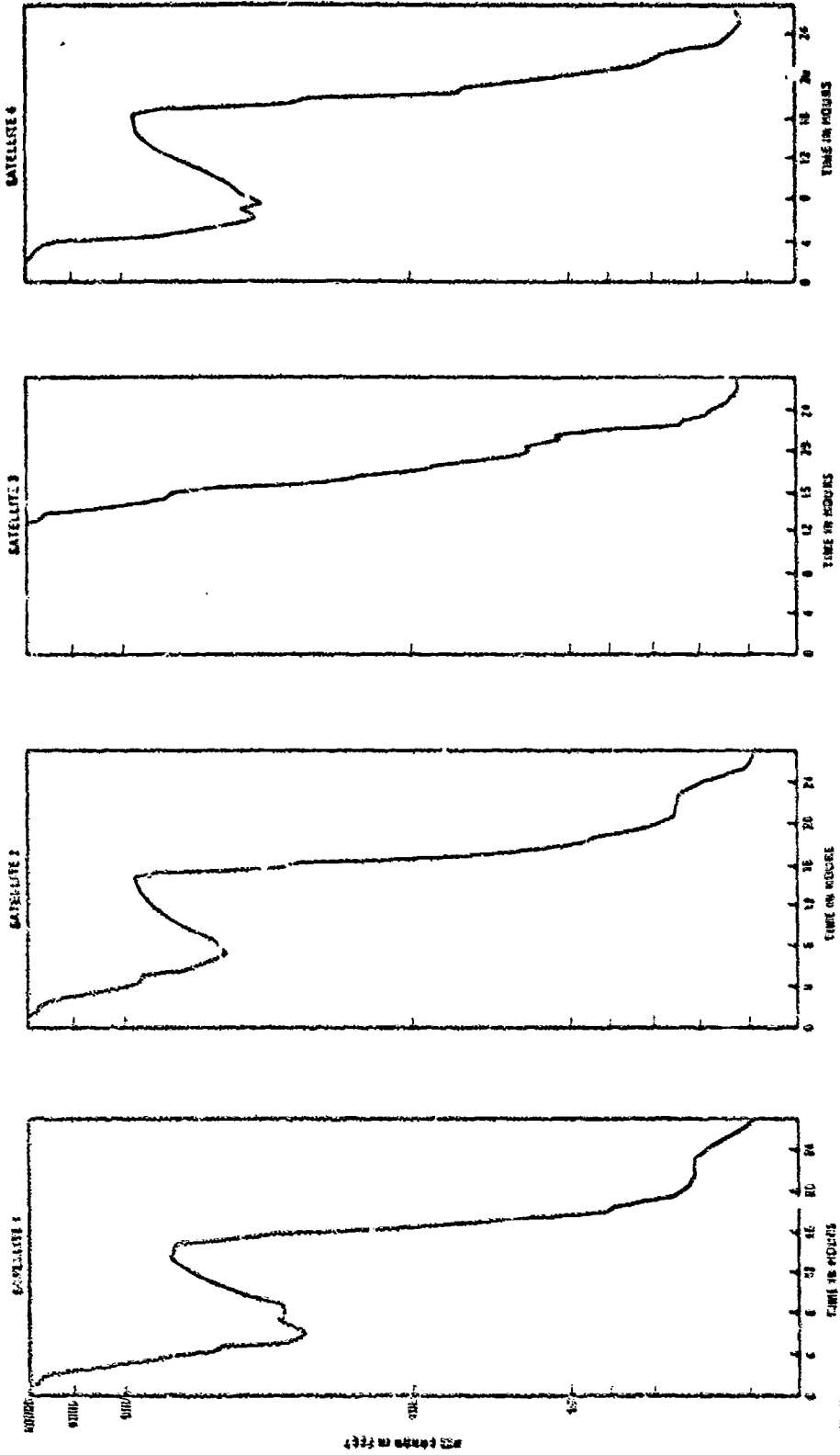


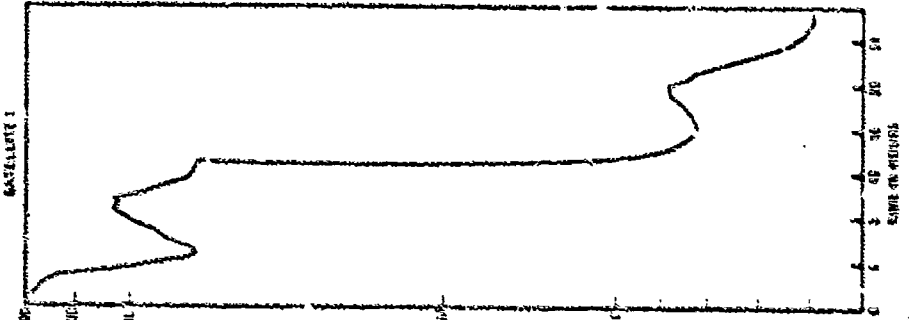
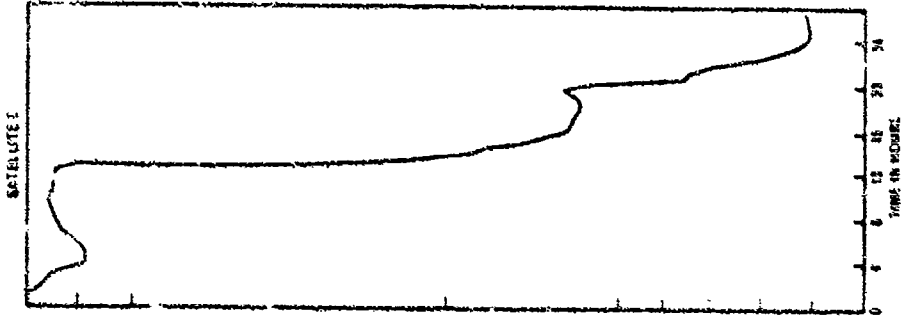
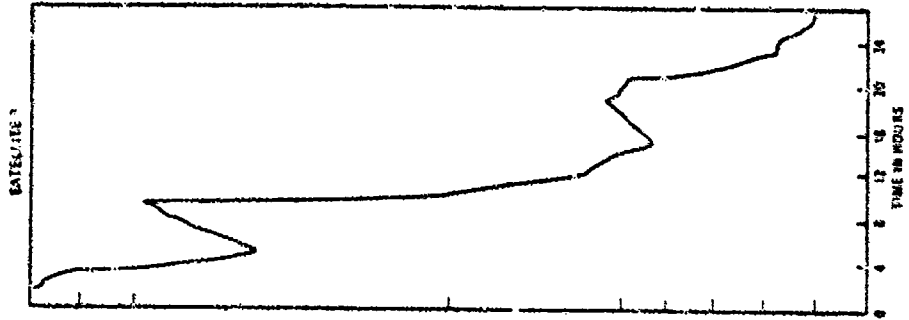
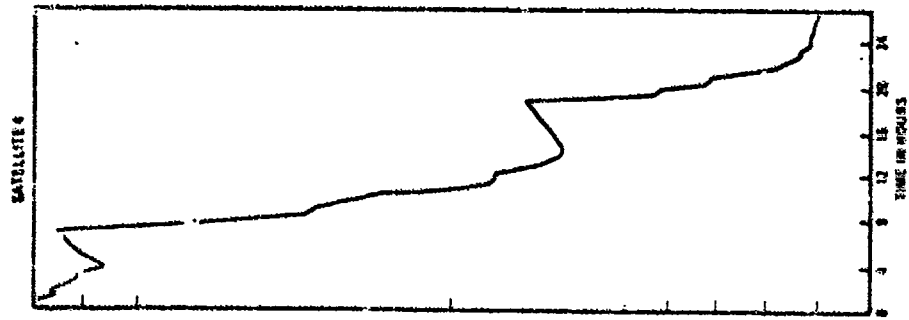
ALTERNATE I

RESP POSITION ENR 2.06



NSIP POSITION ERROR





POSITION ERROR

TRADE STUDY NO. 4

CONTROL SEGMENT COMPUTER SELECTION

W. R. GILLS



**GENERAL DYNAMICS**

*Electronics Division*

P.O. Box 81127, San Diego, California 92138 714-279-7201

## 1. INTRODUCTION

### 1.1 Purpose

This document identifies the rationale and evaluation criteria for choosing appropriate candidate computer systems for the computational, communications, and control requirements of the GPS Control System Segment.

### 1.2 Overview of Selection Concepts

A diagram showing the various computer systems and the interconnecting telecommunication lines for the Control System Segment network is shown in Figure 1.2-1. All computers within this network will be evaluated and selected from the standpoint of integrated hardware/software systems.

The performance of a computer is dependent upon both the quality of the systems software and hardware. From the standpoint of the applications programmer, the hardware and software provide a set of services which are inseparable and indistinguishable components of the system. Software maintenance and systems support are required just as hardware maintenance and support are required. Emphasis on evaluating the total hardware/software/support services capabilities of the competing vendors will be a basic objective in Control System Segment computer system selection.

### 1.3 Impact of Phases II and III on Computer Selection

As stated in SS-GPS-101A, the computer systems selected for Phase I must be expandable to the point of accommodating the requirements of the Phase II 12 satellite constellation. The highly developmental and experimental nature of Phase I also makes the ability to increase internal speeds, central and mass memory and telecommunication handling capacity an absolute necessity. This growth potential will be a highly weighted factor in the selection of computer systems. Growth potential will be more inclusive than having the ability to add on additional or faster devices for improving hardware characteristics. It means that software systems must be available to exploit these features while remaining as adaptable as possible to GPS applications programs.

Phase III will have security, reliability and loading requirements above the capabilities of the initial phases. These, together with the expected advances in computer technology during this period, will undoubtedly result in major, if not total, computer systems replacement. The influence of Phase III requirements on initial computer system selection should not be understated, however. The computer systems, and particularly the MCS system, selected for Phase I should have all the major attributes and capabilities required by the later phases. This subject is discussed further in the Selection Criteria section of this report.

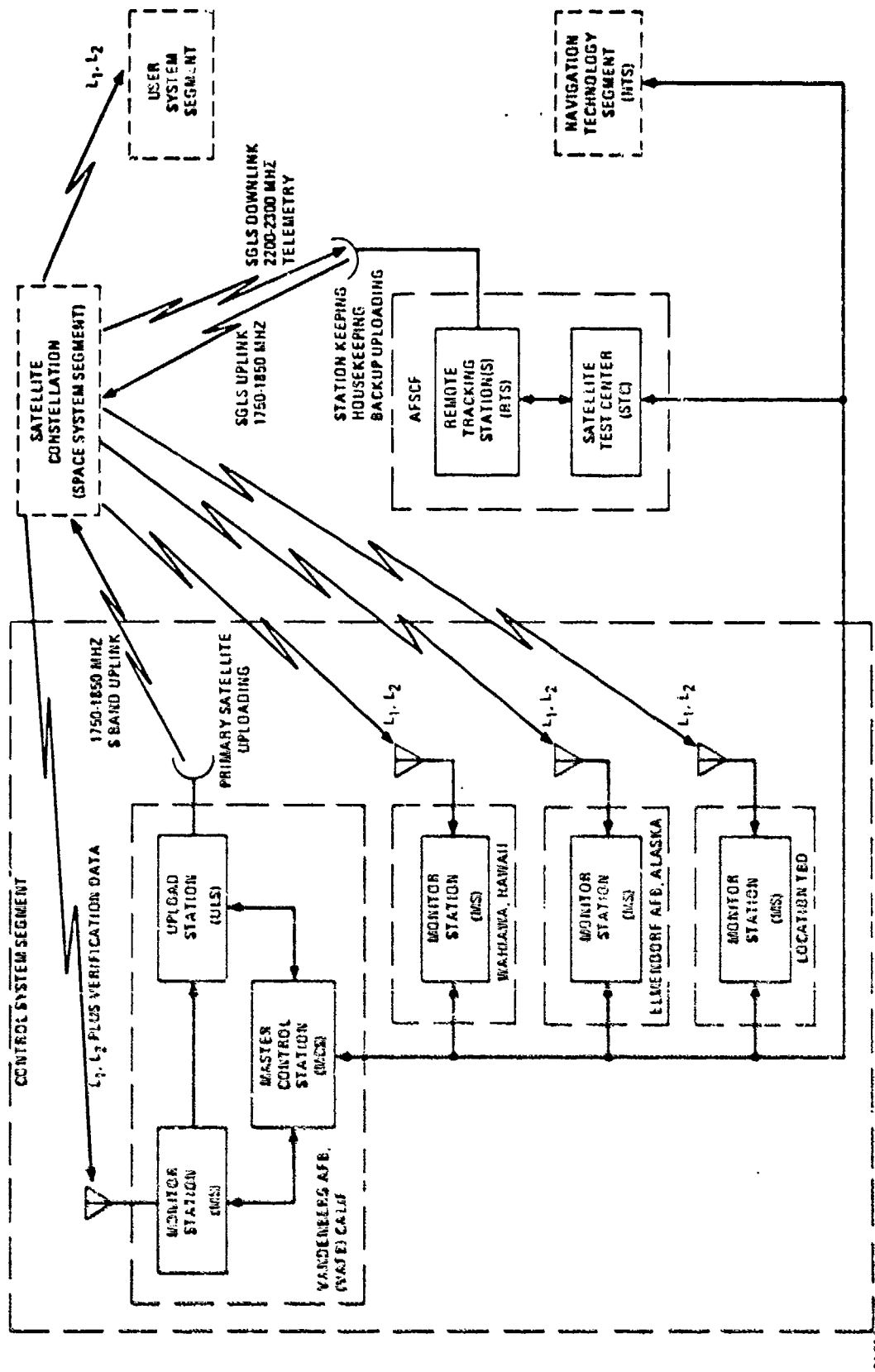


Figure 1.2-1. Global Positioning System (GPS) Overview Interface

## 2. REQUIREMENTS

### 2.1 MCS Computer Functional Requirement

The computational equipment at the MCS shall be sized in speed and memory capacity to support the operation of GPS Phase I software. The equipment will be selected to accommodate expansion to support the operation of twelve closely-space satellites. Responsiveness as indicated by operational time lines for 12 satellites shall be considered in determining the needed computer throughput rate. Source: SS-GPS-101A, para. 3.2.1.2.2.1.

The MCS functional requirements may be categorized as separate computational, communications and control/display functions. Each of the categories is discussed in the following sections.

#### 2.1.1 Computational Functions

The MCS computer must have the speed, central memory and mass storage capacity as well as the extended precision capability to perform the following GPS computational tasks:\*

- Satellite Ephemeris Upgrade
- Satellite Load Data Preparation
- Satellite Polynomial Generation
- System Clock Update
- Tracking Data Processing
- Meteorological Data Processing

#### 2.1.2 Communications Handling Functions

The MCS computer system will handle the routing of all data throughout the Control System Segment network with the exception of the telemetry verification messages from the Monitor Station to the co-located Upload Station. The following data transfers and capabilities will be required:\*\*

- MS to MCS, SV range, environmental and status data
- MCS to Upload Station data set transmission

---

\* Detailed information on the MCS computational requirements may be found in DRB D9000569B.

\*\* Detailed information on MCS computer communications may be found in DRB D9000562B.



- MCS to AFSCF upload data set transmission
- MCS to MS, scheduling and initialization data
- AFSCF to MCS, SV health and status data
- Auto dial-up and answer back capability for all lines
- Capability to initiate dead-start procedures at MS's

### 2.1.3 Control and Display Requirements

All Control System Segment command and control functions will be initiated at the MCS either under the automatic control of the MCS computer system or by the system operator through interaction with the MCS computer system. Displays of system control, status, performance and scheduling information will be provided to the system operator for analysis or information purposes. System control and display functions will be implemented at the MCS on commercially available CRT or hard-copy peripheral devices. Operator control will be through keyboard messages to the system.

### 2.2 MS Computer Functional Requirements

The monitor station hardware and software for GPS Phase I shall be upward compatible from a configuration that will support four satellites to a configuration that will support a constellation of twelve satellites. Source: SS-GPS-101A, para. 3.2.1.2.1.1.

The major functional requirements of the MS computers are as follows:

- A) Controlling receiver sequencing of space vehicle (SV) monitoring
- B) Collecting SV tracking information for determining orbiting parameters of each SV
- C) Determining ionospheric propagation delay corrections
- D) Supporting data communications between the MCS and MS

### 2.3 MCS Computer Design Requirements

The master station computer shall provide the data processing environment needed to host the software; display of system control, status, performance and scheduling; development of new computer programs; and generating hard copy of status, performance, and scheduling information. Source: SS-GPS-101A, para. 3.7.3.1.1.

The MCS Computer System must have sophisticated capabilities to perform the Control System Segment functions described in the preceding sections. These requirements delineate a system which should have the following general attributes and capabilities:

- A) A multi-programming real-time system designed for a range of applications where a number of processes must be monitored concurrently.

- B) Provide simple coupling to on-line processes through a variety of real-time interfaces.
- C) Provide dynamic allocation of system resources for optimum real-time response.
- D) Provide large-scale data management capability through an extensive set of file processing techniques.
- E) Provide an assembler and high-level language compiler.
- F) Provide for straight-forward application program development through on-line editing and debugging techniques.

#### 2.4 MS Computer Design Requirements

The MS computer shall provide the data processing environment needed to host the software for accomplishing the tasks listed in Paragraph 3.7.3.2.2 of SS-GPS-101A.

In addition, the MS computer systems will be designed to operate with a minimum of manual intervention. The hardware/firmware design will include the capability of receiving transmissions from the MSC which will initiate dead-start, loading, testing and execution procedures under the control of the MSC computer or operation. MS software and hardware will have the further mandatory requirements described in Section 4 of this report.

As stated above, software systems and computer hardware must be considered as inseparable components of a computer system. The design requirements for the MS computer will include software, central processor, peripheral equipment and services required to perform the Phase I MS computer tasks. A detailed description of mandatory requirements and desirable features is given in Section 4 of this report.

### 3. GROUND RULES AND REQUIRED INFORMATION

It is reasonable to assume that the Uploading Station and AFSCF Magnetic Tape Terminal will be supported by equipment common or compatible with the MCS computer system. However, the question of whether or not the User Segment, US, and MS common functional requirements should be implemented on the same or compatible computer system is not resolved. Assuming that the US computer is not a compatible member of the same family as the MCS computer, then one of the following approaches must be selected:

- A) US/MS commonality outweighs the commonality of the MCS/MS implementations and the selection of the MS computer will be determined primarily by the selection of the US computer.
- B) Common or compatible systems throughout the Control System Segment outweighs US/MS commonality and requires separate implementation of US functions on the MS computers.

Other ground rules are:

- A) The method of computer selection will be evaluation of bids from vendors responding to RFPs.
- B) RFPs will state specifications of the tasks to be performed, rather than specific means of doing the tasks.
- C) Certain requirements will be considered mandatory: each mandatory requirement must be satisfied or the vendor will be eliminated from further consideration.

To develop specifications for the various tasks to be performed in the computer systems the following information must be provided:

- A) Sequence and maximum time allowable for completion of each computational task.
- B) Precision required for the arithmetic operations of each computational task.
- C) Types, quality, and quantity of all hardcopy documents and display messages to be presented.
- D) The sequence, volume, frequency of transmission and kind of information to be transmitted through all points of the Control System Segment network.
- E) How soon the various kinds of information must arrive to be useful. What intervals the information is to be transmitted and when. How much delay is permissible and the penalty for delays.
- F) How the total system is going to grow and the rate of growth from the initial installation in Phase I on through later phases of the GPS program.

Most of this information will be available from the MCS and MS computer hardware specifications in sufficient detail to be incorporated in the RFP for potential vendors.

#### **4. EVALUATION CRITERIA**

For purposes of evaluating vendors, the GPS Control System Segment computer specifications are divided into mandatory requirements and desirable features. All mandatory requirements must be satisfied or the vendor is eliminated from further consideration. The desirable or discriminatory features form the basis for selecting the winning proposal. The degree of the vendors' ability to satisfy the desirable features will be the principle means of evaluating the proposals.

##### **4.1 Systems Software Mandatory Requirements**

The capabilities outlined in Section 1 and in SS-GPS-101A require that the MCS computer be supplied with an operating system capable of supporting a number of complex software functions. The applicability, soundness and maintainability of this must be insured by making the following mandatory requirements:

- A) The systems software supplied by the manufacturer will have been in use at installations of at least 10 separate organizations for a period of at least one year prior to its initial installation for program development.
- B) The manufacturer must be capable of supplying a resident systems analyst trained and experienced with the supplied software in applications having requirements similar to the GPS Control System Segment.
- C) Complete detailed documentation on the systems software as well as source listings, flow-charts and source decks must be available from the vendor.
- D) USAS FORTRAN IV compiler and symbolic assembler must be supplied under the real-time operating system.

##### **4.2 Systems Software Desirable Features**

Some of the following features could be considered requirements for implementing MCS computer applications. They are defined as desirable features in order to evaluate their implementation under each vendors systems software. These features and a short definition of each follows:

- A) **Disk Operating System.** A disk-based system uses random access peripherals as an extension of Executive main memory, and as the principal data interchange medium. This capability is required at the MCS and Uploading Station computers only.

- B) **System Generation.** The process by which a collection of system services are tailored to meet the local physical constraints and performance requirements of the end-user. If MCS and MS use members of a compatible family, the MS system generation will be done on the MCS computer.
- C) **Task Overlay Structure.** A segmented task in which the segment currently being executed may overlay the memory occupied by a previously executed segment belonging to the same task.
- D) **Multiprogramming.** The process of multiplexing two or more resident tasks competing for resources in a single processor.
- E) **Multi-Tasking.** Multi-tasking is the multiprogramming of two or more tasks having a common applications objective. Such tasks need to communicate among themselves and synchronize their activities.
- F) **Shareable Libraries.** A shareable library consists of subroutines that are coded such that they may be interrupted, asynchronously, service another request, either for the current or a different task; then resume later at the point of interruption.
- G) **Foreground/Background.** A foreground/background system is one in which core is partitioned into two separate regions, one for executing real-time tasks and one for execution of low priority, pre-emptible tasks not involved in system operation.
- H) **Power Failure Restart.** Power failure restart is the ability of a system to smooth out intermittent short-term power fluctuations with no apparent loss of service, without losing data, all the while maintaining logical consistency within the system itself and the application tasks.
- I) **Priority Scheduling.** Priority scheduling is the method by which system resources are distributed to active tasks, based solely on the task's priority. With many units executing in parallel, the system must schedule more than just the CPU. As a result, scheduling can be viewed as a 3-step process:
  - 1) Providing tasks with the resources they request
  - 2) Selecting requests to be issued to shared resources (memory pool, and public disks, for example)
  - 3) Selecting tasks for control of the CPU
- J) **Error Reporting.** A centralized error reporting facility is a system service designed specifically for reporting error conditions via a standard interface, available to all tasks in the system.
- K) **Device Independence.** A system which provides the necessary services to make it possible for tasks to process the same type of data on different device types without requiring a program change supports device independence.

- L) **Contingency Exits.** Subroutines automatically entered as the result of an unanticipated synchronous condition, or as the result of an asynchronous condition (anticipated or unanticipated) are contingency exit routines, and the conditions which triggered their entry are contingency exit conditions.

Synchronous exit conditions are those which, if they occur, are the result of a specific instruction encountering an unanticipated event, and if the code sequence up to and including the instruction were repeated under identical conditions, the same unanticipated event would occur. An example is floating point underflow.

- By contrast, asynchronous conditions are not associated with a specific instruction execution and the point of exit for the condition in the code is unpredictable. An I/O termination is an example of an asynchronous condition.

- M) **Common File System.** A File System is the collection of system services which permits a user to view his I/O as a transaction between his program and a name, protected collection of records.
- N) **System Operator Control.** A system which assumes the presence of a human operator and centralizes the functions of initiation run-time control and shutdown through a uniquely identifiable device (or devices) under the direct, exclusive control of the human operator provides operator console system control.
- O) **Batch Job Stream Operation.** Single-stream batch is the facility whereby the system processes a single job, described by a job control language and entered into the to-be-processed queue, requiring no operator intervention except stream initiation. Such a facility consists of:
  - 1) Job Control Language
  - 2) Job Scheduler
  - 3) Reader/Writer
- P) Others may be added.

#### 4.3 Central Processor - Mandatory Requirements

- A) The central memory must initially be equivalent to 64K words of 16-bit memory with field expandability to at least 128K for the MCS computer and field expandability to at least 32K for all other computers in the Control System Segment.
- B) The central processor internal speeds must be capable of at least a 50% increase over the initial configuration by field installed options such as faster memory modules or a second CPU sharing central memory.

- C) The field installed memory expansion and internal speed improvement components must be fully supported by, or transparent to, all supplied systems software.
- D) All the models of central processors used in all Control System Segment stations must have been installed in at least five other separate user installations for a period of at least six months prior to its installation for GPS program development.
- E) CPU's must allow for mass storage expandability by the addition of units to at least 100% above initial configuration.

#### 4.4 Central Processor-Desirable Features

- A) Integer multiply/divide hardware as options if not supplied as standard equipment.
- B) Single precision and extended floating point hardware with a 64-bit floating point operand precision either as options or as standard equipment.
- C) Both program-controlled and high-speed (DMA) data transfer between memory and peripherals.

#### 4.5 Peripheral Equipment-Mandatory Requirements

- A) All peripheral devices and interfaces must be fully supported under the supplied systems software and be designed to be directly compatible with the central processor hardware.
- B) All peripheral device controllers and interfaces must be supplied by the manufacturer of the device or the manufacturer of the central processor.
- C) All peripheral devices must be standard, commercially available equipment and must have been installed in at least 10 installations for at least one year prior to installation of the GPS development configuration.

#### 4.6 Peripheral Equipment-Desirable Features

- A) Central processors manufacturer is capable of supplying all peripherals, controllers and interfaces.
- B) Disk drives with removable disks having at least 1 million 16-bit word capacity per disk with a transfer rate no less than 1 million bits per second.
- C) Industry standard magnetic tape drives capable of producing compatible 7-track, 200, 500 and 800 bits per inch recording density.
- D) Line printer with print speed of at least 300 lines per minute of 132 column lines.
- E) Card reader with read speed of at least 300 full 80 columns punched cards per minute.

- F) CRT display with ability to display at least 20 lines of at least 72 alphanumeric characters per line, per screen page.
- G) Teletypewriter. Model 33 ASR, or similar printer should be supplied with central processor for system operators and hardware maintenance service.

#### 4.7 Services and Support-Mandatory Requirements

- A) Maintenance service must be supplied by the service organization either by MCS resident service personnel or within a period TBD.
- B) Complete documentation of all software/hardware and interfacing will be available.
- C) Applications and system software consulting by manufacturers' systems specialists must be available.

#### 4.8 Services and Support-Desirable Features

- A) All maintenance of all computer equipment supplied by one service organization.
- B) Programming training supplied by manufacturer.
- C) Spare parts and back-up configurations within 100 miles distance from MCS and response to services calls made within 2 hours. MS response time to service calls must be made within 24 hours.



## 5. COMPUTER MANUFACTURES CANDIDATES

The following manufacturers either meet, or are likely to meet by installation date, all the preceding mandatory requirements. This list is limited to manufacturers capable of supplying all computers employed in the GPS Control System Segment network. This limitation is imposed by the assumption that program development for all other computers will be accomplished on the MCS computer system. If US computer selection determines MS computer selection, it is still desirable to have compatible equipment at the MCS, Uploading Station, and the AFSCF Terminal.

Two obvious omissions from the candidate manufacturers above are Interdata Inc. and System Engineering Laboratories. The Interdata 7/32 does not meet the mandatory requirement of having its operating system in use for one year prior to installation. The SEL 80 series appear to be excellent machines but are overpowered and overpriced for Phase I of GPS Control System Segment application. Moreover, SEL provides no compatible machines suitable for the MS or Uploading Stations.

## 6. ANALYSIS

The comparison matrix shown in Table 6-1 gives some of the hardware and software characteristics of the MCS computer candidates. Compatible computers in the same family would be chosen for the MS computers. For instance, if the Data General 840 were selected as the MCS computer, the Data General Nova 2 would be selected as the MS computer. Each of the MS computer candidates are capable of performing the MS tasks and compatibility with

Table 5-1. Candidate Computers

Manufacturer	MCS Candidate	MS Candidate	Possible US Candidate
Data General Corp.	840	Nova 2	Relm Rugged Novas
Digital Equipment Corp.	11/45	11/40	11/20R
Hewlett-Packard	3000	2100	2100*
Modular Computer System	IV	II	N/A
Varian Associates	V73	V73 or 620	R620

\*NOTE: The H-P 2100 is not ruggedized but undergoes more stringent testing and has been successfully used in more airborne and maritime applications than any of the other standard versions of microcomputers.

Table 6-1. MCS Computer Comparison Matrix

Characteristics	Data Gen <sup>1</sup> 840	Dec 11/45	H/P 3000	Mod Comp IV	Varian V73
<u>Central Processor</u>					
Number of Registers	6	16	Stack	240	16
Add Time, sec/word	.80	.75-1.90	1.05	.80 (32B)	1.32
Hdw. Extended Precision	64 Bits	64 Bits	48Bits*	64 Bits	64 Bits
Hdw. Byte Manipulation	Std.	Std.	Std.	Std.	Std.
Real-Time Clock	Opt.	Opt.	Std.	Opt.	Std.
Pwr. Failure Protect	Opt.	Std.	Std.	Std.	Std.
MCS Suitability	Good	Good	*Marginal	Good	Good
<u>Central Memory</u>					
Cycle Time, sec	.80	.85	.90	.64	.66
Max. Capacity, Words	131K	124K	65K*	262K	262K
Parity Checking	No	Std.	Std.	Std.	Opt.
Storage Protect	Std.	Opt.	Std.	Std.	Opt.
MCS Suitability	Good	Good	*Marginal	Good	Good
<u>Peripheral Equip.</u>					
Mag. Tape, 7 Track, 200 BPI	Yes	Yes	Not Std. *	Yes	Yes
Interchangeable Disk	Yes	Yes	Yes	Yes	Yes
Card Reader, LPM	225/400	300	600/1200	300/1000	300/1000
Line Printer	245*	300/1200	300/1200	300/1200	245/1200
MCS Suitability	*Fair	Good	*Fair	Good	Good
<u>I/O Control</u>					
I/O Word Size, Bit	16	16	16	16	16
DMA Channel	Std.	Std.	Std.	Opt.	Std.
Max. Xfer Rate, Words	1.25M	1.16M	1.40M	1.56M	1.50M
Interrupt Levels	16	Variable	253	8-16	8-64
MCS Suitability	Good	Good	Good	Good	Good
<u>Systems Software</u>					
Real-Time Op. System	RDOS	RSX-11Z	TBD	MAX BI	Vortex*
Fortran IV ASCII Std.	Yes	Yes	Yes	Yes	Yes
Macro Assembler	No	Yes	Yes	Yes	No
MCS Suitability	Good	Excel.	Good	Good	*Fair
Preliminary Ranking	2	1	5	3	4

the MSC system would outweigh any advantages other MS computer candidates might have. The foregoing assumes that US computer selection will not necessarily determine the selection of MS computers. The ideal situation would be that optimum computer systems for MCS, MS and US could all be chosen from the same manufacturer's compatible line.

The MCS computer complex will be supplied with a full line of peripheral equipment for satisfying all MCS operational requirements as well as for program development for the MCS, Uploading Station and AFCE Terminal. The MS computer program development will also be accomplished on this system if compatible MS computers are chosen.

The preliminary ranking in the Comparison Matrix does not take into consideration some vital factors which will weigh heavily in the analysis and evaluation of the various manufacturers before final selections are made. Some of these are as follows:

- A) Financial status and stability of the vendor
- B) Ability to provide the support functions outlined in Sections 4.7 and 4.8
- C) Reliability of hardware and software

Weighted scoring and cost-value analysis techniques are being developed for evaluating competent vendors' bids on the Control System Segment computer systems. These will weigh all factors from the importance they play in the developmental and operational success of the program.

## 7. SELECTION

Computer system selection will be based on thorough analysis and evaluation of all hardware, software system and service capabilities of the vendors who meet all mandatory requirements for the GPS Control System Segment. RFP's will be issued to all competent vendors with a deadline of no more than four weeks for reply. The final selection should be made within two months of this deadline. It is assumed that preliminary tests such as the running of representative benchmarks or kernels will have been made.

TRADE STUDY NO. 5

USER SEGMENT COMPUTER

E. Martin



**GENERAL DYNAMICS**

*Electronics Division*

P.O. Box 81127, San Diego, California 92128 714-273-7301

## 1. INTRODUCTION

Selection of the computer for the GPS User Segment involves a survey of a number of existing computer candidates which may be viable contenders to meet the requirements determined or defined to fulfill the user processor function. This selection is a trade study in that the result is constrained to be cost effective in terms of total procurement dollars for the hardware and development dollars for the software. An additional constraint of low technical risk is also a factor in that the computer hardware and software should be reliable during tests and readily modified to meet the changing demands of the development program.

The eventual emphasis of the GPS program will be on the development and delivery of low cost user equipment which meets the varied operational requirements of each user class, and which also exhibits low cost of ownership, hence, is easily maintained and extremely reliable. The forerunner of this concept will be the Class C computer prototype which represents a unique set of requirements and trades since it will be a model design-to-cost effort different from the general scope of the other equipment development. The future Class C design and selection is excluded from this trade study for this reason. It should be noted that the trade study is also concerned with computers which are truly presently available and is not intended to be valid beyond the Phase I time frame, and is certainly not concerned with the potential computer options expected to be available during Phase II or Phase III due to expanding technological developments.

## 2. REQUIREMENTS

### 2.1 Functional Requirements

The user equipment computer functional requirements consist of two major areas: 1) software and 2) hardware and I/O. The software has been divided into eight task areas:

1. Executive Control
2. Software Initialization
3. Space Vehicle Selection
4. Measurement Processing
5. Navigation
6. Display
7. Self-Test
8. Navigation Aids

All of the tasks are described in paragraph 3.7.2.3 of SS-GPS-101A dated 29 January 1974.

The remainder of the functional requirements are:

1. The receiver accepts navigation signals and processes them to provide digital data from which the computer will calculate position and velocity.
2. The computer outputs digital data to the receiver for code changing.
3. Information is able to flow from the computer to the receiver.
4. The computer can accept data from the receiver and auxiliary sensors.
5. The computer is able to provide inputs to other navigation devices.
6. The user computer is reprogrammable and permits expansion in an economical manner.
7. Processor capability consistent with a double precision add time on the order of 5 microseconds.

These requirements are basically the general functional characteristics delineated in the Annex 1 attachment to the RFP as presented in paragraphs 6.5 and 6.6.

## 2.2 Derived Design Requirements

The basic computer design requirements derived from study of the system development and technical performance concepts are summarized at the highest level by the general system requirement which is:

- a. Computer shall be consistent with a low cost user equipment concept.
- b. Computer will provide the developmental Phase I user equipment with high conditional availability during the validation test programs.
- c. Flexibility should be deliberately maintained to provide for modifications during the development testing.

A study of system computer functions by potential user classes and by operating mode configurations has been performed (DRB D9000598B "User Equipment Computer Programs".) This effort established the basic memory storage and execution time requirements for the computer. It should be noted that execution time is determined by the size of the estimation filter employed and the estimation update rate in conjunction with the basic machine speed which is a hardware restriction. Memory requirements by mode are summarized in Table 2.2-1.

Throughput estimates for the computer programs were derived on the basis of a 12 state Kalman filter whose update rate is once each 5 seconds. Maximum required baseline throughput was estimated at 220-250 KOPS (K operations per second) with the assumption of a 1.0 to 2.0 microsecond machine cycle time with a contemporary instruction speed set. Baseline

Table 2.2-1. Baseline Memory Sizing

Mode	Memory Allocation 16 Bit Words
Continuous IMU Aided Class A, B, F	15,800
Continuous AMDR Aided Class A, B	11,500
Sequential Class C, D, E	6,800

design requirements dictated a computer which would have the following characteristics shown in Table 2.2-2.

### 2.3 Ground Rules

With the large number of candidate systems which are encountered in the current computer technology (approximately 170 military or quasi-military computer designs were initially surveyed). A set of ad hoc ground rules was used to initially establish a manageable sorting

Table 2.2-2. Baseline Computer Characteristics

Memory Capacity	4K, 8K, 16K
Cycle Time	1.0 Microsecond
Stored Program	General Purpose
Organization	Parallel 16 Bit Processor
Data Word	16/32 Bit
Arithmetic	Binary, Fixed Point, Floating
Instructions	16/32
Input/Output	16 Bit Parallel I DMA
Interrupts	External and Internal
Execution	2.0 Microsecond Add 10-20 Microsecond Multiply

of design information. (The initial constraints are documented in DRB 9000597B "User Equipment Computer Selection".) These initial constraints were used to establish the following set of ground rules:

- 16-bit x 16K memory for airborne aided applications
- Avionic computer design with viable MIL-SPEC operation
- Previous or imminent military avionic application to insure availability and producibility
- Demonstrated or visible potential for IMU integration
- Sufficient thruput for high filter rate
- Floating point hardware

Changes to these ground rules is continually possible because the basic design requirements really must be responsive to the technical objectives of the program and to the operational constraints defined for the system. Feedback and changes as a function of preliminary design constraints and varying software requirement tend to alter the computer design requirements with time.

#### 2.4 Evaluation Criteria

Using the design requirements discussed above the selection process still requires a set of given evaluation criteria to make comparisons between the potential candidate computers. The selected criteria employed at present for the design trades are:

1. Higher Order Language  
Much of the time and money spent for any new computer related program is in the area of programming costs. Employment of a higher order language offers the potential for reducing excessive software programming delays and provides better visibility of the computer program and functions. Many candidate languages exist such as FORTRAN, CMS, JOVIAL, BASIC, and ALGOL plus many others. The use of a higher order language, HOL, requires that software packages must be developed for the computer and a compiler or interpreter must also be employed.
2. Hardware Multiply/Divide  
This criteria is a restriction on performance of the computer hardware. In addition to the hardware multiply, an add time of 3  $\mu$ seconds was also included to handle the real time control and computations anticipated in the program.
3. Floating Point Hardware  
Generally the cost of floating point hardware can be justified by the reduction in software programming difficulties.



4. Environmental Qualification

Two basic forms of qualified computer hardware designs are presently employed. In the military hardware, the computers are tested to applicable MIL SPEC such as MIL-E-5400, MIL-E-16400, or MIL-E-4158 for airborne, shipborne or ground based equipments. The commercial hardware utilizes a "ruggedized" category of limited testing which is in excess of benign laboratory conditions.

5. Reliability (Predicted or Demonstrated)

Data on reliability of the equipment would establish its capability for being available during extended testing conditions which will be encountered during the development program.

6. Cost

For the present exercise only costs associated with the basic computer and a "standard" I/O capability is indicated based on budgeting estimates for 10 to 20 units. Expanded cost comparisons based on full complements of peripherals will be accomplished later.

3. CANDIDATE COMPUTERS

The compilation of viable computers has been grouped into two distinct categories which are the military computers and the commercial minicomputers. The military computer candidates are given in Table 3-1.

Commercial minicomputer candidates were also considered but since the list of machines is so extensive only the computers listed in Table 3-2 were initially selected based on having a FORTRAN capability as a qualifying requirement.

Table 3-1. Listing of Military Candidates

Manufacturer	Model Number
Singer Kearfott	SKC 2000
International Business Machine	4P1-CP2
International Business Machine	4P1-TC2
International Business Machine	4P1-AP1
Univac	1830A
Univac	1832
Univac	MPC-16
Univac	AN/UYK-20
Control Data Corp.	469
Control Data Corp.	ALFA 1
General Electric	CP32A
Magnavox	MAXAL
Lear Siegler	LS52
Rohm	NOVA-1602
Teledyne	TDY 43
Rockwell International	D216

Table 3-2. Established Minicomputer Candidates

Manufacturer	Model Number
Computer Automation	Alpha 16, Naked mini 16
CDC	1700, SC-1700
Data General	Nova 800, 820, 1200, 1210, 1220, Super, Super SC
DCC	D-116 (same as Nova)
DEC	PDF 11 - 03, -05, -10, -15, -20, -35, -45
Digital Scientific	META-4
Electronic Associates	PACER
FMR	6145
General Automation	SPC-16, 1930
General Electric	3010/2
GTE	Tempo 1, 11
Hewlett-Packard	2100A, 3000
Honeywell	316, 516, 700
Interdata	70, 80
Lockheed	MAC 16, MAC Jr., SUE-1110
Modular Computer Systems	MODCOMP-1, -11, -111
Omnitac	BIT 483
Raytheon	703, 704, 706
ROLM Corp.	Rugged Nova -1601, -1602
System Eng. Lab	-71, -72
TI	960A, 980
VARIAN	620A, 1100, L, L-100, RL, 73
Westinghouse	2500
Xerox Data Systems	CP16A

## 4. ANALYSIS

Material investigated and derived from the trade analyses and studies is summarized in this section by comparing the candidates against the evaluation criteria. Additional supportive data and trade study factors which will influence the final selection are also presented.

### 4.1 Evaluation Comparison

Comparison of the military and commercial minicomputer candidates is provided in separate comparison arrays. The military (Table 4.1-1) and commercial (Table 4.1-2) computers are separately listed but are evaluated against the same criteria.

The commercial minicomputer list is selectively reduced as one applies the various evaluation criteria. This attrition is indicated in Table 4.1-2. The imposition of a ruggedized or partially operationally qualified commercial version lead to only two potential candidates, the Honeywell 516 and the Rugged Nova-1602R. Further evaluation in terms of reliability and cost of these candidates is still being presently pursued.

### 4.2 Supportive Data

In addition to the specific design requirements and evaluation criteria presented, there are a large number of suggested parameters which influence computer selection. A brief summary of these cogent factors is given in the following paragraphs. These factors are grouped into areas of hardware considerations, software considerations, and technological considerations.

#### 4.2.1 Hardware Considerations

##### 4.2.1.1 Word Length

<u>Word Length</u>	<u>Advantages</u>
8	Compatible with byte I/O
12	Divisible by 2, 3, 4, 6, 8, and 12
16	Most popular, low cost, software available
24	Two word floating point accurate enough for navigation, Kalman filter
32	Most powerful in computation

##### 4.2.1.2 Memory Parity

<u>Memory Parity</u>	<u>Advantages</u>
Yes	Increases reliability of system
No	Lower cost

Table 4.1-1. Military Evaluation Matrix

TRADE CATEGORY	TRADE CATEGORY	HIGHER ORDER LANGUAGE	HARDWARE MULTIPLY/DIVIDE 3 #SEC ADD	FLOATING POINT HARDWARE	ENVIRONMENTAL QUALIFICATION	RELIABILITY MTBF (HRS)	COST (PER 1 UNIT AND STANDARD I/O)
ENGINE	SEC 2000	FORTRAN	✓	✓	MIL-E-5400	8000	140K
IBM	CP1-CP2	NONE	✓	NO	MIL-E-5400	2000	65K
	CP3-CP7	NONE	5.0 ADD	SOFTWARE ONLY	MIL-E-5400	6000	65K
	CP1-CP4	NONE		NO	MIL-E-5400	6000	65K
	CP5-CP7	NONE		NO	MIL-E-5400	2000	160K
CITEAC	1620A	FORTRAN IV	✓	NO	MIL-E-16400	7000	205K
	1622	CMS MONVAL	✓	✓	MIL-E-16400	4000	73K
	1620-16	FORTRAN IV	✓	✓	MIL-E-5400	2000	TBD
	AN/CVR-26	CMS	✓	PROPOSED	MIL-E-16400	2000	TBD
CIC	609	NONE	NO	NO	MIL-E-5400	7000	30K
	ALFA I	FORTRAN	✓	NO	TBD	7000	350K
GI	ALPHA	FORTRAN	✓	OPTIONAL	MIL-E-5400	8000	160K
MACRAVON	MACAL	EASY	✓	NO	MIL-E-16400	12000	30K
LIFE EVIDER	1602	NONE	✓	✓	MIL-E-5400	8000	45K
	1604-1609	FORTRAN BASIC	3.25 ADD	✓	MIL-E-5400	8000	50K
PHILIPINE	TD-03	NONE	NO	SOFTWARE	MIL-E-5400	TBD	TBD
ROCKWELL	1616	(FORTRAN DEV.)	TBD	TBD	MIL-E-5400	TBD	TBD

Table 4.1-2. Commercial Minicomputer Evaluation Matrix

MANUFACTURER	MODELS WITH FORTRAN I/O	OPTIONAL HARDWARE MULT/DIVIDE PLUS 3 μSEC ADD TIME	OPTIONAL FLOATING POINT	RUGGEDIZED QUALIFICATION
Computer Associates	Alpha 16, Naked mini 16			
DEC	P100, BK-1700	(1700)		
Digital Equipment	Nova 800, 810, 1200, 1210, 1220, Super, Super BC	(Nova 800, 810, 1200, 1210, 1220, Super, Super BC)		
DEC	D-116 (same as Nova)	(D-116) (same as Nova)		
DEC	PDP 11-05, -05, -10, -15, -20, -25, -45	(PDP 11-05, -05, -10, -15, -20, -25, -45)	PDP 11-35, -45	PDP 11-520
Digital Scientific	META-4	(META-4)	META-4	
Electronic Associates	PACER	(PACER)	PACER	
EMC	6145	(6145)	6145	
General Automation	SPC-16, 1630	(SPC-16, 1630)		
General Electric	3010/2	(3010/2)	3010/2	
CYR	Tempo 1, 11	(Tempo 1, 11)		
Hewlett-Packard	2100A, 3000	(2100A, 3000)	3000	
Honeywell	316, 516, 700	(316, 700)	516	516
Integrals	70, 80	(70, 80)	70, 80	
Intelcor	MAC 16, MAC Jr., SUE-1110	(MAC 16, MAC Jr., SUE-1110)		
Leitch Computer Systems	MODCOMP-1, -11, -111	(MODCOMP-1, -11, -111)	MODCOMP-111	
Cometec	BIT 483	(BIT 483)	BIT 483	
Parsons	704, 706, 708	(704, 706)		
NEC Corp.	Rugged Nova - 1601, -1602	(Rugged Nova - 1602)	(Rugged Nova - 1602)	Rugged Nova - 1602
Systems Eng. Inc.	71, 72			
TI	930A, 930B	(930)		
VATLASH	6510/1, 1100, L, L-100, RL, 73	(6510/1, 1100, L-100, 73)	73	R-620/L
Whalingham	2500	2500	2500	
Novas Data Systems	CF-16A			

Comments:

1. Core Memory rarely has parity errors hence the requirement is not mandatory.
2. Military environment requires parity.
3. Solid state memories being unproven should have parity.

4.2.1.3 Programmable Environment in CPU

Programmable Environment

Advantages

Accumulators/Index Registers

1. Older concept (more experience available).
2. Easier to program and debug on an in-experienced level.
3. Less time and storage required generally to switch environment in an interrupt driven, multiprogramming situation.

Register File

1. Execution of loops and subroutines generally faster.
2. High level language compilers are easier to write and understand.
3. Any register can be used as accumulator or index register.

Comment: HOL on an inexperienced level hide any differences from the programmer.

4.2.1.4 Hardware Stack

Hardware Stack

Advantages

Yes

1. Subroutine reentrance automatic.
2. Interrupt handling and nesting automatic.
3. Hardware maintenance of system queues automatic.
4. Compiler translation almost at run time.

No

1. Less confusing for programmer.

4.2.1.5 Interrupt System

Methods

Advantages

Vectored (encoded)

1. Automatic device identification (low software overhead).
  2. Environment switching accomplished faster.
  3. More reliable.
  4. In conjunction with stack architecture, operates well within a operating system.
1. Greater flexibility for unusual applications.

Discrete (unencoded)

#### 4.2.1.6 I/O Bus Definition

<u>Methods</u>	<u>Advantages</u>
Common in GPS	<ol style="list-style-type: none"><li>1. Low second sourcing cost.</li><li>2. High legacy.</li><li>3. Low production cost.</li><li>4. Hardware commonality</li></ol>
Different from CPU to CPU	<ol style="list-style-type: none"><li>1. Lower initial cost.</li></ol>

Comment: It might be highly desirable to define each I/O Bus for standard I/O devices.

#### 4.2.1.7 Directly Addressable Words

<u>Size</u>	<u>Advantages</u>
256 or 1024 (page size)	<ol style="list-style-type: none"><li>1. Instruction including address fits in one memory word, hence every memory word can be interpreted as an instruction.</li><li>2. Small programs more compact.</li></ol>
All of Memory	<ol style="list-style-type: none"><li>1. Much greater flexibility for programmer.</li><li>2. Possibility of running out of directly addressable memory does not exist.</li><li>3. HOL compilers greatly simplified.</li><li>4. Linking loader greatly simplified and more reliable. (No indirect references needed.)</li><li>5. Large programs more compact.</li><li>6. Programs easier to debug and understand.</li></ol>

Comment: Best of all: Allows local (256 or 1024) addressing for program transfer instructions and all of memory addressing for memory data referencing instructions.

#### 4.2.1.8 Hardware Floating Point

<u>Hardware Floating Point</u>	<u>Advantages</u>
Yes	<ol style="list-style-type: none"><li>1. Speeds up computations (important in real or near-real time environments)</li></ol>
No	<ol style="list-style-type: none"><li>1. Less hardware, hence greater reliability.</li></ol>

Comment: As with any system that has not been specified completely, a danger exists of exceeding the capability of the MS computer. Should at least have floating point hardware as an option that can be added later. FORTRAN compiler should generate code to drive the optional floating point hardware.



#### 4.2.1.9 Hardware Byte Manipulation

##### Hardware Byte Manipulation

##### Advantages

Yes

1. Allows addressing down to an 8-bit level.
2. Simplifies and speeds up certain "list" handling operations.
3. Simplifies compilers, assemblers, human message handlers.
4. Simplifies byte oriented I/O operation.

No

1. Allows larger addressable (word) memory.
2. Shortens instruction list of a CPU, hence easier to learn.
3. One less confusion factor in debugging.

Comment: Hardware byte manipulation tends to be more important in data storage/retrieval, business data processing than in real-time control-type systems.

#### 4.2.1.10 Microprogrammable vs Hardwired

##### Method

##### Advantages

Microprogrammable

1. Certain algorithms can be performed considerably faster on a "micro"-level. (Important for real-time).
2. CPU hardware is simpler more reliable, easier to service.
3. Greater potential of future LSI construction; hence lower cost, greater software nonrecurring recovery.
4. Less expensive.
5. Older architectures can be profitably emulated on a machine instruction level.

Hardwired

1. Easier to operate under operating system environment.
2. Certain instructions can be faster due to specialized hardware.

#### 4.2.2 System Software Considerations

##### 4.2.2.1 Family of CPUs Availability

<u>Type</u>	<u>Advantages</u>
Commercial a. System b. Micro-LSI	1. Low cost ground station $\leq$ \$150K. Micro-LSI in user equipment $\leq$ \$1,000 potentially.
Ruggedized	1. Can be flown and shipboard tested without great expense.
Military	1. Can be used in tactical environment.

Comment: Best of all. Need a family that is software compatible across all above categories. Unfortunately that restricts the selection.

##### 4.2.2.2 Multi-processor Configuration Availability

<u>Approach</u>	<u>Advantages</u>
Yes	1. Needed when single CPU runs out of computing power.
No	

Comment: This capability is valuable in an unspecified future growth R/D program such as master control station. Unfortunately there are few CPUs that support this capability with hardware and software, hence this might be too restrictive.

#### 4.2.3 Techno-Political Considerations

##### 4.2.3.1 Multi-source Availability

<u>Options</u>	<u>Advantages</u>
Yes	1. Improves manufacturing competition. 2. Eases logistics.
No	

Comment: Only PDP-11 and NOVA have a second source manufacturer. Hence requirement is restrictive.

#### 4.2.3.2 Virtual Memory

<u>Alternatives</u>	<u>Advantages</u>
Yes	<ol style="list-style-type: none"><li>1. No need to worry about running out of memory while writing program.</li><li>2. Automatic overlaying and swapping of core for free.</li></ol>
No	<ol style="list-style-type: none"><li>1. Less hardware, less operating system software, hence more-reliable easier-to-debug system.</li></ol>

Comment: Nice to have especially in MS equipment; however not many manufacturers support it yet.

#### 4.2.3.3 Real Time Operating (RTO) System

<u>Alternatives</u>	<u>Advantages</u>
Yes	<ol style="list-style-type: none"><li>1. Speedy creation of organized real-time computer systems.</li><li>2. Allows background/foreground operation, hence allows use while operating on line (controlling in real time) if spare CPU time is available.</li><li>3. Improves efficiency of resource allocations.</li></ol>
No	<ol style="list-style-type: none"><li>1. Lower cost procurement.</li></ol>

Comment: RTO disc based, is a must in MS developmental mode equipment. Abbreviated versions will also exist in user equipment (Micro). FORTRAN, FORTRAN Loader, run time library should cooperate with RTOs.

### 5. SELECTION

Final selection of the user computer candidates has not been completed. One conclusion that may be drawn from the analysis at this point however is that a very small number of final candidates will result from the imposition of a higher order language capability, floating point double precision hardware, low cost, and proven reliability. At this time the one outstanding candidate is the ROLM Rugged-Nova 1602R. Other critical selection parameters are being investigated at this time for this candidate such as its ability to interface with the auxiliary sensors and the capability to provide the monitor station function as a user equipment.

In terms of potential candidates the following machines have been identified:

ROLM Rugged-Nova 1602R

General Electric CP32A

Univac MPC-16

Honeywell 516

Rockwell D216

TRADE STUDY NO. 6

USER COST/PERFORMANCE

E. Martin



**GENERAL DYNAMICS**

*Electronics Division*

P.O. Box 81137, San Diego, California 92138 (619) 275-7301

## 1. INTRODUCTION

The purpose of this trade study is to identify specific design techniques that have a significant effect upon the cost and performance of User Segment equipments. It is apparent that all techniques will not be equally applicable to all user classes. This is because of power constraints, form factor, user scenario, and type of environment.

The primary emphasis on the user equipment design is to develop a minimum cost set of user systems that will provide adequate operational capability for a specified military mission. The particular technical performance objectives and requirements are a direct result of the particular mission and obviously may conflict with a lowest cost user equipment objective. The trade between cost and performance then becomes, in reality, a shopping list that identifies what improved performance costs.

Primary restriction and emphasis for this analysis is on the projected Phase III or operational portion of the GPS program and secondary trade issues relevant to Phase I or Phase II are not discussed. The impact of design-to-cost restrictions is not considered as a constraint on the analysis since such an issue would tend to distort the alternatives pursued by the study.

Particular design and performance requirements can be categorized for the trade study as follows:

### Technical Requirements

- Direct P signal acquisition
- High Anti-Jam margin
- Maintain lock and tracking for high dynamics
- Minimize search and acquisition time
- Position accuracy of 10 feet
- Velocity accuracy of 0.2 feet/sec
- Establish Satellite alert

### Environmental Requirements

- Maintain performance in temperature variation
- Maintain performance by hardness design

Several other requirement factors which will influence cost but are not specifically addressed in this report are:

- Packaging
- Reliability
- Maintenance concepts
- Acquisition option

## 2. REQUIREMENTS

### 2.1 Functional Requirements

Basic user equipment requirements for performance are derived from paragraphs J and K of Annex I of the RFP for the study. Both functional and detail user segment performance is defined in the preliminary User Segment specification SS-US-101 submitted on January 26.

## 2.2 Design Requirements

Numerous system design studies involving detail requirements imposed on the User Segment have been documented in a series of Design Review Bulletins (DRB' s). Rather than attempt a detail performance summary, the following DRB' s are referenced as the source file for the User Segment performance studies.

D9000582B	UE EMC Requirements
D9000583B	UE Hardness Criteria
D9000585B	UE Error Budget
D9000586B	UE Reliability/Maintainability
D9000587B	UE Equipment Commonality
D9000588B	Digital vs. Analog Implementation
D9000589B	Software vs. Hardware Implementation
D9000591B	Continuous P-Signal Receiver Performance
D9000592B	Sequential P-Signal Receiver Performance
D9000593B	Clear Code Receiver Performance
D9000594B	Integration with AMDRU/IMU
D9000595B	UE Antenna Description
D9000596B	UE Displays
D9000597B	UE Computer Selection
D9000598B	User Computer Programs
D9000599B	UE Physical Environment

## 2.3 Evaluation Criteria

Fundamental criteria for this trade study is the cost of a candidate implementation technique contrasted with the performance requirement delta which is implied by the candidate. Cost figures are 1974 dollars and are given under the stated assumptions of 3,000 unit level quantities where appropriate. Applications with smaller visualized quantities are stated as necessary.

## 3. CANDIDATE TECHNIQUES

Several specific candidate techniques have been established which indicate significant cost and performance differentials. The present candidates are not to be considered exhaustive or final since other relevant candidates will be evaluated.

### 3.1 Oscillator Stability and Design vs. Direct Acquisition

User equipments which demand operational capability to directly acquire the P signal will be driven to oscillator quality and design configurations which are obtained by additional expense. A large amount of functional characterization of the candidate quality, design, packaging and resulting performance is detailed in DRB D9000599AB, Oscillator Stability Study. The oscillator stability versus cost and performance are covered in Table 3.1-1.

### 3.2 Oscillator Standards

Maintenance and repair of user equipment will require test equipment which generate high quality timing references. Selection of a standard 5, or 10 Mhz clock will be compatible

TABLE 3 1-1 - Oscillator Stability vs. Cost and Performance

Candidate Technique	Cost Elements	Performance Elements	
		Short Term	Long Term
Oscillator Stability for Direct Acquisition	TCXO Costs *      \$ 61	$1 \times 10^{-9}$	$5 \times 10^{-9}$
	4th Grade ovenized Quartz      \$ 134	$1 \times 10^{-10}$	$1 \times 10^{-9}$
	1st Grade ovenized Quartz      \$ 271	$1 \times 10^{-11}$	$1 \times 10^{-10}$
	* Cost based on 1,000 units in 1975		
	Cost Delta      \$ 53	Yields 10 times longer interval of operation	
	Cost Delta      \$ 190	Yields 100 times longer interval without calibration	



with existing test equipment. A non-standard oscillator (5.1125) will imply additional cost in test equipment modification or synthesis. The GPS signal structure requires the use of a non-standard oscillator. Note that the study indicates that no fundamental cost factors are identified with procurement of a non-standard oscillator provided sufficient quantities are procured. Table 3.2-1 shows the potential impact of non-standard oscillators.

### 3.3 Error Correcting Codes

Encoding data words for error correction requires the use of alternate receiver demodulation techniques. This requires additional receiver hardware and costs as shown in Table 3.3-1.

### 3.4 Higher Anti-Jam Margins

Higher Anti-Jamming margins may be obtained through the use of an accurate inertial system calibration and aiding concept. This imposes restrictions on the form of the filter algorithm, computer size and computer through-put. Additional IMU model verification testing and validation is also implied or basic improved IMU accuracy is demanded. Table 3.4-1 shows the cost impacts for improved anti-jam margins.

### 3.5 IMU Dynamic Aiding

Incorporation of an IMU in the design concept to provide user equipment initialization, acquisition search, and reacquisition under dynamic conditions is a technique of some utility. The technique requires additional interfacing and computational penalty in the processor function of the design. Table 3.5-1 shows the cost versus improvements.

### 3.6 Dual Ionospheric Measurement

Propagation vagaries associated with the ionosphere can be measured in real-time by use of dual frequency processing of the group delay encountered at the  $L_1$  and  $L_2$  carrier frequencies. Dual frequency implementation requires redundant receiver circuit implementation. Table 3.6-1 shows the impact of dual frequency implementation.

### 3.7 Computer Memory Hardening with Plated Wire

Provision for hardening may be included for stored memory terms which establish the computation base for the processor. Complete memory hardening of both fixed and volatile storage is not considered but rather a capability to resume operation following a nuclear event. The costs for memory hardening are shown in Table 3.7-1.

### 3.8 Kepler Alert Program for Satellites

Identification of the visible SV's for the user based upon a stored program for establishing the optimum set is defined using a Kepler orbit mechanization. The costs associated with this implementation are shown in Table 3.8-1.

### 3.9 Analog vs. Digital Design of Receiver

Detailed investigation of potential functions of the receiver which may be allocated between the use of analog or digital hardware is given in DRB D9000555B. Potential digital implementation envisioned for the receiver design is detailed in the DRB. Table 3.9-1 addresses this trade study.

TABLE 3.2-1 - Oscillator Standardization vs. Cost

Candidate Technique	Cost Elements	Performance Elements
Standard Oscillator Frequency selection of 5, 10 MHz.	Baseline (No Cost Δ)	No performance impact
vs. Non Standard Oscillator 5.1125 Mhz.	Cost Delta \$ 200 Per laboratory or aircraft/ ship test equipment.	Logistic Supply System affected but not user equipment. Logistic system performance hard to quantify.
	Assume: 1,000 units affected Total non-recurring cost is about \$200,000.	

TABLE 3.3-1 - Error Correction Code vs. Cost

Candidate Technique	Cost Elements	Performance Elements
<p>Error Correcting Code utilization in receiver design.</p>	<p>Recurring Cost of Additional Hardware per 5,000 units  - \$200</p>	<p>Lowers Data Demodulation Threshold up to 3dB.  Lowers carrier tracking threshold by 1-2dB.</p>

TABLE 3.4-1 - Anti-Jam Margin vs. Cost

Candidate Technique	Cost Elements	Performance Elements
Higher Anti-Jam Margin by Utilizing		
1. Extensive Software Modeling and Calibration	Cost of expanded computer RAM memory of \$2K. Delta cost \$ 100*	Improve AJ Margin from 58 to 60 dB Delta Improvement 2dB
2. Higher Quality IMU	Cost of Geans system vs. contemporary IMU Geans Cost (unknown) TBI, Military Platform \$50 - 100K	Minimal performance difference since IMU calibration is limited by receiver measurement noise of 0.1 ft/sec.
* Recurring cost for 5,000 units in 1980.		

TABLE 3.5-1 - IMU Dynamic Aiding

Candidate Technique	Cost Elements	Performance Elements
<p>IMU Dynamic Aiding to improve receiver performance.</p>	<p>Additional interface costs for IMU \$200</p> <p>Computational memory (RAM \$2K) \$100</p> <hr/> <p>TOTAL DELTA \$300</p>	<p>Lower Acquisition time TBD</p> <p>(Requires detail assumptions of times, missions)</p>
	<p>Assumption: Does not amortize the IMU cost of \$30K to \$50K.</p>	

**TABLE 3.6-1 - Two-Frequency Ionospheric Correction vs. Costs**

Candidate Technique	Cost Elements	Performance Elements
Dual Ionospheric Frequency Measurement	Additional RF Hardware and Signal Processing Hardware Delta Cost                      \$680	Ranging Accuracy Improvement which reduces the ionospheric error from 50* or 25** feet to less than 10 feet.  * Error with no modeling and average conditions. ** Error with simple ionospheric modeling.

TABLE 3.7-1 - Memory Hardening vs. Costs

Candidate Technique	Cost Elements	Performance Elements
<p>Plated Wire Memory Hardening of GPS Computers</p>	<p>Cost differentials involved in employing plated wire memory for volatile and non-volatile storage. Cost data is still TBD.</p>	<p>Performance differential is operational capacity to re-institute the navigation function following a nuclear event.</p>

TABLE 3.8-1 - Kepler Alert Program vs. Costs

Candidate Technique	Cost Elements	Performance Elements
Kepler alert program for satellites.	<p>RAM memory costs associated with Kepler constants storage and conversion.</p> <p>Delta cost                      \$60</p>	<p>Satellite search mode without alerts would increase sequential receiver time to first fix by factor of 6 (24 satellites).</p>



TABLE 3.9-1 - Analog vs. Digital

Candidate Technique	Cost Elements	Performance Elements
<p>Analog vs. Digital Designs of Receiver Circuits</p>	<p>Detail Cost Projections for suggested implementation are TBD.</p> <p>Potential implementations have been identified. DRB D9000588B.</p>	<p>To Be Determined</p>

### 3.10 Hardware vs. Software Design

Certain functions of the receiver lend themselves to software implementation within the processor. The inclusion of functions for code search, coarse and fine frequency estimation, carrier and code loop tracking demand a portion of the processor memory and timing capability. A detailed discussion of the techniques is given in DRB D9000589B. The cost trade-offs are shown in Table 3.10-1.

### 4. SELECTIONS

Many of the cost versus performance study trades remain to be finalized in the design effort and pricing exercise. One of the prime outputs revealed by numerous study trade elements is that incorporation of functions into and by the processor provides an economical way of increasing system performance be it for alert modes, expanded IMU calibration, or transfer of complete receiver capabilities. This axiom will only hold true insofar as the predicted computer technology cost declines actually do occur in the 1980 time frame projected for GPS. To a great extent, the final selection of any performance growth which carries with it an inherent cost increase must be made by the operational user or potential customer who applies his own unique set of weighting factors to the performance differentials.

TABLE 3.10-1 - Hardware vs. Software

Candidate Technique	Cost Elements	Performance Elements
<p>Hardware vs. software design concepts for receiver/processor.</p>	<p><u>Options</u>                      1. Code correlation PA Memory 120 words                      2. Coarse Frequency estimation 40 words                      3. Fine Frequency estimation 90 words                      4. Third order tracking loop 120 words</p>	<p>Total performance impact is loss of 1 - 0.5 dB due to quantization noise effects introduced by Digital implementation.</p>
	<p>Computer Cost Delta &lt;\$100                      Expanded I/O \$100                      Cost Increase \$200                      Cost decrease due to replaced hardware functions is TBD.</p>	

TRADE STUDY NO. 7

USER IONOSPHERIC MODEL

R. B. Bennett

R. Westervick

H. Navoy



**GENERAL DYNAMICS**

*Electronics Division*

P.O. Box 91127, San Diego, California 92138 (619) 279-7300

## 1. INTRODUCTION

There are two general approaches that appear feasible for correcting range measurements made on signals transmitted from satellites to user equipments for the delay introduced by the ionosphere. One approach, "modeling", is to develop a mathematical model of the ionosphere from past data then use this to predict the correction to be applied to measured data. The second approach, called the two frequency method, takes advantage of the fact that the ionospheric delay varies with frequency in a known manner so that the measured difference in time of arrival of signals simultaneously transmitted provide a means of determining the delay introduced by the ionosphere.

The purpose of this trade study is evaluate modeling approaches to determine their effectiveness for the GPS. The preferred selection must be compatible with all the phases of the GPS program. In Phase I no specific portion of the user navigation data frame is allocated to ionospheric modeling data. It is expected that the model coefficients or parameters will be transmitted in the spare bits of the user navigation data frame.

## 2. REQUIREMENTS

### 2.1 Functional Requirements

User equipment must perform corrections for ionospheric signal delay by modeling.  
Source: SS-GPS-101A, para. 3.7.2.1.

### 2.2 Design Requirements

No specific design requirement for ionospheric modeling is given by the System Specification for the GPS Phase I.

### 2.3 Ground Rules

The ground rules for this trade study include:

- The reference model of the ionosphere used to generate the data for modeling is the Bent Ionospheric Model\*
- Data transmission capability to the user is assumed to be approximately 200 bits every 30 seconds

### 2.4 Evaluation Criteria

The evaluation criteria for the various ionospheric models are:

- Percent RMS error for a 24 hour period

---

\* Final Report of SAMSO Contract No. F04701-73-C-0207.

- The number of bits transmitted by each satellite to the user
- User equipment storage requirements

### 3. CANDIDATES

Emphasis has been placed on candidate methods that allow minimum transmission of ionospheric data to the satellite, little or no processing of data in the satellite, minimum transmission of data from the satellite to the user. The two aspects of the ionospheric data representation that have to be considered are the allowances for time and space variations of the data and user location.

The ionospheric modeling techniques investigated for the GPS are:

- A) Grid Interpolation — A world wide map of data points consisting of ionospheric height and electron content. The data points are separated 10 degrees (1100 km) and the user employs linear interpolation between nearby points to determine the ionospheric delay along the signal paths.
- B) Series Evaluation — A world wide map of vertical group delay and ionospheric height. The maps are made up of four Fourier series representations consisting of a separate vertical group delay series and ionospheric height series for the northern and southern hemisphere.
- C) Gradient Approach — A world wide map of ionospheric data points spaced at 13.5 degrees (1500 km). Each data point consists of vertical group delay, direction of group delay gradient, magnitude of group delay gradient and ionospheric height. The total electron content near any data point is computed by using the fixed values and gradients.
- D) Cross-Line Technique — There were two transmission approaches investigated for this technique: the world wide model and 30 degree sector maps. The world wide model uses vertical group delay and ionospheric height at 5 degree spacing along a cross line on the earth. This cross line is defined by a magnetic latitude line and a magnetic longitude line. The ionospheric total electron content at any point on earth is obtained by taking proportional ratios of suitable latitude and longitude data points. The 30 degree sector map technique is equivalent except a cross line of data points of 7.5 degree spacing are generated for each sector. A method still under investigation and not reported herein is the use of geographic longitude and latitude data points for sector maps.
- E) Satellite Transmit Delay — This method utilizes a Fourier series model for the area of coverage for a particular satellite. The Fourier series represents the line of sight delay from a satellite at a particular time. The series is a function of the co-elevation angle and an azimuth angle measured from a known subsatellite point. This method permits the user to determine the propagation delay along any signal ray to the satellite directly; thereby eliminating computations of total electron content and the cosecant function.

F) Static Cross-Line Technique -- This technique is similar to D) above except the cross line data values are averages of the electron content and height of the ionosphere. The simple tabulation is with respect to local time of day for a specific grid of magnetic latitude and longitudes. This simple static model can be carried in the user's equipment and could be applied without modification worldwide to all times, seasons, and sections of the solar cycle. The analysis of this approach is not completed however; initial results for evaluations within the same month indicate RMS errors on the order of 55 to 60%. Because of the preliminary nature of this analysis, further discussion of this technique is not presented in this document. As results are available, they will be reported accordingly.

- G) Universal User Model - This technique utilizes a fixed, user-based set of data for determining ionospheric delay. The model consists of a fixed set of zenith ionospheric delays averaged over all contributing independent variables except local time of day, i.e., earth location, solar activity, and day-to-day variations are normalized to a mean value. The local time of day values would nominally be one hour and time adjustment would be performed by linear interpolation. An empirical analysis of this approach is not completed and further discussion of this approach is not presented in this document. However, the technique must be considered viable pending the outcome of the analysis because of its great simplicity.

### 3.1 Time Adjustment

The first method that was investigated accounts for the time variation by retransmitting new data of group delay over short intervals of 1/2 hour without applying any corrections for the intermediate time discrepancies. The results are listed in Appendix D, showing that the errors due to the time offset are quite small, less than 1% of the basic prediction at most locations, except in a wide longitude band around sunrise where the ionospheric gradients change very rapidly with time resulting in a RMS error of 33%. The frequency transmission requirement in addition to the inaccuracies eliminates this method from further consideration.

The second method uses the group delay data at a fixed time and rotates it at a rate of 15 degrees in magnetic longitude per hour for continuous time adjustment over anywhere from 1 to 24 hours. This is the most flexible and accurate solution to the problem, resulting in errors of less than 10% around sunrise for  $\pm 1/2$  hour adjustment by rotation, and RMS errors of around 30% of the basic prediction for a continuous 0 to  $\pm 12$  hour rotational adjustment by which a full 24 hour period would be covered. As explained in Appendix H, it is expected that through additional work, this method can still be refined yielding an overall RMS error of 25% and reducing the current maximum individual error of 50% to maybe 40% of the maximum prediction for continuous time adjustments and yielding an overall RMS error of 10% for  $\pm 1$  hour time adjustments.

### 3.2 Space Adjustment

Four methods of representing the space distribution of ionospheric data have been under investigation, all of them using the Bent Model and recoding the obtained ionospheric data for minimum storage and transmission time requirements. Method 1 generates a grid pattern of ionospheric data, and uses linear interpolation in space for all intermediate points. Method 2 determines a set of coefficients that define the series representation of the ionospheric data, and the series is evaluated for each data point. Method 3 generates a wide spread grid point pattern of ionospheric data and matching ionospheric gradients which are used to determine the data for all intermediate points. Method 4 expands data values along a single magnetic latitude-longitude cross line to cover the whole world. The accuracies achieved by these methods are described in detail in the individual reports listed in Appendices D, E, F, and G respectively.



### 3.3 Method 1 - Grid Interpolation

Ionospheric data points cover the world at 10 degree (1100 km) spacing, resulting in a total of 421 points. The data requirements for each point are: 4 bits for vertical group delay leaving an error of  $\pm 2.6$  nsec, and 3 bits for the height of the ionosphere leaving  $\pm 18$  km inaccuracy. The combined 7 bits per point result in a total of 2947 bits of data covering the world.

The transmission to the satellite consists of two types of data: Once per day a correction factor of 7 bits allowing numbers between 0 and 127 is transmitted for the purpose of updating the 10 day world map of group delay. Every 10 days new prediction values of vertical group delay and height are transmitted for the worldwide grid. This data consists of 2947 bits.

The processing by the user involves linear interpolation for the space adjustment, coordinate rotation at a rate of 15 degrees in magnetic longitude per hour for time adjustment, and updating with the daily correction factor. The user can see the ionosphere within a 21 degree radius of his site, resulting in a 42 degree geographic latitude coverage, and he can continuously adjust for time by rotating the magnetic latitude, longitude system, requiring continuous magnetic longitude coverage. Since the magnetic equator varies about  $\pm 11.5$  degrees from the geographic equator, the user has to store all the data within a 65 degree latitude band around the globe centered at the latitude of his site. An observer on the pole has to store 197 bits of data, and for an equatorial observer the storage requirement is at its maximum of 1583 bits of data.

The accuracy tests to this approach are described in Appendix D. The RMS errors due to the space adjustment alone are about 10% in the equatorial zone and still lower outside. The maximum individual percent errors are of about the same size as the RMS percent error. If it is desired to improve the accuracy of this method leaving less than 5% error in the equatorial zone, the point pattern of world coverage could be densified by spacing it at 5 degrees between  $\pm 30$  degrees latitude and at 10 degrees outside. This would result in 1035 points or 7245 bits of data. To retain the higher accuracy the number of bits for vertical group delay might have to be increased from 4 to 5 reducing the error due to the data coding to  $\pm 1.26$  nsec and raising the total number of bits even more to 8280.

### 3.4 Method 2 - Series Evaluation

Ionospheric world maps are represented by 2 sets of coefficients, one for the northern and one for the southern hemisphere with 10 coefficients each. There will have to be a coefficient set for the vertical group delay as well as for the height of the ionosphere. The coefficients for vertical group delay take up 7 bits of data each allowing numbers between 0 and 127 and the coefficients for height use 6 bits allowing numbers between 0 and 63. This results in a total data requirement of 1040 bits for world coverage.

The transmission to the satellite consists of two types of data: Once per day a 7 bit correction factor is transmitted to update the world map. Every 10 days new coefficient sets describing the worldwide predicted values of vertical group delay and height are transmitted. This data consists of 1040 bits at a rate of 10 bits per second.

The processing by the user includes series evaluation involving trigonometric functions for space adjustment, coordinate rotation at a rate of 15 degrees in magnetic longitude per hour for time adjustment, and updating with the daily correction factor. A user located roughly 30 degrees north or south of the magnetic equator will only need to store one coefficient set of 520 bits, but users located closer to the equator have a storage requirement of the total 1040 bits for both sets. There is a possibility, however, to make this double storage unnecessary, if the coefficients were chosen to represent the ionospheric variations for an area 20 degrees larger than each hemisphere.

The accuracy tests to this approach are described in Appendix E. The RMS errors due to the space adjustment alone are between 14 and 24% of the basic predictions for different combinations of coefficients. However, the maximum individual errors are extremely large in some cases 73% and higher. This indicates that by minimizing the residuals between the model predictions and the coefficients estimates, the ionospheric conditions are well approximated over most of the area, but result in a very bad fit at one relatively small location. Such maximum errors can not be tolerated, but it should be possible through more work in this area to come up with the best choice of coefficients that produce RMS errors between 11 and 21% or even smaller and bring down the maximum percent error to values smaller than twice the RMS percent error. It might also be possible to represent the ionospheric variations by only 20 well chosen coefficients in each the northern and southern hemisphere. This would result in only 520 bits of data.

The most satisfactory approach would be for each satellite to transmit the coefficients which would enable a user to compute the angular delay time along the line of sight to the satellite which would include ionospheric and tropospheric refraction. By changing the equations used in the tests shown in Appendix E, it would probably be possible to cover each satellite's visibility area with 28 x 8 bit coefficients for the angular delay time. By these means a user could receive the tropospheric and ionospheric delay times along the line of sight to the satellite within the half frame of normal transmissions. The input to the users package would be the 28 coefficients, azimuth, and elevation. The only major problem would be the positional rotation of the satellite over the ionosphere; a satellite could not economically store coefficients for time periods greater than 2 hours throughout the day (2048 bits). The data would, therefore, be in error by  $\pm 1$  hour of the satellite's path movement through the ionosphere ( $\approx 3500$  km) which could provide very large errors near the equator where the ionospheric changes are greatest. Perhaps added coefficients could account for this satellite movement effect on ionospheric delay, or the overall area covered by the satellite could be made very much larger enabling the user to move his effective position in both time and space.

### 3.5 Method 3 - Gradient Approach

Ionospheric data points and matching gradients cover the world at 13.5 degree (1500 km) spacing. The data requirement for each point are: 4 bits for vertical group delay leaving an error of  $\pm 2.6$  nsec, 4 bits for the direction of the group delay gradient leaving an uncertainty of  $\pm 12$  degrees, 3 bits for the amount of the group delay gradient leaving an error of  $\pm 7\%$ , and 3 bits for the height of the ionosphere leaving an error of  $\pm 18$  km. The combined 14 bits per point result in a total of 3178 bits of data covering the world.

The transmission to the satellite consists of a 7 bit correction factor once per day for the purpose of updating the 10 day world map. Every 10 days new predictions for vertical group delay, gradient and height are transmitted consisting of 3178 bits.

The processing by the user involves the gradient evaluation for the space adjustment, coordinate rotation at a rate of 15 degrees in magnetic longitude per hour for time adjustment, and updating with the daily correction factor. The user can see the ionosphere within a 21 degree radius of his site, and a tolerance of  $\pm 11.5$  degrees in latitude is allowed for the rotation of the magnetic latitude, longitude system required for the time adjustment. Thus the user has to store the data within a 65 degree latitude band around the globe centered at the latitude of his site. An observer on the pole has to store 212 bits, and a user at the equator has to store the largest amount of data consisting of 1797 bits.

The accuracy tests to this approach are described in Appendix F. The RMS error due to the space adjustment alone is about 12% of the prediction in the equatorial zone, and the maximum individual percent error is about 47%. The higher errors only occur at a few locations where the gradient does not represent the ionospheric variation very well. Through careful evaluation, better gradient estimates could be found and the overall RMS error could be reduced to 10% in the equatorial zone, and the maximum error could be reduced to values smaller than twice the RMS error.

### 3.6 Method 4 - Cross-Line Technique

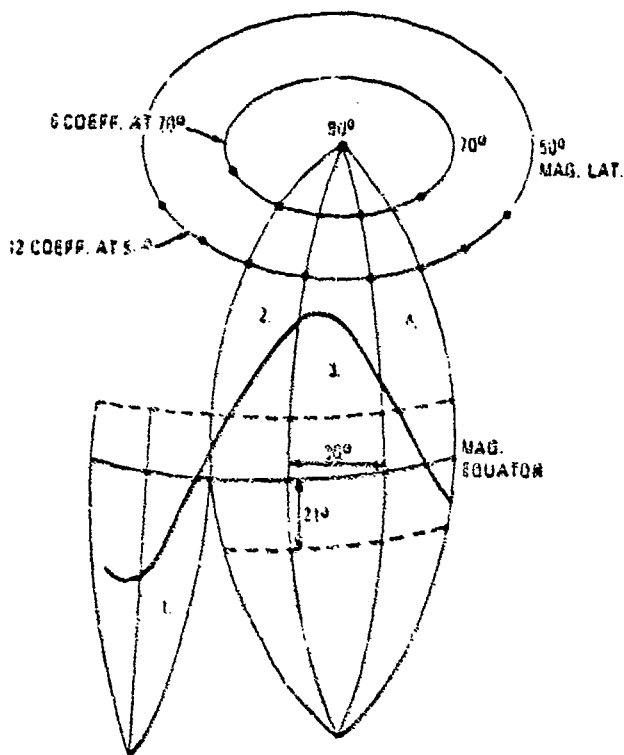
Ionospheric data points at 5 degree (550 km) spacing along one magnetic latitude line, the magnetic equator, and along one magnetic longitude line that passes through the densest section of the equatorial anomaly are assumed to be representing the typical ionospheric variation for the whole world. The data requirements for each point are: 4 bits for vertical group delay leaving an error of  $\pm 2.6$  nsec, and 3 bits for the height of the ionosphere leaving  $\pm 18$  km inaccuracy. The combined 7 bits per point result in a total of 770 bits of data.

The transmission to the satellite consists of a 7 bit correction factor once per day for the purpose of updating the 10 day world map. Every 10 days new predictions for vertical group delay and height are transmitted consisting of 770 bits.

The processing by the user involves forming of proportional ratios for the space adjustment, coordinate rotation at a rate of 15 degrees magnetic longitude per hour for time adjustment, and updating with the daily correction factor. The storage requirement for the user is 770 bits of data.

The accuracy tests to this approach are described in Appendix G. The RMS errors due to the space adjustment alone are between 33% and 75% for the different cases, and the maximum individual percent errors are between 33% and 100%. The high RMS and maximum errors only resulted in the case in which the effect from the dipole magnetic equator used instead of the true magnetic equator caused distortions in the group delay contour lines at high density areas. It appears that through more investigations, the simple technique could be somewhat refined that it would yield RMS errors between 20 to 35% and maximum errors of about the same percentage or only slightly higher.

A variation on this technique using a 7° spacing could probably provide a very satisfactory approach, see Figure 3.6-1. We understand that as one satellite frame is being read by a user's equipment, another satellite is being located. A suggested approach to transmitting



7-31

Figure 3.6-1. Grid Pattern

ionospheric group delay could, therefore, be as follows. If a satellite was over position 2, it would sequentially transmit ionospheric group delay and height for zones 1, 2, and 4, etc. Even though satellites may be transmitting three different zones, they would be sequentially coded so that if there is a common zone, it would be transmitted by both satellites at the same time. If these zones are each  $30^\circ$  in longitude width, a user would need no more than 3 zones to obtain his ionospheric information; near the equator he may need only two zones which he could obtain from satellites transmitting zones for the northern or southern hemisphere. This is because of a  $21^\circ$  equatorial overlap providing a  $30^\circ \times 42^\circ$  duplicated zone for each equatorial longitude belt (north or south). The user could obtain information for each zone in a  $1/2$  minute frame and because of the sequential coding, obtain all his ionospheric information after tuning in to no more than three satellites within a normal 90 second listening period.

Problems occur when a user is in the polar region and his 'visible' ionosphere would reach over many or all of the northern hemisphere zones. This problem can be overcome by transmitting a grid of points for the magnetic pole area about  $50^\circ$  magnetic latitude. In this zone where ionospheric gradients are reasonably symmetrical a  $20^\circ$  grid provides good accuracy for interpolation. To cover a polar zone above  $50^\circ$  latitude 19 coefficients are needed or 133 bits of information. The user who has to obtain ionospheric information from four (4) satellites can therefore receive sequentially the polar zone plus the three  $30^\circ$  cross-line zones. One zone being transmitted during one satellite frame with a maximum of 133 bits plus 5 bits time reference = 138 bits maximum per frame. The satellite storage would be 2 polar zone at 2 times of the day plus 12 cross-line zones at 3 daily times per zone plus time and space reference bits making 4789 bits for a 24 hour period. Additional investigations are still ongoing for this method.

### 3.7 Method 5 — Satellite Transmit Delay

The satellite transmit delay method described in DRB 90000572B by II. Navoy consists of generating an empirical grid of the ionospheric delay for each satellite's field of view using the reference Bent ionospheric model. The resulting delay grid is then represented by a functional in time and user location. The process of generating the delay correction is shown in the flow diagram of Figure 3.7-1. The grid pattern and definition of terms is given in Figure 3.7-2.

First, an empirical grid of ionospheric "delay" is generated about the subsatellite position at some time,  $t$ . The grid pattern is a series of evenly spaced locations in concentric circles out to the satellite's field of view and about the subsatellite position. Above each grid point is calculated the vertical group delay (GD) and height of the  $f_oF_2$  layer ( $H_m$ ). Satellite time and position as well as the Bent Global Ionospheric Delay Model serve as inputs to the computer program which generates the group delay and height data for each grid point. The grid locations are defined by earth central angle and azimuth from the subsatellite point. A sample of the grid density is as follows:

<u>Concentric Ring Sub Satellite Pt.</u>	<u>Earth Central Angle</u>	<u>N No. of Grid Pts. per Ring</u>	<u>Azimuth (=360°/N)</u>
Subsatellite point	0°	1	--
1	7.5°	4	90°
2	17.5°	10	36°
3	27.5°	16	22.5°
4	37.5°	21	17.14°
5	47.5°	26	13.85°
6	57.5°	30	12°

108 Locations

The vertical group delay data are converted to line-of-sight (LOS) delay and the grid locations are referenced to elevation angles and azimuths of potential users, based on the following relationships:

$$\text{LOS Delay} = \frac{\text{Vert. GD}}{\cos \beta}$$

$$E = \cos^{-1} \left( \frac{R_e + H_m}{R_e} \right) \sin \beta$$

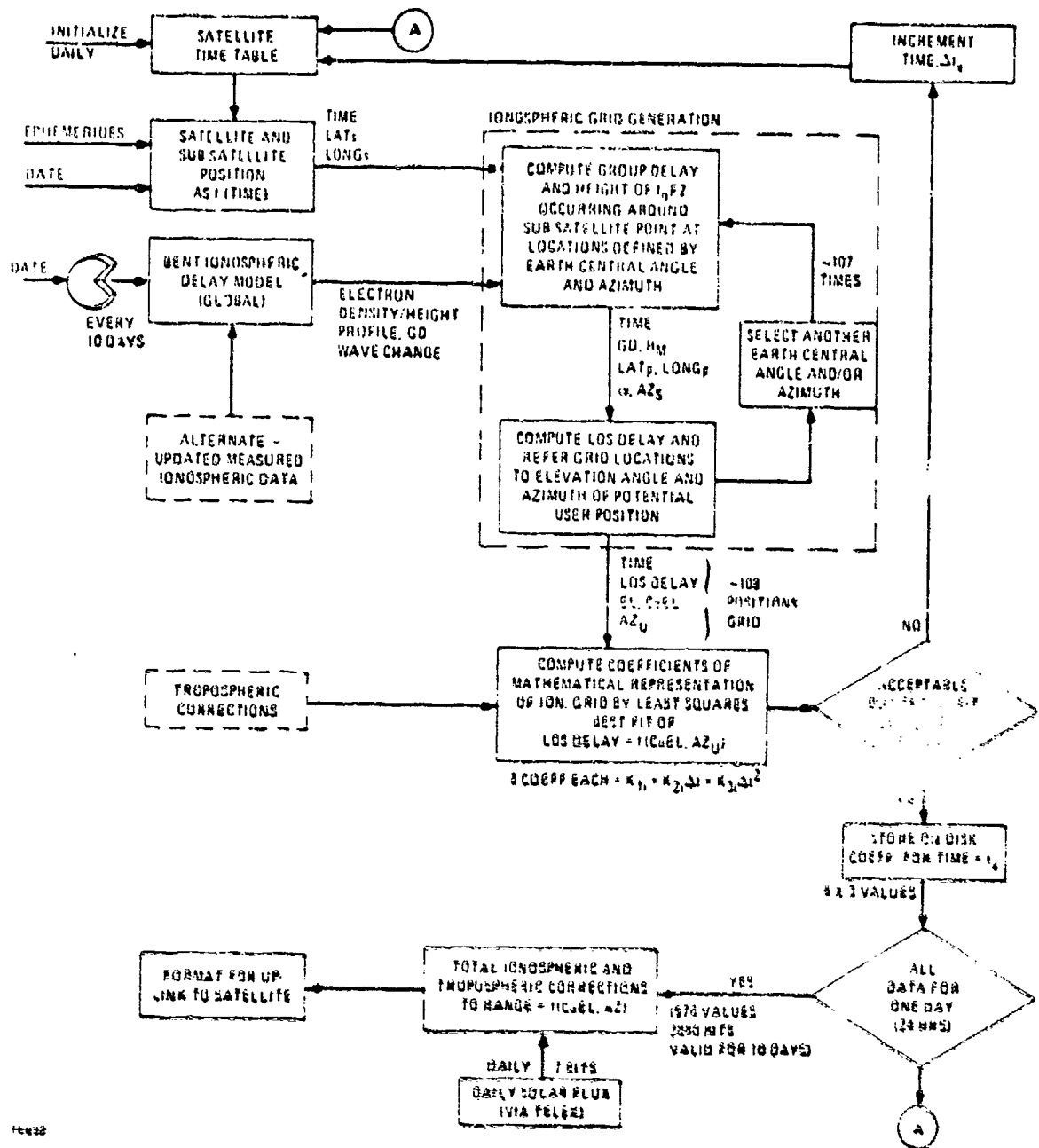
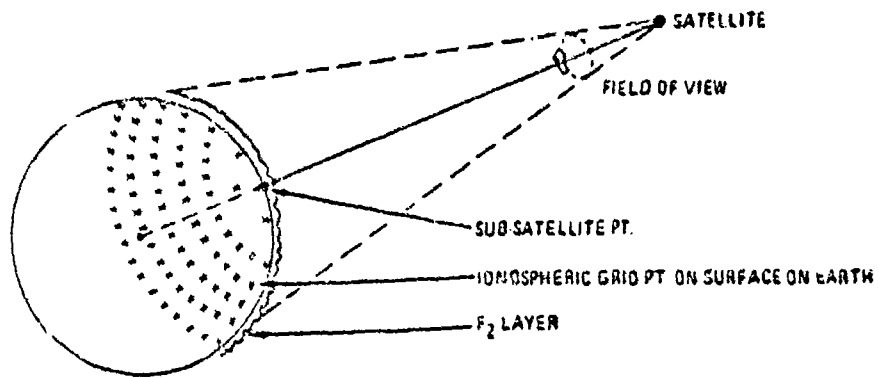
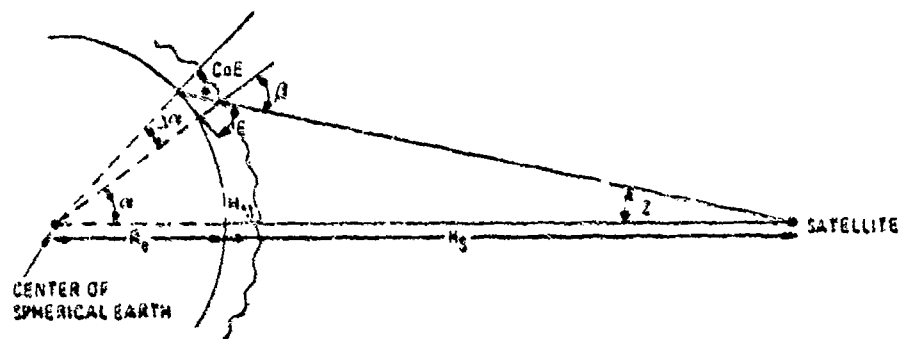


Figure 3.7-1. Range Correction Processing, Flow Diagram

A SATELLITE FIELD OF VIEW & IONOSPHERIC GRID PATTERN



B ANGULAR AND LINEAR DEFINITIONS



- $R_0$  = MEAN RADIUS OF EARTH (APPROX. 3442 N.MI)
- $H_s$  = HEIGHT OF SATELLITE ABOVE EARTH (APPROX. 11,000 N.MI)
- $H_m$  = HEIGHT OF MAXIMUM ELECTRON DENSITY OF  $F_2$  ABOVE EARTH
- $\alpha$  = EARTH CENTRAL ANGLE FROM SATELLITE TO  $F_2$  LAYER
- $\Delta\alpha$  = EARTH CENTRAL ANGLE FROM GND OBSERVER TO  $F_2$  LAYER
- $\alpha + \Delta\alpha$  = EARTH CENTRAL ANGLE FROM GROUND OBSERVER TO SATELLITE
- $\epsilon$  = ELEVATION ANGLE OF GROUND OBSERVER TO SATELLITE
- $\text{CoE} = \frac{\pi}{2} - \epsilon$
- $z$  = ZENITH ANGLE OF SATELLITE TO EARTH
- $z'$  = ZENITH ANGLE AT  $F_2$  LAYER =  $\alpha + z$

7-12

Figure 3.7-2. Grid Pattern and Definitions



$$C_oE = \frac{\pi}{2} - E$$

$$A_z \text{ user} = \pi \pm A_z \text{ sat.}$$

where  $\beta = d + Z$ ; also  $\beta = C_oE - \Delta\alpha$ ;  $\alpha$  is selected and  $Z$  is calculated where two sides ( $R_c + H_s$ ,  $R_c + H_m$ ) and the included angle ( $\alpha$ ) are known.

A three-dimensional, polar plot of the ionospheric grid is CoE vs  $A_z$  vs LOS Delay; a sketch of a cutaway portion is shown below:

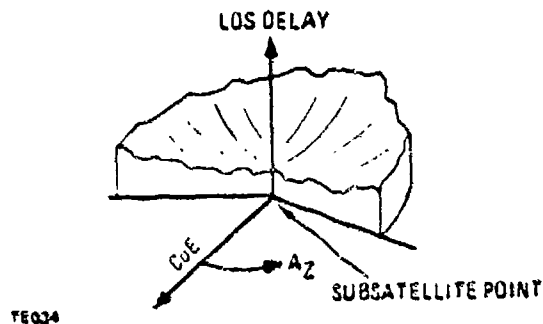


Figure 3.7-3. LOS Delay with Respect to Subsatellite Point.

This empirical ionospheric grid can be represented mathematically in terms of power series of CoE and multiple angle trigonometric functions of the azimuth angle, such that

$$\text{LOS Delay} = K_{00} + \sum_{j=1}^n (C_oE)^j (K_{0j}) + \sum_{i=1}^m (K_{1i}) \cos (i A_z) + K_{2i} \sin (i A_z)$$

Sample calculations indicate that  $n = 1$  and  $m = 3$  are deemed adequate for the mathematical representation, thus reducing the above equation to

$$\text{LOS Delay} = K_{00} + C_oE (K_{01}) + \sum_{i=1}^3 (K_{1ii}) \cos (i A_z) + K_{2ii} \sin (i A_z)$$

LOS delay (in nanoseconds) may be rewritten in terms of  $\Delta R$ , range correction (in feet), as follows:

$$\Delta R = A_0 + C_0 E (A_{01} + \sum_{i=1}^3 (R_i \cos (i A_2) + S_i \sin (i A_2)))$$

since  $\Delta R$  in ft = Velocity of Light X LOS Delay in sec

$$= .98208 \times \text{LOS Delay in nano-sec.}$$

The eight coefficients  $A_0$ ,  $A_{01}$ ,  $R_1$ ,  $R_2$ ,  $R_3$ ,  $S_1$ ,  $S_2$ , and  $S_3$  reflect the changes due to time and satellite position; each one expressed as a quadratic function of time was found to be adequate, so that

$$A_0 = a_{00} + a_{01} \Delta t + a_{02} \Delta t^2$$

$$A_{01} = a_{010} + a_{011} \Delta t + a_{012} \Delta t^2$$

$$R_1 = r_{10} + r_{11} \Delta t + r_{12} \Delta t^2$$

⋮

$$S_3 = s_{30} + s_{31} \Delta t + s_{32} \Delta t^2$$

to which a least square best fit process is applied. The coefficients are evaluated for a period of time, assume one hour, and are stored on disk. The process is repeated until all the coefficient data for a 24-hour span are obtained. These data are valid for 10 days before requiring a Bent model update. In order to increase the accuracy of the data and reflect the daily solar radiation condition requires the insertion of the daily solar flux expressed as a multiplication factor.

The data uplinked to the satellite are comprised of 24 sets of 24 coefficients (assuming each set is good for one hour). The entire data set takes 2880 bits (24 x 24 x 5 bits per value) and is valid for a 10-day period before requiring a Bent modeling update. To increase accuracy requires a daily update of the specific day's solar flux count which can be expressed in 7 bits. The accuracy of predicting the range correction is estimated to be:

$$\text{RMS} \approx 7 \text{ ft. due to Bent modeling}$$

$$\text{RMS} \approx 7 \text{ ft. due to above technique and assumptions}$$

$$\text{RSS} \approx 10 \text{ ft}$$

## 4. ANALYSIS

### 4.1 Comparison Matrix

Table 4.1-1 summarizes the requirements and accuracies for the methods using minimum transmission, storage, and processing. One of the methods described is illustrated with two different approaches making 6 ionospheric data representations.

During 24 hours the satellite orbits the earth twice, but traces out one "two-cycle" track on the surface of the earth. The world coverage requirements are shown for 4 of the cases whereas the other two cases show the storage requirements for the sectors beneath the satellite during a 24 hour period. The data can remain unchanged, apart from one 7 bit update number, for a period of 7-10 days when new maps should be transmitted to the satellite.

The maximum storage a user requires is listed along with the number of bits he must receive from each of four satellites if data from them was sequentially coded. It is assumed that when a user is receiving data from one satellite, the equipment is locating a second satellite. It is also assumed that a normal frame or "listening period" per satellite is 30 seconds and that approximately 200 ionospheric bits can be transmitted in this 30 second period. With sequential coding of satellite information a user can receive 800 bits of ionospheric information from 4 satellites in the normal "listening period." Should he miss one frame due to loss of lock, he may have to remain on a satellite for an extra period to regain his last information.

The errors shown are in percentages as this measure remains reasonably constant irrespective of ionospheric delay magnitude. The magnitude of these errors for different sites are shown in Figure 4.1-1 where the results are for diurnal annual residuals. The daytime monthly residuals are approximately twice as large as these during local afternoon and occasional excursions to ten times these values will occur. Appendix A describes these daily errors in more detail and Figure 4.1-2 shows how the percentages remain reasonably constant.

The basic error in the model has been shown to be 15-30% (SAMSO TR 72-239). Further errors in the methods described are due to time and space interpolation. Time interpolation is large when the satellite map covers a 24 hour period due to geographic and geomagnetic effects and has been shown in Appendix H to be 23%, whereas the error for  $\pm 1$  hour interpolation is only 10%. Spatial interpolation is discussed separately for each method in the respective Appendices. The final column of Table 4.1-1 summarizes the overall RSS of the three preceding columns relating to model, time, and spatial errors. The error figures given for the 4 worldwide cases include improvements that can be expected to be made in time and space interpolation. The remaining two methods 4b and 5 appear to be the ones most suitable to be used in the proposed navigation satellite system.

Table 4.1-1. Summary of Ionospheric Data Representation Methods - Comparison Matrix

Method For Space Adjustment	Coverage	Maximum User Storage (bits)	Approx. Data Received From ea. of 4 Satellites	% RMS Errors Due to			Expected Total % Error (RSS of 3 Preceding Columns)
				Space Adj. (Equatorial Zone)	Time Adjustment	Basic Prediction	
<sup>1</sup> Grid Interpolation	World-wide map (10° spacing)	1583	400	10	25	15-30	31-40
<sup>2</sup> Series Evaluation	World-wide map (vertical) (SMO coeff)	520	130	14-24	25	15-30	32-46
<sup>3</sup> Gradient Approach	World-wide map (13.5° spacing)	1707	430	10	25	15-30	31-40
<sup>4a</sup> Crossline Technique	World-wide map (5° spacing)	660	165	20-35	25	15-30	35-52
<sup>4b</sup>	30° sector maps (7° spacing)	451	140	14	10	15-30	23-35
<sup>5</sup> Satellite Transmit Delay	Satellite coverage area ≈ 57.5° sector	508	127	14	10	15-30	23-35

Group Delay (nanoseconds)

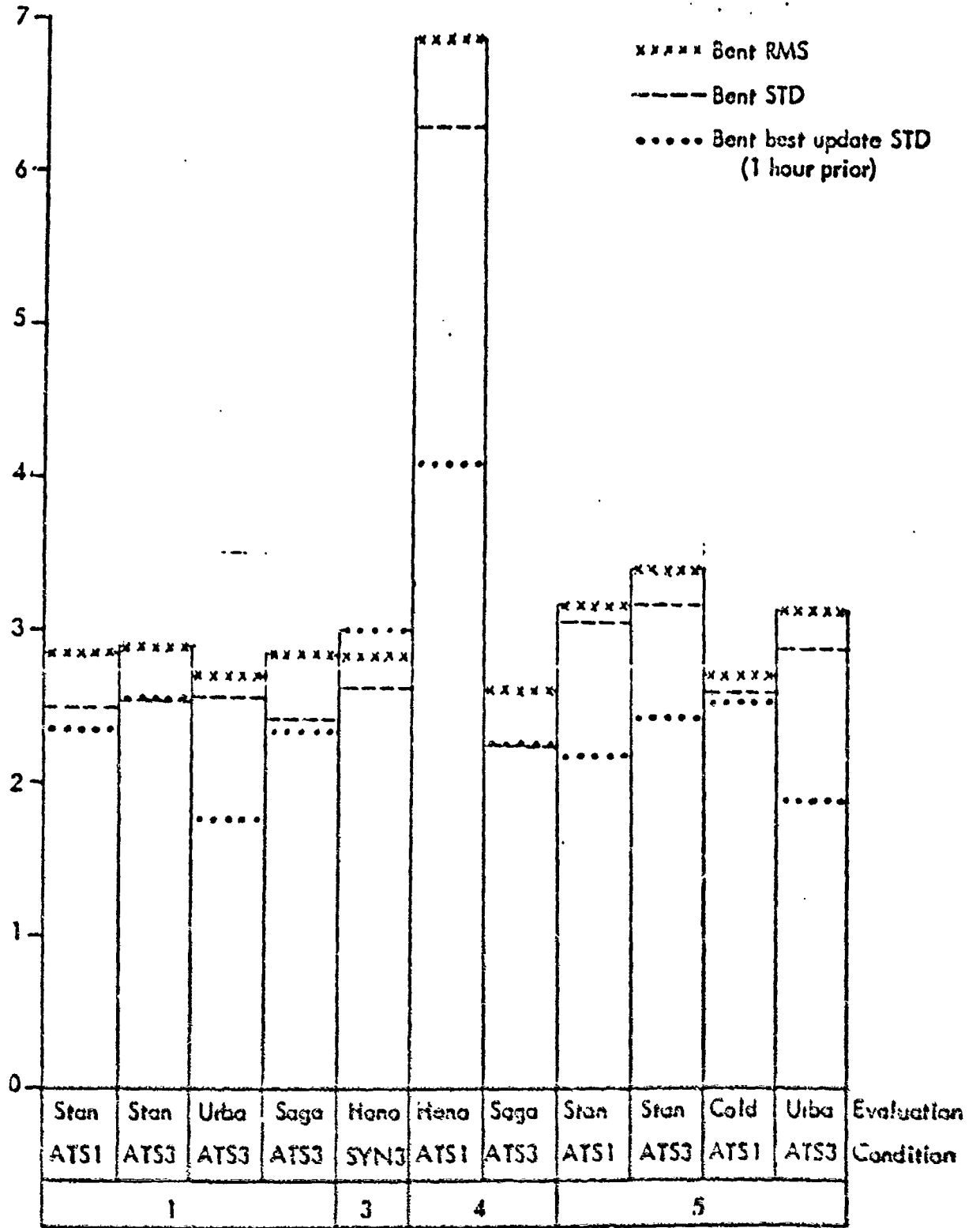


Figure 4.1-1. Overall RMS and STD of Residual Group Delay for Each Evaluation Condition

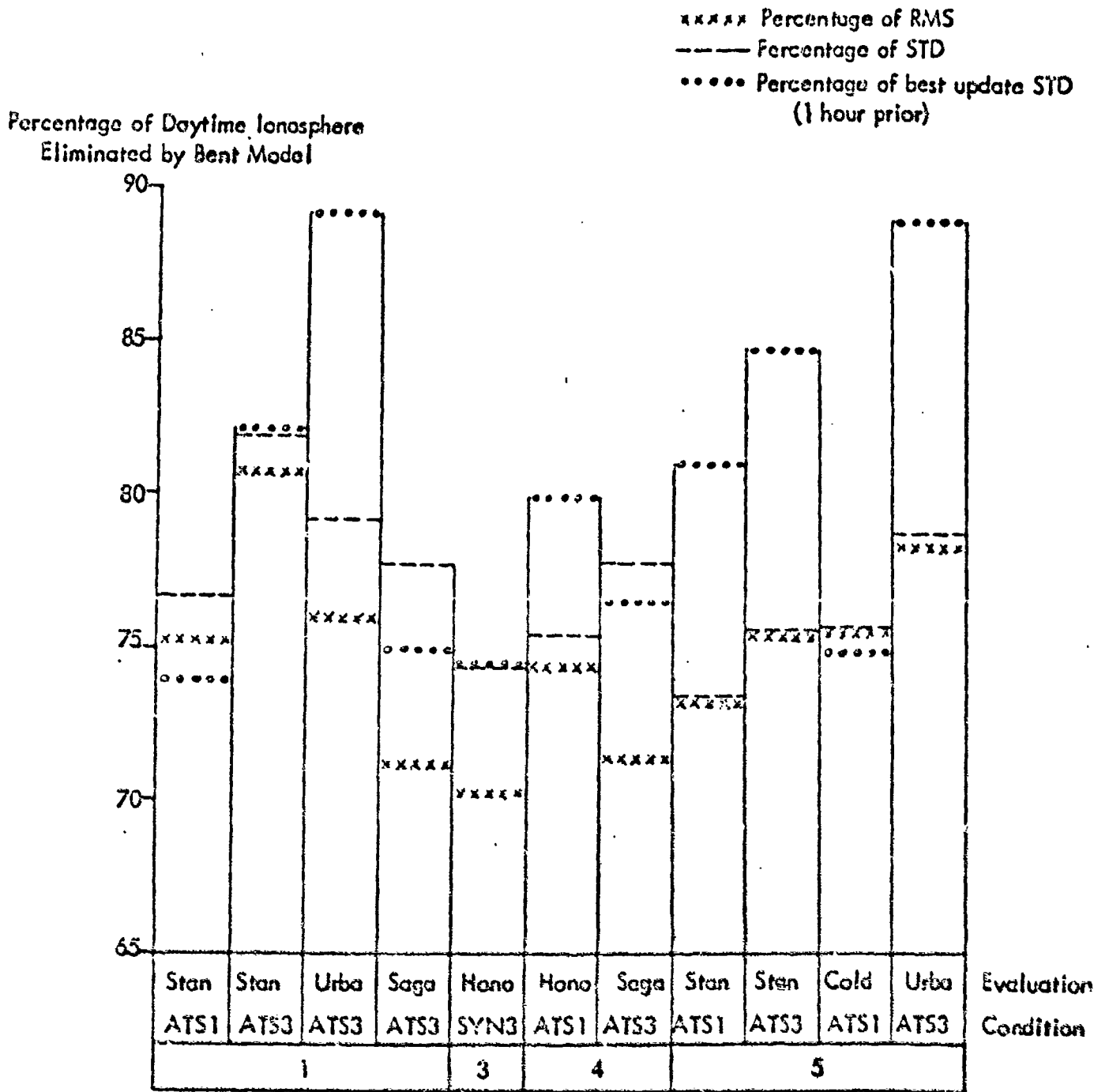


Figure 4.1-2. Percentage of Daytime Ionosphere Eliminated for Each Evaluation Condition

## 4.2 Derivation of Results

The analysis for the results given in the preceding comparison matrix is given in Appendices A through H.

## 5. SELECTION

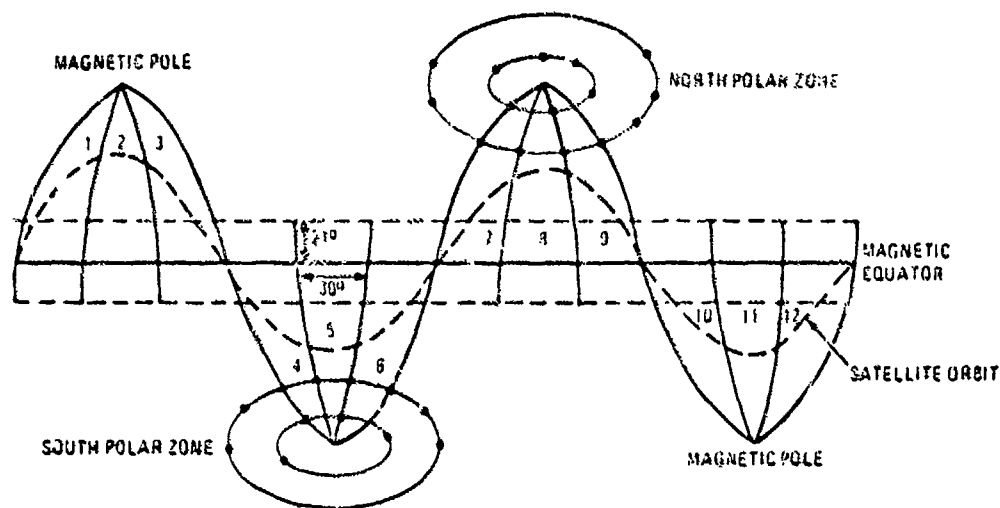
Before a particular recommendation of ionospheric techniques to be used in the navigational satellite system can be made we must consider a number of items that affect the simplicity of the overall system. Both the satellite and user storage should be kept to a minimum; the satellite stored data can only be updated once per day; the satellite to user transmission time should be kept to a minimum; the final results should be as accurate as possible and the users reduction should be simple. It is understood that approximately 200 bits per half minute frame can be used for ionospheric data transmission and if the information can all be obtained in this period of time, the user will not need any extra time in order to obtain his ionospheric data. We also believe that when a user is receiving data from the first satellite, his equipment is already searching for the second satellite thereby removing any "lock on" delay time. The user requires data from four satellites to obtain his final position and therefore the ionospheric information could be sequentially coded into four parts, with all satellites in a particular sector of the globe transmitting the same sectors at the same time. The only major problem with such a technique would be that a user who lost lock during a frame may have to wait two minutes to obtain his lost ionospheric data frame.

A major factor in ionospheric errors in the simple approach is the time factor causing relative ionospheric rotation. If a satellite stores a complete world map of the ionosphere, the map must be rotated in time up to  $\pm 12$  hours which gives over 25% error. A better system is for the stored data to be divided into segments that are much nearer to the time required. This reduces the 25% time error to 10%. In view of all these factors, two techniques are recommended, one of which is still under investigation by General Dynamics and may prove satisfactory. In addition to these dynamic models, the two static versions of ionospheric modeling discussed in Section 3 are also viable candidates.

### 5.1 Cross-line Technique for 30° Longitude Segments

This concept is still under investigation, but preliminary results presented here indicate the method as a modification is a viable candidate.

During a 24 hour period a satellite's path on the earth's surface will be two cycles as in Figure 5-1. It has been shown (Figure 1a, Appendix G) that the earth's ionosphere shows considerable symmetry to the earth's magnetic field and therefore implies that for simplicity we should assume the satellite is moving in a magnetic not a geographic environment. Figure 5-1, therefore, represents a magnetic projection where a satellite orbit can be  $\pm 12^\circ$  latitude in error over a geographic illustration. If we are to divide the globe up into segments in order to reduce the time error which is larger near the equator and in order to reduce the user's storage requirements, we will have a problem over the poles. In this



TE038

Figure 5-1. Satellite Path

region a user may need to receive all the earth's segments of information to provide his total coverage. It is therefore necessary to transmit a separate polar cap zone to eliminate the need for a large storage of information.

A user requires approximately a  $\pm 16^\circ$  earth central angle zone to cover his visible ionosphere to a  $5^\circ$  cut-off angle. He, therefore, would require three consecutive  $30^\circ$  zones to cover his field of view if he is at  $50^\circ$  magnetic latitude. At higher latitudes the polar zone would be sufficient although a combination of  $3 \times 30^\circ$  segments and a polar zone may be necessary. Let us assume the user is in segment 8. The satellite whose path is displayed on the diagram would sequentially transmit data (1/2 minute or approximately 140 bits) for the polar zone, and zones 7, 8, and 9. All satellites in this sector of the earth would transmit the same zones at the same time. For example:

TIME AND ZONES TRANSMITTED

		30 sec	60 sec	90 sec	120 sec	150 sec	180 sec
Satellite A	N. Pole	7	8	9	N. Pole	7	8
Satellite B	N. Pole	10	8	9	N. Pole	10	8
Satellite C	S. Pole	7	8	9	S. Pole	7	8



For the time error due to the earth's rotation to be limited to 10% it is necessary for the zones away from the pole to be accurate to  $\pm 1$  hour and then the user to rotate his position with respect to time within this zone. Because the satellite takes 2 hours to cross a particular zone and because it is transmitting a zone for 6 hours, it is necessary for the satellite storage to contain data for each zone at 3 different times, each 2 hours advanced from the other. The total satellite storage is therefore 12 zones  $\times$  3 for 24 hours plus 2 polar zones  $\times$  2. The polar zone can be in error by  $\pm 6$  hours as the ionospheric gradients are less severe. An overlap of  $21^\circ$  is provided at the equator in each direction so that a user may obtain his information from either a southern or a northern hemisphere satellite.

Let us now consider the way the information in each sector is to be transmitted. It is shown in Appendix G that a  $30^\circ$  zone can be very well represented by a cross-line technique. Each of these zones will therefore be transmitted in a way described in Figure 5-2.

A  $7^\circ$  spacing of group delay will describe the magnetic equator and a seven degree spacing of ratios will describe the latitude effect from  $-21^\circ$  to  $49^\circ$  magnetic latitude. Above  $50^\circ$  latitude the polar zone will dominate. Fifteen (15) coefficients will adequately describe each zone, although a reference longitude and a reference time will be needed. The reference longitude could be a number between 1 and 12 which describes on which multiple of  $30^\circ$  the initial longitude line lies. The time reference should be accurate to 5 minutes and be related to the time the satellite is at the center of a zone. The number of bits per zone is made up of 4 bits for the group delay and 3 for the height per coefficient. The longitude reference needs 4 bits and the time reference 5 bits. One zone is therefore made up of  $(15 \times 7) + 4 + 5$  bits = 114 bits.

The polar zone can satisfactorily be made up of a  $20^\circ$  grid as shown in Figure 5-3.

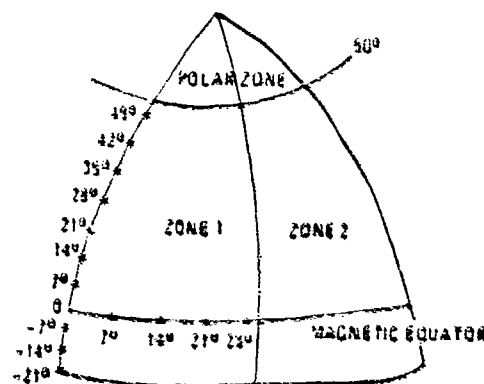
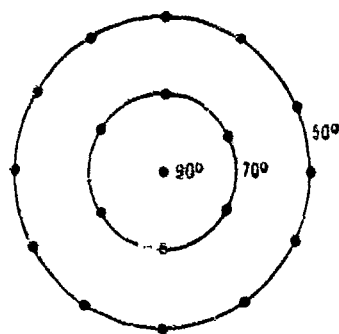


Figure 5-2.  $30^\circ$  Zone



7-22

Figure 5-3. Polar Zone

The coefficients can be fixed in longitude with  $30^\circ$  longitude steps at  $50^\circ$  latitude and  $60^\circ$  longitude steps at  $70^\circ$  latitude. The 19 coefficients will need only a time reference of 6 bits making a total of 139 bits. Linear interpolation will be performed in the polar zones.

In summary we can list the important features:

<u>User storage</u>	3 equatorial $30^\circ$ zones plus 1 polar zone = 481 bits.
<u>Satellite Transmission</u>	Approximately 140 bits per 30 second user navigation data frame.
<u>Technique accuracy</u>	Results show this approach to have the following RMS errors: <ol style="list-style-type: none"> <li>a) Model error 15-30%</li> <li>b) Time error 10%</li> <li>c) Space error 14%</li> <li>d) OVERALL RSS ERROR 23-35%</li> </ol>

### 5.2 Satellite Transmit Delay - Series Approach

With this approach, the series representation of the polar plot of line of sight delay will provide coverage of the satellite's field of view for a one hour interval. Empirical results indicate that 24 coefficients, each of 5 bit resolution is required to adequately represent the desired accuracy for a one hour period. Because of the minimum satellite transmission, simpler user processing and the series longevity of one (1) hour this method is the recommended approach when using a dynamic model.

Simpler user processing is obtained because of the type of model used. The series representation is for the delay between any user location and the satellite. This saves considerable computation over other approaches that model the ionosphere's electron density and height. The reason is that ionosphere model require addition steps of computing total electron content along the ray path of the signal.

In summary, the important features are:

User Storage

127 bits from each of four satellites for a total of 508 bits.

Satellite Transmission

127 bits per 30 second user navigation data frame, with a data change every hour.

Technique Accuracy

Results show this approach to have the following RMS errors:

Model Error	15 - 30%
Time Error	10%
Space Error	14%
Overall RSS Error	23 - 35%

APPENDICES

Trade Study No. 7

These results were extracted from the  
"Final Report on Ionospheric Modeling"  
prepared for General Dynamics Electronics  
Division by Atlantic Science Corporation

## APPENDIX A

### The size of ionospheric errors that can be expected after application of a good ionospheric model

The size of ionospheric group delay errors at 1600 MHz remaining after application of several ionospheric models has been discussed in a number of SAMSO reports. On average it is assumed that over the continental United States a residual RMS group delay (measured-predicted) for high solar activity varies between 2.6 and 3.3 nano-seconds using a good ionospheric model. For a point nearer the magnetic equator, however, such as Honolulu, this value can be as high as 6.8 to 9.0 nano-seconds. The purpose of this short report is to point out the real information on group delay that is hidden by these deceptive figures.

Let us look initially at the ionospheric characteristics above Hawaii during 1968 when the solar activity was at its height during the last solar cycle. During the month of January and November large values of total ionospheric content existed. Figures 1 and 2 show the minimum, mean, and maximum values recorded during these months where the total electron content has been converted to group delay at 1600 MHz. It is immediately obvious that even with the best ionospheric model, without daily update, the predicted value can be 27 nano-seconds in error. It is highly unlikely that an ionospheric model will produce the same value as the mean and so the likely errors may be well in excess of 30 nano-seconds at vertical incidence.

Studying these two months in more detail brings us to Figures 3 and 4. These figures show during one hour in the local afternoon for January and November, the actual value of vertical group delay on a day by day basis. Also displayed are the corresponding predictions and updated values using the Bent Ionospheric Model. It is obvious that the predictions are very low, but we will show later that this is related to a critical frequency very much

higher than predicted. Using daily updates of critical frequency one hour old at Maui, the predicted values are significantly correlated to the actual values. Updating with Faraday data from Stanford provides very little improvement in November, but a significant amount in January.

These two figures indicate that vertical group delay times of 70 nano-seconds or more were measured. Converting this value to the delay at 5° elevation we must expect line of site delays of 210 nano-seconds. One may ask the question, what would the maximum value be during a solar cycle where the activity was much higher as was the case during the previous cycle? With ionospheric 'no-update' predictions during these months, it is still possible to have a residual error (measured-predicted) of 40 nano-seconds at vertical incidence (see November 24 at 0 hours UT). At 5° elevation, therefore, the residual error after application of a mean ionospheric model will be 120 nano-seconds. With update from a nearby station, this residual was reduced from 40 nano-seconds to 2 nano-seconds.

Figures 5 and 6 show the corresponding predicted and measured  $f_oF_2$  value and we immediately see the measured value is considerably higher than the predicted value at all times except the last week of January. During that week when the predictions for  $f_oF_2$  were reasonably accurate, Figure 3 shows us that the predictions of group delay were also accurate. The values of 10.7 cm. solar flux are also displayed in Figures 5 and 6, but on this occasion it seems to bear little correlation to the magnitude of  $f_oF_2$ . In fact, Figure 7 illustrates the residual group delay at 0 hours UT versus the daily value of solar flux. This demonstrates that absolutely no correlation exists between solar flux and the residual group delay.

One must bear in mind, however, the inaccuracies of the Faraday rotation measurements used to compute the measured group delay, particularly during periods of disturbed conditions. D.H. Smith (JGR Feb 1970) indicates a 50% change in the mean diurnal Faraday factor at Aricebo existed during an experimental period in January 1969 which would be directly

proportional to the total content and hence group delay. More commonly a diurnal variation of  $\pm 4\%$  exists in the Faraday factor, but using the Bent Ionospheric Model and a magnetic field model, an average seasonal variation of 9% has been shown to exist at a specific time over Hawaii in 1969. These variations were not included in the basic reduction of the data and we must, therefore, assume that they have been fed into the reduction of the group delays shown here. Atlantic Science Corporation are at present working for the National Aeronautics and Space Administration (NASA) on a contract to model such a factor on a worldwide basis thereby providing a more accurate reduction of Faraday rotation data.

In summary, Figure 8 shows the RMS residual group delay after application of the Bent Ionospheric Model for Hawaii in 1968. Values in excess of 20 nano-seconds are evident in November and January without update. These values drop significantly with a local update. The figure also shows the basic no-update value for August to be low indicating considerable seasonal variation of group delay. As an indication that the results are not a function of the Bent Ionospheric Model, the results from a Stanford Model are shown in Figure 9 for January 1968. This model was built by totally different techniques and still showed the same large diurnal variation in the RMS residual. Figure 10 shows the improvement that can be obtained by ionospheric modeling with and without update under the worst conditions.

The continental United States has a much more stable ionosphere as it is some distance from the magnetic equator. In this region the maximum monthly RMS residual after applying a good ionospheric model will be about 6-7 nano-seconds during local afternoon. The actual daily residual, however, may rise to 4 times this value.

Honolulu looking at ATS-1 for 31 days of January 1968

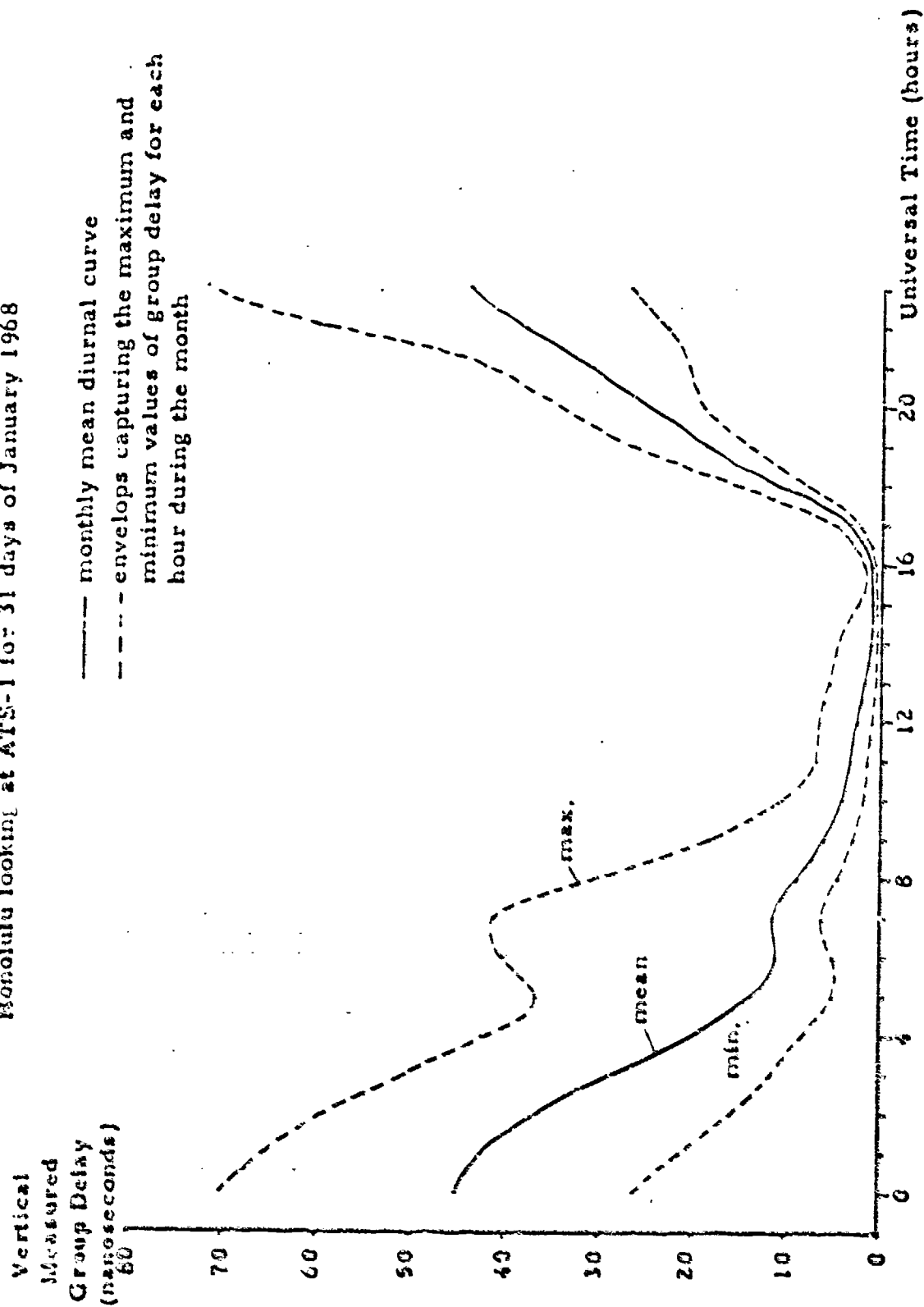


FIGURE 1.



Vertical Measured Group Delay (nanoseconds)

Honolulu looking at ATS-1 for 30 days of November 1968

— monthly mean diurnal curve  
- - - envelopes capturing the maximum and minimum values of group delay for each hour during the month

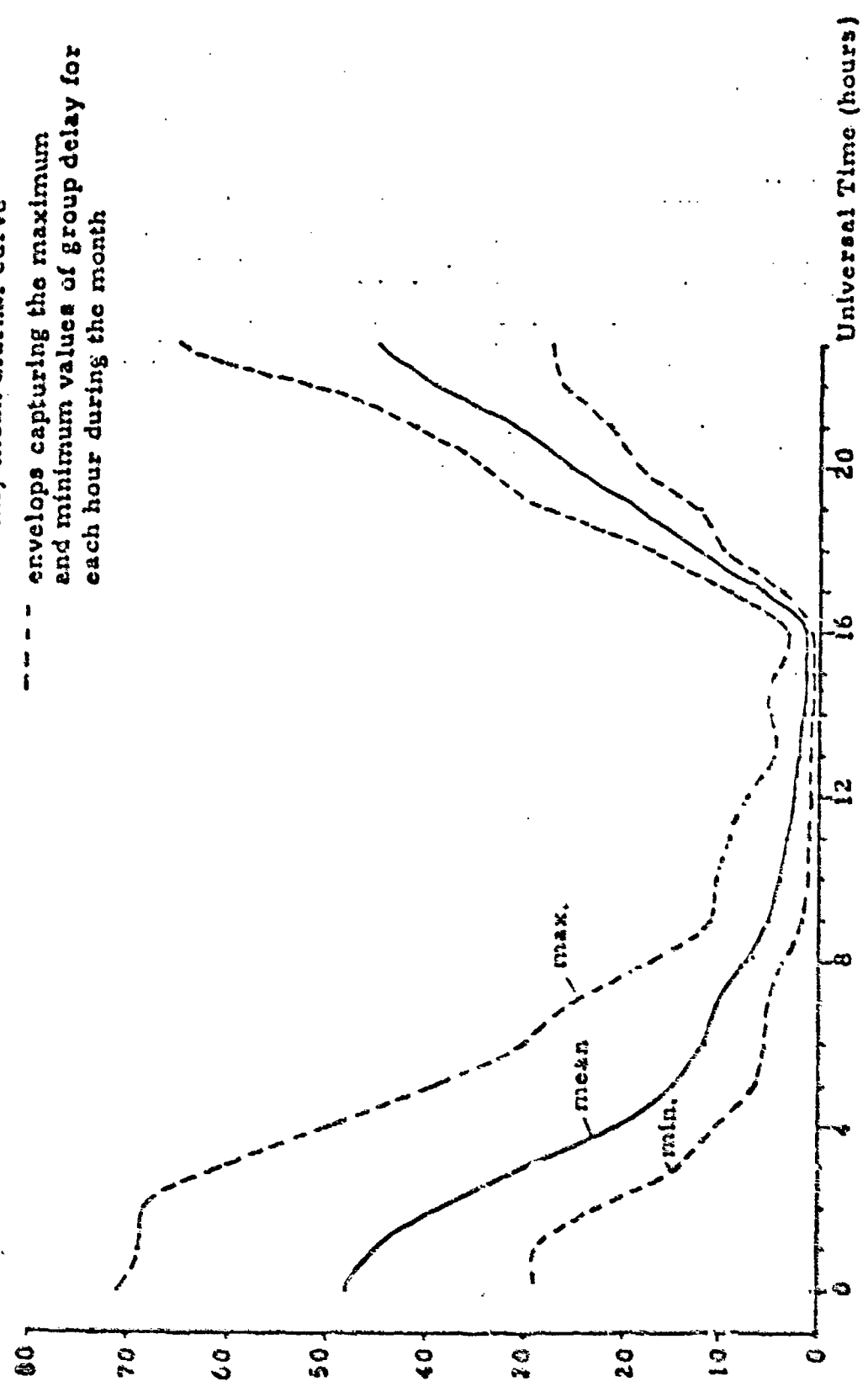
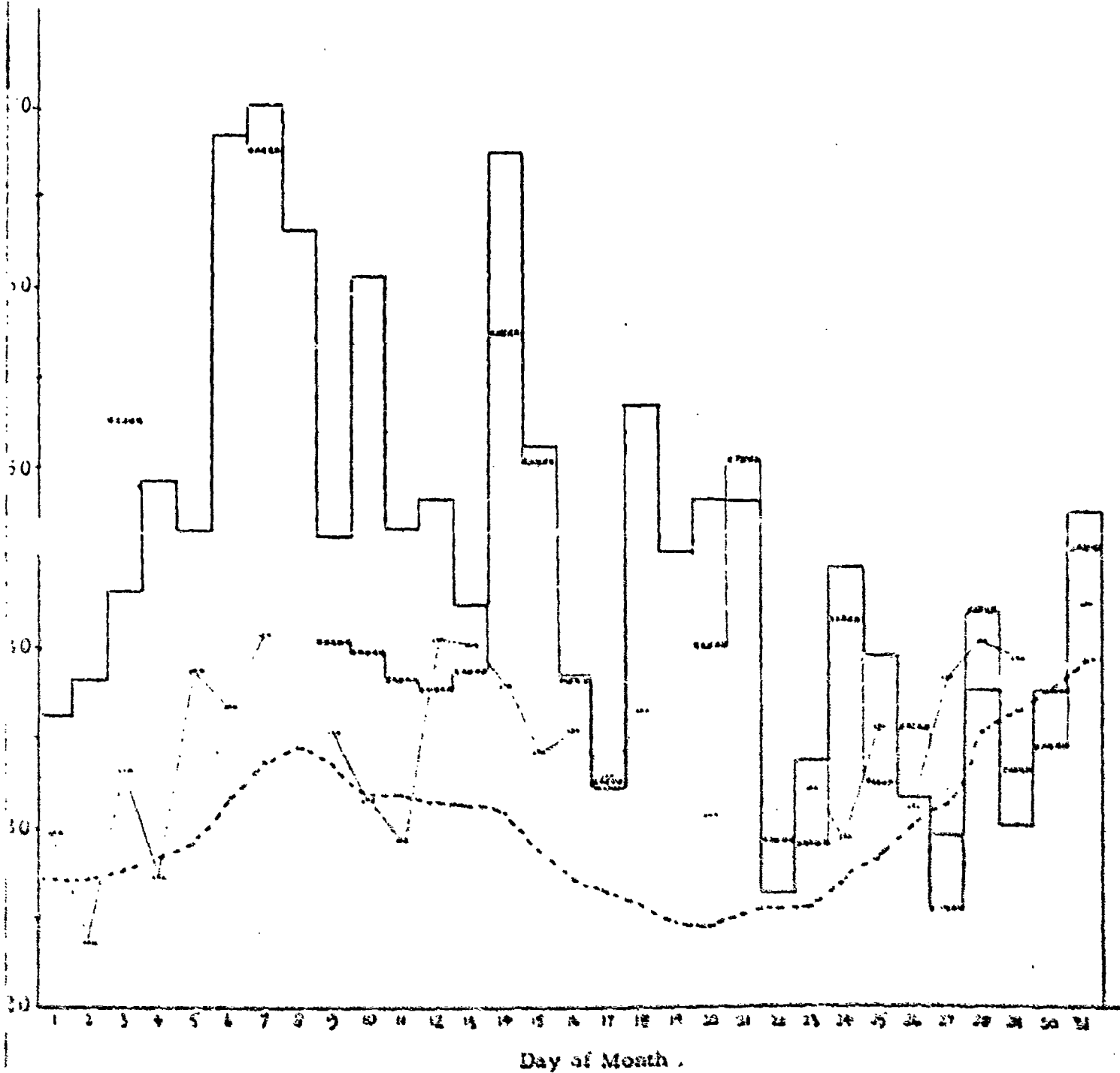


FIGURE 2.

January 1968 0 hours UT  
 Honolulu ATS-1

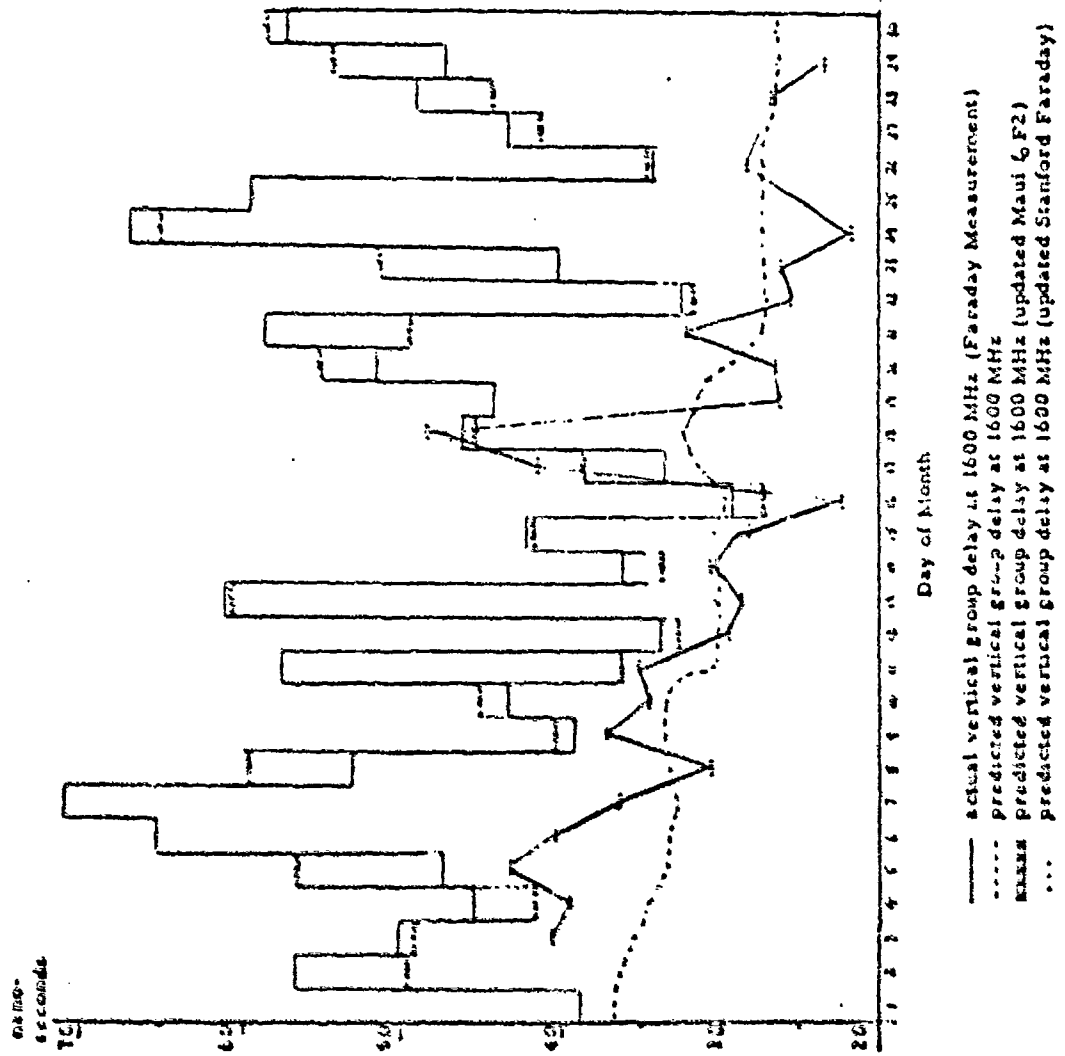
nano  
 seconds



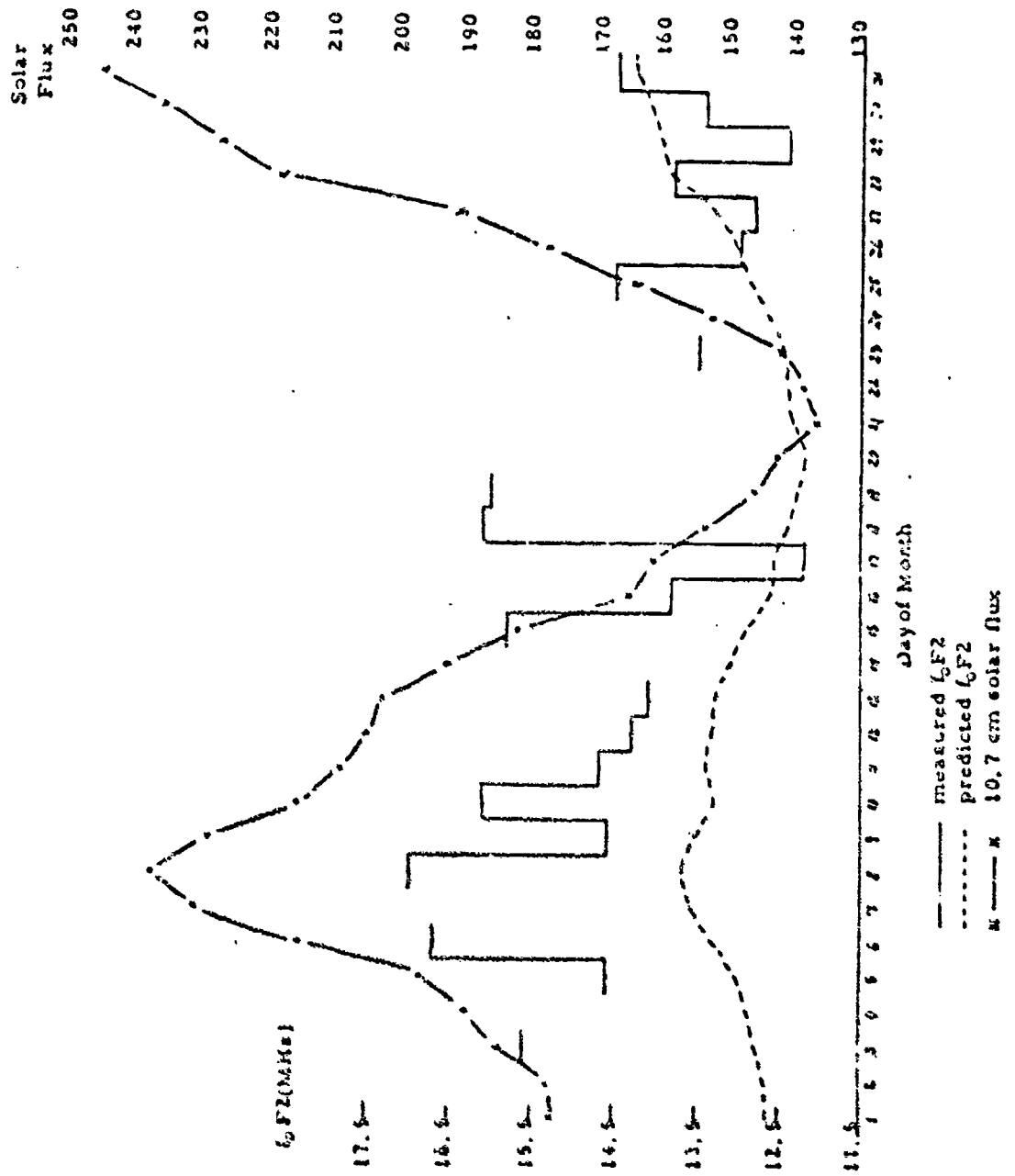
- actual vertical group delay at 1600 MHz
- predicted vertical group delay at 1600 MHz
- xxxxxxx predicted updated vertical group delay at 1600 MHz (Maui L F2)
- ... predicted updated vertical group delay at 1600 MHz (Stanford Faraday)

FIGURE 3.

IONOSPHERICAL DELAY AT 1600 MHZ  
HONOLULU ATS-1, NGV 1968 0 HOURS UT



# JANUARY 1968 0 HOURS UT MAUI



November 1968 0 hours UT  
Maui.

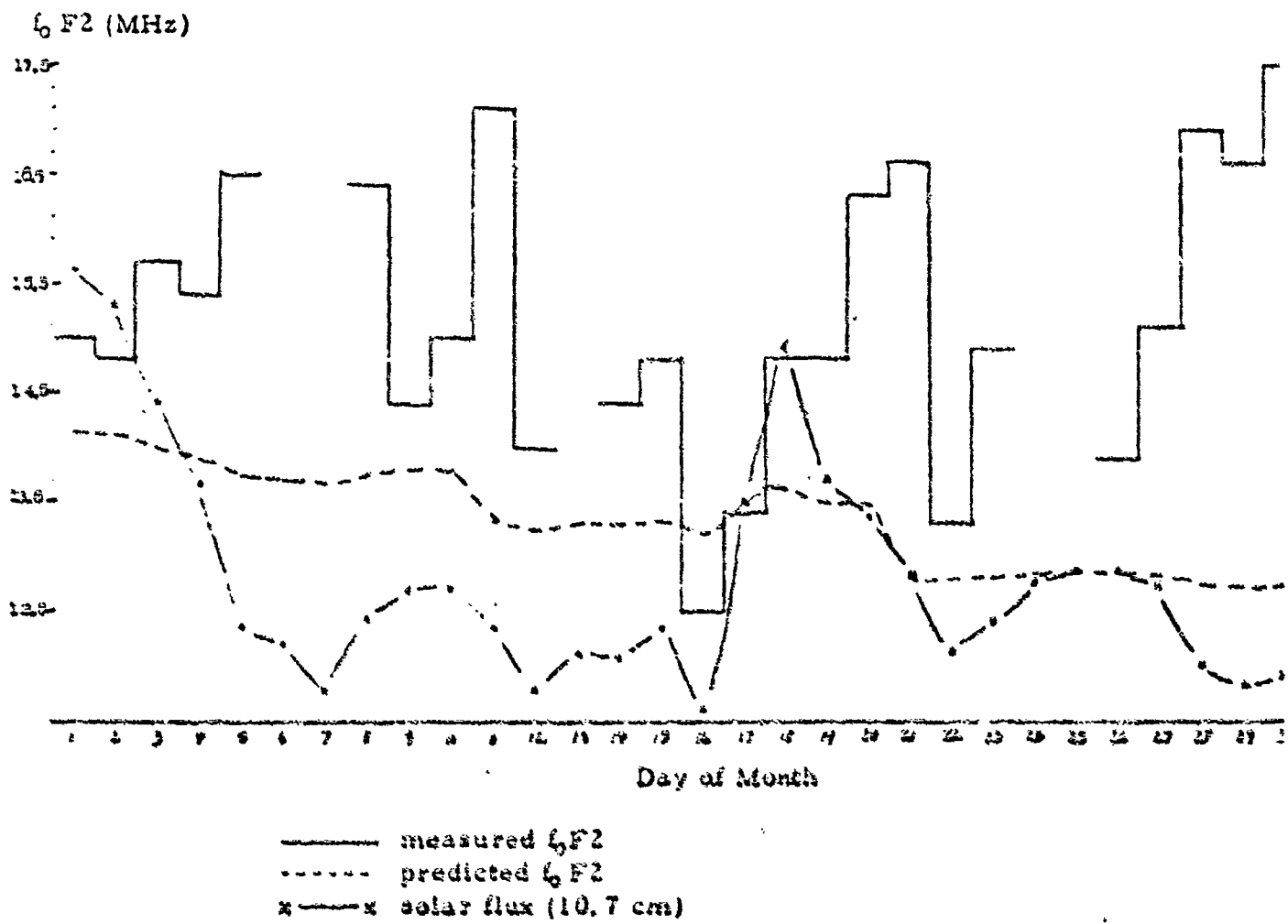
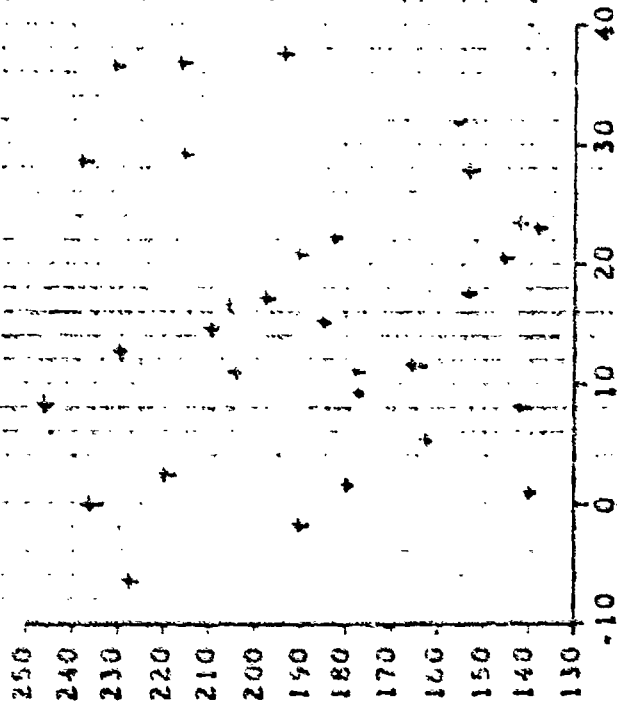


FIGURE 6.

Daily Solar Flux



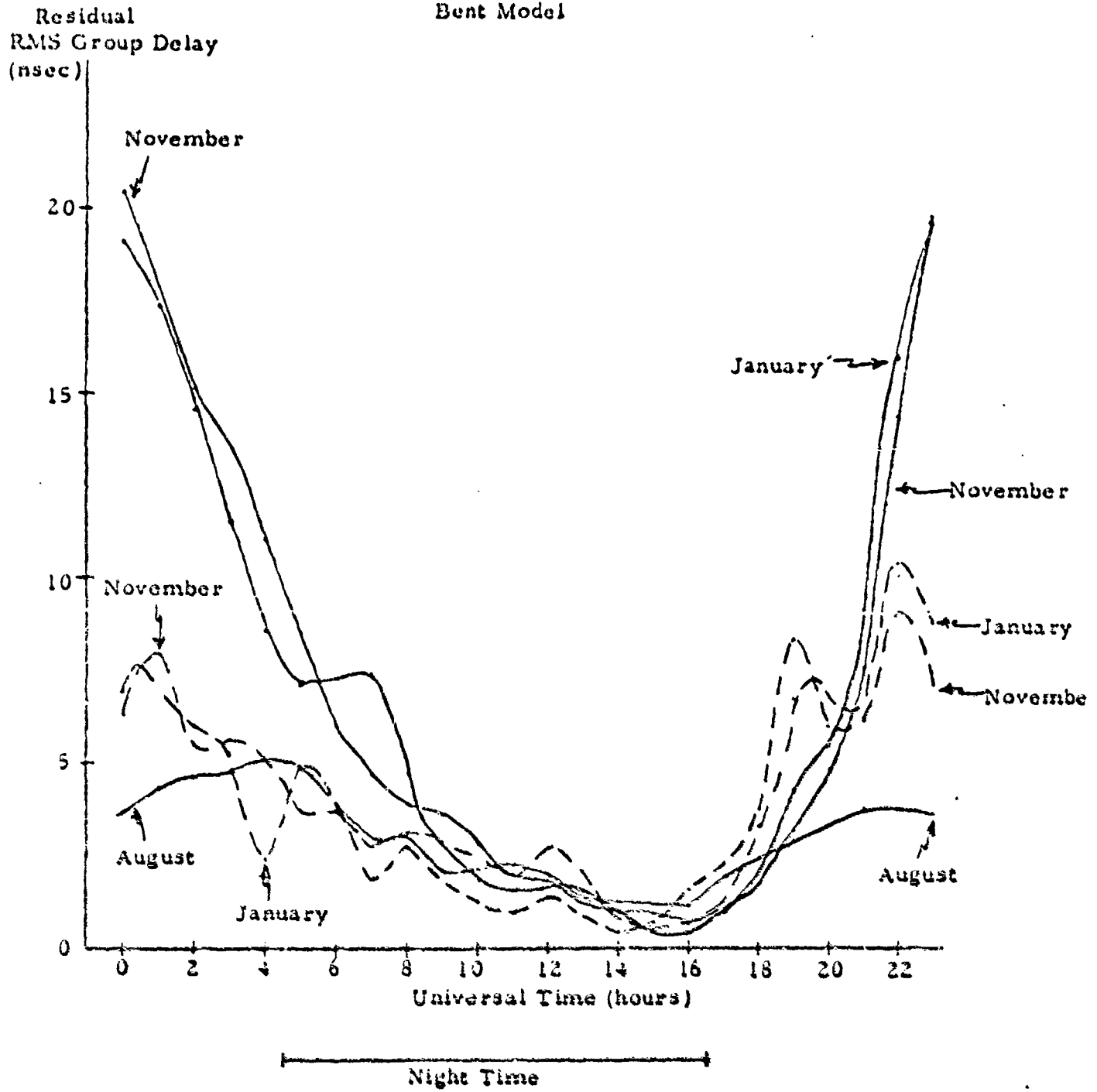
The plot for the 31 days of Jan 1968 of the residual group delay at hour 0 versus the daily value of solar flux demonstrates that there is no solar flux relationship that could be used to correct the predictions of group delay.

Measured - Predicted Residual vertical Group Delay (nanoseconds) at (P UT for 31 days in January 1968 and station Honolulu looking at ATS-1

FIGURE 7.

# Hawaii Group Delay for 1968

Bent Model



— Residual RMS of Group Delay for Honolulu ATS-1  
- - - Residual RMS of Group Delay for Honolulu ATS-1  
Updated with  $f_2$  from Maui

FIGURE 3.

Hawaii Group Delay for 1968  
Stanford Model

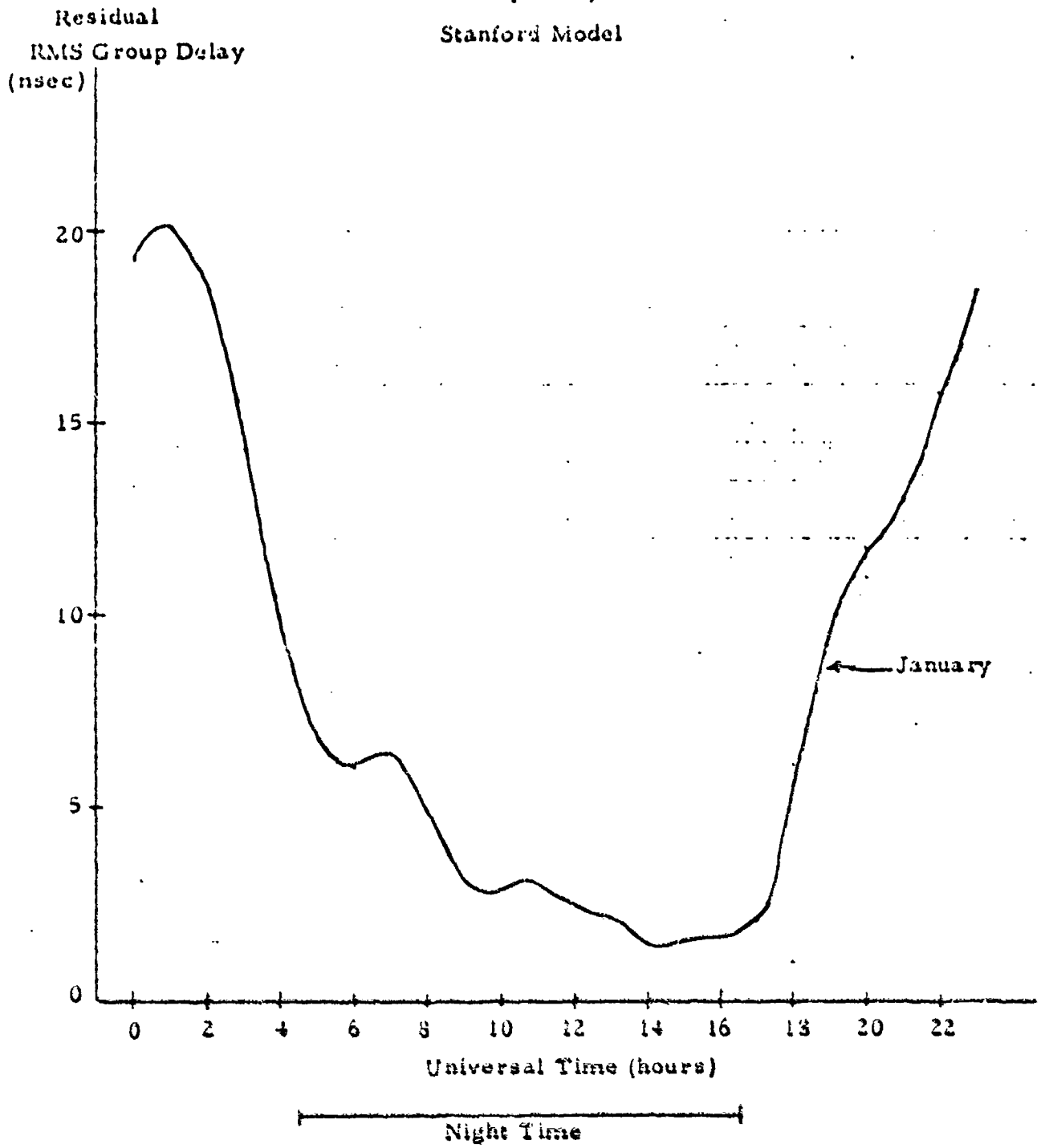


FIGURE 9.



Honolulu looking at ATS-1 for 30 days of November 1968

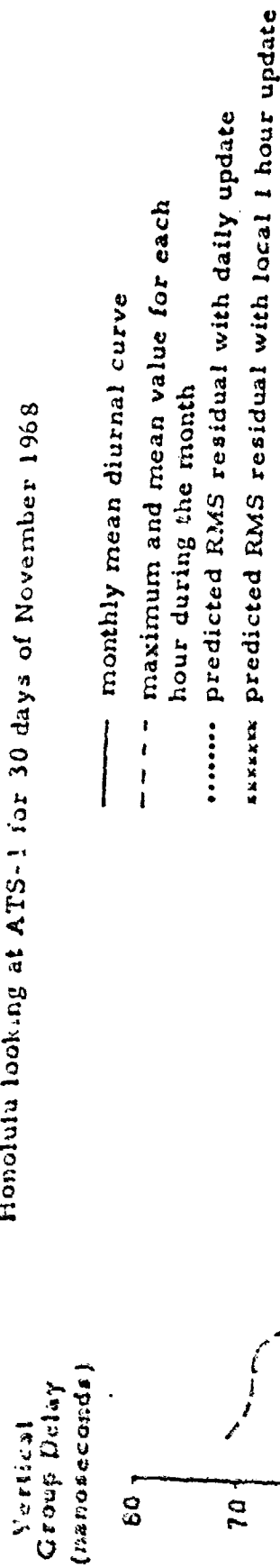


FIGURE 10.

## APPENDIX B

### The feasibility of using two frequency group delay measurements to eliminate the ionospheric retardation of signals from satellite to ground

Radio signals from artificial earth satellites propagated through the earth's ionosphere are subjected to group delays. These effects cause uncertainties in the determination of distance between transmitter and receiver; the uncertainties being a function of the frequency of transmission and the electron densities in the ionosphere.

For a single transmission frequency where only group delay is being measured, it is necessary to model the ionospheric electron content in order to account for time delay within the ionosphere. Modeling the ionosphere which has many uncertainties, can still lead to errors which are unacceptable. It is possible to monitor both group delay and phase delay to account for ionospheric problems or, more accurately, it is possible to monitor the source with two frequencies if these frequencies are well separated and are high enough.

An explanation of the two frequency approach is given below:

The electromagnetic path of a radio wave is defined by Fermat's principle as that particular path, of all possible paths the ray might follow, that results in the minimum group path length. The quantity is obtained by integrating the refractive index along the group path

$$L(t) = \int_g n(r, f, \theta) ds$$

where  $g$  represents the group path. The limits on the integral are understood to be time dependent.

The electromagnetic path length of the geometric or straight line path is obtained by integrating the refractive index along the geometric path

$$C(t) = \int_s n(r, f, \theta) ds$$

where  $s$  represents the straight line path.

The group path length can be expressed

$$L(t) = G(t) + \left[ \int_0^{\infty} n(r, r, \theta) ds - \int_0^{\infty} n(r, r, \theta) ds \right]$$

or  $L(t) = G(t) + \Delta L$  where  $\Delta L$  is the correction for bending (1)

An expression for the square of the refractive index of the ionosphere was derived by Sir E. V. Appleton in the 1920's and is given as (Appleton, 1932)

$$n^2 = 1 - X / \left\{ 1 - \frac{Y_r^2}{s(1-X)} \pm \left[ \frac{Y_r^2}{4(1-X)^2} + Y_L^2 \right]^{1/2} \right\}$$

where

$$X = (Ne^2) / (4\pi^2 \epsilon_0 m f^2)$$

$$Y_L = Y \cos \alpha$$

$$Y_r = Y \sin \alpha$$

$$Y = (\omega_e H_e) / (2\pi m f)$$

This equation includes the effects of the earth's magnetic field, but neglects the effects of the collision between particles.

Assuming the quasilongitudinal approximation (Budden, 1961), the Appleton-Hartree equations becomes

$$n_o^2 = 1 - X \left( \frac{1}{1 \pm Y_L} \right) \text{ for phase index of refraction and}$$

$$n_g^2 = 1/n_o^2 = 1 + X \left( \frac{1}{1 \pm Y_L} \right) \text{ for group index of refraction}$$

For  $f > 40$  MHz, and  $Y_L \ll 1$ , the terms  $1/(1 \pm Y_L)$  can be approximated by a series expansion, so that the square of the refractive index becomes

$$n_g^2 = 1 + X \pm X Y_L + X Y_L^2 \quad (2)$$

For  $n_g^2 = 1$ , an equation for the refractive index is obtained from equation (2) by the binomial expansion and is given as

$$n = 1 + \frac{X}{2} \pm \frac{X Y_L}{2} + \frac{X^2}{8} + \frac{X Y_L^2}{2} + \dots \quad (3)$$

Substituting the physical constants for X and Y<sub>1</sub>, equation (3) becomes

$$\begin{aligned}
 n_g(r, \Gamma, \theta) = & 1 + \frac{e^2}{2(2\pi)^3 m \epsilon_0 f^2} N(r, \Gamma, \theta) \pm \frac{|e|^2 \mu_0}{2(2\pi)^3 m^2 \epsilon_0 f^3} N(r, \Gamma, \theta) H(r, \Gamma, \theta) \cos \alpha \\
 & + \frac{e^4}{8(2\pi)^4 m^2 \epsilon_0^2 f^4} N^2(r, \Gamma, \theta) + \frac{e^4 \mu_0^2}{2(2\pi)^4 m^3 \epsilon_0 f^4} N(r, \Gamma, \theta) H^2(r, \Gamma, \theta) \cos^2 \alpha \\
 & + \text{terms of the order of } \frac{1}{f^5} \text{ and higher.} \quad (4)
 \end{aligned}$$

In MKS units this may be re-written as

$$\begin{aligned}
 n_g(r, \Gamma, \theta) = & 1 + \frac{A}{f^2} N(r, \Gamma, \theta) \pm \frac{B}{f^3} N(r, \Gamma, \theta) H(r, \Gamma, \theta) \cos \alpha + \\
 & \frac{C}{f^4} N^2(r, \Gamma, \theta) + \frac{D}{f^4} N(r, \Gamma, \theta) H^2(r, \Gamma, \theta) \cos^2 \alpha + \dots
 \end{aligned}$$

where  $A = 40.365$ ,  $B = 1.4200 \times 10^6$ ,  $C = 8.1465 \times 10^2$ ,  $D = 4.9952 \times 10^{10}$

Substituting equation 4 into equation 1 and letting

$$L_0(t) = \int_0^t ds$$

$$L_1(t) = A \int_0^t N(r, \Gamma, \theta) ds$$

$$L_2(t) = \pm B \int_0^t N(r, \Gamma, \theta) H(r, \Gamma, \theta) \cos \alpha ds$$

and

$$L_3(t) = C \int_0^t N^2(r, \Gamma, \theta) ds + D \int_0^t N(r, \Gamma, \theta) H^2(r, \Gamma, \theta) \cos^2 \alpha ds$$

$$+ f^2 \left[ \int_0^t n_g(r, \Gamma, \theta) ds - \int_0^t n_g(r, \Gamma, \theta) ds \right]$$

the expression for the electromagnetic path length becomes

$$L(t) = L_0(t) + \sum_{k=1}^{\infty} \left( \frac{1}{f^{k+1}} \right) L_k(t) \quad (5)$$

now let us define

$$L_0 = \int_0^r ds$$

$$L_1 = \int_0^r N(r, \Gamma, \theta) ds$$

$$L_2 = \int_0^r N(r, \Gamma, \theta)H(r, \Gamma, \theta) \cos \alpha ds$$

$$L_3 = \int_0^r N^2(r, \Gamma, \theta) ds$$

$$L_4 = \int_0^r N(r, \Gamma, \theta)H^2(r, \Gamma, \theta) \cos^2 \alpha ds$$

$L_0$  is the geometric straight line path in the absence of the ionosphere.

The remaining terms represent the ionospheric contribution to the group propagation path as follows:

$L_1$  is the first order term neglecting magnetic field

$L_2$  is the first order term correcting for magnetic field effects

$L_3$  is the second order ionospheric term

$L_4$  is the second order term with magnetic field

Therefore,

$$G(t) = L_0 + \frac{A}{f^2} L_1 \pm \frac{B}{f^3} L_2 + \frac{C}{f^4} L_3 + \frac{D}{f^4} L_4 + \dots \quad (6)$$

but by the mean value theorem

$$L_2 = \int_0^r N(r, \Gamma, \theta)H(r, \Gamma, \theta) \cos \alpha ds = M \int_0^r N(r, \Gamma, \theta) ds = ML_1$$

$$L_4 = \int_0^r N(r, \Gamma, \theta)H^2(r, \Gamma, \theta) \cos^2 \alpha ds = M' \int_0^r N(r, \Gamma, \theta) ds = M' L_1$$

where  $M' \leq M^2$

and as shown in Appendix A

$$L_3 = \int_0^r N^2(r, \Gamma, \theta) ds = 2N_0 \int_0^r N(r, \Gamma, \theta) ds = 2N_0 L_1$$

where  $N_0$  = maximum electron density along the path of integration

Substituting in Equation 6

$$G(t) = L_0 + \frac{A}{f^2} L_1 \pm \frac{B}{f^2} M I_1 + \frac{C}{f^2} \cdot 2N_s L_1 + \frac{D}{f^4} M' L_1$$

$$= L_0 + \frac{40.365}{f^2} L_1 \left( 1 \pm \frac{3.5179 \times 10^4 M}{f} + \frac{40.364}{f^2} N_s + \frac{1.2375 \times 10^9 M'}{f^2} \right)$$

In order to investigate the maximum and minimum effect of the higher order terms, we will assume the extreme values of  $M$ ,  $N_s$  and  $M'$  to be as follows:

maximum	{	$M = 40$ ampere-turns (corresponds to $H = .5$ gauss) $N_s \leq 5 \times 10^{12}$ electrons/m <sup>3</sup> (corresponds to $f_0 F2 = 20$ MHz) $M' \leq M^2 = 1600$ (ampere-turns) <sup>2</sup>
minimum	{	$M = 40$ ampere-turns (corresponds to $H = .5$ gauss) $N_s = 1 \times 10^{12}$ electrons/m <sup>3</sup> (corresponds to $f_0 F2 = 3$ MHz) $M' \leq M^2 = 1600$ (ampere-turns) <sup>2</sup>

Therefore

$$G(t) = L_0 + \frac{40.365}{f^2} N_s \left( 1 \pm \frac{1.4072 \times 10^3}{f} + \frac{161.456 \times 10^{15}}{f^2} + \frac{1.98 \times 10^{12}}{f^2} \right)$$

Now from (1)

$$L(t) = G(t) + \Delta L \quad \text{where } \Delta L \text{ is the bending correction}$$

therefore

$$L(t) = L_0 + \left( \frac{40.365}{f^2} N_s \cdot \beta(f) \right) + \Delta L \dots \quad (7)$$

The maximum and minimum values of  $\beta$  for various frequencies  $f$  are listed in Table 1

$$\left[ \text{where } \beta(f) = 1 \pm \frac{1.4072 \times 10^3}{f} + \frac{161.456 \times 10^{15}}{f^2} \right]$$

TABLE 1: Ionospheric propagation correction to group path length  
 $\beta$  vs.  $f$

Maximum Values									
$f(\text{MHz})$	50	100	140	200	300	600	900	1200	1600
$\beta_-$	1.053	1.006	1.003	.998	.998	.999	.999	.999	.999
$\beta_+$	1.110	1.034	1.020	1.012	1.007	1.003	1.002	1.001	1.001

Minimum Values									
$f(\text{MHz})$	50	100	140	200	300	600	900	1200	1600
$\beta_-$	.974	.986	.990	.993	.995	.998	.998	.999	.999
$\beta_+$	1.031	1.015	1.010	1.007	1.005	1.002	1.002	1.001	1.001

Note:  $\beta_{\pm}$  correspond to the  $\pm$  sign in the expression for  $\beta$ .  
 The  $\pm$  sign stands for different propagation modes (ordinary or extraordinary) depending on wave polarization.

In Equation 7  $\Delta L$  is a function of elevation angle, maximizing toward the horizon

$$\Delta L = \Delta_0 + \Delta_1 + \Delta_2 + \Delta_3 + \Delta_4 + \dots$$

where  $\Delta_0 = \int_0^r ds - \int_0^r ds$

$$\Delta_1 = \frac{40.365}{f^2} \left( \int_0^r N ds - \int_0^r N ds \right) = \frac{40.365}{f^2} \Delta_0 N_0$$

$$\begin{aligned} \Delta_2 &= \pm \frac{1.42 \times 10^6}{f^3} \left( \int_0^r N H \cos \alpha ds - \int_0^r N H \cos \alpha ds \right) \\ &= \pm \frac{1.42 \times 10^6}{f^3} M \left( \int_0^r N ds - \int_0^r N ds \right) = \mp \frac{1.42 \times 10^6}{f^3} M \Delta_0 N_0 \end{aligned}$$

$$\begin{aligned} \Delta_3 &= \frac{8.1465 \times 10^2}{f^4} \left( \int_0^r N^2 ds - \int_0^r N^2 ds \right) = \frac{8.1465 \times 10^2}{f^4} 2N_0 \\ &\quad \cdot \left( \int_0^r N ds - \int_0^r N ds \right) \end{aligned}$$

$$\Delta_3 \leq \frac{8.1465 \cdot 10^3}{f^4} \quad 2 N_s^2 \Delta_0$$

$$\Delta_4 = \frac{4.9952 \cdot 10^{10}}{f^4} \left( \int_0^{\pi} NH^2 \cos^2 \alpha \, ds - \int_0^{\pi} NH^2 \cos^2 \alpha \, ds \right)$$

$$= \frac{4.9952 \cdot 10^{10}}{f^4} M' \left( \int_0^{\pi} N \, ds - \int_0^{\pi} N \, ds \right)$$

$$\Delta_4 \leq \frac{4.9952 \cdot 10^{10}}{f^4} M' N_s \Delta_0$$

$$\text{hence } \Delta L \leq \Delta_0 + \frac{40.365 N_s}{f^2} \Delta_0 \pm \frac{1.42 \cdot 10^8}{f^3} M N_s \Delta_0 + \frac{1.6293 \cdot 10^3}{f^3} N_s^2 \Delta_0 + \frac{4.9952 \cdot 10^{10}}{f^4} M' N_s \Delta_0$$

For maximum effect we will assume

$$N_s = 10^{12} \text{ e/m}^3$$

$$M = 40 \text{ ampere turns}$$

$$M' = 1600 \text{ (amp turns)}^2$$

$$\text{therefore } \Delta L \leq \Delta_0 \left( 1 + \frac{161.456 \cdot 10^{12}}{f^2} \pm \frac{227.2 \cdot 10^{12}}{f^3} + \frac{6677 \cdot 10^{24}}{f^4} \right)$$

$$\text{Now } L(t) = L_0 + \frac{40.365 N_s}{f^2} \beta(f) + \Delta_0 + \Delta_0 \gamma(f)$$

$$\text{where } \gamma(f) = \frac{161.456 \cdot 10^{12}}{f^2} \pm \frac{227.2 \cdot 10^{12}}{f^3} + \frac{6677 \cdot 10^{24}}{f^4}$$

and  $\gamma(f)$  represents the frequency dependence of the bending correction.

The maximum and minimum values of  $\gamma$  versus  $f$  can be obtained from

$$\text{Table I as } \gamma(f) = \beta(f) - \frac{40.365 N_s}{f^2} \beta(f)$$

$$\text{therefore } L(t) = L_0 + \Delta_0 + \frac{40.365}{f^2} \beta(f) [N_s + N_s] \quad (8)$$



Where  $L_0 = \int_0 ds =$  straight line distance between observer and satellite

$\Delta_0 = \int_0 ds - \int_0 ds =$  difference between refracted path and straight line distance

(the degree of bending depends on the ionospheric conditions, frequency, and elevation angle)

$\mathcal{E}(f) =$  correction factor to group path due to high order terms in expansion of Appleton-Hartree equation for index of refraction

(It depends on maximum electron density along the straight line path, magnetic field, and frequency of transmission)

$$\text{and } \mathcal{E}(f) = 1 \pm \frac{3.5179 \times 10^4 M}{f} + \frac{40.364 N_e + 1.2375 \times 10^9 M^2}{f^2}$$
$$\approx 1 \pm \frac{1.4072 \times 10^6}{f} + \frac{163.436 \times 10^{12}}{f^2}$$

$\mathcal{V}(f) =$  frequency dependent correction factor for the bending correction to a straight line group path

(It depends on maximum electron density along straight line path, magnetic field, and frequency)

$$\text{and } \mathcal{V}(f) \approx \frac{161.456 \times 10^{12}}{f^2} \pm \frac{227.2 \times 10^{18}}{f^3} + \frac{6077 \times 10^{24}}{f^4}$$

$\Delta_0$  must be determined by ray tracing; it depends on frequency and ionospheric conditions

(An order of magnitude effect for a thick ionosphere at 140 MHz and at 5° elevation angle is  $\Delta_0 = 50\text{m}$ )

$\Delta_0 = 0$  as  $E1 \rightarrow 90^\circ$  and

$\Delta_0 = 0$  as  $f \rightarrow \infty$ )

### Glossary

$G(t)$	=	geometric path length (straight line)
$H$	=	earth's magnetic field intensity
$L(t)$	=	minimum group path length
$N(r, \Gamma, \theta)$	=	electron concentration
$N$	=	electron concentration
$N_T$	=	total electron content
$N_m$	=	maximum electron content
$c$	=	velocity of light
$e$	=	electronic charge
$f$	=	wave frequency
$m$	=	electronic mass
$n(r, \Gamma, \theta)$	=	refractive index of ionosphere
$n_p$	=	phase index of refraction
$n_g$	=	group index of refraction
$r$	=	radial distance to differential element
$\alpha$	=	angle between earth's magnetic field vector and ray path
$\Delta L$	=	bending correction
$\epsilon_0$	=	dielectric constant of free space
$\Gamma$	=	geocentric latitude
$\mu_0$	=	permeability of free space
$\theta$	=	geocentric longitude

## APPENDIX C

### Transmission Times for Ionospheric Predictions

To determine the transmission time for the ionospheric predictions, consider first what the maximum acceptable error for the desired data type is; for either vertical electron content or group delay and the height at the maximum electron density or for the angular electron content or group delay for which no height information is required. Using Table 1 the number of bits are determined required for the ionospheric data of specified accuracy at each location.

From Table 2, the earth central angle corresponding to the lowest elevation angle to the satellite can be extracted. If each satellite transmits the ionospheric data for its own region, the second column yields the desired central angle. In this mode angular group delay is preferable as data type. If not all satellites transmit their own data, the user has to get enough data from just one satellite to cover the whole region visible from his sight. For the lowest elevation of the highest elevation satellite transmitting ionospheric data, columns 3 and 4 give the corresponding central angles for users cutting off at 5 and 2 degrees of elevation. For this case it is advantageous to choose the ionospheric data as vertical group delay and height.

Having determined the number of bits required for each point and the central angle from the satellite to which data is needed, Tables 3a-f give the transmission times for a choice of the point densities of 5, 7, and 10 degrees central angle. Columns 3-5 list the total transmission time. Columns 7-9 give transmission times for an alternate approach where the user with low accuracy requirements can pick up a less dense prediction pattern during the first part of the transmission period, and columns 11-13 give the additional times for users with high accuracy requirements to fill in the remaining data during the second part of the transmission interval.

Table 1. Coding of Various Data Types

Data Type	Minimum Value	Maximum Value	#Bits	#Steps	Stepsize	Maximum Error
Vertical Electron Content ( $e/m^2$ )	$1 \times 10^{16}$	$150 \times 10^{16}$	7	127	$1.2 \times 10^{16}$	$.6 \times 10^{16}$
			6	63	$2.4 \times 10^{16}$	$1.2 \times 10^{16}$
			5	31	$4.8 \times 10^{16}$	$2.4 \times 10^{16}$
			4	15	$10.0 \times 10^{16}$	$5.0 \times 10^{16}$
Vertical Group Delay at 1600 MHz (nsec)	0.5	78.8	7	127	.62	.31
			6	63	1.24	.62
			5	31	2.52	1.26
			4	15	5.22	2.61
Angular Electron Content ( $e/m^2$ )	$1 \times 10^{16}$	$579 \times 10^{16}$	9	511	$1.1 \times 10^{16}$	$.6 \times 10^{16}$
			8	255	$2.2 \times 10^{16}$	$1.1 \times 10^{16}$
			7	127	$4.6 \times 10^{16}$	$2.3 \times 10^{16}$
			6	63	$9.2 \times 10^{16}$	$4.6 \times 10^{16}$
			5	31	$18.6 \times 10^{16}$	$9.3 \times 10^{16}$
Angular Group Delay at 1600 MHz (nsec)	0.5	304.0	9	511	.60	.30
			8	255	1.20	.60
			7	127	2.38	1.19
			6	63	3.94	1.97
			5	31	9.80	4.90
Height at Maximum Density (km)	200	450	4	15	17.0	8.5
			3	7	36.0	18.0

Table 2. Elevation Angle to Earth Central Angle Conversion Table

ELEV = ELEVATION ANGLE FROM USER TO SATELLITE (DEG)  
 ALF = EARTH CENTRAL ANGLE BETWEEN SATELLITE AND USER (DEG)  
 A5 = EARTH CENTRAL ANGLE BETWEEN SATELLITE AND MOST DISTANT  
 IONOSPHERE POINT VISIBLE FROM USER AT 5 DEG ELEV. CUTOFF (DEG)  
 A2 = SAME AS A5 BUT USING A 2 DEGREE ELEVATION CUTOFF

ELEV	ALF	A5	A2	ELEV	ALF	A5	A2
89.	.8	17.3	19.9	44.	39.8	56.3	58.8
88.	1.7	18.2	20.7	43.	40.7	57.2	59.7
87.	2.5	19.0	21.6	42.	41.6	58.1	60.6
86.	3.4	19.9	22.4	41.	42.5	59.0	61.5
85.	4.2	20.7	23.3	40.	43.4	59.9	62.4
84.	5.1	21.6	24.1	39.	44.3	60.8	63.3
83.	5.9	22.4	25.0	38.	45.2	61.7	64.2
82.	6.8	23.3	25.8	37.	46.1	62.6	65.1
81.	7.7	24.1	26.7	36.	47.0	63.5	66.0
80.	8.5	25.0	27.5	35.	47.9	64.4	66.9
79.	9.4	25.8	28.4	34.	48.8	65.3	67.9
78.	10.2	26.7	29.2	33.	49.8	66.2	68.8
77.	11.1	27.6	30.1	32.	50.7	67.2	69.7
76.	11.9	28.4	30.9	31.	51.6	68.1	70.6
75.	12.8	29.3	31.8	30.	52.5	69.0	71.5
74.	13.6	30.1	32.6	29.	53.4	69.9	72.5
73.	14.5	31.0	33.5	28.	54.4	70.9	73.4
72.	15.3	31.8	34.4	27.	55.3	71.8	74.3
71.	16.2	32.7	35.2	26.	56.2	72.7	75.3
70.	17.1	33.5	36.1	25.	57.2	73.7	76.2
69.	17.9	34.4	36.9	24.	58.1	74.6	77.1
68.	18.8	35.3	37.8	23.	59.0	75.5	78.1
67.	19.6	36.1	38.7	22.	60.0	76.5	79.0
66.	20.5	37.0	39.5	21.	60.9	77.4	80.0
65.	21.4	37.8	40.4	20.	61.9	78.4	80.9
64.	22.2	38.7	41.2	19.	62.8	79.3	81.8
63.	23.1	39.6	42.1	18.	63.8	80.3	82.6
62.	24.0	40.4	43.0	17.	64.7	81.2	83.8
61.	24.8	41.3	43.8	16.	65.7	82.2	84.7
60.	25.7	42.2	44.7	15.	66.6	83.1	85.7
59.	26.6	43.0	45.6	14.	67.6	84.1	86.6
58.	27.4	43.9	46.4	13.	68.6	85.1	87.6
57.	28.3	44.8	47.3	12.	69.5	86.0	88.6
56.	29.2	45.7	48.2	11.	70.5	87.0	89.5
55.	30.1	46.5	49.1	10.	71.5	88.0	90.5
54.	30.9	47.4	50.0	9.	72.5	88.9	91.5
53.	31.8	48.3	50.9	8.	73.5	89.9	92.5
52.	32.7	49.2	51.7	7.	74.5	90.9	93.5
51.	33.6	50.1	52.6	6.	75.5	91.9	94.5
50.	34.5	51.0	53.5	5.	76.5	92.9	95.5
49.	35.4	51.9	54.4	4.	77.5	93.9	96.5
48.	36.3	52.8	55.3	3.	78.5	94.9	97.5
47.	37.2	53.7	56.2	2.	79.5	95.9	98.5
46.	38.1	54.6	57.1	1.	80.5	96.9	99.5
45.	39.0	55.5	58.0	0.	81.5	97.9	100.0

Table 3a.

## \*\*\* TRANSMISSION TIMES FOR 5 DEGREE GRID \*\*\*

A = EARTH CENTRAL ANGLE (DEG) MEASURED FROM SUB-SATELLITE POINT  
OUTWARDS FOR WHICH ISNOSPHERIC DATA IS TO BE TRANSMITTED

#PTS = NUMBER OF POINTS IN THE GRID COVERING THE GROUND BELOW THE  
SATELLITE UP TO THE CENTRAL ANGLE A

#P1, #P2 = NUMBER OF GRID POINTS ACCUMULATED FROM EVERY SECOND GRID CIRCLE  
#P1 FOR STARTING WITH CENTER POINT FOR FIRST PASS  
#P2 FOR FILLING IN MISSING GRID CIRCLES FOR SECOND PASS

T4, T6, T8 = TIME (MIN) REQUIRED TO TRANSMIT GRID INFORMATION UP TO ANGLE A  
AT A 10 BIT/SEC RATE FOR 4, 6 AND 8 BITS OF INFO. PER GRID POINT

A	#PTS	T4	T6	T8	#P1	T4	T6	T8	#P2	T4	T6	T8
0	1	.01	.01	.01	1	.01	.01	.01				
5	7	.05	.07	.09					6	.04	.06	.08
10	19	.13	.19	.25	13	.09	.13	.17				
15	37	.25	.37	.49					24	.16	.24	.32
20	61	.41	.61	.81	37	.25	.37	.49				
25	91	.61	.91	1.21					34	.36	.54	.72
30	126	.84	1.26	1.68	72	.48	.72	.96				
35	167	1.11	1.67	2.23					95	.63	.95	1.27
40	213	1.42	2.13	2.84	118	.79	1.18	1.57				
45	263	1.75	2.63	3.51					145	.97	1.45	1.93
50	318	2.12	3.18	4.24	173	1.15	1.73	2.31				
55	378	2.51	3.78	5.01					203	1.35	2.03	2.71
60	436	2.92	4.36	5.84	235	1.57	2.35	3.13				
65	503	3.35	5.03	6.71					268	1.79	2.68	3.57
70	570	3.80	5.70	7.60	302	2.01	3.02	4.03				
75	639	4.26	6.39	8.52					337	2.25	3.37	4.49
80	709	4.73	7.09	9.45	372	2.43	3.72	4.96				
85	780	5.20	7.80	10.40					408	2.72	4.08	5.44
90	851	5.67	8.51	11.35	443	2.95	4.43	5.91				
95	922	6.15	9.22	12.29					479	3.19	4.79	6.39
100	992	6.61	9.92	13.23	513	3.42	5.13	6.84				

Table 3b.

\*\*\*\*\* TRANSMISSION TIMES FOR 5 DEGREE GRID \*\*\*\*\*

A = EARTH CENTRAL ANGLE (DEG) MEASURED FROM SUB-SATELLITE POINT  
 OUTWARDS FOR WHICH ATMOSPHERIC DATA IS TO BE TRANSMITTED  
 #PTS = NUMBER OF POINTS IN THE GRID COVERING THE GROUND BELOW THE  
 SATELLITE UP TO THE CENTRAL ANGLE A  
 #P1, #P2 = NUMBER OF GRID POINTS ACCUMULATED FROM EVERY SECOND GRID CIRCLE  
 #P1 FOR STARTING WITH CENTER POINT FOR FIRST PASS  
 #P2 FOR FILLING IN MISSING GRID CIRCLES FOR SECOND PASS  
 T5, T7, T9 = TIME (MIN) REQUIRED TO TRANSMIT GRID INFORMATION UP TO ANGLE A  
 AT A 10 BIT/SEC RATE FOR 5, 7 AND 9 BITS OF INFO. PER GRID POINT

A	#PTS	T5	T7	T9	#P1	T5	T7	T9	#P2	T5	T7	T9
0	1	.01	.01	.01	1	.01	.01	.01				
5	7	.06	.08	.10					6	.05	.07	.09
10	19	.15	.22	.28	13	.11	.15	.19				
15	37	.31	.43	.55					24	.20	.28	.36
20	61	.51	.71	.91	37	.31	.43	.55				
25	91	.75	1.05	1.35					54	.45	.63	.81
30	126	1.05	1.47	1.89	72	.60	.84	1.08				
35	167	1.39	1.95	2.50					95	.79	1.11	1.42
40	213	1.77	2.43	3.19	118	.93	1.38	1.77				
45	263	2.19	3.07	3.94					145	1.21	1.69	2.17
50	318	2.65	3.71	4.77	173	1.44	2.02	2.59				
55	375	3.13	4.39	5.64					203	1.69	2.37	3.04
60	438	3.65	5.11	6.57	235	1.96	2.74	3.52				
65	503	4.19	5.87	7.54					248	2.23	3.13	4.02
70	570	4.75	6.65	8.55	302	2.52	3.52	4.53				
75	639	5.32	7.45	9.58					337	2.81	3.93	5.05
80	709	5.91	8.27	10.63	372	3.10	4.34	5.58				
85	780	6.50	9.10	11.70					408	3.40	4.76	6.12
90	851	7.09	9.93	12.76	443	3.69	5.17	6.64				
95	922	7.68	10.76	13.83					479	3.99	5.59	7.18
100	992	8.27	11.57	14.88	513	4.27	5.95	7.69				

Table 3c.

\*\*\*\*\* TRANSMISSION TIMES FOR 7 DEGREE GRID \*\*\*\*\*

A= EARTH CENTRAL ANGLE (DEG) MEASURED FROM SUB-SATELLITE POINT  
 OUTWARDS FOR WHICH IONOSPHERIC DATA IS TO BE TRANSMITTED  
 #PTS= NUMBER OF POINTS IN THE GRID COVERING THE GROUND BELOW THE  
 SATELLITE UP TO THE CENTRAL ANGLE A  
 #P1, #P2= NUMBER OF GRID POINTS ACCUMULATED FROM EVERY SECOND GRID CIRCLE  
 #P1 FOR STARTING WITH CENTER POINT FOR FIRST PASS  
 #P2 FOR FILLING IN MISSING GRID CIRCLES FOR SECOND PASS  
 T4, T6, T8= TIME (MIN) REQUIRED TO TRANSMIT GRID INFORMATION UP TO ANGLE A  
 AT A 10 BIT/SEC RATE FOR 4, 6 AND 8 BITS OF INFO. PER GRID POINT

A	#PTS	T4	T6	T8	#P1	T4	T6	T8	#P2	T4	T6	T8
0	1	.01	.01	.01	1	.01	.01	.01				
7	7	.05	.07	.09					6	.04	.06	.08
14	19	.13	.19	.25	13	.09	.13	.17				
21	37	.25	.37	.49					24	.16	.24	.32
28	61	.41	.61	.81	37	.25	.37	.49				
35	90	.60	.90	1.20					53	.35	.53	.71
42	124	.83	1.24	1.65	71	.47	.71	.95				
49	162	1.08	1.62	2.16					91	.61	.91	1.21
56	204	1.36	2.04	2.72	113	.75	1.13	1.51				
	249	1.66	2.49	3.32					136	.91	1.36	1.81
	297	1.98	2.97	3.96	161	1.07	1.61	2.15				
77	347	2.31	3.47	4.63					186	1.24	1.86	2.48
84	398	2.65	3.98	5.31	212	1.41	2.12	2.83				
91	449	2.99	4.49	5.99					237	1.58	2.37	3.16
98	499	3.33	4.99	6.65	262	1.75	2.62	3.49				



Table 3d.

\*\*\*\*\* TRANSMISSION TIMES FOR 7 DEGREE GRID \*\*\*\*\*

A = EARTH CENTRAL ANGLE (DEG) MEASURED FROM SUB-SATELLITE POINT  
 OUTWARDS FOR WHICH IONOSPHERIC DATA IS TO BE TRANSMITTED  
 #PTS = NUMBER OF POINTS IN THE GRID COVERING THE GROUND BELOW THE  
 SATELLITE UP TO THE CENTRAL ANGLE A  
 #P1, #P2 = NUMBER OF GRID POINTS ACCUMULATED FROM EVERY SECOND GRID CIRCLE  
 #P1 FOR STARTING WITH CENTER POINT FOR FIRST PASS  
 #P2 FOR FILLING IN MISSING GRID CIRCLES FOR SECOND PASS  
 T5, T7, T9 = TIME (MIN) REQUIRED TO TRANSMIT GRID INFORMATION UP TO ANGLE A  
 AT A 10 BIT/SEC RATE FOR 5, 7 AND 9 BITS OF INFO. PER GRID POINT

A	#PTS	T5	T7	T9	#P1	T5	T7	T9	#P2	T5	T7	T9
0	1	.01	.01	.01	1	.01	.01	.01				
7	7	.06	.03	.10					6	.05	.07	.09
14	19	.16	.22	.28	13	.11	.15	.19				
21	37	.31	.43	.55					24	.20	.28	.36
28	61	.51	.71	.91	37	.31	.43	.55				
35	90	.75	1.05	1.35					53	.44	.62	.79
42	124	1.03	1.45	1.86	71	.59	.83	1.06				
49	162	1.35	1.89	2.43					91	.76	1.06	1.36
56	204	1.70	2.38	3.06	113	.94	1.32	1.69				
63	249	2.07	2.90	3.73					136	1.13	1.59	2.04
70	297	2.47	3.46	4.45	161	1.34	1.83	2.41				
77	347	2.89	4.05	5.20					186	1.55	2.17	2.79
84	398	3.32	4.64	5.97	212	1.77	2.47	3.18				
91	449	3.74	5.24	6.73					237	1.97	2.76	3.55
98	499	4.16	5.82	7.48	262	2.13	3.06	3.93				

Table 3c.

\*\*\*\*\* TRANSMISSION TIMES FOR 10 DEGREE GRID \*\*\*\*\*

A = EARTH CENTRAL ANGLE (DEG) MEASURED FROM SUB-SATELLITE POINT  
 OUTWARDS FOR WHICH IONOSPHERIC DATA IS TO BE TRANSMITTED  
 #PTS = NUMBER OF POINTS IN THE GRID COVERING THE GROUND BELOW THE  
 SATELLITE UP TO THE CENTRAL ANGLE A  
 #P1, #P2 = NUMBER OF GRID POINTS ACCUMULATED FROM EVERY SECOND GRID CIRCLE  
 #P1 FOR STARTING WITH CENTER POINT FOR FIRST PASS  
 #P2 FOR FILLING IN MISSING GRID CIRCLES FOR SECOND PASS  
 T4, T6, T8 = TIME (MIN) REQUIRED TO TRANSMIT GRID INFORMATION UP TO ANGLE A  
 AT A 10 BIT/SEC RATE FOR 4, 6 AND 8 BITS OF INFO. PER GRID POINT

A	#PTS	T4	T6	T8	#P1	T4	T6	T8	#P2	T4	T6	T8
0	1	.01	.01	.01	1	.01	.01	.01				
10	7	.05	.07	.09					6	.04	.06	.08
20	19	.13	.19	.25	13	.09	.13	.17				
30	36	.24	.36	.48					23	.15	.23	.31
40	59	.39	.59	.79	36	.24	.36	.48				
50	86	.57	.86	1.15					50	.33	.50	.67
60	117	.78	1.17	1.56	67	.45	.67	.89				
70	150	1.00	1.50	2.00					83	.55	.83	1.11
80	185	1.23	1.85	2.47	102	.68	1.02	1.36				
90	220	1.47	2.20	2.93					118	.79	1.18	1.57
100	255	1.70	2.55	3.40	137	.91	1.37	1.83				

Table 3f.

\*\*\*\*\* TRANSMISSION TIMES FOR 10 DEGREE GRID \*\*\*\*\*

A	#PTS	T5	T7	T9	#P1	T5	T7	T9	#P2	T5	T7	T9
0	1	.01	.01	.01	1	.01	.01	.01				
10	7	.06	.08	.10					6	.05	.07	.09
20	19	.16	.22	.28	13	.11	.15	.19				
30	36	.30	.42	.54					23	.19	.27	.34
40	59	.49	.69	.88	36	.30	.42	.54				
50	86	.72	1.00	1.29					50	.42	.58	.75
60	117	.97	1.36	1.75	67	.56	.78	1.00				
70	150	1.25	1.75	2.25					83	.69	.97	1.24
80	185	1.54	2.16	2.77	102	.85	1.19	1.53				
90	220	1.83	2.57	3.30					118	.95	1.38	1.77
100	255	2.12	2.97	3.82	137	1.14	1.60	2.05				

Accuracies in Ionospheric Predictions Obtained from Grid Pattern Interpolation

A number of test cases were set up to determine the average and the maximum errors encountered when interpolating predictions at the points of a grid pattern around a central location to obtain the values at the intermediate positions. The date was chosen as August 1968 for high solar activity near the peak of the sunspot cycle. The central locations were chosen as A, B, and C as shown in Figure 1 so that the three test areas covered different regions of the ionosphere capturing the rapid changes of the equatorial anomaly for testing maximum position errors, and the sunrise effect for testing maximum time errors and enclosing a less disturbed area in the mid latitudes for average position and time errors. The areas are defined by a circle of  $21^\circ$  in earth central angle around the location A, B, and C. The predictions were computed for three conditions at points evenly spaced at 5, 7, and 10 degree intervals of central angle and azimuth.

These predictions were interpolated to points which were offset in central angle and azimuth from the original grid pattern by 0,  $\frac{1}{2}$ , and  $\frac{3}{4}$  the size of the grid interval. The  $\frac{1}{2}$  grid size offset, as shown in Figure 2, results in maximum errors due to position, the  $\frac{1}{4}$  offset in average errors, while no offset eliminates position errors. Another contribution to errors comes from time discrepancies. Assuming that the ionospheric data is valid for a time  $\frac{1}{2}$  transmission interval ahead of the actual transmission time, and choosing a transmission interval of 1 hour, the maximum errors are due to time discrepancies of  $\frac{1}{2}$  hour and average errors due to  $\frac{1}{4}$  hour.

Thus the predictions were interpolated in position and no adjustments for the time discrepancies were allowed. The resulting values were compared with the accurate predictions obtained from the Bent Model for the proper time and locations. Table 1a. shows the comparison for predictions of vertical group delay at 1000 MHz, Table 2a. for the height of the maximum electron density. The tables list for each condition the range of the predictions

over the grid pattern by giving minimum, maximum, and mean values. The errors of each point are defined as the deviation of the interpolated value from the prediction computed directly for that point and time. Listed are the RMS values of the errors for the areas around A, B, and C, the percentage of the RMS error to the mean prediction, the largest absolute error incurred at any one point, and the corresponding percentage of error to prediction at that point. It is seen that in all cases the errors due to time exceed the errors due to position.

Tables 1b. and 2b. show the comparison of the same predicted data with values that were interpolated in position and adjusted for the time discrepancy by shifting the original grid pattern at a rate of 15 degrees per hour in longitude. The time errors so dominant in the previous case dropped way below the position errors. To approximately match position and time errors another test was performed assuming a transmission interval of 4 hours with maximum time discrepancies of 2 hours. Again, the predictions at the grid points were interpolated in position and adjusted for the time discrepancy by a longitude shift of the grid along the magnetic latitude line for the central point. The results are shown in Tables 1c. and 2c.

The results in Tables 1 and 2 list as errors the deviation of the interpolated values from the predictions. However, the predictions do not properly represent the ionospheric variations, and to obtain the total errors expected from the interpolation technique, the errors in Tables 1 and 2 have to be combined with the deviations of the predicted from the observed data. Accuracy data for the predictions was available from comparisons of the Bent model results with Faraday rotation measurements defining the actual group delay. To show average errors during a period near the peak of the sunspot cycle, the 1958 yearly RMS values over all hours were chosen as prediction errors at locations A and C, and over two hours at sunrise at location C. To present some maximum possible errors, the monthly RMS values for one hour were taken as prediction errors, selecting

the month and hour with the largest errors during 1968. Since the accuracy data was not available for the exact locations A, B, and C and the corresponding grid point, the data from near stations with similar type ionospheric variations was chosen. The combined prediction and interpolation RMS errors are listed in Table 3.

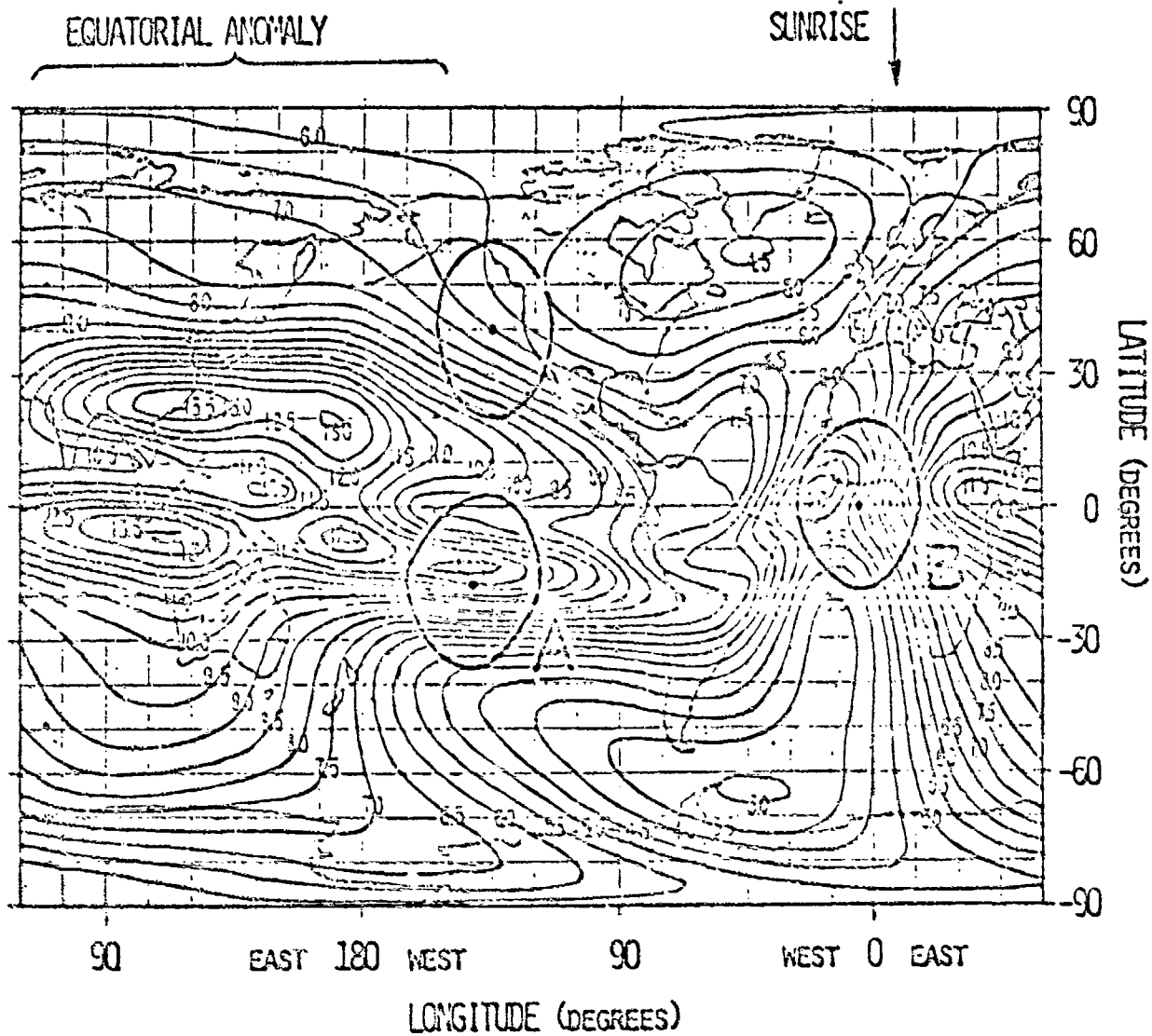


Figure 1. The Predicted Global Status of a Monthly Median  $f_1F_2$  at 6 hours Universal Time Showing the Areas around Locations A, B, and C Used for the Tests.

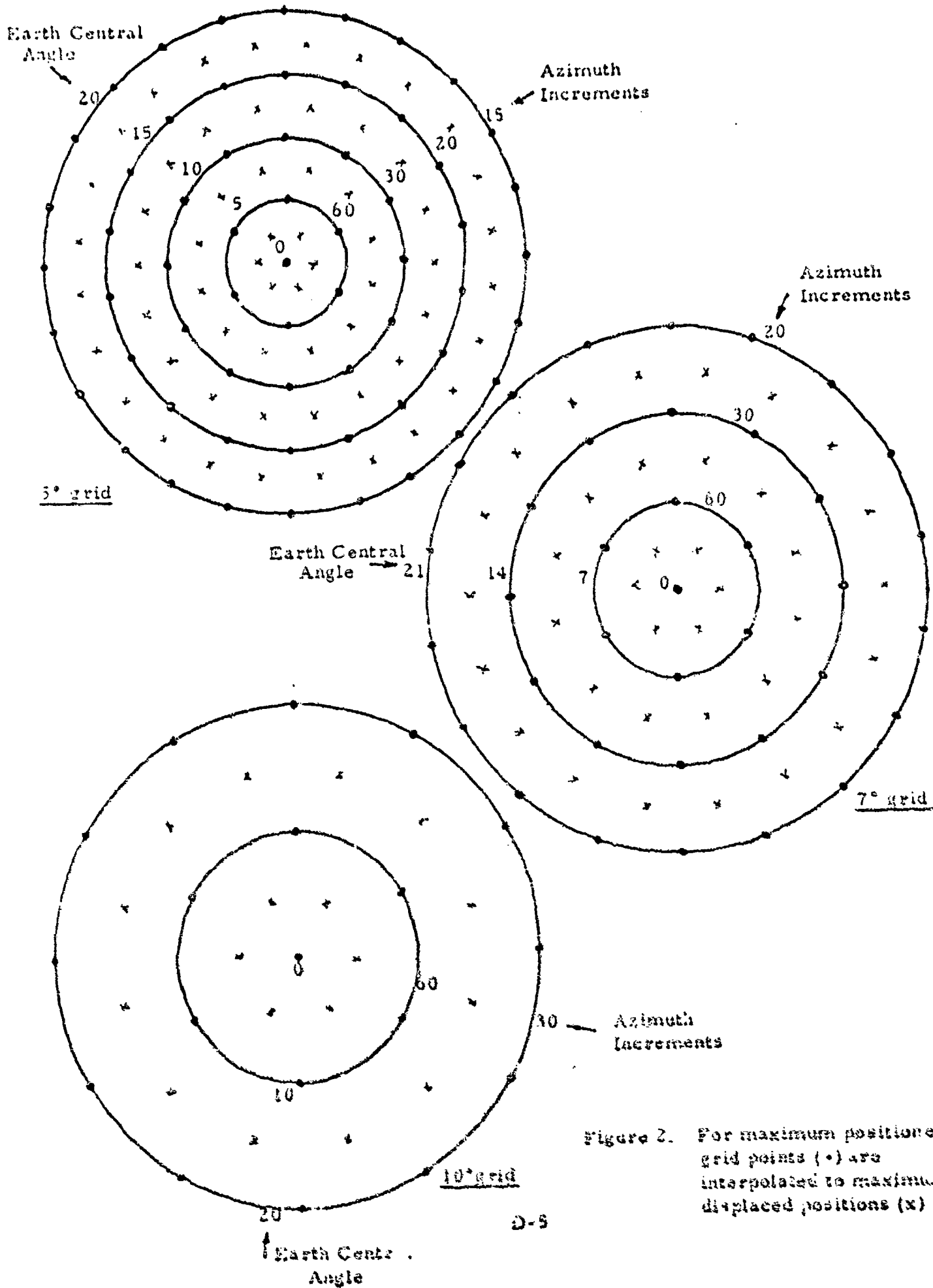


Figure 2. For maximum position error grid points (•) are interpolated to maximum displaced positions (x)



Locations: A - latitude = -17°, longitude = 218°, captures effect of the equatorial anomaly  
 B - latitude = 0°, longitude = 355°, captures sunrise effect  
 C - latitude = 40°, longitude = 225°, represents average density condition

Errors: Maximum/average position errors are due to interpolation over  $\frac{1}{4}$  grid size  
 Maximum/average time error for 1 hour transmission interval is due to  $\frac{1}{4}$  hour discrepancy (no interpolation)

Grid Size	Location	Position Error		Time Error		Prediction		Mean	RMS	Error (Predicted-Interpolated)		No. Points
		Aver.	Max.	Aver.	Max.	Min.	Max.			Overall %	Abs. % of Max. Abs.	
5°	A	Aver.	19.6	Aver.	2.8	Max.	11.8	0.61	5.2	1.21	10.5	60
5°	B	Aver.	16.0	Aver.	1.4	Max.	5.6	1.09	19.6	2.89	18.1	60
5°	C	Aver.	12.1	Aver.	4.4	Max.	7.0	0.33	4.7	0.78	7.0	60
5°	A	Max.	19.2	Max.	2.9	Max.	11.9	0.89	7.4	1.87	16.4	60
5°	B	Max.	17.5	Max.	1.6	Max.	6.5	2.26	34.6	5.24	29.9	60
5°	C	Max.	10.9	Max.	4.3	Max.	6.6	0.57	8.7	1.34	12.7	60
5°	A	None	19.7	None	3.2	Max.	12.5	0.56	4.5	1.20	6.3	60
5°	B	None	18.6	Max.	1.5	Max.	6.7	2.24	33.6	4.78	30.2	60
7°	A	Aver.	19.5	Aver.	2.7	Max.	11.6	0.93	8.1	1.64	14.2	36
7°	B	Aver.	16.1	Aver.	1.6	Max.	5.7	1.14	20.1	2.99	18.6	36
7°	C	Aver.	12.4	Aver.	4.4	Max.	7.1	0.36	5.1	0.80	7.6	36
7°	A	Max.	19.4	Max.	2.9	Max.	11.8	1.24	10.5	2.39	19.3	36
7°	B	Max.	16.6	Max.	1.7	Max.	6.6	2.30	35.1	5.27	32.2	36
7°	C	Max.	10.8	Max.	4.4	Max.	6.6	0.61	9.3	1.36	12.6	36
7°	A	None	19.9	None	3.3	Max.	12.4	0.97	7.8	1.89	9.9	36
7°	B	None	19.6	Max.	1.8	Max.	6.7	2.22	32.9	4.57	23.3	36
10°	A	Aver.	19.3	Aver.	3.1	Max.	11.7	1.48	12.7	2.57	13.3	18
10°	B	Aver.	13.6	Aver.	1.4	Max.	5.6	1.28	22.6	3.29	24.2	18
10°	C	Aver.	11.2	Aver.	4.5	Max.	7.0	0.40	5.7	0.79	8.2	18
10°	A	Max.	19.2	Max.	3.6	Max.	12.2	2.09	17.1	3.42	30.8	18
10°	B	Max.	15.6	Max.	1.8	Max.	6.5	2.41	36.9	6.03	38.7	18
10°	C	Max.	9.7	Max.	4.6	Max.	6.5	0.62	9.6	1.12	12.0	18
10°	A	None	19.7	None	4.1	Max.	12.8	1.88	14.7	2.77	14.3	18
10°	B	None	18.0	Max.	1.5	Max.	6.7	2.20	32.8	4.67	25.9	18

Table 1b  
Accuracy in Group Delay at 1660 MHz (nanoseconds) Obtained from Grid Interpolation

**Locations:** A - latitude = -17°, longitude = 218°, captures effect of the equatorial anomaly  
 B - latitude = 0°, longitude = 355°, captures sunrise effect  
 C - latitude = 40°, longitude = 225°, represents average density condition

**Errors:** Maximum/average position errors are due to interpolation over  $\frac{1}{4}$  grid size  
 Maximum/average time error for 1 hour transmission interval is due to  $\frac{1}{4}$  hour discrepancy adjusted for by longitude shift of grid.

Grid Size	Location	Position Error		Time Error		Prediction		Mean	RMS	Error (Predicted-Interpolated)		No. Points
		Aver.	Max.	Min.	Max.	Overall %	Abs. % of Max. Abs.					
5°	A	Aver.	19.6	2.8	11.8	0.70	6.0	1.34	7.8	60		
5°	B	Aver.	13.4	1.5	4.7	0.27	5.7	0.63	9.9	66		
5°	C	Aver.	12.7	4.6	7.3	0.10	1.4	0.25	3.0	60		
5°	A	Max.	19.1	2.9	11.9	1.13	9.5	2.16	24.3	60		
5°	B	Max.	12.4	1.5	4.6	0.51	11.1	1.21	20.0	60		
5°	C	Max.	11.2	4.6	7.2	0.19	2.6	0.45	5.2	60		
5°	A	None	19.7	3.2	12.5	0.56	4.5	1.20	6.3	60		
5°	B	None	13.6	1.6	4.9	0.50	10.3	1.28	38.0	60		
7°	A	Aver.	19.2	2.8	11.6	0.94	8.1	1.79	10.0	36		
7°	B	Aver.	13.7	1.5	4.8	0.32	6.6	0.79	14.3	36		
7°	C	Aver.	12.9	4.5	7.4	0.10	1.4	0.25	2.2	36		
7°	A	Max.	19.3	2.9	11.8	1.36	11.5	2.33	19.6	36		
7°	B	Max.	12.0	1.6	4.6	0.53	11.4	1.30	25.0	36		
7°	C	Max.	11.8	4.7	7.2	0.17	2.4	0.38	4.1	36		
7°	A	None	19.9	3.3	12.4	0.97	7.8	1.89	9.9	36		
7°	B	None	14.7	1.5	5.1	0.49	9.7	1.23	39.4	36		
10°	A	Aver.	19.5	3.1	11.7	1.50	12.8	2.74	14.1	18		
10°	B	Aver.	10.8	1.6	4.8	0.42	8.9	0.97	26.9	18		
10°	C	Aver.	11.8	4.6	7.3	0.10	1.4	0.20	2.1	18		
10°	A	Max.	19.1	3.5	12.1	2.15	17.8	3.27	29.1	18		
10°	B	Max.	10.0	1.9	4.5	0.71	15.8	1.33	20.0	18		
10°	C	Max.	10.6	4.2	7.1	0.12	1.7	0.24	3.2	18		
10°	A	None	19.7	4.1	12.8	1.88	14.7	2.77	14.3	18		
10°	B	None	13.6	1.8	5.1	0.47	9.2	1.26	20.4	18		

Table 14  
Accuracy in Group B by at 1600 Miles (Longitude) derived from Grid Interpolation

Locations: A - latitude = -17°, longitude = 215°, captures effect of the equatorial anomaly  
 B - latitude = 0°, longitude = 355°, captures sunrise effect  
 C - latitude = 40°, longitude = 225°, represents average density condition

Errors: Maximum/average position errors are due to interpolation over  $\frac{1}{4}$  grid size  
 Maximum/average time error for 4 hour transmission interval is due to 2/1 hour discrepancy adjusted for by longitude shift of grid along magnetic latitude line.

Grid Size	Location	Position Error		Time Error		Prediction		Mean	RMS	Error (Predicted-Interpolated)		No. Points
		Aver.	Max.	Aver.	Max.	Min.	Max.			Overall %	Abs. % of Max. Abs.	
5°	A	Aver.	19.0	Aver.	2.9	Max.	11.5	1.08	9.0	2.76	22.3	60
	B	Aver.	12.0	Aver.	1.7	Max.	4.6	0.69	15.2	1.46	15.4	60
	C	Aver.	11.2	Aver.	3.4	Max.	7.1	0.54	7.5	1.80	16.4	60
	A	Max.	18.6	Max.	3.8	Max.	12.6	1.56	12.4	3.94	28.3	60
	B	Max.	10.4	Max.	2.1	Max.	4.5	0.96	21.3	2.53	29.6	60
	C	Max.	11.0	Max.	4.8	Max.	7.2	0.67	9.3	1.87	18.9	60
	A	None	19.7	None	3.2	None	12.5	0.56	4.5	1.20	6.3	60
	B	None	12.0	Max.	2.1	Max.	4.9	1.07	21.9	3.26	29.6	60
	C	None	19.4	Aver.	2.9	Aver.	11.8	1.15	9.8	2.95	27.1	36
7°	A	Aver.	12.3	Aver.	1.7	Max.	4.7	0.65	13.9	1.36	27.6	36
	B	Aver.	11.5	Aver.	4.4	Max.	7.2	0.57	7.9	1.78	15.7	36
	C	Max.	18.8	Max.	3.8	Max.	12.6	1.51	11.8	4.17	35.4	36
	A	Max.	10.5	Max.	2.1	Max.	4.6	0.91	19.9	2.20	24.8	36
	B	Max.	11.0	Max.	4.8	Max.	7.3	0.67	9.3	1.82	18.2	36
	C	None	19.9	None	3.2	None	12.5	0.97	7.8	1.89	9.9	36
	A	None	12.4	Max.	2.0	Max.	5.1	1.05	20.7	2.59	20.9	36
	B	Aver.	18.3	Aver.	3.3	Max.	11.9	1.44	12.1	3.24	17.9	18
	C	Aver.	9.9	Aver.	2.1	Max.	4.6	0.65	14.1	1.28	39.8	18
10°	A	Aver.	10.6	Aver.	4.5	Max.	7.2	0.55	7.7	1.57	15.4	18
	B	Max.	15.8	Max.	4.7	Max.	12.8	1.38	10.8	3.32	30.4	18
	C	Max.	8.5	Max.	2.4	Max.	4.7	0.84	19.1	1.72	27.3	18
	A	Max.	10.0	Max.	5.1	Max.	7.2	0.59	8.3	1.26	13.5	18
	B	None	19.7	None	4.1	None	12.8	1.88	14.7	2.77	17.3	18
	C	None	12.0	Max.	2.2	Max.	5.1	1.09	21.4	2.23	42.8	18

Table 2a.

Accuracy in Height of Maximum Electron Density (km) Obtained from Grid Interpolation

**Locations:** A - latitude = -17°, longitude = 218°, captures effect of the equatorial anomaly  
 B - latitude = 0°, longitude = 355°, captures sunrise effect  
 C - latitude = 40°, longitude = 225°, represents average density condition

**Errors:** Maximum/average position errors are due to interpolation over  $\frac{1}{4}$  grid size  
 Maximum/average time error for 1 hour transmission interval is due to  $\frac{1}{4}$  hour discrepancy (no interpolation)

Grid Size	Location	Position Error		Time Error		Prediction		RMS	Error (Predicted-Interpolated)		No. Points
		Aver.	Max.	Min.	Max.	Mean	Overall %		Abs. % of Max.		
5°	A	Aver.	390	299	Aver.	329	2.2	0.7	4.4	1.4	60
5°	B	Aver.	306	274	Aver.	284	2.3	0.8	5.3	1.9	60
5°	C	Aver.	346	312	Aver.	327	2.0	0.6	3.2	1.0	60
5°	A	Max.	388	297	Max.	327	4.2	1.3	7.9	2.5	60
5°	B	Max.	300	274	Max.	283	4.3	1.5	10.2	3.5	60
5°	C	Max.	346	314	Max.	329	4.2	1.3	6.3	1.9	60
5°	A	None	390	301	None	329	1.4	0.4	3.1	0.8	60
5°	B	None	303	273	Max.	284	5.3	1.9	11.9	4.0	60
7°	A	Aver.	390	299	Aver.	330	2.6	0.8	5.6	1.8	36
7°	B	Aver.	305	274	Aver.	285	2.5	0.9	5.5	1.9	36
7°	C	Aver.	347	312	Aver.	327	1.9	0.6	3.0	0.9	36
7°	A	Max.	388	297	Max.	327	4.3	1.3	8.7	2.8	36
7°	B	Max.	300	274	Max.	283	4.4	1.6	10.3	3.5	36
7°	C	Max.	346	314	Max.	329	4.0	1.2	6.0	1.8	36
7°	A	None	390	301	None	329	2.5	0.8	5.9	1.5	36
7°	B	None	304	273	Max.	285	5.8	2.0	12.8	4.3	36
10°	A	Aver.	389	301	Aver.	330	4.1	1.3	7.6	2.0	18
10°	B	Aver.	304	275	Aver.	285	2.4	0.8	4.5	1.6	18
10°	C	Aver.	344	313	Aver.	327	1.9	0.6	2.8	0.8	18
10°	A	Max.	381	299	Max.	326	5.5	1.7	11.0	3.4	18
10°	B	Max.	297	274	Max.	282	3.8	1.3	7.7	2.7	18
10°	C	Max.	343	316	Max.	328	3.9	1.2	5.3	1.6	18
10°	A	None	386	301	Max.	328	5.3	1.6	11.9	3.1	18
10°	B	None	301	275	Max.	285	5.9	2.1	11.9	4.0	18

**Table 11**  
**Accuracy in Height of Maximum Electron Density ( $f_oF_2$ ) Obtained from Grid Interpolation**

**Locations:** A - latitude =  $-17^\circ$ , longitude =  $218^\circ$ , captures effect of the equatorial anomaly  
 B - latitude =  $0^\circ$ , longitude =  $355^\circ$ , captures sunrise effect  
 C - latitude =  $40^\circ$ , longitude =  $225^\circ$ , represents average density condition

**Errors:** Maximum/average position errors are due to interpolation over  $\frac{1}{4}$  grid size  
 Maximum/average time error for 1 hour transmission interval is due to  $\frac{1}{4}$  hour discrepancy adjusted for by longitude shift of grid.

Grid Size	Location	Position Error		Time Error		Prediction		RMS	Error (Predicted-Interpolated)		No. Points	
		Aver.	Max.	Aver.	Max.	Min.	Max.		Mean	Overall %		Abs. % of Max.
5'	A	Aver.	391	Aver.	300	331	391	1.6	0.5	3.0	1.0	60
	B	Aver.	306	Aver.	274	284	306	2.0	0.7	4.9	1.7	60
	C	Aver.	345	Aver.	311	325	345	0.5	0.1	0.8	0.3	60
	A	Max.	390	Max.	300	330	390	3.0	0.9	6.4	2.1	60
	B	Max.	302	Max.	274	282	302	4.1	1.5	9.3	3.2	60
	C	Max.	343	Max.	312	325	343	0.9	0.3	1.7	0.5	60
	A	None	390	None	301	329	390	1.4	0.4	3.1	0.8	60
	B	Max.	305	Max.	274	283	305	4.2	1.5	10.2	3.5	60
7'	A	Aver.	391	Aver.	300	332	391	2.3	0.7	5.1	1.3	36
	B	Aver.	307	Aver.	274	285	307	2.0	0.7	4.6	1.6	36
	C	Aver.	346	Aver.	311	326	346	0.5	0.1	0.7	0.2	36
	A	Max.	390	Max.	300	330	390	3.2	1.0	6.3	2.1	36
	B	Max.	301	Max.	274	282	301	4.0	1.4	8.6	3.0	36
	C	Max.	343	Max.	311	326	343	0.9	0.3	1.6	0.5	36
	A	None	390	None	301	329	390	2.6	0.8	5.9	1.5	36
	B	Max.	306	Max.	273	284	306	4.1	1.5	10.4	3.5	36
10'	A	Aver.	390	Aver.	301	331	390	4.0	1.2	9.0	2.3	18
	B	Aver.	305	Aver.	275	284	305	2.2	0.8	5.2	1.9	18
	C	Aver.	343	Aver.	311	325	343	0.6	0.2	1.0	0.3	18
	A	Max.	383	Max.	302	329	383	4.5	1.4	10.1	2.7	18
	B	Max.	297	Max.	274	281	297	3.9	1.4	7.4	2.6	18
	C	Max.	339	Max.	313	325	339	0.8	0.3	1.3	0.4	18
	A	None	386	None	301	328	386	5.3	1.6	11.9	3.1	18
	B	Max.	305	Max.	275	285	305	4.2	1.5	9.3	3.1	18

**Table 2C**  
**Accuracy in Height of Maximum Electron Density (km) Obtained from Grid Interpolation**

**Locations:** A - latitude = -17°, longitude = 218°, captures effect of the equatorial anomaly  
 B - latitude = 0°, longitude = 355°, captures sunrise effect  
 C - latitude = 40°, longitude = 225°, represents average density condition

**Errors:** Maximum/average position errors are due to interpolation over  $\frac{1}{2}$  grid size  
 Maximum/average time error for 4 hour transmission interval is due to 2/1 hour discrepancy adjusted for by longitude shift of grid along magnetic latitude line.

Grid Size	Location	Position Error		Time Error	Prediction		Error (Predicted-Interpolated)		No. Points		
		Aver.	Max.		Min.	Max.	RMS	Overall %		Abs. % of Max.	Abs.
5°	A	Aver.	304	Aver.	388	329	9.6	2.8	14.5	4.6	60
5°	B	Aver.	272	Aver.	299	280	6.5	2.3	13.9	4.8	60
5°	C	Aver.	311	Aver.	342	325	1.9	0.6	4.5	1.4	60
5°	A	Max.	313	Max.	380	342	16.6	4.9	24.9	7.6	60
5°	B	Max.	268	Max.	287	277	10.4	3.7	22.9	7.7	60
5°	C	Max.	314	Max.	339	327	3.8	1.2	8.6	2.6	60
5°	A	None	301	None	390	329	1.4	0.4	3.1	0.8	60
5°	B	None	268	Max.	289	278	11.2	4.0	23.3	8.1	60
7°	A	Aver.	304	Aver.	387	339	9.2	2.7	14.0	4.4	36
7°	B	Aver.	271	Aver.	300	281	6.3	2.2	12.6	4.4	36
7°	C	Aver.	311	Aver.	343	326	1.9	0.6	4.4	1.4	36
7°	A	Max.	314	Max.	380	341	16.0	4.7	24.4	7.5	36
7°	B	Max.	269	Max.	287	278	10.1	3.6	21.1	7.4	36
7°	C	Max.	314	Max.	339	327	3.8	1.2	8.4	2.6	36
7°	A	None	301	None	390	329	2.6	0.8	5.9	1.5	36
7°	B	None	268	Max.	293	279	11.2	4.0	23.5	8.1	36
10°	A	Aver.	305	Aver.	388	339	9.3	2.8	13.6	3.5	18
10°	B	Aver.	272	Aver.	297	230	6.1	2.2	12.1	4.2	18
10°	C	Aver.	312	Aver.	340	326	1.7	0.5	3.8	1.2	18
10°	A	Max.	318	Max.	378	342	15.9	4.6	22.5	6.9	18
10°	B	Max.	269	Max.	286	277	9.4	3.4	18.9	6.8	18
10°	C	Max.	315	Max.	336	327	3.3	1.0	7.1	2.2	18
10°	A	None	301	None	386	328	5.3	1.6	11.9	3.1	18
10°	B	None	268	Max.	288	279	11.4	4.1	20.9	7.3	13

Table 3. Combined Prediction and Interpolation Errors in Group Delay at 1600 MHz (nanoseconds)

Locations: A - latitude = -17°, longitude = 218°, captures effect of the equatorial anomaly  
 B - latitude = 0°, longitude = 355°, captures sunrise effect  
 C - latitude = 40°, longitude = 225°, represents average density condition

Errors: Average combined RMS errors - The prediction errors are taken as the 1968 yearly RMS value over all hours at the approximate locations A and C and over two hours at sunrise at the approximate location B.  
 Maximum combined RMS errors - The prediction errors are taken as the monthly RMS value for one hour at the approximate location. Selected is the month and hour that had the largest errors during 1968.

Grid Size	Location	Average Combined RMS Errors		Prediction Error & Interpolation Error from Table 1a.		Pred. Error & Int. Error from Table 1b.		Maximum Combined RMS Errors		Pred. Error & Int. Error from Table 1c.			
		Daily Update	Hourly Update	Daily Update	Hourly Update	Daily Update	Hourly Update	Daily Update	Hourly Update	Daily Update	Hourly Update		
5°	A	6.89	4.42	6.90	4.44	6.94	4.51	20.51	6.40	20.52	6.44	20.55	6.53
5°	B	2.59		2.36		2.45		5.15		4.65		4.72	
5°	C	2.62		2.60		2.66		6.18		6.17		6.19	
7°	A	6.93	4.48	6.93	4.48	6.96	4.53	20.53	6.46	20.53	6.48	20.55	6.52
7°	B	2.60		2.36		2.43		5.18		4.67		4.72	
7°	C	2.63		2.60		2.66		6.19		6.17		6.19	
10°	A	7.01	4.62	7.03	4.63	6.96	4.61	20.59	6.68	20.61	6.69	20.53	6.49
10°	B	2.67		2.38		2.43		5.22		4.68		4.71	
10°	C	2.63		2.60		2.66		6.19		6.17		6.19	

## APPENDIX E

### Series Representation of Ionospheric Predictions

The problem under investigation is how to use all the information available from the Bent Ionospheric Model and come up with a smaller set of information representing the ionospheric predictions to sufficient accuracy. The first approach investigated earlier utilized a grid pattern of predictions covering an area around a central location and linear interpolation between the grid points. The denser the grid pattern, the higher was the accuracy achieved.

The approach taken here is to express the ionospheric predictions at a fixed time over a selected area around a central location by a series representation. The series expressing the prediction  $p$  is developed in terms of power series in the earth central angle  $\alpha$  from the central location to any point of the selected area, and in terms of multiple angle trigonometric functions of the azimuth  $A$ .

$$p = \sum_{i=0}^n \alpha^i \sum_{j=0}^m (a_{ij} \cos^j A + b_{ij} \sin^j A)$$

The highest power in  $\alpha$  is  $n$  and the largest multiplier of  $A$  is  $m$ . The total number of coefficients  $a_{ij}$  and  $b_{ij}$  is  $l = (n+1)(2m+1)$ , since  $b_{ij}$ , always having a zero multiplier can be eliminated.

The coefficients are to be determined from ionospheric predictions and corresponding central angle and azimuth angle data for points covering the selected area. The equation system to be solved for the coefficients is,

$$P = XC,$$

where  $P$  is the matrix of ionospheric predictions,

$C$  is the matrix of coefficients, and

$X$  is the observation matrix.



The observation matrix contains in each row the functions in central angle and azimuth by which the coefficients of the series are multiplied, and the information from each point is placed in a separate row. The  $k^{th}$  row is defined by,  $(X_{k1} X_{k2} \dots X_{kn}) =$

$$\begin{pmatrix}
 1 & \cos A_k & \sin A_k & \cos 2 A_k & \sin 2 A_k \dots & \cos m A_k & \sin m A_k \\
 \alpha_k & \alpha_k \cos A_k & \alpha_k \sin A_k & \alpha_k \cos 2 A_k & \alpha_k \sin 2 A_k \dots & \alpha_k \cos m A_k & \alpha_k \sin m A_k \\
 \alpha_k^2 & \alpha_k^2 \cos A_k & \alpha_k^2 \sin A_k & \alpha_k^2 \cos 2 A_k & \alpha_k^2 \sin 2 A_k \dots & \alpha_k^2 \cos m A_k & \alpha_k^2 \sin m A_k \\
 \vdots & \vdots & \vdots & \vdots & \vdots & \vdots & \vdots \\
 \vdots & \vdots & \vdots & \vdots & \vdots & \vdots & \vdots \\
 \alpha_k^n & \alpha_k^n \cos A_k & \alpha_k^n \sin A_k & \alpha_k^n \cos 2 A_k & \alpha_k^n \sin 2 A_k \dots & \alpha_k^n \cos m A_k & \alpha_k^n \sin m A_k
 \end{pmatrix}$$

If the number of predictions is equal to the number of coefficients, an exact solution can be formed. To take advantage of the series approximation approach though, the number of predictions should be quite a bit larger than the number of coefficients yielding an overdetermined equation system that is to be solved using a linear regression technique. The small amount of resulting coefficients are then formed from a large data base of predictions, and thus represent the predictions over the whole of the selected area better. As a solution technique, the least square adjustment was used, minimizing the sum of the squared deviations from the fit. Solving for the coefficients yields the matrix equation,

$$C = (X'X)^{-1} X'P.$$

A number of tests were performed in which coefficients for several combinations of  $m$  and  $n$  were determined from selected grid patterns of predictions. A matching set of predictions for the same patterns were then computed by the series approximation utilizing the coefficients to demonstrate the accuracy of the method. Predictions for patterns offset from the original grid patterns were determined by the series approach for an accuracy comparison with the interpolation technique mentioned above.

The date for the tests was chosen as August 1968 for high solar activity near the peak of the sunspot cycle. The central locations were chosen as  $\bar{A}$  and  $\bar{B}$  as shown in Figure 1 so that the two test areas covered the most varied regions in the ionosphere by capturing the effects of the equatorial anomaly and the sunrise. The areas are defined by a circle of 60 degrees in earth central angle around the location  $\bar{A}$  and  $\bar{B}$  enclosing large ionospheric variations from -60 to +60 degrees in latitude. The predictions and corresponding central and azimuth angles for the coefficient determination were generated at 118 points evenly spaced at 10 degree intervals of central angle and azimuth to cover the areas.

Four sets of coefficients were determined for each of the areas around  $\bar{A}$  and  $\bar{B}$ . In the first two sets equal importance was placed on the variation in central angle and azimuth, setting  $m=3$  and  $n=3$  for the 28 coefficient case and  $m=4$ ,  $n=4$  for the 45 coefficient case. A higher azimuth multiplier was allowed in the 44 coefficient case with  $m=5$ ,  $n=3$ , and a higher power of the central angle was included in the 42 coefficient case with  $m=3$ ,  $n=5$ . Ionospheric predictions were then computed utilizing the coefficients in the series approach, and the results are presented in contour maps for comparison with the original predictions. The 118 point pattern is overlaid by the contour lines of the ionospheric predictions of vertical group delay at 1600 MHz in units of nanoseconds. Figures 2a and 3a represent the original predictions in the areas around  $\bar{A}$  and  $\bar{B}$  respectively; Figures 2b-e show the contour maps around  $\bar{A}$  and Figures 3b-3 around  $\bar{B}$  obtained from the different coefficient sets. The results from all cases of the coefficient method visibly approach the general pattern of the original predictions. However, the results from the coefficient approach do not extend to the highest values of the original predictions, and they tend to approximate oblong contour lines by more circular ones. The improvement in the estimates resulting from the increase in the number of coefficients from 28 to 45 can be clearly noted. The higher power of the central angle does not seem to improve the fit, but the larger multiplier of the azimuth angle causes a better match of the oblong contour lines.

The condition of the sunrise around location  $\bar{B}$  is better matched by the series technique than the condition of the equatorial anomaly around  $\bar{A}$ . To clarify the regions just around  $\bar{A}$  and  $\bar{B}$ , the center of Figures 2c and 3c were enlarged to show the detailed contour maps from 0 to 20 degrees in central angle. Figure 5, the enlargement for location  $\bar{B}$ , does not show much change from Figure 3c; but Figure 4, the map around  $\bar{A}$ , shows a great amount of variation not visible in Figure 2c. The coefficients apparently fit very badly right around  $\bar{A}$  and values from 2 to 24 appear where the original predictions ranged from 12 to 18. Looking further into this case might yield a modified approach that eliminates this particular problem.

By utilizing the coefficients in the series approach as well as by interpolating between the original values at the 118 points, ionospheric predictions were computed for 117 points offset from the original grid pattern by 5, 2.5, and 0 degrees in central angle as well as in azimuth. The 5 degree position offset in the 10 degree grid results in maximum errors, the 2.5 degree offset in average errors, while no offset gives the best possible results. Tables 1a and 2 show the comparison for predictions of vertical group delay at 1600 MHz and Tables 2a and b for the height of the maximum electron density. The interpolation method requires use of 118 numbers while the series method only uses 28 numbers in the first case and 45, 42 and 44 numbers in the following cases. The tables list for each condition the range of the prediction over the 117 point grid pattern by giving minimum, maximum and mean values. The errors at each point are defined as the deviation of the interpolated value or of the coefficient obtained value from the prediction computed directly for that point using the Bent Model. Listed are the RMS values of the errors for the areas around  $\bar{A}$  and  $\bar{B}$ , the percentage of the RMS error to the mean prediction, the largest absolute error incurred at any one point, and the corresponding percentage of error to prediction at that point.

For location  $\bar{A}$  the coefficient method yielded the lowest RMS errors in vertical group delay for the case  $n=4$ ,  $m=4$ , and for location  $\bar{B}$  for the combination  $n=3$ ,  $m=5$  with more variation in azimuth than in central angle.

The RMS percent errors for the different cases of the coefficient method are between 9% and 22% larger than those obtained from the interpolation method and while the maximum error for any one case is up to 4.3 times as large as the RMS value for the interpolation method, it is up to 6.5 times as large as the RMS for the coefficient technique. This indicates that overall the coefficient method might yield acceptable errors, but yet the values at a few individual points might still have unreasonably large errors. Comparison of Figure 4 and Figure 2a shows such a problem area of bad estimates right around location  $\bar{A}$ . Further investigations of the choice of coefficients and of grid variation with latitude and longitude rather than central angle and azimuth are desired to find the best conditions for the coefficient method.

The problem of the choice of coefficients was carried one step further. To estimate the importance of each coefficient in the series approach, the correlation coefficients were computed between all possible combinations of columns for the observation matrix X. If  $x_i$  and  $y_i$  are the elements of two different columns in X, and k is the number of rows in X, then the working equation for the correlation coefficient r for these two columns is,

$$r = \frac{k \sum_{i=1}^k x_i y_i - \sum_{i=1}^k x_i \sum_{i=1}^k y_i}{\sqrt{\left[ k \sum_{i=1}^k x_i^2 - \left( \sum_{i=1}^k x_i \right)^2 \right] \left[ k \sum_{i=1}^k y_i^2 - \left( \sum_{i=1}^k y_i \right)^2 \right]}}$$

Evaluating the case with 45 coefficients,  $m=4$ ,  $n=4$ , the resulting correlation coefficients between any two columns clearly separated into two groups; where the first group showed no correlation with  $.00 \leq r \leq .07$  and the second group showed a high degree of correlation with  $.73 \leq r \leq .79$ . Looking at the individual terms in the observation matrix, it was found that all contributions  $\alpha^i$  were highly correlated with  $\alpha_1$  and all contributions

$\alpha^j \cos j A$  and  $\alpha^j \sin j A$  where highly correlated with  $\cos j A$  and  $\sin j A$  respectively. Since the correlations were smaller than 1, but close to 1, the corresponding coefficients add some, but little, to the estimate of the ionospheric predictions. Eliminating all correlated coefficients the series was modified to be,

$$p = a_{00} + a_1 \alpha + \sum_{j=1}^n (a_{0j} \cos j A + b_{0j} \sin j A).$$

The test case of 45 coefficients reduced to 10 coefficients with  $m=4$ ,  $n=1$ . The coefficients were determined based on the same data as all other test cases and the estimates obtained from the modified series approach using the new coefficients were compared with the original predictions. The results are listed in Tables 1b and 2b. The errors for the 10 coefficient cases are not too much larger than those for the 45 coefficient cases; however, it is seen that the 35 eliminated coefficients contribute some amount to the improvements of the estimates.

To refine the series approach of estimating ionospheric predictions further investigation in several areas is necessary. The proper density of points used for the computation of the coefficients should be determined to allow as much accuracy as possible, but to avoid unnecessary detail that cannot be absorbed into the coefficients. Different grid coordinates for the point patterns should be checked out: a latitude-longitude grid could replace the central angle-azimuth grid. Modified series and various combinations of terms should be further evaluated to come up with only a few coefficients of the best combination that yield small overall errors and also reduce the maximum errors.

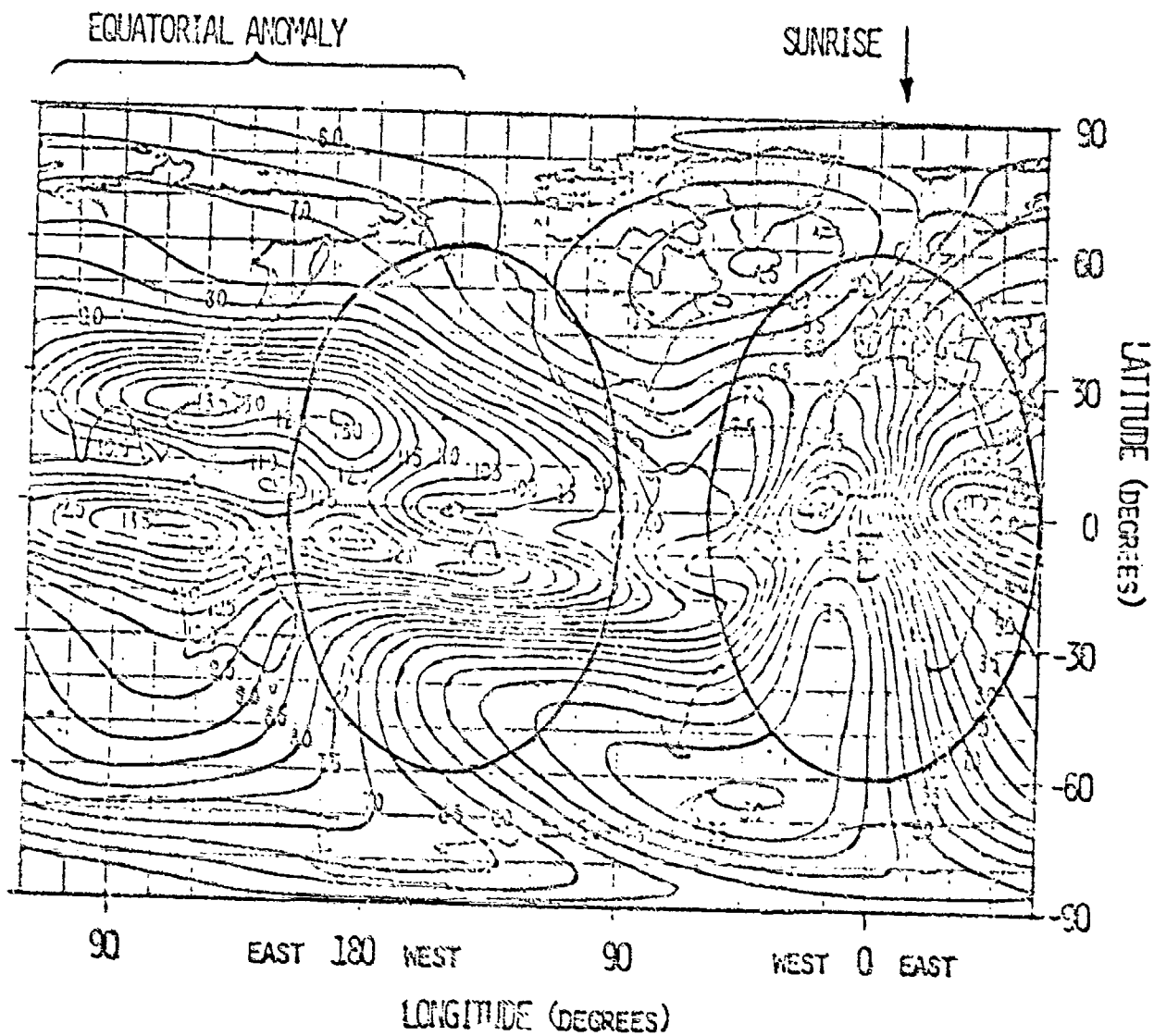


Figure 1. The Predicted Global Status of a Monthly Median  $f, F_2$  at 6 hours Universal Time Showing the Areas Around Locations A and B Used for the Tests.

Central Location  $\bar{A}$  ( $0^\circ, 210^\circ$ ) - equatorial anomaly effect  
Date - 15 Aug 1968, Universal Time: 6 hours

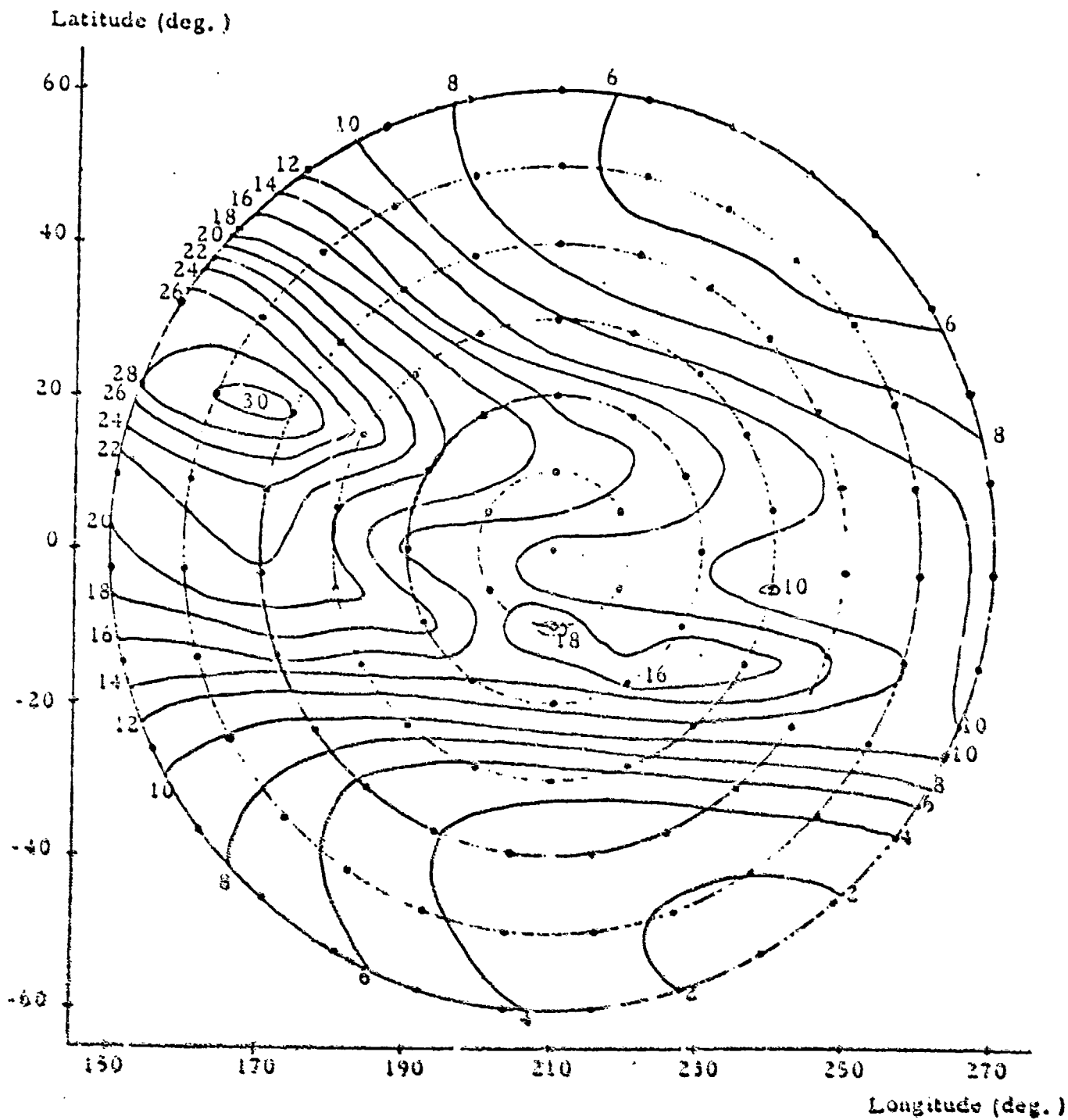


Figure 2a. Contour Map of Group Delay at 1600 MHz Obtained from Ionospheric Prediction Program

Central Location  $\bar{A}$  ( $0^\circ, 210^\circ$ ) - equatorial anomaly effect

Date - 15 Aug 1968, Universal Time: 6 hours

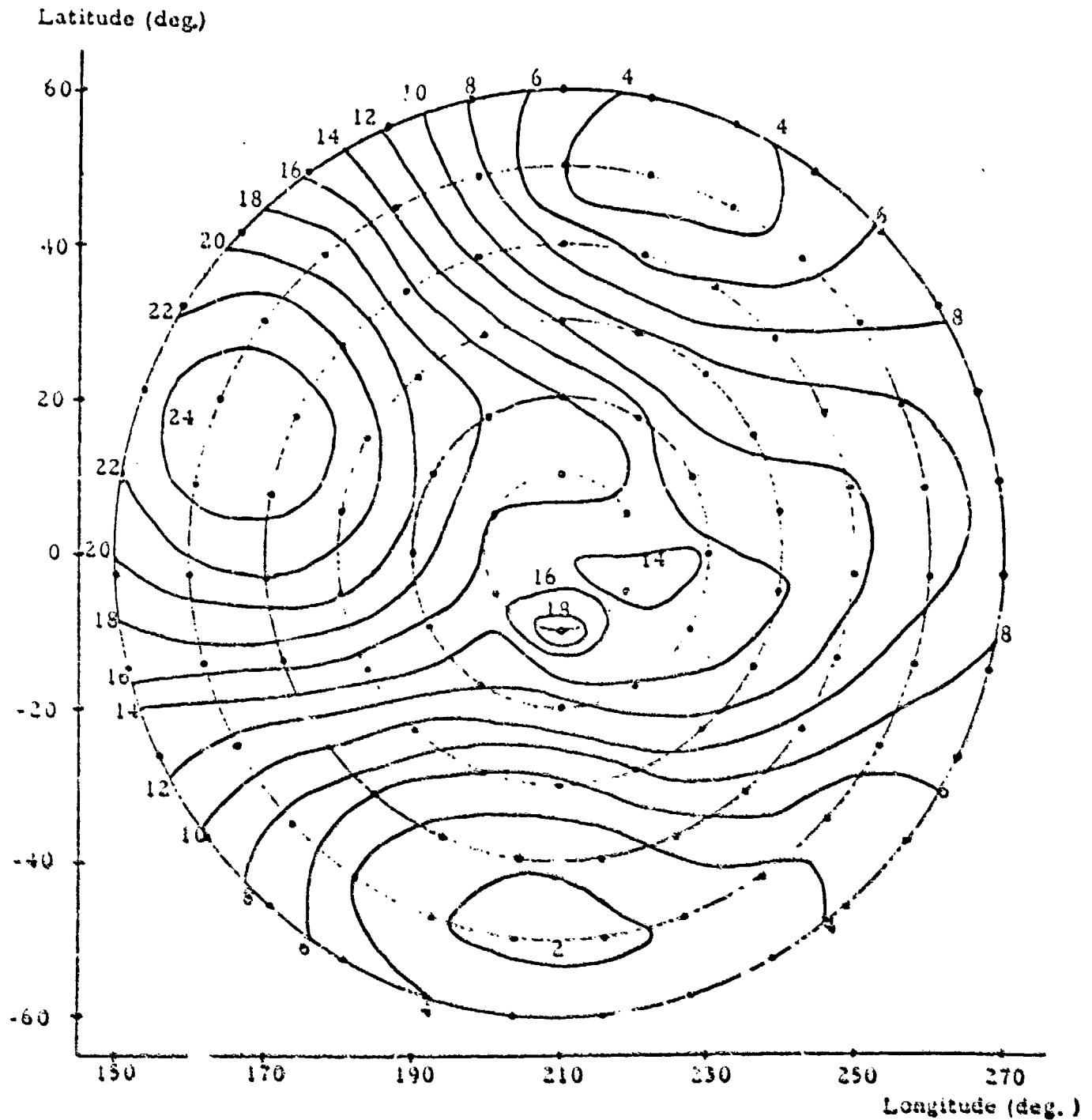


Figure 2b. Contour Map of Group Delay at 1600 MHz Obtained from Coefficient Method Using  $2g$  Coefficients with the Highest Power of the Central Angle  $\mu_3$  and the Largest Multiplier of the Azimuth Angle  $m=3$



Central Location  $\bar{A}$  ( $0^\circ, 210^\circ$ ) - equatorial anomaly effect

Date - 15 Aug 1968, Universal Time; 6 hours

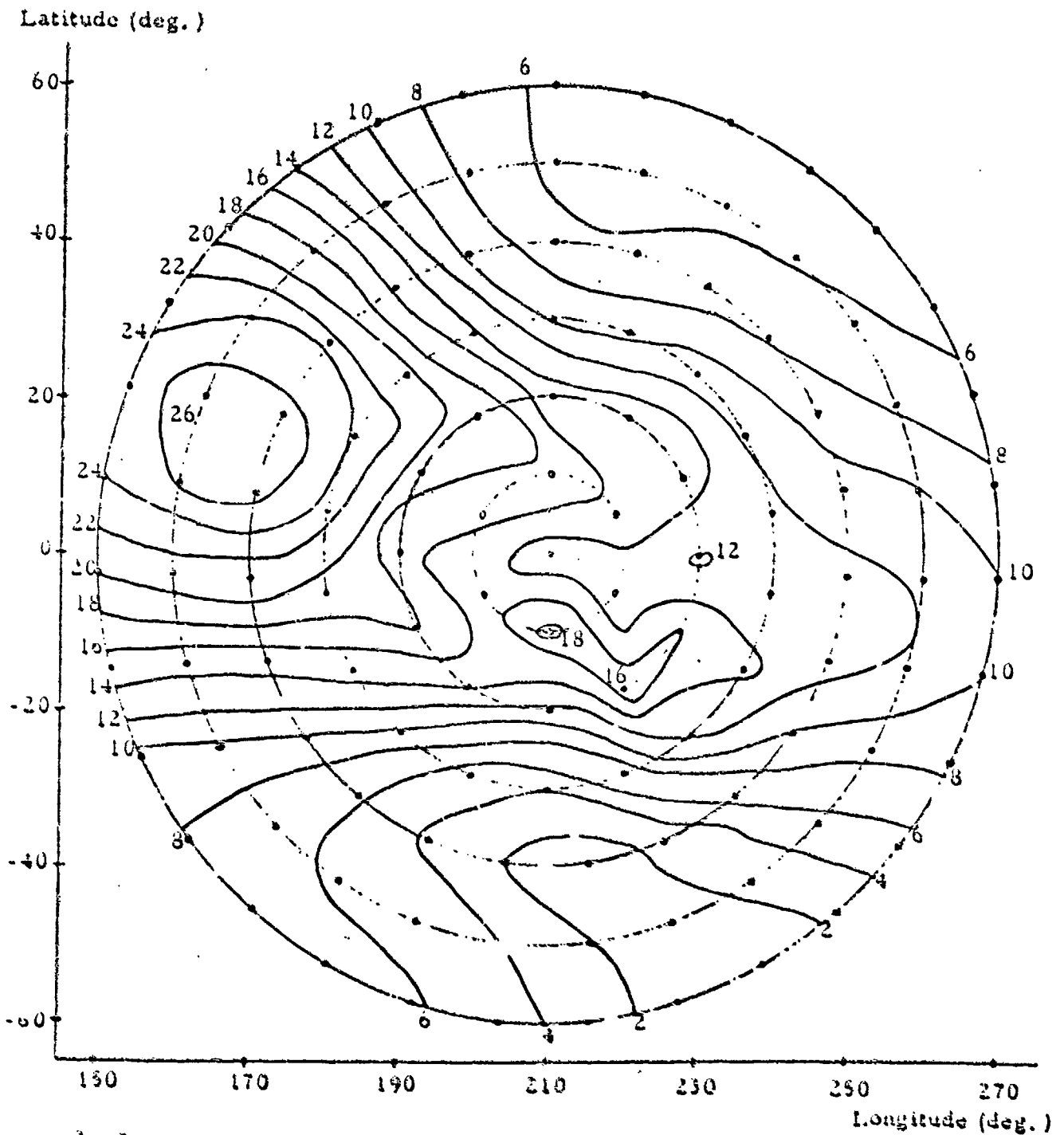


Figure 2c. Contour Map of Group Delay at 1600 MHz Obtained from Coefficient Method Using 45 Coefficients with the Highest Power of the Central Angle  $\underline{m=4}$  and the Largest Multiplier of the Azimuth Angle  $\underline{m=4}$ .

Central Location  $\bar{A}$  ( $0^\circ, 210^\circ$ ) - equatorial anomaly effect

Date - 15 Aug 1968, Universal Time: 6 hours

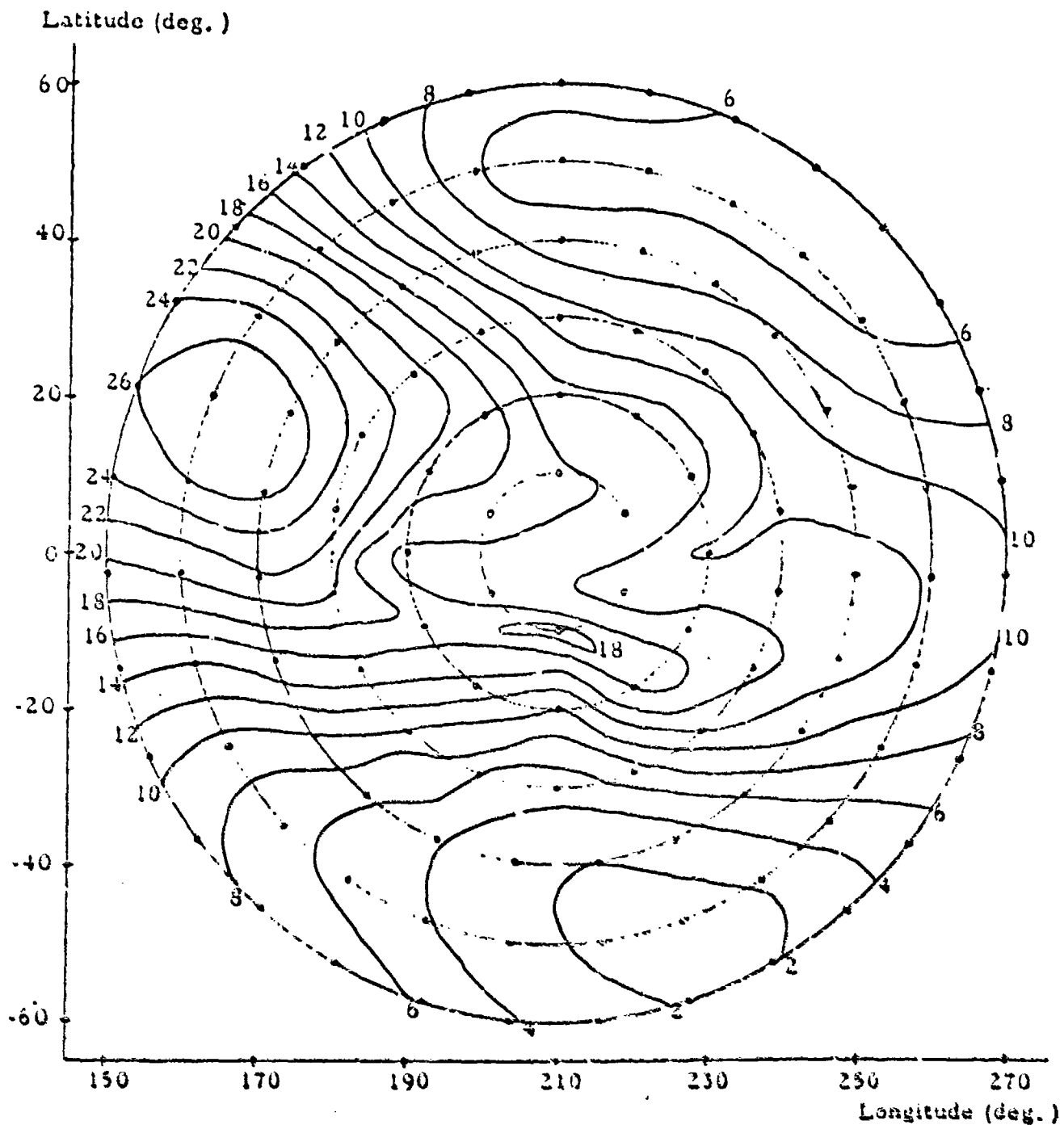


Figure 2d. Contour Map of Group Delay at 1600 MHz Obtained from Coefficient Method Using 44 Coefficients with the Highest Power of the Central Angle  $n=3$  and the Largest Multiplier of the Azimuth Angle  $m=5$ .

Central Location  $\bar{A}$  ( $0^\circ, 210^\circ$ ) - equatorial anomaly effect

Date - 15 Aug 1968, Universal Time: 6 hours

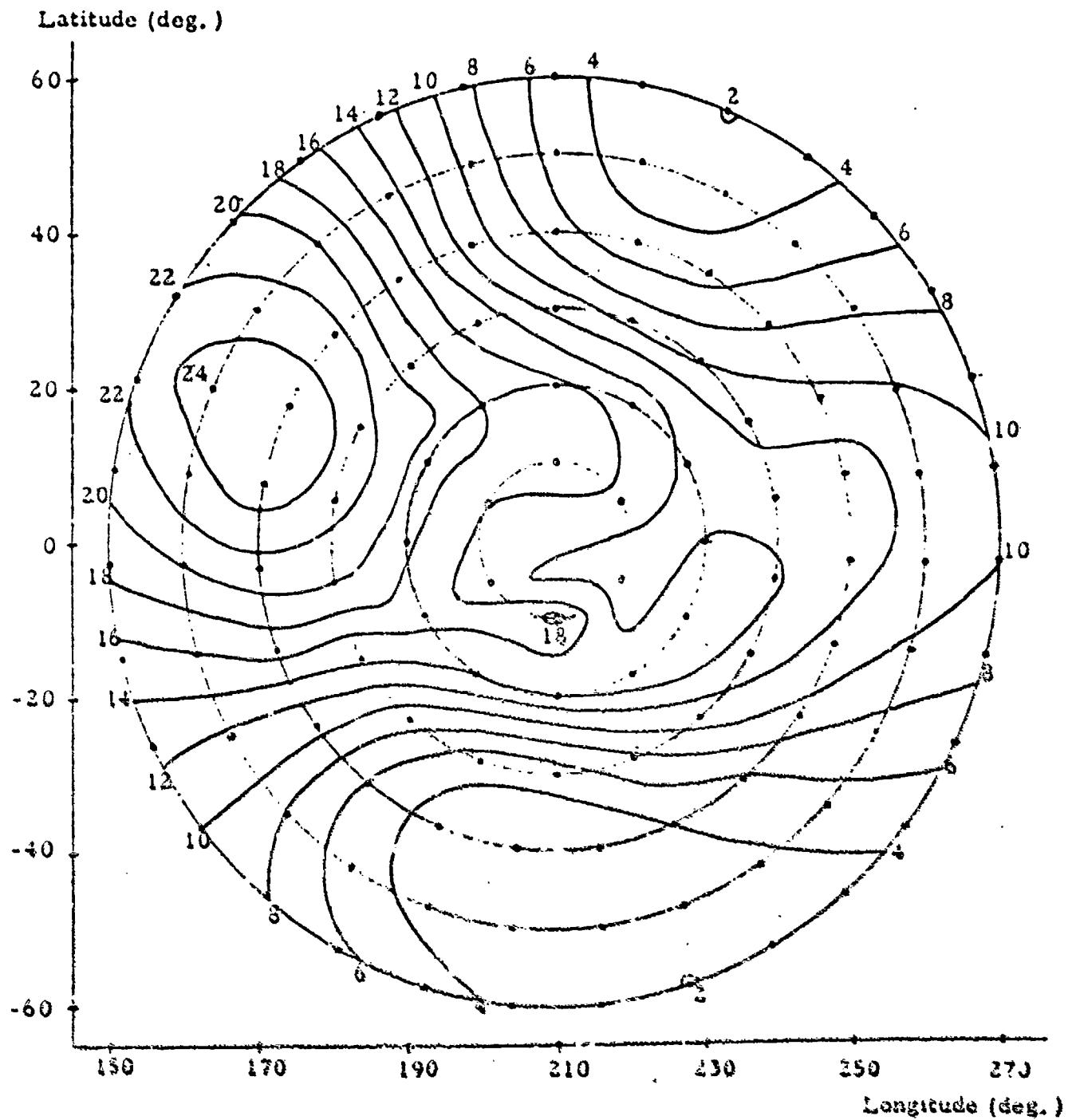


Figure 2e. Contour Map of Group Delay at 1600 MHz Obtained from Coefficients Method Using  $\underline{62}$  Coefficients with the Highest Power of the Central Angle  $\underline{n=3}$  and the Largest Multiplier of the Azimuth Angle  $\underline{m=3}$ .

Central Location  $\bar{B}$  ( $0^\circ, 0^\circ$ ) - sunrise effect  
Date - 15 Aug 1968, Universal Time: 6 hours

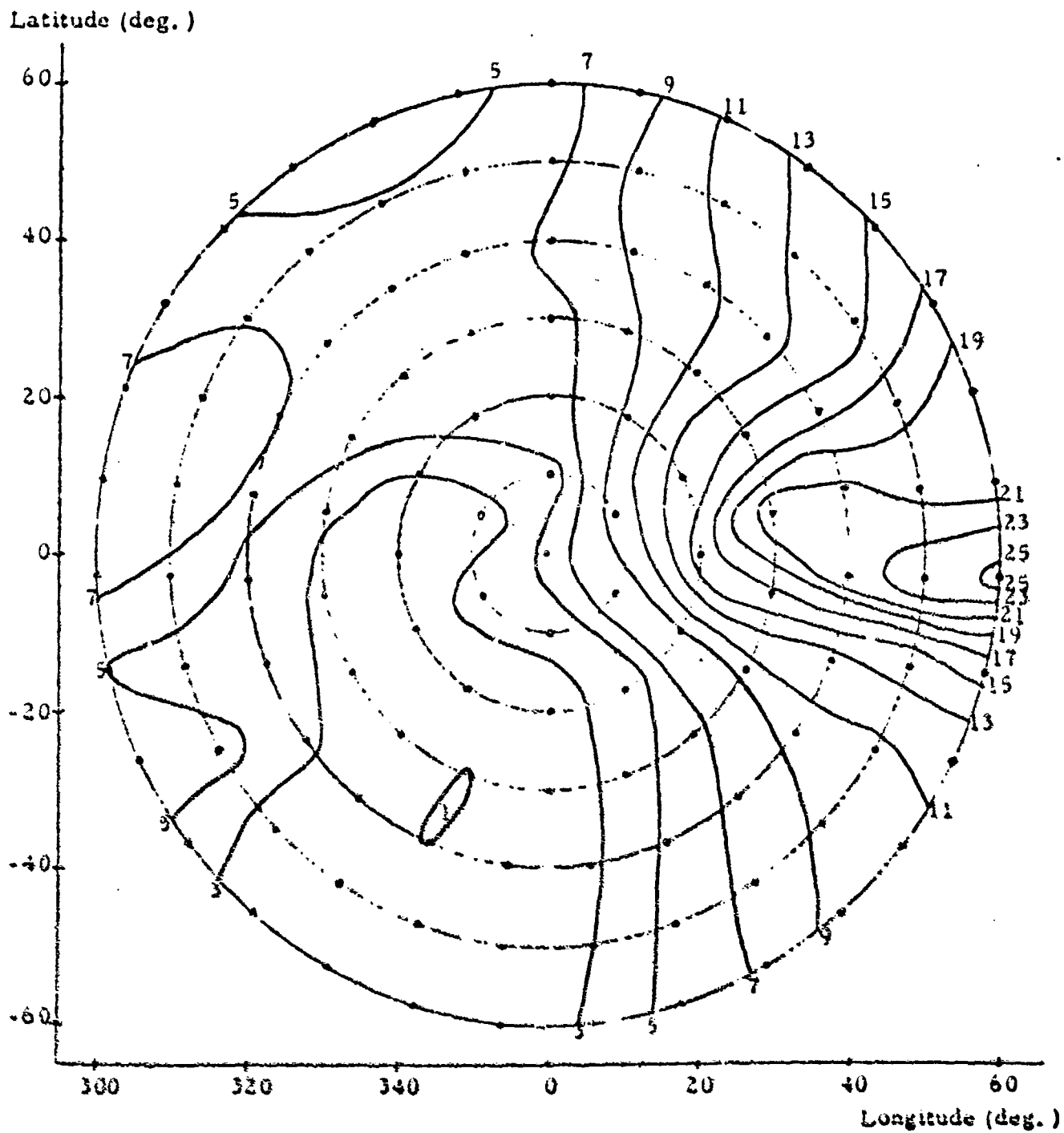


Figure 3a. Contour Map of Group Delay at 1600 MHz Obtained from Ionospheric Prediction Program

Central Location  $\bar{B}$  ( $0^\circ, 0^\circ$ ) - sunrise effect  
 Date - 15 Aug 1968, Universal Time: 6 hours

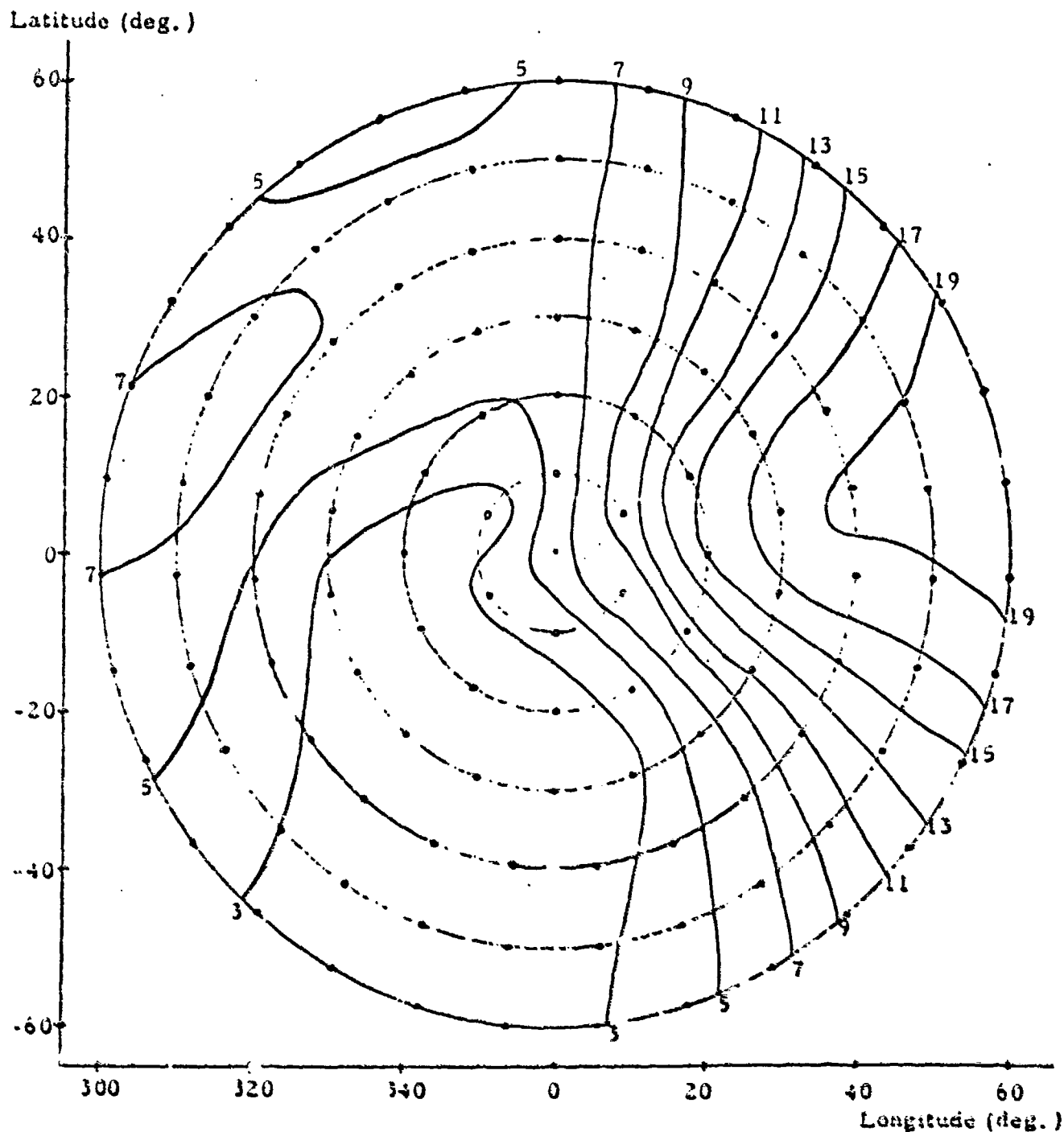


Figure 3b. Contour Map of Group Delay at 1600 MHz Obtained from Coefficient Method Using 28 Coefficients with the Highest Power of the Central Angle  $\alpha=3$  and the Largest Multiplier of the Azimuth Angle  $m=3$

Central Location  $\bar{B}$  ( $0^\circ, 0^\circ$ ) - sunrise effect  
 Date - 15 Aug 1968, Universal Time: 6 hours

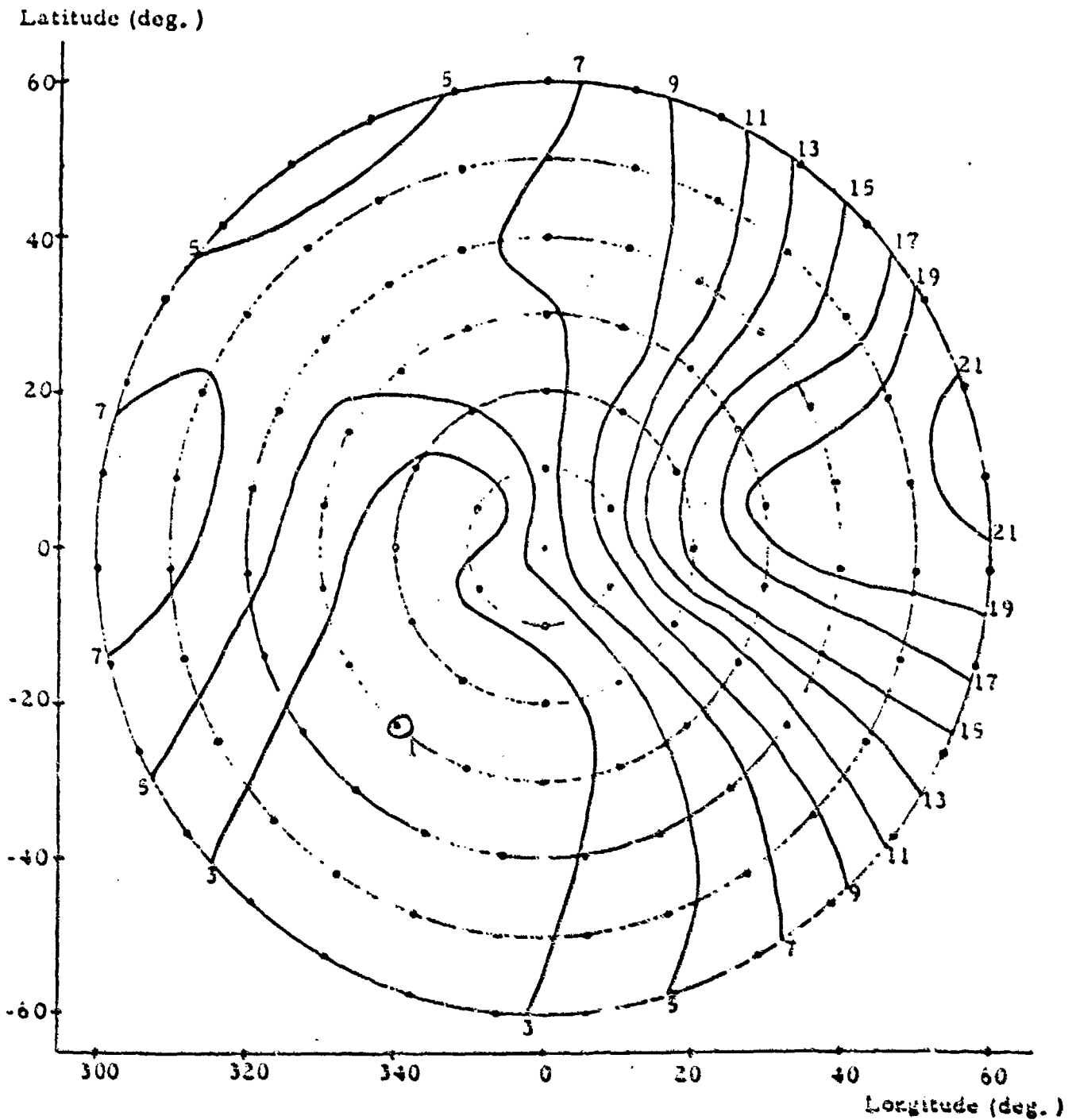


Figure 3c. Contour Map of Group Delay at 1600 MHz Obtained from Coefficient Method Using 45 Coefficients with the Highest Power of the Central Angle  $\alpha_{c4}$  and the Largest Multiplier of the Azimuth Angle  $m_{c4}$

Central Location  $\bar{B}$  ( $0^\circ, 0^\circ$ ) - sunrise effect  
Date - 15 Aug 1968, Universal Time: 6 hours

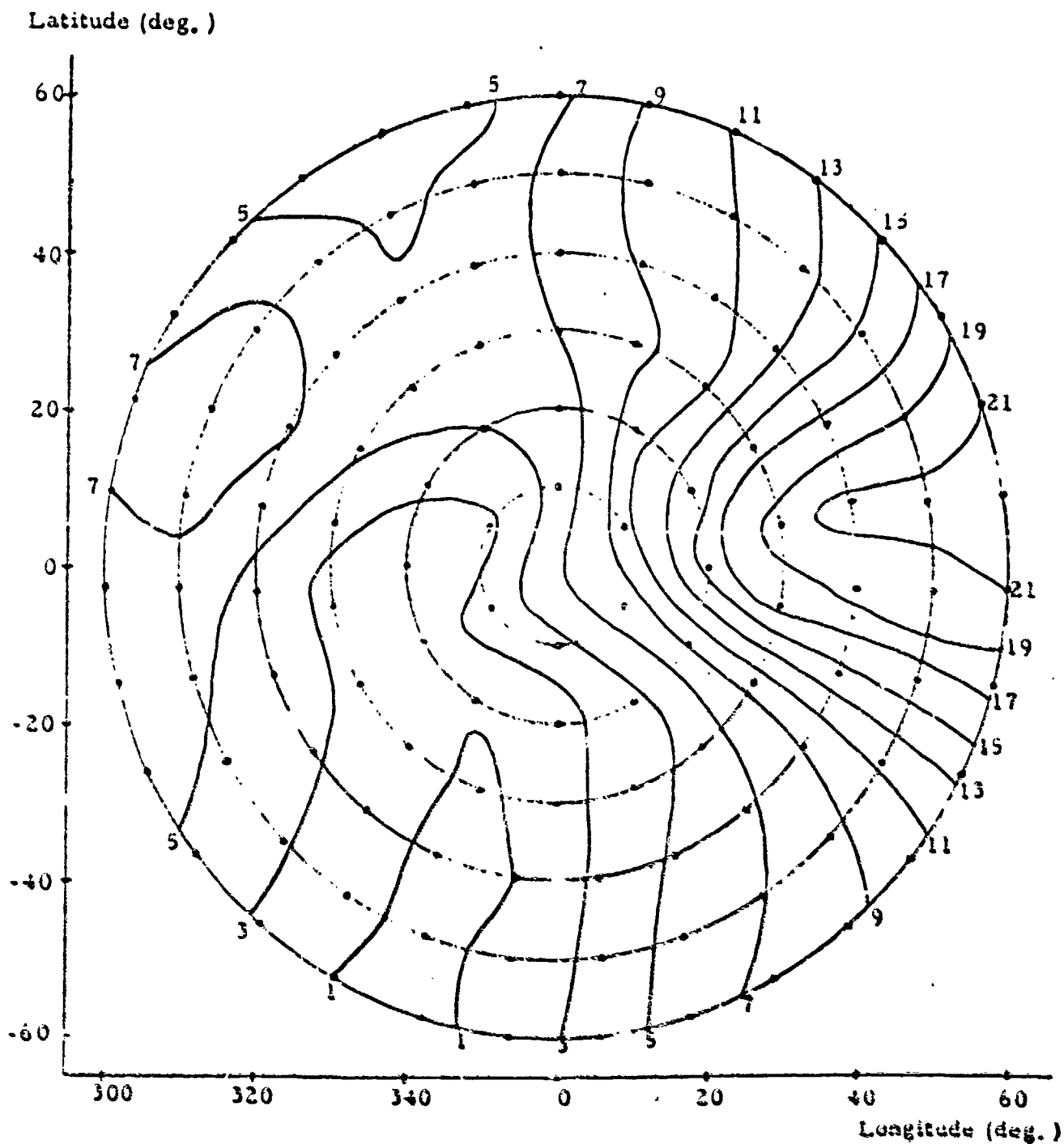


Figure 3d. Contour Map of Group Delay at 1600 MHz Obtained from Coefficient Method Using 44 Coefficients with the Highest Power of the Central Angle  $n=3$  and the Largest Multiplier of the Azimuth Angle  $m=5$ .

Central Location  $\bar{B}$  ( $0^\circ, 0^\circ$ ) - sunrise effect  
 Date - 15 Aug 1968, Universal Time: 6 hours

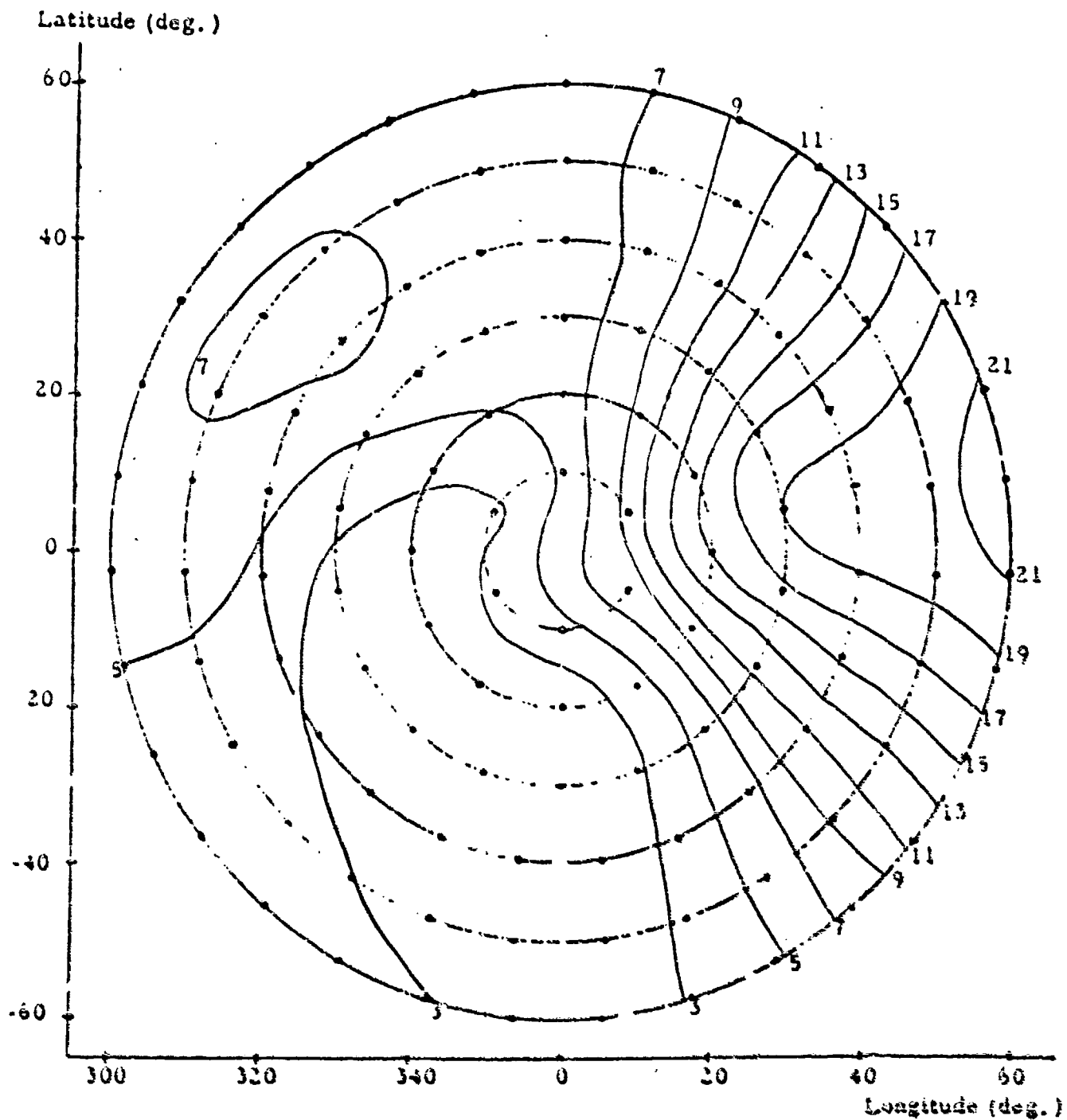


Figure 1e. Contour Map of Group Delay at 1600 MHz Obtained from Coefficient Method Using 42 Coefficients with the Highest Power of the Central Angle  $n_5$  and the Largest Multiplier of the Azimuth Angle  $m_2$ .



Central Location  $\bar{A}$  ( $0^\circ, 210^\circ$ ) - equatorial anomaly effect

Date - 15 Aug 1968, Universal Time: 6 hours

Latitude (deg.)

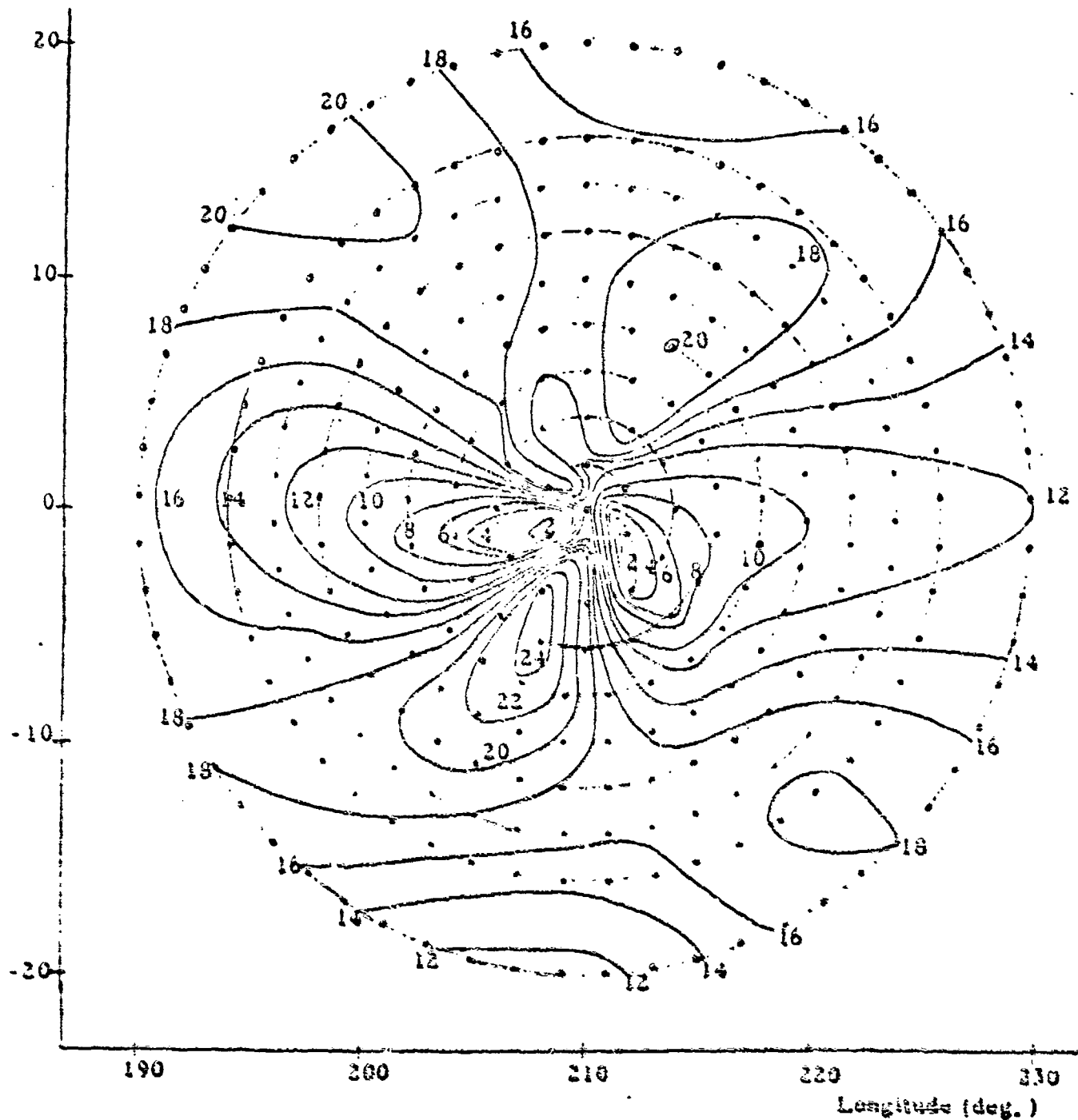


Figure 4. Enlargement of Two Central Circles of Figure 2c Showing the Contour Map of Group Delay

Central Location B (0°, 0°) - sunrise effect  
Date - 15 Aug 1968, Universal Time: 6 hours

Latitude (deg.)

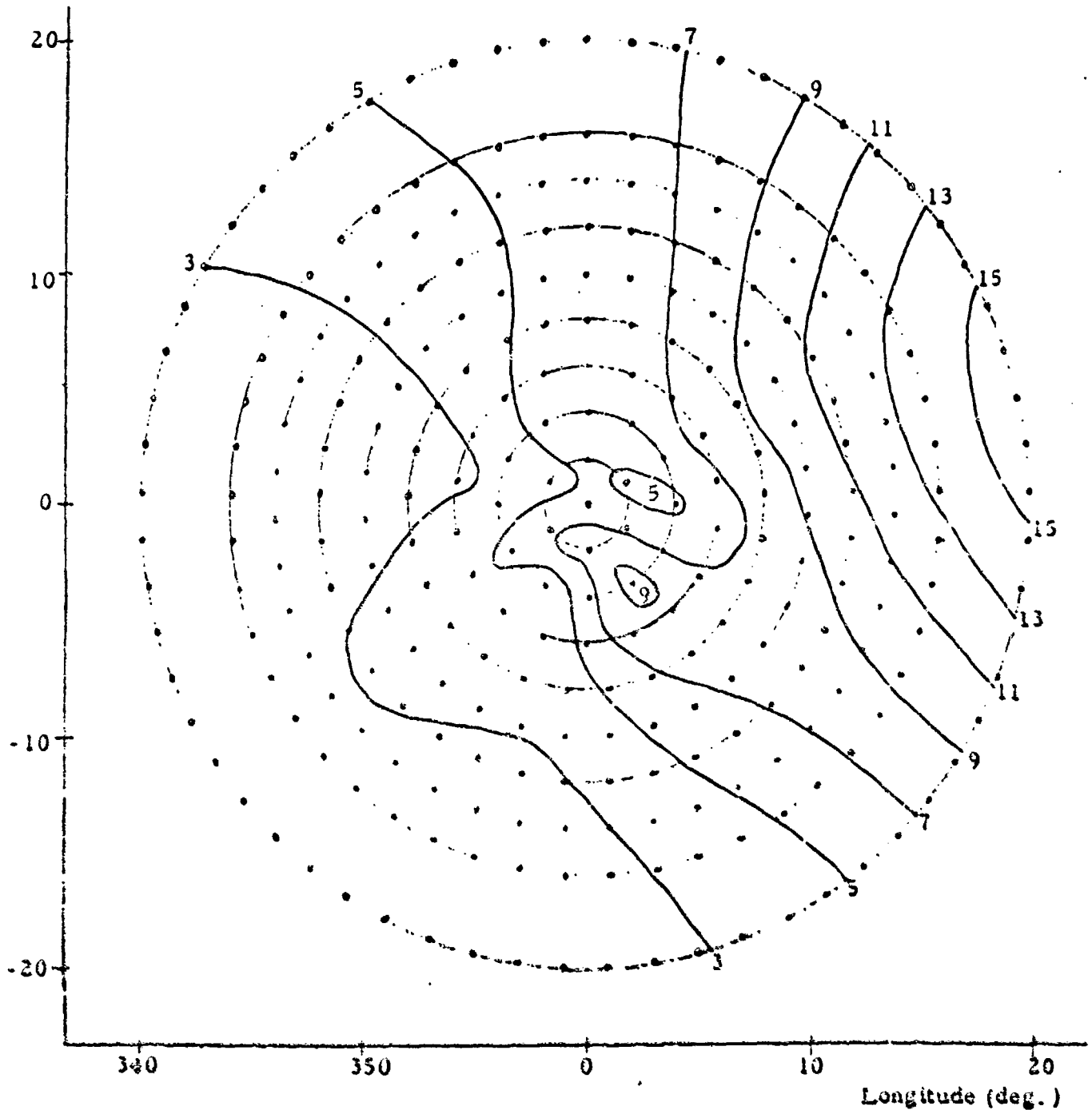


Figure 5. Enlargement of Two Central Circles of Figure 3c  
Showing the Contour Map of Group Delay

Table 1a.

Accuracy in Vertical Group Delay at 1600 MHz (nanosec conds) Obtained from Grid Interpolation or Coefficient Method

Grid Size: 10 degrees

Locations:  $\bar{A}$  - latitude = 0°, longitude = 210°, captures effect of the equatorial anomaly

$\bar{B}$  - latitude = 0°, longitude = 0°, captures sunrise effect

Errors: Time-none, Position-maximum/average/no errors due to point displacement of  $\frac{1}{4} / \frac{1}{4} / 0$  grid size

M - N	Number of Coefficients	Highest Power & Multiple	Largest Multiple	Location	Position Error	Prediction		Error (Predicted-Interpolated or Coefficient)		No. Points			
						Min.	Max.	RMS Overall %	Max. Abs. % of Max. Abs.				
-	-	-	-	$\bar{A}$	Max	1.7	30.1	11.9	1.10	9.2	3.44	17.9	117
					Aver	1.6	30.7	11.6	0.78	6.7	2.51	15.3	117
					None	1.5	30.1	11.4	0.00	0.0	0.00	0.0	117
				$\bar{B}$	Max	1.0	24.5	7.6	0.56	7.3	2.40	10.3	117
					Aver	1.0	23.2	7.8	0.42	5.4	1.82	7.9	117
					None	1.0	25.4	7.9	0.00	0.0	0.00	0.0	117
-	-	-	-	$\bar{A}$	Max	1.7	30.1	11.9	2.25	18.8	9.69	74.4	117
					Aver	1.6	30.7	11.6	2.06	17.7	6.69	42.4	117
					None	1.5	30.1	11.4	1.94	17.1	5.32	19.0	117
					Max	1.0	24.5	7.6	1.32	17.3	5.11	20.9	117
					Aver	1.0	23.2	7.8	1.26	16.2	4.38	18.9	117
					None	1.0	25.4	7.9	1.29	16.3	5.82	22.9	117
				$\bar{B}$	Max	1.7	30.1	11.9	2.14	18.0	12.21	93.7	117
					Aver	1.6	30.7	11.6	1.64	14.1	7.81	49.5	117
					None	1.5	30.1	11.4	1.21	10.7	3.50	19.6	117
					Max	1.0	24.5	7.6	1.16	15.2	4.13	16.9	117
					Aver	1.0	23.2	7.8	1.09	14.0	3.94	17.0	117
					None	1.0	25.4	7.9	1.15	14.5	5.22	20.6	117

Coefficient Method:

Table 1b.

Accuracy in Vertical Group Delay at 1600 MHz (nanoseconds) Obtained from Grid Interpolation or Coefficient Method

Grid Size: 10 degrees

Locations:  $\bar{A}$  - latitude = 0°, longitude = 210°, captures effect of the equatorial anomaly

$\bar{B}$  - latitude = 0°, longitude = 0°, captures sunrise effect

Errors: Time-none, Position-maximum/average/k.o errors due to point displacement of  $\frac{1}{2} / \frac{1}{4} / 0$  grid size

Number of Coefficients	Highest/Largest Power of Multiple	Location	Position Error	Prediction		Error (Predicted-Interpolated or Coefficient)			No. Points		
				Min.	Max.	Mean	RMS Overall %	Max. Abs.		% of Max. Abs.	
42	5	$\bar{A}$	Max	1.7	30.1	11.9	2.19	18.4	9.17	73.3	117
			Aver	1.6	30.7	11.6	1.96	16.8	6.76	22.9	117
			None	1.5	30.1	11.4	1.94	17.0	5.80	20.6	117
	3	$\bar{B}$	Max	1.0	24.5	7.6	1.34	17.6	4.55	18.6	117
			Aver	1.0	23.2	7.8	1.35	17.4	3.64	26.2	117
			None	1.0	25.4	7.9	1.45	18.4	4.53	18.8	117
44	5	$\bar{A}$	Max	1.7	30.1	11.9	3.71	31.1	24.04	185.6	117
			Aver	1.6	30.7	11.6	2.13	18.3	13.85	108.4	117
			None	1.5	30.1	11.4	1.23	10.8	3.48	34.7	117
	3	$\bar{B}$	Max	1.0	24.5	7.6	1.28	16.8	7.46	106.8	117
			Aver	1.0	23.2	7.8	.98	12.6	5.02	51.9	117
			None	1.0	25.4	7.9	.85	10.8	4.28	16.9	117
10	1	$\bar{A}$	Max	1.7	30.1	11.9	3.41	28.6	13.82	106.9	117
			Aver	1.6	30.7	11.6	3.05	26.2	11.06	70.2	117
			None	1.5	30.1	11.4	2.91	25.6	12.06	74.3	117
	4	$\bar{B}$	Max	1.0	24.5	7.6	1.72	22.6	8.59	102.3	117
			Aver	1.0	23.2	7.8	1.60	20.5	7.85	81.1	117
			None	1.0	25.4	7.9	1.53	19.4	5.52	21.7	117

Coefficient Method with Modified Series:

Table 2a.

Accuracy in Height of Maximum Electron Density (m) gained from Grid Interpolation or Coefficient Method

Grid Size: 10 degrees

Locations: A - latitude = 0°, longitude = 210°, captures effect of the equatorial anomaly

B - latitude = 0°, longitude = 0°, captures sunrise effect

Errors: Time-none, Position-maximum/average/no errors due to point displacement of 1/2 / 1/4 / 0 grid size

Number of Coefficients	Highest Power G	Largest Multiple A	Location	Position Error	Prediction		Error (Predicted-Interpolated or Coefficient)		No. Points			
					Min.	Max.	Mean	RMS Overall %		Max. Abs. % of Max. Abs.		
<u>Interpolation Method:</u>												
-	-	-	A	Max	294	402	335	3.5	1.1	10.7	2.7	117
				Aver	293	411	333	2.8	0.8	8.8	2.2	117
				None	293	415	331	0.0	0.0	0.0	0.0	117
			B	Max	260	397	301	2.6	0.9	15.1	3.8	117
				Aver	260	401	303	2.3	0.8	12.5	3.1	117
				None	260	396	305	0.0	0.0	0.0	0.0	117
<u>Coefficient Methods:</u>												
26	3	3	A	Max	294	402	335	10.3	3.1	32.8	8.3	117
				Aver	293	411	333	10.7	3.2	40.2	9.8	117
				None	293	415	331	11.1	3.4	46.2	11.1	117
			B	Max	260	397	301	8.0	2.7	41.9	10.6	117
				Aver	260	401	303	8.6	2.8	41.0	10.2	117
				None	260	396	305	9.3	3.0	39.1	9.9	117
45	4	4	A	Max	294	402	335	7.9	2.3	25.1	6.3	117
				Aver	293	411	333	8.2	2.5	34.0	8.3	117
				None	293	415	331	8.8	2.7	39.9	9.6	117
			B	Max	260	397	301	9.2	3.1	39.0	14.2	117
				Aver	260	401	303	8.5	2.8	38.0	9.5	117
				None	260	396	305	8.9	2.9	34.9	8.8	117

Table 2b.

Accuracy in Height of Maximum Electron Density (m) Obtained from Grid Interpolation or Coefficient Method

Grid Size: 10 degrees

Locations:  $\bar{A}$  - latitude = 0°, longitude = 210°, captures effect of the equatorial anomaly

$\bar{B}$  - latitude = 0°, longitude = 0°, captures sunrise effect

Errors: Time-none, Position-maximum/average/no errors due to point displacement of  $\frac{1}{4}$  / 0 grid size

Number of Coefficients	Highest Power	Largest Multiple	Location	Position Error		Prediction		Error (Predicted-Interpolated or Coefficient)		No. Points		
				Min.	Max.	Min.	Max.	RMS Overall %	Max. Abs. % of Max. Abs.			
42	5	3	$\bar{A}$	Max	294	402	335	15.7	4.7	62.1	15.6	117
				Aver	293	411	333	17.7	5.3	68.9	16.8	117
				None	293	415	331	20.0	6.0	82.7	19.9	117
	3	5	$\bar{B}$	Max	260	397	301	16.4	5.5	53.8	18.4	117
				Aver	260	401	303	18.8	6.2	58.6	19.3	117
				None	260	396	305	21.7	7.1	60.1	21.7	117
44	3	5	$\bar{A}$	Max	294	402	335	5.9	1.8	18.0	4.5	117
				Aver	293	411	333	6.1	1.8	21.7	5.3	117
				None	293	415	331	6.3	1.9	27.6	6.6	117
	4	4	$\bar{B}$	Max	260	397	301	5.3	1.8	24.9	6.3	117
				Aver	260	401	303	5.2	1.7	23.6	5.9	117
				None	260	396	305	5.4	1.8	22.7	5.8	117
10	1	4	$\bar{A}$	Max	294	402	335	14.7	4.4	56.5	14.9	117
				Aver	293	411	333	14.0	4.2	37.9	9.2	117
				None	293	415	331	14.5	4.4	43.7	10.5	117
	4	4	$\bar{B}$	Max	260	397	301	15.3	5.1	54.3	13.7	117
				Aver	260	401	303	15.9	5.3	56.2	14.0	117
				None	260	396	305	15.5	5.1	52.0	13.2	117

## APPENDIX F

### Accuracies in Group Delay Predictions Obtained by Use of the Gradient Method

The purpose of this study is to evaluate the accuracy of the gradient method for predicting group delay. Using a center point value of group delay along with the corresponding gradient magnitude and direction, values of group delay at any point within a  $(1500 \text{ km})^2$  block around the center are estimated. Since the gradient expresses the change in group delay around the center, this method allows estimates to be made over a relatively large area based on data at the center point alone.

To form the data base for this test a world map of contours of equal group delay for different magnetic latitudes and longitudes was plotted (Figure 1). This plot was done using the Bent Ionospheric Model to estimate the group delays occurring on 21 March 1970 at 0 hours universal time. Based on this map, 33 blocks containing  $(1500 \text{ km})^2$  each were constructed. The test blocks were chosen so that areas of most interest and variability would be included. Twenty four blocks were centered around the equator so that the accuracy of this method could be studied in the presence of the equatorial anomaly, and nine blocks were centered around a latitude of -20.25 degrees.

The gradient method for calculating group delay for a grid of points can be summarized as follows: Input data consist of the group delay at the center of the grid, the gradient value of the contours of group delay at the center, and the azimuth defining the direction of this gradient. Using the magnetic latitudes and longitudes at the center point as well as at the point for which an estimate of group delay is to be made, the central earth angle and the azimuth between the center point of the grid and any specified other point are computed. The straight line distance from the center point to the point for which the group delay is to be calculated is computed by the formula

$$d = 2 R_e \sin \frac{\alpha}{2} .$$

where  $R_e$  is the radius of the earth and  $\alpha$  is the central earth angle between

the center point of the grid to the point for which the group delay is to be calculated.

Figure 2 illustrates the geometry of the test blocks. For this test a 5 x 5 grid of points is used.

The distance  $p$  between the center point and the projection of the data point onto the gradient vector is calculated by

$$p = |d \cos (AZ_g - AZ_p)| ,$$

where  $AZ_g$  is the azimuth of the gradient vector and  $AZ_p$  is the azimuth to the point for which the group delay is to be calculated.

The group delay at any given point may be calculated from the group delay at the center and the correction factor

$$\Delta = p \times \text{Grad},$$

where Grad is the value of the gradient at the center point.

A value of group delay for each of the 25 points of the grid is then calculated using

$$GD_p = GD_c + \Delta.$$

where  $GD_p$  is the group delay for each point and  $GD_c$  is the group delay at the center point.

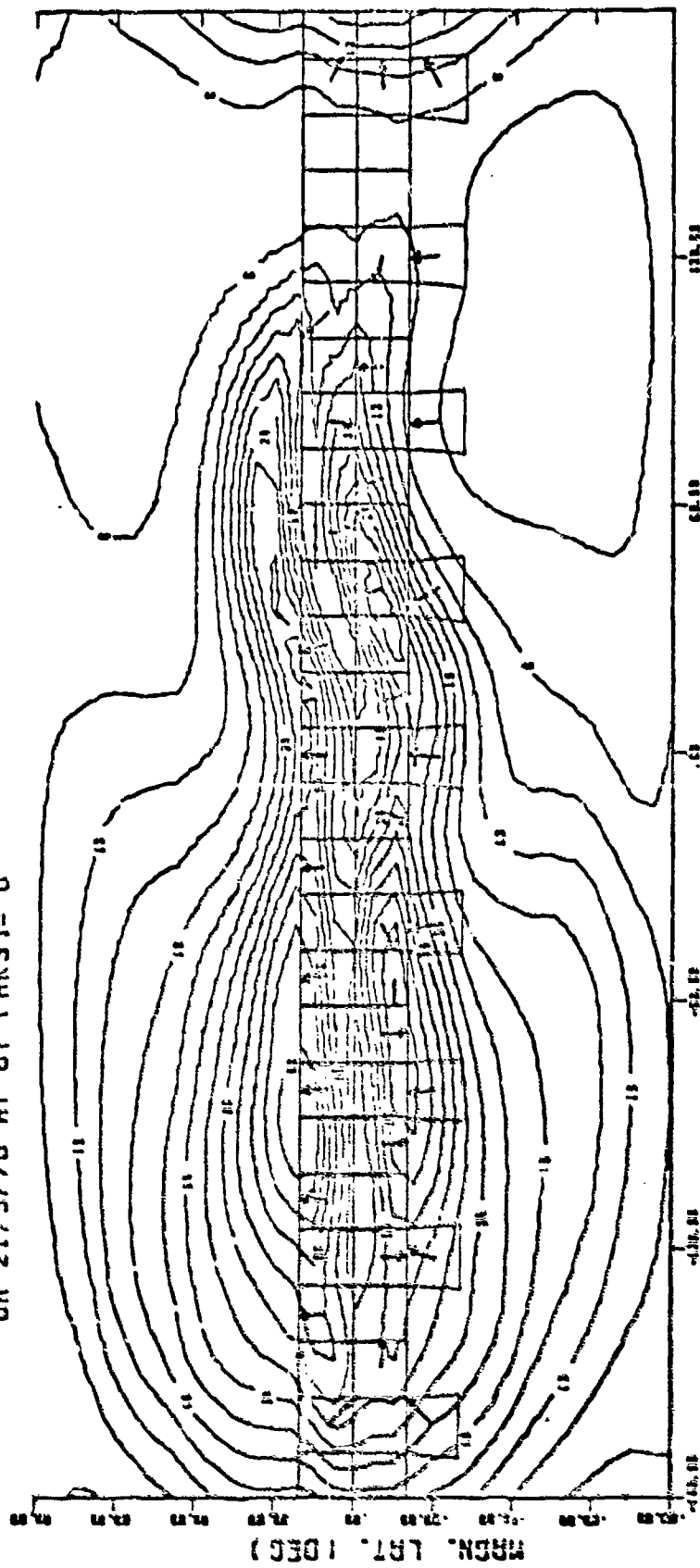
Table 1 is a summary of the results of this study. Data given for each block include the magnetic latitude and longitude for the center point, the mean of the predictions estimated by the Bent Model for the 25 points in the block, and the maximum predicted group delay for the block. Also included is a summary of the errors which are the differences between the values of group delay obtained by the gradient method and the basic predictions. A root-mean-square of these differences is listed for each block as well as the maximum absolute difference. Values for the above statistics are also computed over all blocks and these values are listed at the bottom of the table.



The overall RMS error in the gradient method is listed in Table 1 as 2.6 nanoseconds which is about 12% of the mean prediction computed as 21.5 nsec. For 79% of the individual blocks, however, the RMS errors are below this overall RMS value, and for only a few blocks the overall RMS error is greatly exceeded. Upon examination it is noted that blocks 5, 8, and 20 have very large maximum absolute errors as well as large RMS values. Referring to Figure 1 it may be seen that the configuration of the contours of group delay for these blocks makes it very difficult to compute one estimate of the gradient that can be used to satisfactorily estimate group delay for all the points in the block. By paying special attention to such blocks, estimates of the gradients could be found that will result in more accurate predictions of group delay and hence a reduction in the individual residual RMS. It is possible that these individual residuals may be significantly reduced thereby reducing the overall residual to around 2.0 nanoseconds.

Figure 1.

WORLD MAP OF GROUP DELAY (NSEC)  
 ON 21/3/70 AT UT (HRS)= 0



MAGN. LON. (DEG)

Numbers	13	14	15	16	17	18	19	20	21	22	23	24
for Above	1	2	3	4	5	6	7	8	9	10	11	12
Blocks	25	26	27	28	29	30	31	32	33	34	35	36

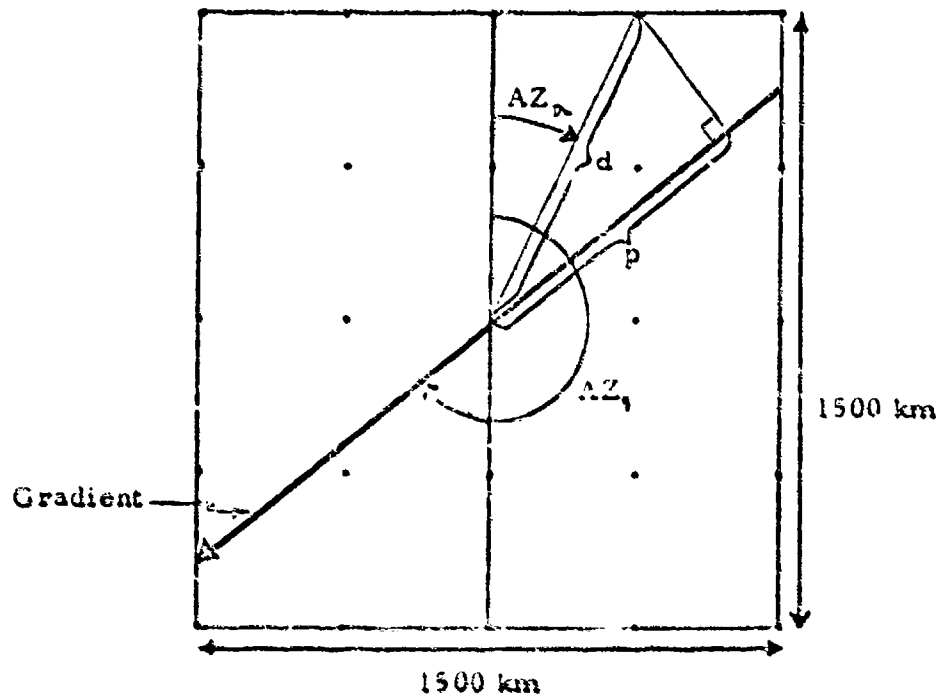


Figure 2. Grid of Points for which Group Delay is Calculated Using the Gradient Method.

TABLE I. ACCURACY IN ESTIMATION OF GROUP DELAY (NSEC) USING GRADIENT METHOD

CHECK NO.	CENTRE POINT MAGN.	PLAN PREDICTION	ERROR IN GRADIENT METHOD	NO. OF
	LATITUDE COMPONENT	PLAN MAXIMUM	RMS MAXIMUM ABSOLUTE	POINTS
1	-14.00	30.87	0.83	25
2	-121.00	33.52	1.90	25
3	-94.00	40.72	2.45	25
4	-67.00	42.08	2.23	25
5	-40.00	41.06	6.20	25
6	-13.00	30.59	2.10	25
7	13.00	29.08	2.45	25
8	40.00	32.64	7.06	25
9	67.00	26.48	1.17	25
10	94.00	16.52	0.80	25
11	121.00	9.30	1.07	25
12	147.00	10.89	0.27	25
13	163.00	30.51	1.81	25
14	179.00	35.09	2.51	25
15	195.00	43.42	3.36	25
16	211.00	45.34	2.11	25
17	227.00	42.37	2.19	25
18	243.00	37.52	2.59	25
19	259.00	30.84	1.40	25
20	275.00	31.41	5.23	25
21	291.00	23.49	3.92	25
22	307.00	21.11	1.80	25
23	323.00	14.74	2.02	25
24	339.00	10.48	0.36	25
25	355.00	26.15	0.43	25
26	371.00	33.52	0.35	25
27	387.00	41.61	0.72	25
28	403.00	36.69	1.42	25
29	419.00	27.63	1.53	25
30	435.00	23.73	1.74	25
31	451.00	5.71	0.50	25
32	467.00	6.57	0.22	25
33	483.00	10.77	0.30	25
34	500.00	45.37	2.63	25
35	516.00	21.52	0.63	25

OFFICE RESULTS

## APPENDIX G

### Accuracies of the Latitude-Longitude Cross Line Technique

A simple technique requiring very little data was tested for producing world wide ionospheric predictions. The basic data consists of values of group delay along one magnetic latitude line, the magnetic equator, and along one magnetic longitude line that passes through the most dense section of the equatorial anomaly. The values along the two cross lines are chosen at 5 degree spacing, which adds up to a total of 107 numbers of 4 to 6 bits depending on the accuracy desired for each world map at a fixed time.

To generate world wide data from these values of group delay it is assumed that the ratios of the value at any given magnetic latitude to the value at the equator are the same along every magnetic longitude line. Specifically, these ratios are equal to the ratios formed for the magnetic longitude line for which data at 5 degree spacing is available. The condition around sunrise, however, does not follow this pattern; here the values of group delay are about the same at all latitudes along the same magnetic longitude line. Thus in this simple cross line technique, the values all along the magnetic longitude line just before sunrise are assumed to be the same as the equatorial value. To allow for a smooth transition between this and the proportionate ratio method, the results from both techniques are combined using linear weighting proportional to the respective distances for 75 degrees in magnetic longitude to both sides of the equal value longitude line.

In all three test cases the magnetic longitude line through the equatorial anomaly and the one just before sunrise were fixed at the same distances from the edges of the plots that are rotated in longitude so that the time dependent pattern appears in the same places. The 4 hour universal time map of group delay for example shows the magnetic longitude line through the equatorial anomaly at 205 degrees and the one just before sunrise at 100 degrees. Figure 1a. shows the map with the basic group delay predictions for the Bent Model. The magnetic latitude and longitude lines that define the data base for the cross line technique are drawn in and

the X defines the location of the equal value longitude line. The contour map resulting from the cross line technique is presented in Figure 1b. and the deviations in the predictions obtained by this technique from the Bent Model values are plotted in Figure 1c. Figures 1a-c. are for 4 hours universal time on 21 March 1970, Figures 2a-c. and 3a-c. are for 20 hours on 21 March 1970 and 21 June 1970 respectively. Table 1 gives a statistical summary of the results; it lists for each test case and for various magnetic latitude regions the mean and maximum values of the Bent Model predictions and the RMS and maximum absolute errors in the cross line technique. The given errors include only the deviation from the basic prediction.

In Cases 1 and 3 this simple model estimates on the average 67 and 58% of the basic prediction and the maximum errors are 1/3 and 1/2 of the maximum prediction, reflecting approximately the same percentage as the average figures for each case. In Case 2, however, only 25% of the basic prediction is estimated and the maximum error is of the same size as the maximum prediction. Upon closer examination of Figures 2a-c., it can be seen that the largest errors occur around 80 degrees magnetic longitude. The approximate symmetry axis of the contours does not completely follow the magnetic equator, and this causes the high equatorial group delay of 30 nsec at 80 degrees longitude, while at -35 degrees where the longitude line passes through the most dense portion of the equatorial anomaly, the equatorial group delay is only 24 nsec. The distortion in the contour pattern is caused by the fact that the axes of the map are the simple dipole magnetic latitude and longitude. The true magnetic equator would follow closer along the actual line of symmetry; thus if an axis of magnetic dip was used around the equator instead of the dipole magnetic latitude, a smaller equatorial group delay would result at 80 degrees longitude and the large errors in Case 2 would be sharply reduced. Another way to improve the results would be to introduce a few extra data values along a longitude line through this dense portion, at roughly 140 degrees east of the most dense part of the equatorial anomaly.

It appears that through more investigations this simple technique could be somewhat refined that it would yield on the average between 65 and 80% of the basic predictions for any fixed time. Time errors due to time discrepancies, interpolation between different sets, or rotation of the maps at a rate of 15 degrees in longitude per hour, as well as the errors in the basic prediction itself, subtract from this accuracy figure.

To reduce the position errors even further another approach was considered that allows cross lines to be used for each of a number of sections of the world, rather than selecting one set of cross lines for the whole world. The sections are 30° in longitude and 70° in latitude, reaching south from 50° north when the satellite is above the northern hemisphere, and north from 50° south when the satellite is south of the equator. With a number of satellites transmitting such data segments all around the world and additional data transmission for the polar caps, complete world coverage can be achieved. Each user can pick up 3 consecutive data segments and data for one polar cap from 4 different satellites to cover his area of visibility. The data for the polar caps can be expressed in the form of a circular grid pattern, the data for all the other segments can be expressed by the data values along two cross lines, one being the magnetic equator, the other the magnetic longitude along the left hand side of the block.

Since the worldwide group delay pattern shows much symmetry in the magnetic latitude-longitude system and the success of the cross line technique as well as the time rotation is dependent on this symmetry, the data blocks are actually defined in the magnetic system as shown in Figure 4, and the satellite orbit being defined in the geographic system will be somewhat offset from the plotted trace. The tests performed give the expected size of the errors in position. The results for blocks both 30° and 60° wide in longitude are summarized for 21 March 1970 in Tables 2a-f and for 21 June 1970 in Tables 3a-f. Listed are the block identification, the RMS and maximum errors along with the mean and

maximum predictions for the individual blocks, and for each hour error and prediction information is summarized for the whole world between  $\pm 50^\circ$  magnetic latitude. The overall RMS error in group delay for the  $30^\circ$  blocks is 18% of the mean prediction, and for the  $60^\circ$  blocks this number has already increased to 26%. Examining the individual blocks often shows that for a particular hour there are 2 blocks at the same longitude north and south for which the RMS errors are considerably larger than for the remaining blocks. These large errors are caused by the distortion due to the inaccurate magnetic equator, as can be seen between  $30$  and  $60^\circ$  in longitude on Figure 4 and Table 2a. By introducing some adjustment for the distortion it is expected that the maximum possible errors are reduced and that an overall RMS error of 14% of the mean prediction can be achieved, which is apparent from errors of 14, 15, and 13% obtained from the data at 4, 8, and 12 hours universal time when the effect of the distortion is relatively small.



Figure 1a. Predictions from Bent Ionospheric Model

WORLD MAP OF GROUP DELAY (NSEC)  
ON 21/3/70 AT UT (HRS.) - 4

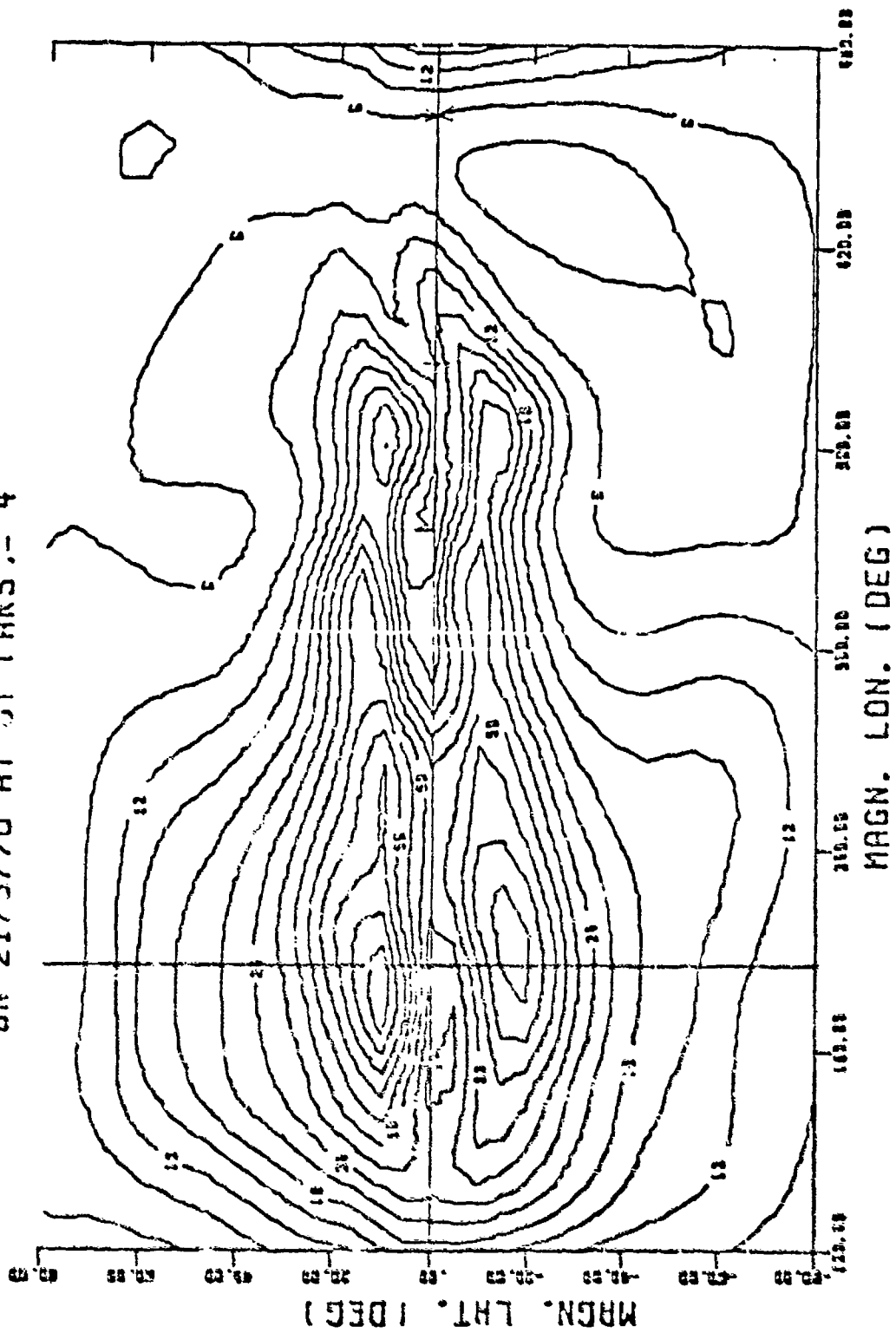


Figure 1b. Predictions from Latitude-Longitude Cross Line Technique

WORLD MAP OF GROUP DELAY (NSEC)  
ON 21/3/70 AT UT (HR5)= 4

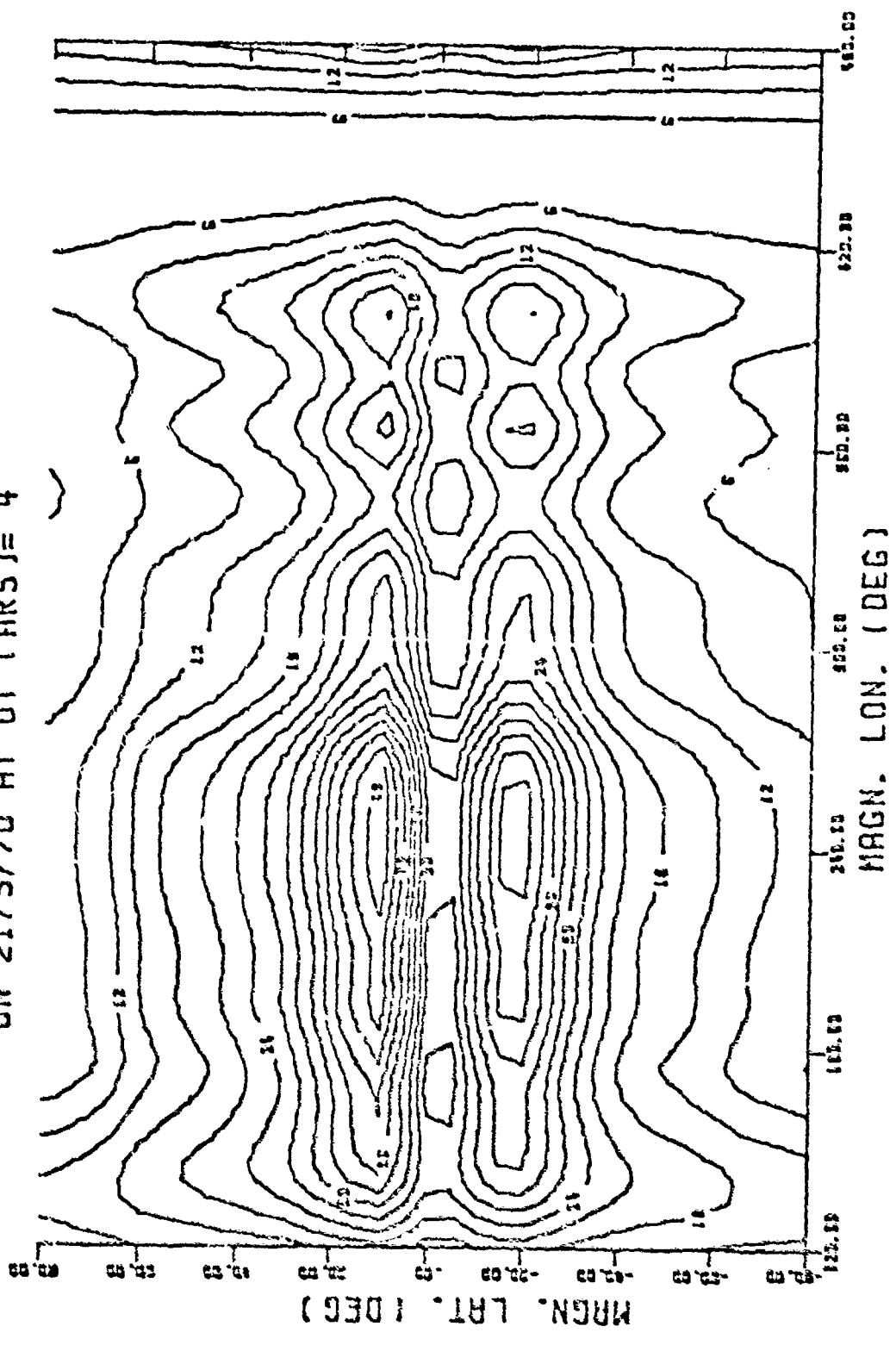


Figure 1c. Deviation in Predictions of Crust. Line Technique from Bent Model Values

WORLD MAP OF DIFF. IN GROUP DELAY (NSEC)  
ON 21/3/70 AT UT (HRS)= 4

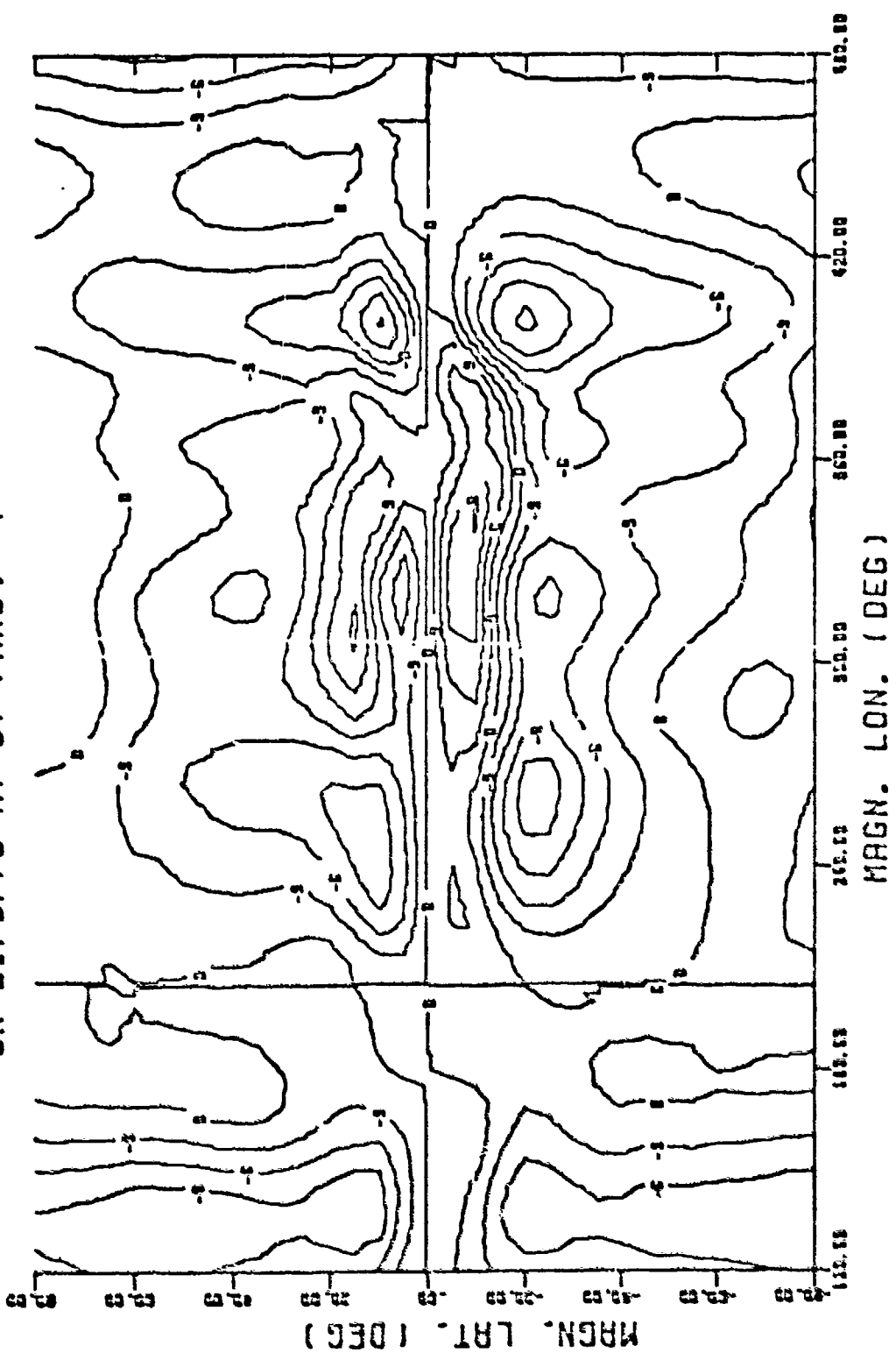


Figure 2a. Predictions from Bent Ionospheric Model

WORLD MAP OF GROUP DELAY (NSEC)  
ON 21/3/70 AT UT (HRS)= 20

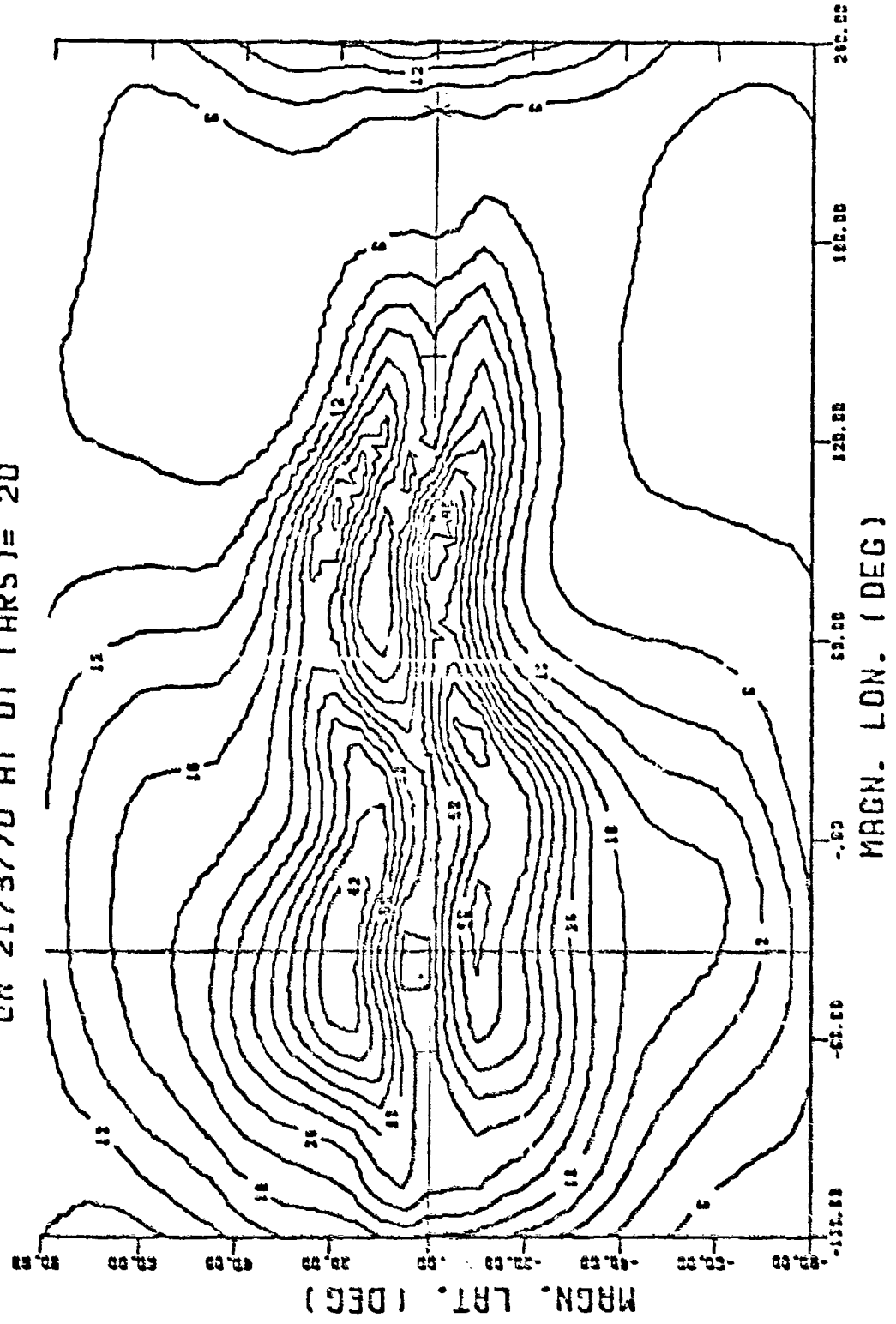


Figure 2b. Predictions from Latitude-Longitude Cross Line Technique

WORLD MAP OF GROUP DELAY (NSEC)  
ON 21/3/70 AT UT (HRS) = 20

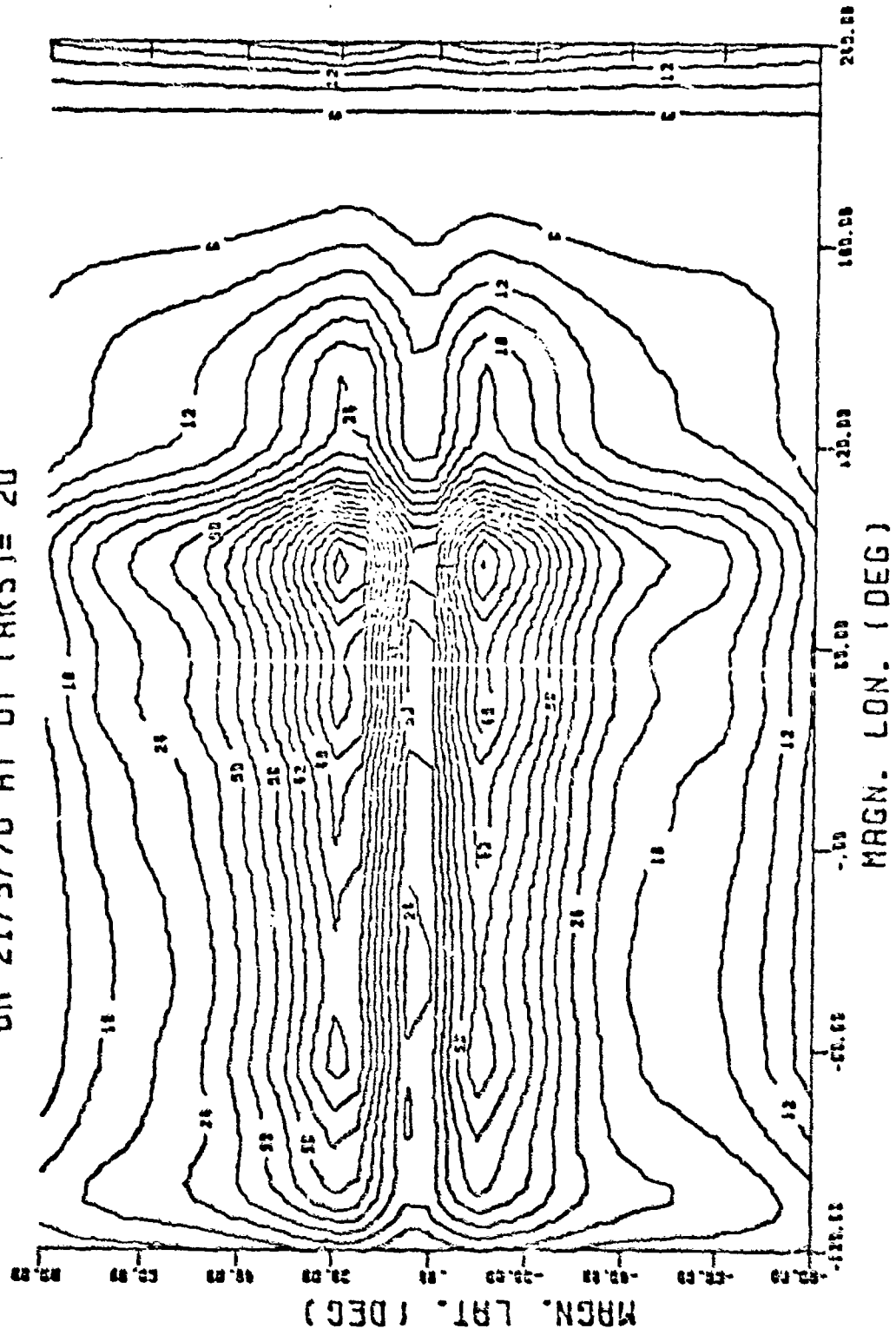


Figure 2c. Deviation in Predictions of Cross Line Technique from Bent Model Values

WORLD MAP OF DIFF. IN GROUP DELAY (NSEC)  
ON 21/3/70 AT UT (HRS)= 20

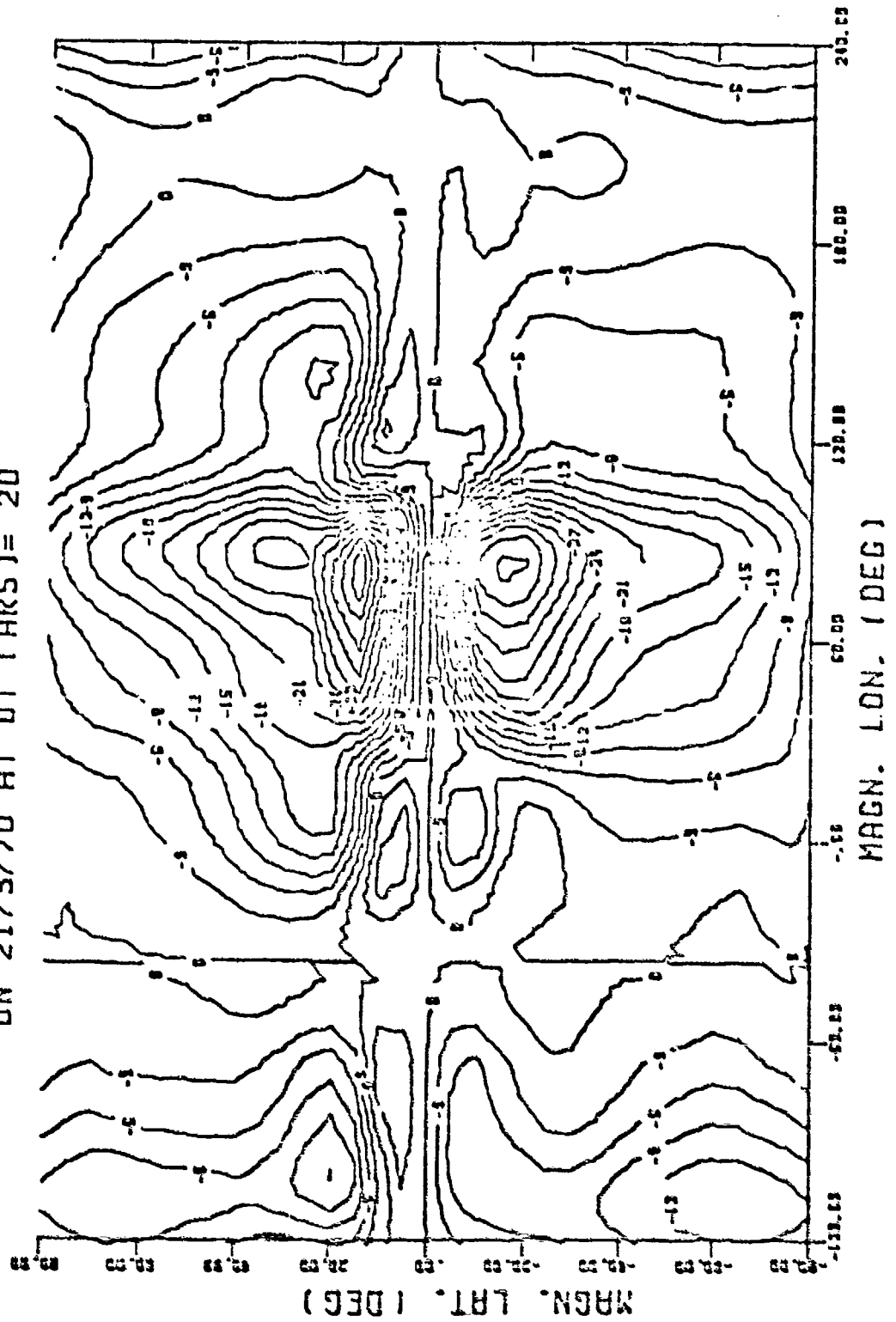


Figure 3a. Predictions from Bent Ionospheric Model

WORLD MAP OF GROUP DELAY (NSEC)  
ON 21/6/70 AT UT (HRS)= 20

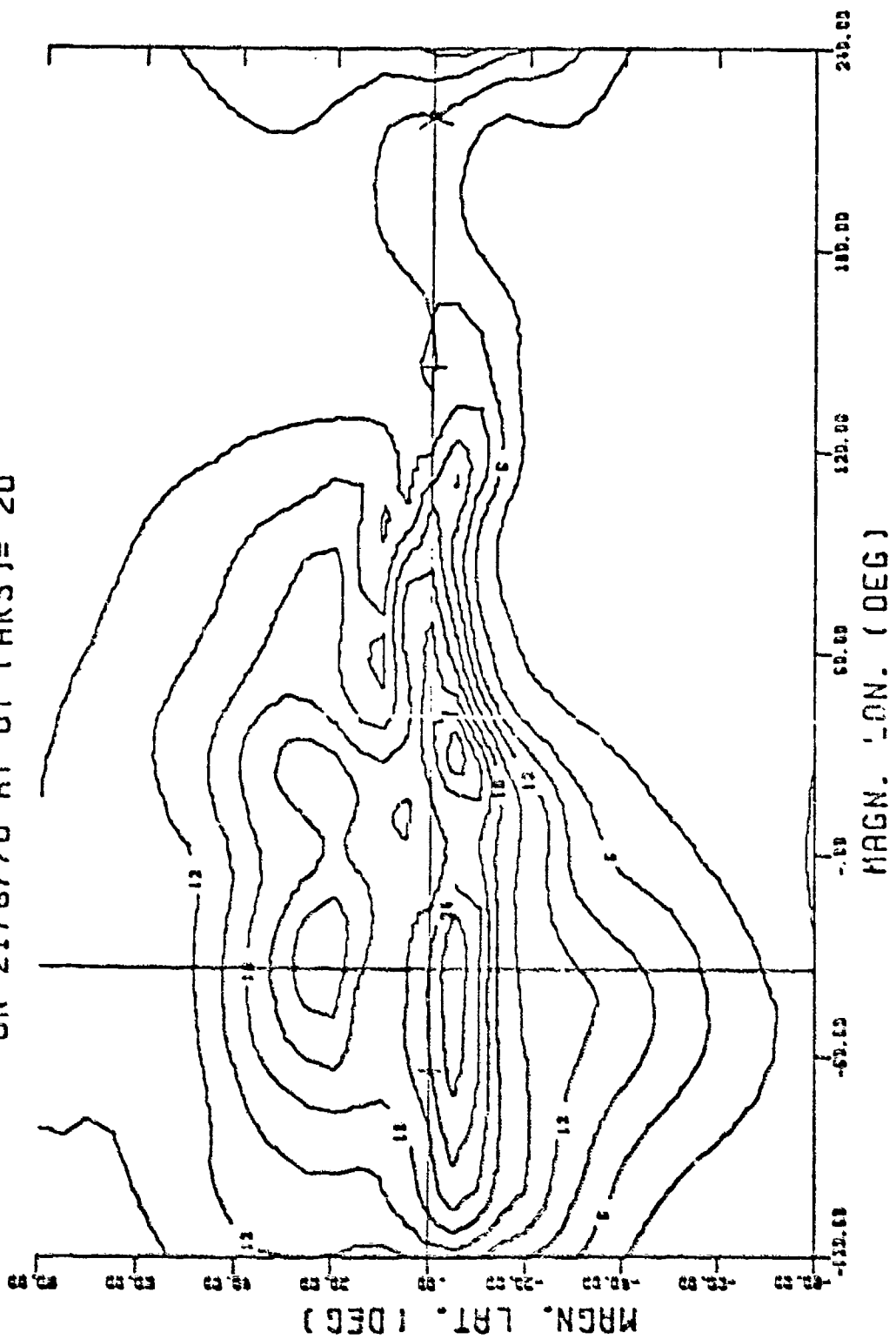


Figure 3b. Predictions from Latitude-Longitude Cross Line Technique

WORLD MAP OF GROUP DELAY (NSEC)  
ON 21/6.70 AT UT (HRS)= 20

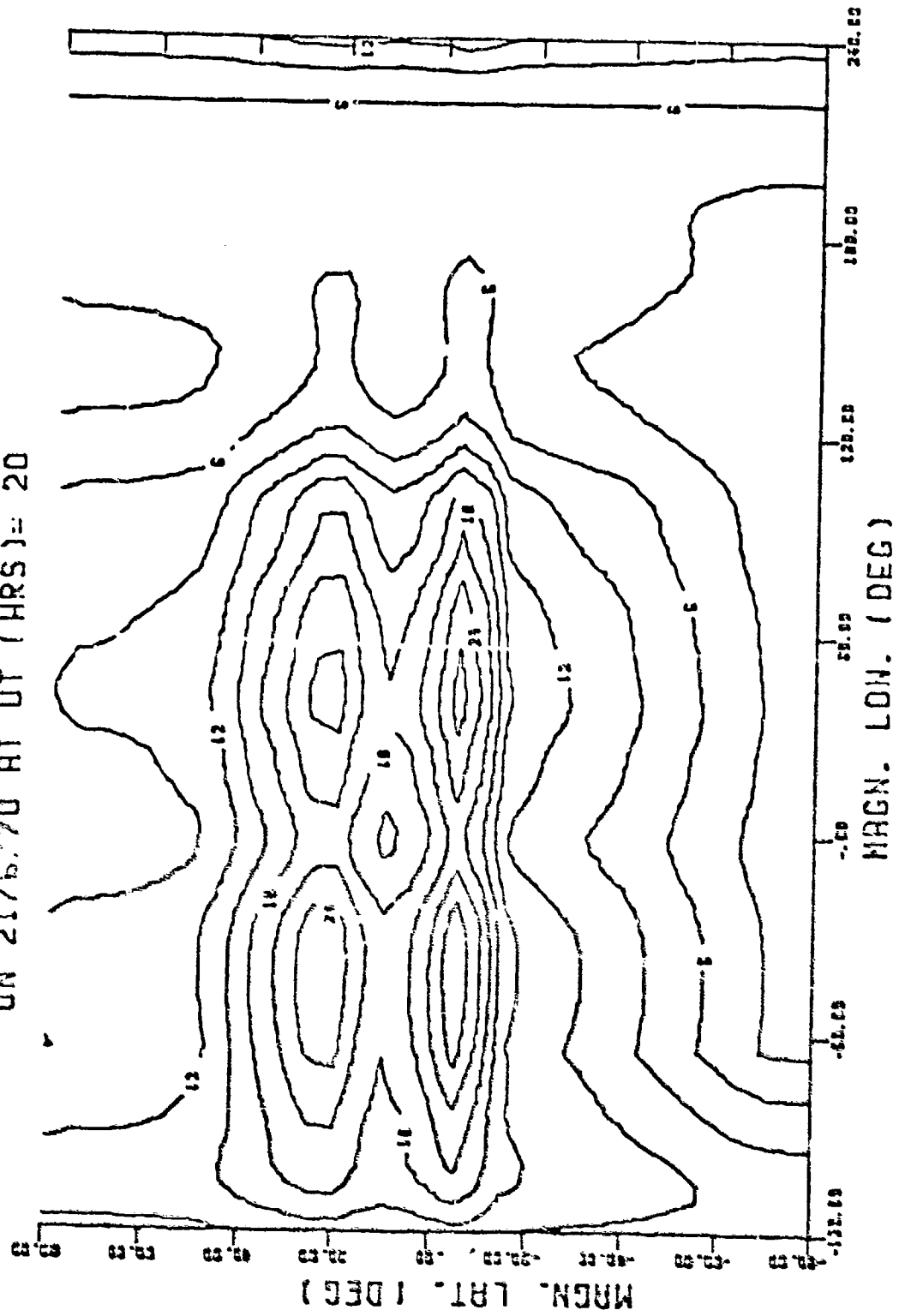




Figure 1c. Deviation in Predictions of Cross Line Technique from Bent Model Values

WORLD MAP OF DIFF. IN GROUP DELAY (NSEC)  
ON 21/6/70 AT UT (HRS)= 20

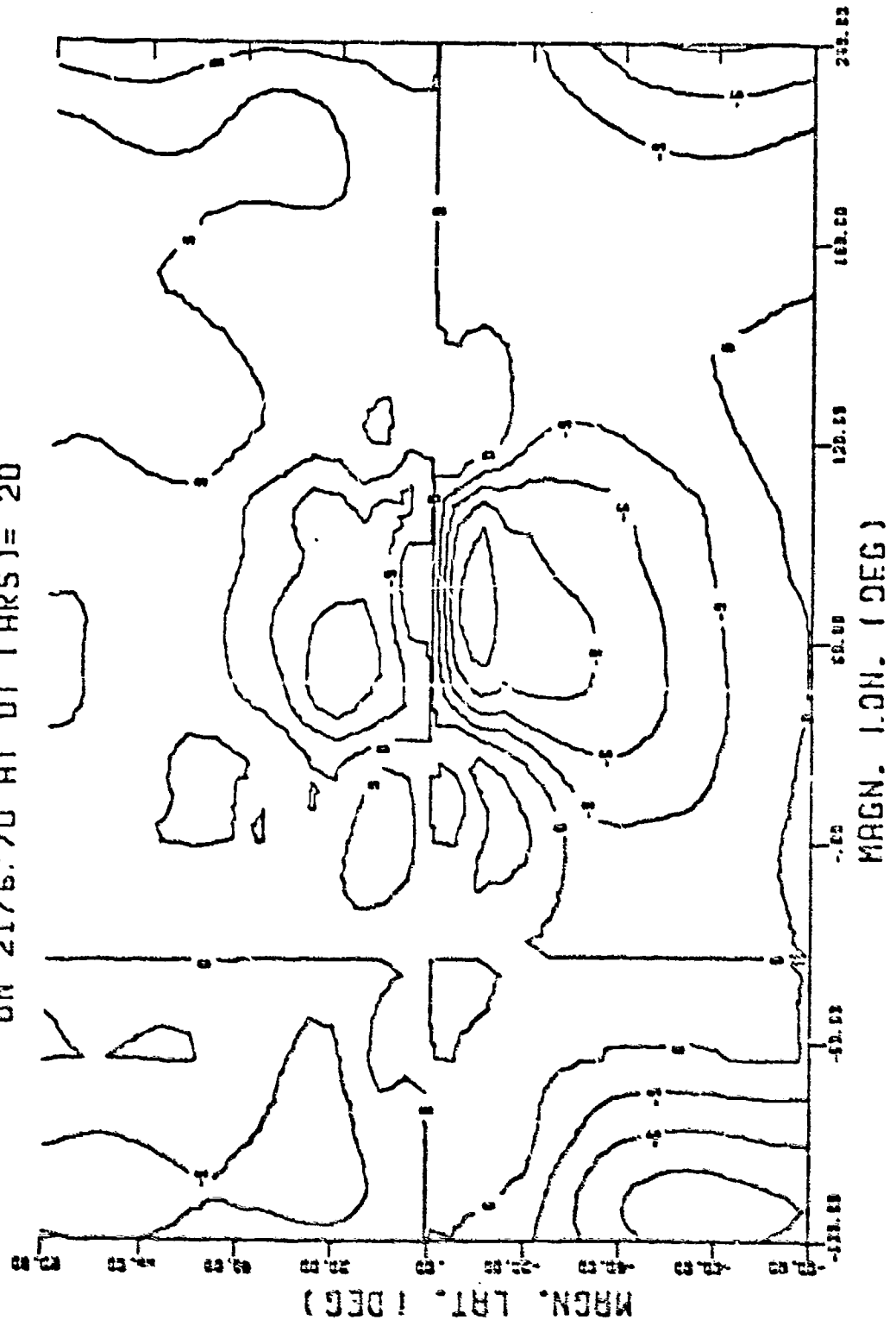


Figure 4. Sections of World Map Transmitted along Satellite Orbit

WORLD MAP OF GROUP DELAY (NSEC)  
ON 21/3/70 AT UT (HRS) = 0

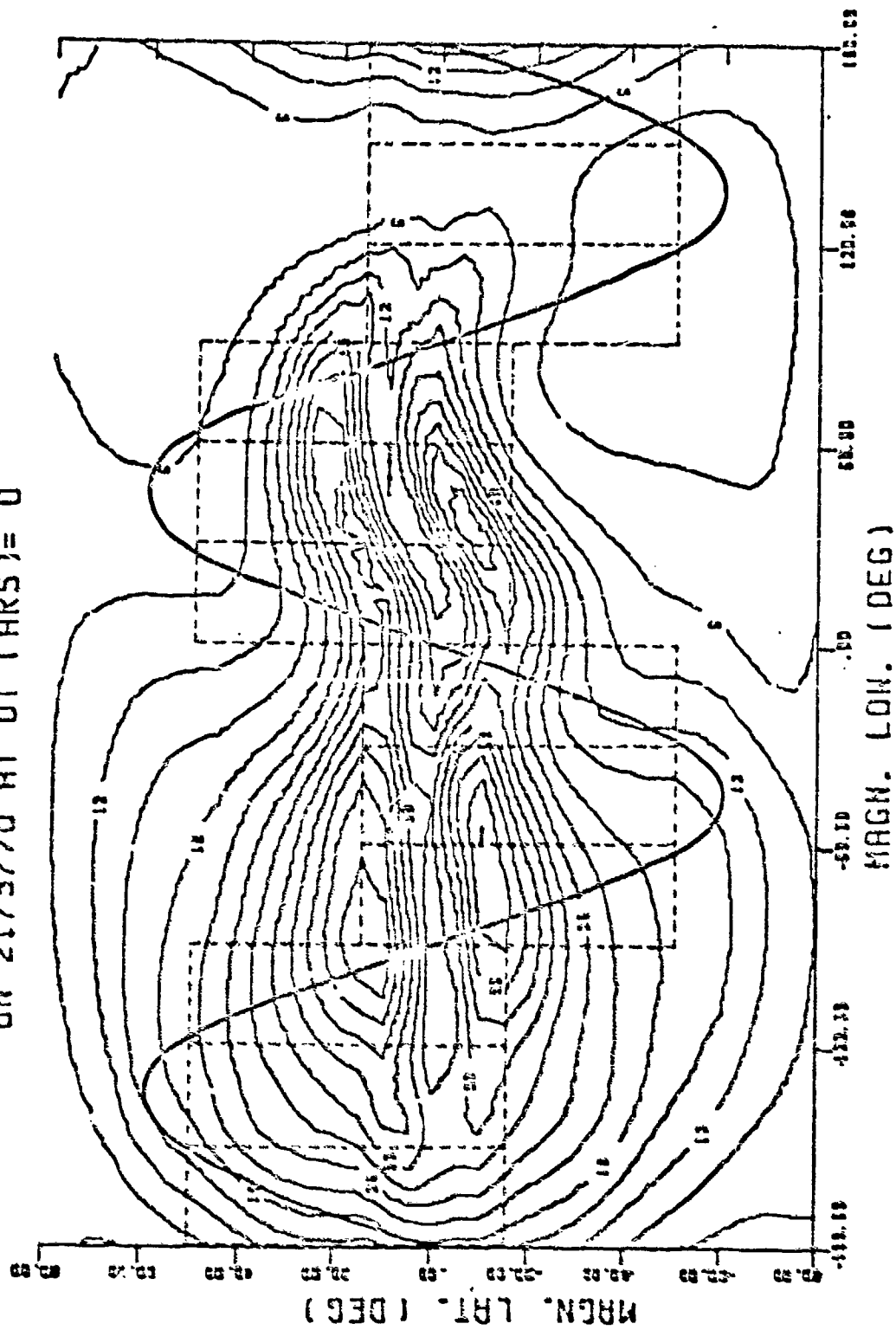


Table 1. Deviations in Group Delay Obtained by the Cross Line Technique from the Basic Predictions

Magnetic Latitude Region	Date=21 Mar 70, UT=4		Date=21 Mar 70, UT=20		Date=21 June 70, UT=20							
	Error RMS Max. Abs.	Prediction Mean Max.	Error RMS Max. Abs.	Prediction Mean Max.	Error RMS Max. Abs.	Prediction Mean Max.						
Inside $\pm 20^\circ$	4.5	15.7	13.5	47.5	0.3	44.7	13.7	44.8	3.6	14.5	8.6	29.5
Inside $\pm 40^\circ$	5.3	15.7	18.2	47.5	12.3	44.7	18.4	44.8	3.3	14.5	11.3	29.5
Outside $\pm 40^\circ$ and Inside $\pm 80^\circ$	3.5	11.3	8.6	20.1	7.8	25.9	8.6	24.2	3.3	10.6	5.7	15.3
Inside $\pm 20^\circ$	5.3	15.7	22.0	47.5	12.3	44.7	21.9	44.8	3.8	14.5	13.1	29.5
Outside $\pm 20^\circ$ and Inside $\pm 80^\circ$	4.2	14.1	10.3	34.5	9.5	34.3	10.6	40.0	3.5	10.6	6.9	26.1

TABLE 2a. COMPARISON OF GROUP DELAY OBTAINED BY CROSS LINE  
TECHNIQUE WITH MODEL PREDICTIONS ON 21/ 3/70

UT	BLOCK SIZE	LATITUDE BLOCK	LONGITUDE		PREDICTION		ERROR	
			START	STOP	MEAN	MAX	RMS	MAX
0	30	NORTH	0	25	18.34	31.14	3.56	11.17
0	30	NORTH	30	55	18.02	32.61	14.34	39.52
0	30	NORTH	60	85	14.14	28.84	2.12	5.53
0	30	NORTH	90	115	9.23	21.56	1.90	4.77
0	30	NORTH	120	145	4.77	8.61	.72	1.64
0	30	NORTH	150	175	7.47	14.11	1.41	4.35
0	30	NORTH	180	205	18.93	30.87	.92	4.25
0	30	NORTH	210	235	27.30	35.63	4.08	10.15
0	30	NORTH	240	265	30.91	44.30	2.75	7.87
0	30	NORTH	270	295	32.14	44.33	1.77	5.14
0	30	NORTH	300	325	29.29	42.06	2.80	6.42
0	30	NORTH	330	355	21.72	35.53	2.15	6.88
0	30	SOUTH	0	25	17.45	31.14	3.20	11.17
0	30	SOUTH	30	55	13.26	32.61	14.66	39.52
0	30	SOUTH	60	85	8.26	26.82	1.45	5.31
0	30	SOUTH	90	115	6.32	16.14	1.80	4.77
0	30	SOUTH	120	145	4.01	8.61	.78	1.78
0	30	SOUTH	150	175	7.01	14.11	.71	2.61
0	30	SOUTH	180	205	18.10	30.87	.89	4.25
0	30	SOUTH	210	235	25.66	35.63	3.66	10.15
0	30	SOUTH	240	265	23.49	44.30	2.53	7.87
0	30	SOUTH	270	295	29.77	44.33	1.74	5.14
0	30	SOUTH	300	325	26.70	42.06	2.89	7.20
0	30	SOUTH	330	355	20.02	35.53	2.48	6.95
0	30	OVERALL STATISTICS			18.22	44.33	4.74	39.52
0	60	NORTH	0	55	18.18	32.61	11.59	42.88
0	60	NORTH	60	115	11.69	28.84	2.55	8.20
0	60	NORTH	120	175	6.12	14.11	1.24	5.69
0	60	NORTH	180	235	23.12	35.63	4.41	14.05
0	60	NORTH	240	295	31.52	44.33	3.85	9.34
0	60	NORTH	300	355	25.30	42.06	2.77	6.42
0	60	SOUTH	0	55	15.36	32.61	13.28	42.88
0	60	SOUTH	60	115	7.29	26.82	2.21	8.20
0	60	SOUTH	120	175	5.51	14.11	1.35	5.69
0	60	SOUTH	180	235	21.88	35.63	3.86	14.05
0	60	SOUTH	240	295	29.13	44.33	3.67	9.34
0	60	SOUTH	300	355	23.36	42.06	2.68	7.20
0	60	OVERALL STATISTICS			18.22	44.33	5.81	42.88

TABLE 2b COMPARISON OF GROUP DELAY OBTAINED BY CROSS LINE  
TECHNIQUE WITH MODEL PREDICTIONS ON 21/ 3/70

UT	SIZE	BLOCK	LONGITUDE		PREDICTION		ERROR	
			START	STOP	MEAN	MAX	RMS	MAX
4	30	NORTH	0	25	14.46	27.04	2.10	8.12
4	30	NORTH	30	55	9.47	18.06	3.60	9.70
4	30	NORTH	60	85	5.10	9.74	1.00	2.18
4	30	NORTH	90	115	6.44	13.65	2.90	8.75
4	30	NORTH	120	145	16.98	28.79	1.90	5.58
4	30	NORTH	150	175	25.64	40.22	4.71	12.65
4	30	NORTH	180	205	29.94	47.50	.95	2.82
4	30	NORTH	210	235	30.72	45.19	2.97	9.32
4	30	NORTH	240	265	27.67	39.56	1.81	4.11
4	30	NORTH	270	295	21.77	37.86	2.33	8.76
4	30	NORTH	300	325	17.76	32.67	1.54	4.64
4	30	NORTH	330	355	14.31	27.28	2.45	7.64
4	30	SOUTH	0	25	13.28	27.04	2.15	8.12
4	30	SOUTH	30	55	7.24	18.06	3.64	9.70
4	30	SOUTH	60	85	3.57	9.74	.87	3.02
4	30	SOUTH	90	115	6.93	13.65	1.66	6.85
4	30	SOUTH	120	145	18.45	28.79	1.62	5.58
4	30	SOUTH	150	175	25.37	40.22	4.01	12.65
4	30	SOUTH	180	205	29.81	47.50	.79	2.50
4	30	SOUTH	210	235	29.96	45.19	3.34	9.32
4	30	SOUTH	240	265	27.08	39.56	1.51	4.06
4	30	SOUTH	270	295	21.54	37.26	2.35	8.76
4	30	SOUTH	300	325	16.75	32.67	1.78	4.64
4	30	SOUTH	330	355	13.80	27.23	2.55	7.64
4	30	OVERALL STATISTICS			18.08	47.50	2.50	12.65
4	60	NORTH	0	55	11.96	27.04	6.73	21.54
4	60	NORTH	60	115	5.77	13.65	1.56	6.63
4	60	NORTH	120	175	21.31	40.22	6.82	19.42
4	60	NORTH	180	235	30.33	47.50	2.53	10.16
4	60	NORTH	240	295	24.72	39.56	2.63	9.58
4	60	NORTH	300	355	16.03	32.67	2.32	7.27
4	60	SOUTH	0	55	10.26	27.04	7.31	21.54
4	60	SOUTH	60	115	5.25	13.65	2.49	7.02
4	60	SOUTH	120	175	21.91	40.22	5.56	19.42
4	60	SOUTH	180	235	29.88	47.50	2.59	10.16
4	60	SOUTH	240	295	24.31	39.56	3.33	9.58
4	60	SOUTH	300	355	15.27	32.67	2.43	7.27
4	60	OVERALL STATISTICS			18.08	47.50	4.30	21.54

TABLE 2. COMPARISON OF GROUP DELAY OBTAINED BY CROSS LINE  
TECHNIQUE WITH MODEL PREDICTIONS ON 21/ 3/70

LT	SIZE	BLOCK	LONGITUDE		PREDICTION		ERROR	
			START	STOP	MEAN	MAX	RMS	MAX
8	30	NORTH	0	25	4.56	7.32	.74	1.63
8	30	NORTH	30	55	7.72	15.10	2.84	9.48
8	30	NORTH	60	85	17.84	26.60	.59	1.75
8	30	NORTH	90	115	24.55	34.82	3.34	12.04
8	30	NORTH	120	145	30.73	46.86	5.15	16.84
8	30	NORTH	150	175	31.08	48.28	3.64	13.34
8	30	NORTH	180	205	28.39	49.75	4.37	8.97
8	30	NORTH	210	235	20.67	36.57	1.78	6.43
8	30	NORTH	240	265	16.81	29.73	1.51	5.57
8	30	NORTH	270	295	15.97	31.08	1.22	4.91
8	30	NORTH	300	325	12.82	26.23	2.28	6.30
8	30	NORTH	330	355	7.61	16.07	1.17	2.75
8	30	SOUTH	0	25	4.76	7.32	.91	2.53
8	30	SOUTH	30	55	7.91	15.10	3.07	8.39
8	30	SOUTH	60	85	17.91	26.60	.54	1.51
8	30	SOUTH	90	115	23.29	33.75	2.67	12.04
8	30	SOUTH	120	145	28.80	46.86	5.80	16.84
8	30	SOUTH	150	175	30.24	48.28	3.08	13.34
8	30	SOUTH	180	205	28.51	49.75	4.43	9.85
8	30	SOUTH	210	235	20.59	36.57	1.58	6.43
8	30	SOUTH	240	265	17.54	29.73	1.54	5.57
8	30	SOUTH	270	295	15.56	31.08	1.69	4.91
8	30	SOUTH	300	325	11.79	26.23	2.14	6.30
8	30	SOUTH	330	355	7.42	16.07	1.46	3.60
8	30	OVERALL STATISTICS			18.05	49.75	2.79	16.84
8	60	NORTH	0	55	6.14	15.10	2.46	11.87
8	60	NORTH	60	115	21.20	34.82	2.50	10.26
8	60	NORTH	120	175	30.91	48.28	6.50	17.95
8	60	NORTH	180	235	24.53	49.75	3.93	8.97
8	60	NORTH	240	295	16.39	31.08	2.53	7.80
8	60	NORTH	300	355	10.22	26.23	2.39	6.30
8	60	SOUTH	0	55	6.34	15.10	2.89	11.87
8	60	SOUTH	60	115	20.60	33.75	1.79	10.26
8	60	SOUTH	120	175	29.52	48.28	7.22	17.95
8	60	SOUTH	180	235	24.55	49.75	3.99	9.85
8	60	SOUTH	240	295	16.55	31.08	2.70	7.80
8	60	SOUTH	300	355	9.60	26.23	2.22	6.30
8	60	OVERALL STATISTICS			18.05	49.75	3.83	17.95

TABLE 2d. COMPARISON OF GROUP DELAY OBTAINED BY CROSS LINE  
TECHNIQUE WITH MODEL PREDICTIONS ON 21/ 3/70

LT	BLOCK SIZE	BLOCK	LONGITUDE		PREDICTION		ERROR	
			START	STEP	MEAN	MAX	RMS	MAX
12	30	NORTH	0	25	19.61	30.94	1.06	4.57
12	30	NORTH	30	55	23.68	38.21	3.13	13.50
12	30	NORTH	60	85	32.03	42.94	1.76	4.44
12	30	NORTH	90	115	31.64	44.72	6.33	19.67
12	30	NORTH	120	145	23.46	40.89	2.50	7.64
12	30	NORTH	150	175	22.72	40.08	1.93	6.98
12	30	NORTH	180	205	17.35	36.85	1.78	3.65
12	30	NORTH	210	235	14.82	31.37	1.51	5.25
12	30	NORTH	240	265	12.16	27.71	1.24	3.50
12	30	NORTH	270	295	7.94	16.13	.75	1.73
12	30	NORTH	300	325	4.96	9.62	.83	2.28
12	30	NORTH	330	355	7.41	13.90	1.58	6.09
12	30	SOUTH	0	25	18.32	30.94	.89	4.57
12	30	SOUTH	30	55	25.94	38.12	3.18	13.50
12	30	SOUTH	60	85	27.25	42.05	2.10	4.77
12	30	SOUTH	90	115	26.97	44.72	6.03	19.67
12	30	SOUTH	120	145	25.87	40.89	2.29	7.64
12	30	SOUTH	150	175	21.03	40.08	2.03	6.98
12	30	SOUTH	180	205	18.01	36.85	.72	2.35
12	30	SOUTH	210	235	15.50	31.37	1.72	5.25
12	30	SOUTH	240	265	13.08	27.71	1.10	3.50
12	30	SOUTH	270	295	8.09	16.13	.50	1.73
12	30	SOUTH	300	325	4.54	9.62	.48	1.41
12	30	SOUTH	330	355	6.69	13.90	.91	3.48
12	30	OVERALL STATISTICS			18.29	44.72	2.43	19.67
12	60	NORTH	0	55	24.14	38.21	2.91	14.15
12	60	NORTH	60	115	31.83	44.72	4.33	19.11
12	60	NORTH	120	175	25.59	40.89	3.90	13.77
12	60	NORTH	180	235	16.08	36.85	2.41	5.35
12	60	NORTH	240	295	10.05	27.71	1.48	3.50
12	60	NORTH	300	355	6.18	13.90	1.57	5.83
12	60	SOUTH	0	55	22.13	38.12	2.55	14.15
12	60	SOUTH	60	115	27.11	44.72	4.14	19.11
12	60	SOUTH	120	175	23.45	40.89	3.93	13.77
12	60	SOUTH	180	235	16.76	36.85	1.53	5.40
12	60	SOUTH	240	295	10.58	27.71	1.20	3.50
12	60	SOUTH	300	355	5.61	13.90	1.39	5.83
12	60	OVERALL STATISTICS			17.29	44.72	2.86	19.11

TABLE 2c, COMPARISON OF GROUP DELAY OBTAINED BY CROSS LINE  
TECHNIQUE WITH MODEL PREDICTIONS ON 21/ 3/70

UT	BLOCK SIZE	LATITUDE BLOCK	LONGITUDE		PREDICTION		ERROR	
			START	STOP	MEAN	MAX	RMS	MAX
16	30	NORTH	0	25	32.35	42.52	3.32	7.72
16	30	NORTH	30	55	34.02	46.76	10.50	26.88
16	30	NORTH	60	85	30.59	44.28	1.30	4.40
16	30	NORTH	90	115	23.17	36.43	4.24	14.28
16	30	NORTH	120	145	16.99	29.39	2.74	7.80
16	30	NORTH	150	175	14.91	29.24	1.90	7.09
16	30	NORTH	180	205	12.49	27.19	1.36	4.38
16	30	NORTH	210	235	8.07	16.14	.76	1.85
16	30	NORTH	240	265	4.97	9.43	1.06	2.94
16	30	NORTH	270	295	8.77	16.99	2.17	7.31
16	30	NORTH	300	325	19.99	30.97	1.03	2.62
16	30	NORTH	330	355	26.81	36.08	1.76	5.02
16	30	SOUTH	0	25	29.52	42.28	2.41	6.82
16	30	SOUTH	30	55	28.37	46.76	10.70	26.88
16	30	SOUTH	60	85	24.29	44.28	.98	2.08
16	30	SOUTH	90	115	19.01	36.43	4.13	14.28
16	30	SOUTH	120	145	15.71	29.39	2.58	7.80
16	30	SOUTH	150	175	14.40	29.24	1.69	7.09
16	30	SOUTH	180	205	12.90	27.19	1.47	4.38
16	30	SOUTH	210	235	8.70	16.14	1.01	2.08
16	30	SOUTH	240	265	5.27	9.43	.48	1.04
16	30	SOUTH	270	295	7.10	16.99	2.26	5.55
16	30	SOUTH	300	325	17.02	30.97	1.02	3.11
16	30	SOUTH	330	355	25.03	36.08	2.57	5.76
16	30	OVERALL STATISTICS			18.35	46.76	3.70	26.88
16	60	NORTH	0	55	33.19	46.76	8.37	31.47
16	60	NORTH	60	115	26.88	44.28	3.79	16.21
16	60	NORTH	120	175	15.93	29.39	3.94	10.46
16	60	NORTH	180	235	10.29	27.19	1.46	4.38
16	60	NORTH	240	295	6.37	16.99	2.20	6.78
16	60	NORTH	300	355	23.40	36.08	1.49	5.28
16	60	SOUTH	0	55	28.94	46.76	9.64	31.47
16	60	SOUTH	60	115	21.65	44.28	3.26	16.21
16	60	SOUTH	120	175	15.06	29.39	3.42	10.46
16	60	SOUTH	180	235	10.80	27.19	1.89	4.38
16	60	SOUTH	240	295	6.19	16.99	1.33	6.78
16	60	SOUTH	300	355	21.03	36.08	3.65	10.64
16	60	OVERALL STATISTICS			18.35	46.76	4.51	31.47



TABLE 2f. COMPARISON OF GROUP DELAY OBTAINED BY CROSS LINE  
TECHNIQUE WITH MODEL PREDICTIONS ON 21/ 3/70

UT	BLOCK SIZE	LATITUDE BLOCK	LONGITUDE		PREDICTION		ERROR	
			START	STOP	MEAN	MAX	RMS	MAX
20	30	NORTH	0	25	28.68	40.63	2.49	9.37
20	30	NORTH	30	55	24.04	40.17	7.32	19.84
20	30	NORTH	60	85	18.86	34.65	2.81	6.44
20	30	NORTH	90	115	17.49	33.96	6.22	19.14
20	30	NORTH	120	145	11.97	24.97	2.66	9.30
20	30	NORTH	150	175	7.75	16.66	.80	2.08
20	30	NORTH	180	205	4.84	8.53	1.12	3.00
20	30	NORTH	210	235	8.44	15.46	2.73	3.52
20	30	NORTH	240	265	19.63	28.53	.99	3.40
20	30	NORTH	270	295	27.39	39.98	4.81	13.56
20	30	NORTH	300	325	32.35	44.24	2.36	5.14
20	30	NORTH	330	355	31.72	44.84	3.73	10.94
20	30	SOUTH	0	25	27.52	40.63	3.09	9.37
20	30	SOUTH	30	55	19.43	40.17	8.20	19.84
20	30	SOUTH	60	85	13.25	34.65	2.31	4.59
20	30	SOUTH	90	115	13.40	33.96	6.10	19.14
20	30	SOUTH	120	145	11.27	24.97	2.11	9.30
20	30	SOUTH	150	175	7.55	16.66	.83	2.08
20	30	SOUTH	180	205	4.50	8.53	.67	1.59
20	30	SOUTH	210	235	7.03	15.46	1.98	5.89
20	30	SOUTH	240	265	18.04	28.53	1.23	4.24
20	30	SOUTH	270	295	24.81	39.98	3.73	13.32
20	30	SOUTH	300	325	27.82	42.52	1.82	4.58
20	30	SOUTH	330	355	28.65	44.84	2.18	6.92
20	30	OVERALL STATISTICS			18.18	44.84	3.64	19.84
20	60	NORTH	0	55	26.36	40.63	9.23	31.80
20	60	NORTH	60	115	18.18	34.65	5.11	19.41
20	60	NORTH	120	175	9.86	24.97	3.07	9.73
20	60	NORTH	180	235	6.64	15.46	2.01	6.08
20	60	NORTH	240	295	23.51	39.98	5.05	17.11
20	60	NORTH	300	355	32.05	44.84	2.71	7.68
20	60	SOUTH	0	55	23.47	40.63	11.62	31.80
20	60	SOUTH	60	115	13.33	34.65	4.42	19.41
20	60	SOUTH	120	175	9.41	24.97	2.63	9.73
20	60	SOUTH	180	235	5.75	15.46	1.19	6.08
20	60	SOUTH	240	295	21.43	39.98	4.95	17.11
20	60	SOUTH	300	355	28.23	44.84	2.01	4.95
20	60	OVERALL STATISTICS			18.18	44.84	5.40	31.80

TABLE 3a. COMPARISON OF GROUP DELAY OBTAINED BY CROSS LINE  
TECHNIQUE WITH MODEL PREDICTIONS ON 21/ 6/70

UT	SIZE	BLOCK	LONGITUDE		PREDICTION		ERROR	
			START	STOP	MEAN	MAX	RMS	MAX
0	30	NORTH	0	25	11.97	14.23	1.11	3.60
0	30	NORTH	30	55	9.31	14.09	4.07	9.06
0	30	NORTH	60	85	7.97	12.65	1.25	3.61
0	30	NORTH	90	115	6.52	10.14	1.62	4.03
0	30	NORTH	120	145	5.32	8.32	.86	1.95
0	30	NORTH	150	175	7.60	12.49	6.85	17.29
0	30	NORTH	180	205	12.44	21.58	1.65	3.74
0	30	NORTH	210	235	15.56	26.09	1.57	5.31
0	30	NORTH	240	265	20.26	29.27	2.46	7.50
0	30	NORTH	270	295	19.87	28.77	1.41	5.95
0	30	NORTH	300	325	19.64	32.76	1.85	4.74
0	30	NORTH	330	355	14.39	25.96	2.91	5.81
0	30	SOUTH	0	25	6.90	13.70	.96	3.60
0	30	SOUTH	30	55	4.63	14.09	3.08	9.06
0	30	SOUTH	60	85	3.85	12.65	.69	2.27
0	30	SOUTH	90	115	2.81	8.45	1.01	3.59
0	30	SOUTH	120	145	2.22	7.00	.37	1.17
0	30	SOUTH	150	175	4.87	12.49	2.37	11.50
0	30	SOUTH	180	205	11.94	21.58	1.58	3.74
0	30	SOUTH	210	235	15.57	26.09	1.38	5.30
0	30	SOUTH	240	265	17.25	29.27	1.25	7.50
0	30	SOUTH	270	295	16.70	28.77	1.34	5.95
0	30	SOUTH	300	325	16.25	32.76	1.86	4.70
0	30	SOUTH	330	355	10.17	25.56	1.69	5.50
0	30	OVERALL STATISTICS			11.02	32.76	2.31	17.29
0	60	NORTH	0	55	10.64	14.23	5.17	12.96
0	60	NORTH	60	115	7.24	12.65	2.21	5.74
0	60	NORTH	120	175	6.46	12.49	4.36	16.28
0	60	NORTH	180	235	14.00	26.09	2.10	4.05
0	60	NORTH	240	295	20.06	29.27	3.00	8.25
0	60	NORTH	300	355	17.01	32.76	2.31	5.88
0	60	SOUTH	0	55	5.76	14.09	4.53	12.96
0	60	SOUTH	60	115	3.33	12.65	1.06	4.36
0	60	SOUTH	120	175	3.55	12.49	2.01	12.29
0	60	SOUTH	180	235	13.75	26.09	1.96	4.05
0	60	SOUTH	240	295	17.26	29.27	1.97	7.71
0	60	SOUTH	300	355	13.21	32.76	2.03	4.70
0	60	OVERALL STATISTICS			11.02	32.76	2.99	16.28

TABLE 3b. COMPARISON OF GROUP DELAY OBTAINED BY CROSS LINE  
TECHNIQUE WITH MODEL PREDICTIONS ON 21/ 6/70

UT	SIZE	BLOCK	LONGITUDE		PREDICTION		ERROR	
			START	STOP	MEAN	MAX	RMS	MAX
4	30	NORTH	0	25	8.34	11.43	1.41	3.86
4	30	NORTH	30	55	6.06	11.12	1.06	2.14
4	30	NORTH	60	85	4.30	8.43	1.04	2.34
4	30	NORTH	90	115	7.25	12.40	6.47	18.74
4	30	NORTH	120	145	14.17	22.29	1.47	5.09
4	30	NORTH	150	175	17.00	25.33	1.15	3.35
4	30	NORTH	180	205	17.07	25.15	1.21	7.16
4	30	NORTH	210	235	17.95	30.50	1.27	4.46
4	30	NORTH	240	265	18.88	30.87	1.10	3.03
4	30	NORTH	270	295	15.82	23.20	1.49	5.15
4	30	NORTH	300	325	11.87	19.91	.84	2.87
4	30	NORTH	330	355	9.63	16.09	1.65	3.66
4	30	SOUTH	0	25	4.43	9.95	.36	1.27
4	30	SOUTH	30	55	2.63	6.52	.79	1.92
4	30	SOUTH	60	85	1.55	3.84	.32	1.14
4	30	SOUTH	90	115	4.29	12.40	1.69	5.81
4	30	SOUTH	120	145	11.93	22.29	1.22	5.09
4	30	SOUTH	150	175	16.74	25.33	1.08	2.82
4	30	SOUTH	180	205	17.85	25.15	1.19	3.16
4	30	SOUTH	210	235	17.43	30.50	1.36	4.46
4	30	SOUTH	240	265	16.37	30.87	.80	2.30
4	30	SOUTH	270	295	12.06	22.98	1.58	5.15
4	30	SOUTH	300	325	8.35	19.91	.98	2.87
4	30	SOUTH	330	355	5.97	16.09	.89	3.32
4	30	OVERALL STATISTICS			11.15	30.87	1.78	18.74
4	60	NORTH	0	55	7.20	11.43	1.96	4.05
4	60	NORTH	60	115	5.77	12.40	4.09	17.51
4	60	NORTH	120	175	15.59	25.33	2.58	7.17
4	60	NORTH	180	235	17.51	30.50	2.40	9.40
4	60	NORTH	240	295	17.35	30.87	1.86	6.53
4	60	NORTH	300	355	10.75	19.91	1.40	3.96
4	60	SOUTH	0	55	3.53	9.95	1.08	3.18
4	60	SOUTH	60	115	2.92	12.40	.95	5.29
4	60	SOUTH	120	175	14.19	25.33	3.33	7.23
4	60	SOUTH	180	235	17.64	30.50	2.36	9.40
4	60	SOUTH	240	295	14.21	30.87	2.23	6.53
4	60	SOUTH	300	355	7.16	19.91	1.11	3.00
4	60	OVERALL STATISTICS			11.15	30.87	2.30	17.51

TABLE 3c. COMPARISON OF GROUP DELAY OBTAINED BY CROSS LINE  
TECHNIQUE WITH MODEL PREDICTIONS ON 21/ 6/70

UT	SIZE	BLOCK	LONGITUDE		PREDICTION		ERROR	
			START	STOP	MEAN	MAX	RMS	MAX
8	30	NORTH	0	25	4.57	7.76	1.48	3.75
8	30	NORTH	30	55	6.93	10.83	5.37	17.33
8	30	NORTH	60	85	13.45	26.64	3.39	8.59
8	30	NORTH	90	115	17.91	28.54	2.21	7.88
8	30	NORTH	120	145	20.14	31.18	3.92	12.81
8	30	NORTH	150	175	19.78	33.17	2.13	6.60
8	30	NORTH	180	205	17.18	32.46	1.73	6.32
8	30	NORTH	210	235	14.44	21.25	.67	2.28
8	30	NORTH	240	265	11.70	16.56	1.27	3.45
8	30	NORTH	270	295	9.99	15.35	.42	1.57
8	30	NORTH	300	325	7.42	12.06	.65	2.71
8	30	NORTH	330	355	5.28	7.43	.80	1.94
8	30	SOUTH	0	25	2.31	5.39	.36	.85
8	30	SOUTH	30	55	4.14	10.83	1.30	5.59
8	30	SOUTH	60	85	11.37	26.64	.82	3.11
8	30	SOUTH	90	115	15.72	28.54	2.08	7.88
8	30	SOUTH	120	145	17.62	31.18	3.67	12.81
8	30	SOUTH	150	175	18.89	33.17	1.16	4.61
8	30	SOUTH	180	205	17.24	32.46	2.02	6.32
8	30	SOUTH	210	235	12.27	21.25	1.42	3.45
8	30	SOUTH	240	265	8.56	16.56	.79	3.45
8	30	SOUTH	270	295	6.70	15.35	.40	1.57
8	30	SOUTH	300	325	4.82	12.06	.64	2.71
8	30	SOUTH	330	355	3.30	7.43	.44	1.42
8	30	OVERALL STATISTICS			11.34	33.17	2.07	17.33
8	60	NORTH	0	55	5.75	10.83	2.02	7.30
8	60	NORTH	60	115	15.88	28.54	5.10	10.56
8	60	NORTH	120	175	19.96	33.17	5.30	15.11
8	60	NORTH	180	235	15.81	32.46	2.37	8.59
8	60	NORTH	240	295	10.85	16.56	1.78	4.68
8	60	NORTH	300	355	6.35	12.06	.92	2.71
8	60	SOUTH	0	55	3.22	10.83	.90	6.34
8	60	SOUTH	60	115	13.54	28.54	2.14	8.48
8	60	SOUTH	120	175	18.26	33.17	5.28	15.11
8	60	SOUTH	180	235	14.75	32.46	3.45	8.59
8	60	SOUTH	240	295	7.63	16.56	1.26	4.68
8	60	SOUTH	300	355	4.06	12.06	.80	2.71
8	60	OVERALL STATISTICS			11.34	33.17	3.10	15.11

TABLE 3d. COMPARISON OF GROUP DELAY OBTAINED BY CROSS LINE  
TECHNIQUE WITH MODEL PREDICTIONS ON 21/ 6/70

UT	BLOCK SIZE	LATITUDE BLOCK	LONGITUDE		PREDICTION		ERROR	
			START	STOP	MEAN	MAX	RMS	MAX
12	30	NORTH	0	25	12.00	24.51	4.23	11.69
12	30	NORTH	30	55	18.39	30.93	2.15	6.05
12	30	NORTH	60	85	20.38	29.76	1.39	6.01
12	30	NORTH	90	115	21.33	33.81	4.23	18.67
12	30	NORTH	120	145	19.77	34.94	2.20	6.15
12	30	NORTH	150	175	15.58	28.59	1.57	6.07
12	30	NORTH	180	205	11.95	18.16	1.11	2.30
12	30	NORTH	210	235	9.54	13.57	.41	1.89
12	30	NORTH	240	265	8.19	10.37	.56	1.94
12	30	NORTH	270	295	6.10	8.84	.78	2.19
12	30	NORTH	300	325	4.30	6.49	.60	1.73
12	30	NORTH	330	355	5.55	8.97	1.25	3.74
12	30	SOUTH	0	25	8.96	24.51	1.78	7.18
12	30	SOUTH	30	55	15.19	30.93	2.12	6.05
12	30	SOUTH	60	85	16.80	29.76	.61	2.27
12	30	SOUTH	90	115	15.95	33.81	3.76	18.67
12	30	SOUTH	120	145	15.93	34.94	1.88	6.15
12	30	SOUTH	150	175	12.61	28.59	1.48	6.07
12	30	SOUTH	180	205	9.23	18.16	.64	1.99
12	30	SOUTH	210	235	6.69	13.57	.52	1.89
12	30	SOUTH	240	265	5.43	10.37	.54	1.94
12	30	SOUTH	270	295	4.06	8.84	.35	.75
12	30	SOUTH	300	325	2.27	4.96	.28	.79
12	30	SOUTH	330	355	2.90	8.43	.54	2.47
12	30	OVERALL STATISTICS			11.22	34.94	1.86	18.67
12	60	NORTH	0	55	15.20	30.93	10.41	21.36
12	60	NORTH	60	115	20.85	33.81	4.35	21.14
12	60	NORTH	120	175	17.68	34.94	2.75	8.90
12	60	NORTH	180	235	10.75	18.16	1.30	2.31
12	60	NORTH	240	295	7.15	10.37	.90	2.54
12	60	NORTH	300	355	4.93	8.97	.89	2.28
12	60	SOUTH	0	55	12.08	30.93	6.70	17.01
12	60	SOUTH	60	115	16.38	33.81	3.13	21.14
12	60	SOUTH	120	175	14.27	34.94	2.20	8.90
12	60	SOUTH	180	235	7.96	18.16	.78	2.07
12	60	SOUTH	240	295	4.77	10.37	.71	1.94
12	60	SOUTH	300	355	2.55	8.43	.62	1.94
12	60	OVERALL STATISTICS			11.22	34.94	3.55	21.36

TABLE 3a. COMPARISON OF GROUP DELAY OBTAINED BY CROSS LINE  
TECHNIQUE WITH MODEL PREDICTIONS ON 21/ 6/70

UT	SIZE	BLOCK	LONGITUDE		PREDICTION		ERROR	
			START	STOP	MEAN	MAX	RMS	MAX
16	30	NORTH	0	25	20.24	30.24	1.58	5.68
16	30	NORTH	30	55	22.54	32.17	4.42	9.86
16	30	NORTH	60	85	21.61	32.91	1.61	7.66
16	30	NORTH	90	115	17.56	30.95	2.49	8.16
16	30	NORTH	120	145	11.47	18.30	1.24	3.52
16	30	NORTH	150	175	9.81	14.75	.85	2.40
16	30	NORTH	180	205	8.58	11.03	.73	1.76
16	30	NORTH	210	235	6.26	9.04	.51	1.62
16	30	NORTH	240	265	5.00	7.63	.86	2.03
16	30	NORTH	270	295	7.51	11.69	3.74	12.06
16	30	NORTH	300	325	13.46	27.42	3.28	6.72
16	30	NORTH	330	355	16.99	30.81	2.87	6.67
16	30	SOUTH	0	25	15.32	30.24	1.61	5.68
16	30	SOUTH	30	55	16.14	32.17	3.53	9.86
16	30	SOUTH	60	85	14.46	31.38	2.05	5.28
16	30	SOUTH	90	115	10.29	27.71	2.40	8.16
16	30	SOUTH	120	145	7.40	18.30	1.04	3.52
16	30	SOUTH	150	175	6.51	14.75	.59	2.29
16	30	SOUTH	180	205	5.67	11.03	.57	1.76
16	30	SOUTH	210	235	4.06	9.04	.29	.76
16	30	SOUTH	240	265	2.55	5.63	.43	1.42
16	30	SOUTH	270	295	3.97	11.22	1.10	4.25
16	30	SOUTH	300	325	10.60	27.42	1.80	5.14
16	30	SOUTH	330	355	14.42	30.81	2.22	6.17
16	30	OVERALL STATISTICS			11.35	32.91	2.08	12.06
16	60	NORTH	0	55	21.39	32.17	5.15	16.75
16	60	NORTH	60	115	19.58	32.91	3.03	12.14
16	60	NORTH	120	175	10.64	18.30	1.35	3.74
16	60	NORTH	180	235	7.42	11.03	1.09	2.82
16	60	NORTH	240	295	6.25	11.69	1.73	8.01
16	60	NORTH	300	355	15.23	30.81	4.05	9.87
16	60	SOUTH	0	55	15.73	32.17	5.51	16.75
16	60	SOUTH	60	115	12.38	31.38	3.53	12.14
16	60	SOUTH	120	175	6.75	18.30	1.17	3.76
16	60	SOUTH	180	235	4.86	11.03	.75	1.78
16	60	SOUTH	240	295	3.26	11.22	1.08	4.89
16	60	SOUTH	300	355	12.51	30.81	3.09	9.87
16	60	OVERALL STATISTICS			11.35	32.91	3.03	16.75

TABLE 31. COMPARISON OF GROUP DELAY OBTAINED BY CROSS LINE  
TECHNIQUE WITH MODEL PREDICTIONS ON 21/ 6/70

LT	SIZE	BLOCK	LATITUDE	LONGITUDE		PREDICTION		ERROR	
				START	STOP	MEAN	MAX	RMS	MAX
20	30	NORTH		0	25	19.42	27.94	1.34	4.70
20	30	NORTH		30	55	16.70	28.98	4.43	13.13
20	30	NORTH		60	85	13.14	21.85	1.12	2.99
20	30	NORTH		90	115	10.76	17.32	2.30	8.16
20	30	NORTH		120	145	8.02	13.18	.79	1.44
20	30	NORTH		150	175	6.23	7.42	.60	2.29
20	30	NORTH		180	205	5.52	8.14	.88	2.13
20	30	NORTH		210	235	7.83	11.37	3.18	8.59
20	30	NORTH		240	265	14.05	23.66	2.11	4.31
20	30	NORTH		270	295	17.59	28.04	.95	3.14
20	30	NORTH		300	325	20.19	29.53	1.04	4.00
20	30	NORTH		330	355	19.91	29.53	1.83	5.32
20	30	SOUTH		0	25	13.81	27.94	1.96	5.44
20	30	SOUTH		30	55	9.79	28.98	4.26	13.13
20	30	SOUTH		60	85	6.73	21.85	.90	2.44
20	30	SOUTH		90	115	5.41	17.32	2.15	8.16
20	30	SOUTH		120	145	4.46	13.18	.57	1.31
20	30	SOUTH		150	175	3.76	7.42	.61	2.29
20	30	SOUTH		180	205	2.74	7.01	.24	.71
20	30	SOUTH		210	235	4.57	10.77	1.42	5.45
20	30	SOUTH		240	265	11.29	23.66	1.29	4.31
20	30	SOUTH		270	295	15.02	28.04	1.07	3.14
20	30	SOUTH		300	325	16.72	29.53	.46	1.16
20	30	SOUTH		330	355	15.38	29.53	1.72	5.32
20	30	OVERALL STATISTICS				11.21	29.53	1.89	13.13
20	60	NORTH		0	55	18.06	28.98	5.48	16.32
20	60	NORTH		60	115	11.98	21.85	1.91	6.94
20	60	NORTH		120	175	7.12	13.18	.92	3.11
20	60	NORTH		180	235	6.68	11.37	1.55	8.46
20	60	NORTH		240	295	15.82	23.04	2.60	8.87
20	60	NORTH		300	355	20.05	29.53	2.15	5.52
20	60	SOUTH		0	55	11.80	28.98	6.23	16.32
20	60	SOUTH		60	115	6.07	21.85	1.67	6.94
20	60	SOUTH		120	175	.11	13.18	.97	3.11
20	60	SOUTH		180	235	3.66	10.77	1.11	5.45
20	60	SOUTH		240	295	13.16	28.04	1.83	4.64
20	60	SOUTH		300	355	16.05	29.53	1.59	5.17
20	60	OVERALL STATISTICS				11.21	29.53	2.85	16.32

## APPENDIX H

### Contour Maps of Group Delay and Height and Error Contours due to Rotation of the Maps for Continuous Time Adjustment

Contours of group delay and height at the maximum electron density are plotted on a world wide magnetic latitude and longitude grid. To allow the similarities of the patterns for maps at different universal times to be easily examined, the magnetic longitude scale is shifted eastward at a rate of 15 degrees per hour out of the 12 hour plot for which the magnetic longitude scale runs from 0 to 360 degrees. In this manner the effects of sunrise and the equatorial anomaly appear in the same portion relative to the edges of the graphs independent of the universal time.

Figures 1a-f. show the world maps of vertical group delay on 21 March 1970 for 0, 4, 8, 12, 16, and 20 hours of universal time; for the same times Figures 2a-f. give the group delay contours on 21 June 1970 and Figures 4a-f. give the contours for the height of the maximum electron density on 21 March 1970. The graphs for the various hours on a fixed date look quite similar except for a distortion of the pattern right around the equator that continuously shifts eastward with increasing time. This distortion is caused by the fact that the simple dipole magnetic latitude and longitude define the axes which give only an approximation to the true magnetic equator. Use of the magnetic dip as an axis around the equator would reduce the irregularities in the patterns for different times.

Since the maps for different times on a fixed date are quite similar, the storage requirement can be significantly reduced if only one map at a fixed time is used and this map is rotated continuously over 24 hours at a rate of 15 degrees in magnetic longitude per hour to account for the diurnal time variation. To estimate the expected accuracy loss due to such a time adjustment, Figure 3 was drawn. The given contour map of the differences in group delay between the 4 hour map and the 8 hour map rotated by 60 degrees to adjust for the time shift shows the distribution of the errors in space. Tables 1, 2, and 3 present a summary of errors



in group delay and height due to time adjustments by rotating the various world maps over 4, 8, and a maximum offset of 12 hours. RMS errors and maximum absolute errors are listed for selected magnetic latitude regions and corresponding mean and maximum values of the Bent Model predictions are given for comparison. The statistics are based on 2376 data values in each map at 5 degree magnetic latitude and longitude increments.

The discrepancies between the values recomputed for the proper time and the numbers obtained from a fixed time map by coordinate rotation for time correction, increase only slightly from a 4 hour to an 8 hour and 12 hour time adjustment. For March 1970 the RMS error in group delay is 26.9% of the mean prediction for the 4 hour rotation, 32.2% for the 8 hour and 32.4% for the 12 hour adjustment. Overall an RMS error of 30.1% exists with a maximum possible error of 46.5% of the maximum prediction. The results for June 1970 look quite similar; the RMS errors in group delay are 27.3%, 34.5%, and 37.0% of the mean prediction for adjustments in time over 4, 8, and 12 hours respectively. The overall RMS error is 32.1% and the maximum error is 52.5%. For ionospheric height data on March 1970 the RMS errors are 5.3%, 6.6%, and 6.9% of the mean prediction for time adjustments over 4, 8, and 12 hours. The overall RMS error for the height data is 6.1% with a maximum possible error of 22.6% of the maximum prediction.

The use of the dipole magnetic latitude instead of the magnetic dip as coordinate causes some distortion around the equator in the pattern of these maps, which in turn results in larger errors in the rotation method for time adjustment. It therefore can be expected that the RMS errors of roughly 30% for group delay and 6% for the height data can be still reduced, if the coordinates were modified or the distortion was corrected for in some other way.

To reduce the time errors even further another approach was considered that allows different sections of the world map to be precomputed for different universal times. This method is described toward the end of Appendix G on the cross-line technique. The moving satellite would transmit each section of the world map at the predetermined median time for 2 hours allowing time discrepancies of only  $\pm 1$  hour. Coordinate rotation for the time correction is then reduced to adjust for only  $\pm 1$  hour.

The tests performed to check out the accuracy of this method are summarized in Table 4. The hourly maps for the tests were chosen from 4 to 8 hours to keep the distortion due to the inaccurate magnetic equator to a minimum; thus the numbers actually reflect the errors to be expected after the distortion has been corrected for in some manner. The method of coordinate rotation to adjust for 1 hour of time discrepancy yields a RMS error in group delay of only 1.37 nsec which is 10% of the mean prediction. But, this value increases rapidly to 2.25 nsec or 17% for a 2 hour time adjustment.

Figure 1a. WORLD MAP OF GROUP DELAY (INSEC)  
ON 21/9/70 AT UT (HRS)= 0

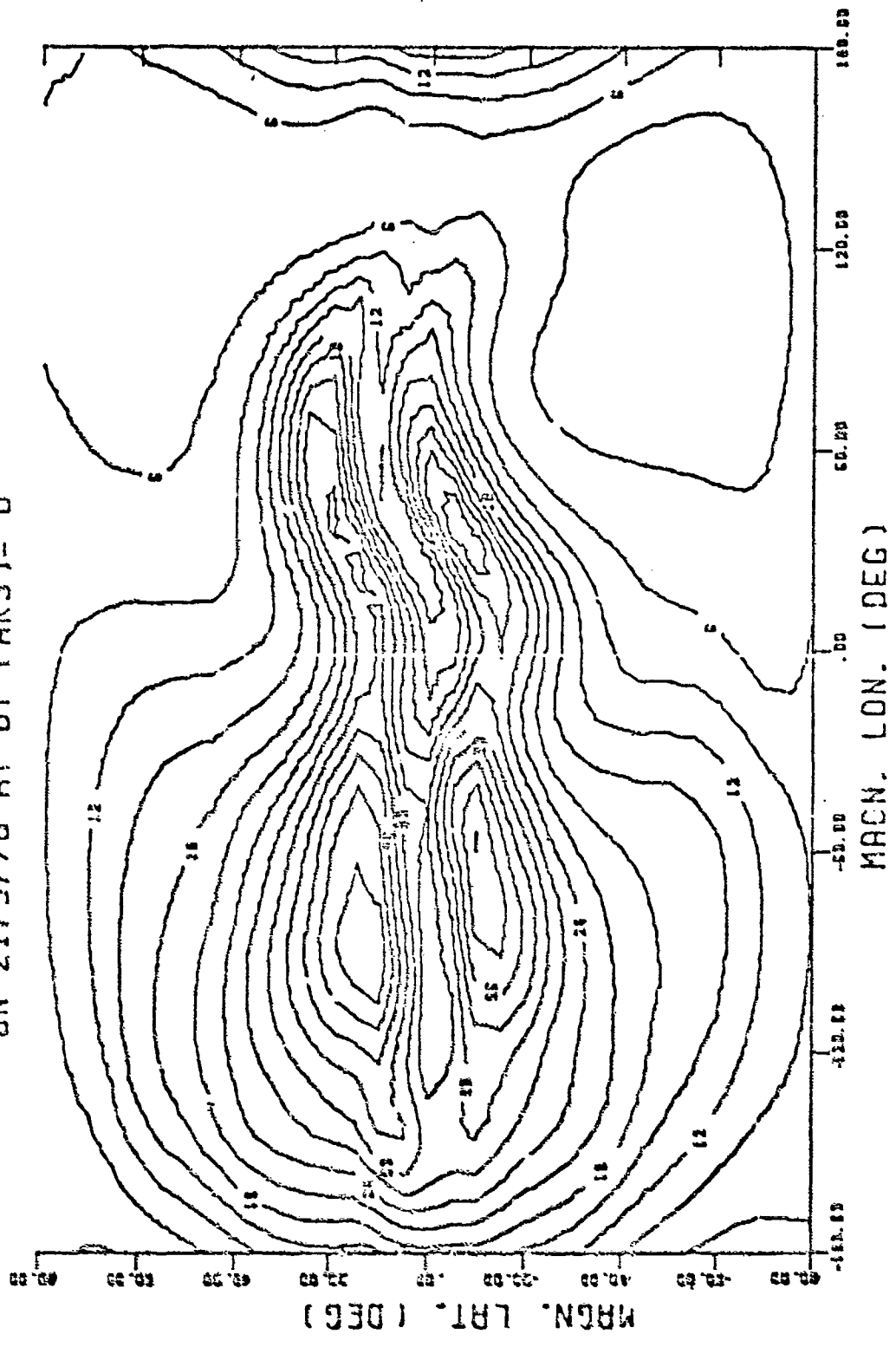


Figure 1b. WORLD MAP OF GROUP DELAY (NSEC)  
ON 21/3/70 AT UT (HRS) = 4

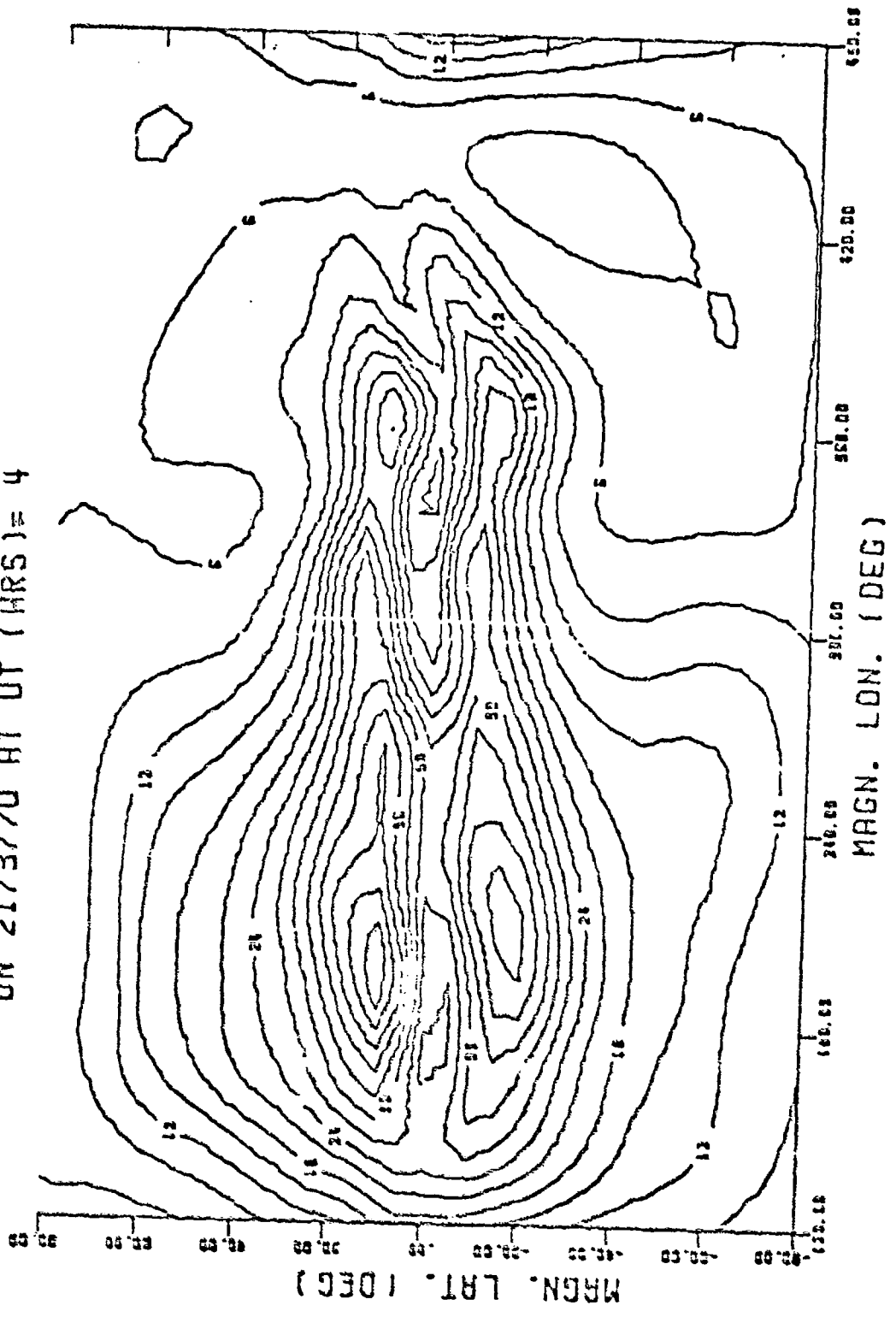


Figure 1c. WORLD MAP OF GROUP DELAY (NSEC)  
ON 21/3/70 AT UT (HRS)= 8

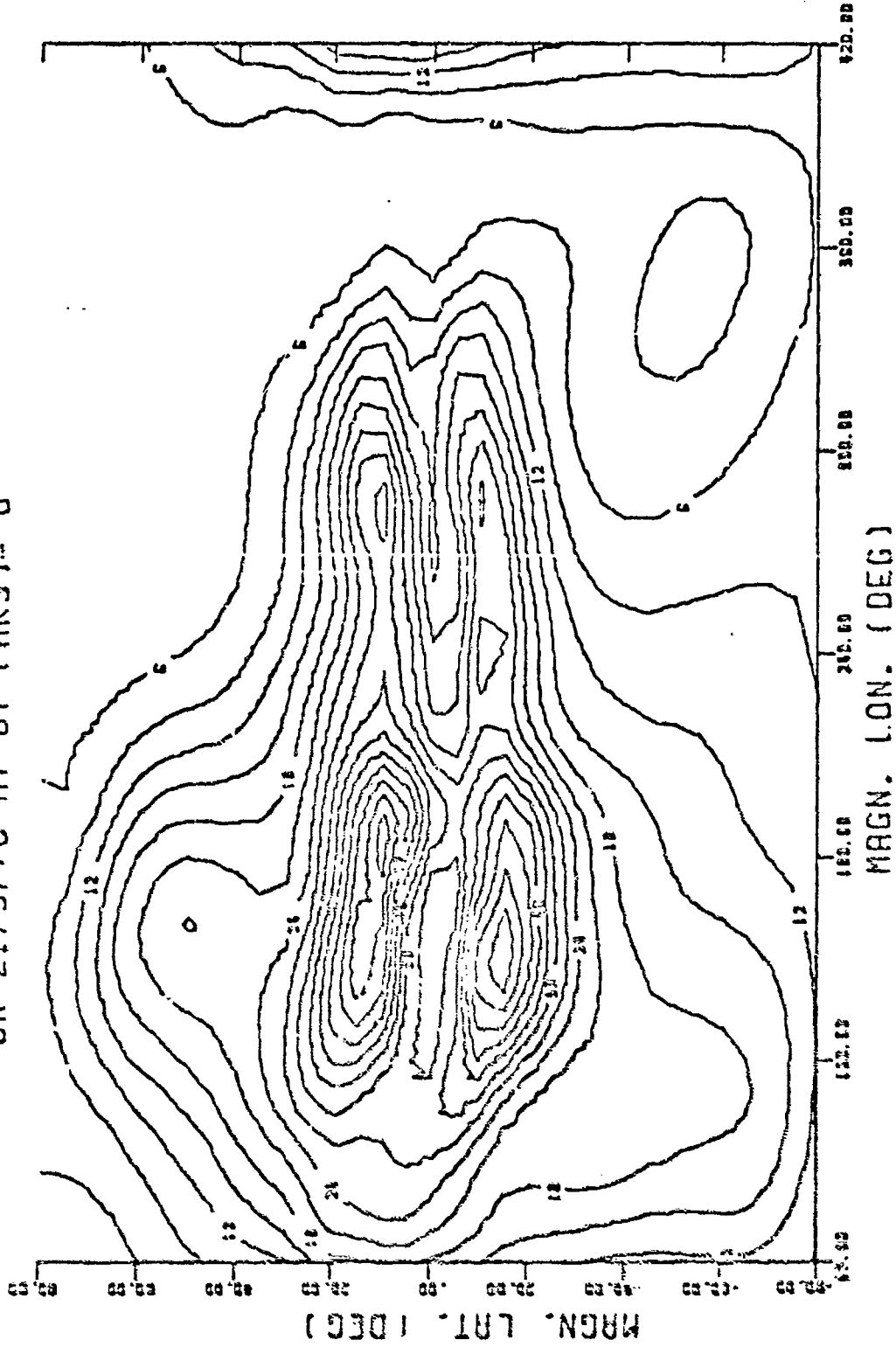


Figure 14. WORLD MAP OF GROUP DELAY (NSEC)  
ON 21/3/70 AT UT (HRS)= 12

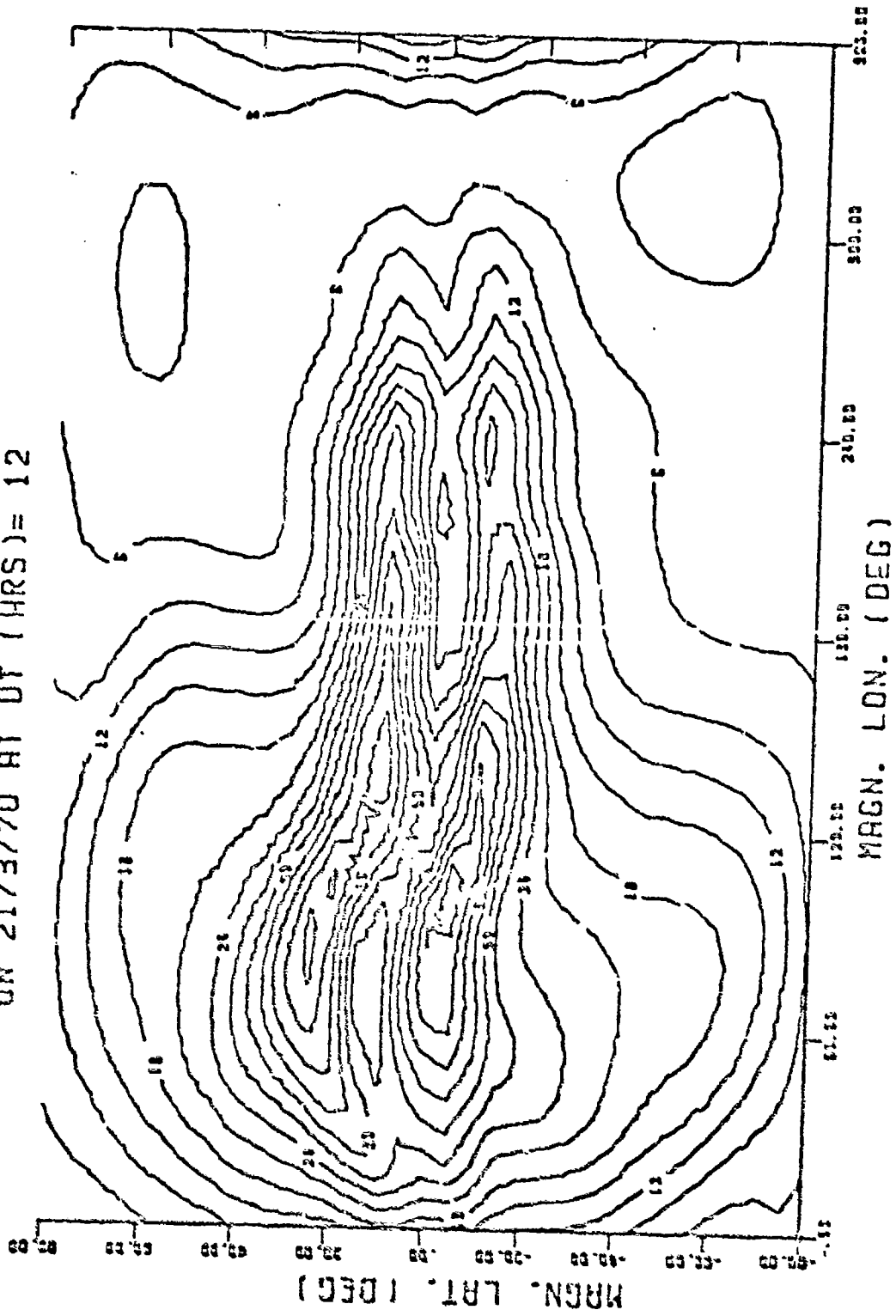


Figure 1e. WORLD MAP OF GROUP DELAY (NSEC)  
ON 21/3/70 AT UT (HRS)= 16

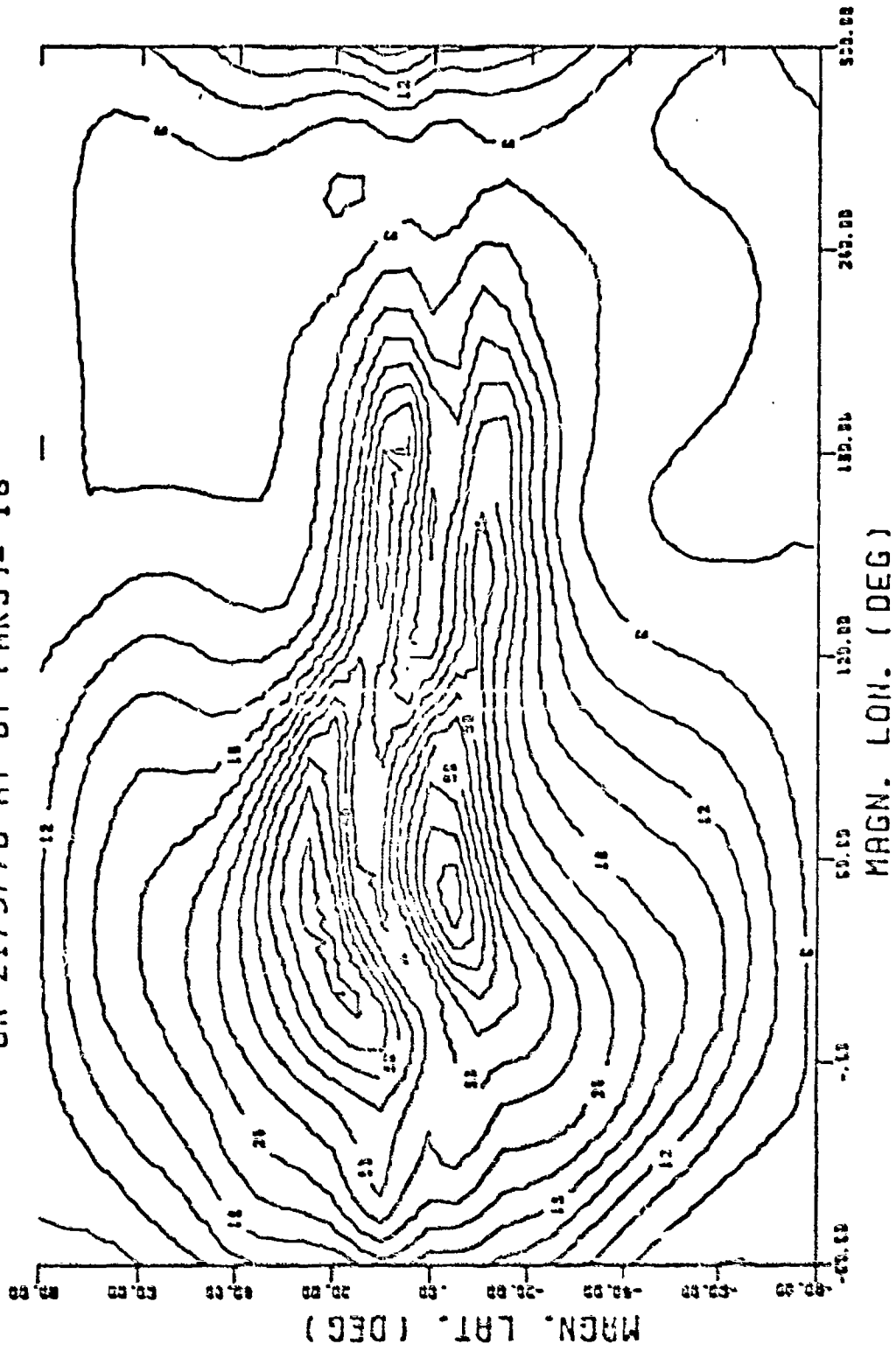


Figure 16. WORLD MAP OF GROUP DELAY (NSEC)  
ON 21/3/70 AT UT (HRS)= 20

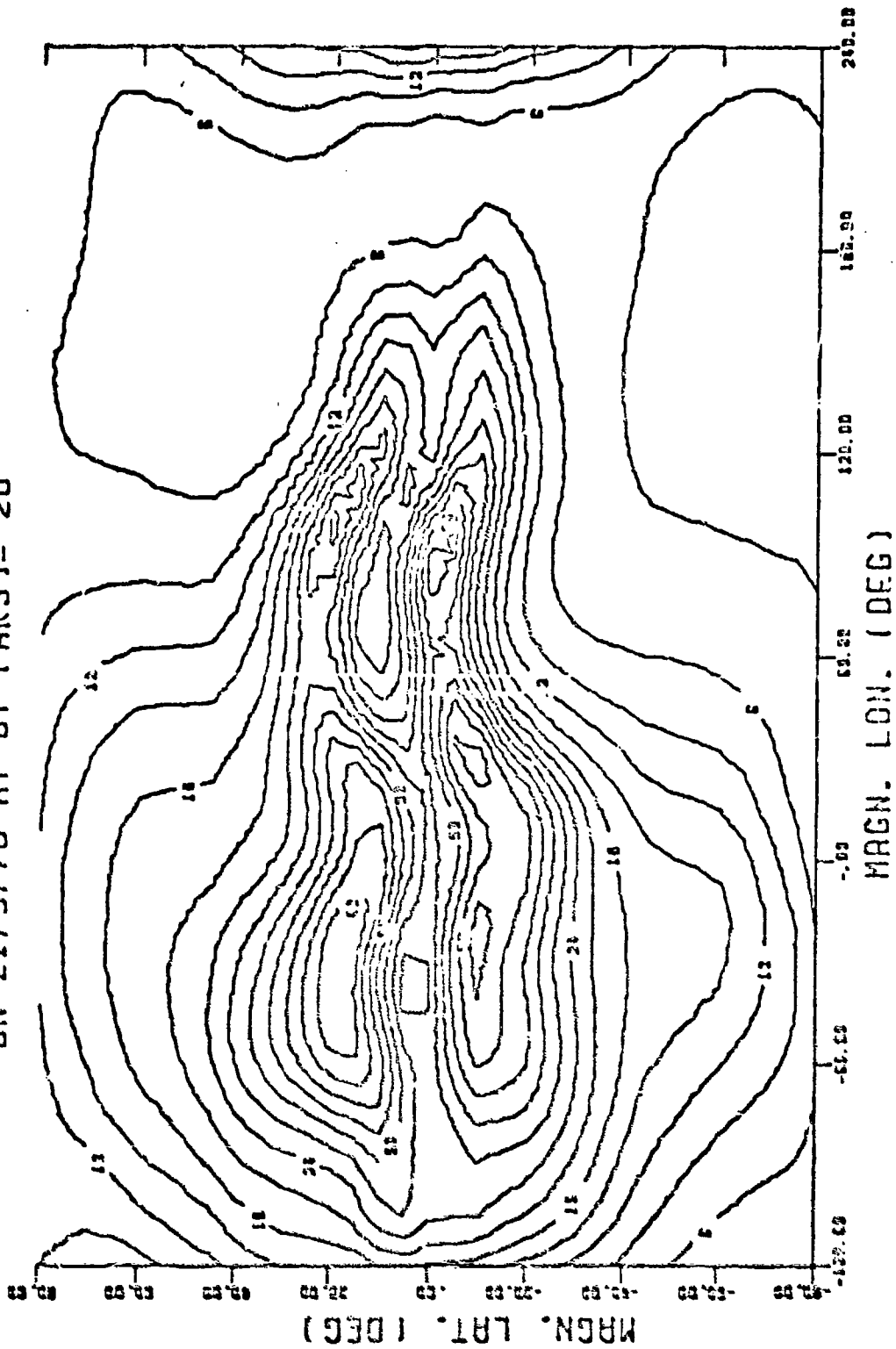




Figure 2 a. WORLD MAP OF GROUP DELAY (NSEC)  
ON 21/6/70 AT UT (HRS)= 0

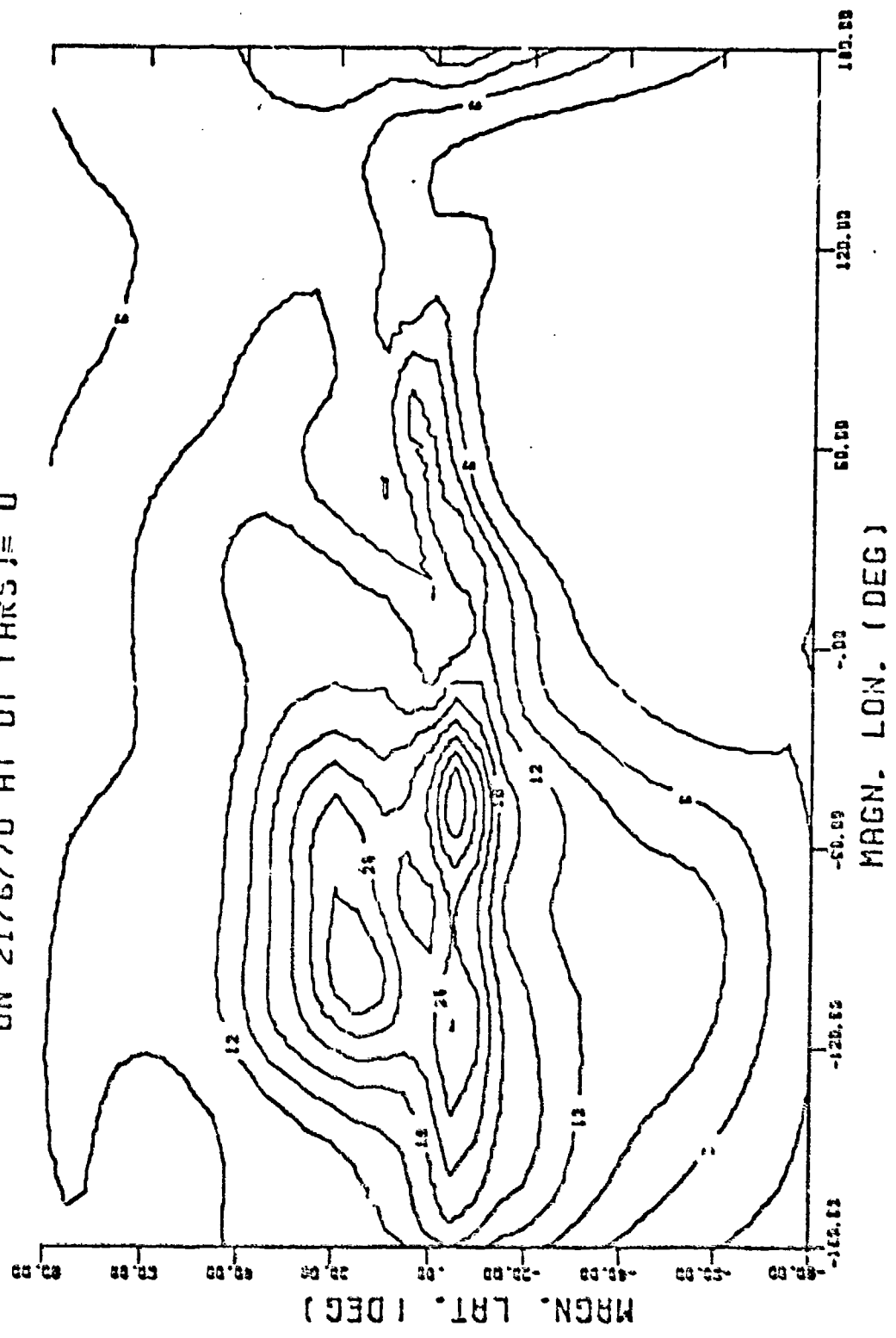


Figure 2 b. WORLD MAP OF GROUP DELAY (NSEC)  
ON 21/6/70 AT UT (HRS) = 4

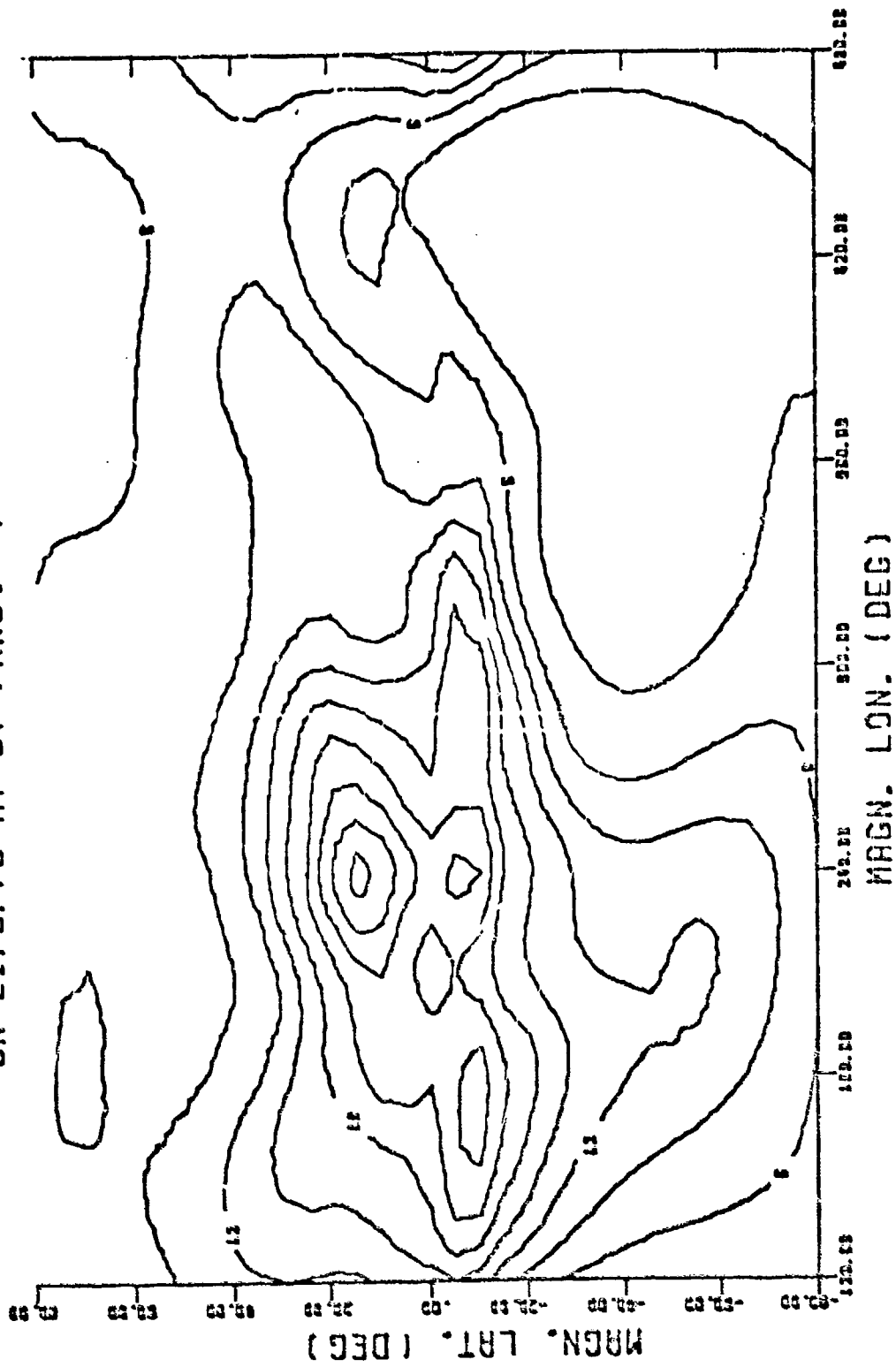


Figure 2 c. WORLD MAP OF GROUP DELAY (NSEC)  
ON 21/6/70 AT UT (HRS)= 8

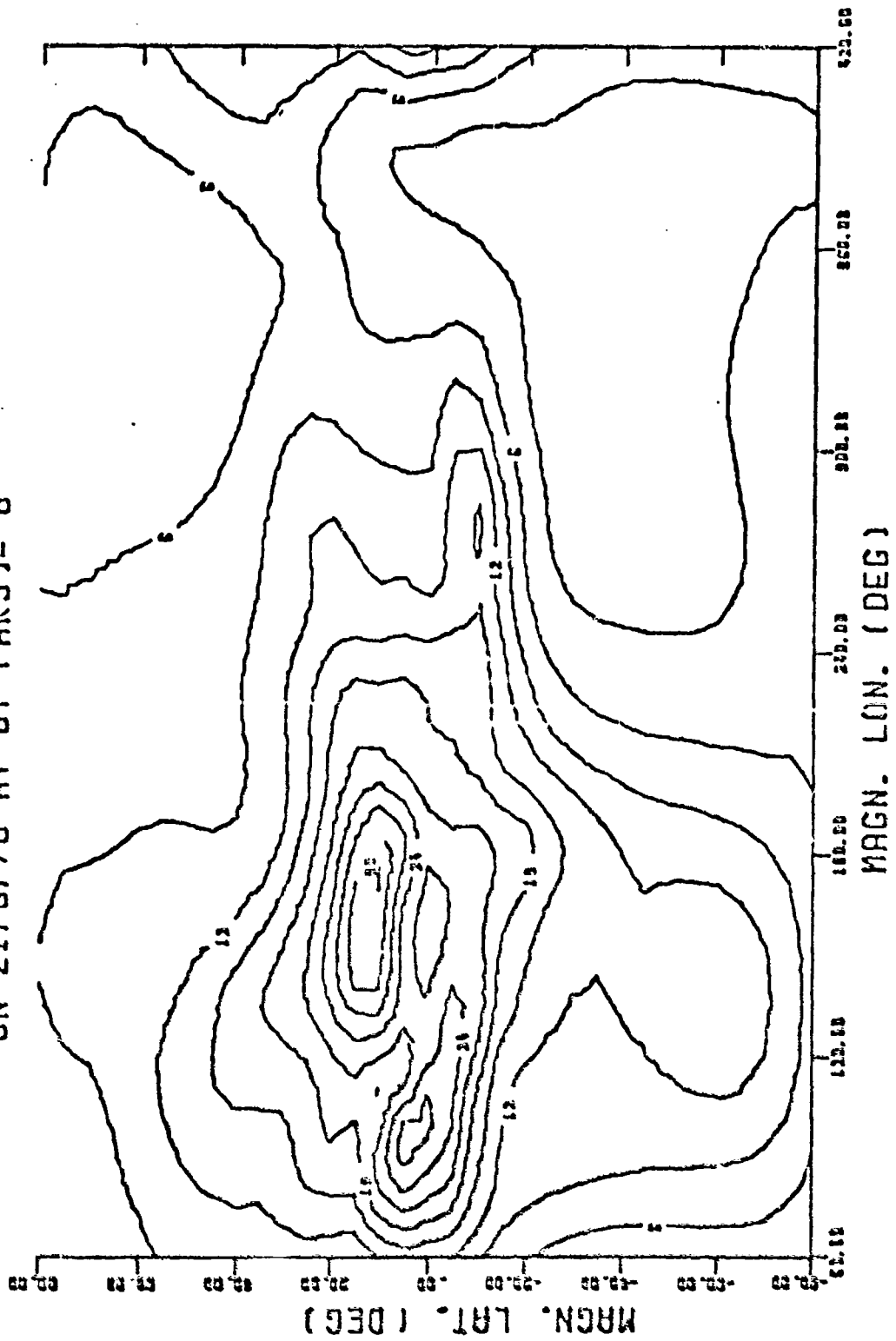


Figure 2 d. WORLD MAP OF GROUP DELAY (NSEC)  
ON 21/6/70 AT UT (HRS)= 12

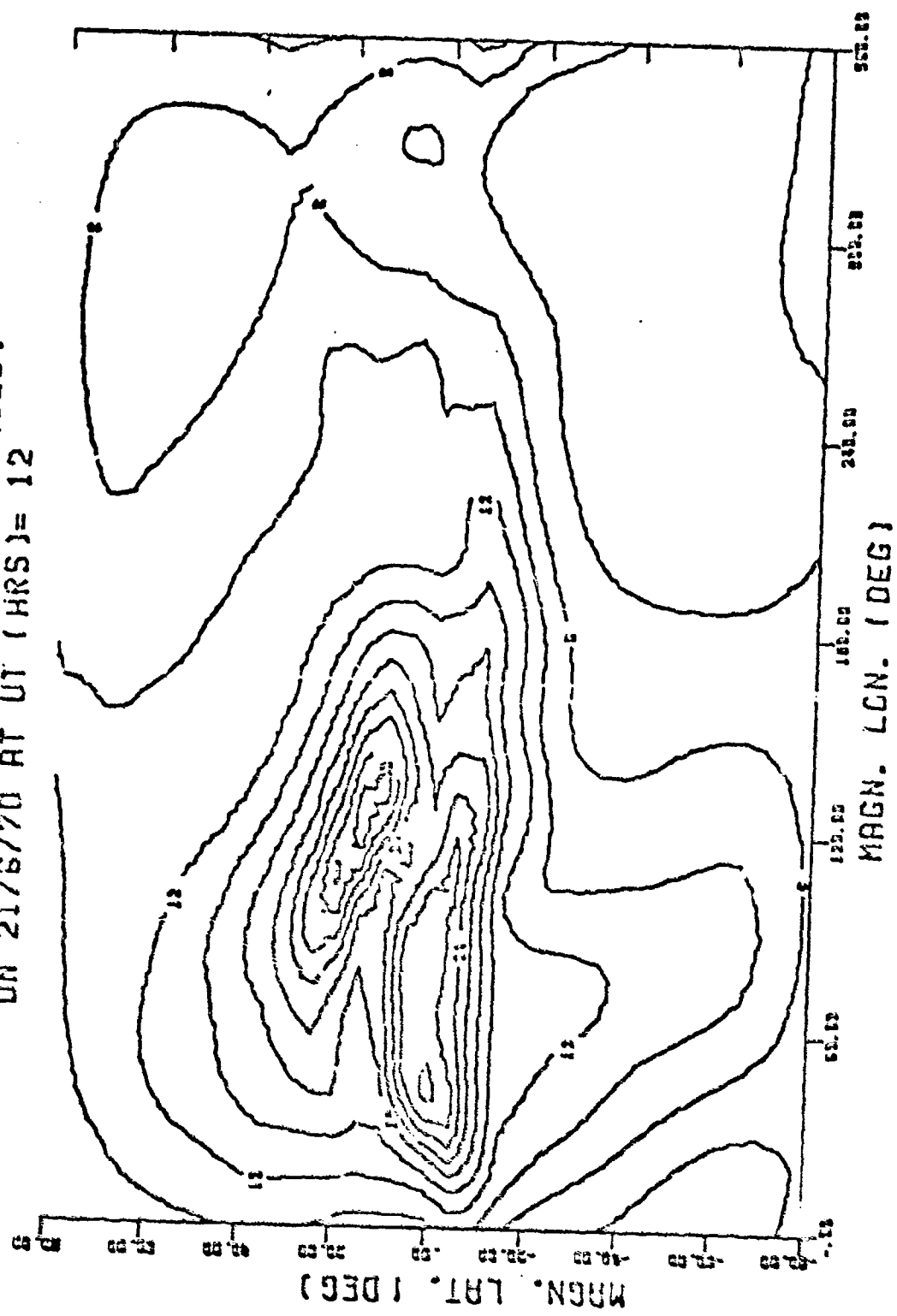


Figure 2 c. WORLD MAP OF GROUP DELAY (NSEC)  
ON 21/6/70 AT UT (HRS)= 16

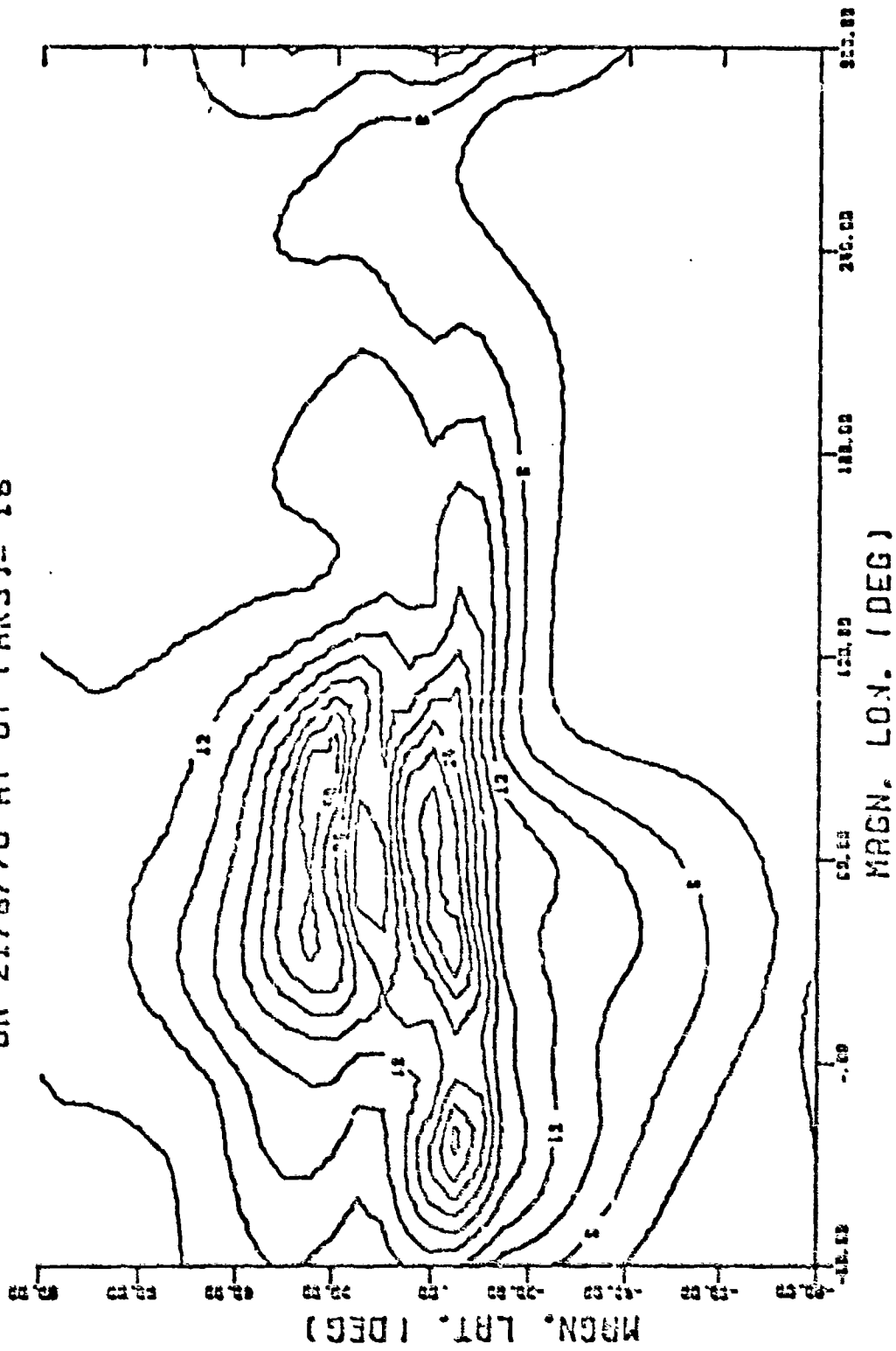


Figure 2 f. WORLD MAP OF GROUP DELAY (NSEC)  
ON 21/6/70 AT UT (HRS)= 20

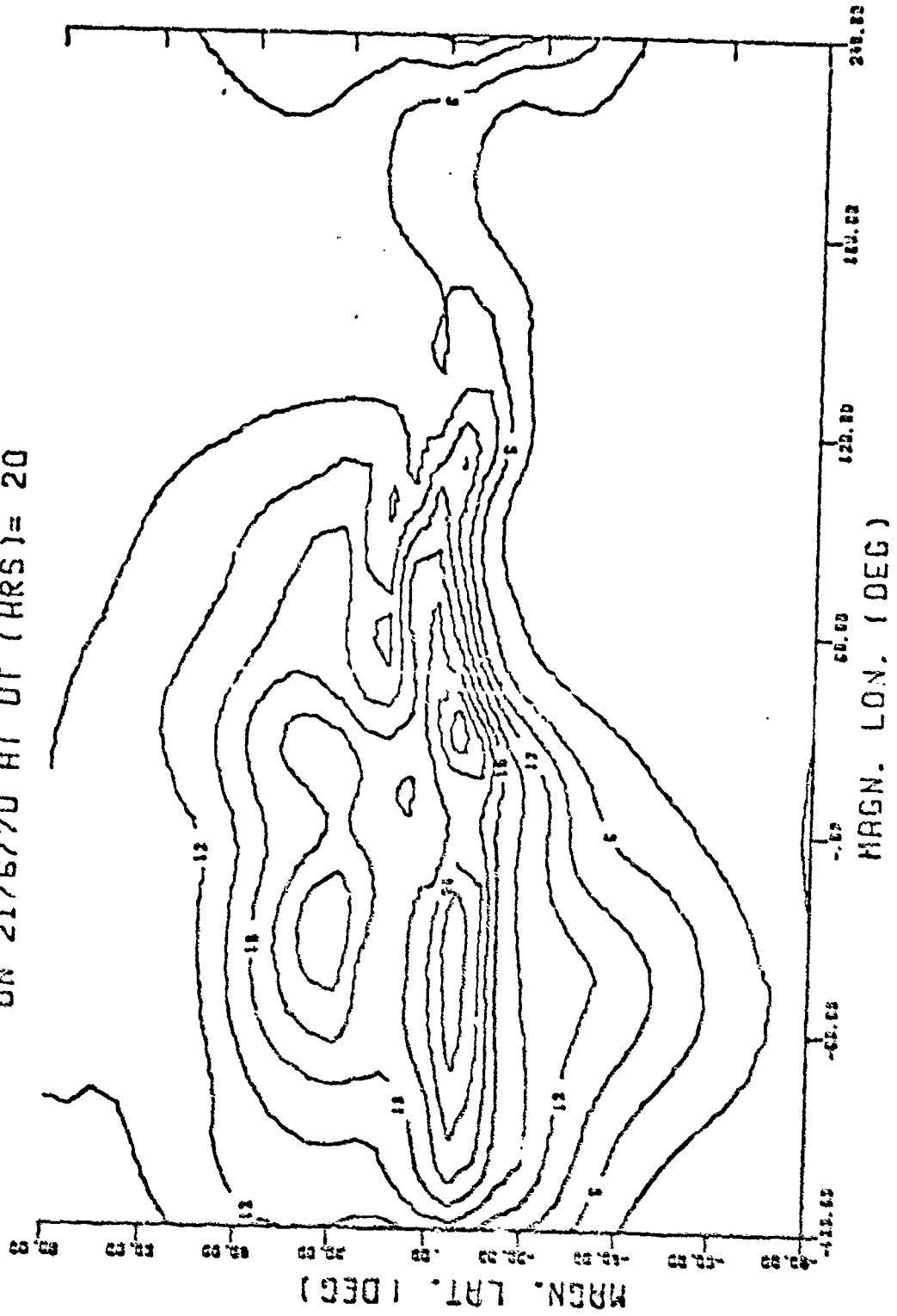


Figure 3. WORLD MAP OF DIFF. IN GROUP DELAY (NSEC)  
ON 21/3/70 FOR UT (HRS)=4 AND 8

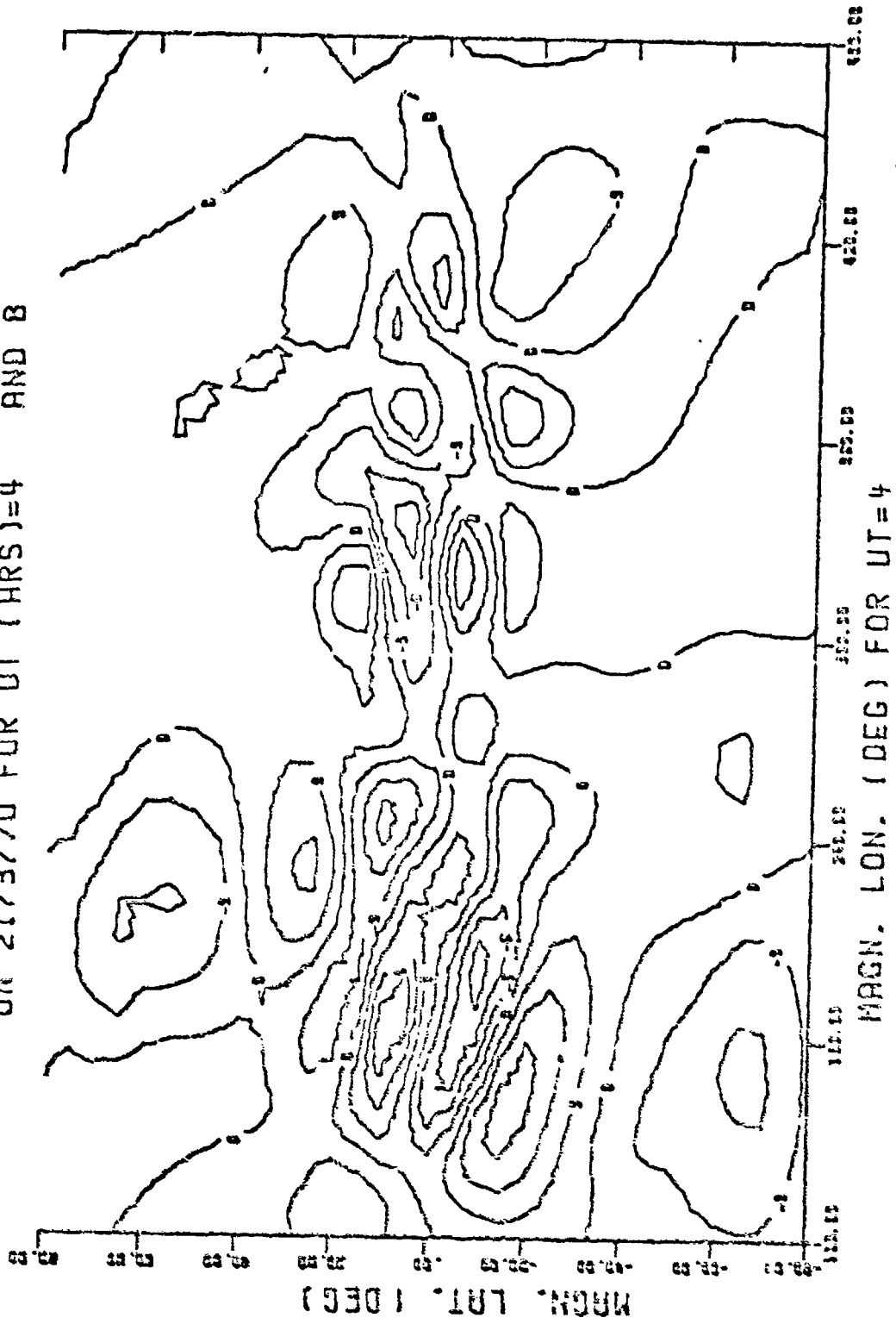


Figure 4a.

WORLD MAP OF HEIGHT OF ION. (KM)  
ON 21, 3:70 AT UT (HRS)= 0

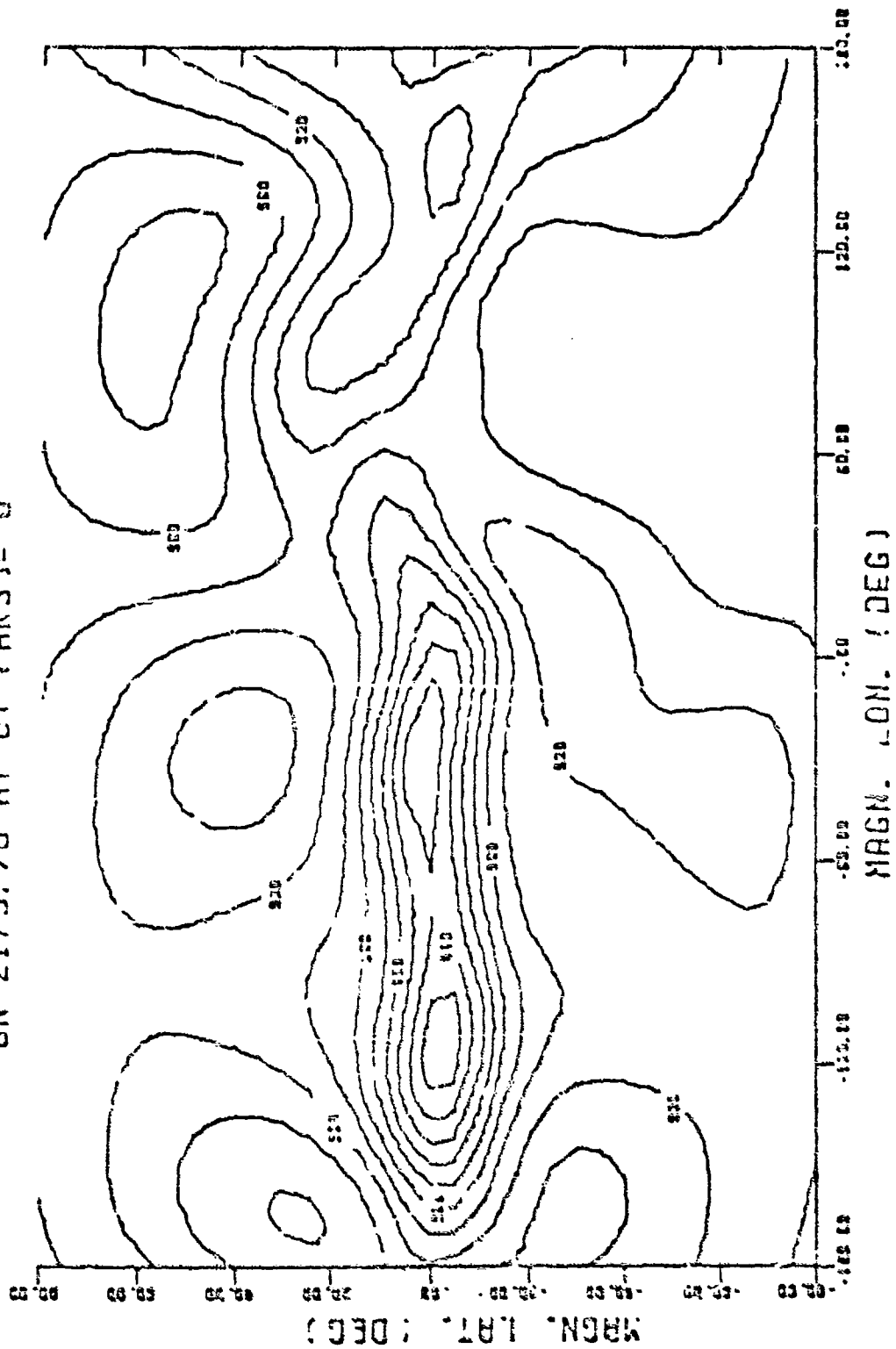




Figure 4b.

WORLD MAP OF HEIGHT OF ION. (KM)  
ON 21/3/70 AT UT (HRS)= 4

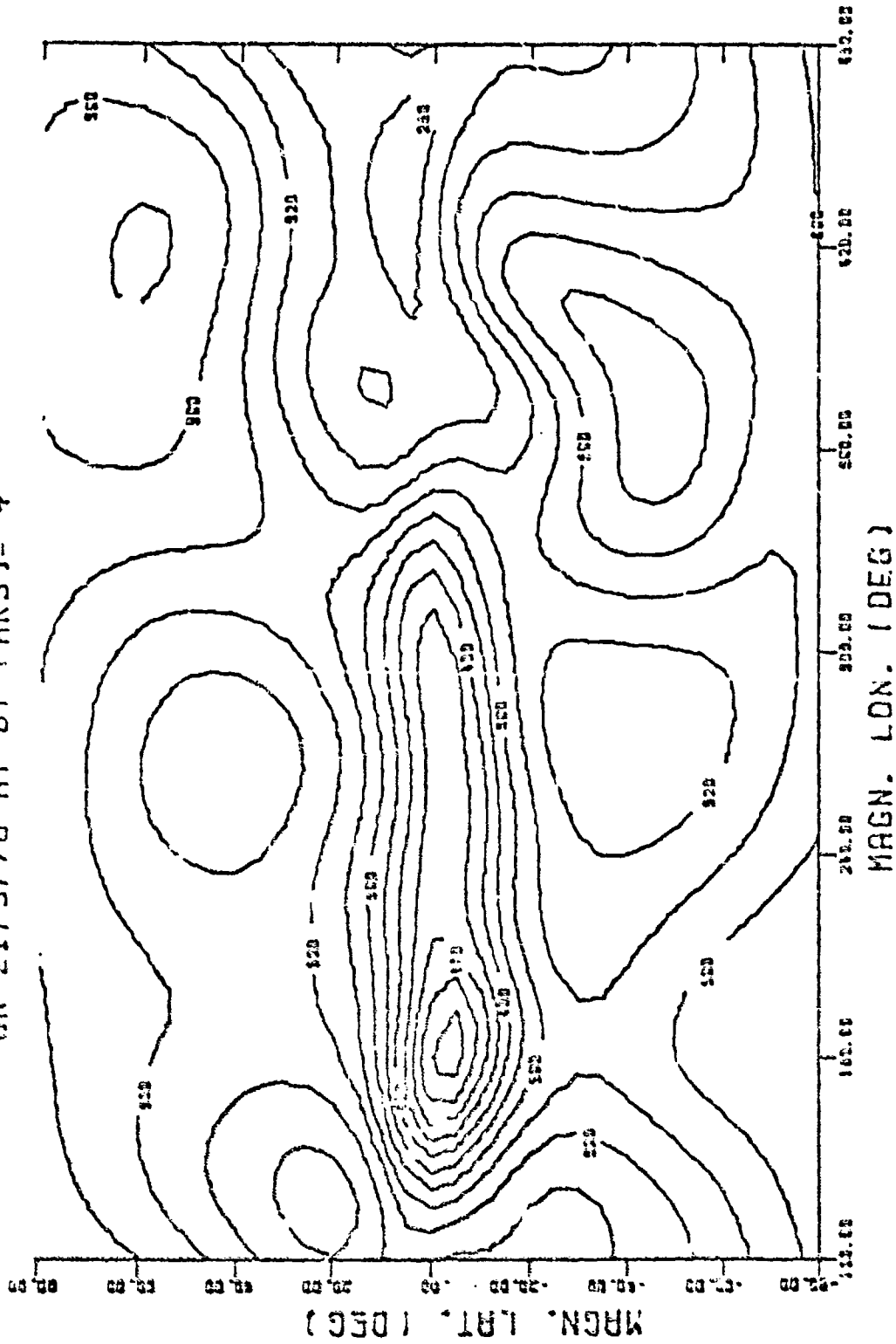


Figure 4c.

WORLD MAP OF HEIGHT OF ION. (KM)  
ON 21/3/70 AT UT (HRS)= 8

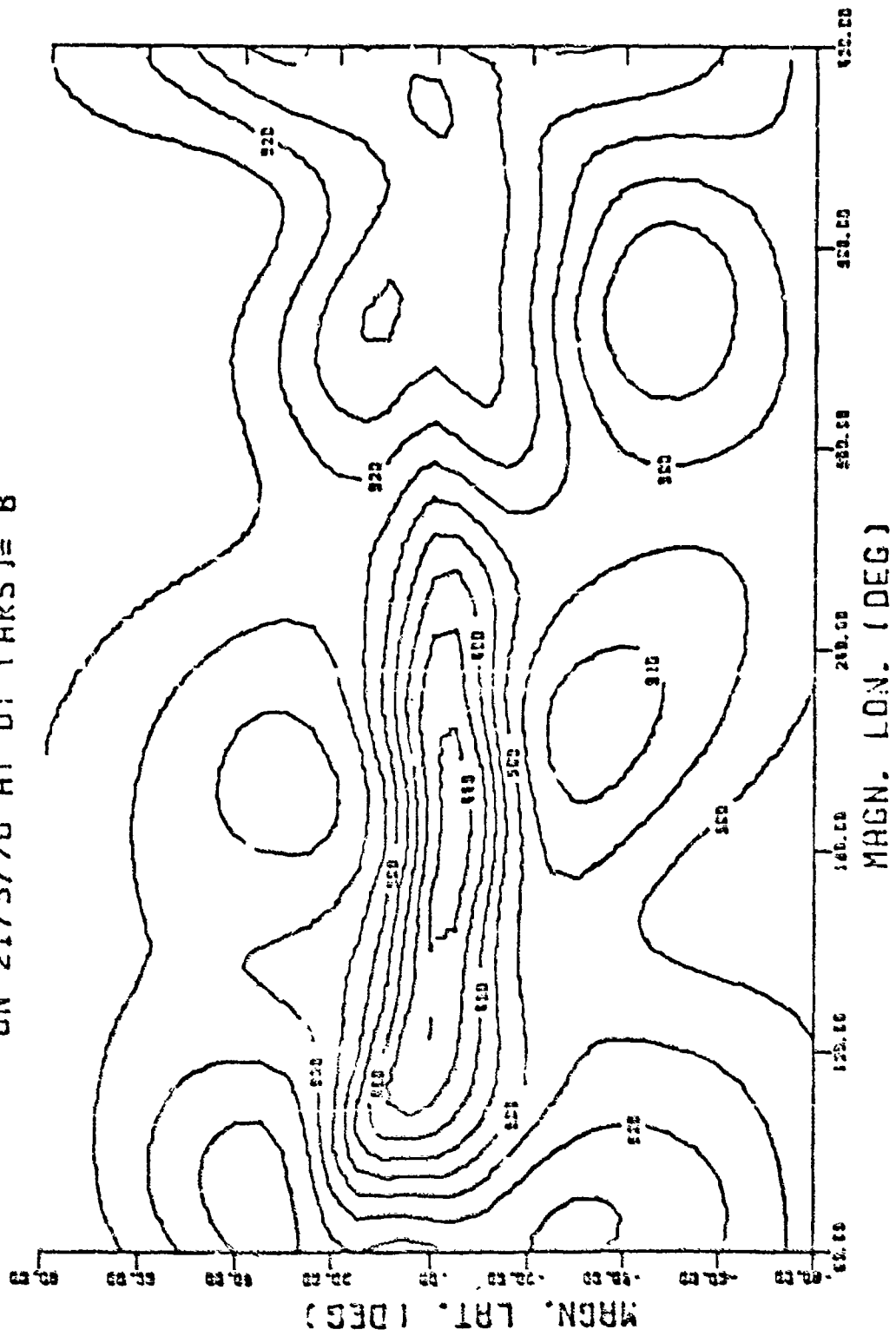


Figure 4d.

WORLD MAP OF HEIGHT OF ION. (KM)  
ON 21/3/70 AT UT (HRS)= 12

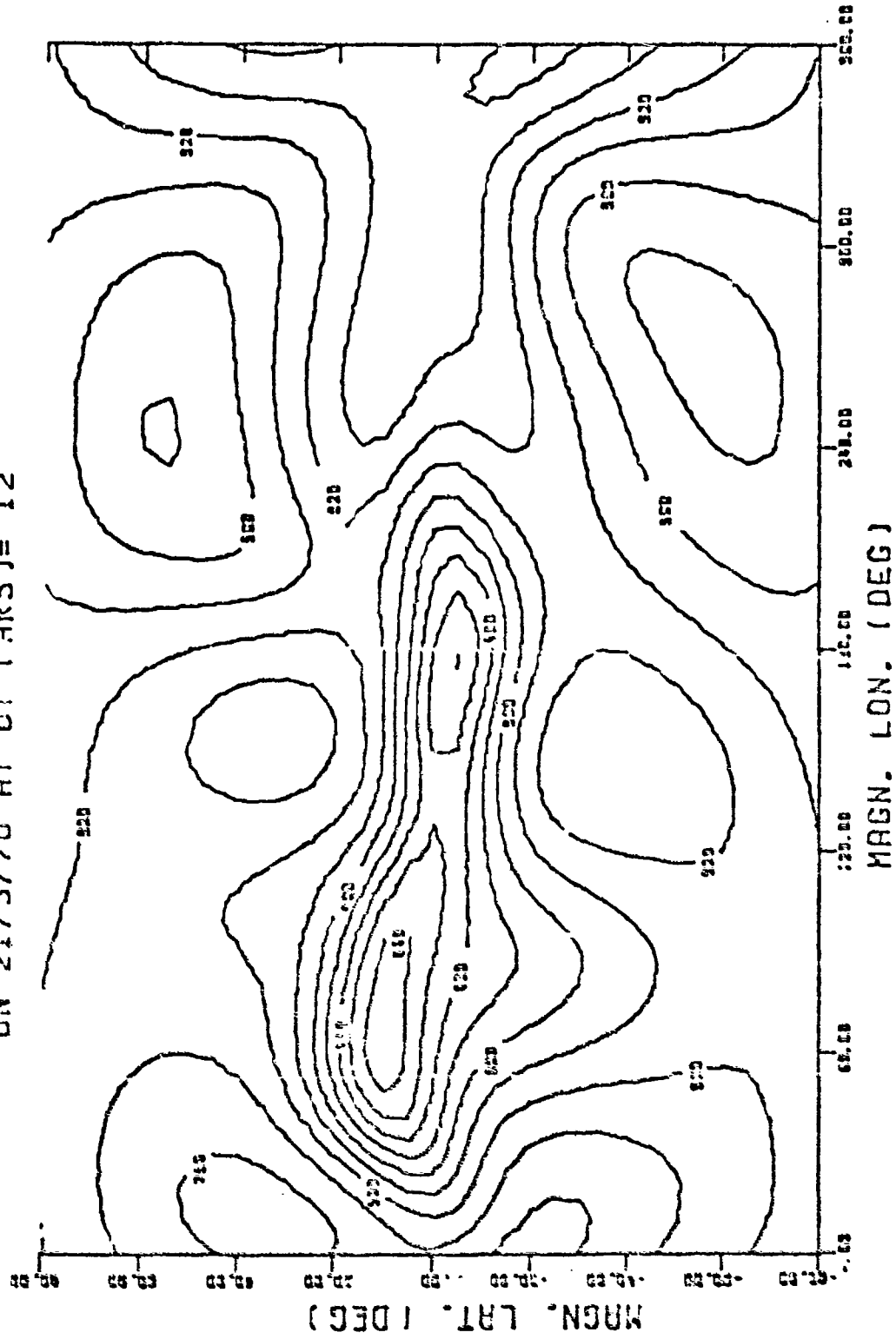


Figure 4e.

WORLD MAP OF HEIGHT OF ION. (KM)  
ON 21/3/70 AT UT (HRS)= 16

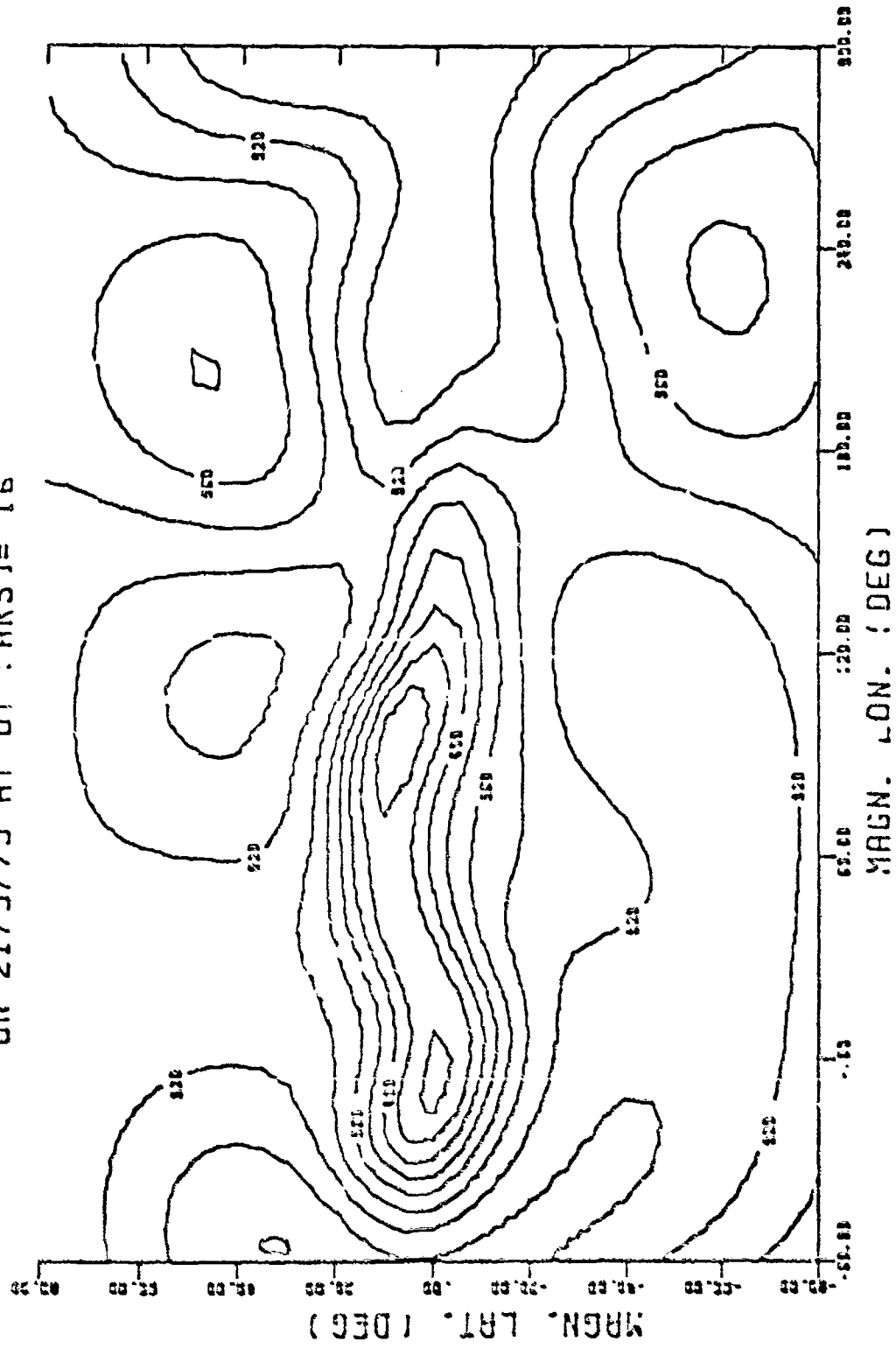


Figure 46.

WORLD MAP OF HEIGHT OF ION. (KM)  
ON 21/3/70 AT UT (HRS)= 20

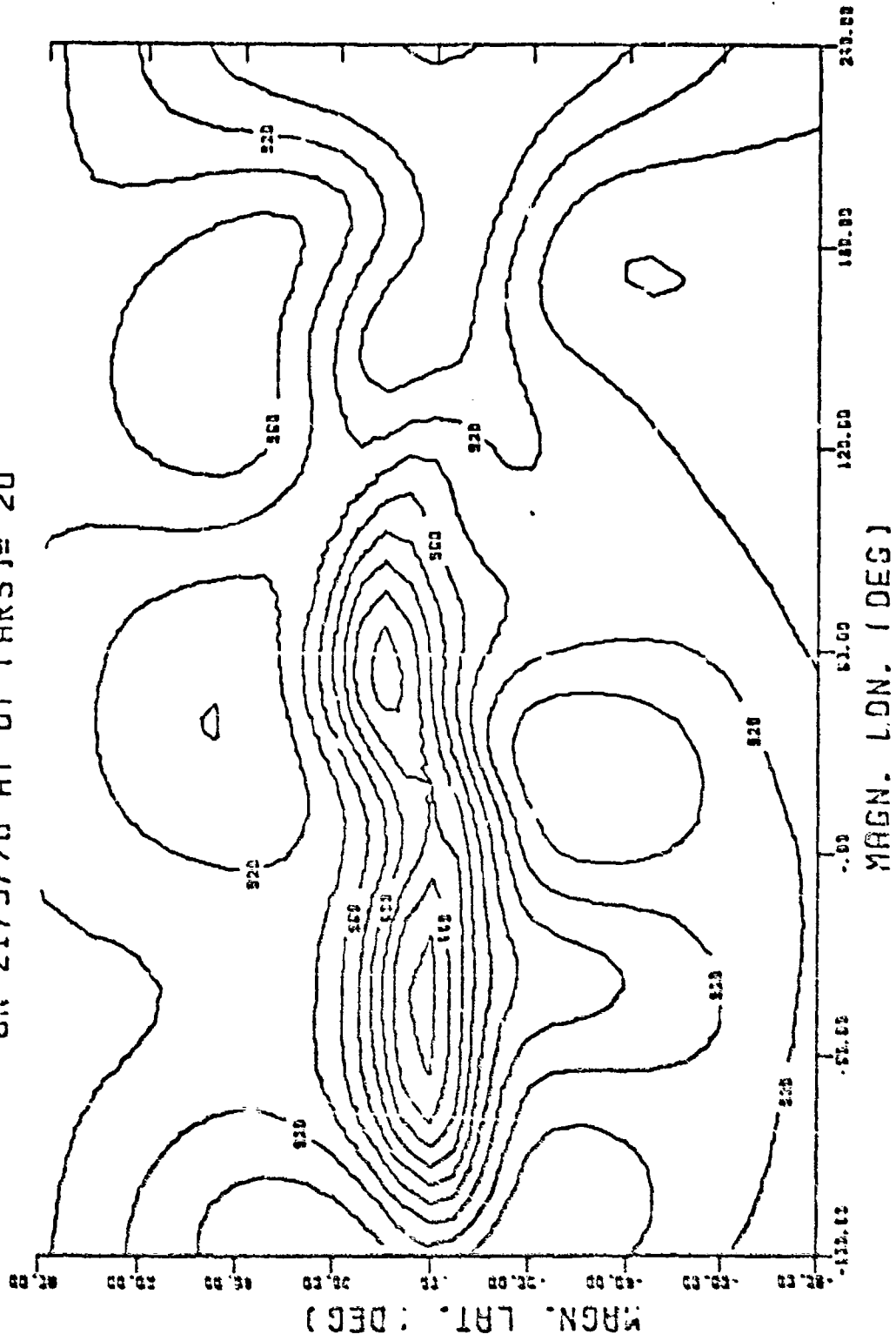


TABLE I. For 21 March 1970

1ST UT	2ND UT	TIME DIFF	DIFFERENCE IN GROUP DELAY FOR WORLD MAPS AT DIFFERENT UNIVERSAL TIMES FOR REGIONS		INSIDE ±80		OUTSIDE ±40		INSIDE ±20		OUTSIDE ±20		RMS	MAX.
			RMS	MAX.	RMS	MAX.	RMS	MAX.	RMS	MAX.				
0	4	4	3.42	19.12	4.33	19.12	2.04	5.51	4.91	19.12	2.65	18.22		
0	8	8	3.57	19.04	4.69	19.04	3.02	8.56	5.27	19.04	3.36	16.91		
0	12	12	4.18	19.81	5.56	19.81	1.80	4.38	6.51	19.41	2.85	19.81		
0	16	8	4.42	21.09	5.76	21.09	2.25	5.68	6.62	18.60	3.23	21.09		
0	20	4	3.96	21.11	5.20	21.11	1.93	5.16	6.05	21.11	2.81	19.77		
4	8	4	2.92	11.09	3.47	11.09	2.19	6.75	4.24	11.09	2.24	8.24		
4	12	8	4.19	22.33	5.12	22.33	2.90	6.74	6.08	22.33	3.20	12.28		
4	16	12	4.50	16.31	5.03	16.31	3.86	8.22	5.60	16.31	4.01	13.89		
4	20	8	4.33	20.89	4.94	20.89	3.57	7.65	5.70	20.89	3.68	14.42		
8	12	4	4.03	21.32	4.82	21.32	2.87	7.92	5.83	21.32	3.10	13.82		
8	16	8	5.02	23.15	5.59	23.15	4.34	11.26	6.12	23.15	4.54	18.92		
8	20	12	4.62	20.05	5.01	20.05	4.16	10.00	5.77	20.05	4.11	14.87		
12	16	4	3.69	16.64	4.70	16.64	2.15	6.19	5.47	16.64	2.74	16.97		
12	20	8	4.47	23.61	5.90	23.61	2.05	6.27	7.19	23.61	2.85	17.74		
16	20	4	4.01	19.58	5.48	19.58	1.08	4.50	6.40	19.58	2.59	18.21		
			Mean	Max.	Mean	Max.	Mean	Max.	Mean	Max.	Mean	Max.		
Basic Prediction:			3.66	49.75	18.29	49.75	8.74	25.98	21.91	42.75	10.57	43.25		

TABLE 2. For 21 June 1970

1ST 2ND TIME		DIFFERENCE IN GROUP DELAY FOR WORLD MAPS AT DIFFERENT UNIVERSAL TIMES FOR REGIONS											
UT	DIFF.	INSIDE $\pm 80$		INSIDE $\pm 40$		OUTSIDE $\pm 40$		INSIDE $\pm 20$		OUTSIDE $\pm 20$		DEG. IN MAGN. LAT.	
		RMS	MAX.	RMS	MAX.	RMS	MAX.	RMS	MAX.	RMS	MAX.	RMS	MAX.
0	4	2.22	10.93	2.62	10.93	1.68	4.44	2.95	10.93	1.87	7.83		
0	8	2.83	12.89	3.16	12.89	2.43	6.23	3.65	12.89	2.45	8.01		
0	12	2.68	13.45	3.36	13.45	1.70	5.22	4.03	13.45	1.96	5.75		
0	16	2.73	12.99	3.34	12.99	1.86	6.23	3.56	12.72	2.34	12.99		
0	20	2.28	12.10	2.70	12.10	1.71	5.41	3.14	12.10	1.85	5.81		
4	4	2.14	10.74	2.61	10.74	1.49	5.32	2.85	10.74	1.80	7.39		
4	8	2.59	12.74	3.18	12.74	1.76	7.17	3.37	11.82	2.23	12.74		
4	12	3.41	15.10	3.79	15.10	2.94	9.47	3.57	14.29	3.35	15.10		
4	16	3.12	11.26	3.28	11.26	2.93	8.40	3.42	11.26	3.00	10.45		
4	20	2.51	13.03	2.99	13.03	1.87	5.32	3.47	13.03	2.04	9.05		
8	4	3.84	18.05	4.17	18.05	3.45	10.47	4.15	15.98	3.72	16.05		
8	8	3.58	12.86	3.63	12.86	3.53	9.34	3.91	12.86	3.45	10.49		
8	12	2.89	18.36	3.51	18.36	2.04	6.08	3.91	18.36	2.40	15.29		
8	16	2.97	14.37	3.55	14.37	2.19	6.74	4.24	14.37	2.32	8.61		
8	20	2.26	12.83	2.98	12.83	1.07	4.57	3.36	12.83	1.68	10.97		
		Mean	Max.	Mean	Max.	Mean	Max.	Mean	Max.	Mean	Max.		
Basic Prediction:		8.72	34.94	11.21	34.94	6.07	17.74	13.22	34.94	7.03	32.91		

TABLE 3. For 21 March, 1970

1ST 2-D TIME		DIFFERENCE IN 16N. HEIGHT FOR WORLD MAPS AT DIFFERENT UNIVERSAL TIMES FOR REGIONS		INSIDE +-40		OUTSIDE +-40		INSIDE +-20		OUTSIDE +-20		DEG. IN MAGN. LAT.	
UT	DIFF	RMS	MAX.	RMS	MAX.	RMS	MAX.	RMS	MAX.	RMS	MAX.	RMS	MAX.
0	4	17.	51.	18.	51.	17.	47.	20.	51.	16.	47.	16.	47.
0	8	20.	62.	20.	62.	20.	54.	24.	62.	18.	54.	18.	54.
0	12	20.	86.	23.	86.	16.	39.	29.	86.	16.	39.	16.	39.
0	16	18.	64.	21.	64.	16.	40.	24.	64.	16.	45.	16.	45.
0	20	17.	90.	21.	90.	13.	33.	24.	90.	14.	42.	14.	42.
4	4	17.	82.	18.	82.	16.	38.	22.	82.	15.	39.	15.	39.
4	8	24.	109.	25.	109.	23.	51.	31.	109.	21.	51.	21.	51.
4	16	26.	92.	27.	92.	24.	62.	30.	92.	24.	62.	24.	62.
4	20	25.	79.	27.	79.	22.	55.	31.	79.	22.	55.	22.	55.
8	4	16.	82.	19.	82.	17.	47.	23.	82.	16.	47.	16.	47.
8	8	24.	108.	26.	108.	21.	57.	29.	108.	21.	57.	21.	57.
8	16	24.	93.	27.	93.	21.	60.	31.	93.	21.	60.	21.	60.
12	4	21.	111.	24.	111.	17.	38.	28.	111.	17.	47.	17.	47.
12	8	22.	110.	26.	110.	18.	38.	32.	110.	17.	48.	17.	48.
16	4	17.	92.	21.	92.	11.	28.	25.	92.	13.	45.	13.	45.
Basic Prediction:		Mean	Max.	Mean	Max.	Mean	Max.	Mean	Max.	Mean	Max.	Mean	Max.
		336.	490.	335.	490.	337.	399.	345.	490.	332.	399.	332.	399.

75



Table 4. For 21 March 1970

1ST UT	2ND UT	TIME DIFF	DIFFERENCE IN GROUP DELAY FOR WORLD MAPS AT DIFFERENT UNIVERSAL TIMES FOR REGIONS									
			INSIDE +8C		+40		OUTSIDE +20 DEG. IN MAGN. LAT.					
			RMS	MAX.	RMS	MAX.	RMS	MAX.				
4	5	1	1.39	7.61	1.62	7.61	.69	1.85	2.30	7.61	.81	3.96
4	6	2	2.21	11.05	2.79	11.05	1.33	4.12	3.48	11.05	1.47	5.55
4	7	3	2.61	12.96	3.16	12.96	1.85	5.70	3.87	12.96	1.93	6.70
4	8	4	2.92	11.09	3.47	11.09	2.19	6.75	4.24	11.09	2.24	8.24
5	6	1	1.32	7.50	1.69	7.50	.76	2.96	2.12	7.50	.86	3.84
5	7	2	2.18	11.91	2.65	11.91	1.51	5.25	3.27	11.91	1.58	6.17
5	8	3	2.63	12.19	3.39	12.19	2.08	6.76	4.17	12.19	2.12	8.84
6	7	1	1.35	8.71	1.67	8.71	.91	3.54	2.08	8.71	.95	5.19
6	8	2	2.35	12.15	2.82	12.15	1.70	5.69	3.51	12.15	1.72	6.94
7	8	1	1.43	8.64	1.77	8.64	.93	3.21	2.23	8.64	.97	4.95

BASIC PREDICTION VALUES

MEAN	MAX.	MEAN	MAX.	MEAN	MAX.	MEAN	MAX.
13.55	53.70	18.10	53.70	8.74	24.16	21.91	53.70
						10.57	43.25

TRADE STUDY NO. 8

USER EPHEMERIS MODEL

T. Stansel



**GENERAL DYNAMICS**

*Electronics Division*

P.O. Box 81127, San Diego, California 92161 714-279-7201

## 1. INTRODUCTION

The GPS Ephemeris Word is used to establish the position, and possibly the velocity of the individual space vehicles (SV) at specific time points or as a continuous function of time. This ephemeris word must be generated or stored in the SV and the data word must be processed by the User Segment equipment. For the user equipment, the primary concern with the ephemeris word format is that the computational aspect of generating the SV state vector (position and velocity) does not place a cost or accuracy burden on the user processor function. It should be noted that the basic accuracy of the users navigation data for the GPS is governed by the user's knowledge of the SV state vector in that the system is never capable of providing navigation to any accuracy greater than the user's knowledge of the SV state vector. This analysis is concerned with the viable mechanization candidates from the user equipment viewpoint. Examination of the ephemeris mechanization has been basically motivated by the change in design concepts for the new satellite altitude (11,000 nautical miles) and by the fact that the satellite configuration is no longer a synchronous orbit.

## 2. REQUIREMENTS

### 2.1 Functional Requirement

General functional requirements for the ephemeris word are derived from paragraph 3.7.2.3 Software Initialization of the System Segment Specification SS-GPS-101A which stipulates that the "current position and velocity of all active satellites" shall be determined by the user processor. A related functional capability is also identified in 3.7.2.3.3 SV Selection which requires that the satellites will be selected to provide the set which yields the best GDOP and the minimum tropospheric error. The requirement also states that the processor data base will be maintained for the SV state vector to establish the anticipated doppler shift and navigation code state. Consideration of the two requirements means that the processor shall have a means of determining the SV state vector from either prior stored data or from data received via the SV ephemeris data word.

### 2.2 Design Requirements

Study of the system design has produced several design requirements which are derived from present ground rules or design concepts. The first design requirement considered is the accuracy of the ephemeris mechanization utilized by the user processor. The system segment error budget defines SV ephemeris error of 5 to 12 feet for which the ephemeris model error allocation is taken as 1 foot. Note that these algorithm errors are the deviation between the ephemeris algorithm and the SV's true trajectory, given that the true trajectory is completely known and defined. The velocity error budget is stipulated to be a value of 0.01 ft/sec. The system specification also includes a basic waveform definition which establishes an ephemeris data format location within the data frame. Fundamentally, Appendix II of SS-GPS-101A states in Paragraph 20.3.2.3, Data Block 2, that an ephemeris word shall be provided within this data block. The actual extent of the ephemeris would be subject to the concepts which are defined in the study.

### 2.3 Evaluation Criteria

Evaluation of the ephemeris mechanization and the resultant ephemeris word data format is seen to be a function of the following criteria:

- a) Processor memory requirements
- b) Processor computation complexity
- c) Number of data word bits required
- d) Accuracy of the selected mechanization
- e) Perturbability of the selected mechanization

Consideration of several pertinent factors which influence the mechanizations and hence must be considered in the analysis using the above evaluation criteria are the following:

- 1) Discrete versus functional position definition
- 2) Selection of reference coordinate frames as inertial or earth-fixed basis systems.
- 3) Data span intervals and data overlap concepts
- 4) Resolution and potential accuracy limitations

Proper choice and selection of these factors must be made to determine the impact of the design on the User Segment, the Control Segment and the Space Vehicle Segment.

### 3. CANDIDATE MECHANIZATIONS

One of the first basic mechanization considerations which may be developed employs the concept of utilizing either discrete or functional formulations of the satellite position and velocity. These two approaches are described in detail in the following specific discussions.

#### 3.1 Discrete Representation

It is possible for the SV to announce its position at regular intervals, e.g., once per second, once every 6 seconds, etc. To achieve a resolution of 0.1 meter, 29 bits plus sign would be required for each of three cartesian coordinates, for a total of 87 bits per position. In addition, the user must verify proper reception by some form of error detection and correction, e.g., majority vote of redundant data or the use of error correcting codes. Thus, the user must receive from 100 to 261 bits per position, and it would be possible to define the SV position at least every 2 to 6 seconds under the assumption of a 50 bits per second data rate.

By having the SV announce its position at discrete time points, there will be no computational burden to the user equipment of converting from a functional form to the discrete positions required for a position fix. On the other hand, the user equipment would be forced to demodulate ephemeris data from each of three or four SV's simultaneously and continuously, rather than sequentially demodulating data from each SV in turn.

The impact on the SV of having to transmit discrete positions would seem to be a very large memory requirement. However, this does not have to be the case. Specifically, the SV memory may be a programmed processor or CPU. All input and output to the memory would be via the CPU. In this way, the Ground Control Segment can load the SV computer memory with algorithms representing SV position as a function of time. Included in the raw data would be the computer program to derive discrete positions from the algorithms and to transmit them in the format expected by the user equipment.

#### 3.2 Functional Representation

Instead of transmitting discrete positions the SV can provide position as a function of time. There are three general methods for functional ephemeris representation: interpolation polynomials, Keplerian inertial orbit elements, and numerical integration techniques.

Representation of satellite position and velocity by either a Taylor series expansion in time or by a polynomial fit such as a Lagrangian are two variations of the first method of interpolation polynomials. The position for a  $n$ th degree Taylor series expansion is given as

$$\vec{R} = \sum_{n=0}^N \frac{\vec{r}^{(n)}(t) \cdot t^{n-1}}{(n-1)!}$$

where

$\bar{r}(\tau)$  = the Kth range derivative

t = system time

$\tau$  = time interval defined between zero and time equal t.

Keplerian orbit coefficients may be employed which establish the satellite in an inertial frame of reference as defined by the classical two body problem of Newtonian mechanics. A set of 13 parameters which are defined in detail in Section 4 is employed.

Numerical integration of the central force field equations may be employed to generate velocity and subsequent position but this method requires both initialization data on each satellite, a recursive formulation of the necessary terms of the central force field equation and the need to transmit the central force field acceleration vector in time as a data polynomial. Numerical integration calculations would be required in the user equipment. Serious consideration was not given to this technique in the analysis.

To contrast the functional representations with the discrete consider the following example. The cartesian coordinates could be defined by three polynomials with time as the independent variable. One estimate\* indicates that no more than eight coefficients would be required to cover a data span of 24 minutes. In this case, there would be 24 total coefficients plus the time reference  $t_0$ . Assuming 29 bits per coefficient, 725 bits maximum would be required to cover 24 minutes. Also assume that half the data bits are used for the ephemeris and that the user must receive three complete ephemeris words for validation through majority vote. By this calculation,  $3 \times 725/25$  bps, we find that the user will receive 24 minutes of orbital data in 87 seconds. The polynomial expansion takes the form:

$$F(t) = (((((((A_7 t + A_6) t + A_5) t + A_4) t + A_3) t + A_2) t + A_1) t + A_0$$

Thus, 21 multiplications and 21 additions are needed for each three dimensional SV position to be computed.

### 3.3 Coordinate Frame Definitions

Two basic coordinate frame selections are considered for the formulation of the ephemeris data: the earth fixed coordinate system and the inertial reference coordinate system.

3.3.1 Earth Fixed Coordinate System — The user will be navigating with respect to an earth fixed coordinate system such as latitude and longitude, northing and easting, etc. The

\*Reference 1: Robinson, J. V., "Optimum Interpolation Interval and Order in Satellite Ephemerides," NWL Technical Report TR-2372, April, 1970.

position of the SV emitter must be defined in an earth fixed coordinate system in order that range measurements to the beacon can be converted to a user position fix. The advantage of providing ephemeris data in earth fixed coordinates is obvious, since it is the coordinate system ultimately required by the navigator

**3.3.2 Inertial Reference System** — The SV orbit is in an inertial plane which remains relatively fixed while the earth constantly rotates. An inertial coordinate system is, therefore, better suited to describing the SV position in space as a function of time. Although, the user would have to convert from the inertial frame to earth fixed coordinates before computing a position fix, there are three primary advantages to using the inertial frame:

- 1) **Alert Calculations** — A number of applications will require that future positions of each SV be computed. For example, a submarine rising to take a position fix with minimum exposure time. Accurate alerts also will be required for direct acquisition of the P signal and for evaluating which of the available SV signals should be tracked to minimize GDOP. Clearly, alert calculations are straightforward when a set of inertial (Kepler) orbit parameters are available; without them alert calculations are very difficult.
- 2) **Minimize Data Transmission and Storage:** Because the SV moves in an inertial frame, its position can be described by a small number of "Kepler Parameters" plus a set of slowly varying, small magnitude, displacement terms defining the SV's deviation from the Kepler orbit. As a result, data storage and transmission time is conserved. These savings may be important in extending the message validity duration before another up-load is required, in permitting greater redundancy in the received message, and in providing message room for other satellite Kepler orbit alert parameters.
- 3) **Duration of Orbit Description** — Figure 3.3.2-1 indicates that it would not be desirable to define more than about 30 minutes of the SV orbit with three polynomials of eight coefficients each. Perhaps this span can be increased by interpolating through non-uniformly spaced orbital positions (Chebychev sampling) so that a span of one hour may be achieved. Thus, 25 coefficients would be required with suitable redundancy every hour. By contrast, the same number of inertial parameters would likely define more than four hours of orbit, and subsequent data requirements would be minimal.

Use of inertial coordinates will have little impact on the sophisticated user because of his extensive computing capacity. However, the requirement for converting from inertial coordinates to earth fixed coordinates could be a substantial burden to the unsophisticated user. Section 4 contains an evaluation of this impact as a fraction of the basic position fix calculation.

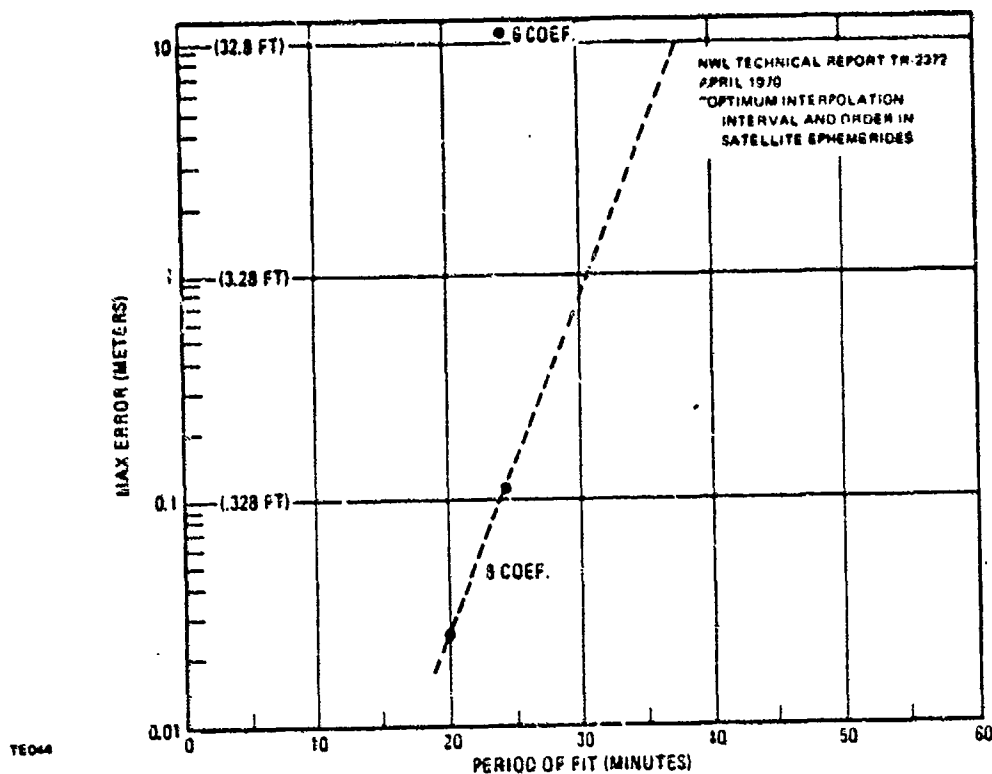


Figure 3.3.2-1. Maximum Interpolation Error for 11,000 nmi Orbit versus Interpolated Interval for Polynomials with 6 or 8 Coefficients

#### 3.4 Data Spans and Overlap

Functional representations provide a capability for defining the satellite orbit for an extended interval of time in contrast to the discrete representation.

Figure 3.3.2-1 shows that there is a limit to the time span over which an orbit can be described by a single set of functional parameters. Reference 1\* examines errors of fitting an orbit span by interpolating through evenly spaced points to produce polynomials describing earth fixed cartesian coordinates. It is well known that a polynomial interpolation through evenly spaced points has minimum error near the central points and increasing error toward the extreme points. The Naval Weapons Laboratory takes maximum advantage of this property by using "central interpolation", i. e., by using the polynomial to describe position only within the central interval. The maximum error from this process is plotted in Figure 3.3.2-1 as a function of number of coefficients and length of the central span for an 11,000 nmi orbit. For a maximum error of one foot, it would appear that eight coefficients are required and a maximum span of about 30 minutes may be possible.

\*Reference 1: Robinson, J. V., "Optimum Interpolation Interval and Order in Satellite Ephemerides," NWL Technical Report TR-2372, April, 1970.



A functional orbit representation must be provided with overlap. This is because a finite time interval is required to acquire and verify a new set of orbit parameters, even assuming simultaneous and continuous demodulation of the message from every SV. In addition, most user equipment will multiplex one or two tracker/demodulator circuits from one signal to the next in order to minimize equipment cost. The result is that most users will demodulate the message only part of the time. Therefore, the functional description of the orbit obtained at one sample time must remain valid at least until the user equipment has the opportunity to sample the message again. It would be very unfortunate if all orbit parameters became "invalid" simultaneously. If central interpolation with either earth fixed or variable portions of the inertial coordinates is employed for the orbital parameters, the functional parameters will continue to be valid and accurate for a considerable period of time after the central interval has been passed and before a new set of coefficients are received. This helpful fact exists because the interpolation polynomial has zero error (within roundoff), when passing through one of the interpolated points.

For a short time beyond the central interval the error will continue to be acceptably small simply because the polynomial approximation is near a point of zero error. This characteristic probably is sufficient to provide the necessary overlap from one functional definition to the next.

#### 4. MECHANIZATION COMPARISONS

Using the criteria defined for the evaluation in section 2.3 the following distinct comparisons are detailed.

##### 4.1 Discrete Versus Functional Representation

The comparison result matrix for the two distinct forms of ephemeris representation may be summarized by the data in Table 4.1-1. Note that accuracy is not included in this comparison since initial accuracy and resolution can be assumed to be equal.

4.1.1 Functional Mechanization Comparison — The use of either a polynomial or a Kepler orbital ephemeris against the evaluation criteria is given in Table 4.1.1-1. The specific polynomial is estimated to be an 8th order to satisfy the accuracy requirements. Accuracy of a Kepler set of coefficients with variable parameters at medium satellite altitudes needs to be researched further but is within the range indicated below.

Estimation of the data word bits for the polynomial versus the Kepler orbit is based on the following derivations. An Everetts polynomial (or basically any other) will employ words for three dimensions of position or velocity of

$$3(n+1) = \text{words}$$

$$n = \text{degree of the polynomial}$$

Table 4.1-1. Representation Comparison

Trade Item	Trade Criteria			
	RAM Memory Requirement	Computation Complexity	Data Bits Required (Per Satellite)	Perishability
Discrete	Minimal to None	None	100-200 for each state	2-6 Seconds
Functional	Up to 200 16 bit words per satellite	Moderate calculation	500 to 1000	20 Minutes to 4 Hours

Table 4.1.1-1. Functional Comparison

Trade Item	Trade Criteria				
	RAM Memory Requirement (Storage & Execution)	Computation Complexity	Data Bits Required (Per Satellite)	Accuracy	Perishability
Polynomial	Fifty 16-Bit words per satellite	Moderate No conversion required	1000 bits for each state	1 foot < 10 <sup>-3</sup> ft/sec	20-30 Minutes
Kepler Orbit :	One-Hundred 16-bit words per satellite	Most extensive but provides inherent alert data	500 Bits	(1 foot) Unknown but within 0.05 ft/sec	Up to 4 Hrs Even longer with reduced accuracy

Assuming that a 32 bit word resolution is employed the resultant bit totals are:

$$3(n+1)(32) = \text{number of bits}$$

For  $n = 8$  as indicated by Reference 1 the polynomial technique will require a maximum 864 bits of data words. Since all coefficients do not require 32 bits, the number of bits transmitted is less than the maximum. In contrast the Kepler orbit method is based on the utilization of 13 basic parameters and hence the data bits for the same assumed resolution will yield

Note that a velocity data parameter is not contemplated since the velocity term can be derived from the positional variations.

The assumption of a full set of 13 parameters which includes the variable parameters is a maximum design concept which may be reduced in scope. By using the inertial coordinate frame to describe the orbit, it will be necessary only to describe the deviation of the satellite from a perfect Kepler ellipse. With a 12-hour orbit, these deviations will be very small in magnitude and will change very slowly. Therefore, it should be possible to describe these variable parameters in a functional format with very few coefficients, having small magnitude, and maintaining accuracy over a very long orbit span. The independent variable may be time, or it may be mean anomaly. A study to resolve these questions is indicated.

#### 4.2 Supportive Analysis

The following information represents additional data relevant to obtaining a definitive selection or corroborating facts relevant to the candidates.

4.2.1 Selection of Specific Polynomials — A comment or two may be in order concerning the method of obtaining the functional orbit representation. These comments will be limited to the process of interpolation to obtain a polynomial approximation of the "true" function. There are many interpolation methods, e.g., various Lagrange interpolation formulas, Aitken's method, Taylor expansion, several Newton difference formulas, Everett's Formula (with and without throwback), Bessel's formula, Thiele's formula, etc. In addition, it is possible to interpolate with a combination of orthogonal polynomials, e.g., Chebychev polynomials. Regardless of the technique, and regardless of how the results may be masked to appear different, "given the  $n+1$  sample points, the corresponding  $n$ 'th degree polynomial passing through these points is uniquely (within roundoff errors) determined, regardless of how it is constructed or the particular notation used." In other words, "The same sample points must lead to the same polynomial".\* The method of interpolation should be chosen at the convenience of the Ground Control Segment. The polynomial seen by the user equipment will be the same regardless of the method of derivation.

The use of Chebychev polynomials has been suggested as a method of interpolating orbits.\*\* It can be shown that the resulting polynomial reduces to a standard power series when  $n+1$  sample points are used to obtain an  $n$ 'th degree polynomial. However, the theory of Chebychev polynomials does offer a method of minimizing the maximum fit error over a long

\*Numerical Methods for Scientists and Engineers, Hamming, R. W., McGraw Hill, 1962.

\*\*Reference 2: Corio, A. J., "The Use of Chebychev Polynomials for Satellite Ephemerides," COMSAT Technical Review, Vol. 3, No. 2, Fall 1973.

interval. This method requires that the resulting polynomial be fit through non-uniformly spaced points which are located at the roots of the next higher order Chebychev polynomial. The result will be to minimize the maximum error at the expense of the overall RMS or average error. This technique runs counter to the concept of central interval interpolation, which provides overlap. It would seem profitable to study and compare these two concepts.

4.2.2 Definition of Kepler Orbit Parameters — A reasonable set of Inertial or Kepler orbit parameters are the following:

#### Fixed Parameters

$t_p$  = time of perigee

$n$  = mean motion

$\omega_0$  = argument of perigee

$\dot{\omega}$  = rate of change of argument of perigee

$e$  = eccentricity

$A_0$  = semi-major axis

$\Omega_0$  = right ascension of ascending node

$\dot{\Omega}$  = rate of change of right ascension of ascending node

$C_i$  = cosine of inclination

$A_G$  = right ascension of Greenwich

$S_i$  = sine of inclination

#### Variable Parameters

$\Delta E_k$  = correction to eccentric anomaly

$\Delta A_k$  = correction to semi-major axis

$\eta_k$  = out of plane orbit component

These parameters may be converted to earth fixed cartesian coordinates for any time  $t$  by the following formulas:

$$t_k = t - t_p$$

$$M_k = n t_k$$

$$E_k = M_k + e \sin M_k + \Delta E_k$$

$$A_k = A_0 + \Delta A_k$$

$$u_k = A_k (\cos E_k - e)$$

$$v_k = A_k \sin E_k$$

$$\omega_k = \omega_0 - |\dot{\omega}| t_k$$

$$x'_k = u_k \cos \omega_k - v_k \sin \omega_k$$

$$y'_k = u_k \sin \omega_k + v_k \cos \omega_k$$

$$z'_k = \eta_k$$

$$B_k = (\Omega_0 - A_G) + \dot{\Omega} t_k$$

$$x_{sk} = x'_k \cos B_k - y'_k C_l \sin B_k + z'_k S_l \sin B_k$$

$$y_{sk} = x'_k \sin B_k + y'_k C_l \cos B_k - z'_k S_l \cos B_k$$

$$z_{sk} = y'_k S_l + z'_k C_l$$

As formulated, these equations require the following number of steps:

15 additions or subtractions

22 multiplications

7 trigonometric (sine, cosine) derivations

Performing these steps manually with a Hewlett-Packard hand calculator would be quite feasible. It is estimated that the entire process could be completed in less than 3 seconds by an HP-65 programmable calculator after entry of the orbit parameters. Calculation of subsequent points would require entry of only the new time  $t$  and the three new variable

parameters  $\Delta E_k$ ,  $\Delta A_k$ , and  $\eta_k$ . In computing alert coordinates, the variable parameters would be ignored.

It is useful to note that the magnitude of the variable parameters is quite small. For example, variable parameters for satellites only 600 nmi above the earth never exceed the following limits:

$$\Delta E_k < 0.1 \text{ degree, or about } 13 \text{ km}$$

$$\Delta A_k < 10 \text{ km}$$

$$\eta_k < 1 \text{ km}$$

All three parameters can be transmitted with a resolution of 0.1 meter with fewer than 51 bits total. For satellites at an orbital height of 11,000 nmi, where the effect of gravity anomalies and their rate of change are many times less than at 600 nmi, the magnitude of these variable parameters will be greatly reduced. Therefore, a simple definition of the parameters as a function of time or of mean anomaly should suffice for many hours, and perhaps for an entire orbit.

Detail examination of these concepts would be a useful extension to the present study.

4.2.3 Kepler Conversion Calculation — The Kepler conversion equations present no problem to even a modest minicomputer. The question is whether they represent a major burden to the very low cost user equipment with minimal computational capacity. To determine this, the equations were coded for the Intel 8080 microcomputer, which represents the type of minimum computer power to calculate a position fix. This type of microcomputer is similar to those in the more sophisticated hand calculators.

The Kepler conversion program assumed availability of an interpretive "math pack" which would perform floating point arithmetic and trigonometric functions when called by single-word pseudo-instructions. This technique significantly reduces the number of program instructions required, at the expense of a slightly longer computing time.

The program requires 169 eight-bit words of program storage in read only memory (ROM) and 34 eight-bit words of storage in temporary random access memory (RAM). The number of each class of instruction and their execution times are:

<u>Function</u>	<u>Events</u>	<u>Time Each (msec)</u>	<u>Time Total (msec)</u>
sine/cosine	7	39.0	273.0
FLD/FST	38	0.05	1.9
FAD	8	0.4	3.2

<u>Function</u>	<u>Events</u>	<u>Time Each (msec)</u>	<u>Time Total (msec)</u>
FSB/FSR	7	0.5	3.5
FMP	23	2.0	46.0
Overhead	84	0.07	5.9
			<u>333.5</u>

4.2.4 Basic Navigation Calculation — In order to scale the difficulty of converting Kepler parameters to earth fixed cartesian coordinates, it is useful to consider the least complex set of navigation equations to be solved. This set assumes:

- 1) A two-dimensional solution is adequate.
- 2) Only three pseudo-range measurements will be made per position fix, i. e., the solution is not over determined.
- 3) Each position fix is independent of all others and of other navigation aids, i. e., no least squares or recursive filtering will be employed.

The parameters available to the position fix calculation are:

#### Input Navigation Parameters

- $x_{s1}, y_{s1}, z_{s1}$  = position of SV No. 1
- $x_{s2}, y_{s2}, z_{s2}$  = position of SV No. 2
- $x_{s3}, y_{s3}, z_{s3}$  = position of SV No. 3
- $\phi$  = estimate of navigator's latitude
- $\lambda$  = estimate of navigator's longitude
- R1 = measured range to SV No. 1
- R2 = measured range to SV No. 2
- R3 = measured range to SV No. 3
- $K_1$  = semi-major axis of the earth
- $K_2$  = semi-minor axis of the earth
- H = height over the spheroid

The minimum complexity position fix calculation involves the following steps:

- 44 add/subtract
- 58 multiply/divide
- 4 trigonometric (sine, cosine)
- 4 square root

Therefore, it is clear that the fix calculation is slightly more complex than the conversion from Kepler to cartesian coordinates. Assuming the following times to perform each calculation step:

- 0.4 msec for add/subtract
- 2.0 msec for multiply/divide
- 39.0 msec for trigonometric
- 14.0 msec for square root

and adding a 3% overhead for data handling, the fix calculation will require 356 msec per iteration, whereas the Kepler conversion required 333 msec per satellite. The total time per fix, assuming one iteration is sufficient, will be approximately 1.4 seconds when using an Intel 8080 microcomputer, exclusive of other computer functions (e.g., control, data acquisition, dead reckoning, etc.). This rate would seem entirely adequate for any low cost application in which a microcomputer would be employed rather than a more expensive minicomputer.

Earlier it was shown that the Kepler conversion program could be implemented in 169 eight-bit Intel 8080 instruction words exclusive of the "math pack" subroutines. A reasonable estimate of the fix program size may be obtained by the ratio of the number of arithmetic steps (110/44) times the Kepler conversion requirement (169), which gives 423 eight-bit words. It would appear that the read only memory (ROM) storage requirements for these two functions is approximately:

$$\begin{aligned} 169 \times 8 &= 1352 \text{ bits for Kepler conversion} \\ \underline{423 \times 8} &= \underline{3384} \text{ bits for fix calculation} \\ 592 \times 8 &= 4736 \text{ bits total for these functions} \end{aligned}$$

Semiconductor ROM's are available today which store 4096 bits of program. Therefore, it seems likely that the entire microcomputer program (including math packs, I/O packs, etc.) could be contained on two or at most three LSI integrated circuit chips.



## 5.0 SELECTION

As a result of the data available at this time the selection of some specific conclusions and approaches is considered below.

### 5.1 Discrete versus Functional Recommendation

The impact on the SV or on the Ground Control System of choosing either the discrete representation or the functional ephemeris format is minimal if the SV memory is implemented as part of a programmable processor. Only through use of a programmable processor will the option remain open to choose either approach throughout the Phase I development and experimental stages.

The impact on the user equipment is a tradeoff between minimum computational requirements on the one hand and the ability to multiplex the data acquisition process from one SV to the next on the other hand, thus saving hardware. Considering the magnitude of the overall position fix calculation and the rapidly decreasing cost of computational capability, it seems clear that the advantages of the functional ephemeris outweigh those of a discrete position ephemeris.

### 5.2 Coordinate Frame Selection

An alert capability will be needed for optimum application of the GPS. It is clear that to be practical, orbit parameters permitting calculation of the SV position hours, days, or months in advance must be referenced to the inertial frame. There are three methods for providing inertial parameters for all GPS SV's:

- 1) Transmit them by means other than the GPS message.
- 2) Include them in addition to earth fixed parameters in the GPS message.
- 3) Transmit only inertial coordinates in the GPS message, including other-satellite alert parameters.

Because we feel that the GPS system should be entirely self-sufficient and not dependent on data entry from other sources, we recommend against the first alternative. Because we have shown that the impact of inertial parameters is negligible and because there would have to be two types of conversion routines, we also recommend against the second alternative.

The following is recommended:

- 1) All orbit parameters should be referenced to an inertial coordinate frame.
- 2) The transmission of other-satellite inertial coordinates should be provided for system-wide alerts. These may consist of coordinates for the "lead" SV in each orbit plane plus phasing parameters for the other satellites in each plane.

3) Several key issues concerning Kepler orbit accuracy at medium altitudes still need to be resolved. Study efforts should be conducted by agencies such as the Naval Weapons Laboratory, Aerospace Corp., or contractor activities which are experienced in precise orbit determination to accomplish the following:

- a) Establish precision requirements of each orbit parameter.
- b) Determine scaling, functional format, and functional duration of the variable parameters required to define position in the 12 hour orbits to within 0.3 to 1.0 foot accuracy.
- c) Compute the alerting accuracy degradation to be expected with the 12 hour orbits when using only a minimal set of fixed inertial parameters.

### 5.3 Kepler Functional Representation

Results of the initial concept evaluation show that the Kepler orbital conversion process is less than half as large as the least complex position fix calculation and that its impact on total system cost and complexity is less than one integrated circuit of read only memory (ROM). It is concluded that the impact is negligible for even the least sophisticated GPS system.

The example problem derived in section 4.2 has established the program storage and computation time requirements to convert Kepler orbit parameters to earth fixed cartesian coordinates. The evaluation has been based on use of a commercially available microcomputer (the Intel 8080) which would be typical of the computer found in the lowest cost GPS user equipment. This level of computing power is equivalent to that provided by recent generations of hand held calculators.

In addition to determining that about 1352 bits of program storage will be required for the Kepler conversion routine and that approximately 333 msec will be required per satellite per position fix, these parameters were compared with the least complex position fix calculation. The fix calculation will be required regardless of the format in which the orbit positions are defined. As shown below, the Kepler conversion requirements are comparable with the required fix calculation:

<u>Fix</u>	<u>Kepler</u>	<u>Parameter</u>
44	15	Add steps
58	22	Multiply steps
4	7	Trip steps
4	0	Square root steps
110	44	Total steps
3,384	1,352	Bits of storage
356 msec	333 msec	Execution time

The conclusion based on the results to date is that although the Kepler data format requires more user calculations than other data formats, the added complexity will be very small when compared with the overall cost of even the least expensive GPS user equipment. The low cost equipment consists of a single-frequency L-band receiver with sequential tracking of three signals PN modulated at about one MHz, coupled to a modest computer system with provision for display to and keyboard input from a human navigator. For low cost equipment a micro computer (or a micro processor) will be employed to perform the position fix calculations. The use of Kepler orbit parameters will require a modest increase in the size of this micro processor memory. The additional memory considered sells today for less than \$10 in 100 lot quantities. The additional computational time of less than one second per position fix seems negligible for the low cost user for whom a fix update every 6 to 10 seconds appears to be more than adequate.

TRADE STUDY NO. 9

EPHEMERIS DETERMINATION

F. Lisenbe

R. Leger



**GENERAL DYNAMICS**

*Electronics Division*

P.O. Box 81127, San Diego, California 92138 714-375-7701

SYSTEM/DESIGN  
TRADE STUDY REPORT  
FOR  
GLOBAL POSITIONING SYSTEM  
CONTROL/USER SEGMENTS

TRADE STUDY NO. 9  
EPHEMERIS DETERMINATION

by

A. J. Van Dierendonck  
R. M. Leger  
F. F. [unclear] nbe

CS/UE DEFINITION CONTRACT  
F04701-73-C-0298

Prepared for  
Space and Missiles Systems Organization  
Los Angeles, California 90045

DATA ITEM A002

ADDENDA

**GENERAL DYNAMICS**

*Electronics Division*

P.O. Box 811 of, San Diego, California 92128 714-279-7301

40 88

## CONTENTS

<b>1</b>	<b>INTRODUCTION</b>	
1.1	Objective . . . . .	1-1
1.2	Approach . . . . .	1-1
1.3	Other Factors . . . . .	1-1
1.4	Document Outline . . . . .	1-1
<b>2</b>	<b>REQUIREMENTS</b>	
2.1	Functional . . . . .	2-1
2.2	Design . . . . .	2-1
2.3	Ground Rules . . . . .	2-3
<b>3</b>	<b>CANDIDATE EPHEMERIS DETERMINATION ALGORITHMS</b>	
3.1	Measurement Sets . . . . .	3-1
3.2	Reference Trajectory . . . . .	3-4
3.3	Kalman Versus Batch . . . . .	3-6
3.4	Partial Derivatives and State Vectors . . . . .	3-7
3.5	Coordinate Frames . . . . .	3-10
<b>4</b>	<b>EVALUATION ALGORITHM</b>	
4.1	Evaluation Criteria . . . . .	4-1
4.2	Cost Functions . . . . .	4-2
4.3	Scoring Algorithm . . . . .	4-4
<b>5</b>	<b>ANALYSIS OF CANDIDATES</b>	
5.1	Preliminary Analysis . . . . .	5-1
5.2	Detailed Analysis . . . . .	5-4
<b>6</b>	<b>SELECTION</b>	
6.1	Candidate Recommendation . . . . .	6-1
6.2	Expandability to 4 and 24 Satellites . . . . .	6-1
6.3	Requirements Imposed on Total System . . . . .	6-2
<b>7</b>	<b>ADDITIONAL MODELING REQUIREMENTS</b>	
7.1	Significance of Additional Modeling . . . . .	7-1
7.2	Clock Models . . . . .	7-2
7.3	Solar Radiation Pressure Models . . . . .	7-10
<b>8</b>	<b>OUTLINE OF FUTURE ANALYSES</b>	
8.1	Planned Analyses Tasks . . . . .	8-1
<b>9</b>	<b>REFERENCES</b>	9-1
	<b>APPENDIX A. APPROXIMATING CLOCK DRIFTS</b>	
	<b>APPENDIX B. SV CLOCK CORRECTION UPLOAD AND DOWNLINK FORMAT AND CS AND US SEGMENT COMPUTATIONAL REQUIREMENTS</b>	

## ILLUSTRATIONS

5-1	Position error of satellite 3. . . . .	5-1
5-2	Velocity error of satellite 3. . . . .	5-2
5-3	Time base error in clock in satellite 3. . . . .	5-2
5-4	Time base rate error in clock in satellite 3. . . . .	5-2
5-5	Time base error at monitor 1 for satellite 3. . . . .	5-2
5-6	Time base rate at monitor 1 for satellite 3. . . . .	5-3
5-7	Actual vs possible measurements for satellite 3. . . . .	5-3
5-8	Sigma and residual of user measurement from satellite 3. . . . .	5-3
5-9	Sigma and residual of range measurement monitor 1 to satellite 3. . . . .	5-3
7-1	Satellite clock standard deviation vs time. . . . .	7-4
7-2	Satellite clock rate standard deviation vs time vs Allan variance specification. . . . .	7-4
7-3	Comparison of monitor clock phase model standard deviations. . . . .	7-6
7-4	Typical solar radiation pressure – body axes. . . . .	7-11
7-5	Forces on a box plus solar panels due to solar radiation. . . . .	7-11
7-6	Box model fit to normal force of Figure 7-4. . . . .	7-12
7-7	Linear momentums along inertial axes due to solar radiation. . . . .	7-12

## TABLES

2-1	GPS Error Budget . . . . .	2 2
2-2	Clock Stability . . . . .	2 2
3-1	Measurement Sets . . . . .	3 1
3-2	Epochs and Coordinate Frames . . . . .	3-11
5-1	Preliminary Analysis Matrix . . . . .	5-1
6-1	Final Scoring Algorithm for System Candidates. . . . .	6-1

# 1

## INTRODUCTION

The GPS ephemeris determination procedure is required to provide accurate GPS satellite ephemeris and clock correction data for computing the navigation data to be loaded into the satellites. Ranging data collected at four monitor stations must be processed and combined with reference trajectory data prepared by an off-line computational facility to produce refined trajectory and clock update data for navigation data computations.

The GPS satellite complement will comprise four satellites in Phase I, up to twelve satellites in Phase II, and up to twenty-four satellites in Phase III. The ephemeris determination procedure utilized must therefore be expandable to handle the 24 satellites of Phase III, and must provide accuracies consistent with the Phase I and Phase III error budgets.

### 1.1 OBJECTIVE

This trade study was undertaken to identify the ephemeris determination technique most compatible with the GPS objectives of maximum legacy with minimum technical risk. Other factors considered were:

1. Computational load
2. Core storage requirements
3. Time line requirements
4. Ease of implementation
5. Expandability
6. Accuracy requirements

### 1.2 APPROACH

The approach utilized was to identify the candidate measurement sets and data processing algorithms, perform a preliminary evaluation to eliminate obviously undesirable candidates and, finally, to evaluate the

remaining contenders in terms of a set of weighted "cost" functions. The leading contenders were evaluated by computer simulation to aid in the final selection.

### 1.3 OTHER FACTORS

In addition to the tradeoff on the various ephemeris determination techniques, the error and force models used, or to be used, in the algorithms were reviewed. The clock models were updated to be more representative of the real world. Solar radiation force models were postulated for future analysis tasks.

Finally, future analysis tasks were formulated which will further substantiate the algorithm selected and reduce risks in its implementation.

### 1.4 DOCUMENT OUTLINE

This trade study report comprises eight sections. Section 2 reiterates the requirements and ground rules on which this study was based. Section 3 describes the candidate measurement sets, the estimation and prediction techniques, the coordinate frame systems traded off, and certain pre-tradeoff rationalizations. Section 4 presents evaluation criteria and the scoring algorithm for trades yet to be made; Section 5 describes the analysis methodology for these trades, primarily between three different measurement sets. Discarded candidate trades are scored in Section 6 along with a discussion of their ephemeris determination impact on the rest of the system. In Section 7, some modeling deficiencies are reviewed, new models generated or postulated are described, and their impact is determined. Section 8 outlines future analysis tasks. References are provided in Section 9.



# 2

## REQUIREMENTS

### 2.1 FUNCTIONAL

The Master Control Station (MCS) software performing this (ephemeris generation) function shall be designed to support the following:

a. Retrieval of reference ephemeris and corrected measurement data file.

b. Processing of retrieved data to refine reference ephemeris and support user navigation with an effective user receiver ephemeris error of no more than that specified in the GPS Error Budget (see Section 2.2).

c. Generation of the refined ephemeris data file.

*Source: SS-GPS-101A, para. 3.7.3.1.2.2.1*

The reference ephemeris generation function may be satisfied by a Government facility such as the Naval Weapons Laboratory. The software performing this function shall be capable, at a minimum, of supporting the following:

a. Editing of raw measurement data.

b. Correction of pseudo-range and range rate measurement data for atmospheric effects.

c. Generation of reference ephemerides that are valid for at least 14 days for all GPS satellites. In this case, valid means that the reference ephemerides are accurate enough so that linear corrections to the reference ephemerides can be made on a daily basis to satisfy the GPS error budget.

*Source: SS-GPS-101A, para. 3.7.3.1.2.2.6.*

The MCS software performing the SV clock update function shall support the following:

a. Retrieval of the refined ephemeris file and the most current corrected measurement data file received from each SV.

b. Processing of retrieved data to generate a clock update (e.g., clock bias, clock

frequency offset, and relativity effect) for each SV accurate to the level specified in the GPS Error Budget.

c. Generation of a clock update file.

*Source: SS-GPS-101A, para. 3.7.3.1.2.2.2.*

### 2.2 DESIGN

The Master Control Station (MCS) and Monitor Station (MS) real time system shall be responsive to the time line requirements of system operation and calibration.

*Source: SS-GPS-101A, para 3.3.8.8.b.*

The MCS and MS software systems shall support GPS system development and operation by allowing for rapid changes in software elements. They shall be designed to minimize and localize the impact of changes or additions to the data base, operational functions and non-central hardware.

*Source: SS-GPS-101A, para. 3.3.8.8.c.*

The MCS and MS software system shall capitalize on existing software and software design to the maximum extent possible (consistent with system operation and accuracy).

*Source: SS-GPS-101A, para. 3.3.8.8.d.*

The elements of the Control System Segment provide the SV tracking, information processing, and communications needed to provide updating of each SV navigation subsystem as required to support accurate user navigation.

*Source: SS-GPS-101A, para 3.7.3*

User navigation error is the statistical estimate of the error in computer user position when the user is uniformly distributed in time and position. The navigation error is the uncorrelated portion of the observed user range error multiplied by the Geometric Dilution of Precision (GDOP) for the user's position. This uncorrelated portion of the observed range error is called "User Equivalent Range Error".

*Source: SS-GPS-101A, para 6.3*

The GPS error budget is defined in terms of User Equivalent Range Error (UERE). The components of UERE for Phase III and Phase I of the GPS are shown in Table 2-1. The Phase I error budget shall be applicable for two hours after all SVs are updated. All values are the one sigma (1 $\sigma$ ) errors given in feet.

Table 2-1. GPS Error Budget

	Phase III	Phase I
Space Vehicle Ephemeris	5	12
Atmospheric Delay	8 to 17*	8 to 17*
Space Vehicle Group Delay	3	8
Receiver Noise and Resolution	5	5
Multipath	4 to 9*	4 to 9*
Total R.S.S.	12 to 21	18 to 25

\*These error quantities represent the use of different atmospheric delay correction methods and different user environmental conditions.

Source: SS-GPS-101A, para. 3.2.1.

The computational equipment at the MCS shall be sized in speed and memory capacity to support the operation of GPS Phase I software. The equipment will be selected to accommodate expansion to support the operation of twelve (12) closely-spaced space vehicles. Responsiveness as indicated by operational time lines for 12 SV's shall be considered in determining the needed computer throughput rate.

Source: SS-GPS-101A, para. 3.2.1.2.1

Data transmission between the Monitor Stations and the Master Control Station shall be accomplished at the minimum rate acceptable for providing the data communications for operation of 24 GPS Space Vehicles.

Source: SS-GPS-101A, para. 3.2.1.2.2

World-wide real-time three-dimensional capability will be achieved by deploying additional satellites (i.e., three orbital planes of eight satellites per plane).

Source: Defense Navigation Satellite Development Program Joint Program Office System Description and Development Plans, 16 September 1973, page 3.

All signal rates and carrier frequencies shall be derived coherently from the same space vehicle clock.

Source: SS-GPS-101A, Appendix II, para. 20.6.

The clock which is used to generate the navigation signal shall exhibit the stabilities listed in Table 2-2. Thermal or other changes in the SV electronics group delay shall not exceed 1 nsec over any non-eclipsed orbit period.

Table 2-2. Clock Stability

Time Since Last Calibration (sec)	Time Deviation from Prediction (nsec)	Maximum RMS RF Phase Deviation (mrads)
10 <sup>-1</sup>	0.01	160
10 <sup>0</sup>	0.01	250
10 <sup>2</sup>	1	TBD
10 <sup>4</sup>	10	TBD
10 <sup>5</sup>	100	TBD

Source: SS-GPS-101A, Appendix II, para. 20.6

The monitor station frequency standard shall be a cesium beam standard (Hewlett-Packard Model 5016A Cesium Beam Standard with Option 004) exhibiting the following characteristics:

Accuracy:  $\pm 7 \times 10^{-12}$  over a temperature range of 0 to 50 C  
 Reproducibility:  $\pm 7 \times 10^{-12}$   
 Frequency Stability:  $\pm 1 \times 10^{-13}$

Long-Term Stability:  $\pm 3 \times 10^{-12}$   
Short-Term Stability:

Time (Seconds)	Frequency Stability
$10^{-3}$	$8.2 \times 10^{-10}$
$10^{-2}$	$1.5 \times 10^{-10}$
$10^0$	$5 \times 10^{-12}$
$10^1$	$2.7 \times 10^{-12}$
$10^2$	$8.5 \times 10^{-13}$
$10^3$	$2.7 \times 10^{-13}$
$10^4$	$8.5 \times 10^{-14}$

Source: DRB D90005618, March 5, 1974  
GD/E.

### 2.3 GROUND RULES

The following ground rules were utilized in performing the ephemeris determination trade study:

a. Four monitor stations (Vandenberg AFB, Wahiawa, Elmendorf AFB, and Guam,) are utilized in tracking the GPS satellites.

b. The off-line computational facility which generates reference trajectories shall also provide accurate locations for the four monitor stations.

c. The test site against which UERE is evaluated is Holloman AFB.

d. Monitor station time, with the exception of time at the system master clock, is not required external to the GPS system.

e. The monitor station receivers are Type X user receivers.

# 3

## CANDIDATE EPHEMERIS DETERMINATION ALGORITHMS

### 3.1 MEASUREMENT SETS

The GPS provides two basic types of measurements; pseudo range based on the pseudo random code modulation, and pseudo range rate based on carrier doppler. Other derived measurements are also possible, such as pseudo range rate obtained by differentiating code-derived pseudo ranges, and pseudo range change obtained by counting carrier cycles or fractions of cycles over some specified time interval.

Under the ground rule that the monitor station receivers should be essentially user receivers of appropriate classes, receiver capabilities are dictated by user requirements. The user's requirement for a precise, rapid position fix is met by providing code ranging with two-frequency compensation for ionospheric delays. The requirement for velocity information is adequately met by carrier doppler measurements without two-frequency compensation. Therefore, the receivers do not provide for two-frequency compensation of the carrier tracking delays and the full accuracy potential of carrier tracking is not available unless the receivers are redesigned. Since receiver redesign entails considerable cost, approaches requiring extensive accuracy from the carrier channels must be charged with this cost.

Table 3-1 shows the various measurement sets considered along with data on the number and sizes of the solution vectors involved. In this table,  $S$  represents the number of satellites in the system while  $M$  represents the number of monitor stations. When  $M$  is used as a subscript in place of  $j$ , it denotes the Master Station which is defined as having a perfect (reference) clock. For each of the nine cases

shown in Table 3-1, the number of satellites,  $S$ , appears either in the column giving the number of states in the solution vector or in the column giving the number of solution vectors in the system. The computational load on the computer tends to vary approximately as the square of the number of states in a solution vector, but increases only linearly with the number of solution vectors. Thus it is desirable to avoid large solution vectors even if this means an increase in the number of solution vectors to be found.

Table 3-1. Measurement Sets

Case Measurement Set	Code	Carrier	M	No. of States for		No. of Solution Vectors	Measurements	Remarks
				4 State Solution	24 State Solution			
1 Pseudo Range	C	C	M	3S	3S	1	$R_j$	Large solution vector
2 Range Differences	C	C	M	3S	15S	1	$R_j, R_k$	Large solution vector
3 Pseudo Range Differences	C	C	M	2S	14S	1	$R_j, R_k$	Large solution vector
4 Carrier Doppler	C	C	M	3S	3S	1	$R_j$	Small solution vector
5 Carrier Doppler Differences	C	C	M	3S	3S	1	$R_j, R_k$	Small solution vector
6 Range Rate	C	C	M	3S	3S	1	$R_j, R_k$	Small solution vector
7 Range Rate Differences	C	C	M	3S	3S	1	$R_j, R_k$	Small solution vector
8 Range Rate Differences	C	C	M	3S	3S	1	$R_j, R_k$	Small solution vector
9 Range Rate Differences	C	C	M	3S	3S	1	$R_j, R_k$	Small solution vector

All the cases shown in Table 3-1 involve the solution for the three dimensional position and velocity of each satellite, the clock offset and clock rate in each satellite, and the clock offset and clock rate in each monitor station

except the master. Fixed biases such as monitor station locations and gravity harmonic terms are assumed to be adequately handled in the off-line reference trajectory computation. It is recognized however that other satellite parameters may eventually be required in the state vector for each satellite, and therefore that the complexity considered here is a lower bound.

In principle, the best accuracy solution can be achieved by exploiting all available measurements in a single large solution which takes all the correlations and interactions into account. Case 1 in Table 3-1 is an approach to such a formulation. The principal degradation from absolute optimum in Case 1 arises from neglecting the rate measurements. Early work indicated that the quality of the rate measurements was such that their inclusion improved the final solution accuracy by only a few percent while essentially doubling the computational load. Thus Case 1 is considered as a reference for accuracy against which the other cases can be compared.

From a computational point of view, Case 1 is rather expensive because of the large number of states in the solution vector. It is already expensive with the four satellites of Phase I, but it becomes entirely unreasonable for the 24 satellites of Phase III. Although Phase III could possibly be handled in a Case 1 manner by breaking the entire constellation into several groupings of satellites, this is still expensive and appears to have little advantage over a more complete breakdown of the problem into single satellite cases, as in Cases 4 and 5, etc. Thus, Case 1 is considered as an accuracy reference and the four satellite version is a viable candidate, but more than four satellites is thought to be unreasonable.

Case 2 is somewhat similar to Case 1 except that the solutions for the satellite clocks have been partitioned into separate two state vectors. This was done by using the range differences to each satellite from two monitor stations as the basic orbital measure-

ment, which now is independent of the satellite clock. Since the satellite clock solution is needed for the GPS state vector, it must then be determined separately on the basis of pseudo range from the master station (perfect clock) and the solved-for orbit. Although the number of available measurements is reduced somewhat by the requirement that two monitor stations be in sight of the satellite simultaneously, the accuracy performance of this case was close to that of Case 1. Although the maximum size of the solution vector is reduced somewhat compared with Case 1, it is still awkwardly large, especially in Phase III.

The primary cause of coupling between the various satellite orbit solutions is the fact that common monitor clock solutions are used for all satellite solutions and thus introduce correlations among the latter. The Case 2 arrangement does nothing to eliminate this coupling.

Case 3 does eliminate the coupling of the monitor clocks into the orbit solutions. In this case, a single derived measurement is defined out of all four combinations of pseudo ranges between two monitors and two satellites. The combination is such that all clocks cancel out to give a pure orbit solution. The satellite clocks are then solved-for separately on the basis of pseudo ranges from the Master Station (reference clock) and the other monitor station clocks are found by the use of pseudo ranges from them to the satellites. The requirement for simultaneous viewing by two monitors and two satellites further reduces the number of measurements available. The monitor clocks are decoupled from the orbit solutions but the orbit solutions themselves are now tightly coupled together through the derived measurements. Although a slight further reduction of the maximum size of the solution vector is achieved, it is still uncomfortably large in Phase III and awkward to divide further.

Case 4 permits a substantial reduction in the number of states in the solution vector by treating each satellite separately - as if the

other satellites were not present. The 14 states in the solution vector are: the six elements for position and velocity of the satellite, two elements for the satellite clock, and two elements for each of the three monitor clocks. As more satellites are added to the constellation, the number of 14-element solutions increases, but the size or make-up of these individual solutions is unaffected. Both the strength and the weakness of Case 4 stem from the fact that each satellite solution vector contains a solution for all monitor clocks based on measurements to the satellite in question and ignoring all other measurements. Thus, if there are  $S$  satellites, there will be  $S$  different solutions for each monitor clock, each one based on a fraction of the total number of measurements made by the monitor in question.

When Case 4 was tried in simulation and compared with Case 1, it was found to almost match Case 1 in accuracy of orbits, satellite clocks, and user navigation errors due to clocks and orbits. It was noticeably poorer in the solution for the monitor clocks because of the dilution of the measurements into the  $S$  separate solutions, but the system performance of the GPS was not noticeably degraded. If more precise monitor solutions are desired, these can be achieved by combining the  $S$  separate solutions in an auxiliary procedure. However, if these combined solutions are reinjected into the basic system solutions, this reintroduces the coupling between satellite orbits via the monitor clock solutions. Thus any such reinjection must be done with care to avoid upsetting the statistics of the main solution.

Case 5 of Table 3-1 achieves a further reduction in the size of the solution vector by eliminating the multiple solution for the monitor clocks which was used in Case 4. This is accomplished by taking some liberties with the statistics of the solutions. It is the correlations between the monitor clock solutions and the solutions for the satellite orbits plus-clocks that couple the satellite solutions to each other. The extent of these correlations can be

observed in the covariance matrix of the solutions for Case 1. Examination of these correlations shows that after the initial start-up, most are less than 10-20% with an occasional isolated term on the order of 50%. This suggests that perhaps these correlations could be ignored without substantially degrading the accuracy of the final solution, although the rate of convergence might be decreased somewhat. In Case 5 this is done by setting up a basic solution algorithm with ten states consisting of six orbit terms, two satellite clock terms, and two monitor clock terms. The six orbit terms and two clock terms associated with each satellite are combined into an eight-state vector with a corresponding  $8 \times 8$  covariance matrix and placed on a "bookshelf" in memory along with 2-state clock vectors and corresponding  $2 \times 2$  covariance matrices for each of the monitor stations (other than the master). Each pseudo-range measurement involves one satellite and one monitor station. For a measurement,  $R_{ij}$ , the 8-state vector and  $8 \times 8$  covariance matrix for the  $i^{\text{th}}$  satellite are picked from the "bookshelf" along with the 2-state vector and  $2 \times 2$  covariance matrix for the  $j^{\text{th}}$  monitor. These are combined into a 10-state vector with corresponding covariance matrix and the  $R_{ij}$  measurement is applied to produce an improved estimate after which the results are again broken into 8-state and 2-state pieces and replaced on the "bookshelf" where they are available for the next measurement. With this arrangement, coupling between various satellite orbits occurs on a sequential basis through the common use of the monitor solutions; but the cross correlations between monitors and satellites within any one measurement are ignored. The degree of approximation involved in doing this becomes smaller as more satellites are added to the constellation because a single measurement is less able to influence a monitor clock estimate that is already weighted by measurements from many other satellites. When this case was simulated with four satellites, the covariance estimates looked very

favorable but the estimated residuals exhibited some initial transients which pushed the monitor clocks into erroneous estimates from which they recovered only very slowly. On the other hand, performance was good once the transients died out and the preliminary attempts at speeding up the convergence appear to be promising. Case 5 can be seen, in principle, to be almost equivalent to Case 4 with reinjection of the combined monitor clock solutions at every step. However Case 5 is more efficient because of the smaller state vector, provided the convergence can be improved.

Case 6 is somewhat like Case 5 except that different measurements are used and the 8-state and 2-state vectors are not combined into 10-state vectors. The 8-state satellite orbit-and-clock vector is solved by the use of pseudo range rate measurements and pseudo ranges from the master station. The latter are needed to set the satellite clock phase and they strengthen the orbit solution. This scheme recovers quickly from the initial transient because the use of rate measurements involves one less integration in the solution loop than is the case with the pseudo range measurements of Case 5. The principal drawback to Case 6 is the fact that in order to get adequate accuracy in the orbit solution, the pseudo range rate accuracies must be of the order of 5 millifeet per second or better and this would require a redesign of the user receiver. Thus it represents an expensive solution to the problem.

Case 7 is a cross between Cases 2 and 6. It has the same accuracy problem as Case 6, and is slightly inferior because two range rate measurements are combined into each range rate difference measurement.

Case 8 is entirely analogous to Case 6, except that effective rates are obtained through differences of ranges taken at different times instead of direct differentiation of carrier data. If the time intervals are long enough, adequate accuracy is achieved in spite of the relatively large errors of the individual pseudo-range

measurements. Thus, the advantages of Case 6 are achieved without the requirement for an expensive receiver redesign. Simulation results show good transient recovery and an accuracy which, although adequate, is inferior to that obtained with pseudo ranges directly.

Case 9 is analogous to Case 7. Although it would undoubtedly perform acceptably, it does not offer enough advantages over Case 8 to be worth the additional complication.

### 3.2 REFERENCE TRAJECTORY

The question here is whether or not to split the overall orbit determination process into two parts, one consisting of the computation in a laboratory environment of a long-term reference orbit, and the other consisting of an on-line refinement of this orbit estimate (on the basis of current field measurements) to a quality suitable for the navigation application.

The GPS orbit determination task involves the prediction of very precise satellite ephemerides and atomic clock calibrations on the basis of intermittent field measurements which compare the readings of satellite-borne clocks with others on the ground. The refined orbits must be obtained to high precision and used to update the system on an on-line basis, including calibration of the clocks. At the same time a very precise dynamic model is required in order to yield the needed predictability of the orbits.

The use of a long-term reference trajectory permits these two critical aspects of the problem to be split up into an off-line laboratory handling of the latter along with an on-line refinement process. Since the "know-how" and software for precise dynamic modeling and long-term orbit determination already exist at installations such as the Naval Weapons Laboratory, a considerable savings in software development cost and on-line computer requirements can be achieved in Phases I and II of the GPS program by using this existing capability.

On the basis of measurements from the field, the NWL facility would periodically

generate a long-term reference trajectory using a very detailed force model to include all the fine-grain perturbations which might be expected. Although this trajectory will gradually drift away from the true trajectory it will retain the fine-grain short-term behavior of the true trajectory so that it can be used as an interpolating function. Furthermore, it may be used in this capacity until its deviation from the true trajectory grows to the point where second-order perturbation terms cease to be negligible. This condition holds for deviations up to 1000 feet or so and should make the reference trajectory useable for several weeks.

The off-line reference trajectory computation can account for detailed gravity models including earth zonal and tesseral harmonics, sun, moon, etc., as well as such fixed parameters as the locations of the monitor station antennas. Drag should be negligible at the GPS altitudes but solar radiation pressure is critical. The latter will need to be carefully modeled — to the order of 1% or so for Phase III. The parameters affecting the force on the satellite from solar radiation flux are no better known during the on-line tracking phase than they were when the reference trajectory was generated. Therefore the modeling of this force should also be made a part of the off line computation.

The reference trajectory emanates from some epoch time,  $t_0$ , from which the dynamic model is integrated in detail to yield the trajectory, projected into the future. At the same time, variational equations are integrated to yield partial derivatives of the trajectory at any later time,  $t$ , with respect to conditions at the epoch time. As long as the refined trajectory computed by the on-line facility stays within the linear range of the reference trajectory (1000 feet or so), points at different times along the refined trajectory can be related to each other through the use of these partial derivatives and the reference trajectory. This technique achieves the desired relationships to the full detail of the dynamic model

used in the integration of the reference trajectory without requiring any integration at all by the on-line facility. Thus the on-line computation is relieved of the necessity of evaluating or integrating the detailed force model and can concentrate on its on-line functions.

A two-way interface is required between the on-line and off-line facilities. The on-line facility collects the field measurements and uses them to refine the reference trajectory in terms of a "prediction for tomorrow" or perhaps somewhat longer. It also periodically forwards these measurements to the off-line facility (e.g., once a day). The off-line facility processes these measurements for several days or weeks and periodically (e.g., once every two weeks) issues a new long-term reference trajectory. This is forwarded to the on-line facility for day-by day refinement.

During the first phase of the GPS program the activity level of the off-line reference trajectory computation should be low enough to be absorbable in the existing NWL facility without serious interface problems. During the third phase, the level of activity and interface will rise to a point where it would probably be more feasible to provide the off line capability alongside the on line facility. The basic software design used in Phases I and II could be retained. Phase II represents an in-between case with a moderate work load and the handling of this phase should depend on the availability of the necessary resources at NWL.

A possible difficulty with the separate reference trajectory in Phase I and perhaps Phase II, could arise out of station keeping operations. It may be assumed that such operations would be preplanned and would be included in the reference trajectory supplied prior to performing the maneuver. A typical station-keeping maneuver may consist of a single impulse of approximately 1 ft/sec. in approximately the direction of the velocity vector. The uncertainty with which this impulse can be applied determines how rapidly the trajectory will deviate from the predicted



one. For example: let the magnitude of the impulse be controllable to within 0.1%; let the attitude of the earth-pointing axis be known to within 10 milliradians; and let the yaw attitude be known to within 25 milliradians. This yields velocity uncertainties in the down-range, vertical, and cross-range directions of 0.001, 0.01, and 0.025 ft/sec, respectively. The corresponding maximum partial derivatives of position within the next 24 hours with respect to the above velocity errors are 25,000, 28,000, and 7000 ft per ft/sec, respectively. The maximum position uncertainties within the next 24 hours due to the three components of velocity error are then 250, 280, and 175 ft. For additional days, these maximum deviations may increase at a rate no greater than linear. This will still cause a deviation of the trajectory out of the linear neighborhood of the reference trajectory within a few days. Thus a new reference trajectory will probably be needed within a few days of each station-keeping maneuver.

### 3.3 KALMAN VERSUS BATCH

With the small state vectors involved in the most attractive measurement sets of Section 3.1, the amount of arithmetic involved in the solutions becomes almost trivial and this ceases to be a significant factor in the choice of Kalman versus batch processing.

More pertinent is the behavior of the solutions in the two techniques, particularly in the presence of process noise. If the process noise is very low so that a long span of data can be included in a single batch, then the batch process works very well. If, on the other hand, the process noise is somewhat higher, a dilemma develops in the batch process. If the data span is too long, the state vector changes from one end of the span to the other due to process noise, so that measurements at the two ends of the span are not measuring the same thing and the accuracy of the solution decreases. On the other hand, if the span is too short, there may not be enough exercise of system parameters (e.g., geometry) over the

span to permit the separation of some of the similar parameters in the solution. In this case the  $H^TWH$  matrix becomes nearly singular and cannot be accurately inverted.

In a Kalman filter there need never be a singular matrix to invert and high process noise is handled very naturally by the addition of the  $Q$  matrix to the projected covariance matrix. This has the effect of exponentially de-weighting or "forgetting" old measurements in proportion to their current age and the amount of process noise present. This exponential forgetting function is sometimes approximated in batch processing by adding a fraction of the results of the previous batch to the estimate of the current batch in a process called recursive batching. It can be done in a way which makes it mathematically identical to the forgetting function in a Kalman filter; this is rather expensive computationally and is usually only approximated. Without recursive features, the batch process assumes zero process noise within the batch but no memory to data outside the batch. For a continuous process, the exponential weighting is more reasonable unless the process noise is very low.

In the GPS solution vector there are two kinds of parameters: orbit parameters, and clock parameters. The process noise for the orbit parameters must be kept very low if the orbits are to be adequately predictable into the future. Furthermore, at the GPS altitudes there is essentially no drag and the gravity terms are very computable. The principal remaining uncertainty is solar radiation pressure; attempts will be made to predict this as accurately as possible so as to minimize the orbital process noise. The period of a GPS orbit with respect to the set of monitor stations on the rotating earth is 24 hours. Thus, a 24 hour batch will contain essentially all the exercise of geometry available to the system so that there is no need to extend a batch to longer than 24 hours except to take advantage of data accumulation from day to day. Such accumulation could be accomplished with a recursive batch process

with daily batches. This is particularly appealing since the plan is to load the state vector of "tomorrow's orbit prediction" into the satellite only once a day so that a daily batch solution would fit well.

However, the situation is complicated by the clocks. Although atomic clocks are remarkably stable, in terms of the requirements for GPS their process noise is rather high. For example, a clock whose frequency is accurate to within one part in  $10^{12}$  can drift enough in 24 hours to cause an error of 102 feet in pseudo-range measurement. This is clearly not negligible when compared with measurement instrument errors of just a few feet. Furthermore, these clock parameters affect all the system measurements. Although orbital solutions are needed only once a day, measurements are occurring throughout the day and these measurements need clock corrections. Therefore, clock solutions are needed more or less continuously through the day instead of just once as for the orbits. This is a situation which clearly favors the Kalman filter on two counts - high process noise, and continuous output requirement.

It might appear, then, that the most appropriate approach is to use a Kalman filter for the clocks and a recursive batch for the orbits. This is indeed possible for Case 3 where orbit solutions are isolated from the clocks, but not in the other cases since the same measurements apply to both the orbits and at least some of the clocks. Even for Case 3 the use of a batch orbit is of questionable merit because the batch solution is not available until the end of the data span. Since the continuous clock solution needs to work its measurements against an orbit solution and today's orbit solution will not be available until the end of the day, today's clock solution is forced to work against an orbit solution extrapolated from yesterday. Thus the clock solution is always working against orbit data based on measurements which are, on the average, 24 hours old instead of always using orbit

information based on the latest measurements as would be the case with Kalman orbits. If the orbits are stable enough (low process noise) this may not make much difference, but it seems to be an unnecessary penalty, however small, for no real benefit.

One possible drawback of the Kalman formulation might be the potential for drift of the solution due to numerical processes in the filter computations. This is more of a problem with Kalman filters than with batch processes because, whereas in the latter the past measurements enter the current solution explicitly, with the Kalman filter their effect is carried only implicitly as accumulations of the terms in the state vector and associated covariance matrices. Thus a very large number of operations have been performed on old measurements before they are finally applied to current results. In the current application, the number of operations is minimized by the use of small state vectors. At the same time, if it should prove to be desirable, it would be possible to greatly improve the accuracy of the Kalman filter by using a square root formulation. Although this causes some increase in the amount of computation required, it is still not a critical factor because of the small-size of the state vectors being used.

### 3.4 PARTIAL DERIVATIVES AND STATE VECTORS

There are two basic types of partial derivatives in the on-line processing operation, namely, measurement partials,  $H$ , and propagation partials,  $\phi$ . If  $\bar{X}$  is the desired  $n$ -state solution vector, the matrix of measurement partials is defined as:

$$H = \frac{\partial \bar{m}}{\partial \bar{X}}, \text{ max: } H_{ij} = \frac{\partial m_{ij}}{\partial X_j}, (1 \times n)$$

where  $\bar{m}$  is the  $m$ -component vector of available measurements. If the measurements are applied one at a time, the  $H$  matrix is used one row at a time as the row matrix  $H_{ij}$ . The complexity of the terms of  $H$  depends on the

nature of  $\bar{X}$  and  $\bar{m}$ . For the GPS, the partial of current clock offset,  $\tau$  with respect to pseudo range is simply +1 for satellite clocks and -1 for monitor clocks. Similarly the derivative of clock rate,  $\dot{\tau}$ , with respect to pseudo range rate is +1 and -1 for satellites and monitors respectively. The cross terms between clock offsets and range rates and vice versa are zero. The clock partials are seen to be very simple and straightforward.

In the case of orbital measurement partials, however, there are several choices which may have considerable effect. The basic measurements are again pseudo-range and range rate but there are several choices as to how to characterize the orbit in the solution vector. Let  $\bar{X}_0$  represent the orbital portion of the state vector and  $H_0 = \partial \bar{m} / \partial \bar{X}_0$ .  $H_0$  takes on its simplest form when  $\bar{X}_0$  is expressed as the current position and velocity of the satellite in a coordinate system fixed in the rotating earth. In this case, the position portion of the  $H_{0ij}$  for a pseudo-range measurement from the  $j$ th monitor to the  $i$ th satellite is simply the unit vector along the line joining the two points. The partial of pseudo range with respect to velocity is zero. The partials of pseudo range rate with respect to  $\bar{X}_0$  are somewhat more complex but they are still purely geometric and easily computed vector functions.

An alternate possibility would be to represent the orbit as current  $\bar{R}$  and  $\bar{V}$  in inertial coordinates. This requires that a time-dependent earth rotation transformation be applied either to the H matrix above, or to the monitor station locations used in the solution.

A further alternative would be to represent the orbit in the state vector as the current orbit propagated back in time to some previous epoch time  $t_0$ . At epoch, it might be represented in terms of  $\bar{R}(t_0)$  and  $\bar{V}(t_0)$  or as some set of orbital elements at  $t_0$ . The definition of  $\bar{X}_0$  as the values at epoch requires that

the H matrix now also involve the propagation partials  $\phi(t_0, t)$  which relate the orbit parameters at  $t_0$  with those at  $t$ . An advantage of the use of  $\bar{X}_0$  at epoch is that  $t$  now becomes a constant so that the orbit solution becomes a solution for a constant. This is a requirement for a batch solution but is optional in a Kalman formulation. When the state vector is defined at an epoch in a Kalman filter, the propagation of the state vector from one time point to the next reduces to an identity.

If current orbital positions and velocity are desired from the epoch solution, they must be propagated by means of the dynamic model from the solution at epoch to the current time. In the case of a representation with a reference trajectory as described in Section 3.1, the propagation need be applied only to deviations from the reference trajectory. If these are small enough to satisfy linearity constraints, the propagation of these deviations can be carried out by means of the propagation partial derivatives,  $\phi(t_0, t)$ . Thus, both the state vector and the covariances can be propagated by use of the reference trajectory and the corresponding set of partial derivatives. These are both provided by the off-line facility and represent all that the on-line facility needs for the detailed dynamic model.

Let  $\phi(t_1, t_2)$  represent the partial derivatives which propagate a deviation from the reference trajectory from time  $t_1$  to  $t_2$ . In principle, such partials can be used to relate any two points along a trajectory which is close to the reference trajectory. With a detailed force model, the computation of the partial derivatives is a major operation. This is carried out by the off-line facility and supplied along with the reference trajectory.  $\phi(t_1, t_2)$  is a function of two variables and would be very cumbersome to produce and transmit in its full extent. Therefore, the off-line facility reduces it to a function of a single variable by limiting  $t_1$  to the epoch time,  $t_0$ .

Thus, at any time,  $t$ , there is published

$$\bar{X}_{ref}(t) = \begin{bmatrix} \bar{R}(t) \\ \bar{V}(t) \end{bmatrix},$$

$$\phi(t_0, t) = \left. \frac{\partial \bar{X}(t)}{\partial \bar{X}(t_0)} \right|_{\text{along } \bar{X}_{ref}}$$

In the batch process used by the CELEST program at the NWL, these are exactly the partial derivatives needed to propagate the measurement partials to the epoch point and to propagate the epoch solutions to other points in the future where predictions are needed.

If, for some reason a partial derivative is needed for propagation from  $t_a$  to  $t_b$  where  $t_a$  is not  $t_0$  this may be computed by

$$\phi(t_a, t_b) = \frac{\partial \bar{X}_0(t_b)}{\partial \bar{X}_0(t_a)} = \frac{\partial \bar{X}_0(t_b)}{\partial \bar{X}_0(t_0)} \cdot \frac{\partial \bar{X}_0(t_0)}{\partial \bar{X}_0(t_a)}$$

$$= \phi(t_0, t_b) [\phi(t_0, t_a)]^{-1}$$

This involves a  $6 \times 6$  matrix inversion and a matrix multiply of two  $6 \times 6$  matrices.

If it is desired to solve for the orbit in a Kalman filter, as described earlier, while using data from NWL to avoid handling the detailed dynamic model, it becomes necessary to use the NWL reference trajectory along with suitable partial derivatives for propagating the solution from point to point. Consider the case where the orbital solution vector consists of the latest estimate of current  $\bar{R}(t)$  and  $\bar{V}(t)$ . There are actually two levels of reference trajectories available and two corresponding tasks for orbit propagation partials. The long-term reference trajectory from NWL has already been described. It extends from some epoch,  $t_0$ , over a span of several weeks. The true trajectory remains within a thousand feet or so of this trajectory so that linearity assumptions are valid. Once a day the on-line facility must predict a refined trajectory with

accuracy suitable for the navigation application and extending at least one day into the future. This refined trajectory prediction is obtained by using the NWL propagation partials to propagate the most recent estimate of the required corrections to the NWL reference trajectory over the desired time span. If the NWL partials are to be used directly for this purpose, then the orbit solution must be defined in terms of  $\bar{R}$  and  $\bar{V}$  or orbital elements at the NWL epoch time,  $t_0$ . It could either be defined there originally and solved in that domain or it could be solved in some other domain and transformed there prior to the prediction operation.

In order to maintain accuracy with the above approach when there is a several week interval between  $t_0$  and the current time,  $t$ , it is necessary to be very careful when handling the solution in the epoch domain and during the transformation to and from epoch. This is because the large derivatives arising from the secular terms can cause a serious loss of precision unless care is taken to prevent it. A possible alternative approach is that of staying in the current time domain and propagating the latest estimate ahead for a day or more on the basis of computed partials  $\phi(t_0, t) = [\phi(t_0, t_a)]^{-1}$ . Inversion would be carried out only once a day but the matrix multiple would be needed for each predicted time point. The significance of this problem has not really been eliminated with this approach but it has been concentrated into the subroutine which computes the modified partials,  $\phi(t_a, t)$ , and does not involve the rest of the process. If the partials are accurate in the first place and their conversion to the  $t_0$  epoch is carefully carried out, accuracy should be maintained.

The other point in the process where propagation partials are used is in the solution for the best estimate of the orbit. With the usual Kalman formulation, the orbit solution would be in terms of the current  $\bar{R}(t)$  and  $\bar{V}(t)$ . Once a measurement is processed, the solution is propagated to the next measure-

ment time by means of the partial derivatives  $\phi(t, t + \tau)$ . To do this with the NWL partials involves going through the inversion and matrix multiple at each measurement time. For  $6 \times 6$   $\phi$  matrices this is not a very substantial task.

There are, however, several other alternatives. The first is to define the orbit solution  $X_0$  in terms of a daily epoch,  $t_a$ . By choosing the daily epoch as the time  $t_a$ , from which the daily prediction is propagated, the converted partials used for prediction can also be used for the subsequent solution by using them with the geometric H matrix to propagate the measurements to the daily epoch. The orbit solution itself need not be propagated during the solving process since it remains defined at  $t_a$ . This approach should not be confused with a batch process. It is a Kalman solution, continuously updated. The only difference is that the solution is referenced to  $t_a$  instead of current time,  $t$ . Any time a current solution is desired at time  $t$  it can be obtained by simply multiplying the solution by  $\phi(t_a, t)$ .

Another approach which permits  $\bar{X}_0$  to be defined in current time without continually converting NWL partials consists of doing a standard current-time Kalman solution and using simple two-body partial derivatives to propagate the solution between measured times. This approach has a chance because the deviations being propagated can be kept very small. During each day, not only is the NWL reference trajectory available but the predicted trajectory transmitted to the satellites for the navigation application is also available. The true trajectory must stay within a very few feet of this predicted trajectory in order to fulfill the navigation requirements. Thus, if the solution is developed in terms of deviations from the predicted navigation trajectory, these deviations will always be very small so that the partial derivatives which operate on them need not be highly accurate.

Preliminary analysis has shown the principal terms of the partial derivatives beyond two-body to be the second zonal

harmonics, with 2nd order tesserals and higher zonals and tesserals down by at least a factor of 100. The seriousness of neglecting the contribution of the second zonal harmonics to the  $\phi$  partials was investigated by integrating the second zonal harmonic terms of the variational equations over a 24-hour period and plotting the results. Plots were made for GPS type orbits with a variety of starting points to ensure that all pertinent cases were covered. It was assumed that the deviations to be propagated would not exceed 30 ft and 0.003 ft/sec with respect to the precision orbit predicted for navigation purposes. These deviations were then multiplied by the maximum values of the plotted integrals to get the maximum error build-up within 24 hours due to the neglect of the second zonal harmonics in the  $\phi$  partials. The maximum orbital position error so obtained within 24 hours was 0.28 ft and the maximum velocity error obtained was  $2.8 \times 10^{-5}$  ft/sec. These are both insignificant within the context of the daily orbit refinement operation. Since there are many measurements each day, these will correct for accumulating errors so that no consideration need be given to error build-up beyond 24 hours. Predictions of future orbits are not affected since they would still be done with the precision partials supplied by NWL.

### 3.5 COORDINATE FRAMES

There are two basic coordinate frames inherent in the orbit determination process:

- a. An earth-fixed set of coordinates is needed since the measuring instruments are fixed in the earth and the measurements are originally made in the earth-fixed system.
- b. An inertial set of coordinates is needed for handling the dynamics of the satellite since the basic equations of motion act with respect to such a non-rotating coordinate frame.

A choice must be made as to which coordinate frame is to be used for the least-squares solution in the orbit determination process. This, however, is also tied up in the

question of whether to define the orbital solution in terms of current time, as is the usual practice with Kalman filters, or in terms of some sort of epoch as is more usual in batch processing. A choice of earth-fixed or inertial coordinates is also available when predicting the "trajectory for tomorrow" to be placed in the state vector transmitted to the satellites.

In principle, the various cases are mathematically equivalent, but they do involve different amounts of computation and they may have some effect on the required precision with which the computations must be carried out. The main impact of the choices is in the computation and application of the various partial derivatives needed for system operation. This, in turn, is strongly affected by the fact that NWL, which supplies the long-term reference trajectory and propagation partials can supply the trajectory in either earth-fixed or inertial coordinates. The corresponding partials are partials of position and velocity in the corresponding (earth-fixed or inertial) coordi-

nate system at time  $t$ , with respect to orbital elements or position and velocity in inertial coordinates at epoch time,  $t_0$ .

Table 3-2 shows some of the more pertinent possibilities. Three sets of partials must be computed:

- Partials to propagate the solution vector from one measurement time to the next
- Partials to relate the solution vector to the measurements
- Partials to project the final solution ahead for a day or more for use in the navigation application.

Table 3-2 shows seven or eight possibilities for each of these three sets of partials, depending on the various choices of coordinate systems and epochs. Each bin of the table contains an expression for the required orbit partial derivative in terms of defined and available parameters to show the process involved in forming the derivatives. In the lower left corner of each bin is a number indicating approximately the num-

Table 3-2. Epochs and Coordinate Frames

SOLUTION EPOCH	ADDITIONAL PARAMETERS	SOLUTION PROPAGATION PARTIALS				MEASUREMENT PARTIALS		PREDICTION PARTIALS	
		SOLUTION COORDINATES				SOLUTION COORDINATES		PREDICTION COORDINATES	
		Earth Fixed		Inertial		Earth Fixed	Inertial	Earth Fixed	Inertial
		Form 1	use	Form 2	use	Form 3	Form 4	Form 5	Form 6
CURRENT TIME	2 Body	$M_2 \left[ \frac{\partial \mathbf{r}(t)}{\partial \mathbf{v}_0} \right]$		$\mathbf{v}(t)$		$M_2 \mathbf{F} = \mathbf{F}_1^T M_2$			
	Partials	836	468	760	468	5	14		
	NWL	$\mathbf{r}_{EFC}(t) \left[ \frac{\partial \mathbf{r}_{EFC}(t)}{\partial \mathbf{v}_0} \right]$		$\mathbf{v}_{EFC}(t) \left[ \frac{\partial \mathbf{v}_{EFC}(t)}{\partial \mathbf{v}_0} \right]$		$M_2 \mathbf{F} = \mathbf{F}_1^T M_2$		$\mathbf{r}_{EFC}(t) \left[ \frac{\partial \mathbf{r}_{EFC}(t)}{\partial \mathbf{v}_0} \right]$	$\mathbf{v}_{EFC}(t) \left[ \frac{\partial \mathbf{v}_{EFC}(t)}{\partial \mathbf{v}_0} \right]$
	Partials	504	468	538	468	5	14	216	216
DAILY EPOCH	Solution in Earth Fixed Coordinates	$\mathbf{r}_{EFC}(t) \left[ \frac{\partial \mathbf{r}_{EFC}(t)}{\partial \mathbf{v}_0} \right]$		$\mathbf{v}_{EFC}(t) \left[ \frac{\partial \mathbf{v}_{EFC}(t)}{\partial \mathbf{v}_0} \right]$		$M_2 \mathbf{F} = \mathbf{F}_1^T M_2$		$\mathbf{r}_{EFC}(t) \left[ \frac{\partial \mathbf{r}_{EFC}(t)}{\partial \mathbf{v}_0} \right]$	$\mathbf{v}_{EFC}(t) \left[ \frac{\partial \mathbf{v}_{EFC}(t)}{\partial \mathbf{v}_0} \right]$
	Solution in Inertial Coordinates	$\mathbf{r}_{IN}(t) \left[ \frac{\partial \mathbf{r}_{IN}(t)}{\partial \mathbf{v}_0} \right]$		$\mathbf{v}_{IN}(t) \left[ \frac{\partial \mathbf{v}_{IN}(t)}{\partial \mathbf{v}_0} \right]$		$M_2 \mathbf{F} = \mathbf{F}_1^T M_2$		$\mathbf{r}_{IN}(t) \left[ \frac{\partial \mathbf{r}_{IN}(t)}{\partial \mathbf{v}_0} \right]$	$\mathbf{v}_{IN}(t) \left[ \frac{\partial \mathbf{v}_{IN}(t)}{\partial \mathbf{v}_0} \right]$
NWL EPOCH		$\mathbf{r}_{EFC}(t) \left[ \frac{\partial \mathbf{r}_{EFC}(t)}{\partial \mathbf{v}_0} \right]$		$\mathbf{v}_{EFC}(t) \left[ \frac{\partial \mathbf{v}_{EFC}(t)}{\partial \mathbf{v}_0} \right]$		$M_2 \mathbf{F} = \mathbf{F}_1^T M_2$		$\mathbf{r}_{EFC}(t) \left[ \frac{\partial \mathbf{r}_{EFC}(t)}{\partial \mathbf{v}_0} \right]$	$\mathbf{v}_{EFC}(t) \left[ \frac{\partial \mathbf{v}_{EFC}(t)}{\partial \mathbf{v}_0} \right]$

ber of multiplications involved in forming that type of orbit partial from the available inputs. In the case of the measurement partials, the numbers given are for pseudo-range measurements. Other types of measurements increase these numbers somewhat. In the lower right corner of each bin is a number showing the number of multiples involved in applying the partial to the orbit determination process wherever this number is not the same for all cases. In general, these numbers of multiples are required for each point in the process at which the partial is applied.

Three solution epoch cases are shown in Table 3-2:

- a. A current running solution
- b. a daily epoch solution
- c. the NWL epoch solution

The current-time solution yields the simplest measurement or H partials, particularly in earth-fixed coordinates. With the current-time solution, the solution propagation partials must propagate from the time of one measurement to that of the next. NWL partials all propagate from the NWL epoch to some time,  $t$ . Thus, an inversion and matrix multiply is required at each measurement time to convert NWL partials into a form useable in the current-time mode.

When working against an accurate reference trajectory (e.g., yesterday's prediction for today's navigation) the solution propagation partials are accurate enough if computed by two-body mechanics. However, a one-day prediction against the NWL reference trajectory is of marginal accuracy with two-body partials and a prediction of more than one day is definitely inadequate. Thus, the NWL partials are needed in any case for the current solution modes. Furthermore, the computation of two-body partials involves more work than the conversion of the NWL partials. Therefore, the two-body partials do not appear to offer any overall benefit.

In the current-time mode, the solution propagation partials must be used to compute the  $\phi^T X$  propagation of the orbit solution vector and also the  $\phi^T P \phi^T$  propagation of the

covariance. These add up to 468 multiples per measurement time as shown in Table 3-2. If, on the other hand, the solution is carried out at the NWL epoch or either of the daily epoch modes, the above propagations of the solution from measurement to measurement drop out. The least overall computation is involved with the NWL epoch because the NWL partials are then directly applicable to the orbit prediction function, the solution propagation operation drops out, and the measurement partials involve a mere 41 multiples per measurement.

The daily epoch cases are basically similar except that the NWL partials must be converted to shift the reference point from the NWL epoch to the daily epoch point. As before, this requires a  $6 \times 6$  inversion plus the product of two  $6 \times 6$  matrices. The inversion is done for the epoch point and, thus, is common to an entire day's set of partials. It is therefore done only once a day and has accordingly been omitted from the multiply count. The modified prediction partials also constitute the major portion of the measurement partial computation. Thus the measurement partials require only an additional 41 or 83 multiples per pseudo-range measurement depending on whether earth-fixed or inertial NWL partials are being used.

With a solution at an epoch, whether daily or NWL, no  $\phi^T P \phi^T$  operation is required. However, there may be a need to operate on the Q matrix to make it represent the dynamic process noise in orbit. Since the dynamic uncertainties apply to the vehicle where it is in orbit, this, in principle, needs to be propagated back to the epoch before addition to the covariance matrix of the solution. If this propagation should turn out to be necessary in practice, the partial is the inverse of the one used for predictions. This partial is indicated by the  $(\phi^{-1})$  in the appropriate boxes of Table 3-2. The numbers in parenthesis in the lower left corners are the number of multiples required for the  $6 \times 6$  inversion while those in the lower right corners are the number of multiples required to implement the  $\phi^{-1} C \phi^{-1T}$  on the assumption that Q is diagonal.

The NWL epoch solution with earth-fixed coordinates for the prediction is the most efficient computationally, requiring only 41 multiples from Table 3-2 if the Q propagation is ignored or 581 if it cannot be ignored. When the measurement times are far from the epoch however, the secular terms of the partial derivatives tend to cause high correlations between positions and velocities at the epoch and these could possibly have a detrimental effect on the numerics of the solution. If this should turn out to be serious, one of the daily epoch solutions could be used instead. The daily epoch solution totals 257 or 795 multiples per measurement depending on whether or not Q is propagated. Simulation studies have shown that if the epoch-to-current-time interval does not exceed one day, the Q can be applied at current time or at epoch with nearly equivalent results so that Q need not be propagated. On the other hand, if the interval extends to many days, the secular terms in the propagation partials cause fixed Q's at epoch to reflect increasingly large uncertainties into the current time estimate. Thus the use of the NWL epoch demands the use of propagated Q's whereas daily epochs permit the use of unpropagated Q's applied directly to the

epoch solution. We are thus left with 257 multiples per time point with the daily epoch and 582 multiples per time point with the NWL epoch.

On the other hand, since the Q's are very small they could be accumulated and applied to the solution at infrequent intervals (e.g., every 3 hours) and treated as zero at other times. With such an approach the Q propagation becomes less significant and the NWL epoch solution again becomes the minimum computation case. The problem of high correlation between position and velocity at the NWL epoch remains, however. It is therefore recommended that the daily epoch solution be used but that the on-line computer be sized to permit the handling of the current-time solution since this is not a severe extra demand and it would permit the handling of any of the viable alternatives. Since it is desired to provide the user's state vector in terms of slowly varying two-body orbital elements, these must be based on inertial  $\bar{R}$  and  $\bar{V}$ . Thus the prediction should be done into inertial coordinates. This can best be done with the inertial NWL partials and this, in turn, leads to an inertial solution at the daily epoch.



# 4

## EVALUATION ALGORITHM

Given the system candidates, the next step was to define and describe the criteria by which they could be evaluated. This section describes the evaluation criteria, a cost function for each criterion, and a weighting function for each of the various criteria.

### 4.1 EVALUATION CRITERIA

We can partition the criteria into essentially independent groups as follows:

- Computer impact
- System accuracy
- System convergence

**4.1.1 COMPUTER IMPACT** - Since each system candidate defines a distinct set of computer systems necessary and sufficient to accomplish it most efficiently, the aim here is only to describe those general criteria which have a sizable influence on the type of computer system ultimately chosen. In no particular order, these may be described as:

- Expandability
- Time line
- Core size, word length, cost (hardware)
- Mechanizational simplicity (software)

**Expandability** - Expandability measures the candidate system's ability to handle more satellites without serious impact on the computer. In handling 24 satellites instead of four, some changes must be made to the computer no matter what the candidate is. Handling 24 satellites should require more memory, more computing time, and some programming changes. To this extent, expanding any candidate to handle more satellites will affect the computer used. "Serious impact" would indicate a radical change to the computer such as a different CPU, a large increase in memory requirements, an increase in computing speed or memory access requirements, massive pro-

gramming changes, or even a whole new computer system.

**Time Line** - This criterion measures the candidate's ability to get the job done on time. GPS system computing requirements are not constant as a function of time. There will be times when the computer is idle and times (e.g., just before satellite uploading) when it has a large workload. The time required to do this peak load work is a function of both the computer and the candidate. By being capable of doing some of the peak load work during idle time or simplifying peak load requirements, the system candidate can ease computer speed and size requirements; this capability will be measured by the time line criterion.

**Core Size, Word Length, Cost (Hardware)** - In general terms this deals with a candidate's hardware impact. Different candidates may require or be most suitable to different hardware configurations - specific word lengths, a certain number of registers, varying amounts of RAM and ROM memory, and so forth. The guiding criteria here will be hardware costs. Those candidates that can handle the general Phase I and II requirements at the least hardware cost should have preferential weighting.

**Mechanizational Simplicity (Software)** - In this case the general subject is software cost. A candidate that is straightforward as far as programming, checkout, maintenance, and ease of modification are concerned must be considered preferable to one that requires fewer words but more work and worry. An overall indication of software cost is as important as an overall indication of hardware cost.

**4.1.2 SYSTEM ACCURACY** - According to the system specification, accuracy is more important than computer cost. On the other

hand, it appears that several of the candidate systems will be capable of attaining the required system accuracy. In this case the topics of expandability and time line dominate the selection process. Definite advantage must be awarded to candidates that offer the greatest accuracy but any candidate that meets the specified accuracy must be considered acceptable. To this end there are two essentially different types of accuracy to be considered: user and ephemeris.

**User Accuracy** — The system specification deals most directly with user accuracy or user equivalent range error (UERE). As such it recognizes a basic difference between the accuracy of the satellite orbit and clock determinations and their effect on the user. If the satellite parameters could be determined exactly, the two would be equivalent; but a large error in satellite orbit need not reflect a large error to the user. Geometries have a sizeable effect on the portion of satellite orbit errors that the user sees. Since the GPS system is dedicated to user accuracy, what the user sees is the most important part of the system. The candidates that afford greatest user accuracy will take precedence over all others in terms of system accuracy.

**Ephemeris Accuracy** — Given the importance of user accuracy, ephemeris accuracy cannot be neglected entirely. User accuracy in Phase I is limited to the test site and may be considerably better than ephemeris accuracy since the measurement directions which are pertinent to the user have been measured by the monitor stations. Correlations which were unresolvable from the monitor stations are similarly indistinguishable to the user because of his relatively similar geometry and do not add much error to his solution. These unresolved correlated errors, however, change their interrelationships at different points in the orbits; they may add substantially to the errors experienced by a user at some location far from the test site. Thus, although ephemeris errors per se are not critical in Phases I and II, they do have a probable

consequence for Phase III and should be minimized in the choice of a solution technique.

**4.1.3 SYSTEM CONVERGENCE** — When a satellite is first placed in orbit or when a station-keeping maneuver is undertaken, there is a larger positional uncertainty than when orbit estimation has been going on for some time. Each candidate must recognize this increased uncertainty and, over a period of time, eliminate it. The length of time a candidate requires to reduce a relatively large uncertainty (the convergence time) indicates how soon after a directed maneuver the system can be expected to be within specified tolerances. For some candidates convergence time will be a few hours, for others it may be several days. Suboptimal candidates whose convergence times may be long enough to be a problem must be deweighted.

## 4.2 COST FUNCTIONS

The cost function for a given criterion is a guideline for measuring each of the system candidates against that criterion. Each cost function will have similar form. There will be three gross levels of "cost":

- Unacceptable (-)
- Gradable (0)
- Completely acceptable (+)

**4.2.1 UNACCEPTABLE (-)** — This will be taken to mean that the candidate "fails" this requirement. It does not necessarily imply that the candidate could not be improved with respect to this criterion. Rather, it is meant to imply that other candidates are enough better from the standpoint of performance and simplicity to warrant disregarding this candidate because of it.

**4.2.2 GRADABLE (0)** — Where unacceptable would imply prohibitive "cost", gradable will mean that a candidate's performance to this criterion is acceptable but differs from the performance of other candidates. As such, this difference in acceptable performance is a basis for comparison. After a preliminary evaluation

of all candidates, a second evaluation will be performed to assess and compare specific differences. A final evaluation, recognizing that there is no clearly objective way to measure intrinsic merit, will adjudicate their comparative impact on the system.

**4.2.3 COMPLETELY ACCEPTABLE (+) –**  
This category reflects a candidate's acceptability beyond which no further gradations of merit make sense. Completely acceptable candidates may differ in their performance on a given criterion, but the differences are no longer meaningful to differentiation.

**4.2.4 INDIVIDUAL COST FUNCTIONS –** For each of the seven criteria described in Section 4.1, a corresponding cost function is described below.

**Expandability Cost Function –** All system candidates are easily expandable in that none requires complete restructuring to accommodate 24 satellites. Each will handle an arbitrary number of satellites with simple parameter changes. The major differences arise when considering whether the changes necessary to accommodate 24 satellites require increase of the solution vector size or cardinality. Computation, accuracy, and memory requirements increase linearly with the *number* of solution vectors but increase something like the square of the solution vector *size*. The former is completely acceptable and the latter is unacceptable in going from 4 satellites to 24.

**Time Line Cost Function –** The time line requirements are in one sense a subset of the expandability requirement. Any increase in the number of computations affects the computer's ability to get all of the computations done on time. To the extent that increased number of computations cannot be spread out over the time line, the increase has a direct effect on the time line. Actual time line "cost" is most directly tied to the solution vector size. Rough calculations for various computer candidates indicate that solution vectors of dimension 50 are approaching saturation of the current-time

line. Since current candidates are well under this value anything over it will be considered unacceptable. Any candidates with solution vectors of dimension 10 or less are completely acceptable and anything up to 20 will easily fit the time line.

**'Hardware' Cost Function –** The ephemeris determination computations are by no means the only responsibility of the Master Control Station computer. In general, the final computer selected for the MCS should allow some margin for the ephemeris determination hardware impact. Within that tolerance all candidates should be completely acceptable and any candidate that requires extra hardware should be unacceptable. In general, the candidate requiring the least hardware will be enough similar in hardware impact to the several closest competing candidates that this is a reasonable cost function.

In order to separate the problem of expanding the hardware to accommodate 24 satellites from the problem of sizing the Phase I computer, the former will be addressed by the expandability cost function and only the latter will be measured by the 'hardware' cost function.

**'Software' Cost Function –** This function attempts to measure the 'cost' of programming a given candidate. It will include subjective trade-offs between the size of the program required and the mechanizational simplicity of the program in terms of checkout and modification ease. In general, all candidates will tend to require approximately the same size program and major software costs will be influenced mainly by how simply the candidate can be described and programmed. Any candidate requiring excessive contingencies or decision processes will be de-weighted. Only a candidate that requires very special and complex software capabilities or a much larger program will be considered unacceptable.

**User Accuracy Cost Function –** Any candidate producing a user equivalent range error greater

than the system specification limit for Phase I of 12 feet is certainly unacceptable. All others are acceptable and can be ordered between 0 and 12 feet so that a UERE half as big as another is worth twice as much. Since the GPS system is dedicated to user accuracy, very good user accuracies should be weighted accordingly. Accuracies better than the Phase III specified limit will be judged completely acceptable.

**Ephemeris Cost Function** - No specific requirements are placed on the actual orbit determination accuracies. However, in general, they will correspond fairly closely in ranking to the UERE accuracies. Since they will be used in general to choose between candidates with similar UERE accuracies, a linear cost function based on a simple numerical comparison of results should be entirely sufficient.

**System Convergence Cost Function** - Any candidate that requires several days for convergence will be unacceptable. Some candidates may, in their simplest form, take several days to converge, but with modifications can be made (at the expense of mechanizational simplicity) to bring their convergence behavior to acceptable limits. In this case their convergent behavior will be said to be acceptable (or gradable) and the associated complexity will show up in the 'software' cost function.

Any candidate whose convergence to within reasonable tolerances occurs within two days on start-up or one day on a station-keeping or related maneuver will be classified completely acceptable.

### 4.3 SCORING ALGORITHM

Given inner-criterion costs for each candidate on each criterion there must still be some method

of determining how important a specific evaluation criterion is to the overall system. This is again a very subjective evaluation but most evidence indicates that computer system impact (particularly in going to 24 satellites) is slightly more important than system accuracy (since all three final candidates appear to be capable of meeting accuracy specifications). All other criteria are essentially equal and much less important than these two.

Assuming all cost functions are normalized to the same scale (arbitrarily at 5 for 'completely acceptable' candidates), observe what assigning equal weight to each criterion does:

a. Since expandability, time line, and hardware all have essentially to do with a candidate's impact on the physical computer system, this tends to weight that impact by three times the weight given any other single criterion.

b. Since user and ephemeris accuracy combine to define the system accuracy, this tends to weight the system accuracy at two-thirds the computer system impact and at twice that of any other criterion.

c. The two remaining criteria, convergence rate and mechanizational simplicity, have only a 2/7 effect on the entire system and are weighted equally.

Since these results correspond fairly well to the subjective impacts implied above, the scoring algorithm will be assigned an equal weight for each evaluation criterion.

# 5

## ANALYSIS OF CANDIDATES

Measurement set candidates were analyzed and evaluated. A preliminary analysis using the -/C/+ grading system was employed to reduce the number of candidates. Remaining candidates were evaluated qualitatively and quantitatively in some detail. The final evaluation, however, is delineated in Section 7.

### 5.1 PRELIMINARY ANALYSIS

Table 5-1 summarizes the results of a preliminary analysis of the nine measurement sets described in Section 3. Those candidates with minuses were dropped from further consideration; the following subsections describe the analyses leading to these decisions. Computer simulations were performed to aid in the evaluation of the more viable candidate ephemeris determination procedures. The error budget utilized in the simulations is described in "Contract Definition Final Report for Global Positioning System Control/User Segments," Volume II, System Error Performance, CS/UE Definition Contract FO4701-73-C-0298, General Dynamics Electronics Division, April, 1974. The simulation program results were obtained in the form of plots to facilitate rapid analysis. Example plots are shown in Figures 5-1 through 5-9. Quantities plotted are the differences between the simulated real world and the filter estimates of typical solve-for parameters as a function of time. For each parameter, the square root of the appropriate diagonal element of the solution covariance matrix is plotted as an envelope defining the expected error of the solution.

**5.1.1 FULL SIMULTANEOUS PSEUDO RANGE** - This is the most optimal accuracy solution. All orbits and clocks are solved simultaneously. The results of simulations done for this case served as a baseline for comparison with the simulations of other candidates. The computation for this case will satisfy the time

Table 5-1. Preliminary Analysis Matrix

Measurement Set	Evaluation Criteria	Ultimate Accuracy					Convergence Rate
		Time Required	Line Hardware	Software	User Effort	Ephemeris	
1 Full Simultaneous Pseudo Range							
2 Range Differences							
3 Double Range Differences							
4 100 Satellites w Separate Monitors							
5 100 Satellites w Common Monitors							
6 Range Rate							
7 Range Rate Differences							
8 Range Intercepts						0	0
9 Range Intercept Differences						0	0

line for Phase I but the corresponding solution vector for 24 satellites would require a different computer system for handling. Suboptimizing this case by solving for two, three, or four satellites at a time (for Phase III) appeared promising but did not produce sufficient

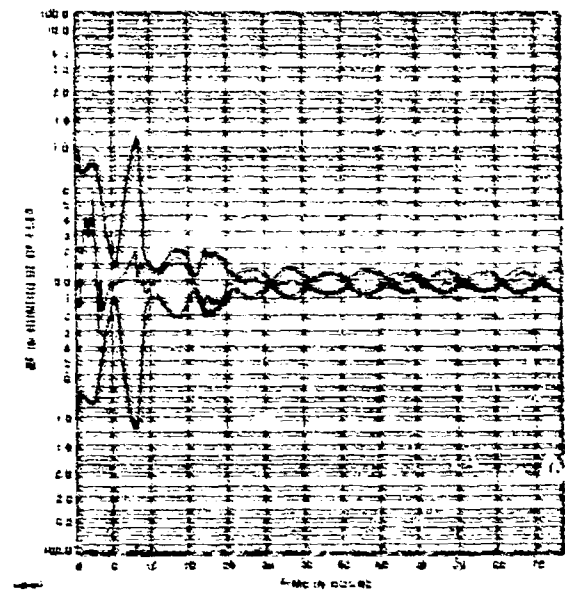


Figure 5-1 Position error of satellite 3

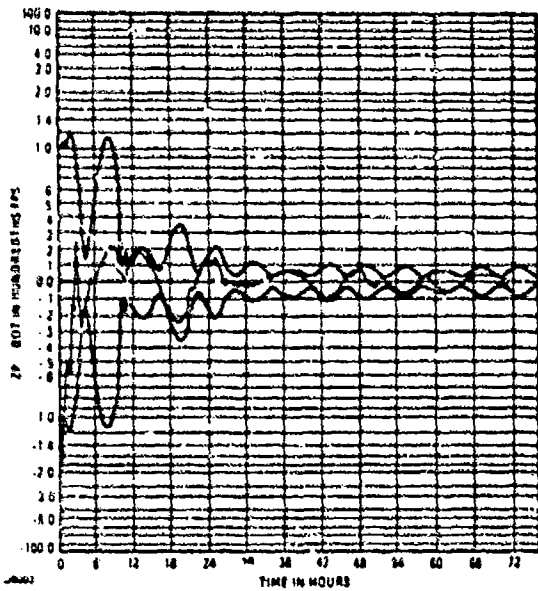


Figure 5-2. Velocity error of satellite 3.

improvement over other suboptimizations to warrant the increased workload.

**5.1.2 RANGE DIFFERENCES** — Range differences from two monitors to a single satellite give a solution independent of the satellite's clock. These clocks can then be solved as a separate calculation involving pseudo-range measurements from the master station to the satellite.

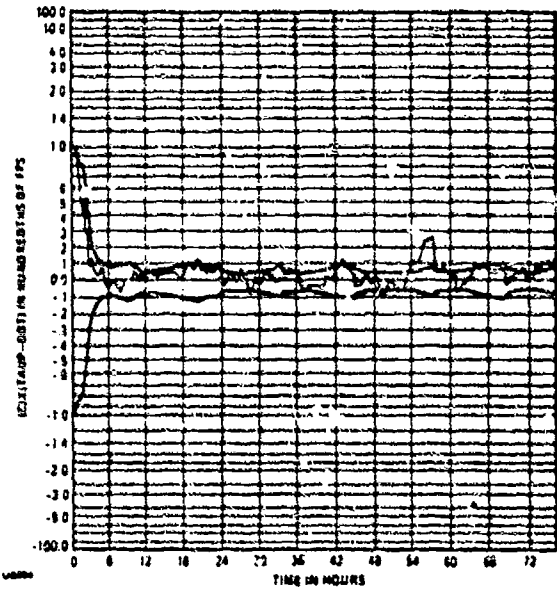


Figure 5-4. Time base rate error in clock in satellite 3.

Simulations were run on this case using a 30-state solution vector and results closely paralleled those for the full 38-state case. The major drawback at this stage was that, though the computational load was decreased, it was not decreased enough to handle 24 satellites using the same technique. Attempts were made to separate the satellite solutions but the strong coupling through the monitors produced enough

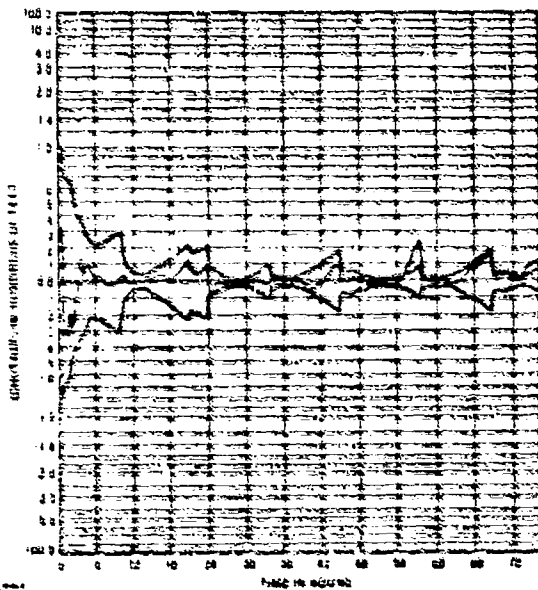


Figure 5-3. Time base error in clock in satellite 3.

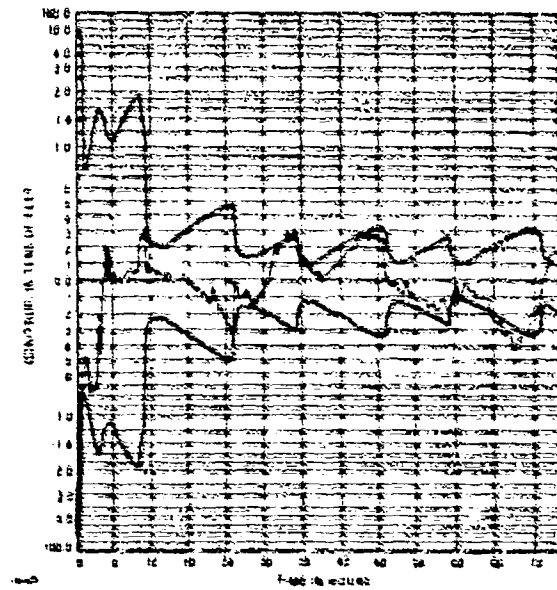


Figure 5-5. Time base error at monitor 1 for satellite 3.

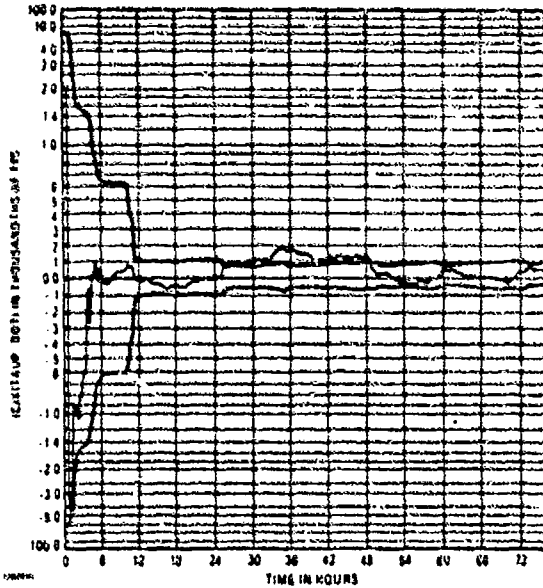


Figure 5-6. Time base rate at monitor 1 for satellite 3.

coupling in the satellite solutions to cause convergence problems when this coupling was ignored. At this point other suboptimal candidates appeared more promising and this case was excluded from further consideration.

5.1.3 DOUBLE RANGE DIFFERENCES - In attempting to entirely separate all clocks from

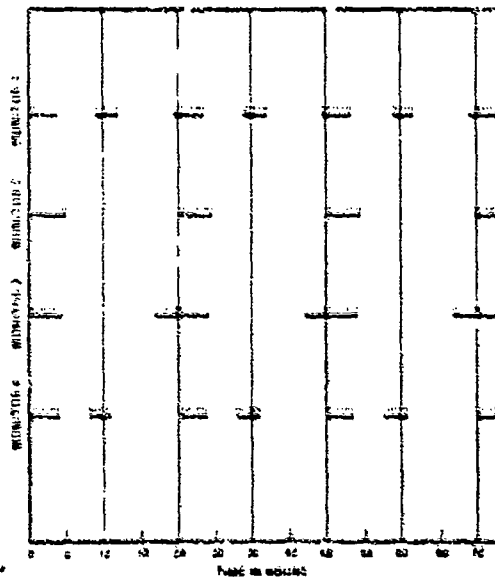


Figure 5-7. Actual vs possible measurements for satellite 3.

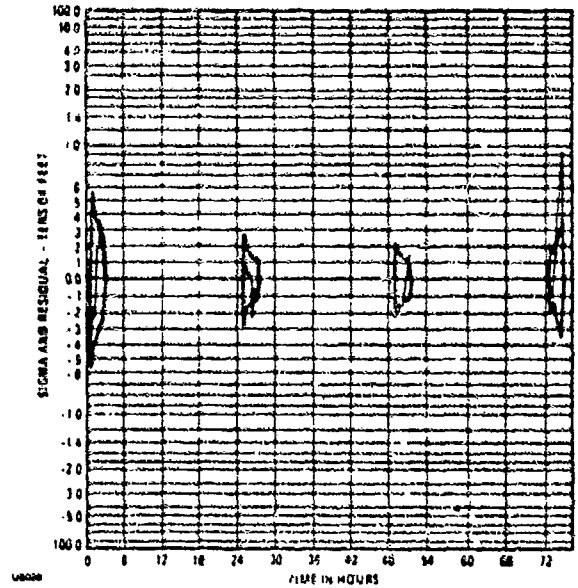


Figure 5-8. Sigma and residual of user measurements from satellite 3.

the satellite orbit solutions, a combination of simultaneous pseudo ranges between two monitors and two satellites was taken as the measurement set. This indeed separates the clocks from the orbits but strongly couples the orbit solutions of the two satellites involved. Very good results could be obtained by solving for all satellite orbits simultaneously, but again the

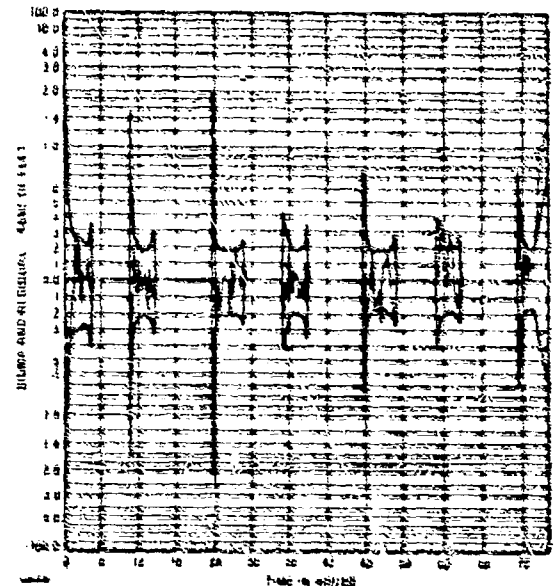


Figure 5-9. Sigma and residual of range measurement monitor 1 to satellite 3.

computational load becomes prohibitive for Phase III. Some method whereby just two satellites are solved simultaneously at each step and then some combination of the satellite solutions is performed would help reduce the computational load but would cause convergence problems due to unmodeled correlations. Another drawback to this solution is that it requires the simultaneous visibility of two satellites by the same two monitors, thus further reducing the small satellite viewing time. The numerous drawbacks for this case conspired to eliminate it from contention.

At this point it seems appropriate to mention another possible measurement set — range differences from a single monitor to two different satellites. This would uncouple the monitor clocks from the satellites but again would strongly couple the satellite solutions as above. For that reason this measurement set was never given serious consideration.

**5.1.4 RANGE RATES** — In looking at the covariance matrix for the most optimal solution two things were noticed. One, the satellite solutions were weakly coupled. Since the satellite orbits should be independent and the only mechanism for coupling them is the monitor station clocks, it appeared that the key to allowing the satellite orbits to be solved for individually was to eliminate the monitor/satellite coupling. Previous attempts had uncoupled the monitors from the satellites, but ended up coupling the satellites directly. The other observation was that there is one less integration between the physical processes of the system and a measurement of pseudo range rate than there is for a measurement of pseudo range itself. Thus, although the correlation of monitor clock rates with orbit velocities is roughly comparable to the correlations of monitor clock time offset with orbital positions, the neglect of the former is much less serious than the neglect of the latter.

Using presently envisioned range rate measurement accuracies of 0.05 ft/sec, simulations were run using range rates as the measure-

ment set and ignoring correlations between monitor clocks and the orbits. Behavior was good but the accuracies were unacceptable. Using measurement accuracies ten times as good in the simulations gave good behavior and acceptable accuracy. Another improvement factor of ten in the measurement accuracies gave good behavior and good accuracy. Design analysis indicated that the latter measurement accuracies could probably be achieved but would require hardware redesign. For this reason, and the fact that other candidates appeared promising enough, the range rate case was disregarded.

**5.1.5 RANGE RATE DIFFERENCES** — The attractiveness of this case stems from the fact that it completely uncouples the satellite clocks from the satellite orbits and substantially uncouples the monitor clocks from the orbits as above. This allows complete uncoupling of orbits, satellite clocks, and monitor clocks and represents the maximal possible partitioning (hence the minimum possible computational load). It was disregarded for the same reasons as the range rate case.

**5.1.6 RANGE INCREMENT DIFFERENCES** — Although Table 5-1 shows no minuses for this case, it was disregarded because of its similarity to the range increment case and its lack of distinct advantages over that case. It does have the advantage of again completely separating all clocks from the orbits in much the same way the range rate difference case did but this advantage is not substantial and is counterbalanced by the reduction in the number of measurements available, since a measurement is possible only when two monitors can see the satellite simultaneously. Furthermore, each difference measurement contains the errors of two pseudo-range measurements. In the interest of simplicity in the following discussions, it will essentially be incorporated into the discussion of the range increment case.

## **5.2 DETAILED ANALYSIS**

Three potentially viable measurement sets were selected for more detailed analysis in the paragraphs which follow.



### 5.2.1 INDIVIDUAL SATELLITES WITH SEPARATE MONITORS

- In this case each satellite is treated as if three distinct monitor stations (and the master station) were tracking it. The solution vector has fourteen states: six for the satellite orbit, two for the satellite clock, and two each for the three monitor station clocks. The measurements are pseudo ranges and the partial derivatives are easily described. The mechanization is very straightforward, then, and would be 'optimal' if only one satellite were being used.

For more than one satellite, the same technique is maintained. Each satellite ephemeris (whether there be four or twenty-four satellites) is calculated as if that were the only satellite in the sky. This leads to a redundancy of monitor clock solutions so that for  $n$  satellites there will, in general, be  $n$  solutions for each monitor clock. If these solutions are very similar, this technique should yield not only good ephemeris data but good user data. If the monitor clock solutions are very different, then a way of 'optimally' combining them for a single monitor clock estimate must be implemented.

The impact of this candidate on the computer is very minimal. It clearly expands very easily to 24 satellites. The number of equivalent multiples required to do one satellite solution for one pseudo range is about 2000. For a computer with a 20  $\mu$ sec multiply time, this corresponds to 40 milliseconds; the full process could easily be done in 0.1 seconds. Compared to an upload time of at least three minutes this candidate easily fits the time line. Therefore, the fact that it requires a few more storage locations for matrix computations (and for the extraneous clock solutions) has very little impact on the hardware and, as has been alluded to earlier, it is very easy to mechanize.

The only remaining doubt is what effect the multiple monitor clock solutions have on the accuracy and the convergence rate. Simulations run on this case indicate that the redundant monitor solutions have very little effect. Accuracy and convergence rate appear very similar to

the full simultaneous pseudo-range case. A close look at the behavior of the four solutions for a single monitor clock indicates strong similarities. The solutions stay within the expected covariances and an overall comparison of clock phases shows them to agree to within two or three nsec.

With behavior this good there is very little reason to obtain more accurate monitor clock solutions. However, given the need to, there is a very simple approach. The four (or twenty-four) monitor estimates can be combined in the natural way where the covariances of the estimates determine the weight for the estimate in a weighted average. The resulting value can be used as the 'best estimate' for the clock parameters wherever it is needed.

This 'best estimate' can also be fed back into the overall system in some way to provide a system 'tie-in'. Runs in which the clock estimates were combined and injected back into the system showed no major benefits to the orbit solution over runs without combining the clock estimates. On the other hand, combining the clock solutions did substantially improve the monitor clock estimates by bringing more data to bear on each solution. It was found that when the strength of the orbit solution was decreased by, for example, limiting the measurements to those where the elevation angle of the line of sight exceeded 15°, the orbit estimates without combined monitors degraded somewhat faster than those in which the monitors were combined. Furthermore, an attempt to combine the monitor clocks at each measurement step from start-up on reintroduced the monitor/orbit couplings without properly accounting for the correlations involved. This tended to upset the convergence of the solution and its recovery from transient disturbances. When monitor solutions are combined at every step this scheme becomes almost equivalent in behavior to the one discussed in the next section. The convergence problems are discussed in more detail there. On the other hand, there is no need to combine clock solutions so often. A combination every 12 hours worked well with no

convergence problems and combinations every few hours should also be feasible if desired.

In general this candidate appears very promising. It yields good ephemeris and user accuracies, good convergence, little computer impact, and simple mechanization. Its drawbacks are a slight increase in computation time (over completely partitioned cases) and a multiplicity of monitor clock solutions.

**5.2.2 INDIVIDUAL SATELLITES WITH COMMON MONITORS** - This case has been rather completely described as Case 5 in Section 3.1 and that description will not be repeated here. It can be thought of as derivable from the full simultaneous solution (Case 1 of Section 3.1) by simply ignoring any correlations developed in the covariance matrix between the individual monitor clock solutions and the rest of the process. If these correlations did not exist, the simultaneous solutions could be broken into a series of separate solutions performed in sequence with each solution accounting for one measurement involving one satellite and one monitor station - namely, the Case 5 solution.

The covariance solution of Case 5 behaves very well and yields expected accuracies essentially equivalent to those for the Case 1 simultaneous solution. However, the covariance solution is based on the assumption of a system in which the above correlations are truly missing. If this were in fact the situation, the entire Case 5 solution should work well. The problem is that the ignored correlations do actually exist in the data, and the data behavior does not conform to the statistics predicted by the covariance solution which ignores them. The size of the ignored correlations can be examined by looking at the covariance matrix of the Case 1 solution where they are not ignored. When this is done it is found that after the first few hours the correlations in question are quite low and thus could probably be ignored with impunity. The problem is that high correlations are encountered during the initial start-up before there is enough exercise of geometry to distin-

guish between orbit effects and clock effects, and it takes the system a long time to recover from the original bad estimates arising from the neglect of the correlations during this initial period. Simulations in which the correlations were accounted for during the first two days and then dropped, worked well yielding accuracies comparable to Case 1 solutions.

The mechanism of the slow convergence stems from the fact that the covariance solution, being unaware of the initial high correlation, improves too rapidly before there is enough exercise of system geometry to properly distribute the corrections between the monitor clocks and the satellite clocks-and-orbits. The result is that we are left with errors in some of the solution vector estimates which are many times the estimated sigmas for these quantities. Small sigmas on the solution vector parameters inhibit the capability of further measurements to change their estimates so that the large existing errors are reduced only very slowly.

There are several ways to alleviate the slow convergence problem of the Case 5 solution, most of which have been demonstrated by simulation to be effective, but the optimum combination has not yet been established. These techniques will now be considered.

The recovery from initial bad estimates can be greatly speeded up by increasing the Q values added to some elements of the covariance matrix of the solution, thus counteracting the over-optimistic covariances which were impeding the convergence. Q values high enough to produce rapid convergence from large initial errors are, however, also large enough to impair the quality of the final solution. Thus, some provision should be made for reducing the Q values as the convergence is achieved.

A second way to improve the convergence rate is to add some range rate or range increment measurements. The latter are more effective because of their higher accuracy with the current receiver design. Range rate or range increment measurements also involve correlations between the monitor clock rates and the orbit

velocities. In fact, these correlations are of comparable order of magnitude to those between monitor clock phases and orbital positions. However, the fact that there is one less integration between the physical processes of the system and the measurement enables such measurements to contribute substantially to the rate of convergence. This technique in no way degrades the ultimate accuracy, but it does add somewhat to the computing load by requiring the handling of the extra measurements.

A third possible technique would be to carry a portion of the previously ignored correlation. In the  $10 \times 10$  covariance matrix used for each measurement solution, there is a place for a single  $8 \times 2$  cross-correlation submatrix. Instead of inserting a zero here, a saved submatrix could be used. Three such submatrices would have to be saved for each satellite — one for each monitor other than the master. Since the couplings are not very tight, it is probable that a less than complete accounting of all the couplings involved would produce a worthwhile improvement without unduly complicating the computations. This technique has not yet been tried in simulation so it is not yet possible to establish how much can be gained with any given degree of additional computation.

Besides the above techniques for improving the speed of convergence, it is to be expected that the convergence properties of the Case 5 solution will improve spontaneously as more satellites are added to the total constellation. This is because the additional satellites will add weight to the monitor clock solutions so that they are less affected by any individual satellite effect. Thus, the monitor clock solutions will be stabilized so that they provide less of a mechanism for coupling the satellites together. When there are few satellites, the computational load is light and extra computations to improve convergence can be tolerated. As more satellites are added, the need for the extra computations decreases and the full computational capacity can be devoted to the basic Case 5 solution.

Although optimum details have not yet been completely worked out, the Case 5 approach clearly appears to be a viable approach with better accuracy than Case 8 and with several avenues available for overcoming the convergence problems.

**5.2.3 RANGE INCREMENTS** — In this case the measurements are pseudo ranges and range 'increments'. A range increment is the difference between a pseudo range from one monitor to one satellite at one time and a pseudo range from the same monitor to the same satellite at a different time. Though the range increments have the dimension of range (or range change) they have the behavior of range rate. To appreciate this consider the following: Let  $R_{ij}(t) + c [\tau_i(t) - \tau_j(t)]$  describe the pseudo range  $R'$  from satellite  $i$  to monitor  $j$  at time  $t$  in terms of the actual range  $R$  from satellite  $i$  to monitor  $j$  at time  $t$ , and the two clock phase offsets  $\tau_i$  for satellite  $i$  and  $\tau_j$  for monitor  $j$  at time  $t$  ( $c$  converts from time to distance). Ignore for the moment any measurement noise. The measurement  $M_{ij}(t)$  may be described by

$$\begin{aligned} M_{ij}(t) &= R'_{ij}(t) - R'_{ij}(t - \Delta t) \\ &= R_{ij}(t) - R_{ij}(t - \Delta t) + c [\tau_i(t) \\ &\quad - \tau_i(t - \Delta t)] - c [\tau_j(t) - \tau_j(t - \Delta t)] \\ &= R_{ij}(t) - R_{ij}(t - \Delta t) + c \dot{\tau}_i \Delta t - c \\ &\quad - c \dot{\tau}_j \Delta t \end{aligned}$$

because the clock frequencies are so stable. The solution with these measurements should thus behave more like a range rate solution than a range difference solution; that is, it should have the advantage of being easily expandable to twenty-four satellites and it should have the disadvantage of decreased ephemeris accuracy. Like the range rate solution it should functionally uncouple the monitor clock time offsets from the satellites and will thus also need individual pseudo-range measurements to solve for the monitor clocks offsets. Unlike the range rate case it should not require hardware redesign

to achieve acceptable accuracies, and it should improve rather than degrade with longer gaps between range increment measurements. This is because the range increments are actually integrations of range rate so that the longer the 'integration' time the better the results, at least to a point when too few measurements degrade the solution.

The impact of this candidate on the computer is rather small. For each measurement an eight-state solution vector for satellite position, velocity and clock and a two-state solution vector for a monitor clock need to be solved. This is approximately one-half to one-third the computational load for the individual satellites with separate monitors. Solution software mechanization is very straightforward and the small size of the matrices involved would make Kalman filter checkout much easier. The principal complication is the requirement to store and keep track of the previous data at  $t-\Delta t$  and to make use of this in forming  $M_{ij}(t)$  and  $H_{ij}$ .

One characteristic of range rate and range increment simulations was a continued slow improvement in accuracy. Though this characteristic is present throughout most of the simula-

tions, it is more noticeable in the range rate and range increment cases because of the greater room for improvement. Because the magnitude of this improvement is significant it is possible to ascribe part of the accuracy problem as a residual problem in convergence.

Actual simulations on the range increment case concentrated at first on discerning the effects of various patterns of pseudo-range and range increment measurement usage. In general, the results improved with increased usage of pseudo range and decreased usage of range increments. Long steps — where the range increment was formed from the last pseudo range before the satellite went out of view and the first pseudo range as it came back into view — were included and exhibited a very beneficial effect on the satellite clock rate solutions.

The overall results would seem to indicate that pseudo ranges rather than range increments should be used as the primary measurement set. On the other hand, range increments have shown themselves to be very useful for improving the satellite clocks when used in conjunction with pseudo-range measurements. This thought is further explored in Section 7.1.

# 6

## SELECTION

This section describes an evaluation and selection process based on the simulations and analysis to date. A specific candidate recommendation is made based on the scoring algorithm described in Section 4. The candidate's effect and the requirements it imposes on the total system are discussed.

### 6.1 CANDIDATE RECOMMENDATION

Table 6-1 shows the final cost functions and scoring algorithm applied to the remaining three candidates from Section 5. As indicated, precedence devalues upon the case with the individual satellites and separate monitors. The only drawback indicated for this case is the time line; in this instance, a drawback only, in comparison to the other two candidates. The final recommendation is *not*, however, simply that the case with individual satellites and common monitors be implemented.

Table 6-1. Final Scoring Algorithm for System Candidates.

	Expand- Bility	Time Line	Hard ware	Soft ware	Accuracy		Com- pense Rate	Final Score
					User	mis		
Individual satellites with separate monitors	5	4	5	5	5	5	5	34
Individual satellites with common monitors	5	5	5	4	5	5	4	32
Range increments	5	5	5	5	5	4	4	32

\* The final score really reflected just how close the first approach (separate monitors) is a little bit better method.

Morphologically the final three candidates are very similar. What shortcomings they have are complementary in the sense that at least one of three candidates is completely acceptable for each criterion. This suggests the following approach: For the time being accept the 'winner' as a safe and completely acceptable mechanization for ephemeris determination. If all else fails this will provide the GPS with the

accuracy, predictability, and stability necessary for required operation.

In addition, since the two 'losing' candidates are so similar to the winner, explore combinations of the final three candidates that may reasonably eliminate all significant drawbacks. It may well be, for instance, that the case for early stability of the individual satellites with separate monitors can be combined with the case for steady-state computational reduction afforded by the individual satellites with common monitors. The similarity of the two mechanizations suggests that a switchover from one to the other (and back again in case of a station-keeping maneuver or similar directed orbit alteration) would not complicate the mechanizational simplicity unduly. Another possibility is that range increments could be used in a separate (or combined) computation to provide a single estimate vector for each monitor clock.

Notwithstanding improvements derived from considerations of this type, however, a specific acceptable candidate mechanization for ephemeris determination has been developed.

### 6.2 EXPANDABILITY TO 4 AND 24 SATELLITES

Although all discussions above were referenced to minimizing computations and memory by dealing with satellites on a separate basis, the full simultaneous solution for four satellites at a time is indeed acceptable, and is also a more optimum approach. In fact, 24-satellite solutions could well be solved for four-at-a-time, as 4-satellite solutions are one-at-a-time. Intermediate numbers and combinations are also possibilities - say, two-at-a-time, or three-at-a-time with one alone, etc.

The exercises above proved the feasibility of solving for smaller numbers of satellite

ephemerides at a time. Intermediate numbers at a time and four-at-a-time are natural expansions, while the performance of these expansions would surely lie somewhere between the one-at-a-time and the four-at-a-time performance. Thus the obvious candidate mechanization selection is an expandable solution vector which includes one to four satellites.

### 6.3 REQUIREMENTS IMPOSED ON TOTAL SYSTEM

The ephemeris determination procedure does not impose any unreasonable requirements on the total system. The combination lines between the Master Control Station (MCS) and the Monitor Stations (MS) are dedicated lines capable of handling 2400 bits per second. The off-line computational facility which computes the reference trajectory is expected to require data at the rate of about one sample each two minutes. A reasonable approach to data collection appears to be to perform data editing and smoothing at the MS, making one sample of smoothed range available to the MCS every two minutes for each visible satellite. This data could be buffered at the MS and sent to the MCS

infrequently in blocks for recording and delivery to the off-line facility.

Requirements imposed on the Air Force Satellite Control Facility (AFSCF) are for the initial ephemerides as the satellites are placed in orbit. In addition, certain information pertinent to stationkeeping operations and attitude adjustments will be required from the AFSCF. It is anticipated that the required information will result in minimal impact on the communication lines.

Requirements imposed on the MCS computer are of significance only in respect to the impact on the time line due to computational demands just prior to satellite uploading. The upload data for each satellite is divided into two parts:

1. Satellite position data
2. Clock correction data

The satellite position data is essentially non-perishable, so that the computation of this data can be accomplished well before the upload time. Clock correction data may be computed from a small amount of tracking data so that the computational load on the computer just prior to upload can be minimized.

# 7

## ADDITIONAL MODELING REQUIREMENTS

### 7.1 SIGNIFICANCE OF ADDITIONAL MODELING

Certain error and force models which affect ephemeris determination have been excluded or simplified in the simulations. The significance of this can only be qualitatively rationalized now. However, future analysis studies should include different models, or verify that the exclusions and simplifications have negligible impact. Here we will summarize the exclusion and simplifications and discuss their impact on the ephemeris determination accuracies.

**7.1.1 MODELING NOT INCLUDED IN ANALYSIS** – The analysis performed and discussed in Section 5 did not include the following important error or force models, it being assured that they were adequately treated in the reference trajectory or with auxiliary calculations outside the Kalman subroutine:

- General relativistic effect on the clocks
- Geopotential harmonics
- Solar radiation pressure models
- Planetary gravitational attractions

Other error and/or force sources not included were deemed negligible for ephemeris determination<sup>(1)</sup>. This does not include stationkeeping and outgassing, which must be modeled and dealt with one way or another; they could be treated as on-off biases and exponential decays, with interface with NWL for updated reference trajectories. This is to be discussed elsewhere. The models excluded and their impact are discussed in more detail in following paragraphs.

**7.1.2 SIMPLIFIED MODELING INCLUDED IN THE ANALYSIS** – The analysis performed and discussed in Section 5 included models for random variations in the clock frequencies.

These models were, however, simplified somewhat for the analysis performed to date. These models and their impact are discussed in more detail in following paragraphs.

**7.1.3 IMPACT OF USING REFERENCE TRAJECTORIES** – It has been proposed that on-line ephemeris determination be performed about a batch processed reference trajectory, thereby operating in the linear world, and "fine tuning" the ephemeris on-line with reference trajectory partial derivatives. If this is the case, much of the modeling excluded thus far (Section 7.1.1) would be included in the reference trajectory computation. The clock effects would not be. In this case, the ephemeris errors simulated *without* these models would be representative of those to be expected in the real world provided that the reference trajectory does a good job of including them. This is the case for both geopotential harmonics and planetary gravitational attractions. To some extent, solar radiation pressure models include these effects in their reference trajectory.

**7.1.4 IMPACT OF SIMULATED CLOCK MODELING** – The random nature of the clock frequency variations was modeled in a convenient way to fit the formulation of a Kalman estimation algorithm – that is, white noise passed through a linear filter. In the real world, however, the filter would be nonlinear. The linear filter generates a pessimistic variation with respect to its form, and is sometimes optimistic in its constants. Thus, with this blend, it is felt that a real-world clock model would not seriously impact the results of the analysis performed to date. More details about the simplified clock model and proposed real-world model will be discussed in later paragraphs.

## 7.2 CLOCK MODELS

The clock models for the satellites should exhibit three types of important errors: random fluctuations of frequency, long-term drifts, and general relativistic effects (not an error, actually).

The ground station clocks are proposed to be of better quality and thus the long-term drift is smaller, as are some of the longer time-constant random frequency variations.

**7.2.1 RANDOM VARIATION MODELS** – The random variations in frequency for both the satellite and the ground station clocks modeled for the analysis given in Section 5 were modeled as integrated white noise (phase is doubly integrated white noise) plus white noise. The variances of the noises sometimes differed from those described here; however, their impact on ephemeris accuracy is minimal. An integrated white-noise frequency variation does produce a significant long-term drift in frequency; however, the models include some adaptive variation in the noise variances to limit the drift.

An integrated white-noise frequency variation is more conservative, in a long-term sense, than either the clock specifications as much of the literature imply. However, with the adaptive variances the conservatism can be removed. The selection of constants also will affect how conservative the model is.

Atomic clock random variations are normally described as a sum of frequency white noise and frequency flicker noise. Frequency flicker noise has a variance proportional to the natural logarithm of time, while integrated white noise has a variance proportional to time. Thus, integrated white-noise variations would be expected to be worse as time goes along, implying a more conservative approach.

The problem in modeling flicker noise arises from the fact that it cannot be generated as a Markov process (white noise through a linear filter), except approximately. It can be modeled as noise through a set of cascaded filters<sup>(2)</sup>, which simulates its 1/f spectrum over a frequency range of interest. Normally, this

results in about a fourth-order filter – three orders higher than integrated white noise.

If a Kalman estimator is implemented as the "fine tuner" for the ephemeris determination, this higher-order model would result in a Kalman estimator of higher order, thus complicating its implementation. Hopefully this would not be necessary. Simulations to verify the algorithm should include the higher-order model, however, in the simulation of the real world.

**Satellite Clock** – At this point the satellite clock is assumed to be a Rubidium frequency standard. General Dynamics Convair had such a unit tested by the National Bureau of Standards to determine its statistics. The results of that test<sup>(3)</sup> produced a one-sided power spectral density of:

$$S_V(f) = 1.28 \times 10^{-22} + 4.1 \times 10^{-25}/f \quad (7.1)$$

This spectral density is in good agreement (although a little worse) than Hewlett Packard specifications for a Rubidium standard<sup>(4)</sup>. The tested unit was not manufactured by Hewlett Packard. This spectral density is better than that specified in the GPS system specifications, which yields:

$$S_V(f) = 2 \times 10^{-20} + 7.17 \times 10^{-25}/f \quad (7.2)$$

In addition, they indicated there was some 1/f<sup>2</sup> frequency random walk noise, although a quantitative number was not given. HP predicts a drift of no more than  $\pm 1 \times 10^{-11}$  per month, which does become significant because it could happen any time during the month. This kind of drift could be estimated off-line and accounted for with bias terms if need be. A random walk model would exhibit this kind of drift in the time frames of interest.

There was no appreciable quartz oscillator noise. Any white or flicker phase noise would be eliminated with appropriate averaging times.



A good fifth-order difference equation filter to simulate the integral of the noise (phase noise) described by Equation 7.1 is given as: (5)

$$\begin{bmatrix} y_0 \\ y_1 \\ y_2 \\ y_3 \\ x \end{bmatrix}_{n+1} = \begin{bmatrix} 0 & 0 & 0 & 0 & 0 \\ \gamma - \frac{1}{2} & 1-\gamma & 0 & 0 & 0 \\ \frac{1}{2}(\gamma - \frac{1}{2}) - \frac{1}{4}\gamma & 1 - \frac{1}{4}\gamma & 0 & 0 & 0 \\ \frac{1}{2}(\gamma - \frac{1}{2}) - \gamma & -\frac{1}{2}\gamma & 1 - \frac{1}{16}\gamma & 0 & 0 \\ 0 & 0 & 0 & 1 & 1 \end{bmatrix} \begin{bmatrix} y_0 \\ y_1 \\ y_2 \\ y_3 \\ x \end{bmatrix}_n + \begin{bmatrix} 1 \\ 1/2 \\ 1/4 \\ 1 \\ 0 \end{bmatrix} \sqrt{\frac{h_0 \Delta t}{2}} \eta_{n+1} \quad (7.3)$$

where  $x$  is the phase noise,  $y_3$  the frequency noise,  $n$  is time  $n\Delta t$ ,  $\Delta t$  is the integration time interval,  $h_0$  is the white noise spectral power given in Equation 7.1 as

$$S_y(f) = h_0 + h_{-1}/f \quad (7.4)$$

$\eta_{n+1}$  is the  $(n+1)\Delta t$  random variable with variance of 1, and  $y_0$ ,  $y_1$  and  $y_2$  are intermediate states of the cascaded filter arrangement.  $\gamma$  is given as

$$\gamma = 0.777 \Delta t / \tau_1 \quad (7.5)$$

where

$$\tau_1 = \frac{h_0}{4 \ln 2 h_{-1}} \cdot \tau_1 \gg \Delta t \quad (7.6)$$

is the intercept averaging time on the Allan variance curve for the atomic clock. It can be seen that if  $\gamma$  approaches zero ( $\tau_1$  approaches infinity), the phase noise approaches integrated white noise - a first-order model with no flicker noise.  $\gamma$  cannot approach infinity because the difference equation would not be legitimate ( $\Delta t$  would have to go to zero faster than  $\tau_1$ ). Larger

$\gamma$ 's do, however, bring in higher orders of integration.

For the Rubidium standard of Equation 7.1,

$$\tau_1 = 113 \text{ seconds} \quad (7.7)$$

$$h_0 = 1.28 \times 10^{-22} \quad (7.8)$$

with a  $\Delta t$  of 10 seconds (about as large as could be tolerated) yields the equation

$$\begin{bmatrix} y_0 \\ y_1 \\ y_2 \\ y_3 \\ x \end{bmatrix}_{n+1} = \begin{bmatrix} 0 & 0 & 0 & 0 & 0 \\ -.431 & .931 & 0 & 0 & 0 \\ -.216 & -.0173 & .983 & 0 & 0 \\ -.862 & -.069 & -.0345 & .996 & 0 \\ 0 & 0 & 0 & 1 & 1 \end{bmatrix} \begin{bmatrix} y_0 \\ y_1 \\ y_2 \\ y_3 \\ x \end{bmatrix}_n + \begin{bmatrix} 1 \\ .5 \\ .25 \\ 1 \\ 0 \end{bmatrix} 2.53 \times 10^{-11} \eta_{n+1} \quad (7.9)$$

It can be seen that  $y_3$  is a "nearly integrated" white noise, as are  $y_2$  and  $y_1$ , with something subtracted out. Thus, it is really a doubly integrated white noise with part of the second integration removed. For the limiting case of singly integrated noise, the phase error propagates to a sigma of 6.5 ft in 2 hours and 23 ft in a day without corrections. With flicker noise, it would be somewhat worse.

Simulating the flicker noise would be time-consuming because of the small time interval ( $\Delta t$ ) required to do it. If the model were used for Kalman estimator covariance propagation, it would be best to revert to the continuous time domain to derive the propagation equations for larger time intervals (using exponentials and statistics). For simulation purposes, however, we must honor the time constants. A more detailed

discussion of higher ordered models is left for Appendix A.

The model actually used for the satellite clocks assumed a one-sided power spectral density function of the form:

$$S_y(f) = 2 \times 10^{-20} + A/f^2 \quad (7.10)$$

The variance  $[(2\pi)^2 A]$  of the random-walk term (integrated white noise) will be somewhat less than that for the flicker noise in Equation 7.2. This is to compensate for the fact that the random walk drifts faster than flicker noise.

The constant A may be selected so that the clock phase standard deviation (or variance) drifts the same amount for both models in a specified time. Since the system specification requires the users equivalent range error (UERE) for SV group delay be within 8 feet for two hours after upload, it would be appropriate to select that time to be two hours (7200 seconds). The variances of the phase for the two models versus time are computed from equations derived in Reference 6:

$$\sigma_{XF}^2(t) = \frac{h_0}{2} t + 2h_{-1} t^2 \quad (7.11)$$

$$\sigma_{XR}^2(t) = \frac{h_0}{2} t + \frac{(2\pi)^2 A}{3} t^3 \quad (7.12)$$

Equating them at  $t = 7200$  seconds yields:

$$A = 1.52 \times 10^{-29} \quad (7.13)$$

The comparison of the clock phase standard deviations in feet for these two models appears in Figure 7-1. At 7200 seconds, about 7.5 feet of rms clock phase is realized.

With these models, the standard deviation of the clock phase rates may also be compared. These rates are compared to the Allan two-sample standard deviation in Figure 7-2. As can be seen, there is no comparison to this quantity. The Allan two-sample statistic is convenient to

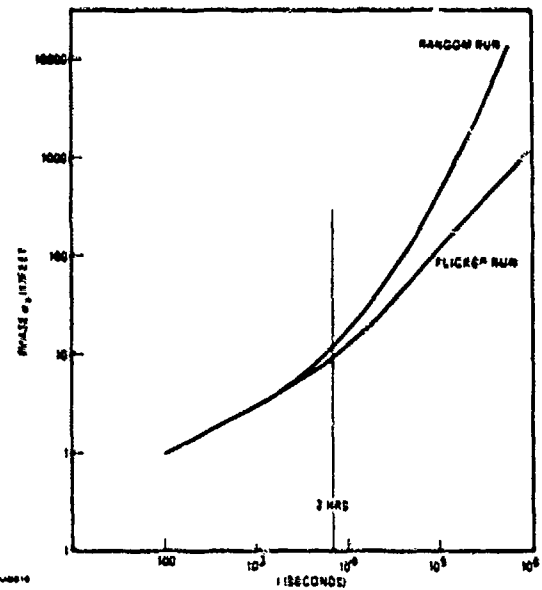


Figure 7-1. Satellite clock standard deviation vs time.

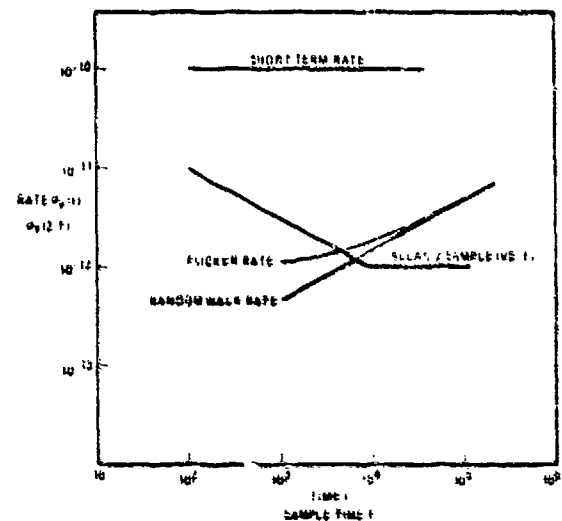


Figure 7-2. Satellite clock rate standard deviation vs time vs Allan variance specification.

represent spectral models such as Equation 7.4, but does not accurately present how the clocks drift versus time.

We can conclude from this discussion, and Figure 7-1 that the random walk model used in the analysis does indeed lean to more pessimistic errors in the satellite clock for long time intervals ( $\Delta t > 2$  hours). (See Appendix A for a further discussion of the approximation of clock drifts.)

The resulting difference equation model for the satellite clock is:

$$\begin{bmatrix} \Delta\tau_{n+1} \\ \Delta\dot{\tau}_{n+1} \end{bmatrix} = \begin{bmatrix} 1 & \Delta t \\ 0 & 1 \end{bmatrix} \begin{bmatrix} \Delta\tau_n \\ \Delta\dot{\tau}_n \end{bmatrix} \quad (7.14)$$

$$+ \begin{bmatrix} \sqrt{\frac{h_0}{2}} \sqrt{\Delta t} & 0 \\ 0 & k\sqrt{(2\pi)^2 A} \sqrt{\Delta t} \end{bmatrix} \begin{bmatrix} \eta_{1n+1} \\ \eta_{2n+1} \end{bmatrix}$$

Where  $\Delta\tau_n$  is the clock phase error at time  $n\Delta t$  and  $\Delta\dot{\tau}_n$  is the normalized frequency offset at that time;  $\eta_{1n}$  and  $\eta_{2n}$  are two independent random numbers with a variance of one generated at a time  $n\Delta t$ ;  $\Delta t$  is the computation interval;  $k$  is a constant greater than zero that adapts the frequency drift to keep the frequency offset within its specified accuracy. (It is normally 1 except in cases where the estimate of  $\Delta\dot{\tau}_n$  begins to approach its upper bound.) Normally, this does not occur for the bounds are quite high.

Measurement noise for measurements of phase on a short time basis is negligible compared to the clock phase error described above, and to the errors modeled for propagation and instrumentation uncertainties.

**Ground Station Clocks** - Cesium atomic clocks are proposed for monitor station timekeeping and, if possible, they would be a high performance type, such as the Hewlett Packard Model 5061A with the Option 004 Tube<sup>(7)</sup>. Using their specifications, the clock would have essentially non-existent frequency flicker noise, having a spectral model of the form:

$$S_y(f) = 1.446 \times 10^{-22} \quad (7.15)$$

(white frequency noise) over the frequency range of interest. However, one would expect some frequency flicker noise to be present. Thus, let us specify

$$S_y(f) = 1.446 \times 10^{-22} + h_{-1}/f \quad (7.16)$$

The  $h_{-1}$  specifies the level of the flicker noise and was selected to be:

$$h_{-1} = 6.46 \times 10^{-28} \quad (7.17)$$

resulting in a  $\tau_1$  of Equation 6.5 of  $8.04 \times 10^4$  seconds (almost a day).

In light of the fact that this still represents a low level of flicker noise, an optimistic model for the phase noise would be

$$x_{n+1} = x_n + 8.5 \times 10^{-12} \sqrt{\Delta t} \eta_{n+1} \quad (7.18)$$

for some computation interval  $\Delta t$ . However, for intervals of one day without correction, the flicker noise specified does cause additional drift in the phase. Thus, it may be modeled.

The process defined in Equation 7.16 could be simulated with a model as in Equation 7.3, and should be used to verify future results. A larger  $\Delta t$  could be used, say on the order to 800 seconds. However, at this point the more pessimistic model using a frequency random walk variation is being used. This has a spectrum of the form:

$$S_y(f) = 1.446 \times 10^{-22} + A/f^2 \quad (7.19)$$

where  $A$  is  $1.35 \times 10^{-32}$  with an adaptive random walk variance to suppress long-term frequency drift within a guaranteed accuracy of  $\pm 7 \times 10^{-12}$ . The variance of the random walk term is again somewhat less than that of the flicker noise of Equation 7.17 to compensate for its faster drift.

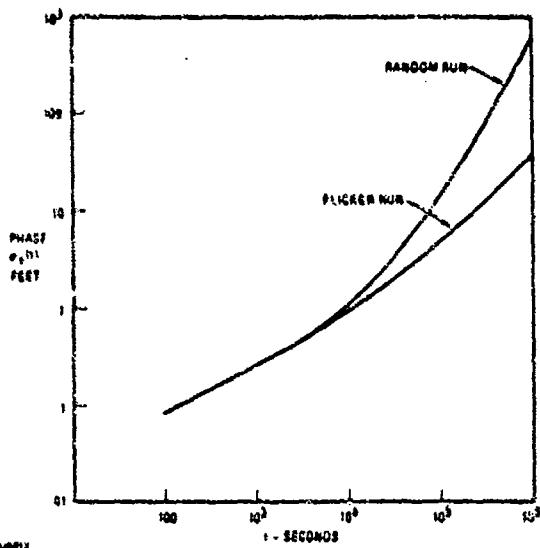


Figure 7-3. Comparison of monitor clock phase model standard deviations.

Comparison of the two models appears in Figure 7-3, using the standard deviation equations:

$$\sigma_{XF}(t) = \sqrt{7.23 \times 10^{-23} t + 1.292 \times 10^{-29} t^2} \quad (7.20)$$

$$\sigma_{XRW}(t) = \sqrt{7.23 \times 10^{-23} t + 1.78 \times 10^{-31} t^3} \quad (7.21)$$

where  $\sigma_{XF}$  and  $\sigma_{XRW}$  are the standard deviations for the phase noise with the flicker model, and phase noise with the random walk model. It can be seen that the deviations compare favorably out to 2-3 hours mainly because the white frequency noise dominates during that time interval, reverting to Equation 7.18 as a possible model.

We may conclude that the random walk model is not at all pessimistic except for time intervals longer than three hours. This could be removed also by limiting the long-term frequency variation with the adaptive random walk variance. (See Appendix A for more discussion of approximating clock drifts.) The resulting difference equation model for the monitor clocks is:

$$\begin{bmatrix} \Delta r_{n+1} \\ \Delta f_{n+1} \end{bmatrix} = \begin{bmatrix} 1 & \Delta t \\ 0 & 1 \end{bmatrix} \begin{bmatrix} \Delta r_n \\ \Delta f_n \end{bmatrix} + \begin{bmatrix} 8.5 \times 10^{-12} \sqrt{\Delta t} & 0 \\ 0 & 4.73 \times 10^{-16} \sqrt{\Delta t} \end{bmatrix} \begin{bmatrix} n_{1,n+1} \\ n_{2,n+1} \end{bmatrix} \quad (7.22)$$

Definitions of the variables are the same as for Equation 7.14 above.

As for the satellite clocks, the measurement noise for measurements of phase is dominated by errors modeled for instrumentation uncertainties.

**7.2.2 LONG-TERM FREQUENCY DRIFT** – Long-term frequency drift appears to be insignificant. The Rubidium standard specification gives a figure of  $\pm 1 \times 10^{-11}$  per month, while the Cesium standard specifications give none at all, except for a guaranteed frequency accuracy of  $\pm 7 \times 10^{-12}$  for the life of the tube (guaranteed for 10,000 hrs –  $3.6 \times 10^8$  seconds). In Reference 5, they experience a drift of about  $1 \times 10^{-13}$  in 2-1/2 years on a standard Cesium clock. These kind of numbers would be buried in the models discussed above, especially the random walk model.

The conclusion is that long-term frequency drift is not important.

**7.2.3 GENERAL RELATIVISTIC EFFECTS IN CLOCKS** – It will be necessary to correct the SV atomic clocks for drifts due to general and special relativity. These drifts arise out of the fact that the satellite clocks are located at different gravitational potentials than the monitor clocks and are moving with respect to them. The relativistic effects cause apparent shifts in the frequencies of the various clocks in the system. The apparent relativistic shift of a satellite clock with respect to a monitor clock can be expressed as:

$$\Delta f_r = \Delta f_{rs} - \Delta f_{rm} \quad (7.23)$$

where  $\Delta f_{rs}$  and  $\Delta f_{rm}$  are the relativistic shifts of the satellite and monitor clocks respectively with respect to some common reference points.

by suitably choosing the reference points, each of the terms can be conveniently computed independently of the other. Thus, in the earth-satellite system, we reference all velocities to earth center, this being the only unaccelerated point in the system, and reference all gravity potentials to a zero value at an infinite distance from earth center. With these ground rules we can proceed to evaluate  $\Delta\dot{\tau}_{rs}$  and  $\Delta\dot{\tau}_{rm}$  individually.

**Satellite Clocks** - The relativity effects act like an additional shift,  $\Delta\dot{\tau}_s$ , in the satellite clock frequency which must be added to the model represented by Equation 7.14. Thus:

$$\Delta\tau_{n+1} = \Delta\tau_n + \Delta t (\Delta\dot{\tau}_n + \Delta\dot{\tau}_{rs}) + \sqrt{\frac{h_0}{2}} \sqrt{\Delta t} \eta_{n+1} \quad (7.24)$$

where

$$\frac{\Delta\dot{\tau}_{rs}}{\dot{\tau}} = \frac{\phi_s}{c^2} - \frac{1}{2} \frac{v_s^2}{c^2} = \frac{1}{c^2 m_s} (V_s - K_s) \quad (7.25)$$

Where  $\phi_s$  is the gravity potential at the satellite locations,  $v_s$  is the magnitude of the inertial satellite velocity with respect to earth center,  $m_s$  is the satellite mass, and  $V_s$  and  $K_s$  are the potential energy and kinetic energy, respectively, of the satellite.

For a Keplerian orbit we have:

$$K_s + V_s = E_s = -\frac{\mu m_s}{2a} \quad (7.26)$$

where  $E_s$  is the constant total energy, and  $a$  is the semi-major axis of the orbit. Solving Equation 7.26 for  $K_s$  and substituting into Equation 7.25 yields

$$\frac{\Delta\dot{\tau}_{rs}}{\dot{\tau}} = \frac{1}{c^2 m_s} \left[ 2V_s + \frac{\mu m_s}{2a} \right] \quad (7.27)$$

But

$$V_s = \frac{-\mu m_s}{r} \quad (7.28)$$

so that

$$\frac{\Delta\dot{\tau}_{rs}}{\dot{\tau}} = \frac{\mu}{c^2} \left[ \frac{1}{2a} - \frac{2}{r} \right] \quad (7.29)$$

For a perfectly circular orbit,  $\Delta\dot{\tau}_{rs}/\dot{\tau}$  is a constant,  $-3\mu/2ac^2$ . If the orbit becomes slightly elliptical (e.g.,  $\epsilon = 0.01$ ), then  $r$  varies in a cyclic manner so that  $\Delta\dot{\tau}_s$  has both a constant and a periodic component. In the orbit determination process the clock periods are integrated to provide time measures. This integration will cause constant terms to grow indefinitely whereas periodic terms with zero mean will remain bounded in the integral. If the biases are known separately they can be added directly to the clock rate as an additional component of the fixed rate offset leaving only a zero-mean time-varying term. It is thus useful to split Equation 7.24 into a bias and a zero mean periodic term. We have shown that for small eccentricity the bias is given by  $-3\mu/2ac^2$ . Subtracting this from Equation 7.29 and simplifying yields the zero mean term. Recombining the two yields:

$$\frac{\Delta\dot{\tau}_{rs}}{\dot{\tau}} = \underbrace{-\frac{3\mu}{2ac^2}}_{\text{Bias Term}} + \underbrace{\frac{2\mu}{c^2} \left[ \frac{1}{a} - \frac{1}{r} \right]}_{\text{Zero Mean Periodic Term}} \quad (7.30)$$

From orbit mechanics we have:

$$r = \frac{a(1 - \epsilon^2)}{1 + \epsilon \cos \theta}$$

where  $\theta$  is the true anomaly of the satellite position. Substituting this into Equation 7.30 yields:

$$\frac{\Delta\dot{\tau}_{rs}}{\dot{\tau}} = -\frac{3\mu}{2ac^2} + \frac{2\mu}{ac^2} \left[ 1 - \frac{1 - \epsilon \cos \theta}{1 - \epsilon^2} \right] \quad (7.31)$$

Expanding the fraction in the brackets by the binomial theorem and dropping all terms beyond the linear term in  $\epsilon$  yields.

$$\frac{\Delta \dot{r}_{rs}}{\dot{r}} = -\frac{3\mu}{2ac^2} + \frac{2\mu}{ac^2} \epsilon \cos \theta \quad (7.32)$$

Bias Term	Zero Mean Periodic Term
--------------	----------------------------

The first term neglected in the above linearization would have subtracted  $2\mu\epsilon^2/ac^2$  from the bias term. For  $\epsilon = 0.01$ , this has a magnitude of the order of  $4 \times 10^{-14}$  and is thus negligible compared with the other drifts of the clock itself; and, being a constant, is absorbed by the solved-for clock models in any case.

To a first approximation with a small  $\epsilon$ ,  $\theta = (2\pi/T)(t-t_p)$  where  $T$  is the orbital period (in seconds) and  $t_p$  is the time of perigee. Thus Equation 32 becomes

$$\Delta \dot{r}_{rs} = -\frac{3\mu}{2ac^2} \dot{r} + \frac{2\mu\epsilon\dot{r}}{ac^2} \cos\left[\frac{2\pi}{T}(t-t_p)\right] \quad (7.33)$$

This can be directly added to  $\Delta \dot{r}_n$ , and integrated by the action of the  $\phi$  clock matrix (as in Equation 24), or the bias term only might be added to  $\Delta \dot{r}_n$  and the second term could be integrated analytically with respect to time with the integral then added to  $\Delta r_n$ .

For a 12-hour GPS orbit the coefficients of Equation 33 may be evaluated yielding:

$$\frac{\Delta \dot{r}_{rs}}{\dot{r}} = -2.495 \times 10^{-10} + 3.327 \times 10^{-10} \epsilon \cos [1.454 \times 10^{-4}(t-t_p)] \quad (7.34)$$

For off-nominal periods the coefficients will change slightly. For  $\epsilon = 0.01$  the integral of the periodic term introduces a peak variation of  $\pm 23$  feet in the pseudo range.

In addition to the above, the satellite clocks are, in principle, also affected relativistically by the various harmonics of the earth's gravitational field and by variations in the gravitational fields of the sun and moon as the satellite proceeds in its orbit. All these effects have been analyzed, and found to be

negligible in the GPS system as compared with the basic clock physical uncertainties.

**Monitor Clocks** - The term  $\Delta \dot{r}_{rm}$  for the monitor clocks can now be evaluated for the same reference points. These clocks are subject to the gravitational potential at the surface of the earth and the inertial velocity of their location on the surface with respect to earth center.

The relativistic shift of a monitor station clock depends on four non-negligible effects: (1) the central force gravity field, (2) the distance from earth center (a function of latitude on the oblate earth and altitude of the station above the geoid), (3) the second zonal harmonic of the earth's gravitational field (a function of latitude), and (4) the velocity of the monitor station with respect to earth center (a function of latitude).

It can be shown that the fourth effect can be treated either as a special relativistic correction or as an additional potential in the general relativity due to the centrifugal acceleration with equivalent results. The latter viewpoint is particularly useful because all four terms then become potential terms and the summation of all the terms is the total potential of the point at which the monitor is located. The gravitational force on a body is given by the gradient of the gravitational potential multiplied by the mass of the body. Since the gravitational force is everywhere perpendicular to the geoid, the geoid must be an equipotential surface. Thus all clocks on the geoid will all run at the same speed, independent of latitude. It is still necessary to determine what relativistic frequency offset applies for clocks on the geoid and how this offset changes with the altitude of the clock above the geoid. The geoidal offset can be conveniently obtained by evaluating the four listed components at either the equator or the pole. When this is done the value  $-6.969 \times 10^{-10}$  is obtained at both the pole and the equator (thus verifying the contention that the result is independent of latitude).

To a first approximation the effect of altitude can be obtained by observing that the predominant effect of altitude is the central force potential; if  $R_e$  is the earth radius to the geoid and  $h$  is the altitude above the geoid we have:

$$\begin{aligned} \frac{\delta_h \Delta \dot{t}_{rm}}{\dot{t}} &= \frac{\Delta \dot{t}_{rm}}{\dot{t}} \Big|_h - \frac{\Delta \dot{t}_{rm}}{\dot{t}} \Big|_{\text{geoid}} \\ &= \frac{\mu}{c^2 R_e} - \frac{\mu}{c^2 (R_e + h)} = \frac{\mu h}{c^2 R_e (R_e + h)} \end{aligned} \quad (7.35)$$

Neglecting the  $h$  in the denominator yields:

$$\frac{\delta_h \Delta \dot{t}_{rm}}{\dot{t}} = \frac{\mu}{c^2 R_e^2} h \quad (7.36)$$

When this is combined with the constant term for the geoid the final result is:

$$\begin{aligned} \Delta \dot{t}_{rm} &= [-6.969 \times 10^{-10} \\ &\quad + 1.10 \times 10^{-13} h] \dot{t} \end{aligned} \quad (7.37)$$

where  $h$  is altitude above the geoid in kilometers.

**Combined Relativistic Effect** – The pertinent relativistic shift is the difference between the satellite clocks and the ground observers. Since the monitor stations are not necessarily all at the same altitude, some reference level must be chosen. Since at least several of the monitors will be close to sea level, let us use the sea level geoid as the reference. Then combining Equations 7.33, 7.37, and 7.23 one obtains for the relative satellite clock shift with respect to the geoidal clock:

$$\begin{aligned} \frac{\Delta \dot{t}_{rsg}}{\dot{t}} &= -\frac{3\mu}{2ac^2} + \frac{2\mu e}{ac^2} \cos \left[ \frac{2\pi}{T} (t - t_p) \right] \\ &\quad + 6.969 \times 10^{-10} \end{aligned} \quad (7.38)$$

whereas for each monitor station the relative frequency offset is simply:

$$\begin{aligned} \frac{\Delta \dot{t}_{rmg}}{\dot{t}} &= 1.10 \times 10^{-13} h \\ &\quad (\text{km above sea level}) \end{aligned} \quad (7.39)$$

For a nominal orbit Equation 7.39 becomes:

$$\begin{aligned} \frac{\Delta \dot{t}_{rsg}}{\dot{t}} &= \underbrace{4.474 \times 10^{-10}}_{\text{Bias Term}} \\ &\quad + \underbrace{3.327 \times 10^{-10} e \cos [1.454 \times 10^{-4} (t - t_p)]}_{\text{Zero Mean Periodic Term}} \end{aligned} \quad (7.40)$$

**User Relativistic Clock Shifts** – The relativistic effects on a user are minimal. If he has a four-channel receiver so that all four pseudo ranges are measured simultaneously, his clock does not enter into his solution except very grossly and relativity is no factor. A stationary user with a sequential receiver uses his clock to tie the various measurements together. His relativistic clock shifts are just like those of a monitor station. With respect to the sea-level reference, his clock offset depends only on his altitude.

A user moving at high speed with a sequential receiver may need to adjust his clock rate for the relativistic shift due to his velocity with respect to the earth's surface. A user fixed on the geoid is moving at a vector velocity  $\bar{V}_e$  with respect to earth center (a function of latitude). His clock is running at the reference rate. If he now moves with a vector velocity  $\bar{V}_u$  with respect to his subpoint on the geoid, his velocity with respect to earth center is  $\bar{V}_e + \bar{V}_u$ . The relative clock rate offset  $\Delta \dot{t}_{rm}/\dot{t}$  for a referenced clock on the geoid contains a term  $V_e^2/2c^2$  due to motion with respect to earth center. For the moving user, this term must be replaced with  $(\bar{V}_e + \bar{V}_u)^2/2c^2$ . Without  $\bar{V}_u$  the user's clock would be running at the reference rate. Therefore, with the motion  $\bar{V}_u$  his relative clock rate offset from the reference would become:

$$\left. \frac{\Delta \dot{t}_{RU}}{\dot{t}} \right|_{\text{motion}} = \frac{|\bar{V}_e + \bar{V}_u|^2}{2c^2} - \frac{V_e^2}{2c^2} \quad (7.41)$$

Combining this with the altitude effect yields the total relativistic user clock rate shift

$$\frac{\Delta \dot{t}_{RU}}{\dot{t}} = 1.10 \times 10^{-13} h + \frac{|\bar{V}_e - \bar{V}_u|^2 - V_e^2}{2c^2} \quad (7.42)$$

where  $h$  is in kilometers and  $\bar{V}_e$  depends on latitude. In most cases, this offset will be small enough to ignore.  $\bar{V}_e$  can be conveniently computed as:

$$\bar{V}_e = \bar{\omega}_e \times \bar{R}_{EU}$$

where  $\bar{\omega}_e$  is the earth's rotation rate vector,  $\bar{R}_{EU}$  is the location on the geoid of the user's subpoint, and  $\times$  is a vector cross product.

Computational and Data Word Requirements for Clock Relativistic Effects – The computational requirements and data transmittal requirements for clock corrections are discussed in detail in Appendix B.

### 7.3 SOLAR RADIATION PRESSURE MODELS

Solar radiation forces on the satellite are important forces to consider and to model. However, if they are handled correctly, they should not create an intolerable problem. A mean force projected from the sun through the satellite should be easy to determine to the accuracy necessary to achieve Phase I goals. Phase III goals may be a little harder to achieve, unless more detailed force models are used. Modeling the perturbations about this mean force also becomes more complex as the goals become more stringent. Again, for Phase I, this modeling need not be complex. Collecting data during the NTS tracking and Phase I tracking will provide for a means for more detailed analysis during Phase III.

7.3.1 SOLAR RADIATION PRESSURE MODEL COMPLEXITY – General Dynamics Convair Aerospace Division performed studies

on their proposed satellite on solar radiation pressure effects. They did so with a 952 element flat-plate model, where for each discrete surface element ( $i$ ), the force vector is defined as

$$F_i = -VA_i [(1 - \gamma_i) \hat{S} + 2\gamma_i (\hat{S} \cdot \hat{N}_i) \hat{N}_i] \max[\hat{S} \cdot \hat{N}_i, 0] \quad (7.43)$$

where

$\bar{F}_i$  = solar radiation force on the  $i$ th element acting at its centroid

$A_i$  = element's area

$\hat{S}$  = unit element-to-sun vector

$\hat{N}_i$  = element's outward unit normal vector

$V$  = solar radiation constant ( $\approx 0.98 \times 10^{-7}$  psf) near earth

$\gamma_i$  = estimated surface reflectivity,  $\gamma_i$  [0, 1]

This model provided for all forces greater than  $0.01 \mu$  lb, which is equivalent to about a 1.5-foot orbital drift per day, if it is always in the same direction. The computation of the total force  $F$  is the sum over all 952 surfaces at each orbit position. These forces were put out in space vehicle (body) coordinates. A typical force variation in these coordinates is shown in Figure 7.4. Here, the solar panels are not aligned exactly to the sun, resulting in more than just residual normal force. This force does, however, give a clue to how one might simplify the model of Equation 7.43 by fitting the force variations to a simpler satellite structure such as a box or hexagonal shape. It is possible, however, that the detailed forces could be stored as a function of satellite, sun, and earth relative positions, and table lookups be used to determine their effect.

7.3.2 THE BOX CONCEPT – NWL, in observing NTS solar pressure forces, noted that treating the satellite as a sphere in their CELEST program was insufficient for long-term predictions of the satellite ephemeris.



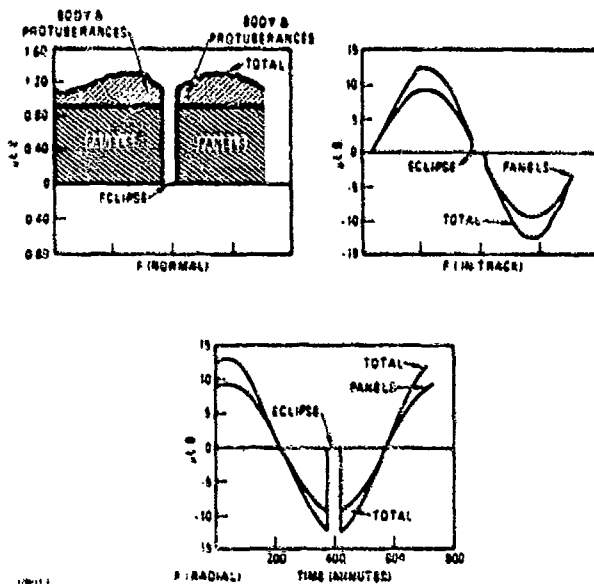
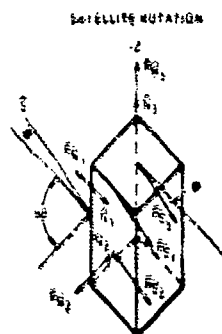


Figure 7-4. Typical solar radiation pressure - body axes.

They found, however, that a simple box model of the satellite gave them considerable improvement in the predictions. This concept appears to have merit here; however, it may not be necessary for Phase I type goals (discussed later).

Let us observe what a box model (plus solar panels) might do to the normal force of Figure 7-4. This normal force would be the Z component of the forces indicated on the box in Figure 7-5. The equations for the total force



$$F = (m_{e1} \cdot e_1 + m_{e2} \cdot e_2 + m_{e3} \cdot e_3) \cdot (E_{s1} |e_1| + E_{s2} |e_2| + E_{s3} |e_3|)$$

$$F_z = (m_{e1} \cdot e_1 + m_{e2} \cdot e_2 + m_{e3} \cdot e_3) \cdot E_{s3} \quad \text{is component of } \vec{F}$$

Figure 7-5. Forces on a box plus solar panels due to solar radiation.

and the force in the normal body direction are given in the figure.

The only reflective force in that direction is  $\vec{F}\hat{N}_3$ . The reflective forces due to the solar panels and the side 3 (top) are constant with the box rotation. Only the absorbing forces on sides 1 and 2 vary with box rotation. Let their incident angles be  $\theta_1$  and  $\theta_2$  in the X-Y plane. But:

$$\theta_2 = 90^\circ - \theta_1 \quad (7.44)$$

and

$$\cos \theta_2 = \sin \theta_1 \quad (7.45)$$

Assuming that the opposite sides are of equal area and equal reflectivity:

$$\begin{aligned} & (\vec{F}\hat{S}_1 + \vec{F}\hat{S}_2) \text{ in x-y plane} \\ & = V [A_1 (1-\gamma_1) |\cos \theta_1| \end{aligned} \quad (7.46)$$

$$+ A_2 (1-\gamma_2) |\sin \theta_1|] \cos \phi$$

for  $-180 \leq \theta_1 \leq 180$

$$\begin{aligned} & (\vec{F}\hat{S}_1 + \vec{F}\hat{S}_2) \hat{S}_z \\ & = V [A_1 (1-\gamma_1) |\cos \theta_1| \end{aligned} \quad (7.47)$$

$$+ A_2 (1-\gamma_2) |\sin \theta_1|] \sin \phi$$

$$= F_{12}$$

for a constant angle. Therefore, the total normal force is:

$$\begin{aligned} F_z & = (\vec{F}\hat{S}_{S.P.} + \vec{F}\hat{S}_3) \hat{S}_z \\ & + |\vec{F}\hat{N}_3| + F_{12} \end{aligned} \quad (7.48)$$

The  $F_z$  is a constant force plus a periodic function of the incidence angle in the x-y plane. If we fit Equation 7.48 to the normal force in Figure 7-4 with  $\gamma_2 = 1$ , and with

$$\theta_1 = \frac{11}{2} = 25^\circ$$

where  $t$  is in minutes and  $1/2$  is in degrees/minute, we have a fit (neglecting the eclipse) resembling Figure 7-6, leaving a residual of no more than about  $\pm 0.05\mu$  lb in that direction ( $\pm 2 \times 10^{-9}$  ft/sec<sup>2</sup> acceleration), which is quite tolerable. At that level, over a two-hour period, it would result in about a 0.6-foot drift error.

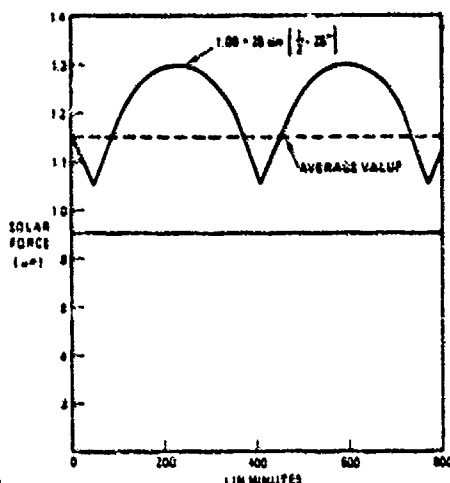


Figure 7-6. Box model fit to normal force of Figure 7-4.

For the radial and in-track forces, the periodic components using this model could be obtained by multiplying Equation 7.46 by either the cosine or sine of  $\theta_1$ . The reflective forces  $\vec{F}_{N1}$  and  $\vec{F}_{N2}$  are also periodic, and vary as a function of the cosine squared of the incidence angle when the side is in view of the sun.

We shall leave the task of verifying the box concept as future analyses (see Section 8).

### 7.3.3 THE TIME VARYING BIAS CONCEPT

The forces discussed above do get integrated twice before they show up as orbital drifts and thus many of the perturbations get integrated out before they do much harm, at least during Phase I. It is conceivable that the solar radiation forces could be treated as biases that vary with time of year (or as the difference between the satellite's orbit inclination and the sun's inclination). Such a bias would be the slope of the plots of Figure 7-7. The eclipse should be easy to keep track of (if nothing else, through

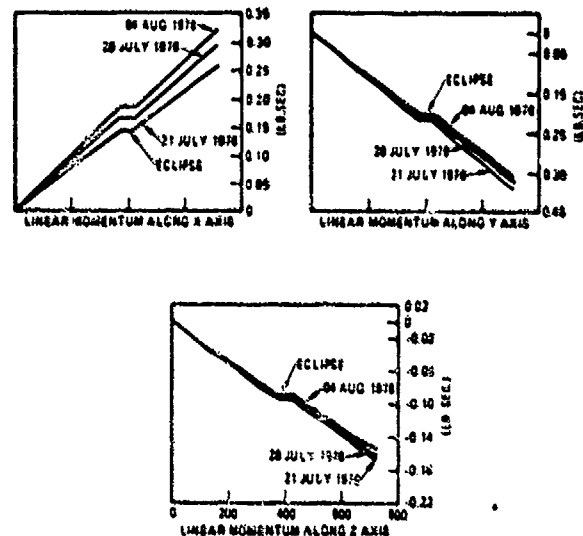


Figure 7-7. Linear momentums along inertial axes due to solar radiation.

telemetry of the temperature), so we could ignore its effect by just shutting off the bias when it occurs.

Dividing the momentums plotted in Figure 7-7 by a mass of 25 slugs results in a velocity buildup in inertial space versus time. To obtain the drift in feet, we multiply the mean velocity at any time by  $t/2$ . Mismodeling this bias by five percent produces an envelope on any one of the plots that would contain the variations in the velocity (or momentum). This would result in a maximum drift error for a day along the x or y axis of about 52 ft, and for two hours of 4.5 ft. This is probably tolerable during Phase I. It is not for Phase III.

### 7.3.4 SUMMARY OF SOLAR RADIATION FORCE MODELING

It is obvious that solar radiation force modeling is one of the fuzzy areas of ephemeris determination modeling. Three concepts were discussed above, going from great detail to a very simple model. The many-flat-plate element approach would probably be prohibitive from the standpoint of computer memory and time line requirements. The latter is questionable with respect to legacy for Phase III, as well as not being acceptable for NWL's purposes. This leaves the box concept, which appears quite feasible, and

would probably be an extension of NWL's work on NTS. Additional studies of each method are planned.

In either case, the expected residual forces should be included in the propagation noise matrix of the Kalman equations.

# 8

## OUTLINE OF FUTURE ANALYSES

The discussions in this trade study indicate that not all trades have been completed, and some analytical questions still need to be answered. Publication of this trade study report does not mean that there is a work stoppage in this area. This section outlines some of the major future analysis tasks which are necessary and are planned in order to reduce the engineering risk in the development of the Global Positioning System.

### 8.1 PLANNED ANALYSES TASKS

The following is a brief description of planned analysis tasks.

**8.1.1 TRADEOFFS ON HANDLING EPOCH SOLUTIONS** - The object of this task would be to answer tradeoff questions with respect to the inverse propagations of the propagation noise matrix  $Q$  to epoch; that is, the effect of ignoring the propagation, or the effects on numerical accuracy if it is not ignored, for both the NWL epoch and the daily epoch.

**8.1.2 FURTHER MEASUREMENT SET TRADEOFFS** - The objective of this task is to continue to evaluate the measurement sets scored in Section 7 with respect to the gradable criteria. Such subtasks would be the following.

**Evaluation of Combining Separate Monitor Station Clock Solutions** - This task is related to Case 4 of Table 3-1, which has  $n$  solutions of the monitor station clocks for  $n$  satellites.

**Improving the Convergence of Common Monitor Solution with Pseudo Ranges and/or the Long-Term Accuracy Using Pseudo-Range Increments** - This task is related to Cases 5 and 8. The convergence of Case 5 can be improved three ways:

1. Adapting the propagation noise as a function of measurement discrepancies
2. Combining the pseudo range measurements with either pseudo range rate or pseudo range increment measurements
3. Using "book shelf" correlations.

The second way could be reversed for Case 8 to improve its long-term accuracy.

**8.1.3 INVESTIGATION OF STATION-KEEPING OUTGASSING COMPENSATION METHODS AND EFFECTS** - This task is designed to define methods of interfacing with the Satellite Control Facility and NWL during station keeping operations, and to investigate the effects of misalignments and misrepresentation of the operations in the estimation models.

**8.1.4 CLOCK MODEL STUDIES** - This task is meant to verify the legitimacy and legacy of the proposed clock models by simulating, as close to the real world as possible, flicker frequency models operating with Kalman gains derived with the random walk models.

**8.1.5 SOLAR PRESSURE MODEL DEVELOPMENT** - By representing the real world with the sophisticated multiple flat-plate element solar pressure models, develop formidable less-complex solar pressure models that would be reasonable and adequate for the GPS algorithms and NWL's algorithms.

**8.1.6 CLOCK RELATIVISTIC EFFECTS REPRESENTATION** - Perform trade studies to determine the best approach in representing the satellite clock relativistic effects to the user, based on orbital parameters presented to him, or included in clock update parameters presented to him.

**8.1.7 ATMOSPHERIC DELAY BIAS MODELING** – Atmospheric delays can be predicted to some extent. However, there are unknown random delays that must be accounted for. The purpose of this task is to

determine the necessity of including these delays, as random biases or highly correlated random processes, in the Kalman estimator equations, or the effects of not including them.

# 9

## REFERENCES

1. "System 621B Force Environment Study Report," Data Dynamics, Inc., 3 October 1973.
2. Barnes, J.A., and Jarvis, S. Jr., "Efficient Numerical and Analog Modeling of Flicker Noise Processes," NBS Technical Note 604, June 1971.
3. General Dynamics' correspondence 624-4-74-12, "Trip Report, Rubidium Frequency Standard Evaluation at National Bureau of Standards," M.A. Treece to J.D. Rhamy, 28 February 1974.
4. "Rubidium Frequency Standard 5065A," Hewlett-Packard Technical Data, 15 April 1971.
5. Allan, David W., et al., "Performance, Modeling and Simulation of Some Cesium Beam Clocks," Proceedings 27th Annual Symposium on Frequency Control, 12-14 June 1973.
6. Barnes, J.A., and Allan, D.W., "A Statistical Model of Flicker Noise," Proceedings IEEE, Volume 54, No. 2, February 1966.
7. "Cesium Beam Frequency Standard 5061A," Hewlett-Packard Technical Data, 1 January 1973.

# A

## APPROXIMATING CLOCK DRIFTS

### GPS CLOCK MODELS

The most significant error source in GPS navigation solutions is presently the drift in the anticipated satellite clocks, at least until the more precise time standards are worthy of being launched into orbit. For the time being, however, it is important that we predict at best we can the ever-present GPS clock drifts.

During the time that the satellites are in view of the monitor stations, and pseudo-range measurements are in use, the impact of the clock models is not quite so significant, since the ephemeris solutions and clock drift estimates are being updated often, and at relatively short time intervals. It is with the longer time predictions that good models are important.

The statistical drift characteristics of such clocks as those to be implemented in the GPS are fairly well-known for the time spans of interest, at least in their form, if not the magnitude. The problem arises from the fact that these characteristics cannot be described in a straightforward way for the Kalman prediction and estimation algorithm; that is, not as white noise passed through a linear filter. The phenomenon that is difficult to describe is flicker frequency noise, which has a  $1/\omega$  spectrum. We can however approximate this characteristic for the SV clocks closely up to about  $10^5$  seconds, something over a day, with a reasonably low-order linear process.

The  $[1+b/\omega]$  spectrum (including the short-term white noise frequency variations) is approximated by passing the white noise through cascade filters of the form

$$\prod_{i=1}^n (s + a_i)/(s + b_i).$$

This produces a spectrum

$$\prod_{i=1}^n (\omega^2 + a_i^2)/(\omega^2 + b_i^2),$$

and approximates  $[1+b/\omega]$  over a range of frequencies.<sup>(1)</sup> Representative approximations were converted to time domain statistics of the satellite clock phase drifts.<sup>(2)</sup> They are presented for comparison purposes in Figures A-1 through A-4 on which the corresponding filters and spectral equations are given. In the figures, the standard deviation (RMS) of the approximate clock phase drift is compared to the expected standard deviation (rms) of a true clock phase drift with the flicker frequency noise spectrum.<sup>(3)</sup>

The first figure represents a comparison to a random walk frequency drift  $[(1+a/\omega^2)$  spectrum] which was used in previous analyses. This drift was designed to match the real-world drift for about two hours (to cover the test site) and then be pessimistic from then on. The thought was that as long as the model is pessimistic, the approach is conservative. This may be true during the estimation process (when the satellites are in view), but during the prediction process, being pessimistic is no better, or no worse, than being optimistic. In

(1) These flicker noise approximations were suggested by J.A. Barnes and Stephen Jarvis, Jr. in the National Bureau of Standards Note 806 entitled "Reference Numerical and Analog Modeling of Flicker Noise Processes," dated June 1977.

(2) The time domain statistics were derived using methods described by J.A. Barnes and G.W. Allen in the February 1968 issue of the Proceedings of the IEEE (Vol 56, No. 2, pp 176-178) in an article entitled "A Statistical Model of Flicker Noise."

(3) The true clock is not suggested by the SV segment clock specifications.

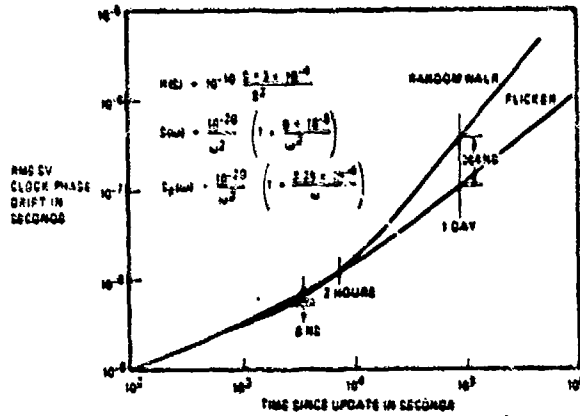


Figure A-1. Random walk approximation.

either case, the prediction is in error.<sup>(1)</sup> The GPS error budget gives no preference to the sign of the error.

The next three figures (A-2 through A-4) illustrate how the phase drift caused by the flicker frequency noise can be approximated with 1st, 2nd, and 3rd order cascaded filter models of the clock frequency offset. All the filters do a satisfactory job out to one day, with some improvement varying with order. The higher-order filters naturally approximate better for a longer period of time. For Phase I purposes, however, there are diminishing returns. The first-order approximation would probably suffice; however, it would not yield an estimate of the second derivative of the clock phase drift, except by the laws of the model. The second order approximation would yield that estimate. Allowing for an estimate of the second derivative would definitely reduce risk in case it were needed, and would define a coefficient for second order polynomial predictions. If it wasn't needed, its estimate would be near zero. One additional state per satellite has negligible impact on computational time lines and computer memory.

<sup>(1)</sup> It should be emphasized here that the errors being discussed are RMS errors due to using approximations. The actual RMS phase drift prediction error becomes the approximation, and is that RMS error expected because of our inability to predict random occurrences.

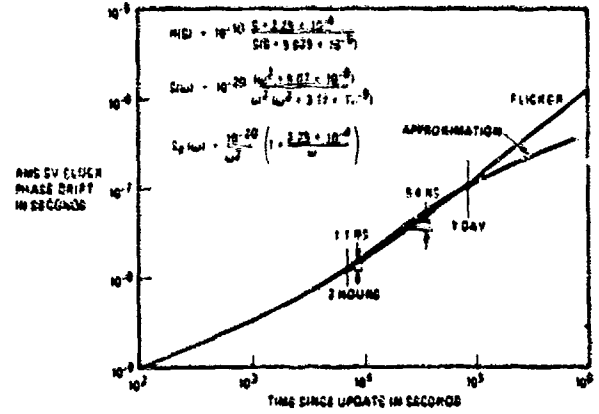


Figure A-2. First-order cascade filter model 3.

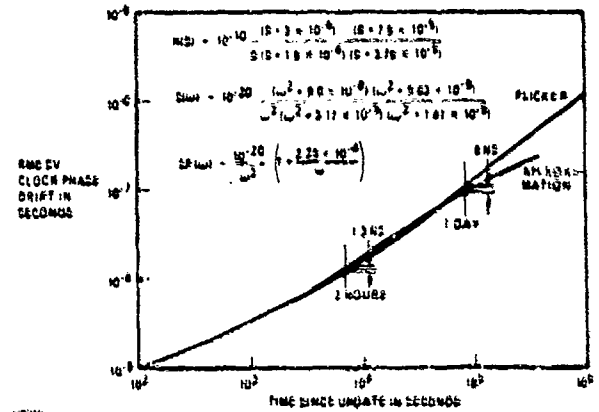


Figure A-3. Second-order cascade filter model 1.

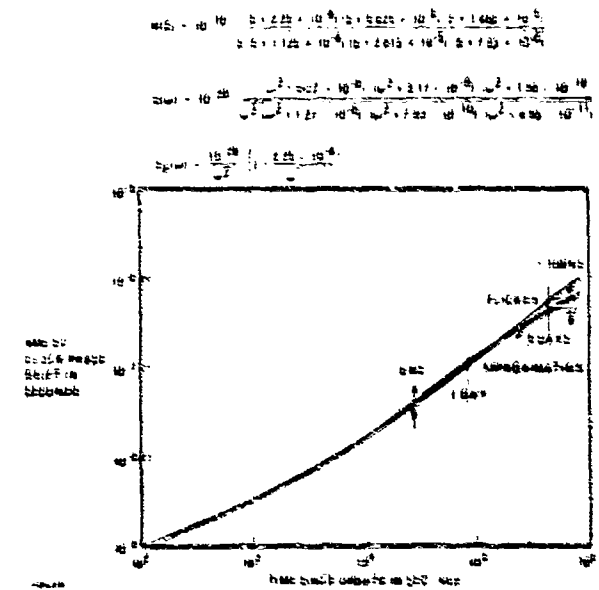


Figure A-4. Third-order cascade filter model 3.



## CESIUM BEAM STANDARDS AND MS CLOCKS

The third order approximation did carry the accuracy out to about 2-3 days, suggesting that it might be useful with Phase III goals. However, it is believed that better clocks would be flyable by then. Cesium beam clocks such as those proposed for the monitor stations could be modeled with the 2nd order approximation to within 2 nanoseconds rms phase drift error out to about 5 days, mainly because of their

increased long-term stability. Even with a constant frequency offset spectral model as an approximation, only about 3.7 nanoseconds rms phase drift error is expected in a day. In this light, a constant frequency offset model is proposed for the monitor station clocks, since their prediction errors over that time are never passed on to the user. For Phase I, any longer time span would result in SV clock drifts that overshadow MS clock drifts. In Phase III, first-order models may be in order.

# B

## SV CLOCK CORRECTION UPLOAD AND DOWNLINK FORMAT AND CS AND US SEGMENT COMPUTATIONAL REQUIREMENTS

### INTRODUCTION

An SV clock correction procedure was defined and computations were split up and allocated to the CS and US segments in a way *minimizing downlink time and user computation*. The computations involve predicting the SV clock drift, propagating the prediction epoch, and computing general relativistic corrections. *The SV manufacturer must offset SV clock frequency for secular relativistic drift.*

### THE DRIFT PREDICTION MODEL

The drift prediction model is a second-order Taylor's Series expansion of the form

$$\Delta t_i(t) = \Delta t_{oi} + \left(\frac{\Delta f}{f}\right)_i (t - t_{oi}) + \frac{1}{2} D_i (t - t_{oi})^2 \quad (B-1)$$

where the subscript  $i$  represents the  $i^{\text{th}}$  page stored in the SV.  $t_{oi}$  is the epoch time of the  $i^{\text{th}}$  page,  $\Delta t_i(t)$  is the predicted SV clock drift with respect to system time  $t$ ,  $\Delta t_{oi}$  is the predicted SV drift at the epoch time  $t_{oi}$ ,  $(\Delta f/f)_i$  is the predicted frequency offset at the epoch time  $t_{oi}$ , and  $D_i$  is the predicted rate of change of frequency offset at that time. The downlink contains 2 bytes for  $\Delta t_{oi}$  for a range of 1 nanosecond to 10  $\mu$ seconds, 1 byte for  $(\Delta f/f)_i$  for a range of  $10^{-13}$  to  $10^{-11}$  seconds/second, and 1 byte for  $D_i$  for a range of  $10^{-16}$  to  $10^{-14}$  seconds/second<sup>2</sup>. Each page is good for one hour of system time. These quantities are computed from the control segment clock predictions for the system time  $t=t_{oi}$ . The user receives that epoch time  $t_{oi}$  in the HOW word for that SV page. An age of data word is also sent in the clock Data Block, which corresponds to the last upload.

### RELATIVISTIC EFFECTS

The SV clock drift due to general relativity since an epoch time  $t_{oi}$  is:

$$\begin{aligned} \Delta t_{iR}(t) = & 6.969 \times 10^{-10} (t - t_{oi}) \\ & + 7.287 \times 10^{-3} (t - t_{oi})^2/a \\ & - 2.9148 \times 10^{-2} \frac{\sqrt{a}}{k} \\ & [E(t - t_p) - E(t_{oi} - t_p)] \end{aligned} \quad (B-2)$$

where  $a$  is the SV orbit semi-major axis,  $k$  is the earth's gravitational constant ( $1.187 \times 10^8 \text{ ft}^3/2/\text{sec}$ ),  $E$  is the orbit's eccentric-anomaly and  $t_p$  is the time of perigee. This drift could be computed in the user software for the parameters are already present for SV position computations.

A problem we encounter, however, is that the secular clock drift is so substantial (about 40  $\mu$ sec/day) that the SV clock time would not be within the specified 10  $\mu$ sec of the system time, unless its time is mechanically updated 4 times a day. The SV clock can, however, be calibrated with a frequency offset  $\Delta f/f_c$  to cancel out this secular drift. It would be necessary to require the SV contractor to do this.\* For a nominal circular orbit, this would be

$$\frac{\Delta f}{f_c} = -4.454 \times 10^{-10} \quad (B-3)$$

making the SV clock run slower than the system clocks to make up for the fact that it runs faster due to relativity.

\*Unless, of course, all manufacturers and users did the opposite in their clocks.

Thus, instead of working with Equation B-2, we must work with perturbations about the offset of Equation B-3. To do this, we must expand the eccentric anomaly about the mean anomaly:

$$M(t) = \frac{k}{a^{3/2}} (t - t_p) \quad (B-4)$$

That is:

$$E(t - t_p) = M(t) + \Delta E(t - t_p) \quad (B-5)$$

$$= M(t) + e \sin E(t - t_p) \quad (B-6)$$

where  $e$  is the eccentricity. Likewise

$$E(t_{oi} - t_p) = M(t_{oi}) + \Delta E(t_{oi} - t_p) \quad (B-7)$$

The last term of Equation B-2 is then

$$\begin{aligned} \text{term} &= -2.9148 \times 10^{-2} (t - t_{oi}) / a \\ &- 2.9148 \times 10^{-2} \frac{\sqrt{a}}{k} \\ &[\Delta E(t - t_p) - \Delta E(t_{oi} - t_p)] \end{aligned} \quad (B-8)$$

The first term of B-8 then combines with the second term of B-2. We then expand  $1/a$  to a good accuracy for  $e \leq 0.01$  as:

$$\frac{1}{a} = \frac{1}{a_0} - \frac{1}{a_0^2} \Delta a \quad (B-9)$$

where  $a_0$  is the nominal semi-major axis ( $8.7 \times 10^7$  ft.), and  $\Delta a$  is the deviation from the nominal. Combining all of this, Equation B-2 is rewritten as

$$\begin{aligned} \Delta t_{IR}(t) &= \left[ 6.969 \times 10^{-10} + 7.287 \times \right. \\ &\quad \left. 10^{-3}/a_0 - 2.9148 \times 10^{-2}/a_0 \right] \\ &(t - t_{oi}) - \left[ 7.287 \times 10^{-3}/a_0^2 \right. \\ &\quad \left. - 2.9148 \times 10^{-2}/a_0^2 \right] \Delta a \\ &(t - t_{oi}) - 2.9148 \times 10^{-2} \end{aligned}$$

$$\frac{\sqrt{a}}{k} [\Delta E(t - t_p) - \Delta E(t_{oi} - t_p)] \quad (B-10)$$

The bracketed quantity of the first term of B-10 is taken care of with the calibration frequency offset in Equation B-3. The second term of Equation B-10 is a smaller secular drift due to semi-major axis difference from nominal. The third term has a time drift at the epoch time  $t_{oi}$  plus a periodic component. We can now expand that third term with:

$$\sqrt{a} \approx \sqrt{a_0} + \frac{1}{2} (a_0)^{-1/2} \Delta a \quad (B-11)$$

as

$$\begin{aligned} \text{term} &= -2.9148 \times 10^{-2} \frac{\sqrt{a_0}}{k} \Delta E(t - t_p) \\ &- 2.9148 \times 10^{-2} \frac{1}{2\sqrt{a_0} k} \Delta a \Delta E \\ &(t - t_p) + 2.9148 \times 10^{-2} \frac{\sqrt{a}}{k} \Delta E \\ &(t_{oi} - t_p) \end{aligned} \quad (B-12)$$

Combining Equation B-12 with Equation B-10, we have:

$$\begin{aligned} \Delta \tilde{t}_{IR}(t) &= \Delta t_{IR}(t) + \frac{\Delta f}{f_c} (t - t_{oi}) \\ &= 2.895 \times 10^{-18} \Delta a (t - t_{oi}) \\ &- 2.29 \times 10^{-6} \Delta E(t - t_p) \\ &- 1.315 \times 10^{-14} \Delta a \Delta E \\ &(t - t_p) + 2.455 \times 10^{-10} \sqrt{a} \\ &\Delta E(t_{oi} - t_p) \end{aligned} \quad (B-13)$$

The first term of Equation B-13 is a secular drift due to off-nominal semi-major axis. The drift rate corresponding to it is on the order of  $10^{-12}$  for  $\Delta a$  of  $10^6$ , thus it is in the ballpark of the clocks mechanical drift rate and can be

included in the corresponding term of Equation B-1.

The next term is a periodic term corresponding to  $\pm 2290e$  nanoseconds drift. It cannot be included in Equation B-1 because of the periodicity. Its higher derivatives are significant. Thus, it would have to be computed by the user in one of two ways. If the user computes the deviation from the mean anomaly to get the eccentric anomaly, he already has it. Otherwise, if he has the eccentric anomaly,  $\Delta E(t-t_p)$  is computed as:

$$\begin{aligned} \Delta E(t-t_p) &= E(t-t_p) - M(t) \\ &= E(t-t_p) - \frac{k}{a^{3/2}}(t-t_p) \\ &= e \sin [E(t-t_p)] \quad (B-14) \end{aligned}$$

In computing the satellite position, he should have it one way or another. The third term of Equation B-13 is negligible ( $\sim 10^{-10}$ ) and can be dropped.

The fourth term is significant ( $\sim 10^{-8}$ ), and can be computed by the control segment, and included in the drift term of Equation B-1.

#### CONTROL SEGMENT COMPUTATIONS FOR UPLOAD

As stated above, the control segment can relieve the user from most of the relativity effects computations by including some of it in the drift model of Equation B-1, leaving only the periodic portion to him. There are some additional computations for the control segment, however, to account for changes in SV clock epoch times.

As far as the user is concerned, his computations are based on the epoch time of the present satellite's page. The control segment has the responsibility of taking care of all previous drift in the  $\Delta t_{oi}$  term of Equation B-1. This includes relativity drift up to that time. Using Equation B-13 to compute the

drift between the time  $t_0$  (time of last used SV measurement) and  $t_{oi}$

$$\begin{aligned} \Delta \tilde{t}_{iR_{cs}}(t_{oi}) &= 2.895 \times 10^{-18} \Delta a \\ &\quad (t_{oi} - t_0) - 2.29 \times 10^{-6} \\ &\quad \Delta E(t_{oi} - t_p) - 1.315 \times \\ &\quad 10^{-14} \Delta a \Delta E(t_{oi} - t_p) \\ &\quad + 2.455 \times 10^{-10} \sqrt{a} \Delta E \\ &\quad (t_0 - t_p) + 2.455 \times 10^{-10} \\ &\quad \sqrt{a} \Delta E(t_{oi} - t_p) \quad (B-15) \end{aligned}$$

including the control segments portion of Equation B-13. The second, third and fifth terms cancel, leaving:

$$\begin{aligned} \Delta \tilde{t}_{iR_{cs}}(t_{oi}) &= 2.895 \times 10^{-18} \Delta a \\ &\quad (t_{oi} - t_0) + 2.455 \times 10^{-10} \\ &\quad \sqrt{a} \Delta E(t_0 - t_p) \quad (B-16) \end{aligned}$$

which is the secular drift for off-nominal semi-major axis since the last SV clock estimation, and the periodic drift between that time and the time of perigee loaded for the epoch  $t_{oi}$ .

Also, as stated before, a drift rate contribution must be included. That is:

$$\left(\frac{\Delta f}{f}\right)_{iR} = 2.895 \times 10^{-18} \Delta a \quad (B-17)$$

due to off-nominal semi-major axis.

The model terms for Equation B-1 are then:

$$\begin{aligned} \Delta t_{oi} &= \Delta t_{oim} + 2.895 \times 10^{-18} \Delta a \\ &\quad (t_{oi} - t_0) + 2.455 \times 10^{-10} \sqrt{a} \\ &\quad \Delta E(t_0 - t_p) \quad (B-18) \end{aligned}$$

$$\left(\frac{\Delta f}{f}\right)_i = \left(\frac{\Delta f}{f}\right)_{im} + 2.895 \times 10^{-18} \Delta a \quad (B-19)$$

\*This quantity can be approximated with  $e \sin [M(t)]$  to within  $10^{-2}$ , which for  $e < 0.01$  is negligible.

$$D_i = D_{im} \quad (B-20)$$

where the subscript m denotes mechanical drift.

#### USER SEGMENT COMPUTATION

When the user receives the clock words  $\Delta t_{oi}$  ( $\Delta f/f$ )<sub>i</sub>, and  $D_i$ , along with the satellite clock time  $t_s$ , he corrects the satellite clock time by subtracting its drift as:

$$t = (t_s - \Delta t_{oi}) - \left(\frac{\Delta f}{f}\right)_i (t_s - t_{oi}) - \frac{1}{2} D_i (t_s - t_{oi})^2 + 2.29 \times 10^{-6} \Delta E (t_s - t_p) \quad (B-21)$$

The fact that  $t_s$  could be off by 10  $\mu$ sec has negligible effect inside the parenthesis of Equation B-21. User clock drifts due to relativity are negligible over the time span that he uses it for a navigation fix.

#### CONTROL SEGMENT COMPUTATIONS FOR PSEUDO RANGE MEASUREMENT CORRECTIONS

The SV clock relativity drift also affects the Control Segment's pseudo range measurements. He must compute the SV Clock relativity drift since the last measurement used which was also corrected. Say this time was  $t_L$ . The governing equation is Equation B-10 with SV  $\Delta f/f_c$  calibration removed. That is, the pseudo range error is

$$c \Delta \tilde{r}_{ij}(t - t_L) = c \left\{ 2.895 \times 10^{-18} \Delta a (t - t_L) - 2.455 \times 10^{-10} \sqrt{5} (\Delta E (t - t_p) - \Delta E \right.$$

$$(t_L - t_p) \left. \right\} - 3.353 \times$$

$$10^{-17} h_j (t - t_L) \quad (B-22)$$

which includes an altitude correction, where  $h_j$  is the  $j^{\text{th}}$  monitor station's altitude above the earth's geoid in feet. This added drift is actually the negative of the monitor station's clock relativity drift, for all relativity drifts are referenced to the earth's geoid. The pseudo range is then

$$\tilde{R}_{ij}(t) = c \Delta r_{ij}(t) - c \Delta \tilde{r}_{ij}(t - t_L) \quad (B-23)$$

where  $\Delta r_{ij}(t)$  is the clock phase difference between the SV<sub>i</sub> and monitor station j clocks. Mechanical drifts are estimated in the ephemeris determination algorithm.

#### SUMMARY

Clock drifts are uploaded to the satellite in 6-byte data blocks (one byte for age of data), in a second-order polynomial format. Assuming the SV manufacturer offsets the frequency of the SV clocks to cancel secular relativity drift, which he must to preserve his time to within 10  $\mu$ sec of system time, the relativistic effects can be included in those data blocks, with the exception of the periodic effect due to eccentric orbits. The user must compute this periodic effect from orbital parameters already available to him from the satellite ephemeris data block. The control segment computes the rest.

The control segment must also compute relativistic effects on its measurements from the satellite. This drift is a function of the orbital parameters and the altitude of the monitor station.